

AD651217

AB

USAALABS TECHNICAL REPORT 67-1

PRELIMINARY DESIGN OF A ROTOR SYSTEM FOR A HOT CYCLE HEAVY-LIFT HELICOPTER

By

J. R. Simpson

March 1967

**U. S. ARMY AVIATION MATERIEL LABORATORIES
FORT EUSTIS, VIRGINIA**

**CONTRACT DA 44-177-AMC-225(T) Task II
HUGHES TOOL COMPANY
AIRCRAFT DIVISION
CULVER CITY, CALIFORNIA**

**Distribution of this
document is unlimited**



ARCHIVE COPY

**D D C
RECORDED
MAY 10 1967
R
C**

**389
F**

Disclaimers

The findings in this report are not to be construed as an official Department of the Army position unless so designated by other authorized documents.

When Government drawings, specifications, or other data are used for any purpose other than in connection with a definitely related Government procurement operation, the United States Government thereby incurs no responsibility nor any obligation whatsoever; and the fact that the Government may have formulated, furnished, or in any way supplied the said drawings, specifications, or other data is not to be regarded by implication or otherwise as in any manner licensing the holder or any other person or corporation, or conveying any rights or permission, to manufacture, use, or sell any patented invention that may in any way be related thereto.

Trade names cited in this report do not constitute an official endorsement or approval of the use of such commercial hardware or software.

Disposition Instructions

Destroy this report when no longer needed. Do not return it to originator.

ACCESSION FOR		
CFSTI	WHITE SECTION <input checked="" type="checkbox"/>	BUFF SECTION <input type="checkbox"/>
DOC	U.S. GOVERNMENT	
3-11-188	Per statement Lm on doc	
S. W. BU BUREAU AVAILABILITY CODES		
CLT.	AVAIL. AND SPECIAL	
/		



DEPARTMENT OF THE ARMY
U. S. ARMY AVIATION MATERIEL LABORATORIES
FORT EUSTIS, VIRGINIA 23604

This report has been prepared by Hughes Tool Company, Aircraft Division, under the provisions of Contract DA 44-177-AMC-225(T), Task II, to present the preliminary design of a hot cycle rotor system.

The report is published for the dissemination of information and the reporting of program results.

Task 1F131001D15701
Contract DA 44-177-AMC-225(T) Task II
USAAVLABS Technical Report 67-1
March 1967

**PRELIMINARY DESIGN OF A ROTOR SYSTEM
FOR A HOT CYCLE HEAVY-LIFT HELICOPTER**

HTC-AD 66-17

by
J. R. Simpson

Prepared by
Hughes Tool Company - Aircraft Division
Culver City, California

for
U. S. ARMY AVIATION MATERIEL LABORATORIES
FORT EUSTIS, VIRGINIA

Distribution of this
document is unlimited

ABSTRACT.

Under the terms of Contract DA 44-177-AMC-225(T) Task II, Hughes Tool Company - Aircraft Division has completed the preliminary design study of a rotor system for a Hot Cycle Heavy-Lift Helicopter.

During the study program, extending from March 1965 to August 1966, accomplishments were as follows. An analytical procedure was developed that permits calculation of fully coupled blade response and dynamic stability characteristics. Parametric and configuration studies to reflect basic characteristics of the rotor system on the design characteristics and mission requirements were conducted. Design layouts, structural design studies, and detailed weight analyses were made. The design and analysis were limited to the integrated lift-propulsion system with emphasis on the rotor system. This effort resulted in the selection, preliminary design, and determination of performance of the optimum rotor for the heavy-lift mission requirements. Also, a fully coupled rotor dynamic analysis of the optimum rotor was made and a full-scale mockup of the rotor hub area was constructed.

The Hot Cycle heavy-lift helicopter with the selected rotor as designed exceeds the performance requirements for a 20-ton heavy-lift mission by as much as 6 tons, a 12-ton transport mission by approximately 2 tons, and a 1,500-nautical-mile ferry range by as much as 600 nautical miles. Fuel utilization (namely, ton-miles of payload per pound of fuel) proved to be outstanding.

FOREWORD

This report was prepared in accordance with Task II of Contract DA 44-177-AMC-225(T) for the U. S. Army Aviation Materiel Laboratories. The contract became effective on 17 March 1965. Work was completed on 31 August 1966. The report summarizes the preliminary design program, including the parametric studies and an integrated preliminary design.

The work was accomplished by Hughes Tool Company - Aircraft Division in Culver City, California, under the direction of Mr. H. O. Nay, Director of Aeronautical Engineering, and Mr. C. R. Smith, Manager, Hot Cycle Department, and under the direct supervision of Mr. J. R. Simpson, Project Engineer, Hot Cycle Heavy-Lift Helicopter.

CONTENTS

	<u>Page</u>
ABSTRACT	iii
FOREWORD	v
LIST OF ILLUSTRATIONS	viii
• LIST OF TABLES	x
LIST OF SYMBOLS	xi
SUMMARY	1
STUDY REQUIREMENTS	7
• AIRCRAFT CONFIGURATIONS STUDIED	10
PERFORMANCE	21
STABILITY AND CONTROL CHARACTERISTICS	31
ROTOR SYSTEM	39
PROPULSION SYSTEM	45
WEIGHTS	51
STRUCTURES	75
PARAMETRIC STUDY	82
COMPOUND HELICOPTER STUDY	129
FULLY COUPLED BLADE RESPONSE AND DYNAMIC STABILITY	
ANALYSIS USING SADSAM IV	135
HUB MOCKUP	149
REFERENCES	160
DISTRIBUTION	163
APPENDIXES	
I Summary Weight Statement and Detailed Weight Calculations	164
II Preliminary Structural Analysis	212
III Rotor Blade Equations	321
IV Computer Circuit Diagram and Input Data for Coupled Analysis	345
V Standard Structural Cell for the Representation of Mechanical Effects in Helicopter Rotor Blades ..	395
VI Typical Samples of Coupled Analysis Unmodified Computer Output	368

LIST OF ILLUSTRATIONS

<u>Figure</u>		<u>Page</u>
1	Hot Cycle Heavy-Lift Helicopter Concept	xix
2	Propulsion System	2
3	Useful Load Comparison	4
4	XV-9A Hot Cycle Research Aircraft	6
5	General Arrangement - Configuration 2 Helicopter	13
6	General Arrangement - Configuration 3 Helicopter	15
7	General Arrangement - Configuration 4 Helicopter	17
8	General Arrangement - Configuration 5 Compound	19
9	Flight Envelope	22
10	Hover Ceiling	24
11	Maximum Rate of Climb Versus Altitude	25
12	Payload Range - Sea Level Mission	26
13	Fuel Utilization Versus Payload - Heavy-Lift Mission . . .	28
14	Fuel Utilization Versus Payload - Transport Mission . . .	30
15	Longitudinal Maneuver Stability Criterion	38
16	Articulated Hub With External Controls	41
17	Blade Assembly	43
18	Propulsion System - Helicopter	46
19	Propulsion System - Compound Helicopter	47
20	Hot Cycle Propulsion System Schematic	48
21	Propulsion System Schematic - Four-Engine	50
22	Total Rotor Group Actual Weight Versus Equation Results	55
23	Fuselage Weight/Rotor Radius Versus Gross Weight \times (Ultimate Load Factor) $^{1/2}$	58
24	Primary Structure Weight Distribution - Configuration 2 .	60
25	Primary Structure Weight Distribution - Configuration 3 .	62
26	Fixed Alighting Gear Group Versus Design Gross Weight	64
27	Flight Controls Versus Design Gross Weight	66
28	Hydraulic and Pneumatic Group Weight Versus Design Gross Weight	67
29	Electrical Group Weight Versus Design Gross Weight . . .	68
30	Time-Temperature Spectrum - GE1 Engine - Heavy-Lift Helicopter	81
31	Configuration 1 Helicopter	86
32	Configuration 2 Helicopter	87
33	Configuration 3 Helicopter	88
34	Configuration 4 Helicopter	90
35	Configuration 5 Compound Helicopter	91

<u>Figure</u>	<u>Page</u>
36 Tilting Hub With Internal Controls	92
37 Tilting Hub With External Controls	93
38 Articulated Hub With Internal Controls	95
39 Articulated Hub With External Controls	96
40 Blade Duct Configurations	98
41 Influence of Blade Chord - Configuration 1	116
42 Influence of Blade Chord - Configuration 2	117
43 Influence of Rotor Radius - Configuration 1	118
44 Influence of Rotor Radius and Tip Speed - Configuration 2	119
45 Effect of Speed on Specific Range Based on Average Gross Weight Out and Average Gross Weight Back - Transport Mission	124
46 Effect of Speed on Specific Range Based on Average Gross Weight Out and Average Gross Weight Back - Heavy-Lift Mission	125
47 Propulsion System Schematic - Two-Engine Compound Helicopter Installation	130
48 Payload Versus Mission Radius for Compound Helicopter	133
49 Productivity - Compound Helicopter	134
50 Flapwise Moment Distribution - Comparison of Theory and Flight Test	143
51 Chordwise Moment Distribution - Comparison of Theory and Flight Test	143
52 Cyclic Flapwise Moment Distribution	145
53 Cyclic Chordwise Moment Distribution	146
54 Maximum Chordwise Moment Distribution	147
55 Maximum Flapwise Moment Distribution	148
56 Plan View of Blade Transition Area	151
57 Blade in Cruise Coning Position	152
58 Blade on Droop Stop (Maximum Positive Feathering)	153
59 Blade on Droop Stop (Maximum Negative Feathering)	154
60 Blade in Maximum Up Flapping Condition	155
61 Droop Stop (Blade in Cruise Coning Position)	156
62 Hub and Duct Configuration	157
63 Lead-Lag Strap Retention	158
64 View Looking Up At Lead-Lag Hinge	159

LIST OF TABLES

<u>Table</u>		<u>Page</u>
I	Performance and Weight Summary	5
II	Preliminary Parasite Drag Estimate of Heavy-Lift Helicopter Configuration	27
III	Dimensional Data	33
IV	Heavy-Lift Helicopter Mass Properties	34
V	Hover Handling Characteristics in Pitch	34
VI	Hover Handling Characteristics in Roll	35
VII	Hover Handling Characteristics in Yaw	36
VIII	Selected Optimum Rotor Characteristics	39
IX	Configuration Weight Summary	52
X	Rotor Group Summary	53
XI	Summary - Optimum Rotor Size for Configurations Studied and Performance	83
XII	Weight of Various Hub Configurations	94
XIII	Weight for Various Blade Sections	99
XIV	Effect of Tilting Hub With Restraint Versus Articulated Hub	113
XV	Effect of Internal Rotor Controls Versus External Rotor Controls	113
XVI	Effect of Blade Duct Shape	114
XVII	Effect of Rotor-Blade Tip Speed	115
XVIII	Effect of Spar Location on Figure-8 Duct Blades	120
XIX	Effect of Fixed Versus Retracted Landing Gear	121
XX	Effect of Blade Thickness	122
XXI	Effect of Engine Installation	122
XXII	Effect of Drag on Performance	123
XXIII	Fuel Requirements and Payload Ton-Miles Per Pound of Fuel - Transport Mission	126
XXIV	Fuel Requirements and Payload Ton-Miles Per Pound of Fuel - Heavy-Lift Mission	126
XXV	Autorotation - Rotor Kinetic Energy Index	128
XXVI	Empty Weight Summary - Helicopter, Compound Helicopter, and Helicopter Having Provisions for Compounding	131
XXVII	Summary - Payload and Ferry Range	132

LIST OF SYMBOLS

<u>Symbol</u>	<u>Identity</u>	<u>Units</u>
A	Area (rotor disc area)	sq ft
A_b	Blade area	sq ft
A_D	Duct area	sq in.
AE	Available energy	BTU/lb
B	Coefficient determined from detailed layout weights	nondimensional
b	Span or number of blades, as applicable	ft
C	Chord	in.
c	Chord length	in.
\bar{c}	Nondimensional coefficient $\left(\frac{c}{45}\right)$	nondimensional
C_L	Lift coefficient	nondimensional
cf	Centrifugal force	lb
C_p	Specific heat at constant pressure	nondimensional
C_r	Chord at root	in.
C_t	Chord at tip	in.
C_v	Velocity coefficient	in.
C_1 and C_2	Constants used in range computations	nondimensional
cg	Center of gravity	nondimensional
D	Drag	lb
D_h	Hydraulic diameter	in.
E	Modulus of elasticity	lb/in. ²
f	Design stress factor or friction coefficient, as applicable	nondimensional
fps	Feet per second	

<u>Symbol</u>	<u>Identity</u>	<u>Units</u>
G	Shear modulus of elasticity	lb/in. ²
g	Gravity	in./sec ²
H	Altitude in nautical miles	nmi
I	Area moment of inertia	in. ⁴
J	Torsional stiffness parameter	in. ⁴
K	Kinetic energy index	ft-lb/sec
KN, kn	Knots	
l	20-percent radius station	
LE	Leading edge	
M	Mach number	nondimensional
m	Exponent determined from statistical data	nondimensional
N	Number of engines	
n	Ultimate load factor, exponent determined from statistical data or station location, as applicable	nondimensional
NMI, nmi	Nautical miles	
OGE	Out of ground effect	
P	Pressure	lb/sq ft
P _T	Total pressure	lb/sq ft
psi	Pounds per square inch	
psig	Pounds per square inch gage	
q	Dynamic pressure	lb/sq ft
q ₀	Dynamic pressure in free stream	lb/sq ft
R	Rotor radius or gas constant for air, as applicable	ft, 53.35 ft-lb/ °R/lb
R _{sp}	Specific range	nmi/lb of fuel
rhp	Rotor horsepower	hp

<u>Symbol</u>	<u>Identity</u>	<u>Units</u>
rpm	Revolutions per minute	
r	Radius of an element	ft
SFC	Specific fuel consumption	lb/hr rhp
SL	Sea level	
STOL	Short takeoff and landing	
T	Rotor thrust or temperature, as applicable	lb or °R
TE	Trailing edge	
t	Thickness	in.
\bar{t}	Thickness ratio	$\frac{\%c}{100}$
t_r	Thickness at root	in.
t_t	Thickness at tip	in.
V_j	Jet velocity	ft/sec
V_{ne}	Design maximum level flight speed	knots
V_T, V_t	Tip velocity	ft/sec
W	Weight	lb
W_8	Flow at exhaust	lb/sec
W_{ac}	Weight of air conditioning and anti-icing group	lb
W_{BU}	Weight of ideal blade	lb
W_b	Weight of fuselage	lb
W_c	Weight of cargo handling equipment	lb
W_{cff}	Weight of cruise fan system - fixed	lb
W_{cfr}	Weight of cruise fan system - removable	lb
W_e	Empty weight	lb
W_{el}	Weight of electrical group	lb
W_{en}	Weight of electronics group	lb

<u>Symbol</u>	<u>Identity</u>	<u>Units</u>
W_f	Fuel flow	lb/hr
W_{fc}	Weight of flight controls	lb
W_{fe}	Weight of furnishings and equipment	lb
W_{ft}	Additional increment of fuel for climb	lb
W_g	Gross weight	lb
W_h	Weight of hydraulic and pneumatic equipment	lb
W_{hy}	Weight of hover - yaw control group	lb
W_i	Weight of instruments and navigational equipment	lb
W_{lg}	Weight of alighting gear	lb
W_{pp}	Weight of propulsion group	lb
W_r	Weight of main rotor group	lb
W_s	Weight at start of climb	lb
W_{scf}	Weight of surface controls	lb
W_{tg}	Weight of tail group	lb
W_w	Weight of wing group	lb
γ	Ratio of specific heat at constant pressure to the specific heat at constant volume	nondimensional
η	Propulsive efficiency	nondimensional
σ	Solidity	nondimensional
ψ	Blade azimuth angle	deg

The following symbols are applicable to Appendix III, Rotor Blade Equations:

<u>Symbol</u>	<u>Identity</u>	<u>Units</u>
\bar{d}	Inboard design station to end of reduced chord section	$\frac{\%R}{100}$
\bar{d}_1	Inboard design station to outboard design station	$\frac{\%R}{100}$
\bar{d}_2	Outboard design station to tip	$\frac{\%R}{100}$
\bar{d}_3	Inboard design station to lead-lag hinge	$\frac{\%R}{100}$
\bar{e}_f	Flap hinge offset	$\frac{\%R}{100}$
\bar{e}_L	Lag hinge offset	$\frac{\%R}{100}$
F_{BU}	Allowable ultimate bending stress	lb/in. ²
F_e	Endurance limit at 0 mean stress	lb/in. ²
F_{TCO}	Steady stress at knee of Goodman diagram	lb/in. ²
F_{CYCO}	Oscillatory stress at knee of Goodman diagram	lb/in. ²
F_{TU}	Allowable ultimate tensile stress	lb/in. ²
f_{CF}	Stress due to centrifugal force	lb/in. ²
\bar{h}	Helicopter center of gravity to rotor centerline	$\frac{\%R}{100}$
I_e	Blade flapping mass moment of inertia about flapping hinge	in. -lb-sec ²
I_p	Section polar mass moment of inertia about center of gravity	in. -lb-sec ² in.

<u>Symbol</u>	<u>Identity</u>	<u>Units</u>
I_x	Flapwise structural moment of inertia	in. ⁴
I_y	Chordwise structural moment of inertia	in. ⁴
J	Section torsional stiffness parameter	in. ⁴
K_c	<u>Chordwise moment</u> (W/b) (R) (C_{11})	nondimensional
K_F	<u>Flapwise moment</u> (W/b) (R) (F_{13})	nondimensional
K_2	$\frac{\bar{x}_c - \bar{x}_f}{\bar{x}_r - \bar{x}_c}$	nondimensional
K_3	$w_{NB} \frac{\bar{x}_{NB} - \bar{x}_c}{\bar{x}_R - \bar{x}_c}$	lb/in.
K_4	$1 + K_2$	nondimensional
\bar{l}	Flap hinge to inboard design station	$\frac{\%R}{100}$
\bar{l}_1	Flap hinge to end of reduced chord station	$\frac{\%R}{100}$
\bar{l}_2	Flap hinge to outboard design station	$\frac{\%R}{100}$
p	Static pressure	lb/in. ²
p_0	Total pressure \times Design factor	lb/in. ²
T	Duct gas temperature	deg. F
\bar{t}_F, \bar{t}_R	Spar depth	$\frac{\%C}{100}$
\bar{t}_t, \bar{t}_2	Airfoil thickness	$\frac{\%C}{100}$

<u>Symbol</u>	<u>Identity</u>	<u>Units</u>
\bar{t}_{SK}	Blade skin thickness	.01 in.
v	Ground wind	kn
w	Helicopter gross weight	lb
w_{BU}	Total blade weight	lb
\bar{w}_{BU}	$\frac{w_{BU}}{12R}$	lb/in.
w_{CA}	Cascade weight	lb
\bar{w}_{CA}	$\frac{w_{CA}}{12R}$	lb/in.
w_t	Tip weight	lb
\bar{w}_t	$\frac{w_t}{12R} x'_t$	lb/in.
w_{NB}	Weight of nonbending material	lb/in.
w_R, w_F	Weight of spars (rear, front)	lb/in.
w_T	Weight of total section	lb/in.
x	Distance from rotor centerline	$\frac{\%R}{100}$
x_A	Lift centroid to rotor centerline distance	$\frac{\%R}{100}$
\bar{x}_C	Blade section center of gravity location	$\frac{\%C}{100}$
\bar{x}_{Ct}	Blade section center of gravity location at the tip	$\frac{\%C}{100}$
\bar{x}_{CA}	Center of gravity location of cascade	$\frac{\%C}{100}$
\bar{x}_F, \bar{x}_R	Spar center of gravity locations	$\frac{\%C}{100}$

<u>Symbol</u>	<u>Identity</u>	<u>Units</u>
\bar{x}_{NB}	Nonbending material center of gravity location	$\frac{\%C}{100}$
\bar{x}_t	Center of gravity location of tip weight	$\frac{\%C}{100}$
x'_t	Center of gravity location of tip weight (flapwise)	$\frac{\%R}{100}$
δ	Structure density	lb/in. ³
λ	<u>Control moment - spring</u> Control moment - lateral force	nondimensional
\bar{r}_F, \bar{r}_R	Spar radii of gyration (area)	$\frac{\%C}{100}$
$\bar{r}_{NB_0}, \bar{r}_{NB_i}$	Nonbending material polar radius of gyration (mass)	$\frac{\%C}{100}$



Figure 1. Hot Cycle Heavy-Lift Helicopter Concept.

SUMMARY

A parametric study and preliminary design program has defined the configuration and characteristics of a rotor for a 12- to 20-ton heavy-lift helicopter utilizing the Hot Cycle propulsion system. The objectives of the program were as follows:

- 1. Develop an analytic procedure that will permit calculation of fully coupled blade loads and dynamic stability characteristics.
- 2. Conduct parametric and configuration studies to determine the optimum Hot Cycle rotor system for a 12- to 20-ton-payload heavy-lift helicopter and investigate, on a limited basis, the features required to increase its cruise speed by a substantial amount.
- 3. Complete the preliminary design of the selected optimum rotor, including design layouts, structural design and weight analysis, stability and control studies, and static and dynamic loads analysis.
- 4. Construct a full-scale mockup of the rotor hub.

To accomplish the above objectives, computer programs were developed for the fully coupled rotor dynamic analysis and the parametric study. For the analysis, a digital computer program that has the capability of solving the full range of helicopter rotor dynamic problems was developed and checked against flight test data. A nonlinear representation of blade loads, including lift and moment hysteresis, is incorporated in the program to provide a more realistic analysis of fully coupled blade loads in forward flight. The development of this program has been summarized and previously submitted (Reference 1). For the parametric study, a computer program to determine the optimum rotor was developed to consider the effect of variables such as blade radius, chord, thickness, tip speed, blade spar location, duct shape, and aircraft configuration. Development and results of this program have been previously reported (Reference 2).

The results of the parametric study were reviewed, and a rotor was selected that was considered most nearly optimum for all the aircraft configurations studied. The selected rotor is a three-bladed, fully articulated rotor with 90-foot diameter and 60-inch chord. The study also included, in addition to the articulated rotors, configurations with

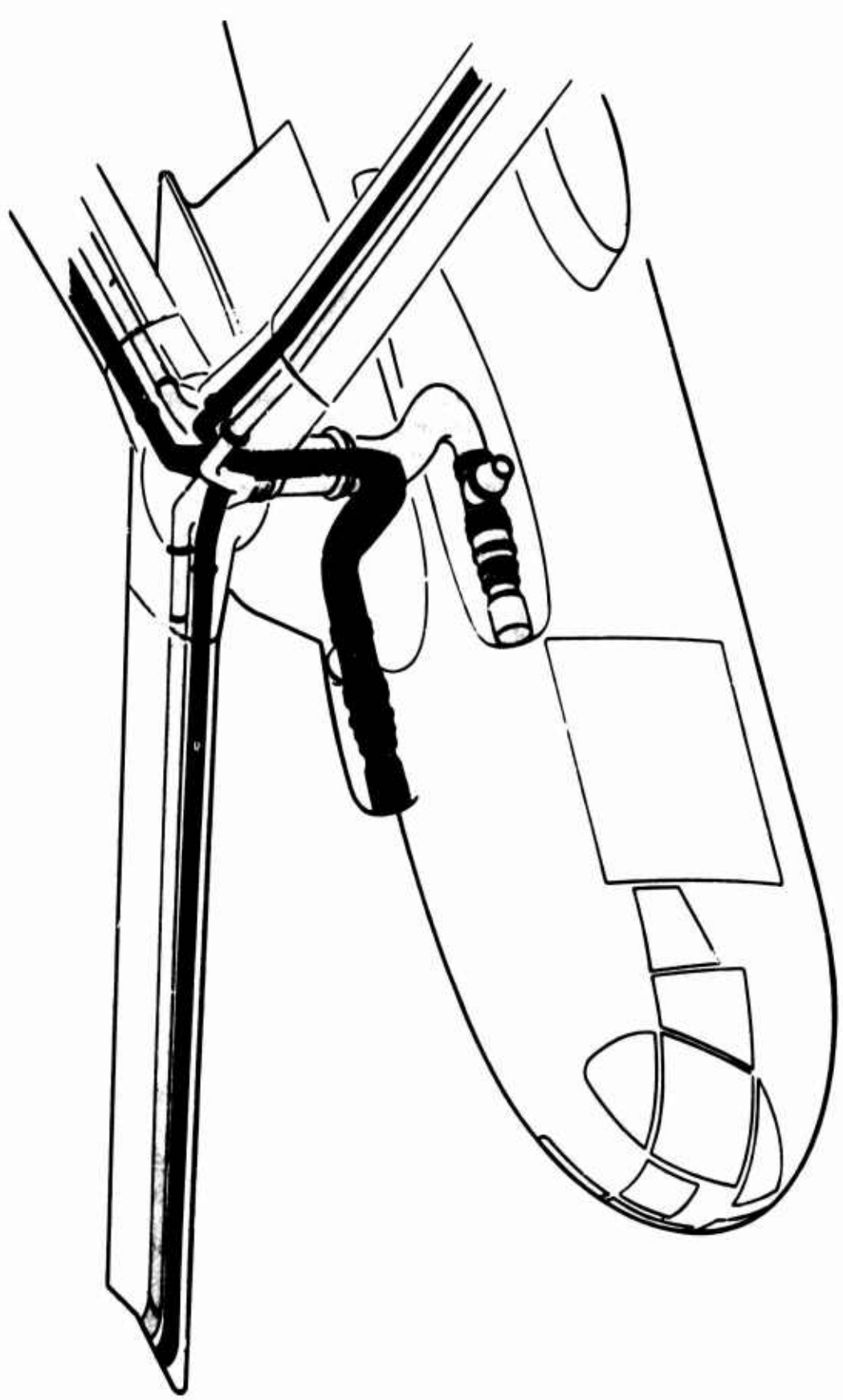


Figure 2. Propulsion System.

in-plane chordwise restraint (akin to a rigid rotor). The rigid type of rotor investigated weighed almost twice as much as the articulated rotor of the same size. Design layouts, structural design and weight analysis, and stability and control studies were completed on this selected rotor. The basic characteristics of this rotor are shown in Table IX in the Rotor Section.

The rotor is powered by the Hot Cycle propulsion system. As shown in Figure 2, the Hot Cycle system transmits power pneumatically by light-weight ducting that directs high-energy gas from turbine engines to the rotor blade tips to drive the rotor as a large reaction turbine. The Hot Cycle rotor is suited to the transport and heavy-lift missions of 12 to 20 tons and up. The favorable characteristics of this rotor are the direct result of the simplicity and light weight inherent in the Hot Cycle propulsion system, which eliminates the weight and complexity of power turbines, shafts, large gearboxes, and clutches. Since there is no rotor shaft drive torque reaction on the fuselage, there is no need for a large antitorque tail rotor; directional control is provided by a small yaw fan located in the vertical stabilizer. The resulting low empty weight, and thus high payload to empty weight ratio, cannot be attained by the conventional shaft-driven rotors with their inherently heavier complex dynamic components. A plot of useful load/empty weight versus useful load (Figure 3) clearly shows an ever-widening gap in favor of the Hot Cycle system over the shaft-driven concept as useful load is increased.

To demonstrate the adaptability of the Hot Cycle principle, the selected optimum rotor in this study is shown installed on a number of helicopter configurations: the minimum-size streamlined conventional fuselage (configuration 2) carrying all cargo externally, a larger conventional streamlined fuselage with a 12-ton internal capacity (configuration 3), and a crane type (configuration 4) with the capability to carry payloads externally or in pods. In addition, the larger conventional fuselage configuration is also shown as a compound helicopter (configuration 5), so that the features required and the benefits obtained by substantially raising the cruise speed by this means can be identified. The parametric study also included a configuration 1 that was identical with configuration 4 except that a pod was included in the empty weight. Configuration 1 was not considered in the preliminary design, because it was not compatible with other heavy-lift studies for comparison purposes.

The selected optimum rotor has overload payload capabilities considerably in excess of those payloads specified in the heavy-lift requirements, as can be seen in Table I. The characteristics of this Hot Cycle rotor provide good hovering and cruise flight efficiency, low noise level, low downwash velocities, and good flying qualities.

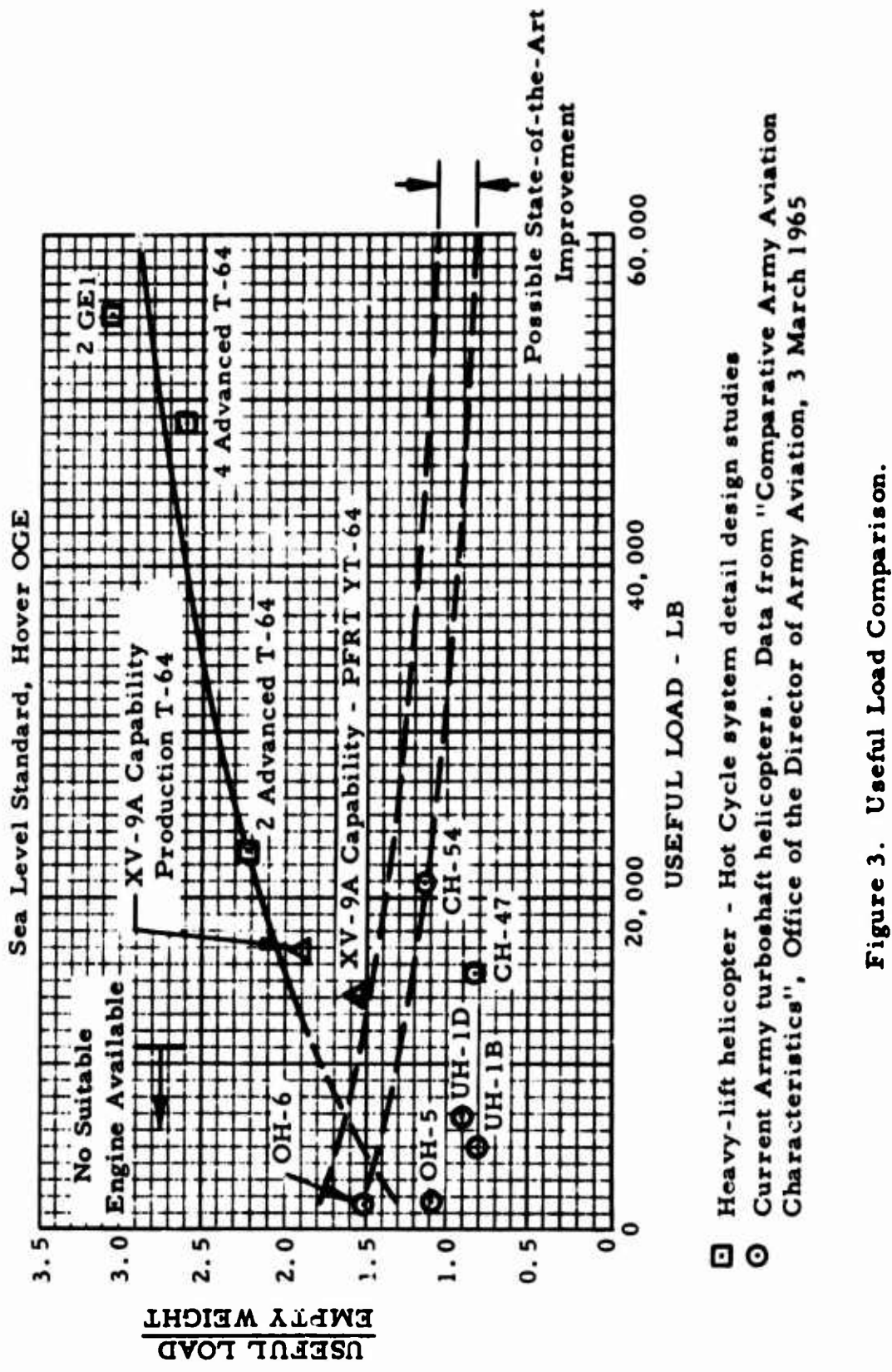


Figure 3. Useful Load Comparison.

TABLE I
PERFORMANCE AND WEIGHT SUMMARY

Item	Heavy-Lift Performance Requirements	Hot Cycle Heavy-Lift Capability Configuration		
		2	3	4
<u>Performance</u>				
Transport mission (100-nmi radius)				
Hover capability with 12-ton payload (95°F OGE)	6,000 ft	8,200	7,800	7,300
Payload capacity (6,000 ft 95°F)	12 ton	14.12	13.79	13.0
Outbound cruise speed (12-ton payload)	110 kn	110	137*	114
Inbound cruise speed (no payload-optimum)	130 kn	134	132	130
Heavy-lift mission (20-nmi radius)				
Hover capability with 20-ton payload (std OGE)	SL	6,000	5,000	4,900
Payload capability (SL, 59° OGE)	20 ton	26.25	25.31	25.1
Outbound cruise speed (20-ton payload)	95 kn	104	103	98
Inbound cruise speed (no payload)	130 kn	134	132	130
Ferry mission (at 2-g load factor)	1,500 nmi	2,172	2,040	1,900
Max ferry range (STOL takeoff with load factor reduced to approx 1.75g)	-	2,308	2,203	2,030
Max speed capability (normal power at lightweight condition)	-	179	178	175
<u>Weights (lb)</u>				
Empty weight		19,599	20,570	21,1
Gross weight				
Transport mission (12-ton payload)	52,260	52,234	54,1	
Heavy-lift mission (20-ton payload)	64,280	65,481	66,1	
Payload/empty weight ratio				
Transport mission (max payload)	1.4	1.3	1.2	
Heavy-lift mission (max payload)	2.7	2.5	2.4	

*Internal load for configuration 3.

The study of the compound helicopter was undertaken on a limited basis to identify the compromises in weight, size, complexity, and performance required to attain a substantial increase in cruise speed. Compounding was accomplished by the addition of wings and ducted fans for thrust. The study showed that the compound helicopter will provide a substantial increase in cruise speed and ferry range. The additional complexity of the compound is confined primarily to the wing and ducted thrust-fan installations, and the required implementation is well within the state of the art.

HTC-AD experience in the design and engineering of the Hot Cycle helicopter spans more than 10 years. The feasibility and attractiveness of the Hot Cycle propulsion system have been established through an extensive research and development program that culminated in the successful flight testing of the U.S. Army AVLabs XV-9A Hot Cycle Research Aircraft shown in Figure 4. During 160 hours of rotor operation and 35 hours of flight testing that was completed in August 1965, structural and mechanical design, weights, and cooling adequacy were verified. Gas leakage was found to be negligible (less than 1/5 of 1 percent) and noise was determined to be essentially equal to that of the quietest type of VTOL aircraft (turboshaft helicopter). The large reduction in maintenance requirements promised by the Hot Cycle system was illustrated by the low logistical requirements during XV-9A flight operations.



Figure 4. XV-9A Hot Cycle Research Aircraft.

STUDY REQUIREMENTS

The preliminary design parametric and configuration study is based on the following vehicle and mission requirements.

VEHICLE

The vehicle shall have the following characteristics:

1. Turbine power.
2. Safe autorotation at design gross weight.
3. Design vertical limit load factor of 2.5 to -0.5 g at design gross weight. * For the integrated preliminary design, the design weight is interpreted to be the heavy-lift mission gross weight carrying a 20-ton payload.
4. Crew minimum of one pilot, one copilot, and one crew chief.
5. All components to be designed for 1,200 hours between major overhauls and 3,600-hour service life.
6. Multiengine installation.

MISSIONS - HELICOPTER

The aircraft shall be able to perform the following missions:

1. Transport mission
 - a. Payload: 12 tons (outbound only)
 - b. Radius: 100 nautical miles
 - c. Cruise speed: 12-ton payload, 110 knots
 - d. Cruise speed: no payload, 130 knots
 - e. Hovering time: 3 minutes at takeoff; 2 minutes at midpoint
 - f. Reserve fuel: 10 percent of initial fuel
 - g. Hover capability: 6,000 feet 95°F (OGE)
 - h. Cruise altitude: sea level standard atmosphere
 - i. Fuel allowance for start, warmup, and takeoff per MIL-C-5011A

*For the parametric study, the design gross weight was taken as the transport mission gross weight, with a resulting design limit load factor of +2.75 for compatibility with the ferry mission load factor of 2.0.

2. Heavy-lift mission

- a. Payload: 20 tons (outbound only)
- b. Radius: 20 nautical miles
- c. Cruise speed: 20-ton payload, 95 knots
- d. Cruise speed: no payload, 130 knots
- e. Hovering time: 5 minutes at takeoff; 10 minutes at destination (with payload)
- f. Reserve fuel: 10 percent of initial fuel
- g. Hover capability: sea level 59°F (OGE)
- h. Cruise altitude: sea level standard atmosphere
- i. Fuel allowance for start, warmup, and takeoff per MIL-C-5011A

3. Ferry mission

- a. Ferry range: 1,500 nautical miles (no payload, STOL takeoff)
- b. Reserve fuel: 10 percent of initial fuel
- c. Fuel allowance for start, warmup, and takeoff per MIL-C-5011A
- d. Minimum design load factor of 2.0
- e. Best altitude for range
- f. Best speed for range

MISSIONS - COMPOUND HELICOPTER

The following missions were selected for the compound study:

1. Transport mission

- a. Payload: both ways, weight to be determined
- b. Radius: 200, 300, and 500 nautical miles
- c. Cruise: 225 knots (minimum)
- d. Hovering time: 4 minutes at takeoff 2 minutes at destination (with payload)
- e. Reserve fuel: 10 percent of initial fuel
- f. Hover capability
 - Basic Hover OGE - initial takeoff at sea level, 59°F; cruise at sea level and best altitude
 - Altitude Hover OGE - initial takeoff at 6,000 feet, 95°F; cruise at sea level and best altitude
 - Overload Initial running takeoff at sea level, 59°F; hover OGE at destination at sea level, 59°F; cruise at best altitude and, alternatively, at sea level

2. Ferry mission

- a. Payload: none
- b. V_{cruise} : for best range
- c. Cruise altitude: for best range
- d. Range: to be determined
- e. Fuel reserve: 10 percent of initial fuel
- f. Initial takeoff: STOL, sea level, 59° F

AIRCRAFT CONFIGURATIONS STUDIED

A wide range of aircraft configurations has been considered in order to show the adaptability of the Hot Cycle rotor to any configuration that might be dictated by operational requirements. By installing the same rotor and propulsion system on the different airframes, the effect of configuration on mission effectiveness can be seen. A brief description of each of the helicopter configurations considered is given in the following paragraphs.

MINIMUM-SIZE CONVENTIONAL FUSELAGE (Configuration 2) (Figure 5)

This configuration utilizes a conventional streamlined fuselage sized to carry the ferry fuel internally. A top-mounted engine installation has been utilized to reduce frontal area. This configuration has been included in the study because it represents the configuration having the lowest empty weight, highest payload-to-empty-weight ratio, and the longest ferry range capability. It is well to note that this configuration has the ability to meet the mission requirements with a rotor smaller than the selected optimum rotor and at a substantially lighter empty weight. The cargo compartment is approximately 6-1/2 feet wide, 7 feet high, and 45 feet long, and will accommodate six standard 54-by-88-inch pallets. Approximately 7 tons may be carried internally at a 10-pound-per-cubic-foot loading. Structural provisions have been included for the 7-ton internal load, though mission performance has been determined based on carrying the transport and heavy-lift mission payloads externally.

CONVENTIONAL FUSELAGE WITH 12-TON INTERNAL CAPACITY (Configuration 3) (Figure 6)

A conventional streamlined fuselage has been used on this configuration, sized to carry 12 tons internally (at 10 pounds per cubic foot). The cargo compartment is approximately 8 feet wide, 7 feet high, and 46 feet long, and will accommodate six standard 88-by-108-inch pallets. The engines have been shoulder-mounted for accessibility and for ease of converting this configuration into a compound helicopter. Performance of this configuration has been determined assuming the transport mission payload to be carried internally and the heavy-lift mission payload externally.

CRANE-TYPE (Configuration 4) (Figure 7)

This configuration is a crane type utilizing a straddle gear and sized to accommodate a pod with a cargo compartment 10 feet wide, 9 feet high,

and 27 feet long. The cross section dimensions were chosen to be the same as those of the C-130 airplane cargo compartment to permit direct reloading between vehicles. The transport and heavy-lift payloads were assumed to be carried externally for the determination of performance. The fuel has been assumed to be carried in a faired pod for the ferry mission.

COMPOUND HELICOPTER (Configuration 5) (Figure 8)

The study of the compound helicopter was undertaken on a limited basis to identify the compromises in weight, size, complexity, and performance required to attain a substantial increase in cruise speed. Configuration 5 is identical with the configuration 3 helicopter (conventional fuselage, 12-ton internal capacity) except that wings and ducted fans for thrust have been added for operation as a compound helicopter. To fly as a compound, the high-energy gas is diverted from the rotor to the ducted fans, with the wing acting to unload the rotor. The increased speed of the compound resulted in an appreciably higher productivity than that achieved by the configuration 3 helicopter.

ENGINE INSTALLATION

Two engine installations were considered in the parametric study, one utilizing two GE1/J1 engines and the other utilizing four GE T64/S4B engines.

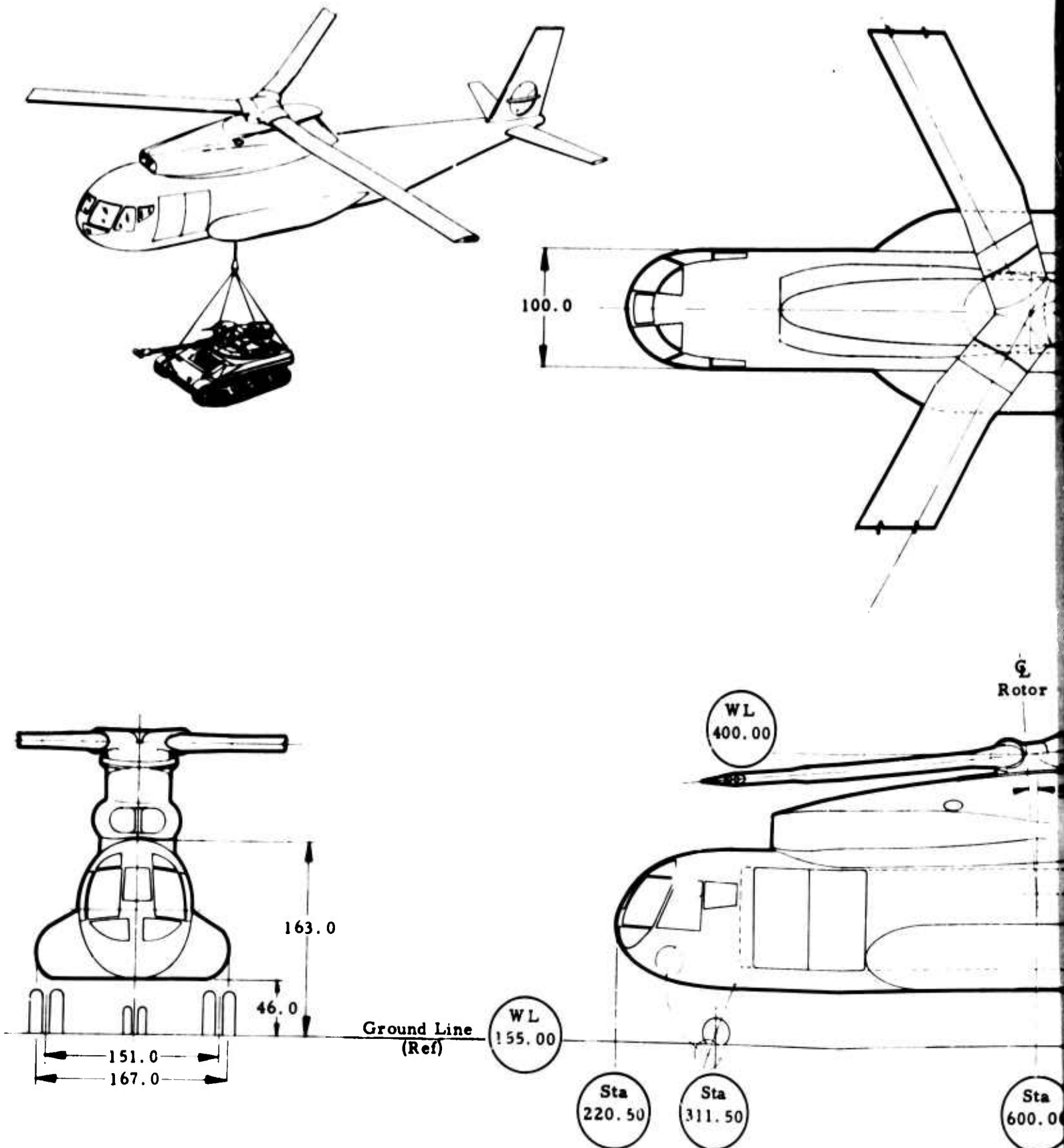
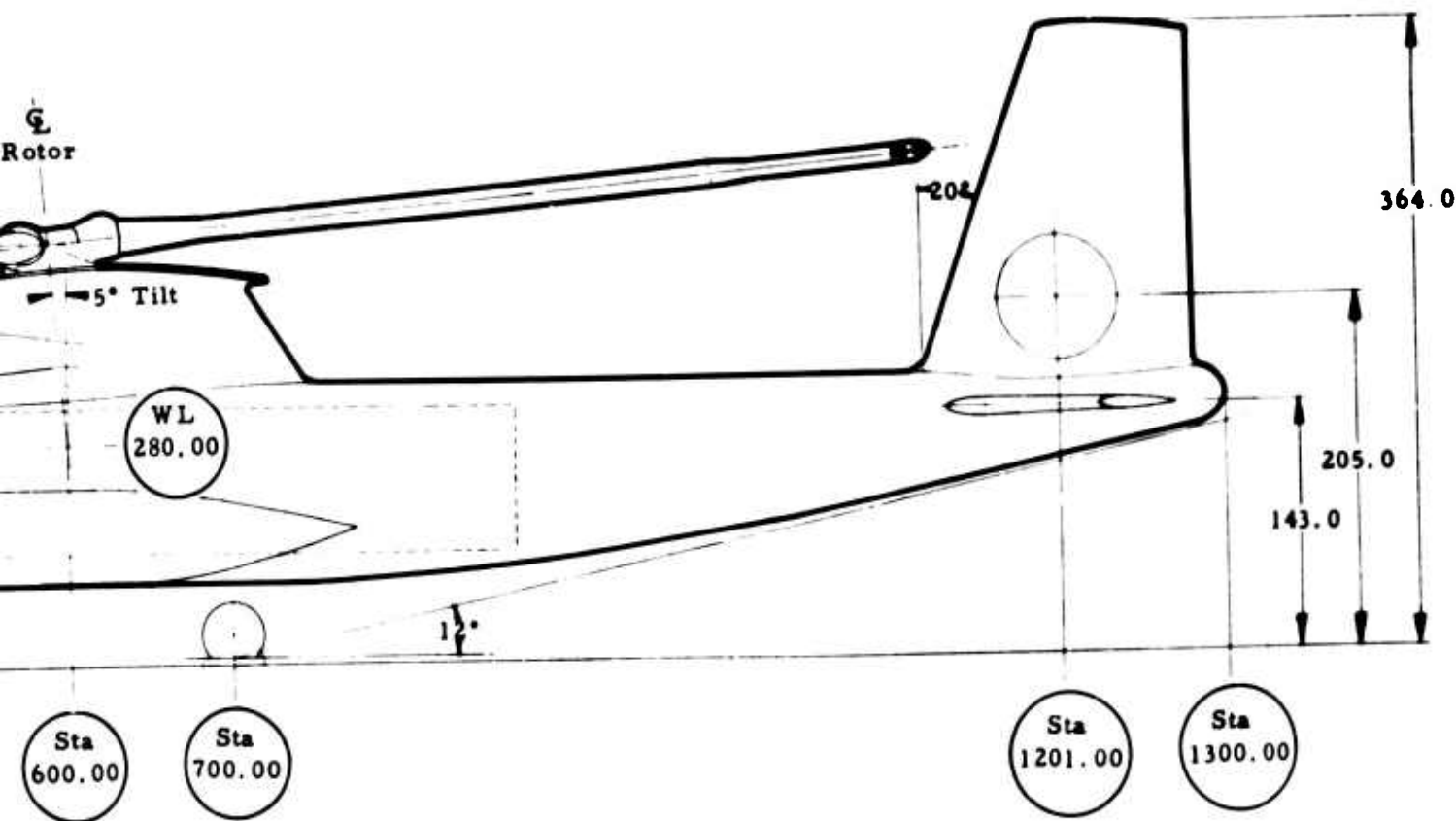
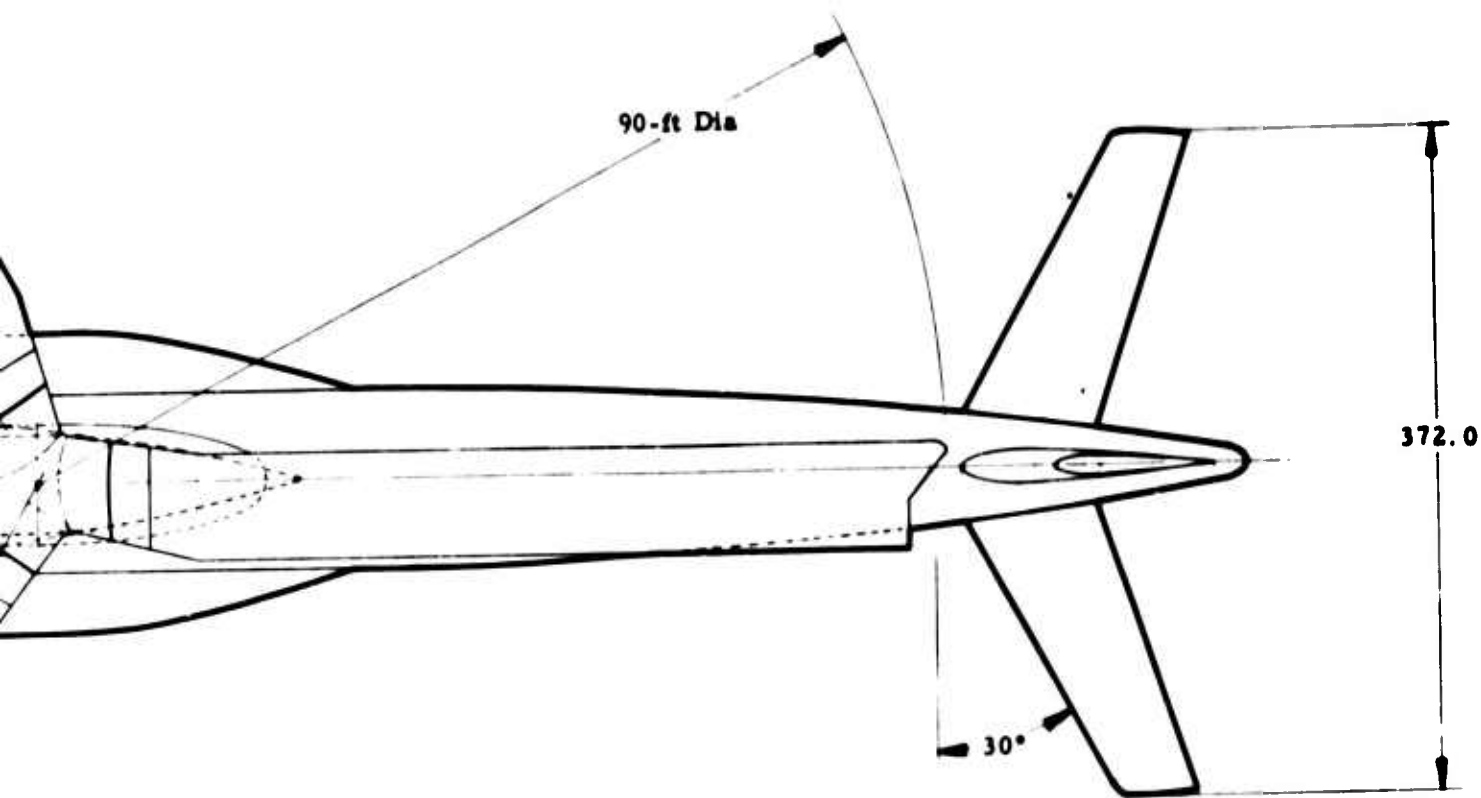


Figure 5. General Arrangement - Con



nt - Configuration 2 Helicopter.

B

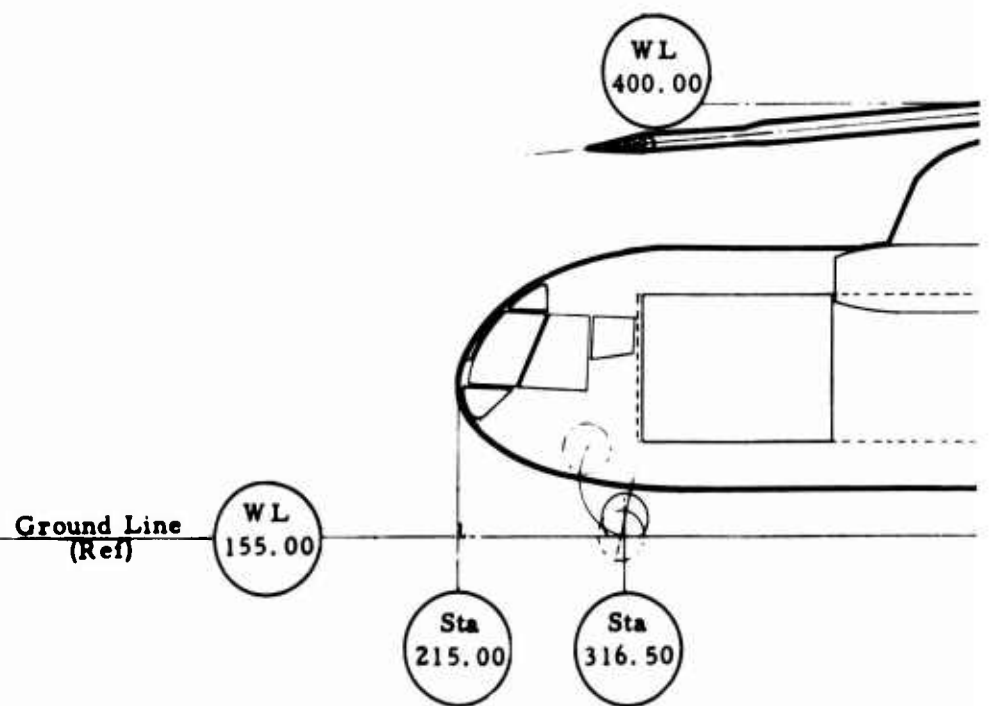
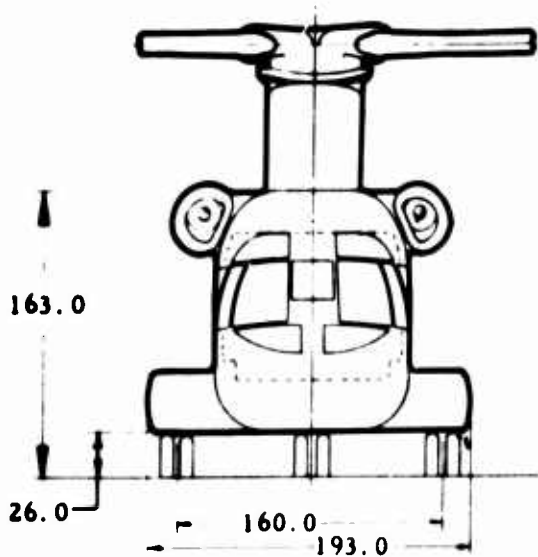
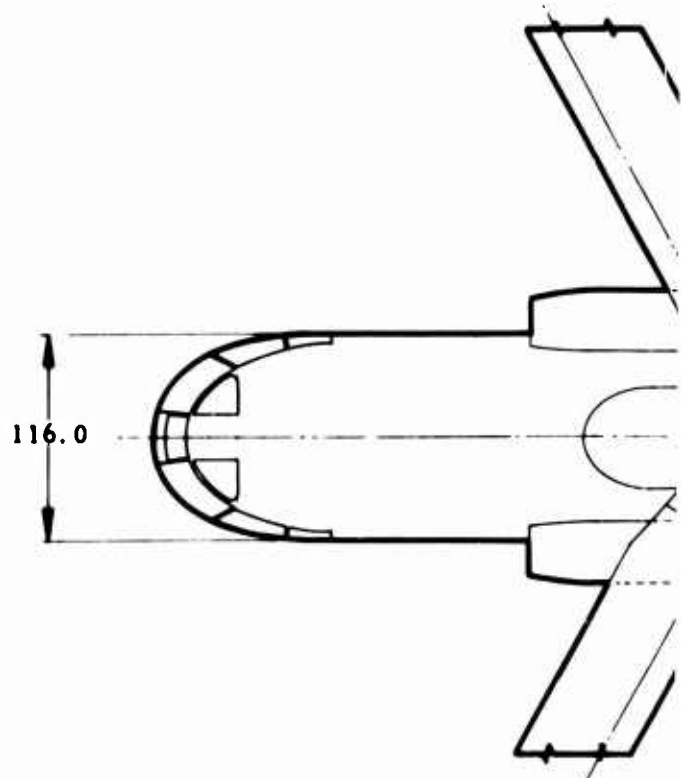
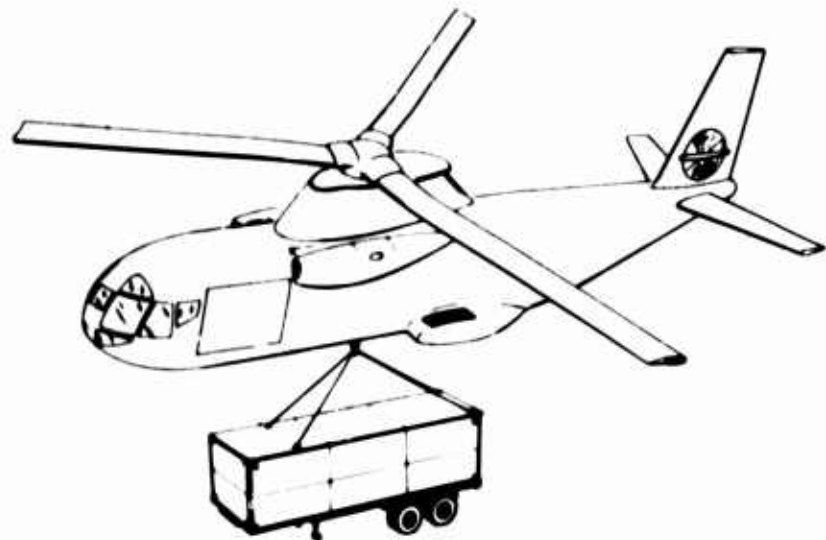
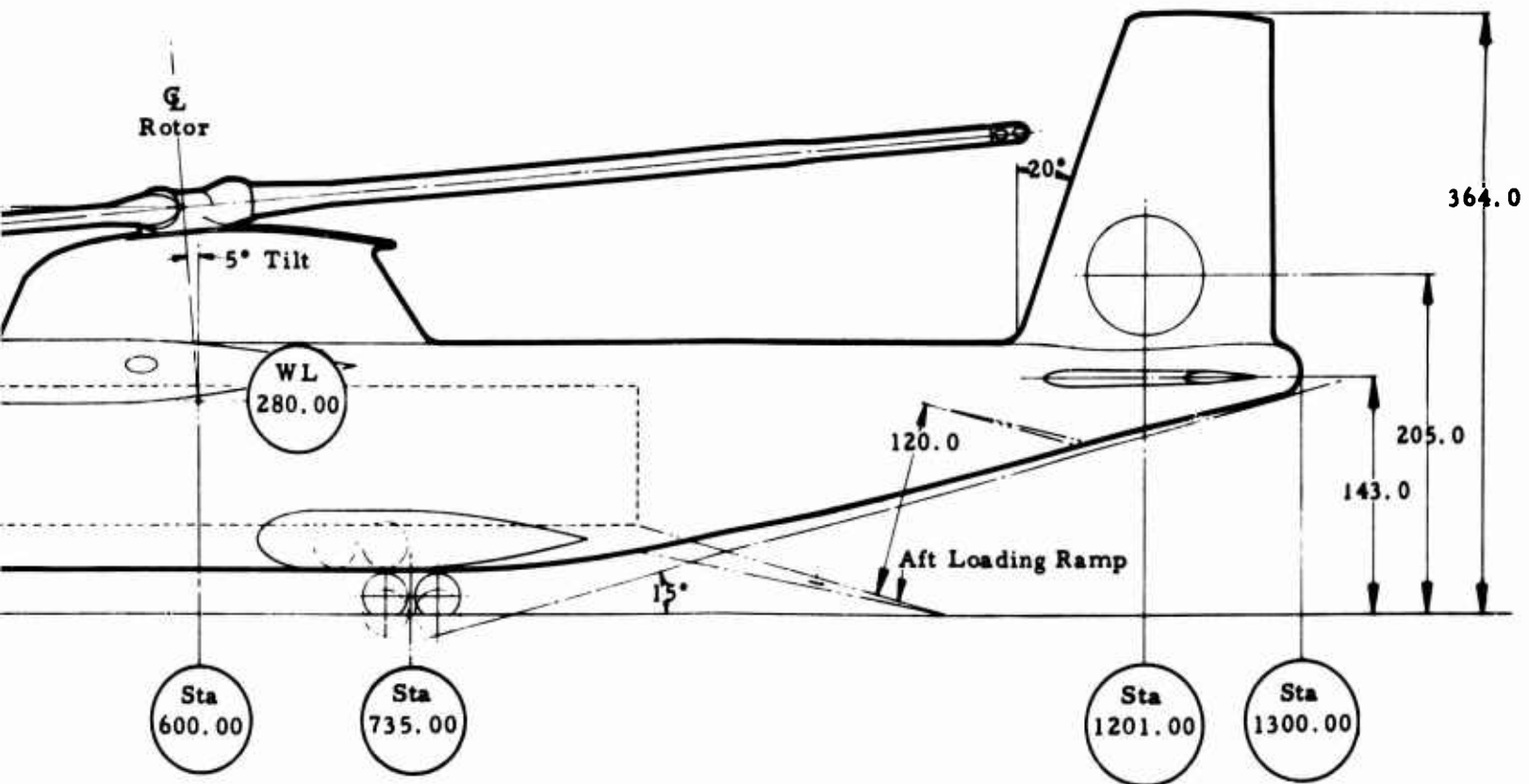
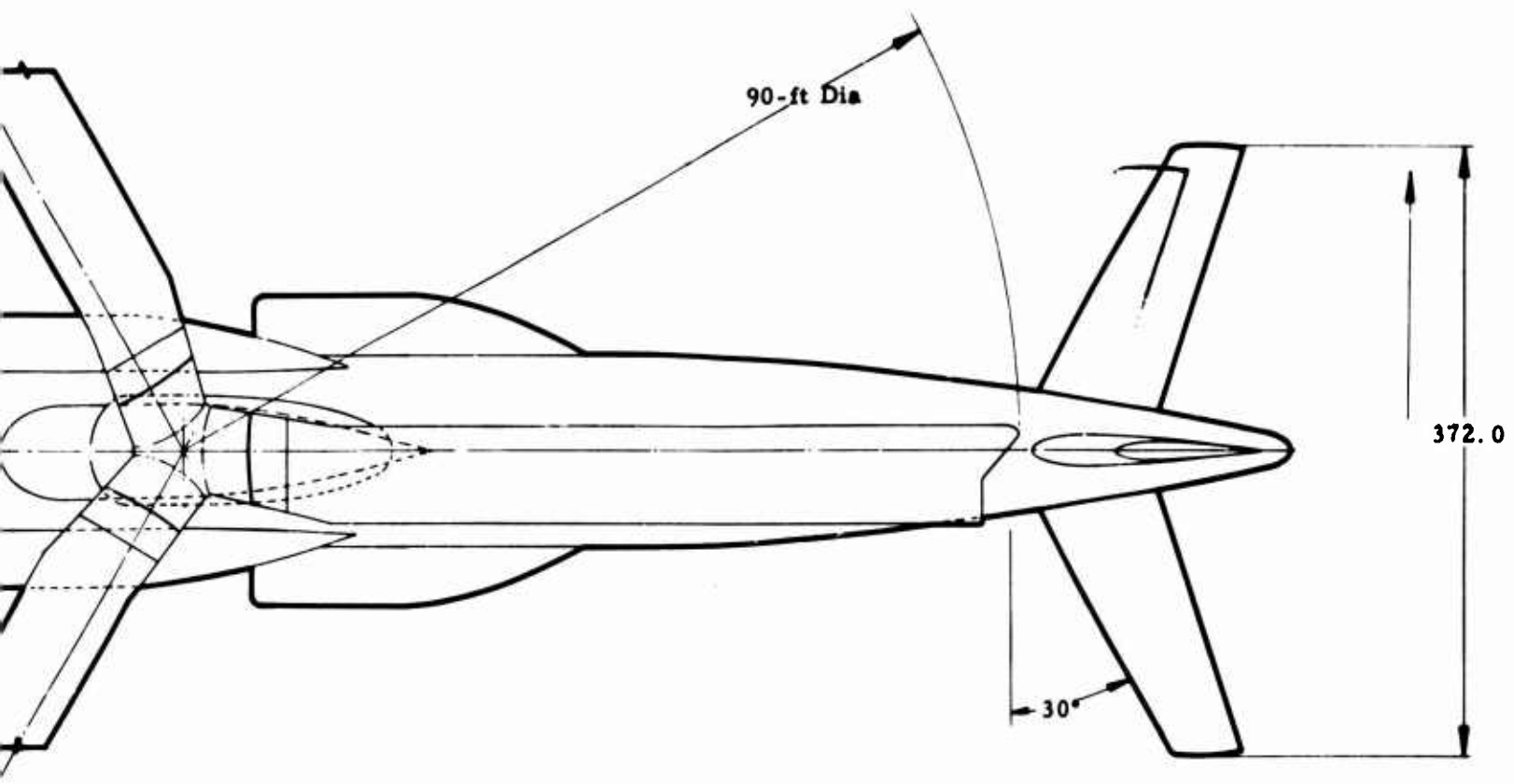


Figure 6. General Arrangement



gement - Configuration 3 Helicopter.

B

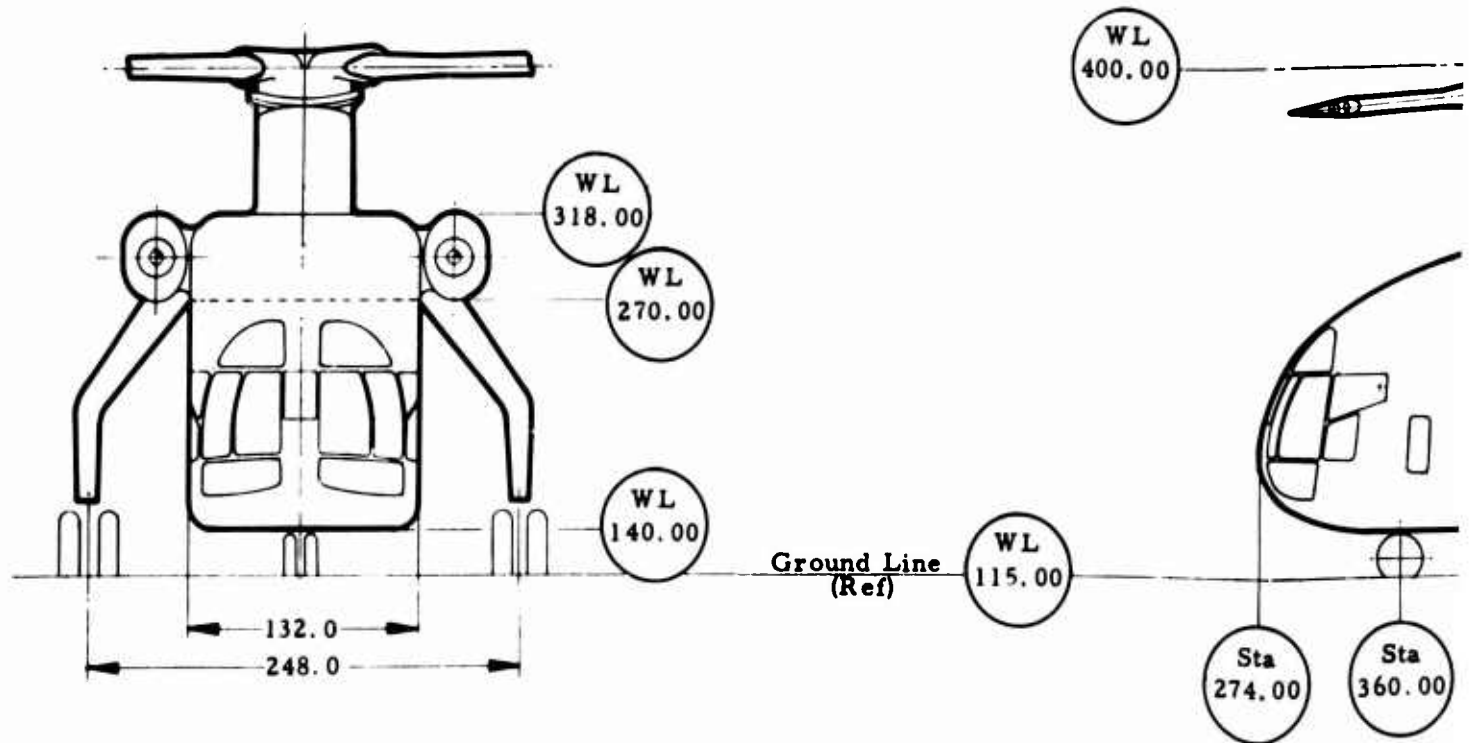
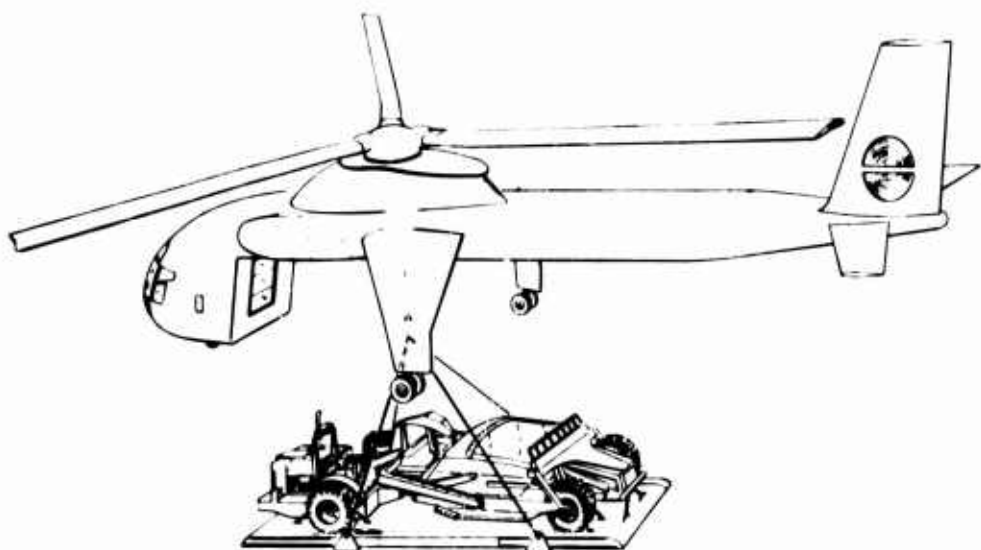
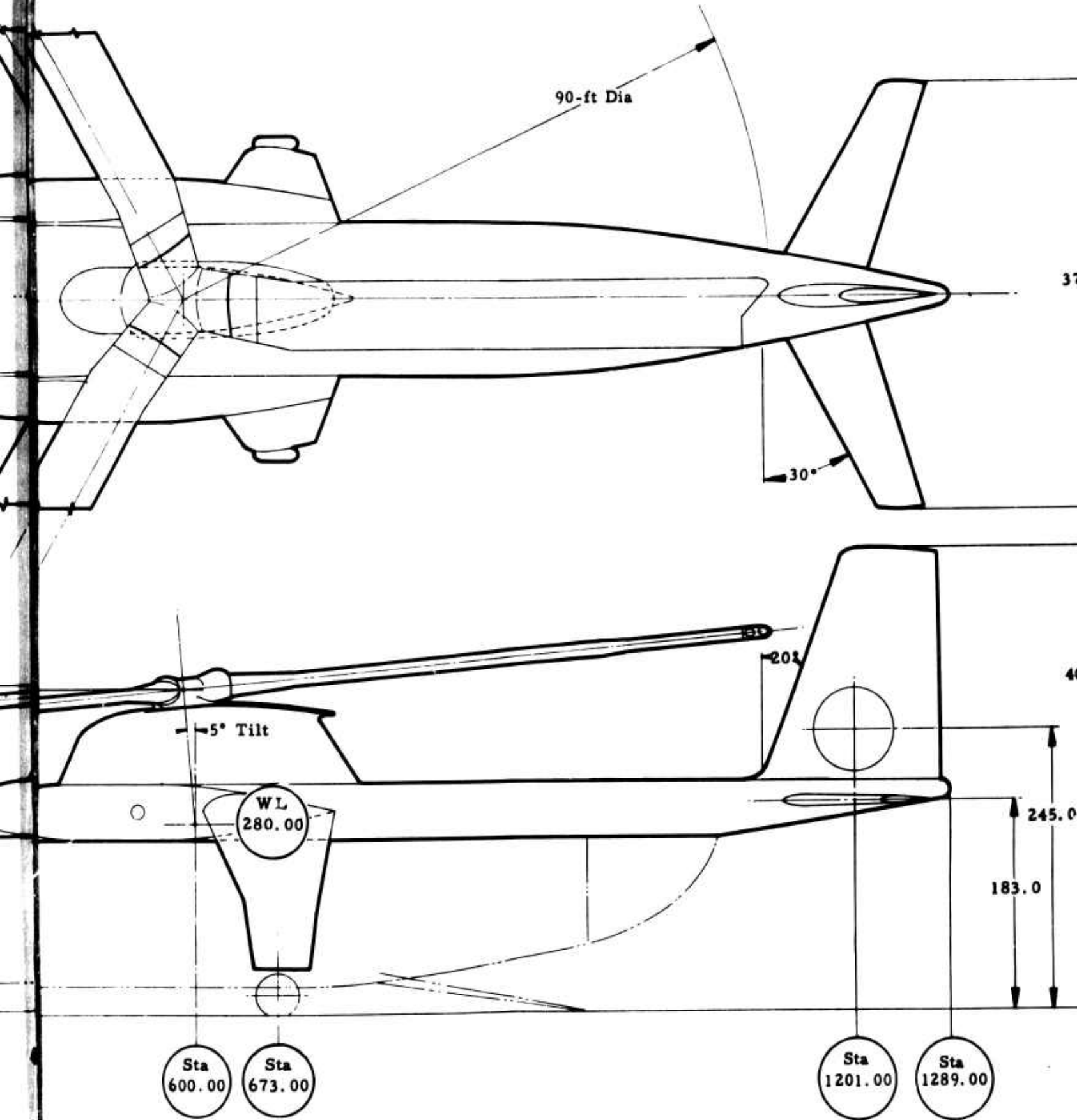


Figure 7. General /



gement - Configuration 4 Helicopter.

P

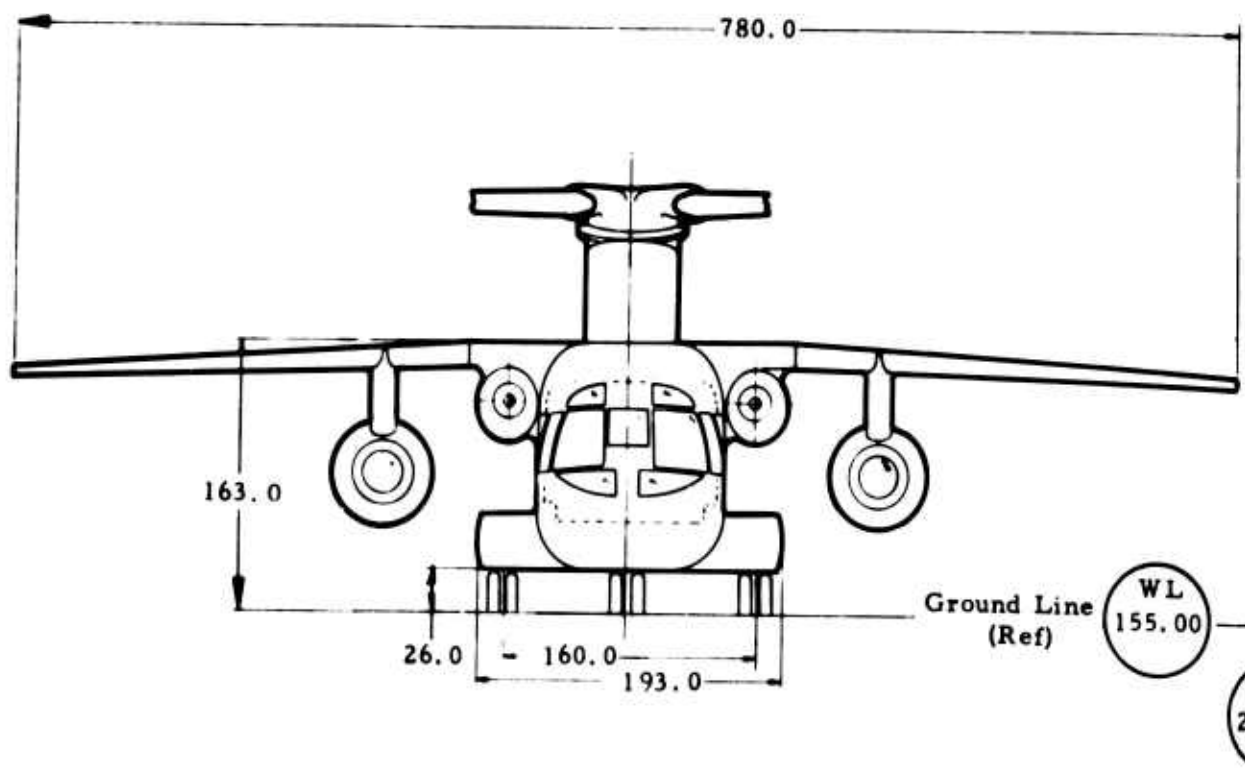
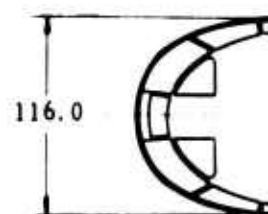
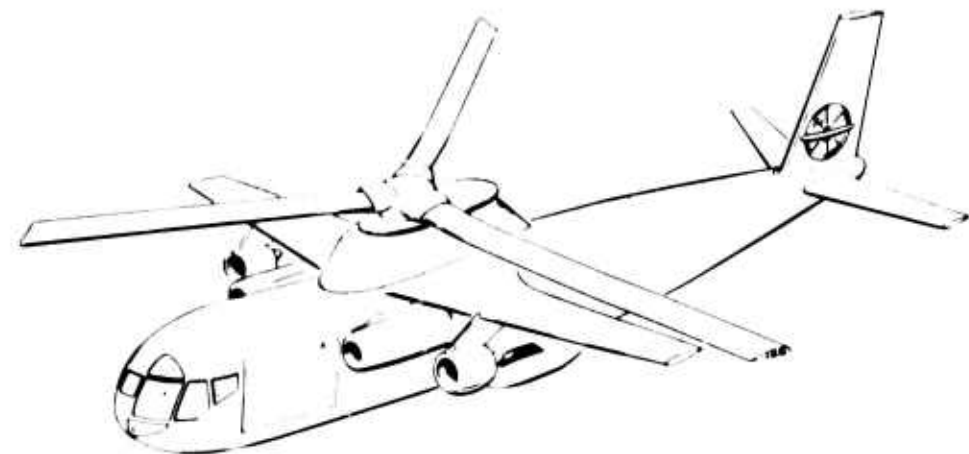
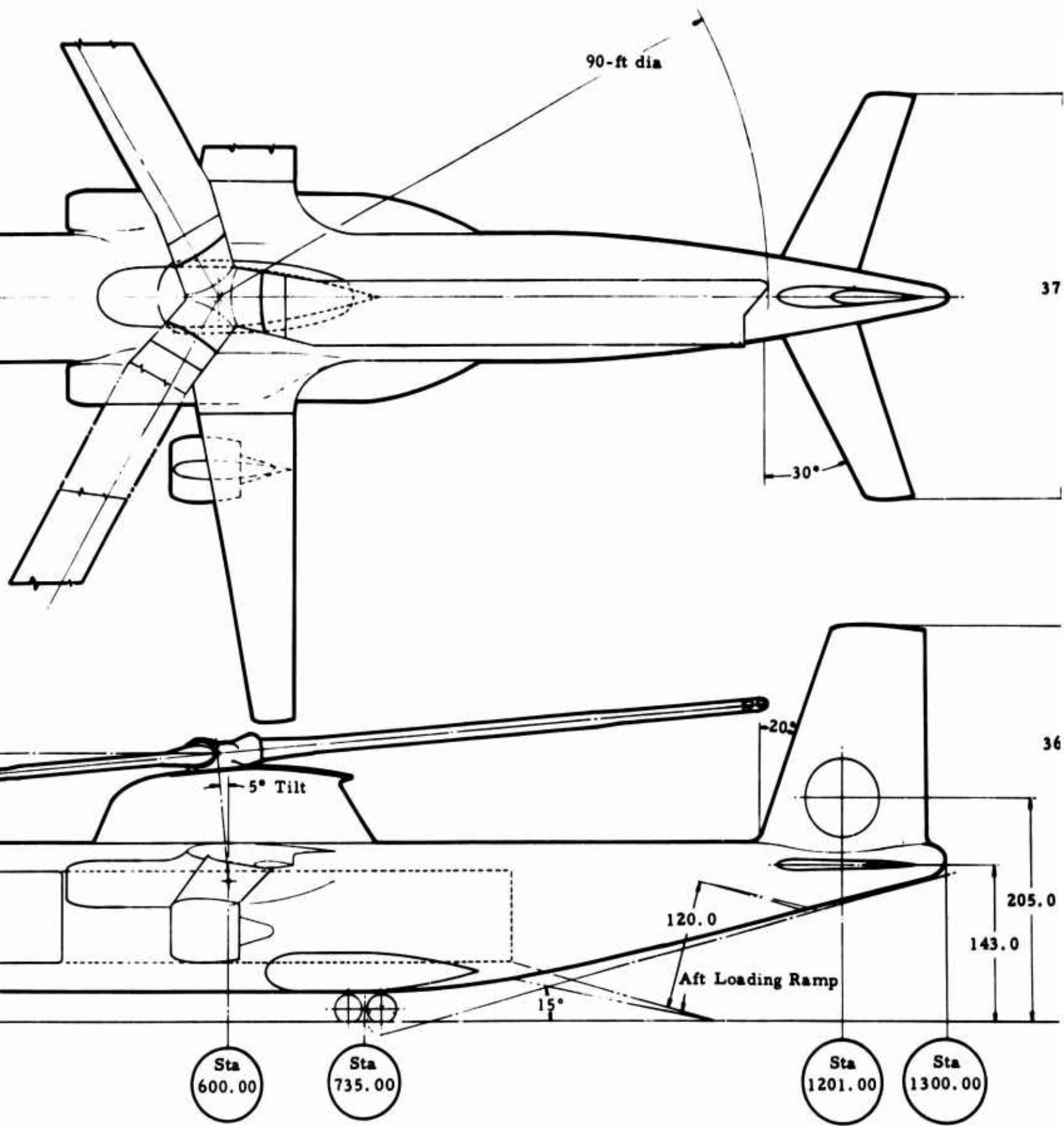


Figure 8. General A



gem - Configuration - Configuration 5 Compound.

B

PERFORMANCE

The performance of the Hot Cycle heavy-lift helicopter meets all mission requirements and exceeds most of the specified requirements by a substantial margin, as can be seen in Table I. Substantial improvement in fuel utilization efficiency over the best current turbine-powered helicopters is attained by the Hot Cycle propulsion system.

The selection of the optimum rotor was based on the results of the parametric study, wherein the effect of the many rotor variables was evaluated on several helicopter configurations. The rotor considered most nearly optimum for all the configurations studied was selected for the preliminary design. As can be seen by comparing the parametric study and preliminary design results (Tables I and XI), the performance of each aircraft configuration with its optimum rotor is somewhat superior to the performance of the same configuration utilizing the rotor selected for the preliminary design. Also contributing to the differences in performance are refinements to the weight and power-available equations as used in the parametric study. Subsequent to completion of the parametric study, the 20-ton heavy-lift mission was designated as the primary mission. This has resulted in a small increase in empty weight, as the design gross weight for the parametric study was initially assumed to be the transport mission gross weight.

PERFORMANCE COMPUTATIONS

All power-required computations are based on standard computation methods developed by NASA, with additional corrections for blade stall and drag divergence. A complete discussion of the computation method is presented in Reference 3.

The induced power in hovering is computed using simple momentum theory, with corrections for tip loss, planform, and twist. The download on the fuselage is also estimated from the induced velocity. The profile power is based on the NACA polar for a 12-percent thickness airfoil, with corrections for blade thickness and practical construction.

The helicopter forward flight power required is computed using the NACA charts given in Reference 4. The profile power of these charts is corrected for thickness and practical construction. Profile power increase as a result of retreating tip stall and advancing tip drag divergence is also included, with the aid of NACA whirl tower model data, Reference 5.

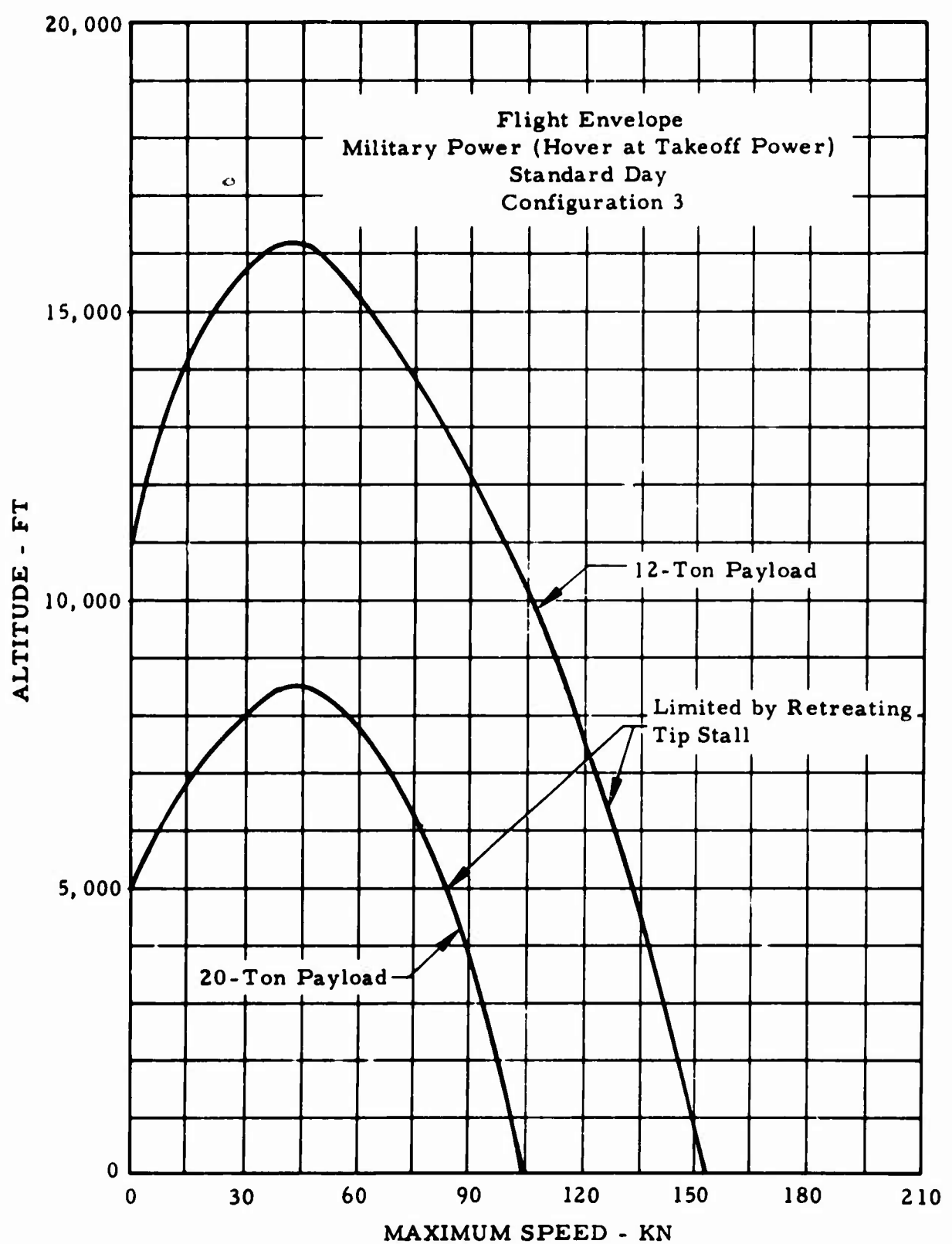


Figure 9. Flight Envelope.

The flight envelope, Figure 9, presents the maximum and minimum air-speeds as limited by military power or retreating tip stall. The retreating tip stall speed is determined as the speed at which the retreating tip drag coefficient is equal to 0.01.

Figure 10 presents the hover ceiling for standard ambient conditions in and out of ground effect as a function of gross weight. Takeoff power was used for the hover ceiling computation. A rotor height equal to one-half rotor diameter was assumed for the in-ground-effect calculations.

Figure 11 presents the maximum rate of climb with military power as a function of altitude.

Figure 12 shows the payload-range curve for sea level standard and 6,000-foot 95°F hover conditions. Payload is outbound only: no return and no reserve fuel.

PARASITE DRAG AREA ESTIMATION

Estimates were made of the parasite drag areas of the basic helicopter configurations with alternate hub arrangements. These estimates were based on References 6 and 7 and on sea level 59°F conditions, with velocity in the 95- to 130-knot range and gross weight in the 55,000- to 90,000-pound range. Results are presented in Table II.

The assumptions are as follows:

1. Fuselage angle of attack remains sufficiently low for all conditions to take it as zero for drag estimates.
2. Empennage parasite drag area (includes trim) constant at 3.98 square feet.
3. Items such as rotor hub, pylon fairing, and landing gear have the same drag when used on fuselages of different configuration; that is, interference effects are taken as the same.
4. All fuselage corners have a radius at least 20 percent of width (or height). This assures lowest drag.
5. External payloads are constant-size cubes with a cargo density of 30 pounds per cubic foot; therefore, 12-ton payload = $9.3 \times 9.3 \times 9.3$. A 50-foot support cable is used.
6. Parasite drag areas for the compound helicopter include additional drag values of 0.01 times wing area, 0.6 square foot for fuselage-wing interference, 2 percent of fan thrust for nacelle drag, and 2 percent of fan thrust for nacelle-wing interference.

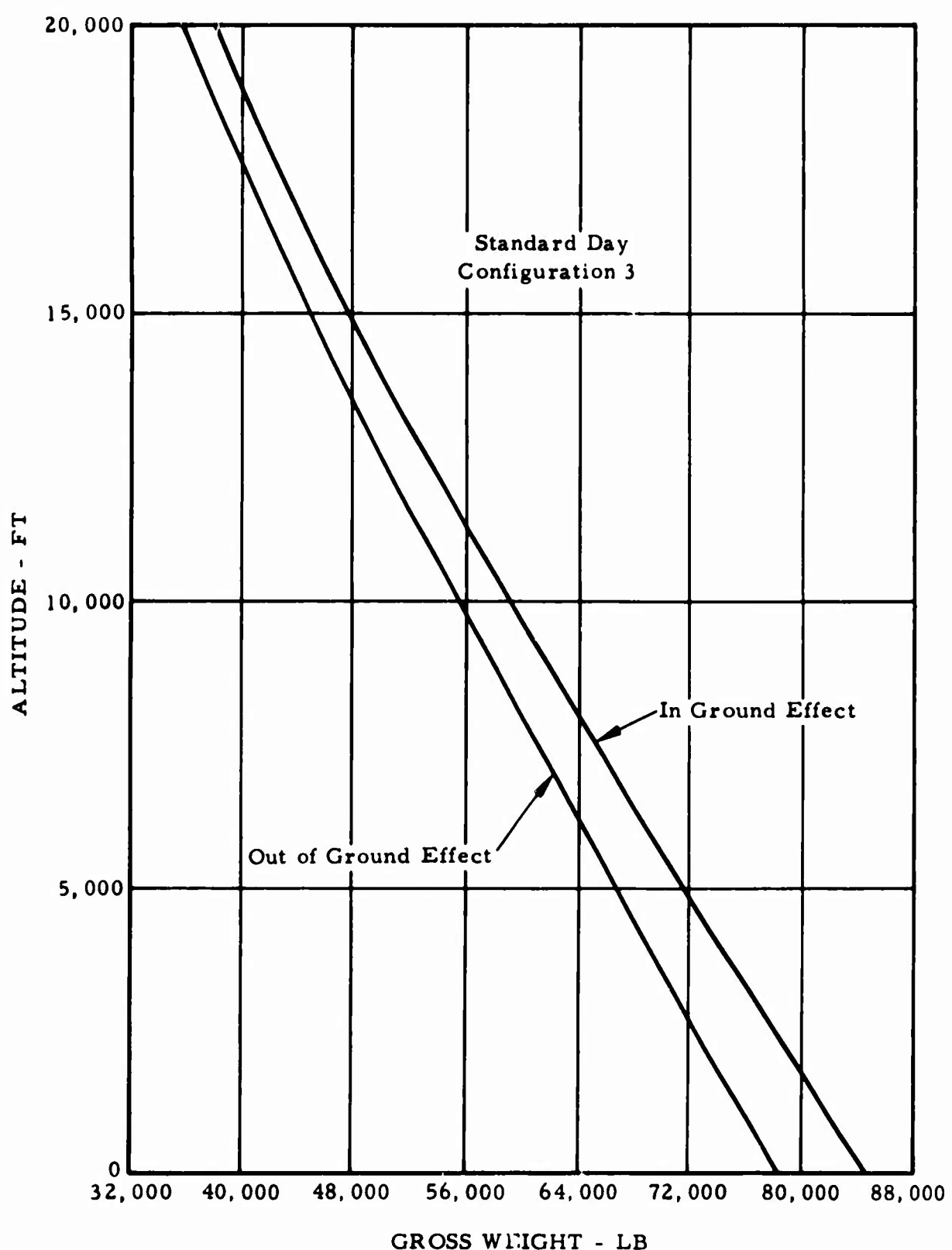


Figure 10. Hover Ceiling.

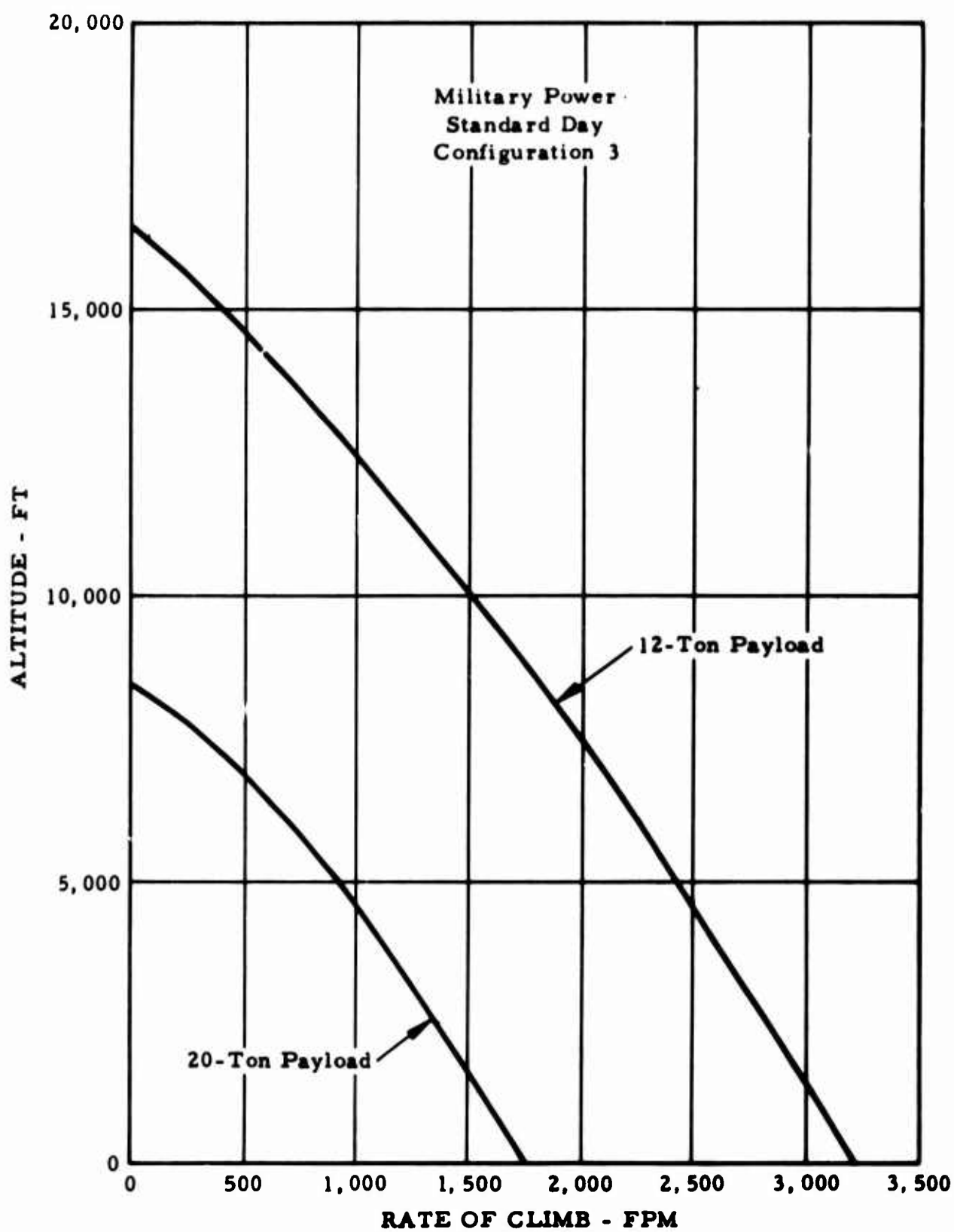


Figure 11. Maximum Rate of Climb Versus Altitude.

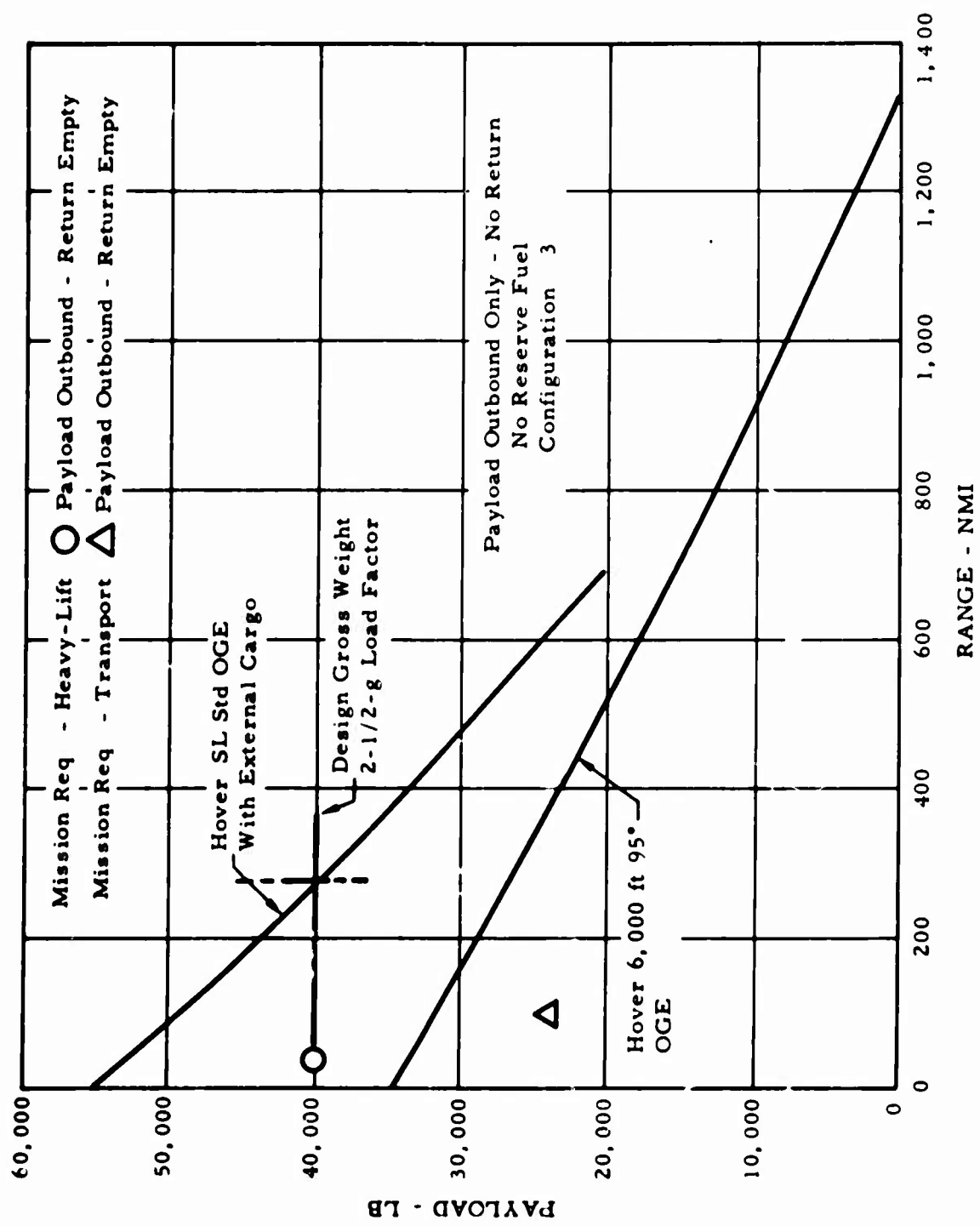


Figure 12. Payload Range - Sea Level Mission.

TABLE II
PRELIMINARY PARASITE DRAG ESTIMATE OF HEAVY-LIFT
HELICOPTER CONFIGURATION

Configuration	Fuselage	Parasite Drag in Square Feet										Total	
		Hub			Tilting			Landing Gear			External Payload		
		Articulated	Exterior Controls	Interior Controls	Exterior	Interior	Controls	Fixed	Retractable	12-Ton (1)	20-Ton (1)	Ferry Mission	Transport Mission
1(2)	26.39	8.06	-	-	-	-	-	3.33	-	-	139	37.78	37.78
1	26.39	8.06	-	-	-	-	-	0	-	-	139	34.45	34.45
1	26.39	-	10.86	-	-	-	-	0	-	-	139	37.25	173.45
1	26.39	-	-	18.76	-	-	-	0	-	-	139	45.15	176.25
1	26.39	-	-	-	23.01	-	-	0	-	-	139	49.40	184.15
4(3)	48.75	8.06	-	-	-	3.33	-	-	33	-	139	60.14	188.4
4	48.75	8.06	-	-	-	-	-	0	33	-	139	56.81	199.14
2	11.03	8.06	-	-	-	-	3.99	-	-	99	139	23.08	195.81
1	11.03	8.06	-	-	-	-	-	1.75	-	99	139	21.04	162.08
2	11.03	-	10.86	-	-	-	-	1.95	-	99	139	23.84	160.04
2	11.16	-	-	18.76	-	-	-	1.95	-	99	139	31.87	170.87
2	11.16	-	-	-	23.01	-	-	1.95	-	99	139	36.12	175.12
3	17.80	8.06	-	-	-	-	2.50	-	-	-	139	28.36	167.36
3	17.80	8.06	-	-	-	-	-	0	-	-	139	25.86	164.86
3	17.80	-	10.86	-	-	-	-	0	-	-	139	28.66	167.66
3	17.80	-	-	18.76	-	-	-	0	-	-	139	36.56	175.56
3(4)	17.80	-	-	-	23.01	-	-	0	-	-	139	40.81	179.81
5(4)	17.80	-	-	-	-	-	-	-	-	-	-	-	-

(1) Drags based on 30-lb/cu-ft density. A decrease to 20 lb/cu-ft would increase $\left(\frac{D}{q_0}\right)$ 23 sq ft for 12-ton load and 36 sq ft for 20-ton load.

(2) Includes pod.

(3) Without pod.

(4) Configuration 5 compound drags may be obtained by adding 0.01 times wing area. 0.6 square foot for fuselage-wing interference to the configuration 3 drags. An allowance of 2-percent fan thrust must also be made for nacelle drag and another 2-percent fan thrust for nacelle-wing interference.

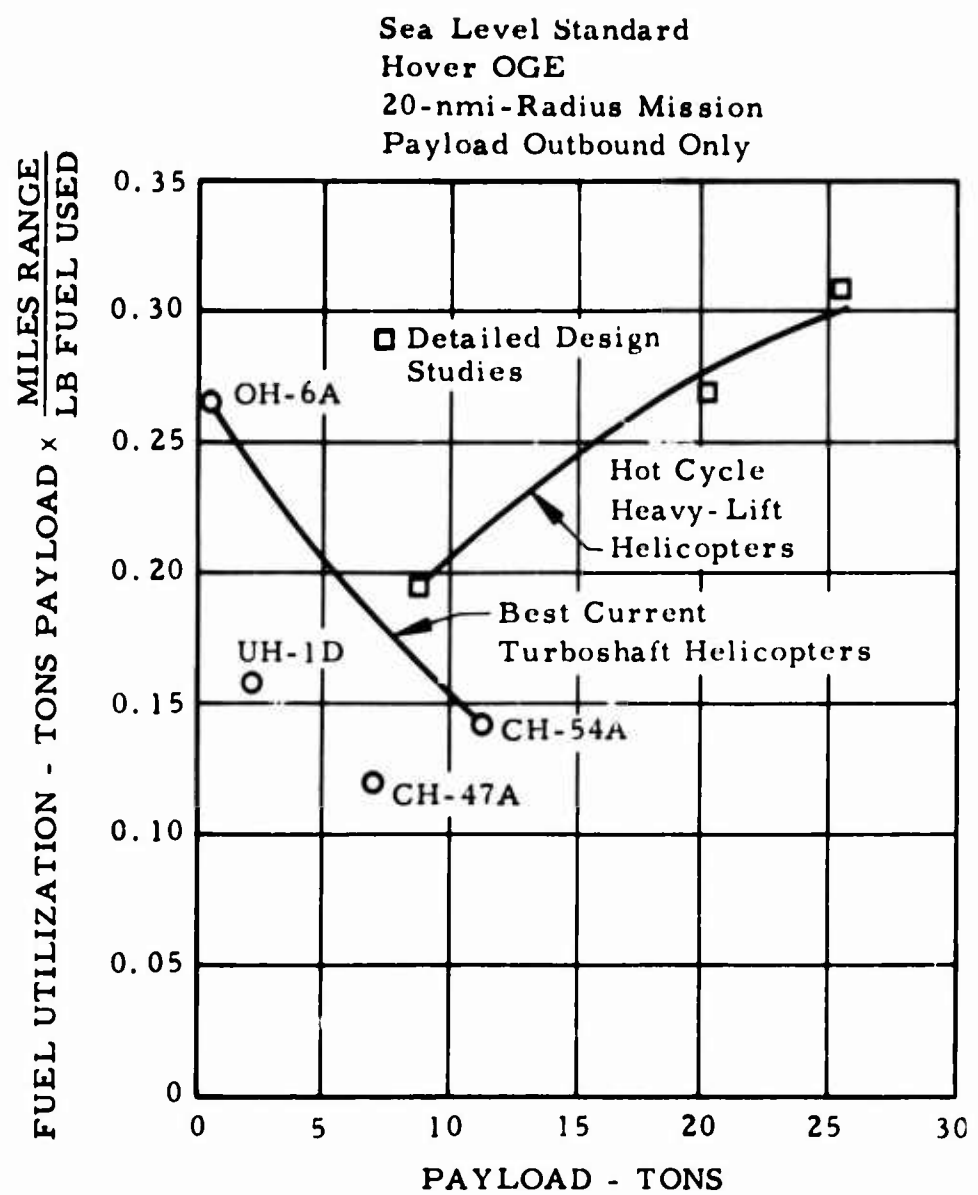


Figure 13. Fuel Utilization Versus Payload - Heavy-Lift Mission.

DISC LOADING

Though not a required part of the study, disc loadings were taken into consideration. The selected optimum rotor installed on the airframe configurations considered in this study results in disc loadings of approximately 10 pounds per square foot for the heavy-lift mission (20-ton payload). Even taking advantage of the large overload capability of the optimum Hot Cycle rotor for the heavy-lift mission results in disc loadings of approximately 12 pounds per square foot. However, this is an external-load condition and downwash hazards are minimized, since the actual disc loading and resulting downwash velocity are very low during hookup and until lift-off. For the transport mission, disc loadings are much more modest.

FUEL UTILIZATION

The results of the fuel consumption study indicate that a breakthrough for the economy of helicopter transports can be expected using the Hot Cycle propulsion system. The fuel utilization (payload ton-mile/pound of fuel) was calculated for the various configurations and missions and is shown in Figures 13 and 14 for the heavy-lift and transport missions, respectively. Fuel utilization based on payload, as opposed to specific fuel consumption, fuel flow/gross weight, and other parameters, is of direct importance for estimating actual fuel costs of specific helicopter operations. These comparisons indicate that for heavy-lift payloads the Hot Cycle offers substantial improvements over the best present turbine-powered helicopters (References 8 through 12). This excellent fuel utilization efficiency of the Hot Cycle helicopter is mainly the result of its excellent payload/empty weight ratio, the empty weight of the helicopter being greatly reduced.

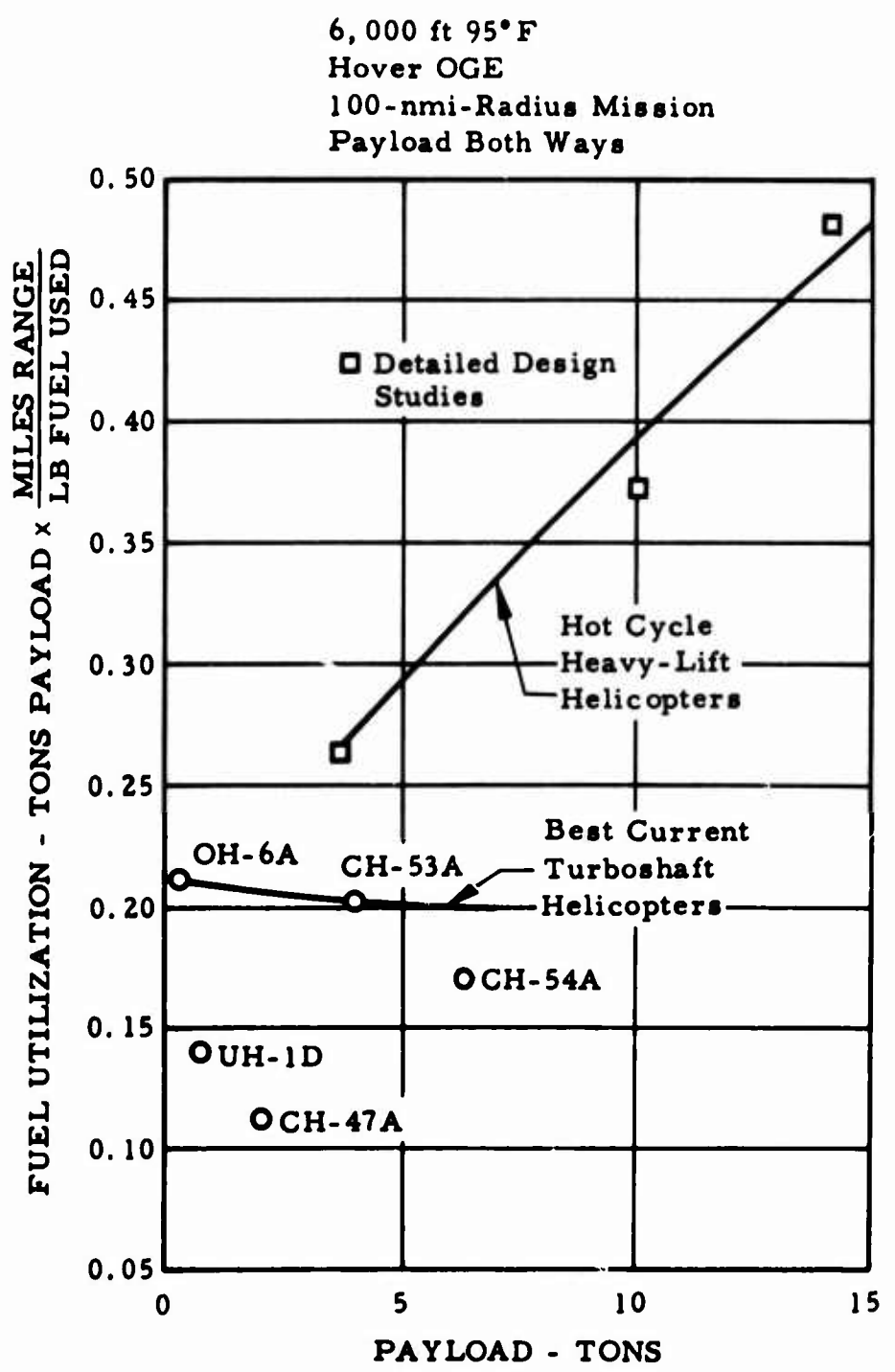


Figure 14. Fuel Utilization Versus Payload - Transport Mission.

STABILITY AND CONTROL CHARACTERISTICS

This section presents the stability and control characteristics of three basic configurations considered for the Hot Cycle heavy-lift helicopter shown previously in Figures 5, 6, and 7.

Efficient utilization of the heavy-lift helicopter, particularly in the external load-carrying conditions requiring pickup, transport, and precise placement of large and heavy loads, dictates that the helicopter possess good handling characteristics under various flight conditions. To ensure this capability of precision flying for the Hot Cycle heavy-lift helicopter, the stability and control requirements of MIL-H-8501A have been considered as a minimum for this design study. The rotor system has been designed to incorporate large blade-flapping hinge offset (4.2-percent blade radius) to provide the high control power and rotor damping necessary for the required good handling characteristics.

In summary, the stability and control analysis has shown the following:

1. With the proposed Hot Cycle rotor design, the heavy-lift helicopter in hover and low-speed flight will possess excellent handling characteristics in pitch and roll, superior to those required by MIL-H-8501A.
2. For cruise flight, the horizontal stabilizer has been sized to provide good longitudinal static and maneuver stability characteristics.
3. The vertical stabilizer has been sized to provide stable directional stability in cruise flight. In hover and forward flight, the proposed yaw fan thrust of 700 pounds per inch of pedal will provide excellent yaw response, superior to that required by MIL-H-8501A.

Since the handling characteristics of each configuration are interdependent on its loading condition (internal or external loading), the two primary mission modes have been considered for each configuration. The configurations and loading conditions investigated for this design study are as follows:

1. Minimum streamline fuselage (close packaged engines on top of the fuselage - configuration 2)

- a. 20-ton external loading (single-point sling)
 - b. 7-ton - internal loading capability
2. Streamline fuselage with laterally-located pylon-mounted engines (configuration 3)
 - a. 20-ton external loading (single-point sling)
 - b. 12-ton transport - internal loading
 3. Crane-type fuselage (configuration 4)
20-ton external loading (single-point sling)

Tables III and IV present the helicopter dimensional data (common to all configurations) and mass properties used in the stability and control analysis of the design configurations considered for the Hot Cycle heavy-lift helicopter.

HOVER FLIGHT CHARACTERISTICS

HANDLING CHARACTERISTICS IN PITCH

Table V presents the hover handling characteristics in pitch for the three basic configurations of the heavy-lift helicopter. The results are also compared with the handling requirements of MIL-H-8501A. As can be seen, the angular velocity damping of the heavy-lift helicopter is superior to that required by MIL-H-8501A for all configurations investigated. It can also be seen that the angular response in pitch per inch of control displacement is three to four times greater than the MIL-H-8501A requirements. For full control displacement from trim, the ratio of angular response available to that required is even greater. This is primarily because of the high control power provided by the large blade flapping hinge offset of the proposed Hot Cycle rotor design. The combination of high rotor damping and control power will provide the heavy-lift helicopter (HLH) with excellent handling characteristics in pitch.

HANDLING CHARACTERISTICS IN ROLL

Table VI presents the hover handling characteristics in roll for the heavy-lift helicopter and compares the results with MIL-H-8501A. Again, as in pitch, the angular velocity damping in roll for the HLH is far superior to that required by MIL-H-8501A. In fact, for all configurations investigated, the damping in roll is approximately twice that required by MIL-H-8501A.

TABLE III
DIMENSIONAL DATA

Rotor	
Diameter	90.0 ft
Disc area	6,359 sq ft
Chord	60.0 in.
Solidity	0.106
Blade twist	-8°
Number of blades	3
δ_3	0
Flapping hinge offset (% blade radius)	4.2%
Rotor shaft tilt, line \perp to fuselage WL	5° fwd
Centrifugal force of rotor blade ($\gamma_T = 750 \text{ ft/sec}$)	221,040 lb/blade
Airfoil section	NACA 0018 from root to 75% radius; NACA 0014 from 75% radius to blade tip.
Rotor tip speed, hovering	750 ft/sec
Rotor tip speed, forward flight	675 ft/sec
Horizontal Tail	
Span	324 in.
Tip chord	44.4 in.
Root chord	88.8 in.
Area	150.0 sq ft
Leading edge sweep	30°
Geometric aspect ratio	4.8
Incidence of tail with respect to fuselage WL	-5° (nose down)
Airfoil section	NACA 0012
Vertical Tail	
Span	200.0 in.
Tip chord	87.8 in.
Root chord	163.0 in.
Area	175.0 sq ft
Leading edge sweep	20°
Geometric aspect ratio	1.58
Airfoil section	NACA 0012
Control Travel	
Longitudinal Stick	
Full aft to full forward	12.0 in.
Cyclic pitch range	14° fwd, 14° aft
Lateral Stick	
Full left to full right	12.0 in.
Cyclic pitch range	6° left, 6° right
Collective Pitch Control Stick	
Full down to full up	9.5 in.
Cyclic pitch range (at 0.75R)	1° to 14°
Pedals	
Full right to full left	±3.25 in.
Pitch range	±25°

TABLE IV
HEAVY-LIFT HELICOPTER MASS PROPERTIES

Condition	Weight (lb)	Center of Gravity (in.)			Inertia (slug feet ²)		
		Fuselage Station	Butt Line	Water Line	Pitch	Roll	Yaw
Configuration 2							
20-ton external - sling	62,900	377.2	0	115.9	203,361	37,418	172,970
7-ton transport - internal	39,900	377.6	0	121.3	279,097	39,562	250,988
Configuration 3							
20-ton external - sling	65,700	385.8	0	113.9	232,812	50,383	204,233
12-ton transport - internal	52,700	386.8	0	110.4	364,095	56,994	335,869
Configuration 4							
20-ton external - sling	66,900	330.2	0	174.1	235,555	49,303	210,644

TABLE V
HOVER HANDLING CHARACTERISTICS IN PITCH

Heavy-Lift Helicopter Configuration	Heavy-Lift Helicopter	Angular Velocity Damping (ft-lb/rad/sec)	Angular Response (Degree of Angular Displacement at End of One Second Per Inch Control)		
		Minimum Requirement per MIL-H-8501A	Heavy-Lift Helicopter	Minimum Requirement per MIL-H-8501A	
Configuration 2					
20-ton external load - sling	73,630	41,995	3.88	1.13	
7-ton transport - internal	58,386	51,896	3.57	1.31	
Configuration 3					
20-ton external load - sling	76,060	46,200	5.39	1.11	
12-ton transport - internal	67,570	63,510	3.24	1.19	
Configuration 4					
20-ton external load - sling	71,170	46,750	4.78	1.10	

TABLE VI
HOVER HANDLING CHARACTERISTICS IN ROLL

Heavy-Lift Helicopter Configuration	Angular Velocity Damping (ft-lb/rad/sec)	Angular Response		
		Minimum	Requirement per MIL-H-8501A	(Degree of Angular Displacement at End of One Second Per Inch Control)
<u>Configuration 2</u>				
20-ton external load - sling	73,630	28,750	3.38	0.68
7-ton transport - internal	58,386	29,736	2.69	0.78
<u>Configuration 3</u>				
20-ton external load - sling	76,060	35,450	2.76	0.67
12-ton transport - internal	67,570	38,510	2.31	0.72
<u>Configuration 4</u>				
20-ton external load - sling	71,170	34,950	2.53	0.66

The angular response in roll for the HLH for all conditions investigated is approximately three times greater than the roll response requirements of MIL-H-8501A, and yet does not exceed the maximum allowable roll rate of 20 degrees per second per inch of stick of that specification. For full control displacement from trim, the roll response available is again superior to MIL-H-8501A requirements. This high control power and corresponding high rotor damping will provide the Hot Cycle HLH with excellent handling characteristics in roll.

HANDLING CHARACTERISTICS IN YAW

Table VII presents the angular response in yaw for the three basic configurations of the HLH based on a common yaw fan thrust of 760 pounds per inch of pedal. As can be seen, in all configurations investigated, the angular response in yaw of the HLH exceeds the MIL-H-8501A requirements. Analysis also shows that the yaw response at the most critical azimuth angle, relative to a 35-knot wind, is superior to MIL-H-8501A requirements.

TABLE VII
HOVER HANDLING CHARACTERISTICS IN YAW

Heavy-Lift Helicopter Configuration	Angular Response	
	(Degree of Angular Displacement at End of One Second Per Inch Control)	
<u>Configuration 2</u>		
20-ton external load - sling	5.41	2.75
7-ton transport - internal	3.79	3.19
<u>Configuration 3</u>		
20-ton external load - sling	4.61	2.71
12-ton transport - internal	2.92	2.91
<u>Configuration 4</u>		
20-ton external load - sling	4.46	2.70

The angular velocity damping in yaw for the Hot Cycle heavy-lift helicopters is low because of the relatively small size of the yaw fan, which is required only for yaw control. This characteristic, which is typical for

all tip-driven helicopters, is not expected to produce any adverse handling characteristics based on company experience with the tip-driven XV-9A helicopter. The heavy-lift helicopter utilizing a yaw fan will have damping superior to that of the XV-9A (with yaw jet control) and will result in greatly improved handling characteristics.

FORWARD FLIGHT CHARACTERISTICS

LONGITUDINAL MANEUVER STABILITY

The longitudinal maneuver stability characteristics of the three basic configurations considered for the Hot Cycle heavy-lift helicopter were determined with the aid of Reference 13. Since the maneuver stability parameter angle of attack stability (M_a) is dependent on cg location, the critical condition of maximum aft cg was considered. Figure 15 presents the results of the maneuver stability analysis for the HLH at $\mu = 0.30$ (forward flight speed of approximately 120 knots). As can be seen, the results show that all three configurations of the heavy-lift helicopter remain on the stable side of the boundary line for all of the representative flight conditions. Thus, the HLH will have good maneuver characteristics. This excellent longitudinal stability is primarily attributed to the relatively large horizontal tail provided in the design.

DIRECTIONAL STABILITY

The combination of the yaw fan control and large vertical tail will provide the Hot Cycle heavy-lift helicopter with good directional stability and control characteristics in cruise flight.

<u>Symbol</u>	<u>Condition</u>	
	Configuration 2	Sea Level Std Day $V_F = 120 \text{ kn}$ $V_T = 675 \text{ ft/sec}$ $\mu = 0.30$
Δ	20-ton external (sling)	
Δ	7-ton internal	
\circ	20-ton external (sling)	
\circ	12-ton transport (internal)	
\square	Configuration 4 20-ton external (sling)	

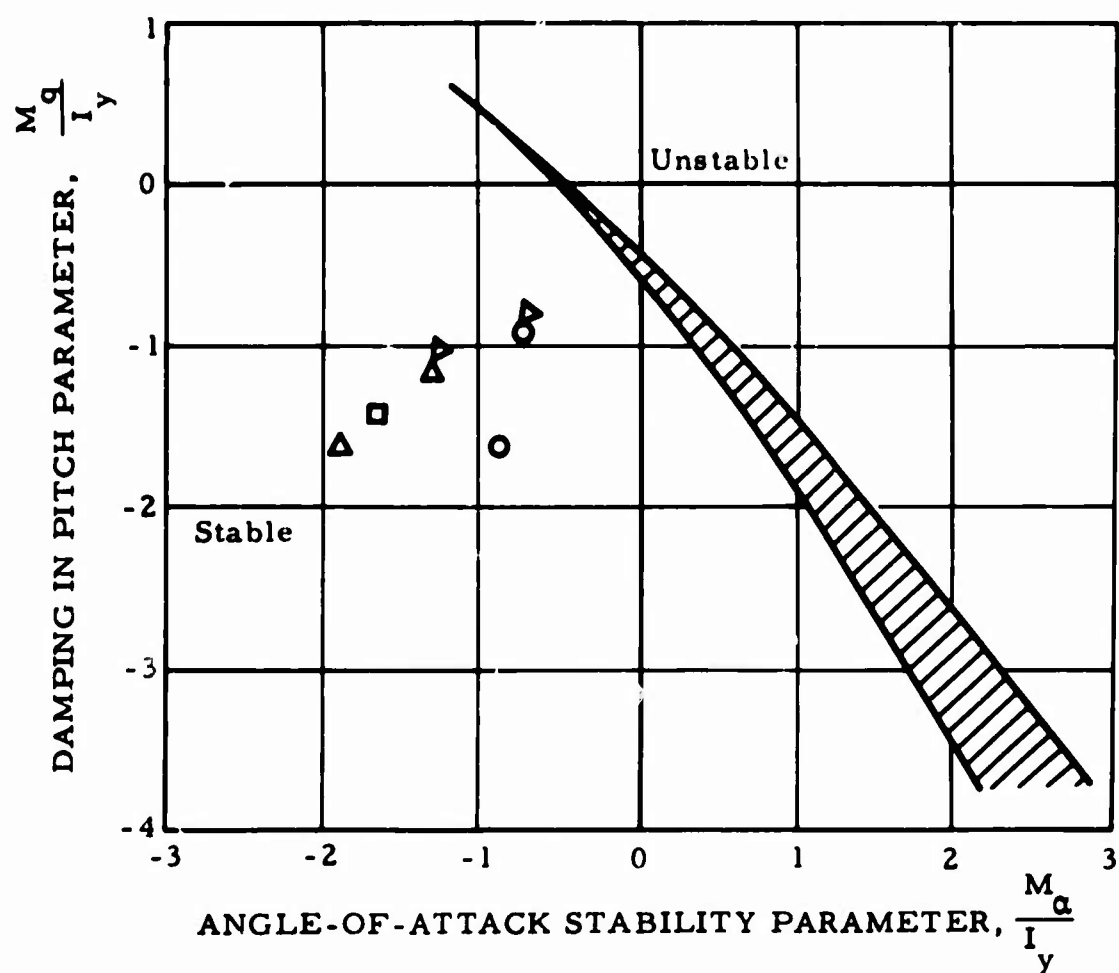


Figure 15. Longitudinal Maneuver Stability Criterion.

ROTOR SYSTEM

The primary objective of this program was to define the optimum Hot Cycle rotor for the heavy-lift helicopter. This objective has been achieved by analyzing the results of a parametric study to determine the effect of varying the many characteristics of the rotor, such as rotor diameter, tilting or articulated type of hub, number and size of blades, tip speed, blade structural arrangement, internal or external flight controls, and airfoil shape. The rotor systems were further evaluated by considering them installed on several aircraft configurations. The results upon which the selection of the optimum rotor was based are discussed in detail in the Parametric Study section of this report. The study has indicated that a rotor as small as 80 feet in diameter, when installed on the minimum airframe, will result in a helicopter that will weigh approximately 18,000 pounds empty and will exceed all mission requirements of range and payload by 20 to 30 percent. However, for the integrated preliminary design, a larger diameter rotor -- 90 feet -- has been selected for disc loading considerations and as the rotor that is more nearly optimum for all of the aircraft configurations studied. The selected rotor is defined in Table VIII.

TABLE VIII
SELECTED OPTIMUM ROTOR CHARACTERISTICS

Type of hub	Articulated
Flapping hinge offset	22-1/2 in.
Lead-lag hinge	Blade station 66-1/2
Controls	External
Rotor diameter	90 ft
Blade chord	60 in.
Blade section	
Root to 0.75R	NACA 0018
0.75R to tip	NACA 0014
Blade spar location	25% chord
Blade duct configuration	Figure-8
Rotor tip speed	
Hover	750 ft/sec
Cruise	675 ft/sec

HUB DESIGN

The parametric study considered two basic types of hub: the fully articulated hub with offset flapping hinges and the tilting type as used on the

XV-9A Hot Cycle helicopter with hub restraint added to provide the necessary control power. Two variations of these basic types -- namely, with internal or external controls -- were also evaluated. A rigid-type rotor was also considered but was abandoned because of its inherent structural problems and the resultant weight increase. The hubs evaluated are described in more detail in the Parametric Study section of this report. The articulated hub was selected for the optimum rotor because of its clear-cut advantage over the tilting type in the areas of light weight and lower drag. The external controls were selected because they were determined to be lighter, less complicated, and more rigid.

The selected hub is shown in Figure 16. This configuration allows coaxial gas ducts to be routed uninterrupted up through the center of the hub assembly. As the ducts approach the blade level, they are split off into three pairs of ducts, one duct from each engine. This arrangement allows the engine output to be completely separated from gas generator to blade tip nozzles.

Located just outside of the coaxial ducts is the rotating housing portion of the hub. Thermal protection is provided by insulation applied to the ducts and by centrifugally pumped cooling airflow between the insulation and housing. A ring gear is installed on the lower rim of this housing to drive the accessory gearbox.

A pair of angular contact bearings offset vertically is used to carry rotor lift loads and moments from the rotating housing into the stationary mast, which in turn is attached to the fuselage through a tubular truss. The vertical offset of the bearings, plus the additional effective distance supplied by the contact angle, provides a generous couple arm to accommodate applied rotor moments. Lift is taken by the lower pair of bearings, and any download is reacted through the single upper bearing. Bearings are lubricated by a circulating oil system.

The stationary mast, in addition to its function as the rotor support, acts as the guide and sliding surface for the spherical bearing on which the swashplate tilts for cyclic inputs and moves vertically for collective motion. The swashplate is of conventional configuration, utilizing an angular contact bearing assembly to provide for the loads between the rotating and stationary swashplates.

The main structural members in the blade retention system and hub assembly provide a direct load path for the centrifugal force and lift loads from the three blades. The retention system consists of a lead-lag strap pack that attaches the inboard end of each blade spar to the flapping

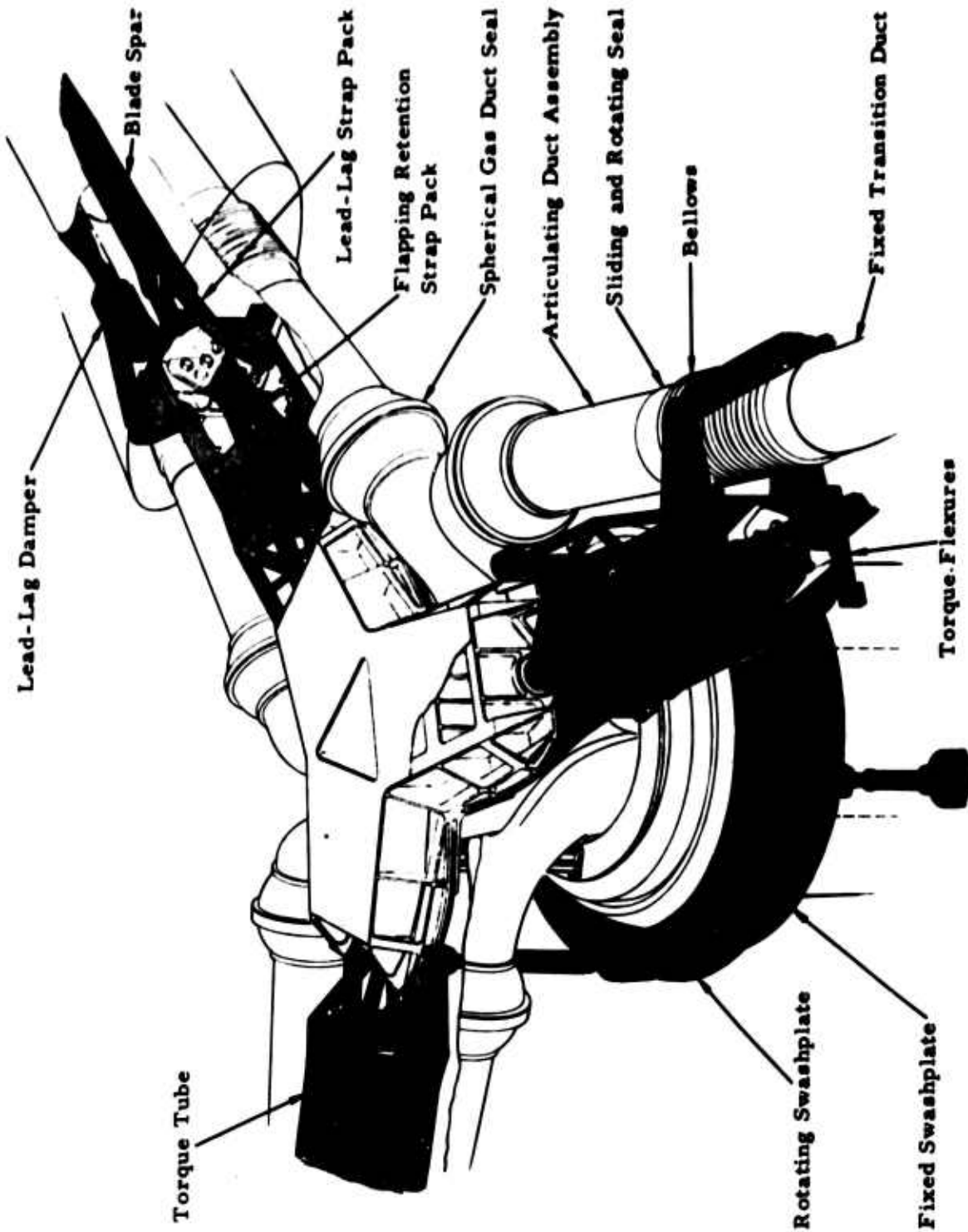


Figure 16. Articulated Hub With External Controls.

retention strap pack and allows lead-lag motion of the blade. The flapping strap packs are attached to the hub plate, wherein the centrifugal loads from the three blades are effectively cancelled out. Only the unbalanced lift and in-plane loads remain to be carried through the support attachment to the mast. A torque box extends from the flapping axis out to the lead-lag hinge point at each blade. This torque box transmits feathering motion from the swashplate to the blade. The torque box is connected torsionally to the blade across the lead-lag hinge points through two flexures offset vertically to provide the torsional load path.

The lead-lag hydraulic damper is installed between the blade leading edge structural member and the torque box. Three stages of damping are provided, so that damping is increased in steps as the lead-lag oscillation increases.

BLADE DESIGN

The blade designs considered in the parametric study were dictated to a large extent by duct configuration. Essentially, the parametric study resolved the tradeoff between duct area and blade weight for the different duct shapes evaluated. Three basic duct shapes were considered. The first configuration considered was the elliptical-shaped ducts as used on the XV-9A Hot Cycle helicopter, where the ducts were an integral part of the blade segment; the second, round ducts; and third, figure-8 ducts. The figure-8 ducts were selected as the most efficient configuration. A more detailed description of these blade duct configurations is to be found in the Parametric Study section of this report.

The structural arrangement of the selected blade is made up of a single spar, leading edge member, and segmented assemblies of sandwich-type skin and ribs joined spanwise by flexible couplings (Figure 17). The pairs of gas ducts are routed through the blades, one forward of the spar and one aft. A segmented trailing edge fairing completes the blade structure. The spar is located on the 25-percent chord and extends the full length of the blade from the lead-lag flexure on the inboard end to the cascade at the blade tip.

The spar area required at each spanwise blade station is determined by and is proportional to the centrifugal force. The flapwise stiffness, that is, moment of inertia, required at each spanwise station is determined by the ground flapping condition. The spar area is apportioned at each spanwise station to meet, but not exceed, the required stiffness. Exceeding the required flapwise stiffness would result in undesirably high in-flight flapwise bending moments. All flapwise shear and moments are taken by the spar. The required chordwise balance weight, located in

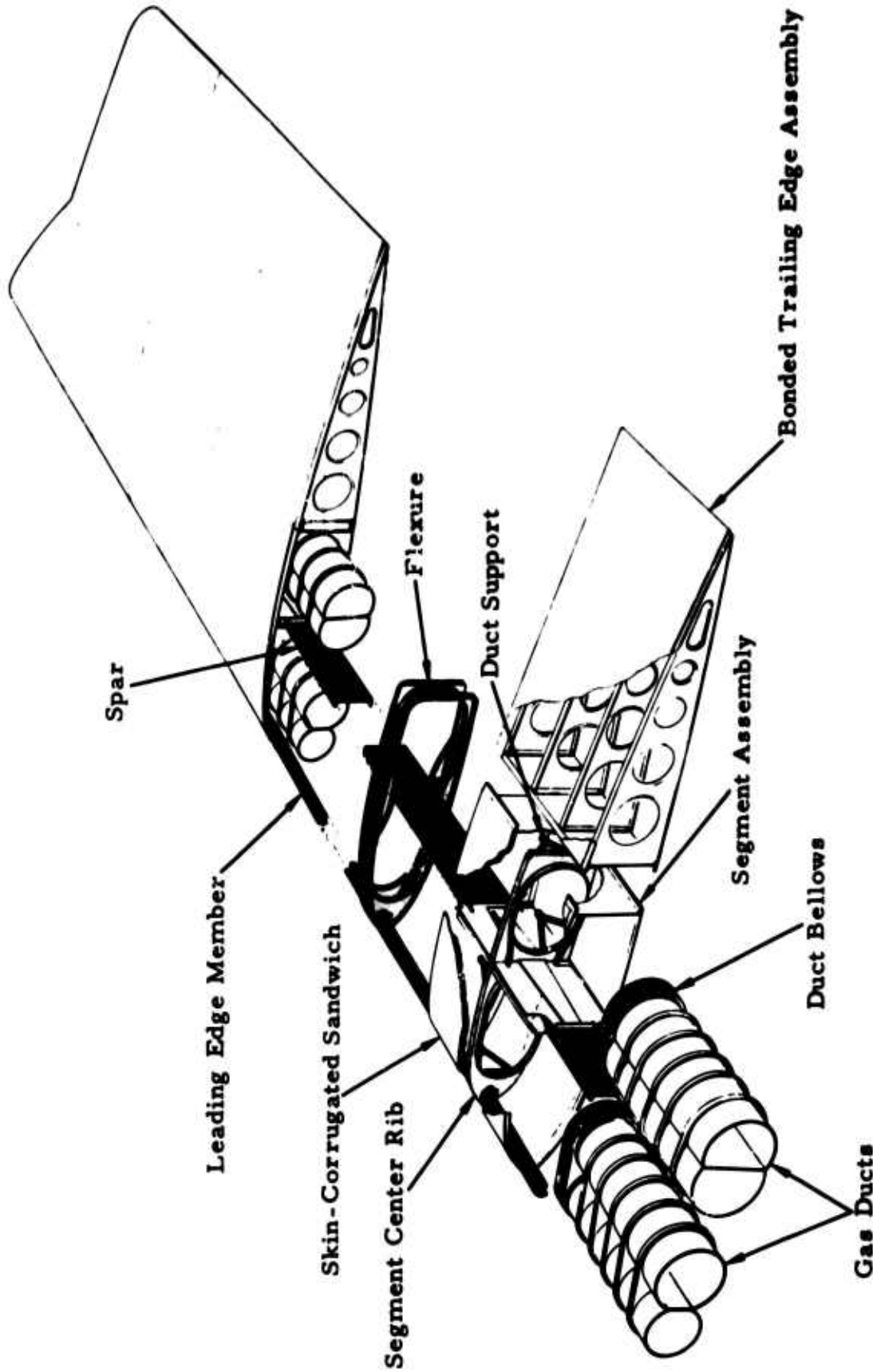


Figure 17. Blade Assembly.

the leading edge, is utilized as a continuous structural member extending from the lead-lag damper at the inboard end to the blade tip. The leading edge member is designed to take chordwise shear and, coupled with the spar, provides a load path for the blade chordwise moment.

The spanwise segments are approximately 20 inches in length and are made up of corrugated titanium skin assemblies and Inconel 718 ribs. The flexures join the segments to each other to provide a load path for blade torsion as well as to provide the necessary flexibility to prevent bending stresses from being induced into the skin panels. Trailing edge fairing segment assemblies are also interrupted spanwise for the same reason, and are fabricated from thin-gage aluminum skin bonded to internal ribs, a configuration similar to the XV-9A.

FLIGHT CONTROL DESIGN

Two basic flight control configurations were considered. One configuration utilized a swashplate located below the rotor with the push rods extending up through the center of the gas ducts to walking beams that were connected to the blade lift links. The other configuration used a swashplate assembly large enough to be installed outside of the ducts and hub structure with the lift link attached directly between the swashplate and blade pitch arm. This latter configuration was selected because of its greater rigidity, simplicity, and resulting lower weight. It also required a smaller fairing, inasmuch as the walking beams increased the size of the required fairing. Three hydraulic servo-controlled cylinders power the flight controls. They are operated in such a manner that for collective pitch they act in unison and for cyclic pitch they act differentially.

PROPULSION SYSTEM

The design of the propulsion system places emphasis on simplicity, reliability, and safety in an easily maintainable twin-engine installation. These factors are inherent in the Hot Cycle propulsion system, in which high-energy gas is diverted from the engine exhaust up through the hub to the tip of each blade, where it is exhausted to drive the rotor (Figure 18). Conversion of the basic helicopter propulsion system to the compound helicopter propulsion system can be accomplished in the manner shown by Figure 19.

DESIGN CHARACTERISTICS

The primary advantage of the Hot Cycle propulsion system is its simplicity, with the resulting advantages of light weight and reliability gained by the elimination of many heavy and complex dynamic components required by other types of propulsion systems. The increased reliability achieved is a significant feature of the Hot Cycle propulsion system. The extreme scatter of failure lifetimes found in conventional drive system elements, such as bearings, gears, couplings, shafts, and clutches, is well recognized throughout the rotary-wing and propulsion industries. Conversely, the low incidence of failure with conservatively designed ducted propulsion systems has been well established, particularly in jet-engine technology. Thus, comparison with the more complex shaft-driven helicopters using the many complex dynamic components emphasizes the simplicity and resulting increase in reliability and safety of the Hot Cycle rotor.

HOT GAS DUCT SYSTEM

The knowledge and experience gained from the successful XV-9A Hot Cycle program have been utilized in the design of the hot gas system. Additional factors of safety have been applied to the design of all pressurized hot gas ducting, and only materials with excellent corrosion resistance and crack-propagation resistance are used. Isolation of both thermal and structural strains is provided in the design of the hot gas ducting system, through proper design of mounts, reinforcements, and flexible joints. In addition to the isolation of both hot and cold components from a structural viewpoint, insulation and cooling airflow preclude any possible detrimental effects from the interaction of the hot and cold components. Further, thermal differential expansion in the primary structure is reduced by using materials of similar thermal expansion rates. Transient thermal effects in the hot gas system are minimized by detail design to assure even heat-up and cool-down of the components. The materials used in

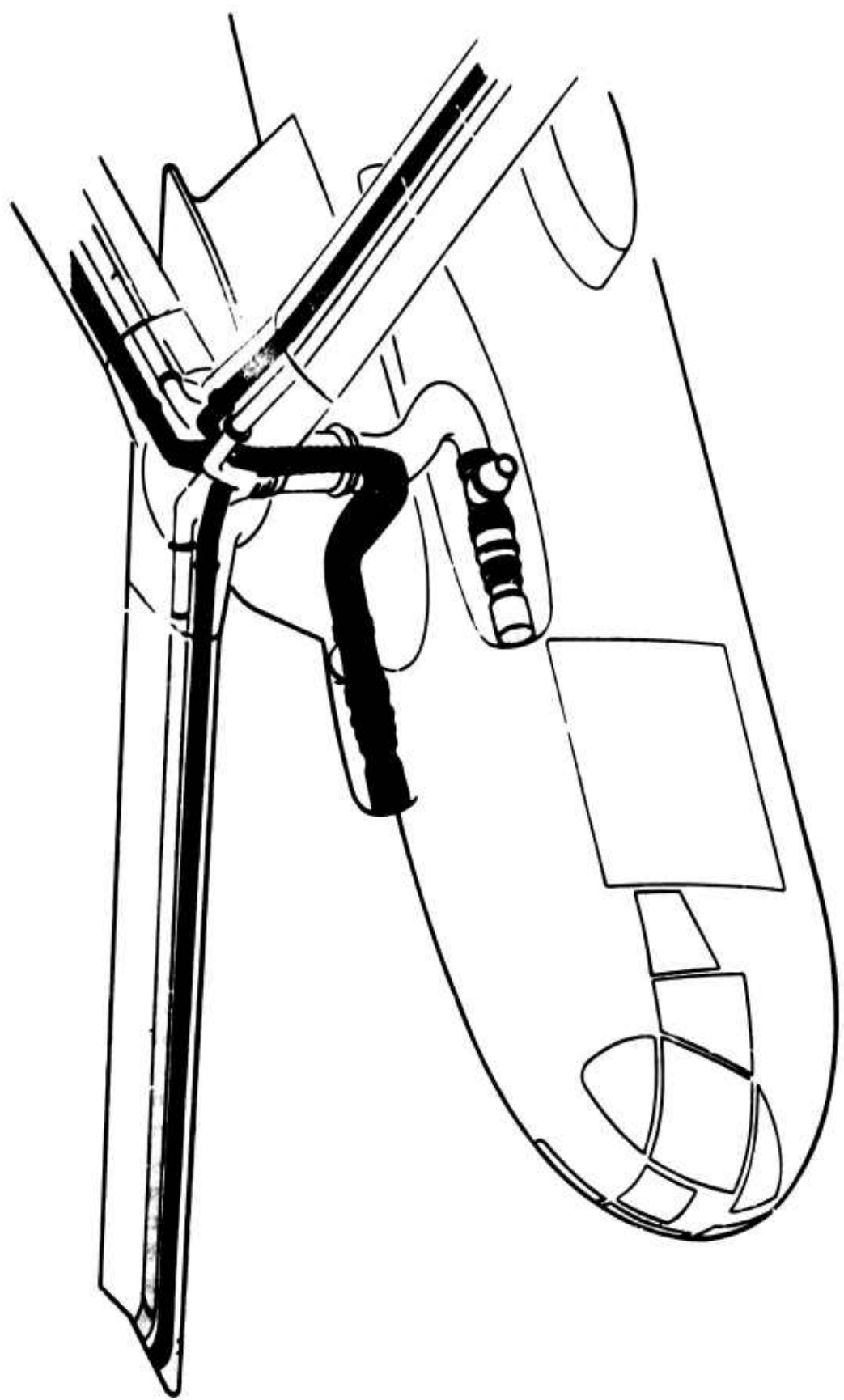


Figure 18. Propulsion System - Helicopter.

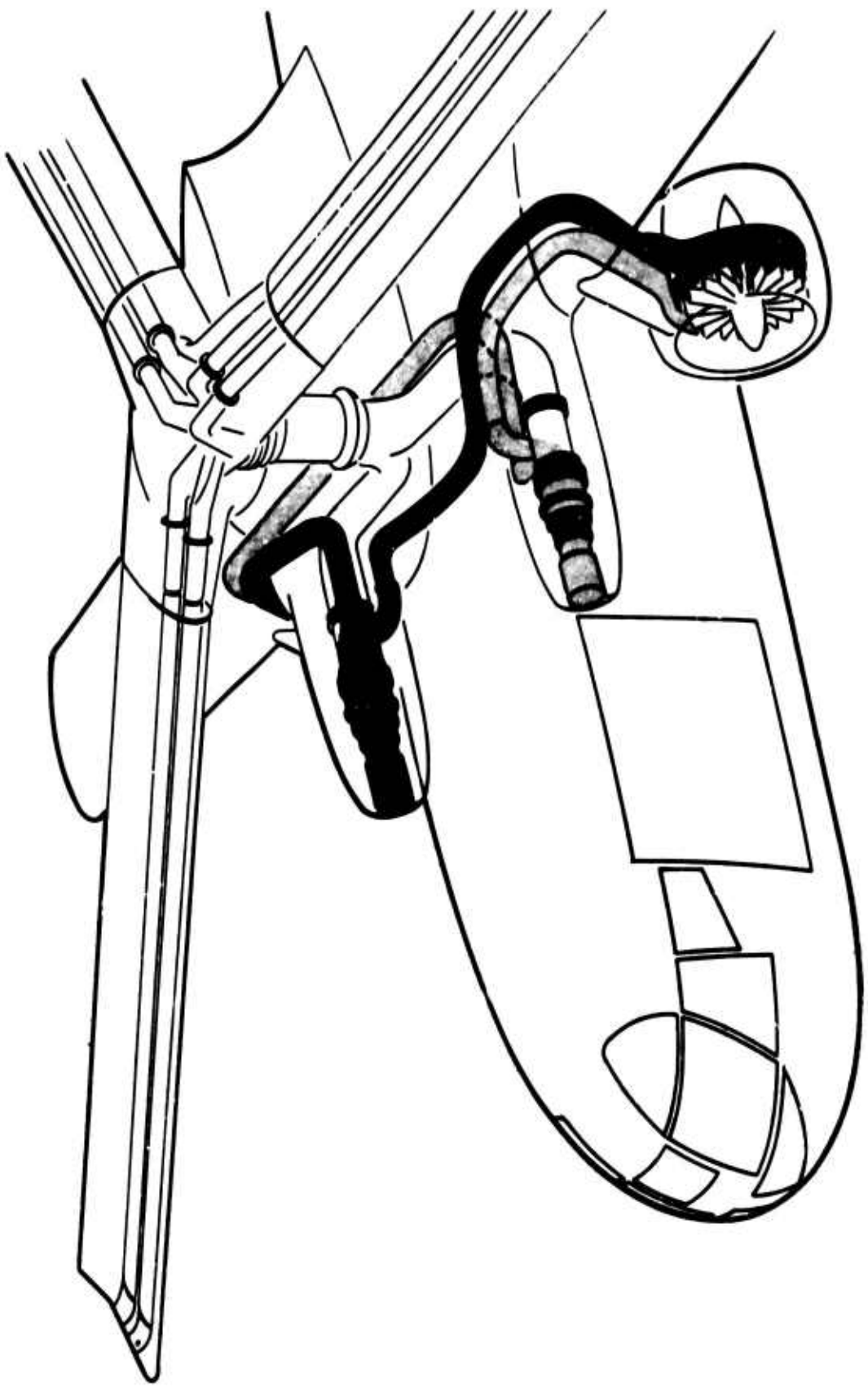
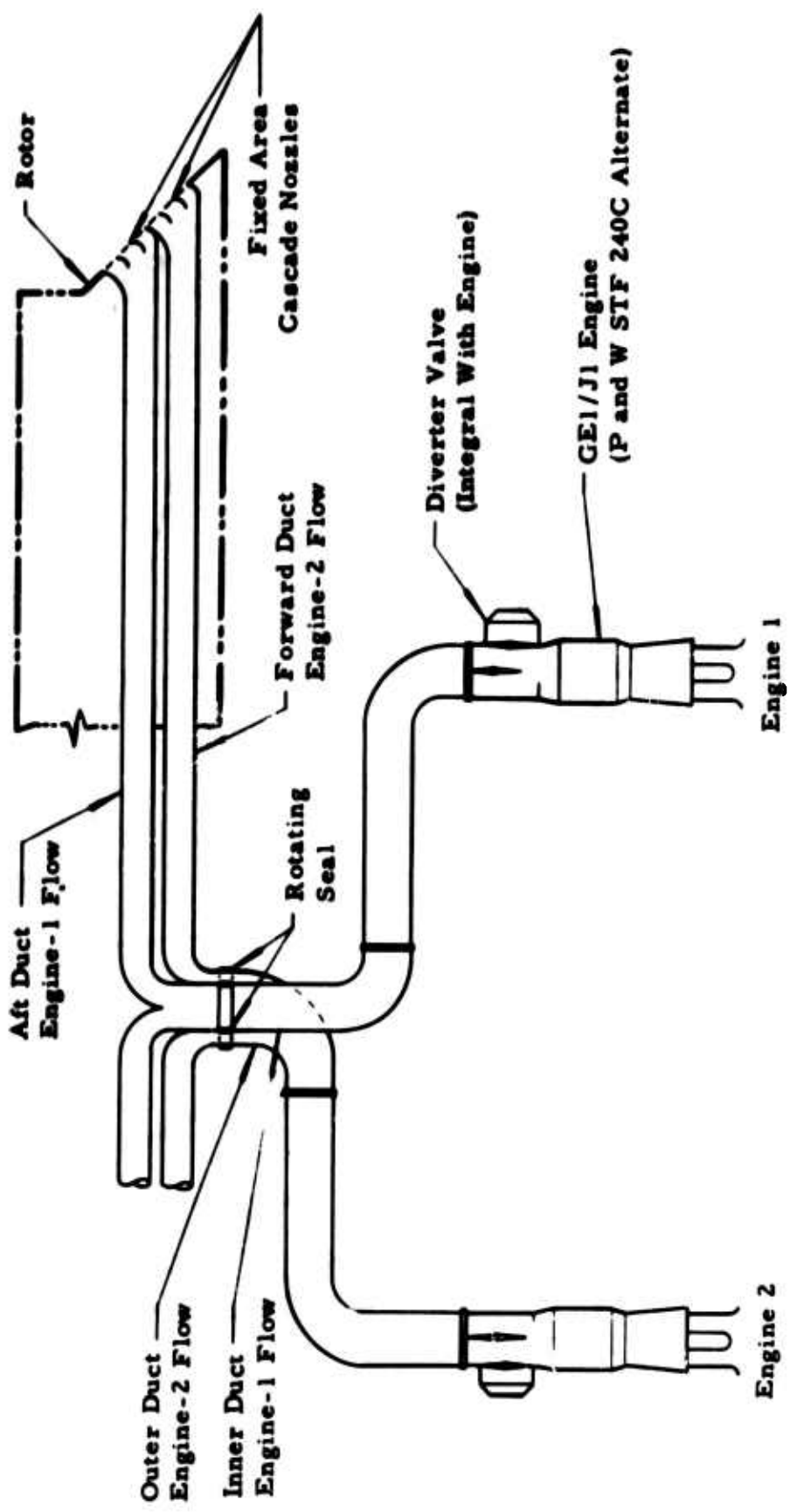


Figure 19. Propulsion System - Compound Helicopter.



Note: Diverter valves are positioned for rotor flow.

Figure 20. Hot Cycle Propulsion System Schematic.

the hot components are standard production materials having wide usage in the jet engine industry and do not require the development of new technology.

The gas output of each engine for the two-engine configuration is ducted separately from engine to blade tip by coaxial gas ducts through the hub and through separate ducting in the blades, shown schematically in Figure 20. The use of separate outlets negates the problems associated with engine mismatch and thereby eliminates the necessity for power matching of engines and the need for blade-tip closure valves.

The exhaust gas flows from each engine through diverter valves that either divert the flow overboard for engine starting or direct the flow up through hub and blades for rotor operation. The engine and diverter valve are an integral unit. The seal above the diverter valve permits rotation between the stationary duct and its counterpart in the rotating system. As it emerges from the hub, the gas flows out three pairs of parallel ducts, separated to provide the necessary clearance for the hub and blade retention straps, through a transition section, and into the blade constant section. At the blade tip, the gas is turned 90 degrees by the cascade vanes and ejected at the trailing edge. All the ducts are insulated to reduce heat flux; bellows are utilized to allow for thermal expansion; articulating ducts and seal assemblies at the blade root are installed to permit blade feathering, flapping, and lead-lag motion.

ENGINE INSTALLATION

Two engine installations were evaluated in the parametric study. The primary power source considered utilized two General Electric GE1/J1 gas generators, shown in Figure 20. An alternate installation utilizing four General Electric GE T64/S4B gas generators was also surveyed and is shown schematically in Figure 21. Subsequent to completion of the parametric study, data on the Pratt and Whitney STF240C gas generator has become available, and it appears to be interchangeable with the GE1/J1 without any major changes to the propulsion system installation or aircraft configuration.

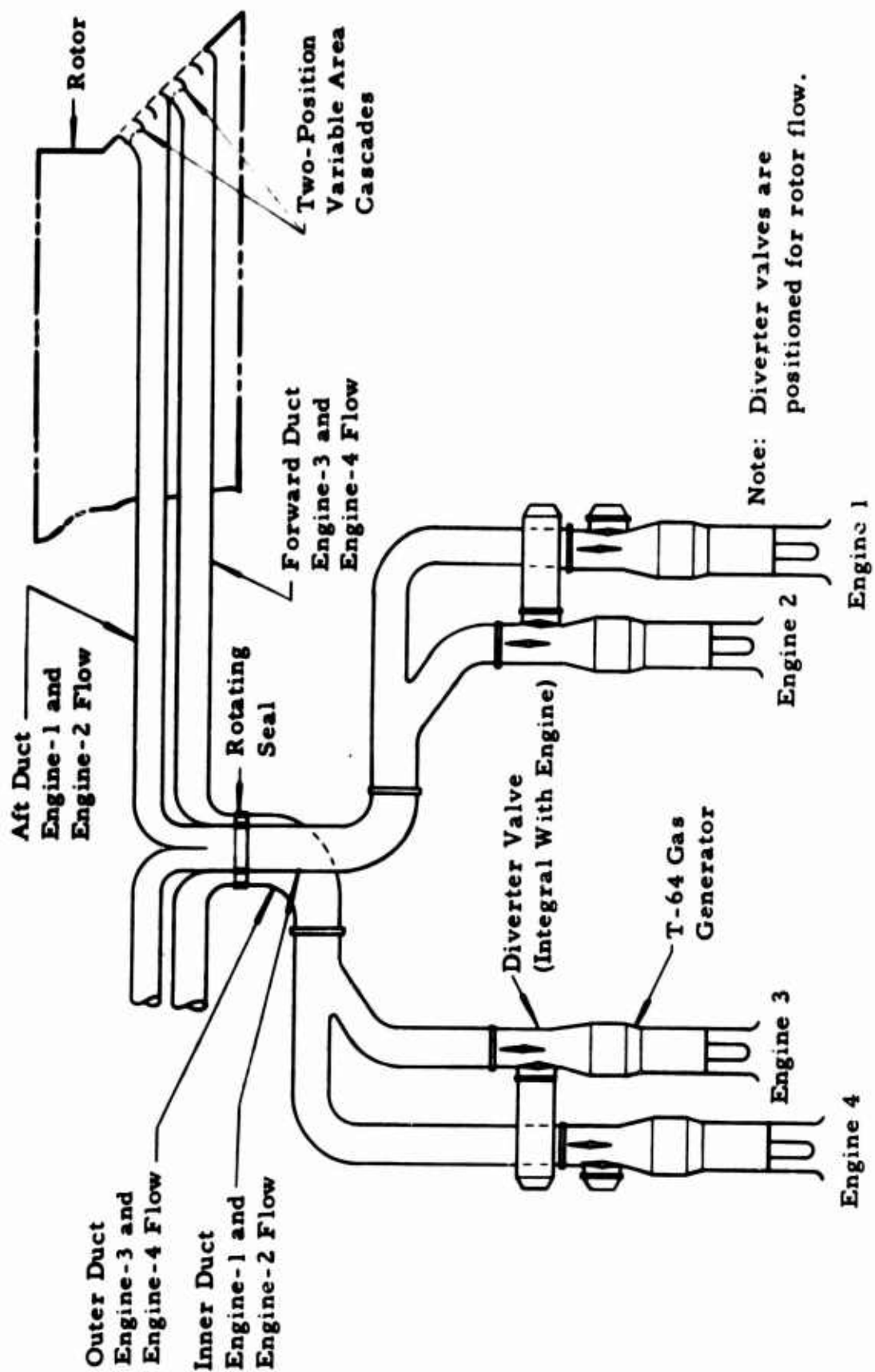


Figure 21. Propulsion System Schematic - Four-Engine.

WEIGHTS

The favorable performance of the Hot Cycle rotor is a direct result of the simplicity and inherent light weight of this propulsion system. Since the propulsion system is lighter, the gross weight is lower and requires a smaller rotor, which results in an even lower gross weight. This compounding effect produces a low empty weight and a high payload-to-empty weight ratio.

The weight estimation for the Hot Cycle heavy-lift helicopter configurations noted in Table IX has been based on data compiled from analytical and statistical studies and was carried out in two parts. The first task was to develop weight equations for the parametric study from existing statistical data and preliminary layouts. The second task was to calculate the weight of the selected optimum rotor detail design. Upon completion of these tasks, it was found that the rotor weight as obtained by the equation using an estimated running blade weight was higher than the rotor weight as obtained by the detailed analysis. This difference was the result of refinement and optimization of blade design subsequent to the development of equations for the parametric study. Good agreement is obtained when the lower running blade weight of the optimized design is used in the weight equation. The detailed weight analysis summarized in Table X shows the selected rotor weight to be 5,440 pounds, and applying the parametric equations to the same rotor results in a weight of 5,475 pounds when the calculated running blade weight is used. The tail group, flight controls, and propulsion group weights for the preliminary design have been changed from those used in the parametric study to reflect a more realistic distribution of weight. A summary weight statement per MIL-STD-451 Part I may be found in Appendix I.

SUBSTANTIATION OF WEIGHT EQUATIONS - HELICOPTER

The helicopter group weights and equations used in the parametric study and preliminary design are based on data compiled from analytical and statistical studies of numerous production and proposed helicopters. Conventional methods have been employed in arranging the various parameters used to obtain meaningful expressions that result in reasonable weight estimates. Also used to the greatest extent possible was the invaluable data and experience gained in the development of the Hot Cycle XV-9A research vehicle. The success achieved in obtaining reasonable correlation with actual data has verified the validity of the equations developed and presented herein.

TABLE IX
CONFIGURATION WEIGHT SUMMARY

	Configuration		
	2	3	4
Rotor radius = 45 ft			
Chord = 60 in.			
Design tip speed, V_t = 750 fpm			
Ultimate load factor = 3.75 (heavy-lift mission)			
Rotor group	5,440	5,440	5,440
Tail group	970	992	998
Hover-yaw group	193	197	198
Fuselage	2,843	3,615	3,575
Alighting gear**	2,185	2,300	2,852
		(2,810*)	
Flight controls	1,414	1,445	1,454
Hydraulic and pneumatic	711	731	735
Electrical	742	749	752
Propulsion (includes 2 each GE-1 engines)	2,971	2,971	2,971
Instruments	180	180	180
Electronics	150	150	150
Furnishings and equipment	300	300	300
Air conditioning and anti-icing	100	100	100
Cargo-handling equipment	<u>1,400</u>	<u>1,400</u>	<u>1,400</u>
WEIGHT EMPTY	19,599	20,570	21,105
		(21,080*)	
Crew (3-man)	600	600	600
Crew kits	50	50	50
Oil	30	30	30
Unusable fuel	<u>100</u>	<u>100</u>	<u>100</u>
OPERATING WEIGHT	20,379	21,350	21,885
		(21,860*)	
Heavy-Lift Mission:			
Payload (20-ton)	40,000	40,000	40,000
Fuel	<u>3,901</u>	<u>4,131</u>	<u>4,312</u>
GROSS WEIGHT	64,280	65,481	66,197
		(65,991*)	
Transport Mission:			
Payload (12-ton)	24,000	24,000	24,000
Fuel	<u>7,881</u>	<u>6,884</u>	<u>8,272</u>
GROSS WEIGHT	52,260	52,234	54,157
		(52,744*)	

*Retractable landing gear.

**Landing gear weight was based on the maximum gross weight associated with a limit load factor of 2-1/2 g. This was obtained by dividing the product of the mission gross weight x load factor by 2-1/2. In all cases, the ferry mission was critical.

TABLE X
ROTOR GROUP SUMMARY

	Weight (lb)
<u>Blade*</u>	
Constant section	848.8
Transition section	57.2
Torque box	92.5
Tension strap (flapping)	40.5
Lead-lag flexure	21.3
Stub spar	28.6
Sealant, finish, etc	5.3
Blade to hub truss	26.2
Droop stop	18.2
Damper	66.0
Damper arm	4.5
Articulated duct	68.0
Fairing over torque box	16.0
Damper attachment	<u>4.8</u>
Total 1 blade	<u>1,298</u>
	<u>x 3</u>
Total 3 blades	<u>3,894</u>
<u>Hub and Shaft</u>	
Hub	369
Hub support	37
Droop stop support	27
Fixed shaft	334
Rotating shaft	280
Upper bearing, seal, retainer	101
Lower bearing, seal, retainer	356
Feathering bearings	17
Hub fairing	<u>24</u>
Total hub	<u>1,545</u>
Total rotor group	<u>5,439</u>

*Blade balanced chordwise 23 percent at the tip to 28 percent at the root.

MAIN ROTOR GROUP WEIGHT EQUATION

The main rotor group equation is based on the statistical and analytical study performed by HTC-AD and published in Reference 14. The equation developed is a power function expression relating total rotor group weight to the total "idealized" blade weight (W_{BU}) and rotor tip speed (V_t). The "idealized" blade weight is defined as the weight of the blade less the weight of the retention system, root fittings, doublers, and so forth. These data were obtained or determined from published detailed weight statement reports of numerous helicopters, based on actual or calculated weights.

A power function analysis was performed on the basis of these data, resulting in the following equation that gives the best fit curve for the plotted points of Figure 22:

$$W_r = B \left(\frac{b W_{BU}}{1,000} \right)^{0.896} \left(\frac{V_t}{700} \right)^{0.80} \quad (1)$$

where

W_r = total rotor group weight, lb

b = number of blades

W_{BU} = ideal blade weight, lb per blade

V_t = rotor tip speed, maximum power on, ft per sec

B = 2,282 = constant for best fit of statistical data

This equation is used as the basis for establishing the relationship of the total rotor group weight to blade weight for each of the Hot Cycle rotor configurations investigated in the parametric study. An estimated rotor size of 94-foot diameter was chosen; and through detailed design layouts and analysis, estimated weights were obtained for the blades, retention system, hub, and rotating controls. From this data, with idealized blade weight (W_{BU}) and total rotor group weight (W_r) being known quantities, the specific value of coefficient B was then determined as follows for the various hub and shaft configurations:

$$B = W_r \div \left(\frac{b W_{BU}}{1,000} \right)^{0.896} \quad (2)$$

when tip speed (V_t) = 700 feet per second.

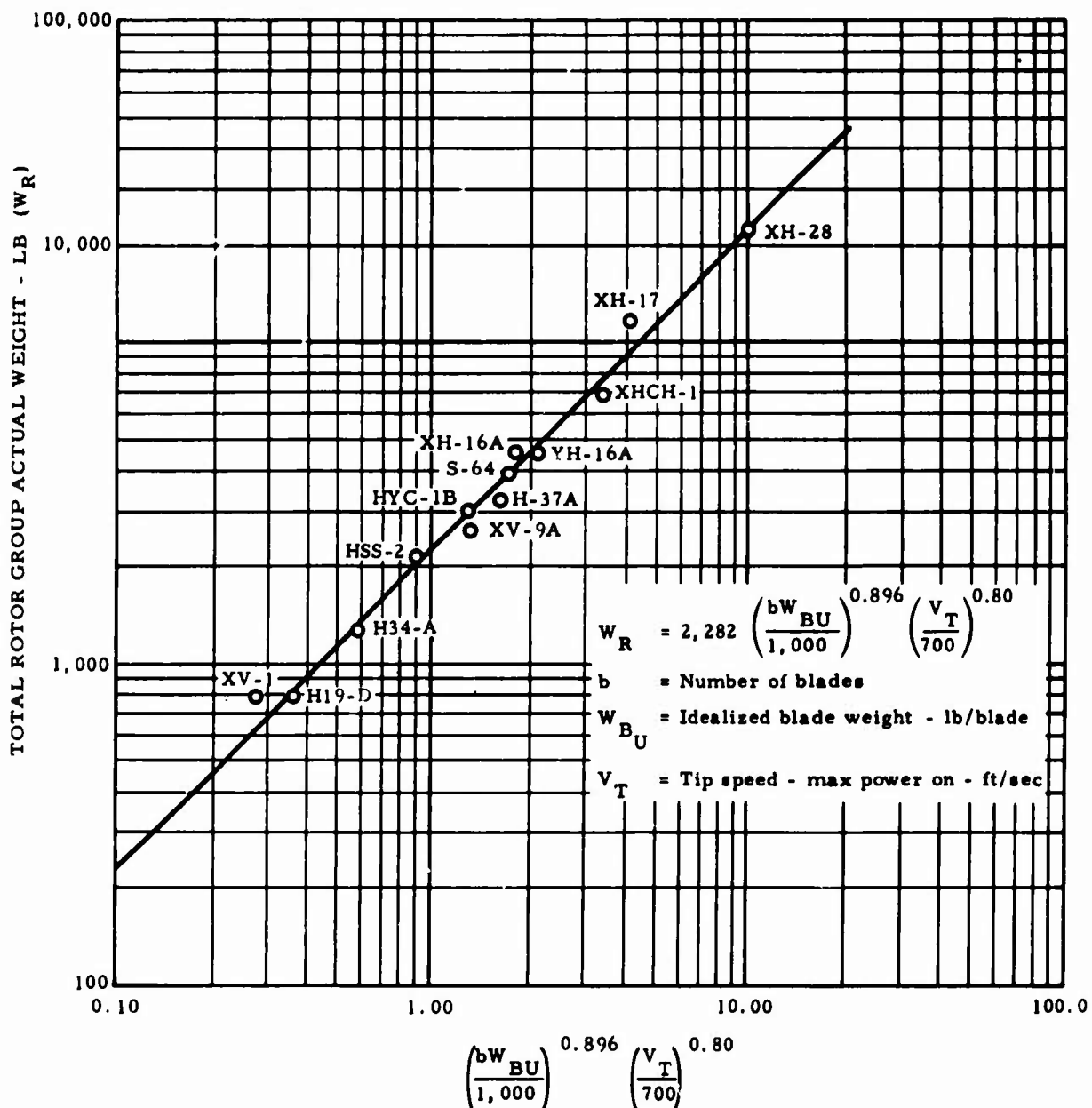


Figure 22. Total Rotor Group Actual Weight Versus Equation Results.

Hub Type	Shaft	bW_{BU^*}	$W_{hub + retention^*}$	W_x	$\left(\frac{bW_{BU}}{1,000}\right)^{0.896}$	B
Tilting	Internal	5,670	4,657	10,327	4.80	2,170
Tilting	External	5,670	5,957	11,627	4.80	2,440
Articulated	Internal	5,160	3,351	8,511	4.36	1,980
Articulated	External	5,160	3,190	8,350	4.36	1,940

The equivalent coefficient for the XV-9A unrestrained tilting-hub internal shaft rotor system is 2,130. The two-percent weight increase obtained in the tabulated value of B for the similar configuration above (tilting-internal) is attributed to the increased loads obtained in a restrained hub. The articulated hub system with its more direct load paths and lower chordwise loads is predictably lighter than the XV-9A system, by as much as nine percent.

TAIL GROUP EQUATION

This equation includes only the weight of the horizontal and vertical surfaces required for flight stability and control.

Qualitative stability studies at HTC-AD coupled with actual experience derived in the testing of the XV-9A Hot Cycle research vehicle indicate that the total surface of the tail should be on the order of 5.50 square feet per 1,000 pounds of gross weight.

The equation used in the parametric study conservatively assumes a unit weight of 3.50 pounds per square foot and is derived as follows:

$$W_{tg} = \frac{5.50 (3.50)}{1,000} W_g = 0.0193 W_g \quad (3)$$

where W_g = design gross weight.

A later review of aircraft tail group data revealed that the unit weight used was too conservative. This conclusion is based on investigation of tail surface weights within the size, gross weight range, and speeds being considered. A more realistic unit weight of 2.75 pounds per square foot would result in a revision of the original equation as follows:

$$W_{tg} = \frac{5.50 (2.75)}{1,000} W_g = 0.0151 W_g \quad (4)$$

*Calculations based on layouts (b = 3 blades).

HOVER-YAW GROUP EQUATION

The equation used in the parametric study was derived by estimating the weight of a tail rotor system required for the tip-driven rotor vehicles being studied. The weights were sized from comparable components used on the OH-6A helicopter. The following data were used to obtain the estimated weight changes noted.

DESIGN DATA

Comparison of Heavy-Lift Helicopter and OH-6A Hover-Yaw Systems

	<u>OH-6A</u>	<u>Heavy-Lift Helicopter</u>
Rotor radius, ft	2.13	4.00
Number of blades	2	6
Design tip speed, fps	694	720
Blade chord, in.	4.81	10.0
Rotor solidity	0.116	0.357
Design gross weight, lb	2,400	60,000
Hover-yaw system weight, lb	25.0	179.7

A rational analysis of the comparative data shown above was performed to obtain weights for the various heavy-lift helicopter hover-yaw components shown, based on the comparable OH-6A weights. The tail rotor and hub weights were determined from blade radius, solidity, and centrifugal force considerations. Drive shafting and coupling weights were based on ratios of transmitted torque and length. The gearbox weights were based on statistical weight studies performed by HTC-AD involving torque, gear ratios, and speeds as parameters. The resulting heavy-lift helicopter weights, obtained by the methods described, totaled 179.7 pounds.

Complexity in a hover-yaw group equation is not warranted, in view of its small influence on gross weight. Assuming, therefore, that the group weight varies directly with gross weight for the heavy-lift parametric study, the equation used is as follows:

$$W_{hy} = \frac{179.7}{60,000} W_g = 0.003 W_g \quad (5)$$

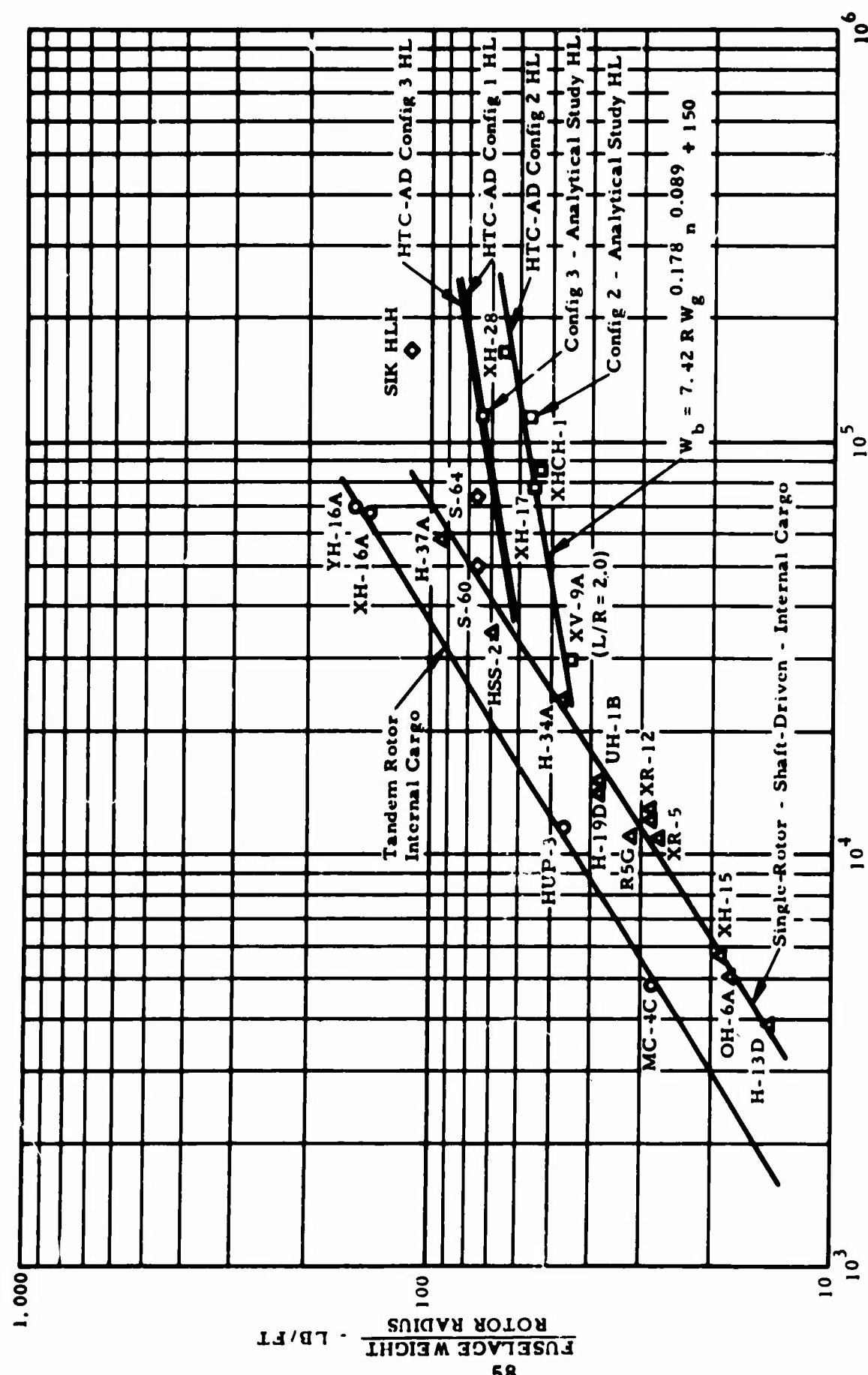


Figure 23. Fuselage Weight/Rotor Radius Versus Gross Weight x (Ultimate Load Factor) $^{1/2}$.

FUSELAGE WEIGHT EQUATIONS

Configuration 2 Fuselage Equation

The original development work of the fuselage weight equations used in the parametric study was performed by HTC-AD under contract AF33 (616)-3149 and published in Reference 15. This report illustrates the correlation between fuselage weight and the fundamental design parameters describing helicopter vehicles; namely, gross weight (W_g), rotor radius (R), and ultimate load factor (n). The three basic fuselage curves developed in the report are shown in Figure 23 for reference. The equation of interest in the parametric study for use on single-rotor tip-driven helicopters carrying cargo externally is:

$$W_b = 7.42 R W_g^{0.178} n^{0.089} \quad (6)$$

The equation for configuration 2 streamlined fuselages with length-to-radius ratios of 2.0 was verified by a preliminary sizing from a structural analysis of the fuselage. A gross weight of 60,000 pounds and a rotor radius of 47 feet were assumed, using an ultimate load factor of 3.75. Floor weight was assumed as 1.5 pounds per square foot. The resultant weight distribution and integration are shown in Figure 24, and the results are plotted in Figure 23. The actual fuselage weight of the XV-9A Hot Cycle research vehicle is also plotted after being adjusted to a length-of-fuselage to rotor-radius ratio of 2.0 from 1.6. The points fall close to the fuselage equation curve, verifying its slope and intercept.

An additional 150 pounds was added to this, and the other equations, to account for the rotor mast fairing unaffected by parametric considerations. The final equation for the configuration 2 fuselage is then revised and used as follows:

$$W_b = 7.42 R W_g^{0.178} n^{0.089} + 150 \quad (7)$$

The relatively low weight of the configuration 2 streamlined fuselage results primarily from the efficient structural shape. In addition, the fuselage is designed to transport a maximum of 7 tons of payload internally.

Configuration 3 Fuselage Equation

The basic difference between this fuselage and configuration 2 is that the fuselage cross section is larger to allow for internal cargo capability to

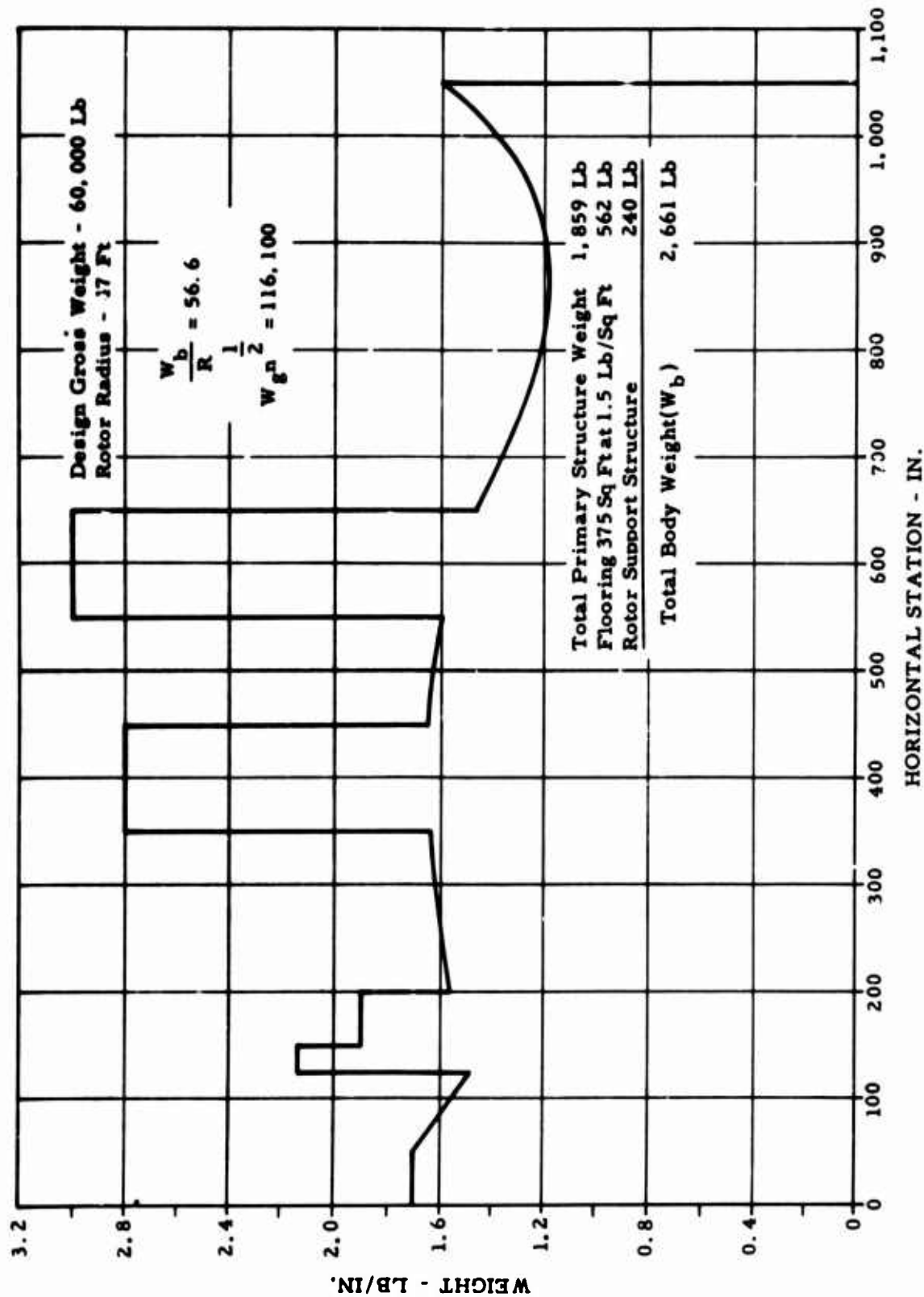


Figure 24. Primary Structure Weight Distribution - Configuration 2.

12 tons. The fuselage equation for configuration 3 was developed from the previous equation by including the effects of the larger fuselage. This was done on the basis of wetted area. On this basis, the configuration 3 fuselage weight would increase 23.4 percent over that of a configuration 2 fuselage of similar length.

An increase in floor structure unit weight to 2.00 pounds per square foot is allowed because of increased floor beam width and floor utilization.

The combined effects of these changes applied to the configuration 2 fuselage equation develop an equation for configuration 3 as follows:

$$W_b = 9.51 R W_g^{0.178} n^{0.089} + 150 \quad (8)$$

An independent structural analysis similar to that performed on configuration 2 produced the weight distribution curve shown in Figure 25. A plot of this weight in Figure 23 shows that close agreement exists between the two methods employed to obtain a fuselage weight.

Configuration 1 and Configuration 4 Fuselage Equation

The configuration 1 and configuration 4 crane fuselages are identical in all respects except in the manner in which the mission payloads are carried; configuration 1 uses a detachable cargo pod in operation.

A weight comparison was made of three crane-type fuselages: the XH-17, S-60, and S-64. Also used was the weight data obtained from detailed design efforts by HTC-AD on the XH-28 heavy cargo crane. The weight study applied the same parameters used to develop the previously discussed equations. The results are plotted in Figure 23.

Two primary design differences are involved in these crane-type ships. First, the shaft-driven cranes require large tail rotors to provide the high reacting torques required to balance out the main rotor transmission torque. These larger tail rotors must be mounted high for ground clearance, and such mounting imposes high torsional loads in the fuselage. These high bending and torsional loads are not present in tip-driven rotor cranes. Second, the tip-driven helicopters used in this comparison have lower ratios of fuselage length to rotor radius than the shaft-driven cranes, since a large tail rotor is not required, and are therefore lighter.

These considerations resulted in the following equation:

$$W_b = 9.39 R W_g^{0.178} n^{0.089} + 150 \quad (9)$$

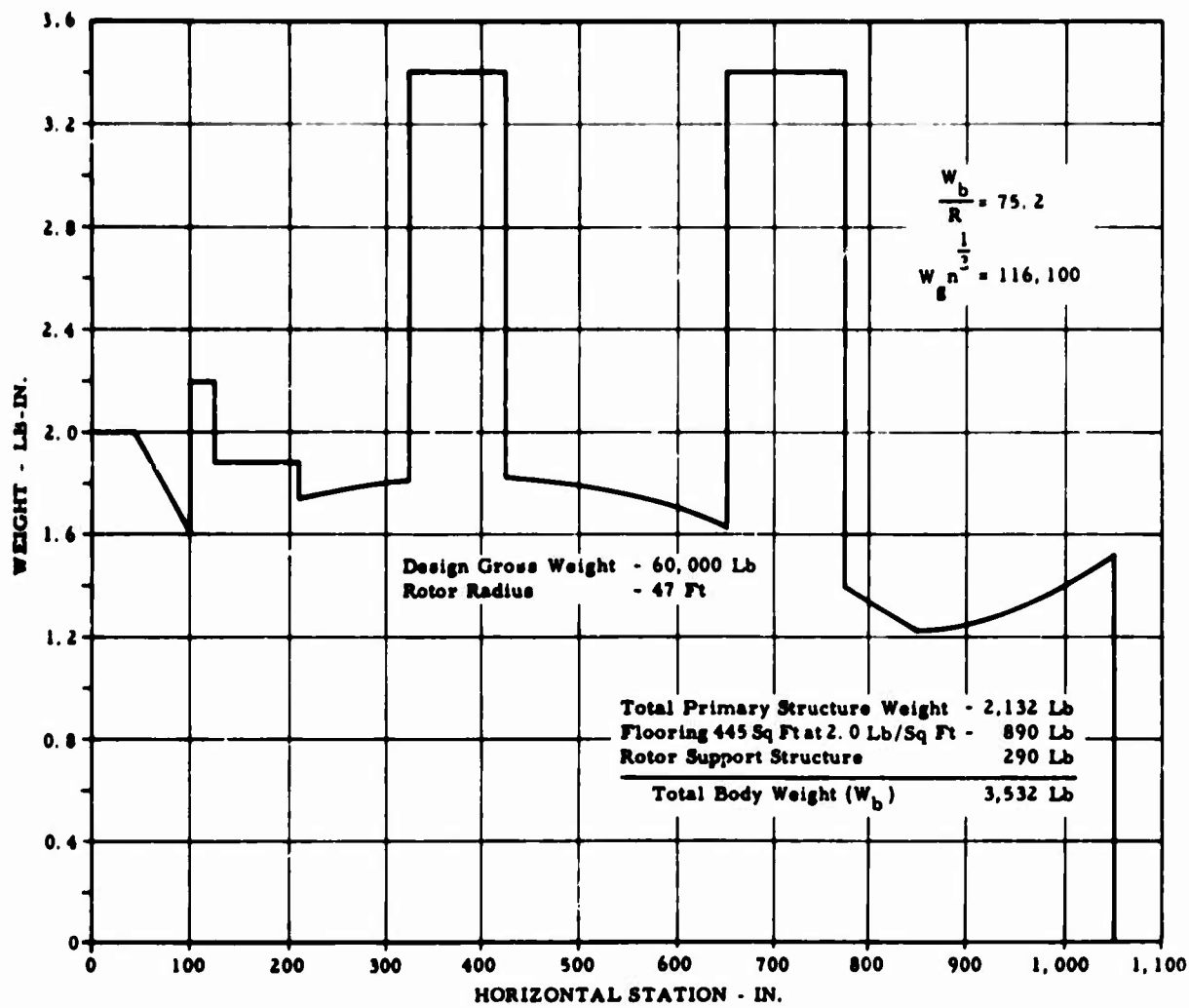


Figure 25. Primary Structure Weight Distribution - Configuration 3.

ALIGHTING GEAR GROUP WEIGHT EQUATIONS

The conventional method of expressing alighting gear weight as a direct function of design gross weight was used in this report. Figure 26 establishes the validity of the fixed landing gear equations based on actual data, which are as follows:

$$\text{Fixed long gear for configurations 1 and 4} \quad W_{lg} = 0.046 W_g \quad (10)$$

$$\text{Fixed short gear for configurations 2 and 3} \quad W_{lg} = 0.035 W_g \quad (11)$$

The retractable landing gear equations assume a retraction system weight penalty of $0.010 W_g$ and $0.013 W_g$ for the short and long gears, respectively. The larger weight penalty for the long gear is based on the increased complexity of the retracting mechanism.

FLIGHT CONTROLS EQUATION

The flight controls equation includes all cockpit controls, rotating and nonrotating rotor controls, and tail rotor and surface controls.

The equation used in the parametric sizing program reflects the preliminary weight estimates of the flight controls system, based on a 60,000-pound-gross-weight vehicle with a rotor radius of 47 feet. The equation assumes a direct relationship with gross weight and was based on design data available at the time that the computer program was being prepared. Since that time, these data have been reviewed, with some weight adjustments being made.

Summarized in the tabulation below is a comparison of this data as well as actual weights on the XV-9A helicopter.

	XV-9A Actual Weight (lb)	Parametric Study Controls Weight (lb)	Preliminary Design Controls Weight (lb)
Cockpit controls	29	30	30
Intermediate linkages and controls - rotor and tail	92	160	160
Hydraulic cylinders and mounts	89	190	340
Rotor head controls	584	620	807
Swashplate assembly	104	492	679
Links, bellcranks, and supports	480	128	128
Total flight controls	794	1,000	1,337

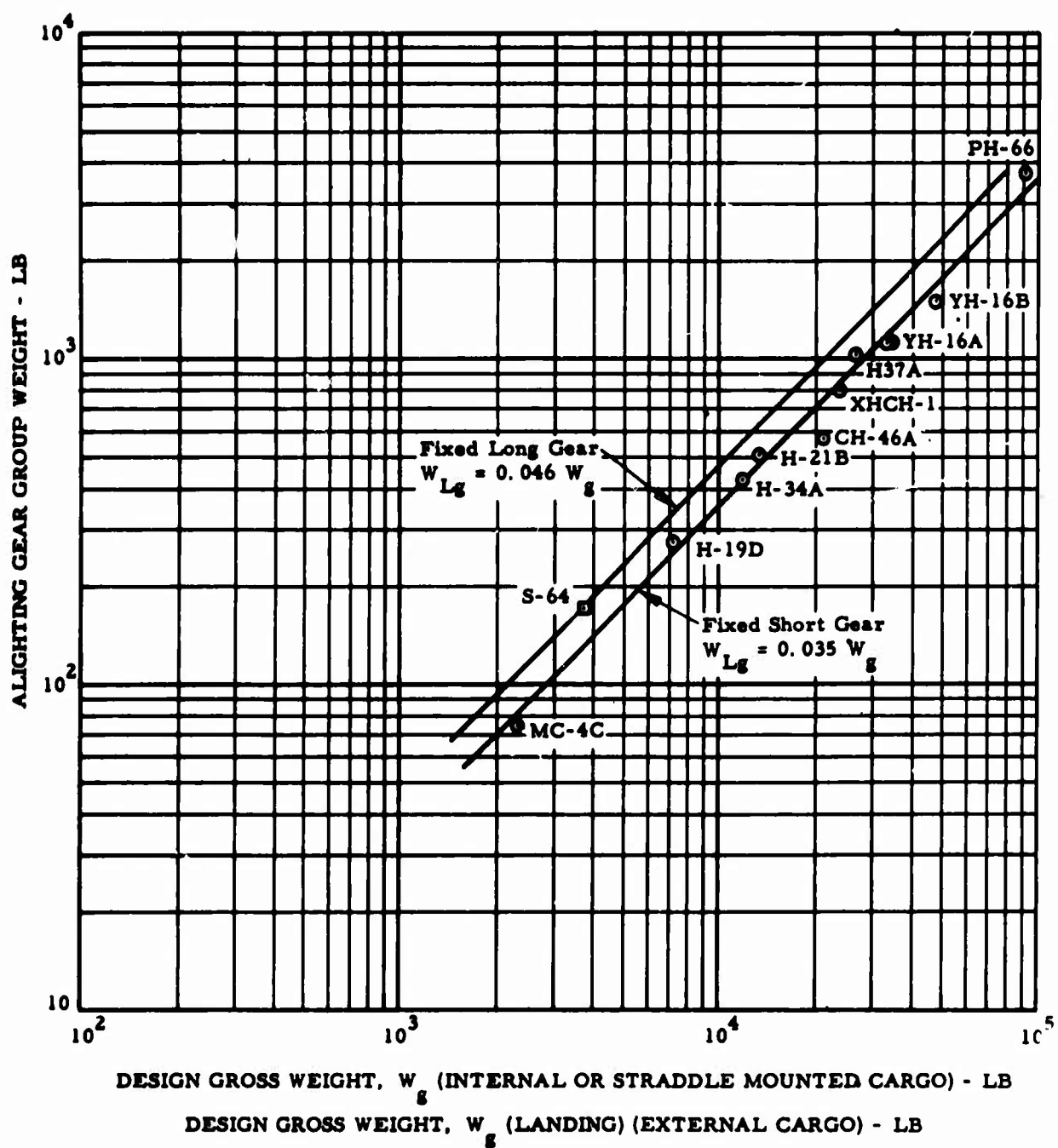


Figure 26. Fixed Alighting Gear Group Versus Design Gross Weight.

The parametric study flight control weight equation based on preliminary weight estimates was derived as follows:

$$W_{fc} = 1,000 \left(\frac{W_g}{60,000} \right) = 0.0167 W_g \quad (12)$$

As a result of later weight data, the equation has been revised as follows for the preliminary design effort:

$$W_{fc} = 1,337 \left(\frac{W_g}{60,000} \right) = 0.022 W_g \quad (13)$$

Figure 27 shows a plot of this equation as well as flight controls weights of articulated single-rotor shaft-driven helicopters.

HYDRAULICS AND PNEUMATICS GROUP EQUATION

The hydraulics and pneumatics group weight equation was derived from weight data plotted versus design gross weight and shown on Figure 28. The equation of the best fit curve is:

$$W_h = 3.45 \left(\frac{W_g}{1,000} \right)^{1.28} \quad (14)$$

Examination of plotted data indicates that this equation adequately represents the weight trend of hydraulic systems with gross weight.

ELECTRICAL GROUP WEIGHT EQUATION

As in the previous equation, the electrical group weights of numerous helicopters were plotted versus gross weight, as shown in Figure 29. The equation of the curve is expressed as follows:

$$W_{el} = 75 \left(\frac{W_g}{1,000} \right)^{0.55} \quad (15)$$

FIXED-WEIGHT COMPONENTS

The following weights, common to all configurations, have been established from preliminary weight estimates and from comparisons with helicopters performing similar missions. These components are assumed to be of constant value for the range of gross weights under consideration.

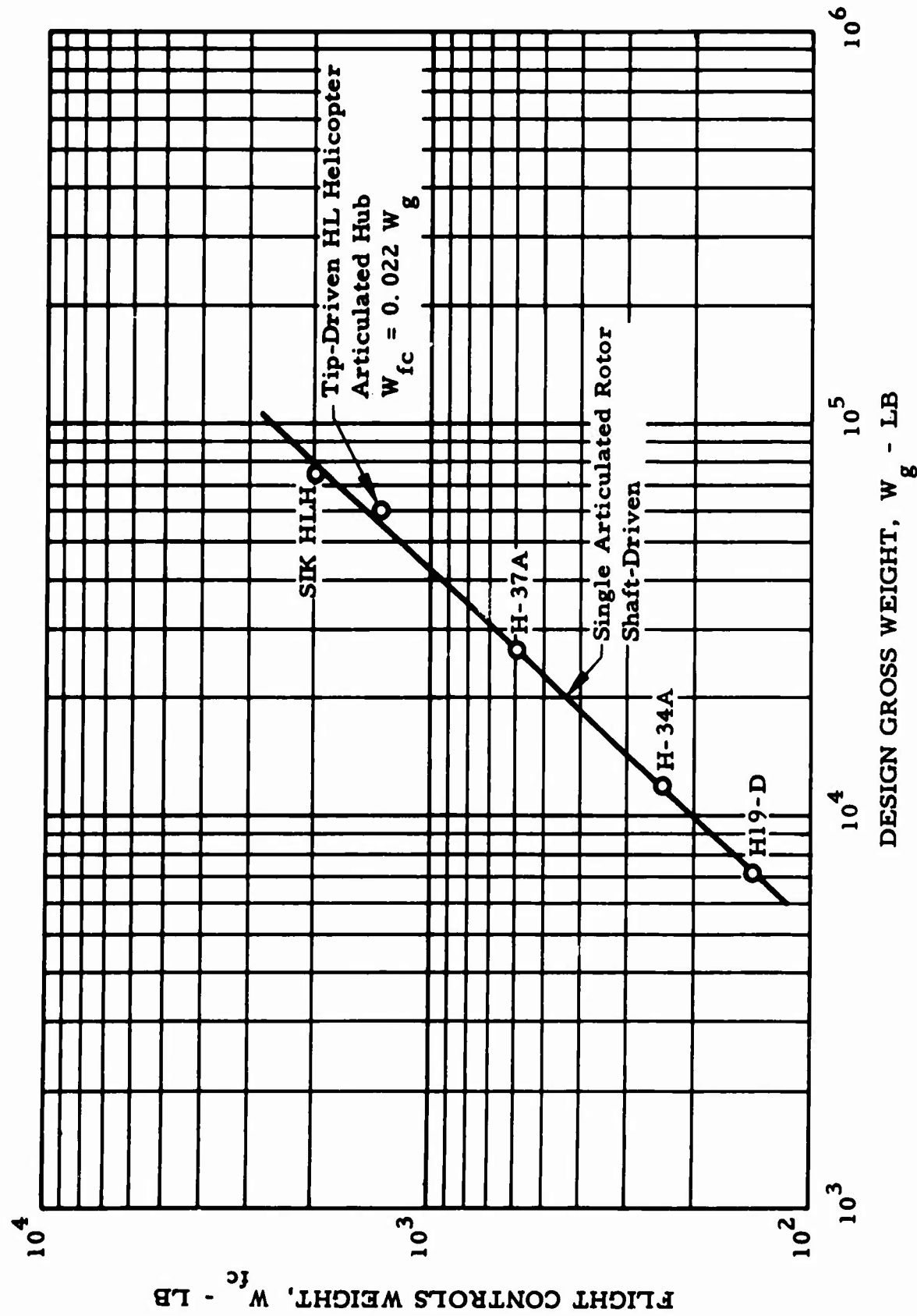


Figure 27. Flight Controls Versus Design Gross Weight.

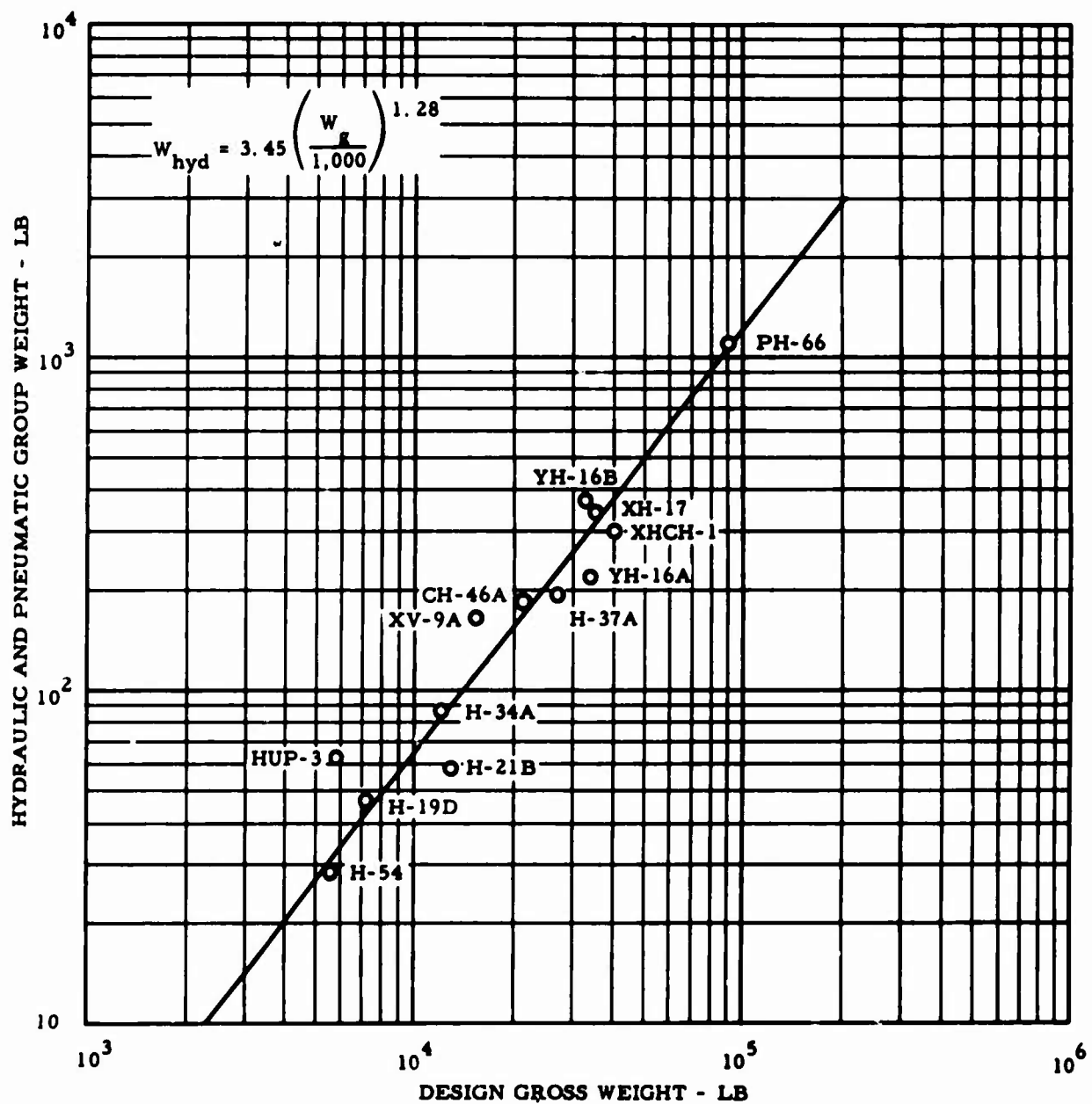


Figure 28. Hydraulic and Pneumatic Group Weight Versus Design Gross Weight.

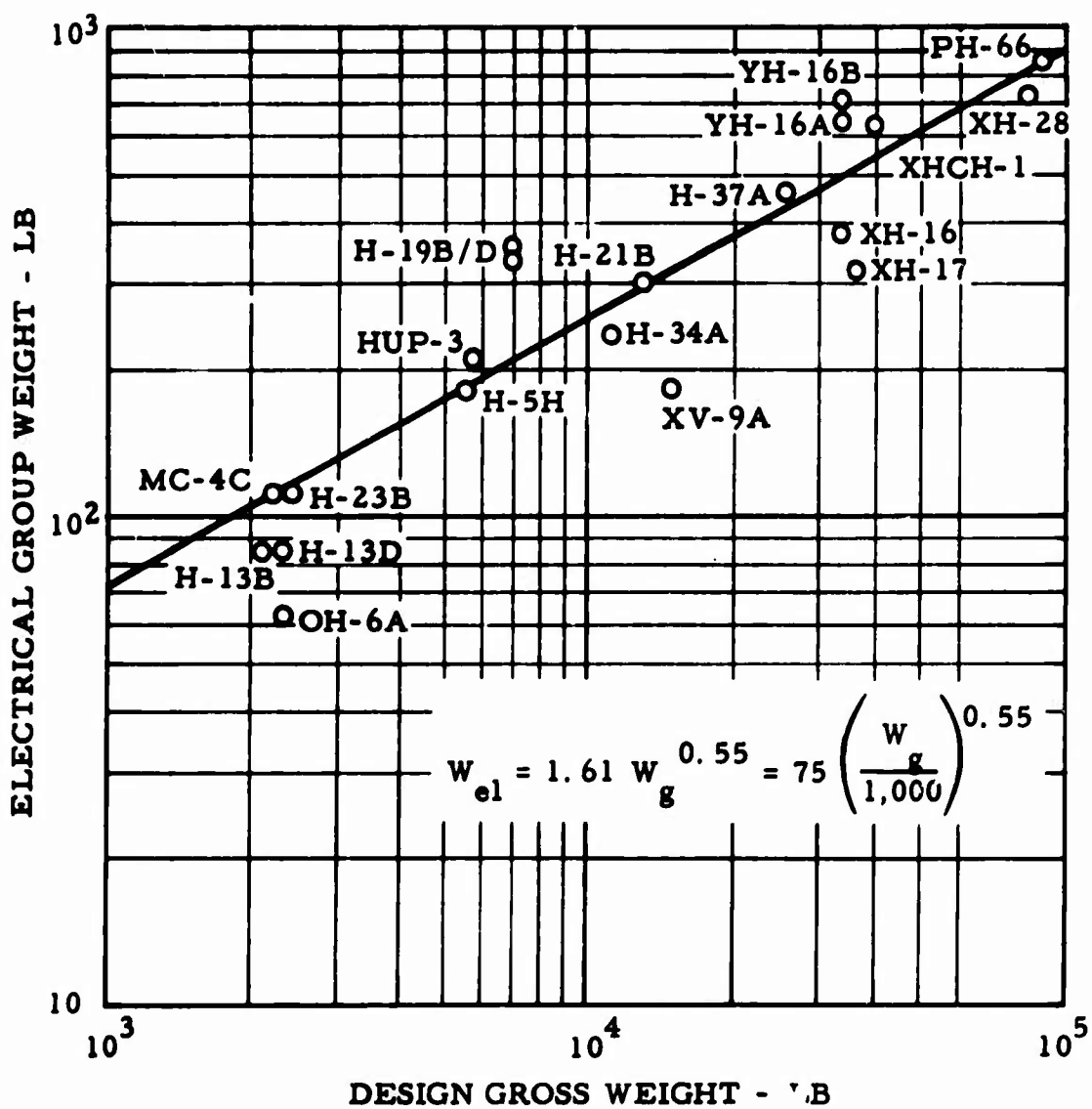


Figure 29. Electrical Group Weight Versus Gross Weight.

PROPULSION GROUP WEIGHT

The propulsion group weight was established from preliminary weight estimates based on design layouts and from sizing of similar components used on the XV-9A helicopter. The weight estimates comprising the group weight of 3,466 pounds used in the parametric study have been revised for the preliminary design to reflect more current information.

A breakdown and comparison of these weights are given below. Included also are actual weights of the XV-9A propulsion group.

	Actual XV-9A Weight (lb)	Parametric Study Weight (lb)	Preliminary Design Weight (lb)
Engine installation (includes engines, induction, exhaust, and fuel systems)	1,537	1,627*	1,627*
Accessory gearbox	74	50	50
Lubrication system	64	64	64
Starting system	10	70	70
Engine controls	83	60	60
Rotor drive system (includes diverter valves, ducting to rotor, joints, seals, and supports)	420	825	480
Engine section nacelles and supports	683	610	460
APU installation		160	160
Total propulsion group	2,865	3,466	2,971

Detailed calculations of the heavy-lift helicopter rotor drive system weights noted in the tabulation above are included in Appendix I.

A review of the propulsion group system using four T64/S4B engines has resulted in a weight change from 4,720 to 4,585 pounds.

INSTRUMENTS AND NAVIGATIONAL EQUIPMENT

$$W_i = 180 \text{ pounds} \quad (16)$$

*Includes weight of GE1/J1 engines.

ELECTRONICS GROUP

$$W_{en} = 150 \text{ pounds} \quad (17)$$

FURNISHINGS AND EQUIPMENT GROUP

$$W_{fe} = 300 \text{ pounds} \quad (18)$$

AIR CONDITIONING AND ANTI-ICING

$$W_{ac} = 100 \text{ pounds} \quad (19)$$

CARGO-HANDLING EQUIPMENT

1 each 25-ton-capacity winch

$$W_c = 1,400 \text{ pounds} \quad (20)$$

Alternate: 4 each 6-ton-capacity winch

$$W_c = 1,700 \text{ pounds} \quad (21)$$

The above weights were based on a manufacturer's proposal for a 20-ton winch.

HELICOPTER EMPTY WEIGHT (W_e)

The empty weight, as defined in this study, is equal to the sum of the following groups:

Main rotor group	W_r
Tail group	W_{tg}
Hover-yaw controls	W_{hy}
Fuselage group	W_b
Alighting gear group	W_{lg}
Flight controls group	W_{fc}
Hydraulics and pneumatics group	W_h
Electrical group	W_{el}

Propulsion group	W_{pp}
Instruments and navigation equipment	W_i
Electronics group	W_{en}
Furnishings and equipment	W_{fe}
Air-conditioning and anti-icing	W_{ac}
Cargo-handling equipment	W_c

USEFUL LOAD ITEMS

This group, as defined in this study, includes the following items.

Crew (3-man)	600 lb
Crew kits	50 lb
Oil	30 lb
Unusable fuel	100 lb
Payload	As determined
Fuel	As required by study
External cargo pod (used on configuration 1, 12-ton maximum gross payload)	4,300 lb
External fuel pod (optional for configurations 1 and 4; 50,000-lb capacity)	2,500 lb
Internal fuel tank cells (optional for configurations 2 and 3; 50,000-lb capacity)	2,500 lb

GROSS WEIGHT (W_g)

The gross weight of the mission being considered is equal to the empty weight (W_e) plus the applicable useful load items.

WEIGHT EQUATIONS - COMPOUND HELICOPTER

The consideration of compound helicopter operation requires modification of some group weight constants and equations and the addition of new

expressions reflecting this conversion. The equations listed below are applied as specified for flight configurations with or without wing installed.

FIXED PROVISIONS

The following equations are used for the compound configuration, wing on or wing off:

Tail Group

This equation replaces the pure helicopter equation for the tail group (3).

$$W_{tg} = 0.025 W_g \quad (22)$$

Surface Controls

Includes all controls required to operate tail surfaces plus wing surfaces controls inboard of the wing joint.

$$W_{scf} = 0.00833 W_g \quad (23)$$

Cruise Fan Duct System

$$W_{cff} = 230 \text{ lb} \quad (24)$$

Hydraulics and Pneumatics System

This equation replaces the pure helicopter equation for the hydraulic and pneumatic systems (14).

$$W_h = 4.47 \left(\frac{W_g}{1,000} \right)^{1.28} \quad (25)$$

REMOVABLE PROVISIONS

The following equations apply when the wing is installed:

Wing Group

The equation shown is the reduced form of the wing weight equation developed by I. H. Driggs and is obtained by assuming the following constants:

$$\frac{C_t}{C_r} = 0.50$$

$$\frac{t_r}{C_r} = 0.21$$

$$\frac{t_t}{C_t} = 0.12$$

design stress factor, $f = 2.7 \times 10^3 W_g^{0.204}$

$$W_w = 0.43 n b \left(\frac{W_g}{10,000} \right)^{0.796} (4.95 + 0.465 AR) \quad (26)$$

Surface Controls

Includes all wing-mounted controls.

$$W_{scr} = 0.00333 W_g \quad (27)$$

Cruise Fan Installation

Includes wing-mounted cruise fan installation and removable ducting

$$W_{cfr} = 2,419 \text{ lb} \quad (28)$$

WEIGHT SAVING FEATURES OF THE HOT CYCLE ROTOR

The large difference between the weight of a heavy-lift helicopter with a tip-driven rotor and that of a heavy-lift helicopter with a shaft-driven rotor may be justified as follows:

1. Rotor Group
 - a. The shaft-driven helicopter requires a larger rotor to support its higher gross weight, which is some 30 percent higher than the gross weight of any of the Hot Cycle configurations.
 - b. The Hot Cycle utilizes strap retention instead of the heavier, more complex pitch housings and bearings.

- c. The Hot Cycle does not have the high steady and cyclic torque loads to transmit through the rotor hub, since it is tip-driven
- d. The Hot Cycle hub provides direct load paths that permit a simpler, lightweight structure.
- e. Blade structure is optimized from root to tip on the Hot Cycle blade, where spar material is arranged to best satisfy the requirements for blade flight loads and ground flapping.

2. Body Group

- a. The Hot Cycle configurations are smaller, with a substantially lower gross weight.
- b. The Hot Cycle fuselages (configurations 2 and 3) are a more efficient structural shape.
- c. The shaft-driven helicopter fuselage must support large gearboxes and associated high torque loads.

3. Landing Gear

- a. The shaft-driven helicopter requires a heavier gear because of its higher gross weight.
- b. The Hot Cycle landing gears are shorter because of the smaller fuselage and lower center of gravity.

4. Flight Controls

- a. The Hot Cycle rotors are smaller, so the lower control loads result in a lighter system.

5. Propulsion Group

- a. The very large and heavy transmission system for the shaft-driven helicopter is not required on the Hot Cycle configurations.
- b. No main rotor shafting is required on the Hot Cycle helicopters -- only the lightweight shafting for the small yaw fan.

STRUCTURES

GENERAL PHILOSOPHY AND DESIGN OBJECTIVES

A discussion of the structural philosophy, features, materials, and design criteria is given in the following paragraphs. Design loads and the detail stress analysis may be found in Appendix II.

The general philosophy used in the design of the heavy-lift helicopter structure is the same as the philosophy used for the OH-6A, TH-55, Models 269 and 300, and the XV-9A Hot Cycle research aircraft. This design philosophy emphasizes simplicity, light weight consistent with desired strength and safety, fail-safe design, long service life, low maintenance, and conservative exploitation of the latest state of the art in materials, processes, and fabrication techniques.

PRINCIPAL STRUCTURAL FEATURES

The following list summarizes the significant structural features of the Hot Cycle heavy-lift rotor:

1. Reliability gains and weight savings over shaft drives with their multiple dynamic elements -- due to the Hot Cycle ducted propulsion system; yaw fan required for maneuver only, since there is no main rotor drive shaft and resulting torque.
2. Fail-safe design features for improved level of safety.
3. Simplest possible functional and structural configuration with a minimum of discontinuities; direct load paths are provided.
4. Minimum structural weight consistent with safety and strength requirements and a conservative application of advanced design.
5. Isolation of hot and cold components.
6. Long service life -- all ducting designed to 0.2 percent creep deformation for 3,600-hour life.
7. No dynamic elements used in the rotor power transmission system; jet aircraft reliability of hot components.

MATERIALS AND ALLOWABLE STRESSES

Materials chosen for the Hot Cycle rotor are fully proven materials with the highest strength-weight ratio for the temperature environment and the static and fatigue loadings to be encountered in this aircraft. Experience gained on the XV-9A has been used in the selection of the following materials.

ALUMINUM ALLOY

Aluminum alloy has been selected as the material for the blade trailing edge fairings and all structural parts that are subject to less than a 200°F temperature environment. It will be used in any structure that is designed primarily by buckling stability, since in this application it is relatively lighter than steel or titanium. In all statically loaded and fatigue loaded structures in which the load is primarily tension, 2024 alloy is used rather than 7075 alloy, which not only has a higher static strength but also has a higher notch sensitivity. Adhesive bonding is used extensively in preference to rivet or bolt attachments to provide excellent fatigue life.

STEEL

Carpenter 455 maraging stainless steel has been selected for the rotor blade spar material and for structural parts in a moderately elevated temperature environment requiring maximum static and fatigue strength properties. For fatigue applications, this steel is considered to be one of the best all-around materials tested to date, showing exceptionally consistent fatigue properties in both longitudinal and transverse grain direction for both smooth specimens and those with holes, and for sheet and bar.

This stainless maraging steel has good resistance to oxidation and pitting. It is highly resistant to stress corrosion cracking at high stress levels, being superior to the semiaustenitic precipitation hardened stainless steels.

The coefficient of linear expansion of Carpenter 455 is slightly higher than that of titanium alloys; therefore, it can be used in combination with titanium at moderately elevated temperatures without developing detrimental thermal stresses.

TITANIUM ALLOY

Titanium alloy is used in sandwich construction for the blade skins and also is used for structural parts in slightly elevated temperature

environment for applications that require high static- and fatigue-strength-to-density ratio.

Two titanium alloys are under consideration: Ti-6Al-6V-2Sn and B-120-VAC. Final selection awaits results of tests currently under way. Ti-6Al-6V-2Sn is similar in many respects to Ti-6Al-4V but has higher strength and greater depth hardenability. Considerably higher toughness with some sacrifice in static strength is attained by reducing the oxygen content. B-120 titanium is an all Beta alloy. It is supplied in the solution-treated condition. A desirable feature of this alloy is that after machining only aging is required to obtain the desired strength level. This alloy is superior to other titanium alloys in bending and cold-forming operations.

The problem of stress corrosion in titanium has also been considered, and it appears that there should be no problem in this application. Stress corrosion has been only a potential problem at temperatures of more than 450°F and a steady stress level of more than 45,000 psi. In the Hot Cycle heavy-lift helicopter application, the temperatures and stress levels are predicted to be well below these limits.

RENÉ 41

René 41 is proposed as the material for the hot gas ducts. It has a superior strength-to-weight ratio for static strength as well as for 0.2-percent creep and rupture properties in the 1,400°F temperature environment. This material performed well as used for blade ducting on the XV-9A.

INCONEL 718

Inconel 718 is proposed for fabrication of parts subjected to temperatures up to 1,200°F, which is higher than can be tolerated by titanium. It has superior static strength properties and elongation values up to 1,200°F. Long-time rupture and creep properties are also superior to those of René 41 up to 1,150°F. This material has good forming qualities with slow response to age hardening, which allows it to be welded in the annealed or aged condition without spontaneous hardening during heating and cooling. It has good corrosion resistance in a wide variety of environments. Inconel 718 proved to be an excellent material as used on the XV-9A for the large duct assemblies in the hub area.

AM355

AM355 is a precipitation hardening stainless steel. This material has been selected for the flapping and lead-lag retention strap packs because of its high static strength, good elongation properties, and excellent fatigue strength. This material is very satisfactorily used for the same applications on the OH-6A and XV-9A.

THERMAL STRESS

The aircraft employs hot gas jets at the rotor blade tips to provide the rotor driving torque. The typical cross section of the blade ducts is formed from the intersection of two circles forming a figure-8. This results in a lightweight system, as all the gas pressure loads are carried by hoop tension. Any additional weight that results from local stiffening is held to a minimum and occurs only in the transition areas where there is a departure from a circular cross section. Thermal considerations are solved in a straightforward, simple manner and do not require complicated or sophisticated systems.

The hot gas system is isolated from the aircraft structure to allow it to grow with temperature without loading the cold structure. The longitudinal elongation due to temperature is taken up by bellows that divide the ducting into appropriate lengths.

These bellows allow the ducting to expand with temperature without introducing high restraining forces in the ducting system. A system of links that fully support each length of duct allows unrestrained growth due to temperature both longitudinally and diametrically. A single thickness of metal forms the duct wall. This eliminates thermal gradients that would exist in a built-up wall having a hot inner wall and a cold outer wall.

The ducts are insulated, thereby reducing the thermal gradients in the primary structure. Isolation of the hot duct from the structure aids in lowering the temperature differential within the cold structure, since less heat is transferred by conduction. The cooling air flowing through the hub and into the blade alleviates the buildup of heat in these structures. The highest structural temperature gradient in the blade is estimated as 260°F, based on XV-9A experience.

STRUCTURAL DESIGN CRITERIA

All limit loads derived from the following criteria shall be multiplied by 1.5 to obtain ultimate loads. The requirements of MIL-S-8698 (ASG) have been used as a guide.

LIMIT LOAD FACTORS

<u>Mission</u>	<u>Load Factor</u>
Design gross weight	+2.5, -0.5
Ferry	+2.00

COMPONENT DESIGN CRITERIA

All components shall be designed for at least 1,200 hours between major overhauls and 3,600-hour service life.

LIMIT DIVING SPEED

$$1.11 V_{ne} = 1.11 \times 135 \text{ kn} = 150 \text{ kn}$$

MAIN ROTOR

The basic rotor data used in the structural design criteria have been previously shown in Table VIII of the Rotor System section of this report.

ROTOR TIP SPEED, DESIGN OPERATIONAL, POWER-ON OR POWER-OFF

The design operational rotor speed shall be consistent with a tip speed of 750 ft/sec in hover and 675 ft/sec in cruise.

ROTOR TIP SPEED, MAXIMUM POWER-ON (RED LINE)

750 ft/sec

ROTOR TIP SPEED, MINIMUM POWER-OFF (RED LINE)

590 ft/sec

ROTOR TIP SPEED, DESIGN MINIMUM POWER-OFF

560 ft/sec

ROTOR TIP SPEED, MAXIMUM POWER-OFF (RED LINE)

750 ft/sec

ROTOR TIP SPEED, LIMIT, POWER-OFF OR POWER-ON (1 g)

786 ft/sec

BLADE DESIGN REQUIREMENTS

Ground flapping - 2.5 g

Ground wind - 40 kn at $C_L = 1.0$

Infinite life at weighted fatigue condition (1.2 x loads in maximum cruise level flight)

HUB DESIGN REQUIREMENTS

Weighted fatigue flapping - $\pm 5^\circ$

Weighted fatigue lead-lag - $\pm 1.25^\circ$

Maximum lead-lag - $\pm 3^\circ$

Weighted fatigue feathering - $\pm 12^\circ$

Maximum flapping - $+25^\circ, -6^\circ$

GAS TEMPERATURE CONSIDERATIONS

Duct wall and skin temperatures with and without insulation are to be based on the following tabulation:

	<u>Basic Structure No Insulation</u>	<u>Basic Structure 1/8-in. Refrasil Insulation</u>
Heat flux - BTU/hr-sq ft	9,500	3,000
Duct wall temperature	1,310°F	1,390°F
Inner skin and inner rib flange temperature	870°F	400°F
Outer skin temperature	225°F	140°F

(Reference - gas temperature = 1,425°F, ambient temperature = 70°F)

GAS TEMPERATURE SPECTRUM

<u>Power Setting</u>	<u>Temperature (deg F)</u>	<u>Pressure (psig)</u>	<u>Remarks</u>
Emergency	1,443	39.6	10 seconds 12 times
Takeoff	1,395	37.9	5 minutes
Military	1,300	33.8	30 minutes
Maximum continuous power	1,225	30.34	

LIMIT STRUCTURAL DESIGN

Maximum temperature
 (occurs at Mach 0.2 SL 103°F) 1,494°F (emergency)
1,415°F (takeoff)

Pressure at maximum temperature
 (Mach 0.2 SL 103°F) 37.7 psig (emergency)
36.3 psig (takeoff)

For 3,600 hours operational use 2 minutes at 1,494°F
20 hours at 1,415°F
40 hours at 1,395°F
100 hours at 1,300°F

See Figure 30 for remainder of spectrum.

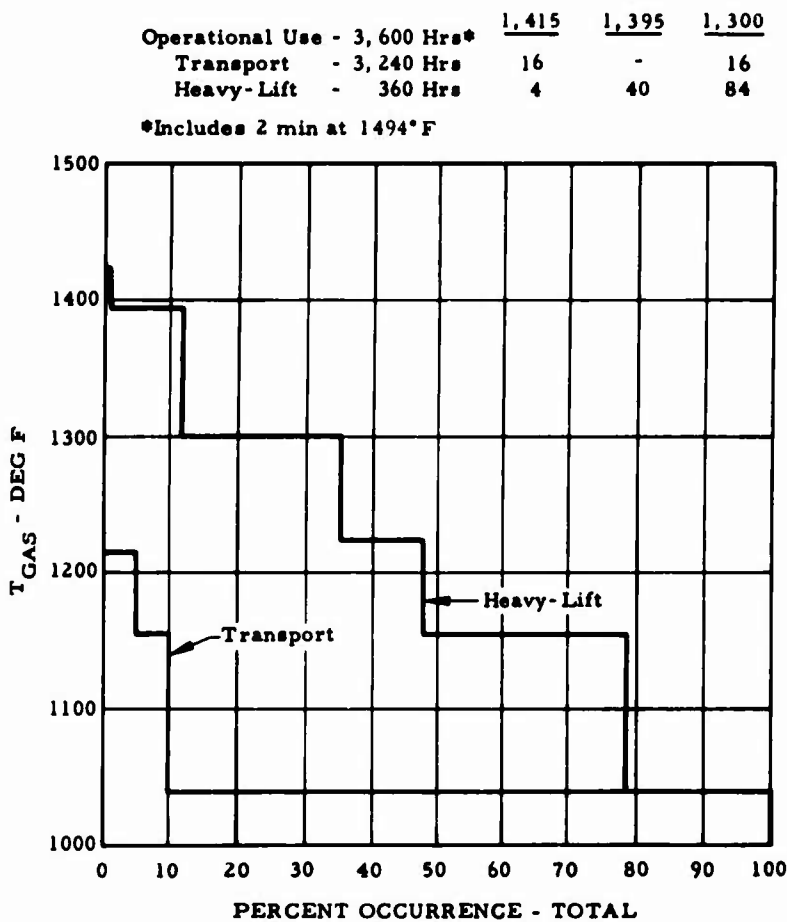


Figure 30. Time-Temperature Spectrum - GE1 Engine - Heavy-Lift Helicopter.

PARAMETRIC STUDY

The parametric study was completed, summarized, and submitted in Reference 2. The following data and discussion of the parametric study are largely direct quotations of the material from that report. The areas covering the compound helicopter and fuel utilization have been revised to reflect the results of additional investigations.

The objective of the parametric and configuration study was to determine the optimum Hot Cycle rotor system for a 12- to 20-ton-payload heavy-lift helicopter, and to investigate, on a limited basis, the features required to increase its cruise speed by a substantial amount. The study indicates that a vehicle with a rotor as small as 80 feet in diameter and with an empty weight of approximately 18,000 pounds will exceed all mission requirements of range and payload by 20 to 30 percent, even though a larger-diameter rotor has been selected as optimum for other considerations.

Five aircraft configurations have been considered in the parametric study. Included are four helicopters and one compound helicopter, which has been investigated as a means of substantially increasing cruise speed. To accomplish the study, statistical and analytical data were integrated into a computer program, and the results were then cross-plotted to arrive at the optimum rotor.

The parametric variables used included four hub configurations; variations in number of blades and their thickness, chord, radius, and spar location; three duct configurations; tip speed; and fixed versus retractable landing gear.

The primary powerplant configuration studied consisted of two GE1/J1 engines; however, an alternate configuration using four T-64/S4B engines was also investigated in the parametric study.

PARAMETRIC STUDY CONCLUSIONS

The following conclusions were reached from the results of the parametric study:

1. The optimum rotors for each of the various configurations, based on the results of the parametric study and on practical considerations, and their performances are shown in Table XI.

TABLE XI
SUMMARY - OPTIMUM ROTOR SIZE FOR CONFIGURATIONS
STUDIED AND PERFORMANCE

Parameter	Configuration				
	1	2	3	4	5**
Number of blades	3	3	3	3	3
Blade radius (ft)	45	40	45	45	45
Blade chord (in.)	55	60	60	55	60
Blade thickness (inboard 0.75R) (%c)	18	18	18	18	18
Blade thickness (outboard 0.25R) (%c)	14	14	14	14	14
Blade spar location (x/c)	0.30	0.25	0.25	0.30	0.25
Blade tip speed - hover (fps)	750	750	725	750	725
Blade tip speed - cruise (fps)	675	675	675	675	675
Blade duct configuration	Fig-8	Fig-8	Fig-8	Fig-8	Fig-8
Hub configuration	*	*	*	*	*
Landing gear	Fixed	Fixed	Fixed	Fixed	Retractable
Ferry mission (nmi)	1,816	2,065	2,034	1,816	2,416
Payload (tons)					
Transport mission	12.03	13.98	14.08	13.72	(See Heavy-lift mission
Heavy-lift mission	25.66	25.40	25.55	25.65	Fig 48)
Weight empty (lb)					
Transport mission	25,898	17,832	20,887	21,598	28,011
Heavy-lift mission	21,598	17,832	20,887	21,598	28,011
Gross weight (lb)					
Transport mission	57,939	54,371	56,788	57,939	54,971
Heavy-lift mission	78,428	73,976	77,368	78,428	74,893
Payload/empty weight ratio					
Transport mission	0.9290	1.5680	1.345	1.2708	-
Heavy-lift mission	2.3758	2.8489	2.45	2.3758	-
Disc loading (lb/sq ft)					
12-ton payload	9.10	10.42	8.25	8.58	-
20-ton payload	10.66	12.60	10.39	10.66	-
Computer run number	1-31	2-15	3-12	4-4	-

*Articulated with external shaft.

**Identical with configuration 3, except that it has been converted to a compound by the addition of wings, fans, ducting, and other required revisions.

2. The rotor selected for the preliminary design for disc loading considerations and as most nearly optimum for all configurations has a 45-foot radius, a 60-inch chord, an 18-percent blade thickness from root to 0.75R and 14-percent from 0.75R to tip, an articulated hub, a 750-fps hover tip speed, and a 675-fps cruise tip speed.
3. The results of the fuel consumption study indicate that a substantial improvement in fuel economy can be expected using the Hot Cycle propulsion system. The numbers of ton-miles per pound of fuel show improvements in the order of 150 to 300 percent as compared with present conventional helicopters.
4. Configuration 1 performance would be improved if a pod of smaller cross section were used. The pod cross section on the ship studied was arbitrarily made the same as that of the C-130. By changing the cross section to one more nearly approximating configuration 3, the range and transport payload would be increased.
5. The weight of the pod is not offset by the saving in fuel from the resulting lower drag; therefore, a detrimental effect on the mission performance results, as shown in a comparison of configuration 1, which has a pod, and configuration 4, which is an identical ship carrying all payloads externally (see Table XI).
6. The optimum rotor size of configurations 2 and 3 could be substantially smaller, if either:
 - a. Single-engine failure only was considered in the autorotational requirements, or
 - b. For configuration 2, internal payload was limited to a lower value than the 7 tons assumed for the autorotational capability check.
7. The Hot Cycle heavy-lift rotor is readily adaptable to any configuration found desirable from an operational standpoint and will produce comparable results in performance and light weight.
8. It is concluded that the compound helicopter will provide a substantial increase in cruise speed and ferry range. It is further concluded that the additional complexity of the compound is confined primarily to the wing and ducted thrust-fan installations, and that the required implementation is within the state of the art.

AIRCRAFT CONFIGURATIONS STUDIED

Five aircraft configurations were studied and are described in the following paragraphs. The propulsion for all configurations is provided by two General Electric GE1/J1 gas generators. An alternate installation using four T-64 engines was also considered. Conversion of the basic helicopter propulsion system to the compound helicopter propulsion system has been accomplished by the addition of wings and ducted fans for thrust.

CONFIGURATION 1 (Figure 31)

This is a crane-pod ship. Its overall size is determined primarily by the cargo compartment, which is 10 feet wide, 9 feet high, and 27 feet long, for a total of approximately 2,400 cubic feet. The cargo compartment cross section dimensions were chosen to be the same as those of a C-130 airplane cargo compartment to permit direct reloading between the vehicles. At 10 pounds per cubic foot, this compartment permits a loading of 12 tons and has cargo floor space for four of the standard 88-by-108-inch pallets. For the parametric study, it is assumed that the 12-ton transport mission payload is carried internally and that the 20-ton heavy-lift payload is carried externally. The engines are shoulder-mounted.

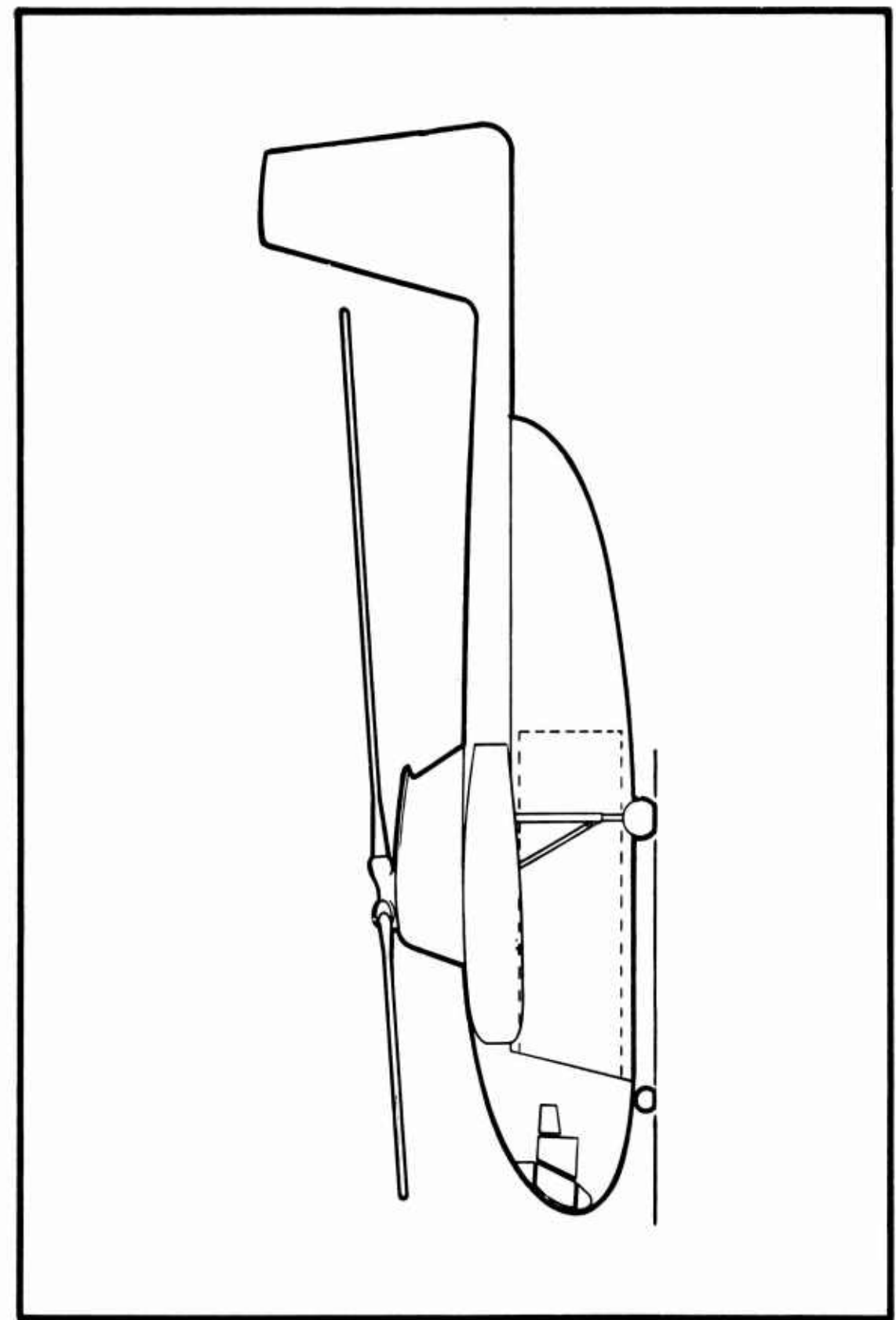
CONFIGURATION 2 (Figure 32)

This aircraft utilizes a streamline body sized to carry the fuel for the ferry mission internally. The cargo compartment is approximately 6-1/2 feet wide (5 feet wide at the floor line), 7 feet high, and 45 feet long. It can carry approximately 7 tons internally at 10 pounds per cubic foot, with a cargo floor area that will accommodate six standard 54-by-88-inch pallets. For the parametric study, it is assumed that both the total transport and heavy-lift payloads are carried externally. The engines on this configuration are top-mounted to minimize frontal area.

CONFIGURATION 3 (Figure 33)

This aircraft utilizes a streamline body sized to permit loading of the transport mission payload of 12 tons (at 10 pounds per cubic foot) internally, with a cargo floor area for six standard 88-by-108-inch pallets. The compartment is approximately 8 feet wide by 7 feet high by 46 feet long. The total heavy-lift mission payload is carried externally. The engines on this configuration are shoulder-mounted to provide for accessibility and for retraction of the landing gear into the nacelle fairing.

Figure 31. Configuration 1 Helicopter.



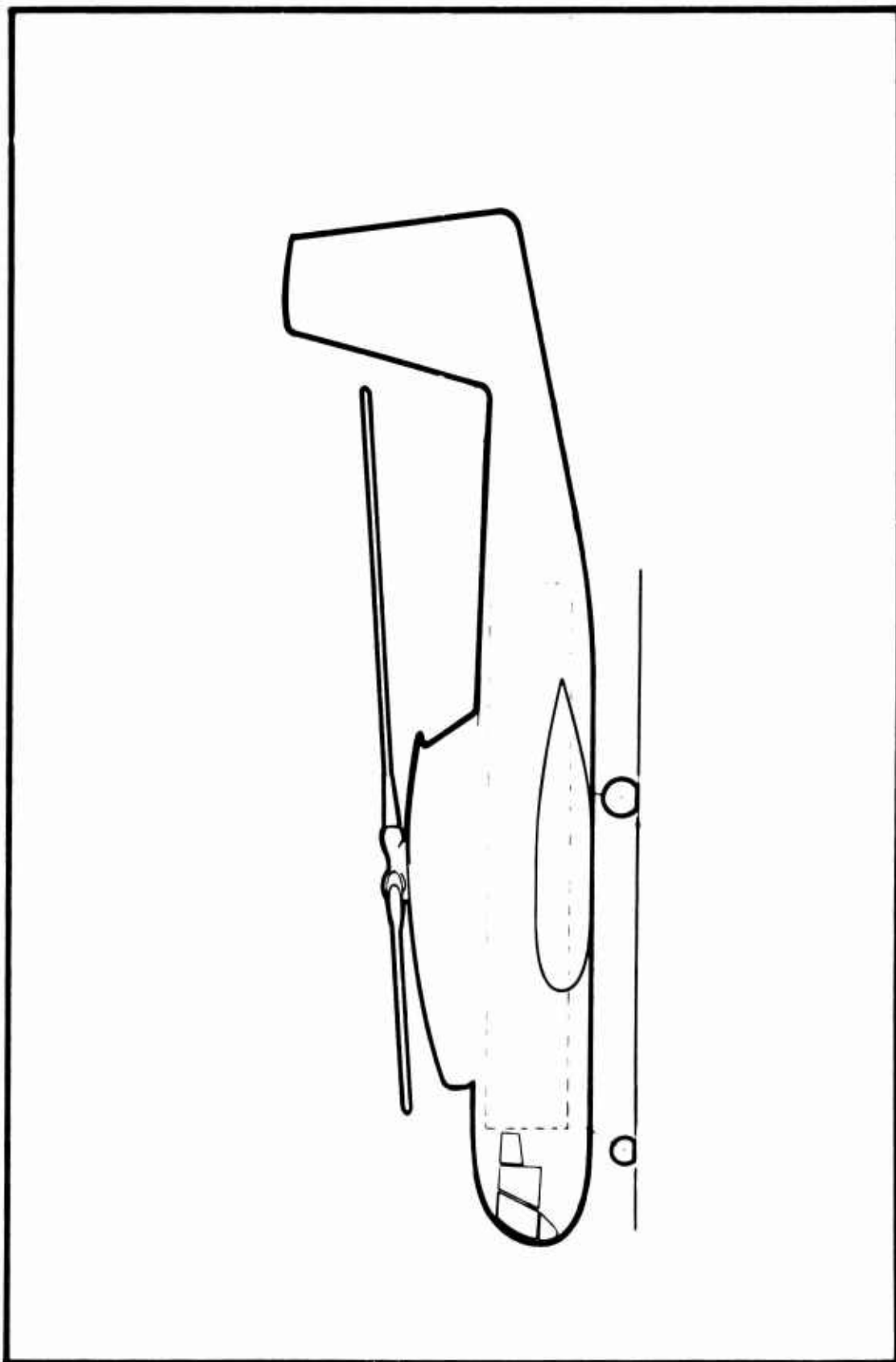
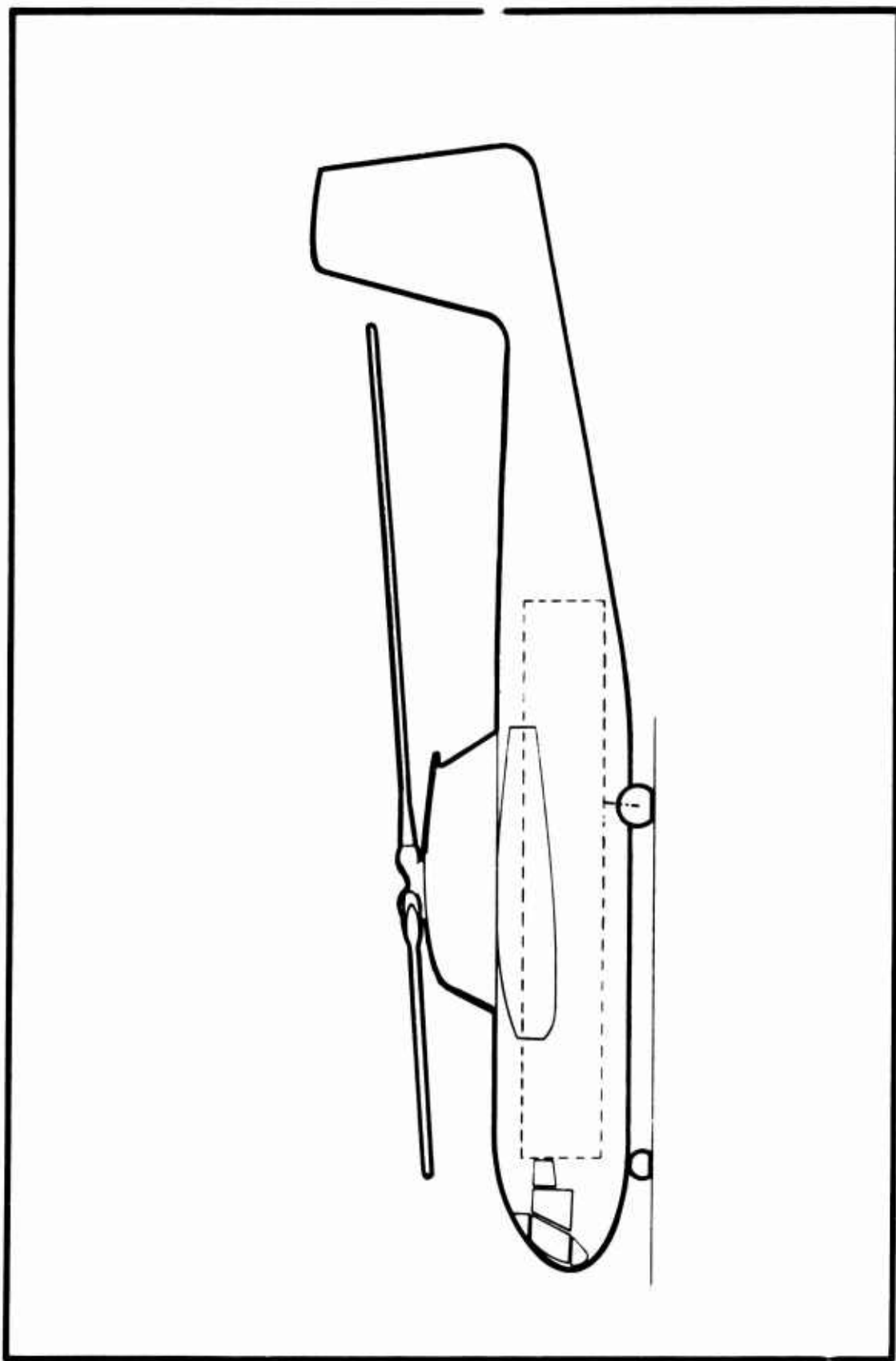


Figure 32. Configuration 2 Helicopter.

Figure 33. Configuration 3 Helicopter.



CONFIGURATION 4 (Figure 34)

This configuration is identical with configuration 1 except that it assumes that both the transport and heavy-lift mission payloads are carried externally (no pod).

CONFIGURATION 5 (Figure 35)

This configuration utilizes the same rotor and fuselage as configuration 3 except that wings and fans have been added for operation as a compound helicopter.

HUB CONFIGURATIONS STUDIED

Four combinations of hub shaft and mast were studied and are described in the following paragraphs. All configurations use blade retention straps to provide flapping and feathering freedom. Weights of these configurations are shown in Table XII.

TILTING HUB WITH INTERNAL CONTROLS (Figure 36)

This configuration, similar to that used on the XV-9A Hot Cycle research aircraft, employs two retention straps per blade, displaced chordwise to provide chordwise rigidity. The retention straps connect the blades to the hub assembly, which in turn is gimbally attached to the rotor shaft. In this hub configuration, the shaft passes through the center of the gas duct, and the flight control push-pull tubes pass from the swashplate, mounted below the hub, up through the center of the shaft to walking beams that transmit the motion to the blade pitch links. Hub restraint for improved controllability is provided in the form of air springs. Because of the necessity of gimbally mounting the tilting hub and the routing of gas ducts between the retention straps, the required hub fairing envelope is larger than that for the articulated hub.

TILTING HUB WITH EXTERNAL CONTROLS (Figure 37)

The tilting hub with external controls is very similar to the tilting hub with internal controls except that the rotor controls, shaft and mast are installed outside the ducts. The swashplate is guided on the outside of the shaft. A heavy "spider" structure is necessary to transmit rotor loads from the gimbal to the external shaft, which results in a heavier hub with a slightly smaller fairing envelope than that of the tilting hub with internal shaft.

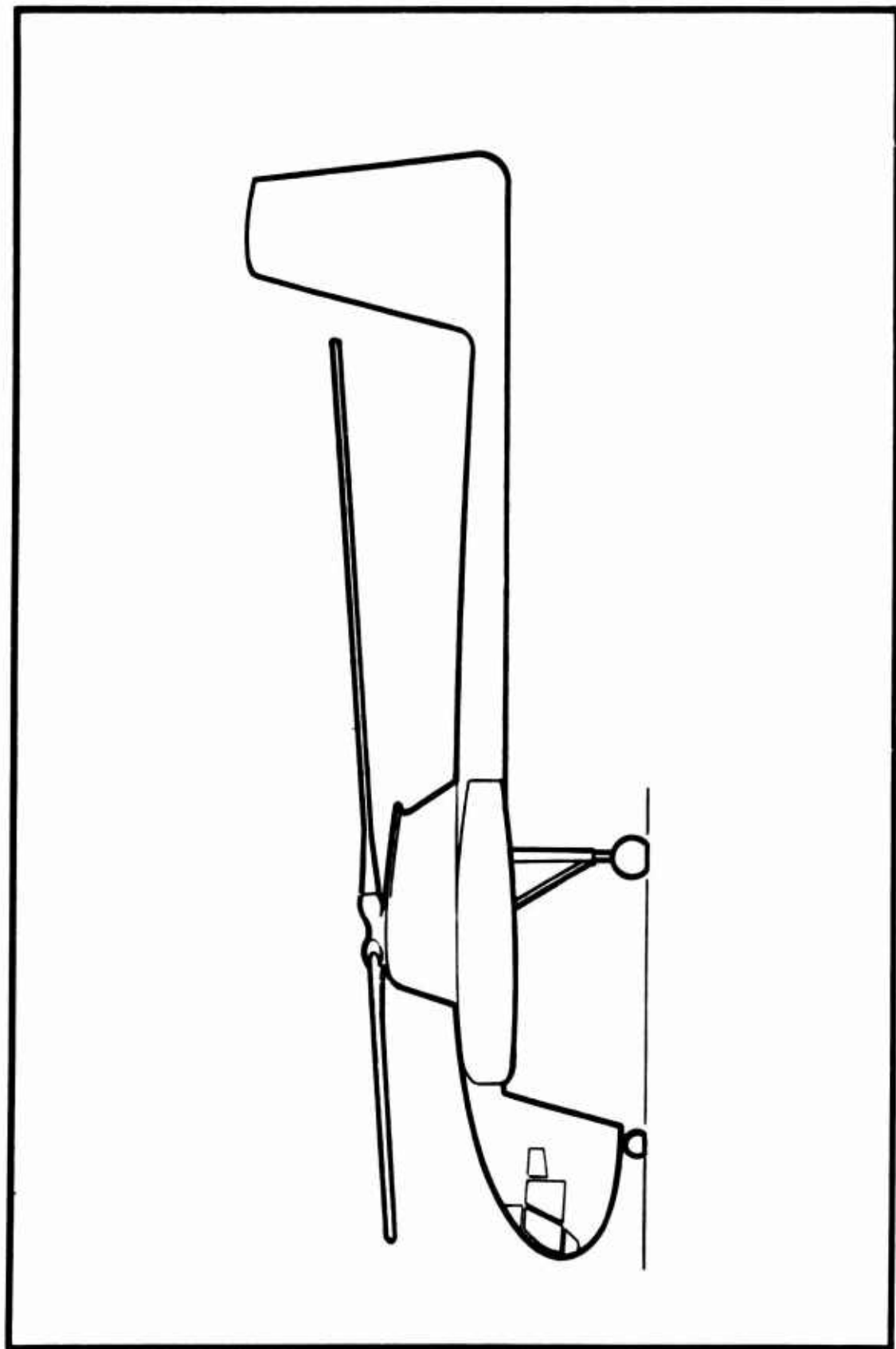


Figure 34. Configuration 4 Helicopter.

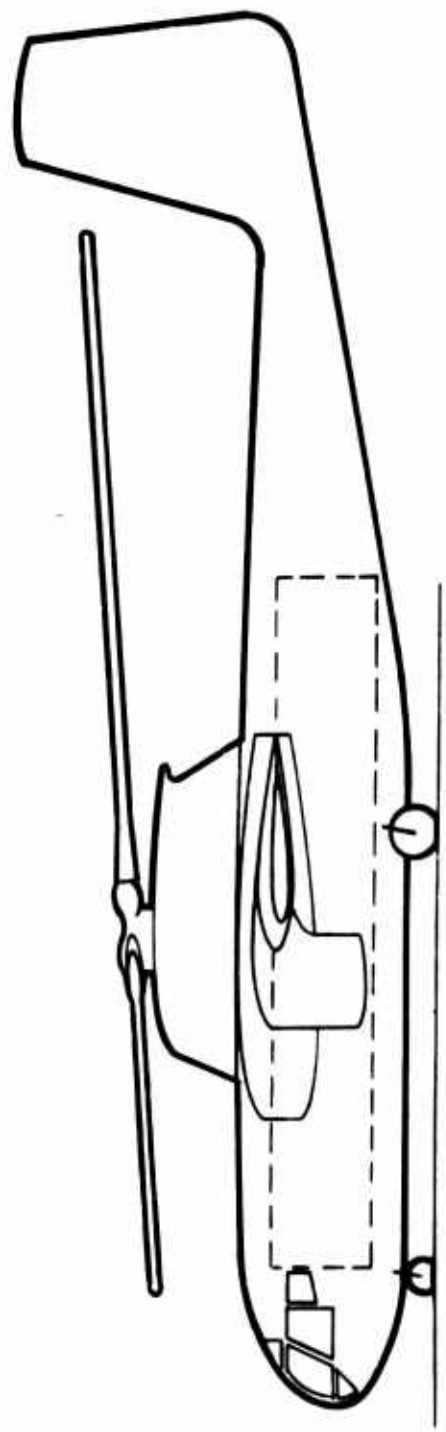


Figure 35. Configuration 5 Compound Helicopter.

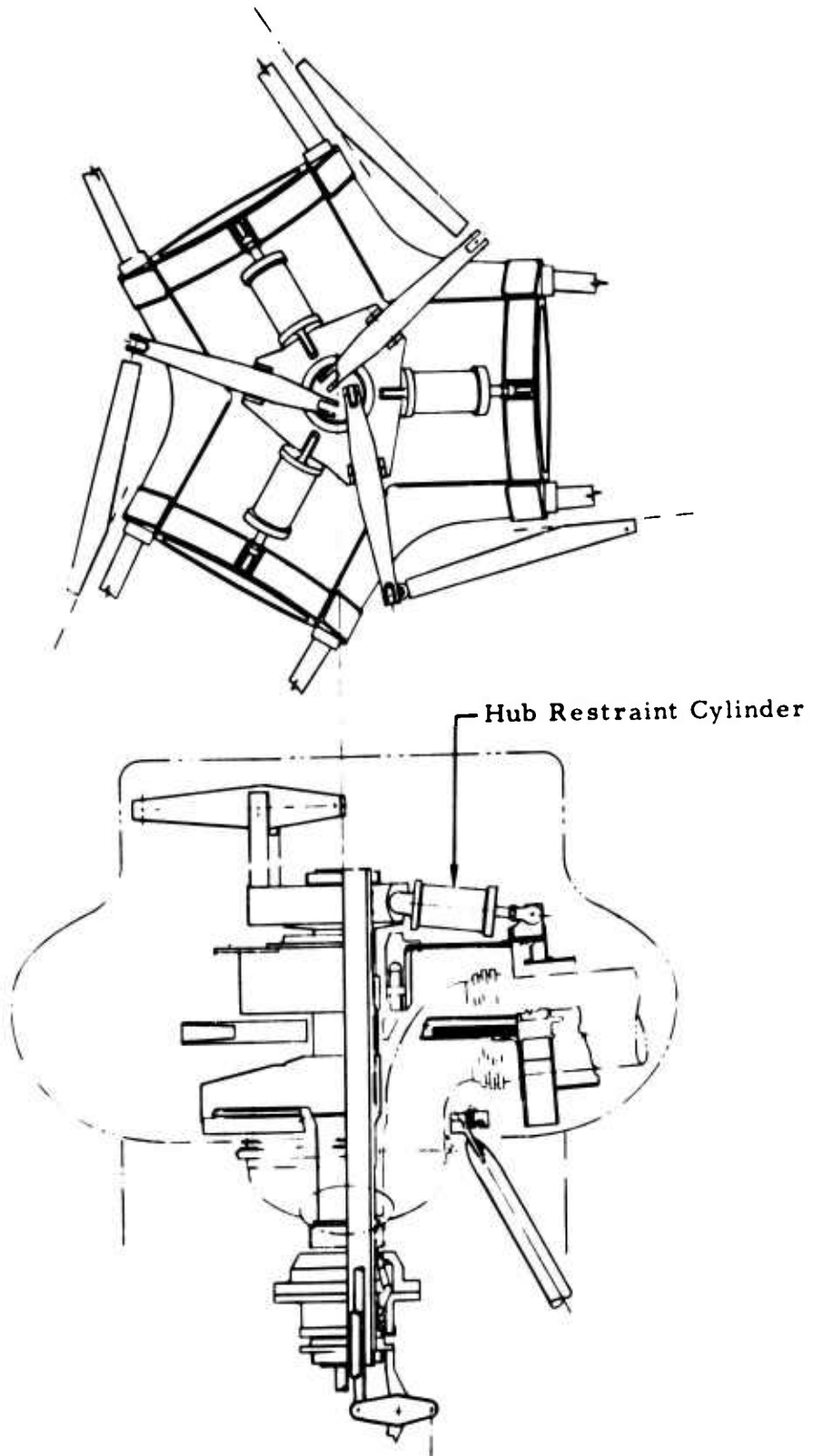


Figure 36. Tilting Hub With Internal Controls.

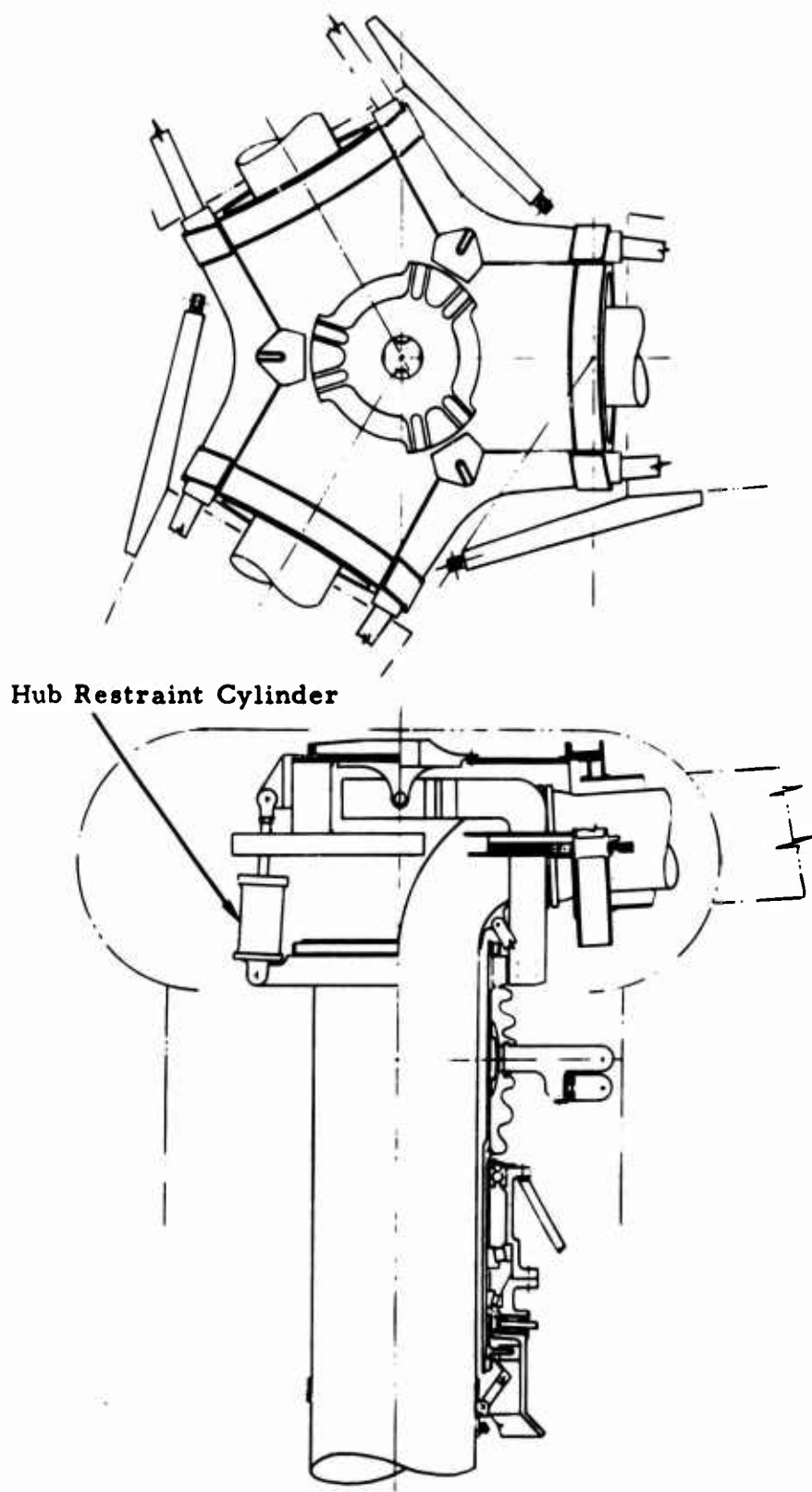


Figure 37. Tilting Hub With External Controls.

TABLE XII
WEIGHT OF VARIOUS HUB CONFIGURATIONS

	Tilting Hub		Articulated Hub	
	Internal Controls	External Controls	External Controls	Internal Controls
	XV-9A*	395-0930**	395-0931**	395-0932**
HUB ASSEMBLY				
Structure	502	1,296	1,296	308
Gimbal	125	436	1,042	-
Bearings, housings, and supports	148	361	1,044	630
Hardware	10	-	-	-
Hub restraint	-	89	122	-
Total	(785)	(2,182)	(3,504)	(938)
MAST ASSEMBLY				
Mast	82	400	460	280
Spoke	33	183	-	-
Spacers and retainers	35	181	234	230
Total	(150)	(764)	(694)	(510)
FAIRINGS				
Hub fairing	8	45	40	30
Total	(8)	(45)	(40)	(30)
TOTAL COMPONENT WEIGHT				
(Excluding blades retention, etc)	964	3,016	4,263	1,503
				1,664

*Based on actual weights of XV-9A components.

**All weights were estimated from drawings 395-0930 through 395-0933; weights were then used as input to the computer program (47-ft rotor radius).

ARTICULATED HUB WITH INTERNAL CONTROLS (Figure 38)

This hub configuration also uses retention straps, as previously noted; however, on the articulated hubs the straps converge as they travel outboard to the lead-lag hinge point, resulting in lower control loads. To permit this convergence, the gas ducts are routed outside the blade retention straps. Flight control push-pull tubes pass from the swashplate, mounted below the hub, up through the center of the shaft to the walking beams that transmit the motion to the pitch arms. Since load paths are

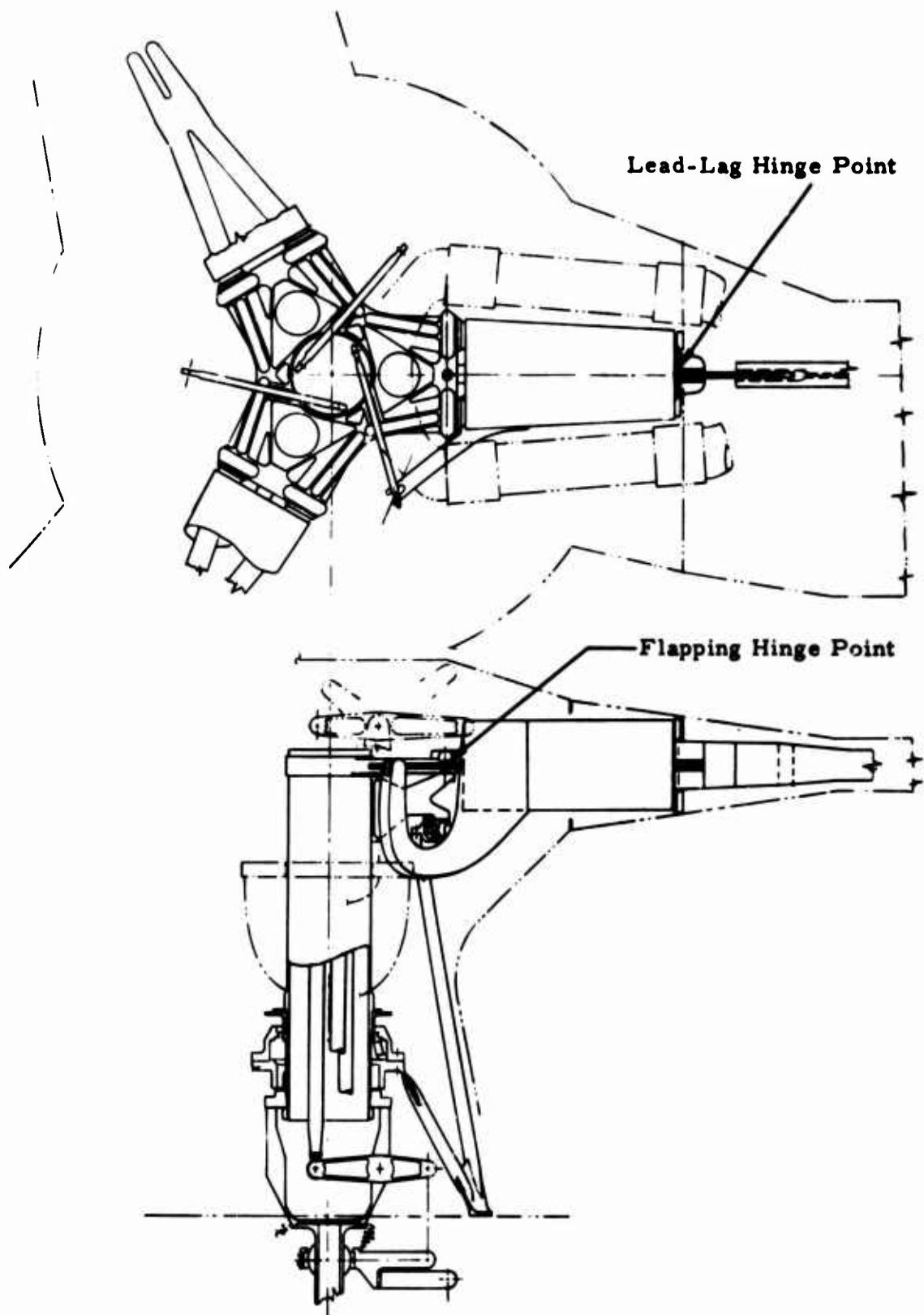


Figure 38. Articulated Hub With Internal Controls.

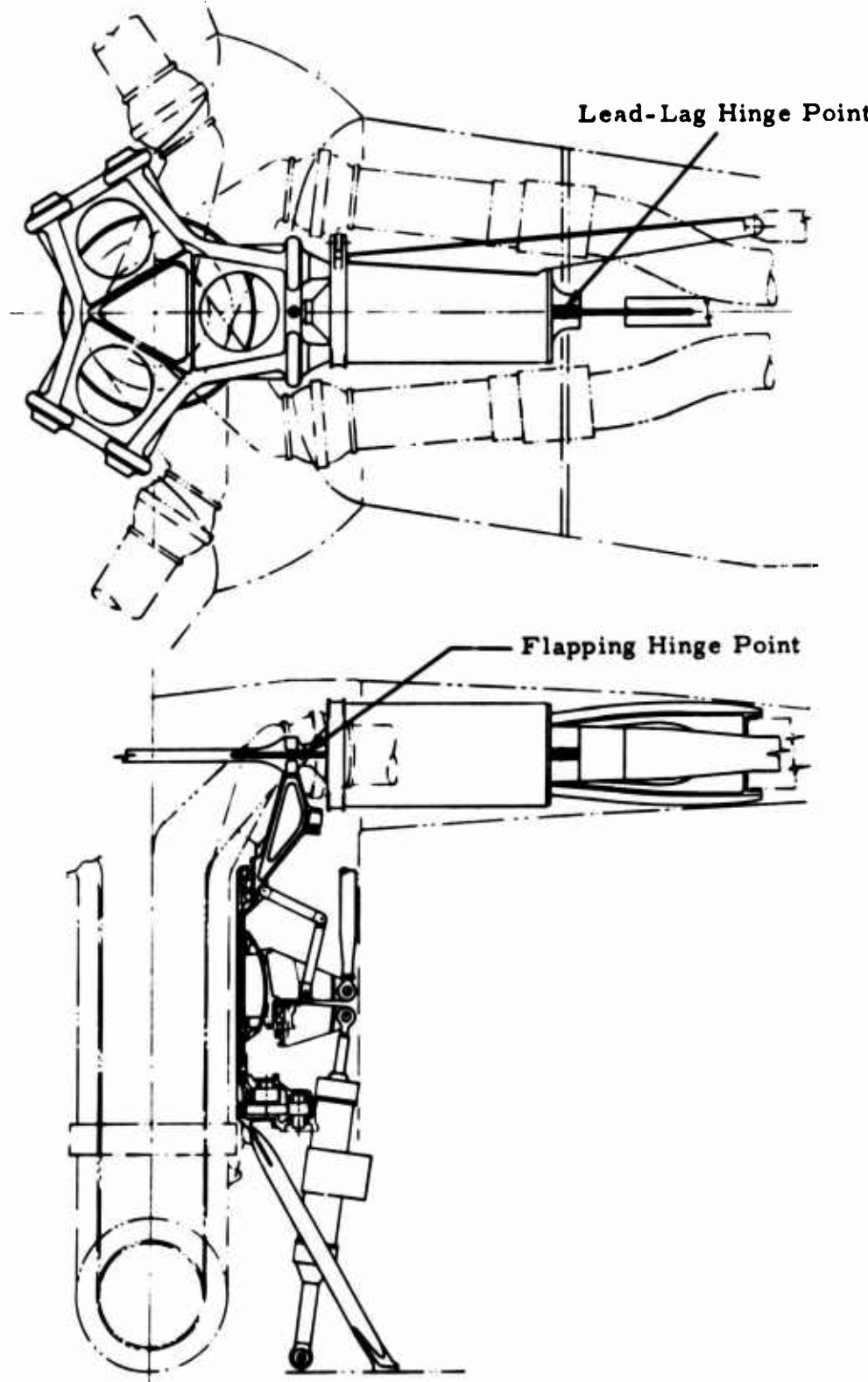


Figure 39. Articulated Hub With External Controls.

direct in the hub structure and hub tilting is not necessary, the weight of this configuration is much lower and the fairing envelope much smaller than for the tilting hubs.

ARTICULATED HUB WITH EXTERNAL CONTROLS (Figure 39)

This configuration is almost identical with the articulated hub with internal controls. The difference is primarily in the relocation of the swashplate assembly, shaft, and mast to the outside of the gas ducts. This configuration is the lightest, as a result of the simpler ducts and flight controls, and has the smallest fairing envelope of all the hubs considered.

BLADE CONFIGURATIONS STUDIED

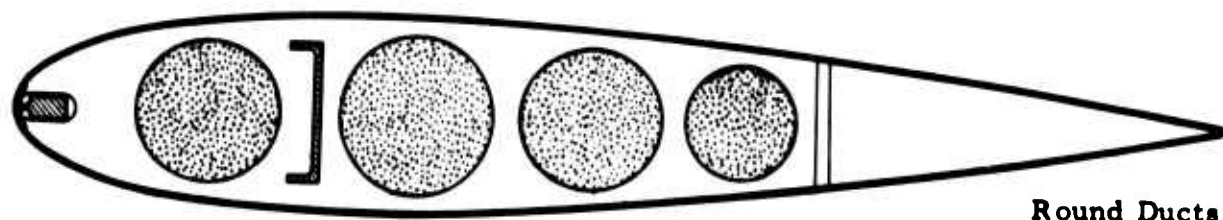
Several blade configurations, their design dictated primarily by gas duct style and shape, were studied and are shown in Figure 40. Common to all these configurations is the structural concept used on the XV-9A of constructing the blades in segments held together with flexures and spars and using nonstructural trailing-edge segments. This type of construction permits carrying all flapwise bending and centrifugal loads in the spars with the segments and flexures providing the load path for blade torsion, chordwise shear, and air loads. This configuration also allows for thermal expansion, minimizing loads in hot parts. In addition to duct shape, the other blade variables introduced into the parametric study were chord, radius, thickness ratio, number of blades, and number and location of spars. The detailed blade weight breakdown used in the computer study is shown in Table XIII. All blades studied use an NACA 0018 section on the inboard 0.75 radius and an NACA 0018, 0016, or 0014 on the outboard 0.25 radius.

ELLIPTICAL DUCTS

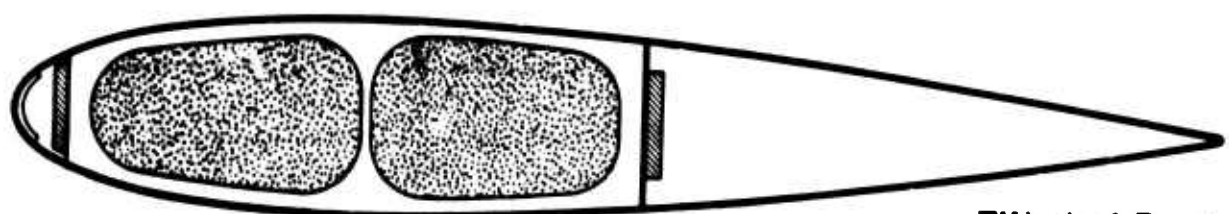
The first blade configuration studied was one dictated by the elliptical duct as used on the XV-9A. This type of duct is an integral structural part of each segment and produces the highest ratio of duct area to airfoil cross section area. To minimize thermal stress problems, a thin duct liner was used to reduce the duct wall temperature.

ROUND DUCTS

The second configuration studied was one utilizing multiple round ducts that are not an integral part of the structure. Gas-tight bellows are installed at spanwise intervals as necessary to provide for duct expansion and to eliminate duct bending stresses. This type of construction minimizes the



Round Ducts



Elliptical Ducts

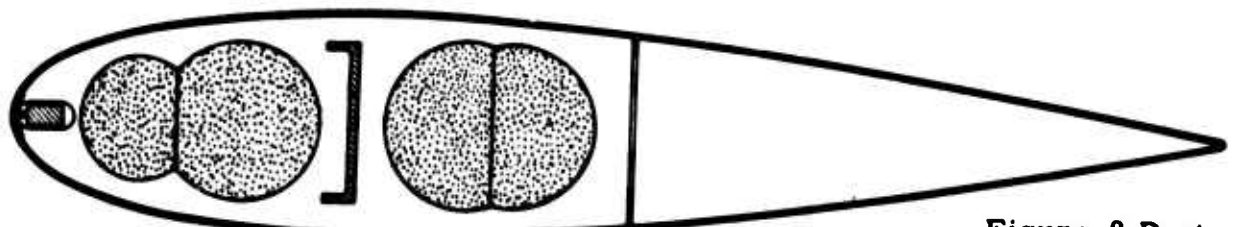


Figure-8 Ducts

Figure 40. Blade Duct Configurations.

TABLE XIII
WEIGHT FOR VARIOUS BLADE SECTIONS*

	Pounds Per Inch				
	395-0907				
	1 Spar				
	at 25%				
	395-0902	395-0903	395-0904	395-0905	
	1 Spar at 28%	2 Spar	XV-9A Type	1 Spar at 30%	Stepped Airfoil
Trailing edge structure	0.1402	0.1286	0.1295	0.1402	0.1523
Main segment skin and corrugations	0.3215	0.2281	0.1573	0.2758	0.2999
Ribs and caps	0.2399	0.2189	0.4518	0.2323	0.2227
Closure channel	0.0288	0.0474	0.1434	0.0260	0.0306
Rib stiffeners	0.0396	0.0294	-	0.0345	0.0196
Flexure	0.1496	0.1364	0.1664	0.1343	0.1210
Duct (forward)	0.1565	0.1541	0.1716	0.1526	0.1401
Duct (aft)	0.1565	0.1541	0.1664	0.1526	0.1401
28 percent or 30 percent channel	0.0660	-	-	0.0570	0.0600
Leading edge	-	0.0450	0.0386	-	-
Total nonbending material	1.2986	1.2420	1.4250	1.2053	1.1863
Front spar (at tip)	0.214	0.143	0.143	0.214	0.214
Rear spar (at tip)	-	0.086	0.086	-	-
Balance (at 23%)	0.5804	0.6954	0.6241	0.6891	0.4264
Total blade weight at tip**	2.0930	2.1664	2.2781	2.1084	1.8276

*Based on full-scale layouts optimized for skin gages and materials.

**Excluding cascade.

NOTE: All sections use the figure-8 duct except 395-0904, which uses the elliptical duct.

thermal stress problems and makes it possible to design a structure that lends itself to ease of inspection and repair. However, this configuration was abandoned because of the poor ratio of duct area to airfoil area and the difficulty in pairing and sizing the ducts to make possible separate engine ducts. It also required more balance weight in the leading edge to provide for an acceptable chordwise center of gravity location.

FIGURE-8 DUCTS

The third configuration considered is identical with the round duct type in principle except that the duct shape has been changed to a figure-8

formed by two intersecting circles. A web connecting the intersection points of the perimeters completes the duct. The figure-8 duct results in an adequate ratio of duct area to airfoil area, as well as two equal-area ducts necessary for separate engine operation. External insulation on the ducts minimizes the thermal stress effects.

ELEMENTS OF THE PARAMETRIC STUDY

WEIGHT EQUATIONS

The weight equations used in the parametric study are based on HTC-AD data compiled from analytical evaluations and statistical studies of numerous production and proposed research aircraft. The weight effects peculiar only to the Hot Cycle rotor system are also reflected in the group weight equations, where applicable.

With few exceptions, these equations were developed from the most basic parameters describing helicopter vehicles; namely, gross weight, rotor radius, and ultimate load factor. The end result produced expressions of simple form that checked reasonably with other estimating methods.

A detailed discussion and substantiation of the equations used may be found in the Weight section of this report.

WEIGHT EQUATIONS FOR ROTOR BLADE

The Hot Cycle rotor employs a unique type of blade construction with rotor diameter and blade chord larger than those of most existing rotors. As a result of this unique design, a method of rotor weight prediction more realistic and reliable than extrapolation of statistical data on existing rotors is necessary.

To meet this requirement, an analytical method using the results of detail layouts and stress analyses of the actual blade structural configurations has been developed. The blade structure is divided into two categories; namely, (1) basic bending structure (spars) carrying flapwise loads, chordwise bending loads, and centrifugal force; and (2) nonbending structure (comprising ducts, ribs, heat shielding, flexures, skins, leading and trailing edge fairings, and miscellaneous hardware) carrying local airloads, duct gas pressures, thermal gradients, chordwise shear, and blade torsional loads.

The analytical method starts with the carefully designed and analyzed nonbending material weight and develops the spar sizes needed to support the

total blade weight in ground flapping and ground wind conditions, to resist the flapwise and chordwise fatigue moments, to prevent proximity of flapwise and chordwise natural frequencies to integer multiples of rotor speed, and to provide chordwise balance as indicated by aeroelasticity considerations.

The method provides for a three-step spanwise variation in exterior skin thickness in order to efficiently fulfill the torsional strength and stiffness requirements along the blade length. In addition, a reduced chord length section may be incorporated on the inboard portion of the blade to minimize torsional divergence problems on the retreating blade. Spars are assumed to have a bilinear taper, thus permitting design of the tip station (station t), the 75-percent radius station (station 2), and the 20-percent radius station (station l) to meet the strength requirements precisely. The spanwise weight distribution established by the foregoing considerations is presented in Appendix III. It is apparent that enough flexibility in choice of parameters is available to provide a very close approximation of actual blade weight distribution.

ROTOR DESIGN LOADS

The most critical item in an analytical weight prediction is the accurate determination of the design loads. Therefore, as much data as possible has been obtained from flight test data on similar blades flown on the XV-9A Hot Cycle research aircraft. For the nonbending material, thermal gradients, which are a major source of structural stress, were based on flight measurements modified to account for the slightly different hot gas conditions associated with the GE1/J1 engines. Torsional loads have been scaled from flight measurements, using a scale factor proportional to gross weight times blade chord. Spar fatigue loads, both flapwise and chordwise, for the tilting-hub rotor have been scaled from XV-9A flight data, using a scale factor proportional to gross weight times radius. For the fully articulated rotor, flight test data from the OH-6A and the CH-34A helicopters have been scaled to be proportional to gross weight times radius. Dynamic effects are accounted for by using a dynamic amplification factor similar to that for a single-degree-of-freedom system, based on first mode natural frequency compared with nearest applied frequency (one per rev chordwise, three per rev flapwise). Natural frequency based on rotating mode shapes has been calculated by computing charts similar to those shown in Yntema (Reference 16). The charts were computed using a Myklestad method and assuming linear mass and stiffness distributions and a distributed tip weight. As Reference 16 uses nonrotating mode shapes and tip weight lumped at the tip of the blade, the frequencies computed herein are more accurate. An additional effect of flapwise stiffness

is accounted for by assuming the bending radius of curvature to be constant for a given centrifugal force. Vibratory flapwise bending stress, as a result, is proportional to spar depth. Maximum cruise speed loads have been increased by 20 percent to obtain design endurance limit fatigue loads. Fatigue stress allowables are based on full-scale tests of the XV-9A blades.

ANALYTICAL PROCEDURE

In outline, the analytical method proceeds as follows (equations referenced may be found in Appendix III):

1. For a given rotor radius and chord, calculate center of gravity and nonbending material weight from equations (53) and (54), which were based on data obtained from detail layouts.
2. From equation (55), compute main spar weight at tip (W_{rt}) required to support the centrifugal force generated by the tip weight and the cascades plus the gas pressure on the cascades.
3. Compute the front spar weight required for chordwise balance (equation 56).
4. Compute nonbending material weight and its chordwise location at station 2 (75-percent radius) from equations (57) and (58).
5. Compute station 2 design fatigue moment from equation (59).
6. The roots of equation (60) give the front spar weight needed at station 2 to meet chordwise balance requirements in conjunction with the flapwise and chordwise fatigue stress requirements in both the front and main spar. Substitute the front spar weight from equation (60) into equation (61) to obtain the total section weight at station 2.
7. Compute nonbending material weight and center of gravity at station 1 (50-percent radius) from the appropriate ones of equations (62) and (63).
8. The dead weight bending moment at station 1, excepting the part contributed by the unknown spar weight at station 1, is given by equation (64).
9. Compute from equation (65) the front spar weight required to balance (1) the nonbending material and (2) the main spar weight necessary to support the ground flapping and ground wind conditions at station 1.

10. Compute the design fatigue moments at station 1 from equation (66).
11. Compute the front spar weight required to take the flapwise fatigue loads and the cf and to provide chordwise balance at station 1 from equation (67). If the spar weight is determined by flapwise fatigue loads, then the depth of the spar is lowered until the blade is designed by ground flapping. In addition, when the front spar is critical for chordwise fatigue stress instead of for chordwise balance, the balance equations are bypassed and the main spar is designed by strength requirements. This results in a favorable chordwise balance further forward than the design requirements specify.
12. Using the largest value of front spar weight at station 1, compute the total section weight at station 1 from equation (68) and extend to total root section weight by equation (69).
13. Total blade weight required to meet all static and fatigue criteria and to meet the prescribed chordwise balance condition is given by equation (70).
14. Blade stiffness and inertial properties are given by equations (71), (72), (73), (74), (75), and (76).
15. Compute the flapwise and chordwise natural frequencies.
16. Compute the dynamic amplification factors from equation (59a) (includes 10-percent damping).
17. Recompute the fatigue moment from equations (59b) and (66a), and repeat steps 6 and 8 through 16. Continue to convergence.

For the compound configuration:

18. Check for bending instability at $\Psi = 180$ degrees. Add tip weight if instability is found. Check for retreating blade torsional divergence. If necessary, increase the blade skin gages for greater torsional stiffness. Check advancing blade flutter, including three modes of vibration -- flapping, first bending, and first torsional. If a disturbance does not damp to one-half amplitude in two cycles or less, move the chordwise balance forward by the addition of tip weight.
19. Repeat steps 2 through 18 until stability is obtained.

ROTOR HORSEPOWER AND CRUISE FAN PERFORMANCE

In order to calculate the rotor horsepower available, it is necessary to determine the conditions at the blade tip. These items depend on the duct

Mach number, duct friction coefficient, and hydraulic diameter of the ducts. The duct Mach number is a function of the engine exit conditions and the duct area. The available duct area and the duct wetted perimeter are determined from blade design drawings. These characteristics are then made into general equations in order to design helicopters of various sizes. Equations are prepared by investigation of blades of various chords, thickness ratios, and rear spar locations. Blade root duct area and hydraulic diameter equations for the figure-8 duct design are as follows:

$$A_D = 200 \bar{c}^2 \left(\frac{t}{c} \right) \left(\frac{x_r}{c} \right)^{1.20} \quad (29)$$

$$D_h = 9.05 \bar{c} \left(\frac{t}{c} \right)^{0.2} \left(\frac{x_r}{c} \right)^{0.93} \quad (30)$$

For the outboard portion of the rotor blade ($t/c = 0.14$):

$$A_D = 205 \bar{c}^2 \left(\frac{t}{c} \right)^{1.5} \left(\frac{x_r}{c} \right)^{1.20} \quad (31)$$

$$D_h = 9.20 \bar{c} \left(\frac{t}{c} \right)^{0.31} \left(\frac{x_r}{c} \right)^{0.93} \quad (32)$$

The corresponding equations for the elliptical (XV-9A) duct area follow.

$$A_D = 106.5 \bar{c}^{2.13} \left(\frac{x_r}{c} \right)^{0.85} \left(\frac{t}{c} \right)^{0.95} \quad (33)$$

$$D_h = 7.717 \bar{c}^{0.94} \left(\frac{x_r}{c} \right)^{0.07} \left(\frac{t}{c} \right)^{0.87} \quad (34)$$

With these equations, use of the proper dimensions will lead to duct area and hydraulic diameter.

The next step is to determine blade duct inlet Mach number. This is found from the following relationships, using consistent values of flow, temperature, and pressure (W_8 , T_8 , and P_8) taken from engine characteristics. These are determined from an IBM deck for engines such as the GE1/J1 or GE T64/S4B.

$$\left(\frac{W}{A_D} \sqrt{T} \right)_9 = \frac{N_{eng} W_8 \sqrt{T_8}}{b A_D \frac{P_9}{P_8} P_8} = \frac{M_9 \sqrt{\frac{gY}{R}}}{\left(1 + \frac{Y-1}{2} M_9^2 \right)^{\frac{Y+1}{2(Y-1)}}} \quad (35)$$

$$\frac{P_9}{P_8} = 1 - 0.04 = 0.96 \text{ based on XV-9A tests}$$

This equation must be iterated to find the blade duct inlet Mach number, which is typically 0.30 to 0.40.

The next step is to find the variation of duct Mach number down the blade. The blade is broken into a number of equal stations (say 20) and is further divided into two thickness ratios at an arbitrary station. The basic relationship of the Mach number change is taken from Reference 17, and assuming constant area over the duct length being checked, the following results:

$$\Delta M = \left[2f \frac{YR}{D_h} \left(\frac{\Delta r}{R} \right) \right] \left[\frac{M^3 \left(1 + \frac{Y-1}{2} M^2 \right)}{1 - M^2} \right] - \left[\frac{V_T^2}{2gRT_8} \left(\frac{\Delta r}{R} \right)^2 \right] (2n+1) \left[\frac{M \left(1 + \frac{Y-1}{2} M^2 \right)^2}{1 - M^2} \right] \quad (36)$$

The first term involves the friction coefficient, f , which is conservatively assumed to be 0.004, as 0.003 was measured during XV-9A tests. The second term is related to centrifugal force.

The total change in Mach number is accumulated from duct inlet to the arbitrary station where the area change takes place. At this location, the total pressure is determined from the following relationship:

$$\frac{P_{T_{9.7}}}{P_{T_9}} = \frac{M_9}{M_{9.7}} \left(\frac{1 + \frac{\gamma - 1}{2} M_{9.7}^2}{1 + \frac{\gamma - 1}{2} M_9^2} \right)^{\frac{\gamma + 1}{2(\gamma - 1)}} \quad (37)$$

and the new flow function is found from

$$\left(\frac{w \sqrt{T}}{A_D P_T} \right)_{9.7} = \left(\frac{w \sqrt{T}}{A_D P_T} \right)_9 \times \frac{1}{\left(\frac{P_{T_{9.7}}}{P_{T_{9.0}}} \right)} \quad (38)$$

A new Mach number on the other side of the area change is found from the change in duct area

$$\left(\frac{w \sqrt{T}}{A_D P_T} \right)_{9.71} = \left(\frac{w \sqrt{T}}{A_D P_T} \right)_{9.7} \times \left(\frac{A_{D_{9.7}}}{A_{D_{9.71}}} \right) = \frac{M_{9.71} \sqrt{\frac{gY}{R}}}{\left(1 + \frac{\gamma - 1}{2} M_{9.71}^2 \right)^{\frac{\gamma + 1}{2(\gamma - 1)}}} \quad (39)$$

which is iterated to find $M_{9.71}$.

A new value of hydraulic diameter, D_h , using equation (32), is also calculated, and then the process of accumulating duct Mach number changes to the blade tip is performed.

At the blade tip, the pressure ratio is finally determined as:

$$\frac{P_{T_{10}}}{P_{T_9}} = \frac{M_9}{M_{10}} \frac{A_{D_{9.0}}}{A_{D_{9.7}}} \left(\frac{1 + \frac{\gamma - 1}{2} M_{10}^2}{1 + \frac{\gamma - 1}{2} M_9^2} \right)^{\frac{\gamma + 1}{2(\gamma - 1)}} \quad (40)$$

With the tip pressure ratio known, it is now possible to determine available energy per degree from the relationship

$$\text{available energy per degree} = \left(\frac{AE}{T} \right) = C_p \left[1 - \left(\frac{1}{\frac{P_{T_{10}}}{P_{T_0}}} \right)^{\frac{\gamma - 1}{\gamma}} \right] \quad (41)$$

and

$$\text{jet velocity} = V_j = 224 C_v \sqrt{\frac{AE}{T} T_8} \quad (42)$$

Velocity coefficient, C_v , is assumed to be 0.98. The XV-9A value was measured at 0.94. It is assumed from available data that with a development program the higher value can be achieved.

Based on measurements of the temperature in the XV-9A blade, the tip temperature is taken as being equal to the engine discharge temperature. (The temperature drop through the duct is approximately equal to the temperature rise due to centrifugal pumping.)

Finally, to get rotor horsepower, the following calculation is performed:

$$rhp = \frac{W_g (V_j - V_T) V_T N_{eng}}{g \times 550} \quad (43)$$

and specific fuel consumption is given by

$$SFC = \frac{N_{eng} W_f}{rhp}$$

where again fuel flow, W_f , is taken from engine data consistent with the other gas conditions.

This value of specific fuel consumption is determined as a function of rotor horsepower over the range of powers.

In addition to the determination of power with all engines, an alternate case was prepared with one engine out. This case checks the potential improvement of specific fuel consumption with reduced duct losses (assuming a variable area nozzle). Another possible improvement of specific fuel consumption might be checked by using four engines instead

of two for the one-engine-out case. The increase in power available with three engines instead of one engine remaining operational permits cruise at a higher altitude and can possibly lead to greater range.

Cruise fan performance was derived from General Electric Report R64FPD155a. Since this report is classified, the data are not included.

INTEGRATION OF ELEMENTS OF THE STUDY WITH MISSION REQUIREMENTS

The integration of the elements of the study and the mission requirements utilized an IBM computer and was based on the program outlined below.

PERFORMANCE COMPUTATION METHOD

The method of computing power required for helicopter performance for both hovering and forward flight is presented in Reference 3. The compound helicopter flight was computed by standard methods with the addition of rotor thrust and drag. Rotor aerodynamic data from References 18 (Figures 19 and 28), 19 (Figure 4), and 20 (Figures 3 and 4) indicate that at advance ratios of more than 1.0 the lift coefficient/solidity ratio is a constant equal to 0.1667 and the drag coefficient/solidity ratio is a constant equal to 0.03888. The thrust of the autorotating rotor is then $T = 0.16667 A_b \times q$, and the drag is equal to $D = 0.03888 A_b \times q$.

Pure Helicopter

The design gross weight (transport mission weight) is computed as the maximum gross weight for hovering out of ground effect at 6,000 feet, 95°F day, with takeoff power. This includes a download factor on the fuselage.

The blade weight and component weights are computed to determine the empty weight and the minimum flying weight.

The heavy-lift weight is defined as the weight for hovering out of ground effect, sea level standard day, or the weight for a design load factor of 2, whichever is lower.

Available rotor horsepower is reduced 2 percent for yaw control requirements.

The payloads for both the 100-nautical-mile transport mission and the 20-nautical-mile heavy-lift mission are determined as follows:

1. Warmup and takeoff fuel for 2 minutes at normal rated power is computed.
2. Power for hover at takeoff weight less warmup and takeoff fuel is determined and fuel for the start hover time is obtained.
3. The fuel flow for cruise at the takeoff weight less hover, warmup, and takeoff fuel is computed. Using this fuel flow, the average weight for the outbound leg is estimated by subtracting the fuel required for one-half the radius.
4. Using the average weight, the cruise fuel flow is recomputed and the fuel for the outbound leg is determined.
5. The hovering power and fuel flow for the landing weight after the outbound leg determine the hover fuel at midpoint.
6. An estimate of the reserve fuel is made, assuming that the fuel for the return leg is the same as that for the outbound leg. This is added to the minimum flight weight to give the mission landing weight.
7. The fuel flow for cruise at the landing weight is used to compute an average weight for the inbound leg. In addition, a more accurate estimate of the reserve fuel and landing weight can be made.
8. Using the average weight, the fuel for the inbound leg is determined.
9. The payload is the takeoff weight less the minimum flight weight and mission fuel, including reserve.

The configurations with internal loading are assumed to require twice the takeoff and warmup fuel, as they would have to shut down to unload at the destination. It is assumed that with external loading, the ship does not land at the destination.

The cruise speed of the outbound leg is 95 knots for the heavy-lift mission and 110 knots for the transport mission, or speed for best range, whichever is larger, unless the retreating tip drag coefficient is greater than 0.06. This value is assumed to be the stall limit of the ship and will be the maximum speed with the required weight and parasite area. The return leg is at 130 knots, or speed for best range, if it is greater, unless the stall limit is reached.

In the program, the ferry range is computed using the following method. The curve of specific range ($R_{sp} = \text{nmi/lb of fuel}$) is assumed to have the following form:

$$R_{sp} = \frac{C_1}{W} + C_2 \left(W - \frac{W_{TO} - W_L}{2} \right) \quad (44)$$

W = weight at given range

where:

W_{TO} = takeoff weight

W_L = landing weight

Integrating this,

$$\text{range} = C_1 \left(\ln \frac{W_{TO}}{W_L} \right) \quad (45)$$

The range is assumed to be a climb cruise; thus, to determine the constants in the equation, the specific range at takeoff weight at sea level and the landing weight at best cruise altitude up to 20,000 feet are used to give two equations in two unknowns, C_1 and C_2 . C_1 can then be used in the range equation. To make an allowance for climb fuel, an energy equation is used:

$$W_{f_t} = (\text{SFC}) \left(\frac{HW_s}{325\eta} \right) \quad (46)$$

where H = altitude in nautical miles

W_s = weight at start of climb

Then one-half of the climb fuel is subtracted from the takeoff weight and one-half is added to the landing weight.

As the ferry mission can be performed with a running takeoff, the takeoff weight is determined by allowable load factor or the maximum weight at which the ship will cruise at 60 knots or greater, as limited by retreating blade stall. In this condition, the ship is never allowed to exceed maximum continuous power. If the ship will not cruise at a speed of 60 knots, the takeoff weight is reduced by 5,000-pound increments until 60 knots can be achieved. As the cruise with takeoff weight is usually stall-limited, hovering tip speed is used, as this greater tip speed results in a higher stall speed.

The specific range at landing weight is determined as follows. The specific range at 20,000-foot altitude with two engines is computed. If this is stall-limited, the specific range at 15,000 feet is computed, and so on, until speed for best range can be achieved. The same procedure is

followed using one engine, and then the largest value of specific range is used in the range equation.

A more detailed computation of ferry range was made for the best rotor for each configuration.

The takeoff weight is determined as the lowest of the following: 2-g load factor or cruise at 60 knots, as limited by retreating tip stall or normal continuous power. The energy equation was used for climb fuel, assuming a final altitude of 20,000 feet and average flight weight. One-half of this fuel was subtracted from the takeoff weight and one-half was added to the minimum flight weight. The minimum flight weight also includes a reserve of 10 percent of the total cruise fuel.

For each weight, the specific range is optimized for hovering or cruise tip speed, altitude, and use of one or two engines. The ferry range was then determined by integrating the specific range using Simpson's rule.

Compound Helicopter

The design weight and heavy-lift weight are determined in the same manner as for the pure helicopter, including the download on the fuselage and wing folded at 60-percent span.

The blade weight computation includes a check (and standard beef-up, if necessary) of bending stability, torsional divergence, and flutter at the high advance ratio conditions appropriate to compound helicopter flight.

The payload is computed for 200-, 300-, and 500-nautical-mile missions at sea level and altitude for best cruise. These missions are computed in the same manner as the helicopter mission.

The heavy-lift and overload weights are checked for ability to perform a transition. If this cannot be achieved, the weights are reduced. The criterion for transition is an overlap of 20 knots between helicopter and autogyro flight and an overlap of 20 knots between autogyro and airplane flight.

In helicopter flight, it is assumed that the flaps are used on the wings to compensate for the download that would result from the nose-down angle of the fuselage, resulting in zero lift. The wing profile drag coefficient is assumed to be raised to 0.03. This is the value with flaps deflected enough to compensate for a negative angle of 5 degrees. As the wing has flaps, a maximum C_L of 2 is assumed for airplane flight.

The method of computing the ferry mission is the same as that used in the helicopter routine.

RESULTS OF THE PARAMETRIC STUDY

The results of the parametric study show the ability of all configurations to meet the mission requirements with a rotor of modest size and remarkably high payload-to-empty-weight ratios. For configurations 2 and 3, the rotor size was determined by the requirement for the ship to have the ability to make a safe autorotational landing at design gross weight. The transport mission is critical for configuration 1, and the ferry mission is critical for configuration 4. It is well to note that the optimum rotor was arrived at by a process of elimination. Thus the tables showing the effect of the parametric variables are examples taken for rotors where comparable data were available and are not necessarily the selected optimum rotors.

EFFECT OF PARAMETRIC VARIABLES ON MISSION PERFORMANCE

Effect of Restrained Versus Articulated Hub

It became obvious early in the program that the articulated hub would provide a substantial saving in weight and hub envelope size. This reduction in weight and drag for a rotor of a given size resulted in an increase in range in the order of 25 percent, an increase in transport payload of 70 percent, and an increase in heavy-lift payload of approximately 20 percent over the restrained tilting hub. The tilting hub, employing rigid chord-wise blade restraint with its attendant higher blade stresses, also results in an empty weight approximately 33 percent greater than that for an articulated rotor of the same size. These differences are shown in Table XIV. The major share of the noted weight difference is in the rotor itself, the restrained tilting rotor with in-plane rigidity being almost twice the weight of the same size articulated rotor.

Effect of Internal Rotor Controls Versus External Rotor Controls

A small improvement in performance is gained by using an external controls instead of the internal controls on the articulated hub, as shown in Table XV. This is because of its smaller envelope and lighter weight.

Effect of Blade Duct Shape

As shown in Table XVI, the figure-8 duct blade proved superior to the elliptical duct blade. Though the elliptical duct area was greater, results

TABLE XIV
EFFECT OF TILTING HUB WITH RESTRAINT
VERSUS ARTICULATED HUB

	Tilting Hub	Articulated Hub
Mission		
Ferry	1, 374 nmi	1, 731 nmi
Transport	7. 02 tons	11. 96 tons
Heavy-lift	22. 57 tons	27. 30 tons
Empty weight	37, 269 lb*	27, 926 lb*
Payload/empty weight		
Transport	0. 3378	0. 7426
Heavy-lift	1. 2112	1. 9552
Computer run number	1-5	1-3
(configuration 1, 55-foot radius, 55-inch chord, V_t hover = 750 fps, V_t cruise = 700 fps)		

*Empty weight for heavy-lift mission only (no pod).

TABLE XV
EFFECT OF INTERNAL ROTOR CONTROLS VERSUS
EXTERNAL ROTOR CONTROLS

	Articulated Hub	
	Internal Shaft	External Shaft
Mission		
Ferry	1, 685 nmi	1, 715 nmi
Transport	11. 96 tons	12. 08 tons
Heavy-lift	26. 58 tons	26. 66 tons
Empty weight (transport mission)	24, 331 lb	24, 189 lb
Payload/empty weight		
Transport	0. 8355	0. 8477
Heavy-lift	2. 1849	2. 2043
Computer run number	1-8	1-4
(configuration 1, 50-foot radius, 55-inch chord, V_t hover = 750 fps, V_t cruise = 700 fps)		

TABLE XVI
EFFECT OF BLADE DUCT SHAPE

	Elliptical Duct	Figure-8 Duct
Mission		
Ferry	1,731 nmi	1,791 nmi
Transport	11.96 tons	12.20 tons
Heavy-lift	27.3 tons	27.47 tons
Empty weight		
(transport mission)	27,926 lb*	26,303 lb*
Payload/empty weight		
Transport	0.7426	0.7974
Heavy-lift	1.9552	2.0887
Computer run number	1-3	1-4
(configuration 1, 55-foot radius, 55-inch chord, V_t hover = 750 fps, V_t cruise = 700 fps)		

*Empty weight for transport mission only (includes pod).

of the study show that this benefit was more than offset by the lighter construction of the figure-8 blade and that its duct area was adequate. Because of this tradeoff and the difficulty of transferring the centrifugal load from the two spars to the lead-lag hinge, the elliptical duct configuration was abandoned early in the study.

Tip Speed

Tip speeds of 750, 725, and 700 feet per second in hover were used with cruise tip speeds of 725, 700, and 675 feet per second. It was determined that, in general, a high tip speed will give better performance for heavy-lift operations and extended hovering times and a lower tip speed is favored for performance at cruise with a lesser payload. Thus, a constant tip speed for all missions can be considered only as a poor compromise, as indicated by the figures in Table XVII, where the results for the best constant tip speed ship are listed in the last column.

Fortunately, the Hot Cycle principle allows for a quick and easy adaption of tip speeds in a rather wide range for best mission performance. In opposition to a gear-driven helicopter, no penalties will result as to

TABLE XVII
EFFECT OF ROTOR-BLADE TIP SPEED

	Tip Speed (fps)				
	Hover = 750 Cruise = 700	Hover = 750 Cruise = 675	Hover = 725 Cruise = 700	Hover = 725 Cruise = 675	Hover = 725 Cruise = 725
Mission					
Ferry	2,038 nmi	2,065 nmi	1,917 nmi	1,949 nmi	1,868 nmi
Transport	13.97 tons	13.98 tons	13.82 tons	13.83 tons	13.77 tons
Heavy-lift	25.39 tons	25.40 tons	25.13 tons	25.14 tons	25.12 tons
Empty weight	17,832 lb	17,832 lb	17,637 lb	17,637 lb	17,637 lb
Payload/empty weight					
Transport	1.5665	1.5680	1.5670	1.5685	1.5612
Heavy-lift	2.0848	2.8489	2.8494	2.8503	2.8482
Computer run number	2-13	2-15	2-13	2-13	-
(configuration 2, 40-foot radius, 60-inch chord)					

gearbox life, fuel consumption, and engine performance, if not operated at the design point. For example, increasing rotor tip speed for improved hover and heavy-lift capability also raises the Hot Cycle propulsion efficiency. This improvement cannot be found in the shaft-driven helicopter.

Effect of Blade Chord Length

Blade chord lengths were varied from a minimum of 45 inches to a maximum of 65 inches. The optimum chord for best performance is nominally 60 inches, depending upon spar location and blade radius. Changing one parameter quite often requires the change of an additional one to approach the optimum rotor. This interaction of spar position, chord length, and blade radius is discussed further under Effect of Spar Position. The effect of varying chord length is shown in Figures 41 and 42.*

Effect of Blade Radius

The effect of varying the blade radius for each rotor configuration is shown in Figures 43 and 44. In general, the performance drops off with any decrease in radius from the minimum selected to meet the mission.*

*The discontinuities of the ferry range curves in Figures 41, 43, and 44 are the result of changes of cruise altitude and/or number of engines operated.

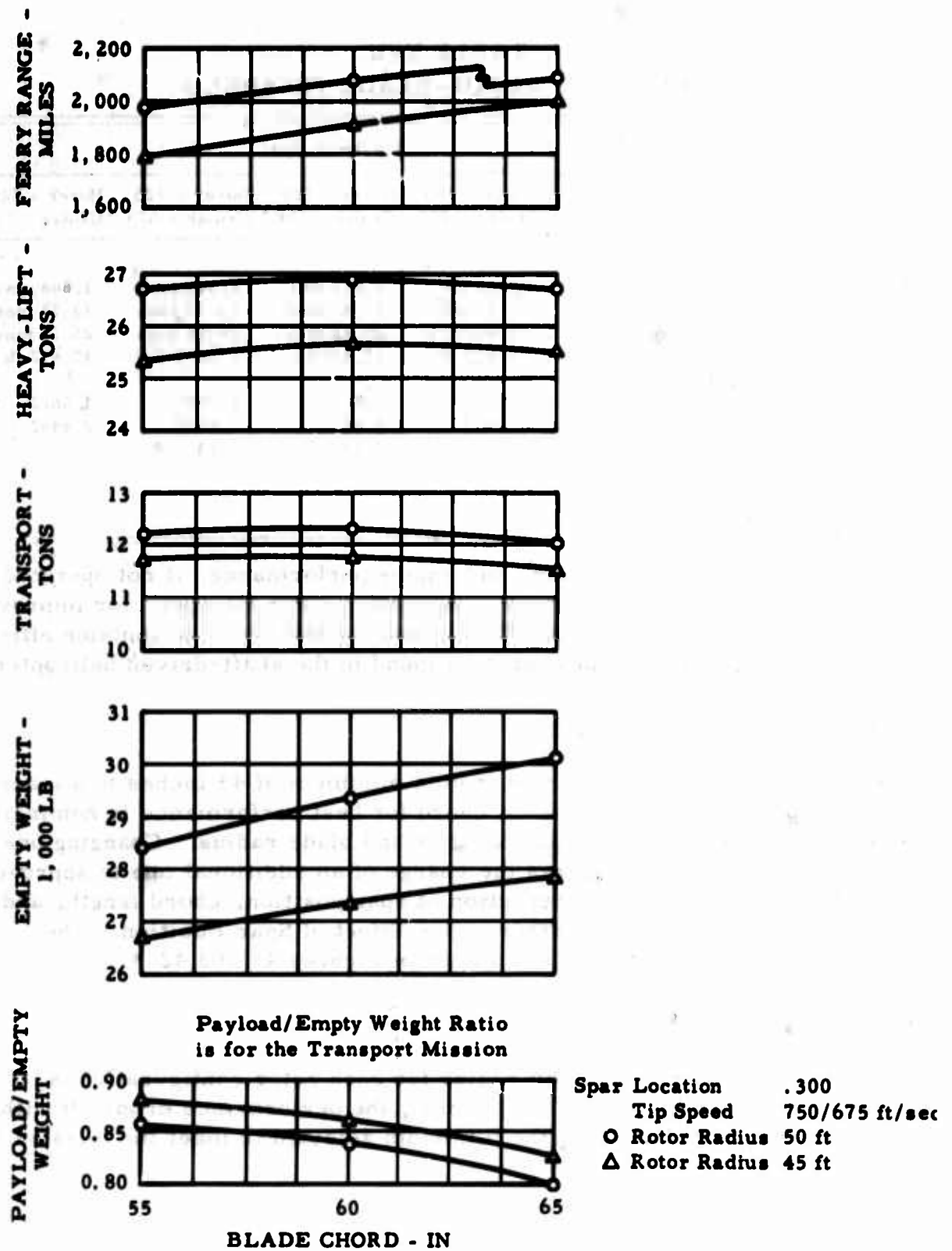


Figure 41. Influence of Blade Chord - Configuration 1.

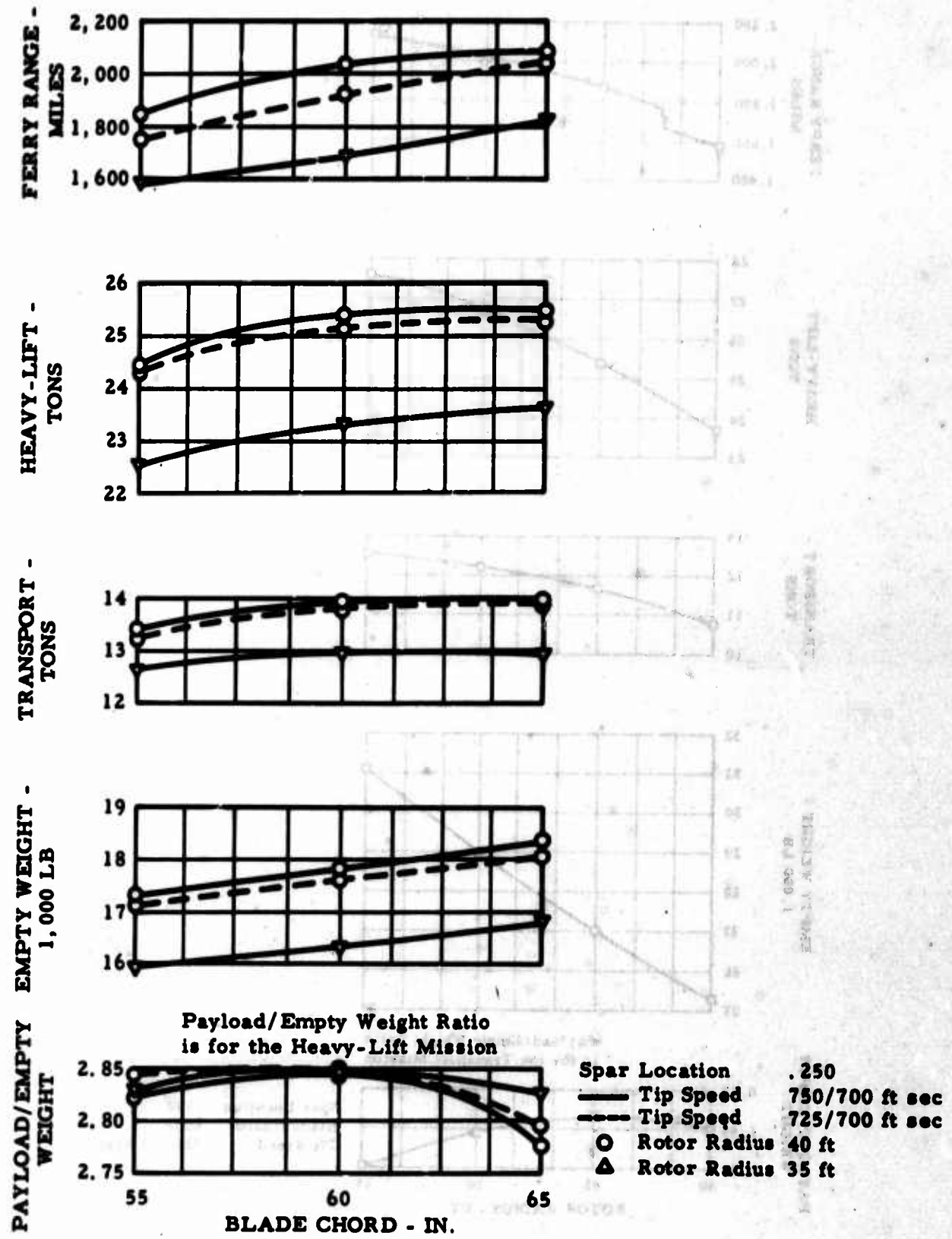


Figure 42. Influence of Blade Chord - Configuration 2.

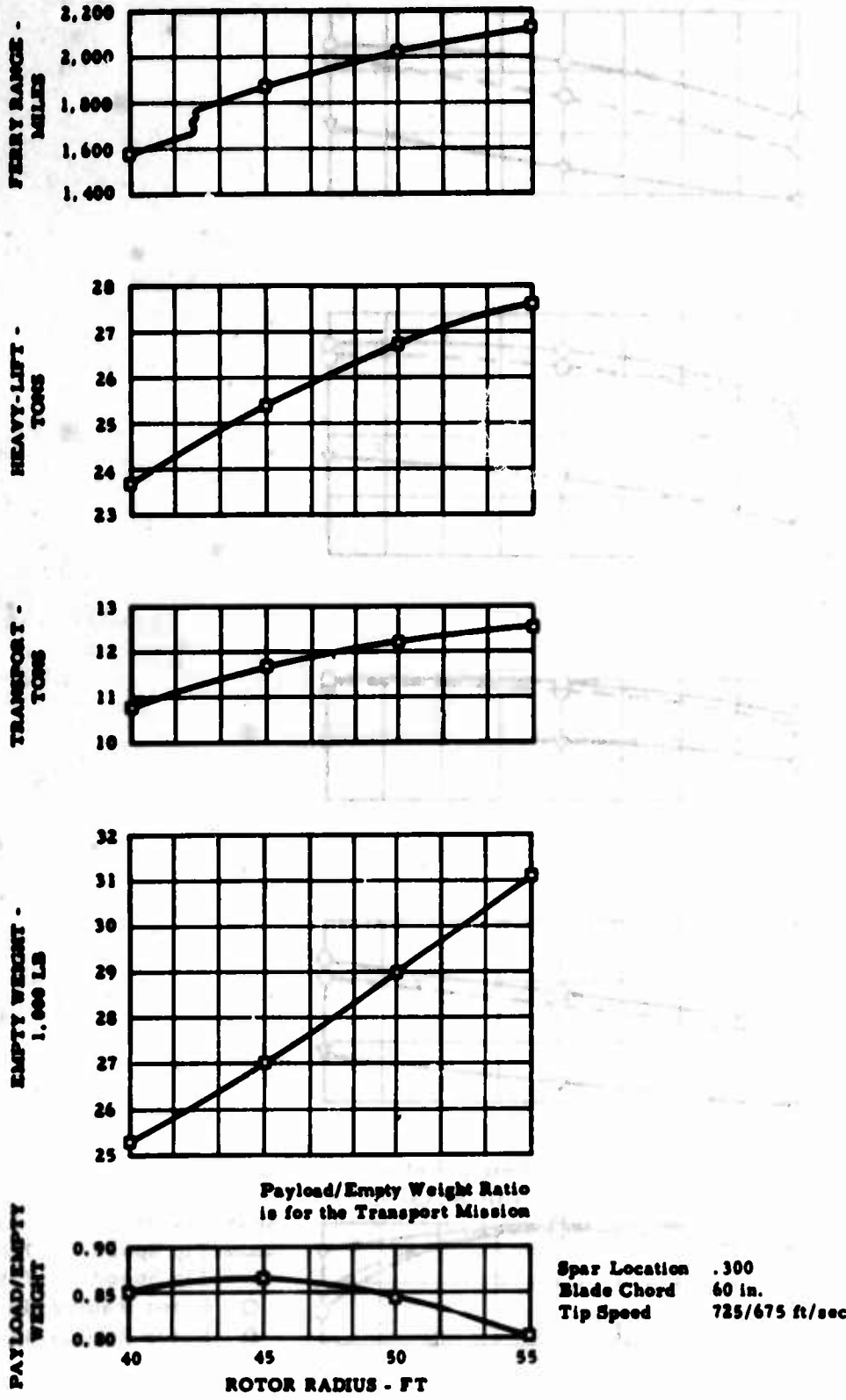


Figure 43. Influence of Rotor Radius - Configuration 1.

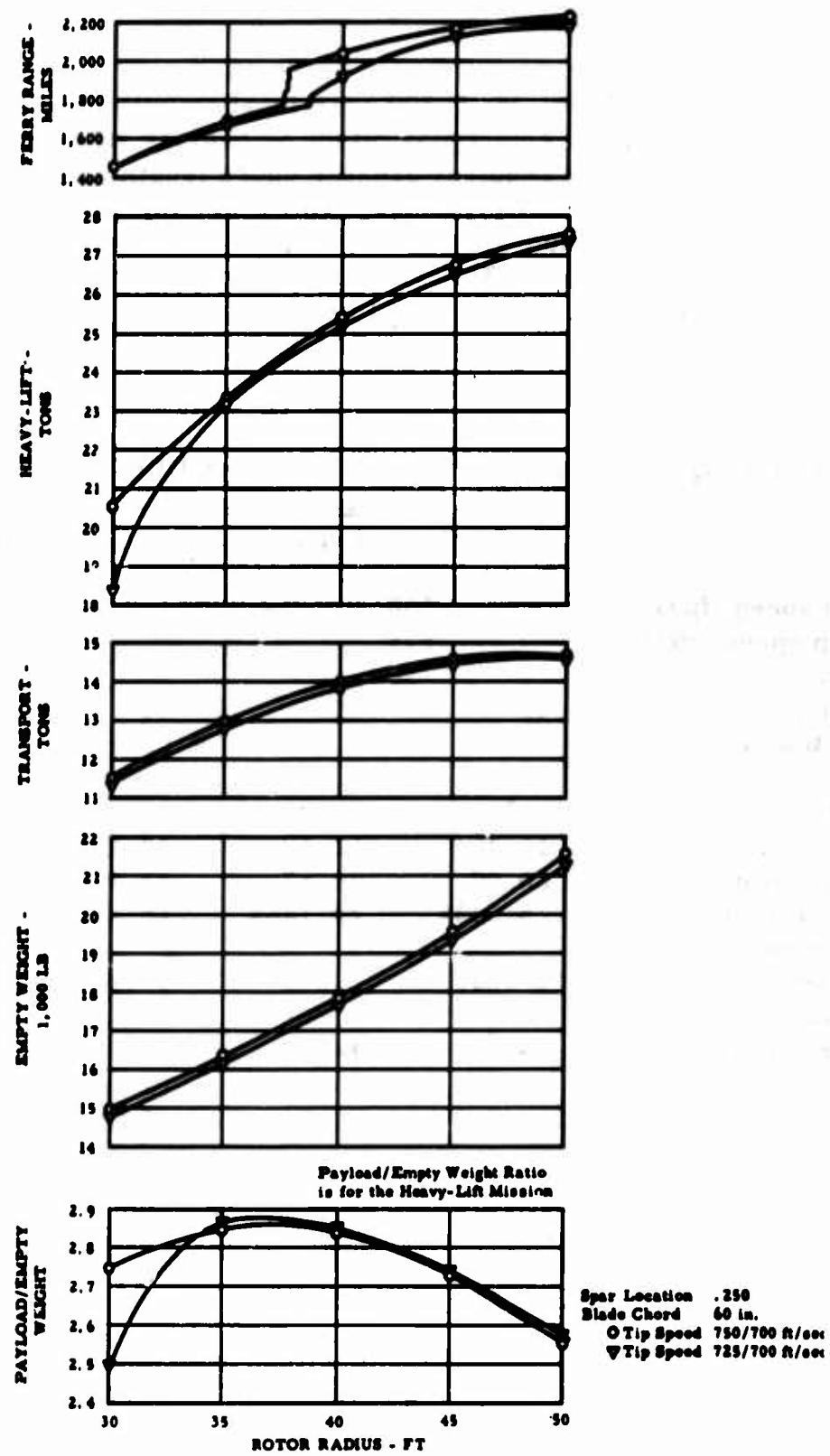


Figure 44. Influence of Rotor Radius and Tip Speed - Configuration 2.

Effect of Spar Position

For the figure-8 duct blades, the 0.300 spar location will permit greater duct area, whose benefit is sometimes offset by heavier structure. The 0.250 spar location usually requires greater chord length to maintain duct area, which also leads to heavier blades. However, for smaller rotor radii, the 0.250 spar location will result in an overall better payload/empty weight ratio and range. This is indicated in Table XVIII, which shows the best rotors of configurations 1 and 2 for the 50- and 35-foot radii and both spar locations.

TABLE XVIII
EFFECT OF SPAR LOCATION ON FIGURE-8 DUCT BLADES

	Configuration 1		Configuration 2	
Hover tip speed (fps)	750		750	
Cruise tip speed (fps)	675		700	
Radius (ft)	50		35	
Chord (in.)	65	55	60	55
Spar location	0.250	0.300	0.250	0.300
Mission				
Ferry (nmi)	2,015	1,965	1,688	1,517
Transport (tons)	11.46	12.17	12.17	13.06
Heavy-lift (tons)	26.00	26.67	23.30	22.87
Empty weight (lb)	25,523*	24,146*	16,349	16,266
Payload/empty weight				
Transport	0.7687	0.8559	1.5863	1.6058
Heavy-lift	2.0377	2.2088	2.8503	2.8121
Computer run number	1-22	1-29	2-13	2-14
			(Sheet 1 of 2)	(Sheet 1 of 2)

*Empty weight for heavy-lift mission.

Effect of Fixed Versus Retracted Landing Gear

All configurations were programmed both with a fixed and with a retracted landing gear. The lighter fixed gear proved to be more efficient. A typical example is shown in Table XIX.

TABLE XIX
EFFECT OF FIXED VERSUS RETRACTED LANDING GEAR

	Landing Gear	
	Retracted	Fixed
Mission		
Ferry (nmi)	1,762	1,772
Transport (tons)	13.81	13.99
Heavy-lift (tons)	25.91	26.11
Empty weight (lb)	19,308	18,881
Payload/empty weight		
Transport	1.4306	1.4818
Heavy-lift	2.6839	2.7657
Computer run number (configuration 2, 45-foot radius, 55-inch chord, V_t hover = 750 fps, V_t cruise = 700 fps)	2-2	2-3

Effect of Thickness Ratio

Blade airfoil thickness ratios of the following combinations were programmed, and the results are shown in Table XX, which shows the thinner blade section to give superior performance.

<u>Inboard 75 Percent Span</u>	<u>Outboard 25 Percent Span</u>
18%	14%
18%	16%
18%	18%

Effect of Engine Installation

Two General Electric GE1/J1 engines were considered as the primary power source. An alternate engine arrangement utilizing four General Electric T64/S4B gas generators was also surveyed. See Table XXI.

Effect of Four Blades

A check was made on the effect of using four blades instead of three. Though the four-bladed configuration showed promise of having adequate performance, it was abandoned as a result of the added difficulties of routing the gas through the hub and into four blades because of space limitation in the hub (reference run 2-7).

TABLE XX
EFFECT OF BLADE THICKNESS

	Airfoil Thickness (% of Chord)		
Inboard 0.75 R	18	18	18
Outboard 0.25 R	18	16	14
Mission			
Ferry (nmi)	1,339	1,376	1,661
Transport payload (tons)	12.25	12.61	12.80
Heavy-lift payload (tons)	20.43	22.82	23.13
Empty weight (lb)	16,178	16,185	16,174
Payload/empty weight			
Transport	1.5141	1.5580	1.5832
Heavy-lift	2.5259	2.8196	2.8602
Computer run number	2-22	2-12	2-13

TABLE XXI
EFFECT OF ENGINE INSTALLATION

	Engine Installation	
	GE1/J-1 (2)	T-64/S4B (4)
Mission		
Ferry (nmi)	2,038	1,782
Transport (tons)	13.97	10.16
Heavy-lift (tons)	25.39	21.26
Empty weight (lb)	17,832	18,297
Payload/empty weight		
Transport	1.5665	1.0103
Heavy-lift	2.8480	2.1154
Computer run number	2-13	2-11
(configuration 2, 40-foot radius, 60-inch chord, V _t hover = 750 fps, V _t cruise = 700 fps)		

Effect of Drag

To evaluate the effect of increased drag on the mission performance, two cases were run on configuration 2 -- one doubling the estimated drag of the helicopter and the other doubling the estimated drag of the external payloads. The results, presented in Table XXII, show the increased fuselage drag to have little effect on any mission except ferry range and the increased payload drag to have a small effect on transport mission payload.

TABLE XXII
EFFECT OF DRAG ON PERFORMANCE

	Estimated Fuselage Payload Drag	Double Estimated Payload Drag	Double Estimated Fuselage Drag
Mission			
Ferry (nmi)	1,587	1,587	1,443
Transport (tons)	13.54	12.87	13.15
Heavy-lift (tons)	24.55	24.31	24.48
Empty weight (lb)	17,364	17,364	17,364
Payload/empty weight			
Transport	1.5591	1.4826	1.5145
Heavy-lift	2.8277	2.8000	2.8200
Computer run number (configuration 2, 40-foot radius, 55-inch chord, V_t hover = 750 fps, V_t cruise = 700 fps)	2-3	2-5	2-6

SPECIFIC RANGE

Figures 45 and 46 show the influence of flight speed on the specific range. It can be seen that at the speeds specified by the requirements, the curves show optimum values for the specific range.

FUEL REQUIRED FOR TRANSPORT AND HEAVY-LIFT MISSIONS

To show the transportation performance achieved by a certain amount of fuel consumed, the payloads in ton-miles per pound of fuel were calculated for the various configurations and missions. These figures, as opposed to fuel flow per hour or miles per pound of fuel, are of major importance for estimating actual costs and logistics of helicopter operations, and are shown in Tables XXIII and XXIV for the transport and heavy-lift missions. Results for an operational helicopter (CH-47A) have been included in Table XXIV for comparison.

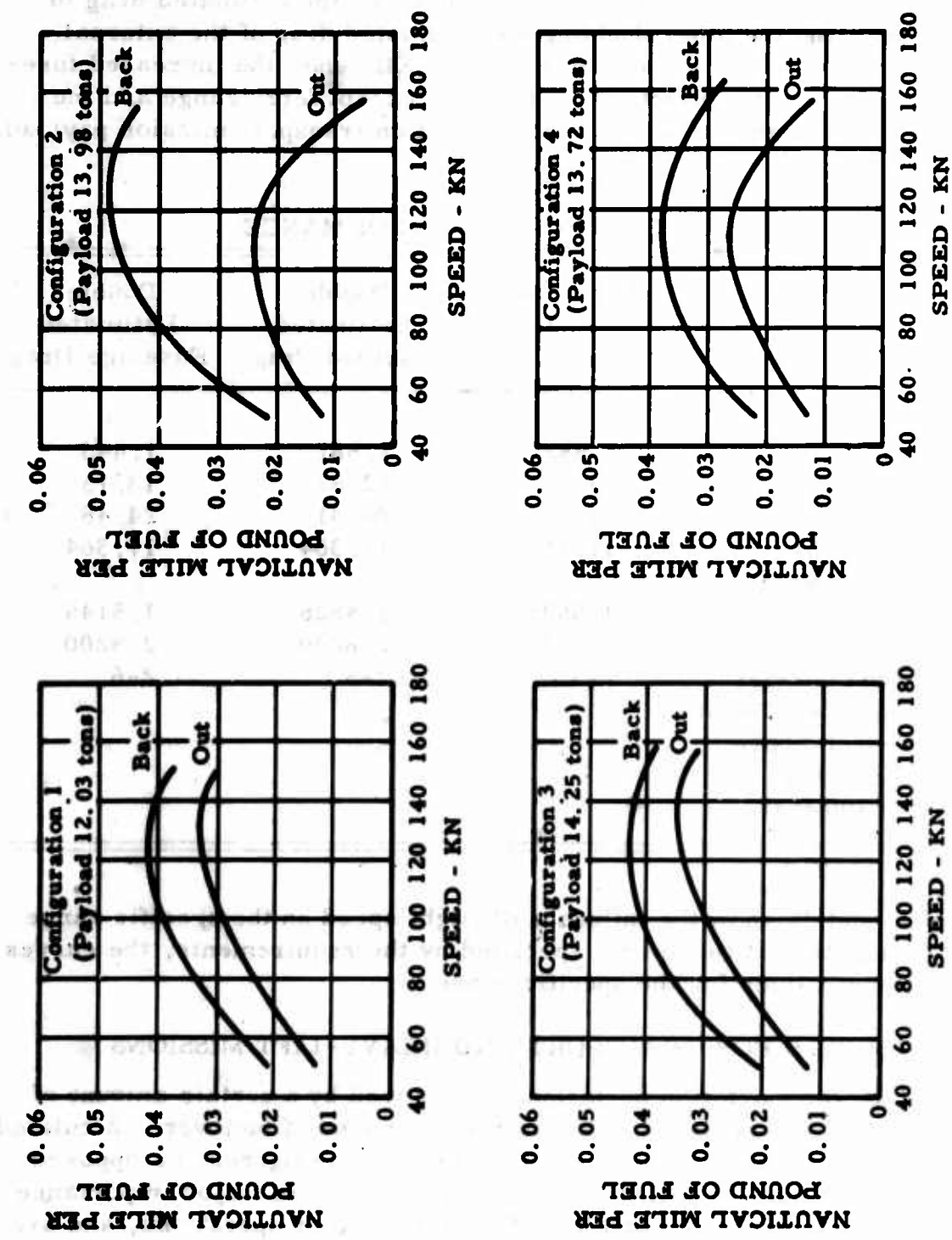


Figure 45. Effect of Speed on Specific Range Based on Average Gross Weight Back and Average Gross Weight Out - Transport Mission.

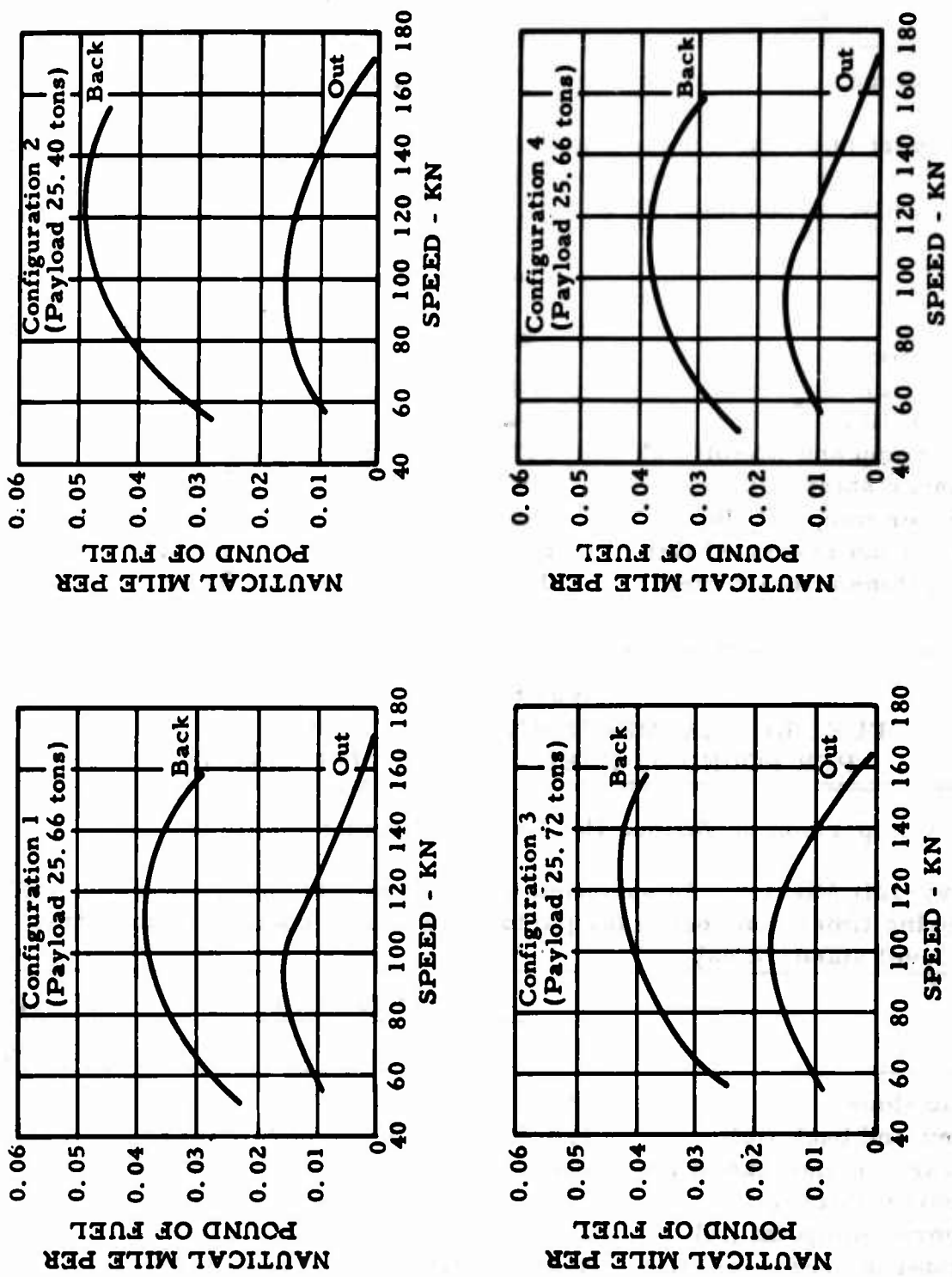


Figure 46. Effect of Speed on Specific Range Based on Average Gross Weight Back and Average Gross Weight Back - Heavy-Lift Mission.

TABLE XXIII
FUEL REQUIREMENTS AND PAYLOAD TON-MILES
PER POUND OF FUEL - TRANSPORT MISSION

Comparison of Various Hot Cycle Helicopter Configurations

Transport Mission: As specified in requirements, but no warmup and hovering times considered for payload ton-miles/pound fuel numbers.
Hover OGE, 6,000 feet, 95°F.

	Configuration			
	1	2	3	4
Payload (tons)	12.03	13.98	14.08	13.72
Fuel out (lb)	3,050	4,142	2,897	3,840
Fuel back (lb)	2,429	2,079	2,350	2,714
Fuel warmup and takeoff (lb)	500	250	500	250
Fuel hover start (lb)	308	307	308	308
Fuel hover midpoint (lb)	186	181	187	183
Fuel total (no reserves) (lb)	6,473	6,959	6,242	7,295
Payload (ton-miles/lb fuel)	0.220	0.223	0.268	0.210

TABLE XXIV
FUEL REQUIREMENTS AND PAYLOAD TON-MILES
PER POUND OF FUEL - HEAVY-LIFT MISSION

Comparison of Various Hot Cycle Helicopter Configurations

Heavy-Lift Mission: As specified in requirements, but no warmup and hovering times considered for payload ton-miles/pound fuel numbers.
Sea level standard day.

	Configuration				CH-47A
	1	2	3	4	(Ref 9)
Payload (tons)	25.66	25.40	25.55	25.66	7.01
Fuel out and back (lb)	1,825	1,650	1,669	1,825	1,170
Fuel warmup and takeoff (lb)	250	250	250	250	-
Fuel hover start (lb)	776	775	775	776	-
Fuel hover midpoint (lb)	1,406	1,422	1,426	1,406	-
Fuel total (no reserves) (lb)	4,257	4,097	4,120	4,257	1,170
Payload (ton-miles/lb fuel)	0.281	0.308	0.306	0.281	0.120

RESULTS OF AUTOROTATION REQUIREMENT STUDY

A spot check was made on several of the configurations studied to estimate the autorotational performance. While autorotation was found to be non-critical on the optimum rotors for configurations 1 and 4, the rotor diameters of configurations 2 and 3 were in fact determined by the autorotational rather than the mission requirements.

Using a method outlined in Appendix III of Reference 2, an index number K was calculated that represents a kinetic energy ratio.

$$K = \frac{\text{usable rotor kinetic energy}}{\text{helicopter sink-rate kinetic energy}}$$

To permit a quick check of the autorotational capability, the following assumptions were made.

1. Safe autorotation is required with all engines failed and at a gross weight associated with the internal payload shown below:

<u>Configuration</u>	<u>Internal Payload (tons)</u>
1	12 (in pod)
2	7
3	12

2. An external payload would be jettisoned in case of emergency.

Table XXV shows the results of this check for configurations 1, 2, and 3 with various rotor radii and gross weights. The comparable index number for some operational helicopters was approximated and added for comparison. It can be seen that the index numbers of the selected rotor radii of 45, 40, and 45 feet for configurations 1, 2, and 3, respectively, fall within the range of the operational helicopter index numbers.

TABLE XXV - ROTOR KINETIC ENERGY INDEX

Helicopter in Operation	Blade Heavy-Lift									
	2,000 rpm OII-SA	High-speed	Medium	Slow-speed	Slowest	Configuration 1	Configuration 1	Configuration 2	Configuration 2	Configuration 3
Gross weight (lb)	1,670	2,460	6,600	7,100	11,700	30,000	50,600	61,800	64,700	33,900
I - rotor (slug ft ²)	1.31	2.15	1.920	2.460	6,470	21,000	59,773	66,975	124,251	22,270
b - number of blades	3	4	2	3	6	3	3	3	3	3
c - chord (ft)	0.562	0.562	1.75	1.364	1.364	1.971	5.0	5.0	5.0	5.0
R - radius (ft)	12.5	13.167	22.0	26.0	36.0	46.0	56.0	56.0	66.0	66.0
A _b - blade area (sq ft)	21.1	29.63	77.0	108.6	153	455	756	825	925	675
A - disc area (sq ft)	691	944.6	1,520.5	2,205	2,463	4,071.5	6,262	7,854	9,503	5,622
D _L - disc loading (lb/sq ft)	3.40	4.41	4.36	3.22	4.03	9.33	9.29	11.97	6.81	7.69
ω - angular velocity (rad/sec)	50.6	69.2	32.9	22.0	23.2	19.3	15.6/16.7	14.0/15.0	12.7/13.6	17.5/18.8
V _T - tip speed (ips)	6.32	6.60	7.24	5.93	6.60	6.96	7.00/7.90	7.00/7.90	7.00/7.90	7.00/7.90
A_{∞} - parasite area (sq ft)	14.0	5.0	22.0	40.0	36.5	120.0	36.5	36.5	23.1	23.1
V for minimum sink rate (ft/s)	41.4	42.6	54.8	95.0	98.0	60.0	103.3	108.7	98.2	106.9
K _{KEA} - kinetic energy index	3.20	3.90	4.61	3.95	3.26	1.61	3.49/3.72	4.40/4.56	5.47/5.69	3.55/3.65
										2.4/2.41
										2.4/2.41
										3.7/3.76

COMPOUND HELICOPTER STUDY

The study of the compound helicopter was undertaken on a limited basis to identify the compromises in weight, size, complexity, and performance required to attain a substantial increase in cruise speed. For this study, the configuration 3 helicopter (conventional fuselage) was compounded and redesignated configuration 5. Compounding was accomplished by the addition of wings and ducted fans for thrust. The resulting increased structural and system requirements were also incorporated into the basic helicopter configuration.

The missions selected to be studied for the compound were transport missions of 200-, 300-, and 500-nautical-mile radii and ferry range. These missions were considered to be run at both sea level and optimum altitude. Three takeoff conditions were studied: hover at sea level standard conditions, hover at 6,000 feet and 95°F, and STOL operation.

In this study, it was determined that the additional complexity required by the compound may be identified as primarily that of adding the wings and thrust fans. Some weight increase is required in the rotor system for dynamic reasons, but this should not affect the blade complexity. The fuselage, of course, is slightly more complex because of the wing loads and increased tail loads and additional ducts to be routed. The flight controls are modified by the addition of aileron controls. Propulsion system controls, valves, and ducting must be expanded in number and complexity for the compound version.

PROPULSION SYSTEM FOR COMPOUND HELICOPTER

The propulsion system for the compound helicopter is shown schematically in Figure 47. For helicopter operation, the gas is ducted up through the rotor in the normal manner. For operation as a compound, the gas is diverted to drive the ducted fans. One-half the output of each engine is routed to each of the ducted fans, to minimize the problems associated with single-engine operation.

WEIGHTS FOR COMPOUND HELICOPTER

The consideration of compound helicopter operation required modification of some group weight constants and equations and addition of new expressions reflecting this conversion, as discussed in the Weight section of this report.

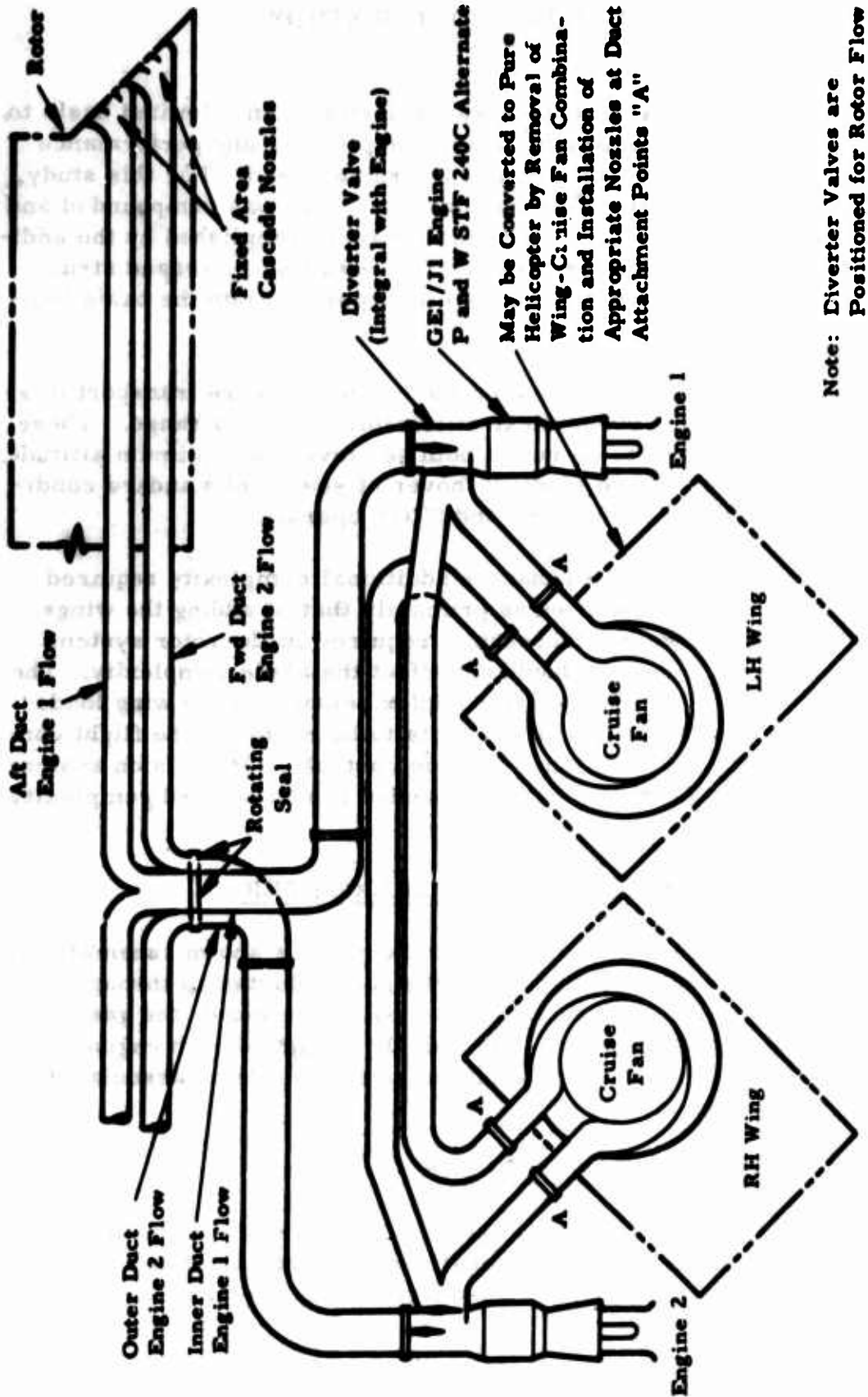


Figure 47. Propulsion System Schematic - Two-Engine Compound Helicopter Installation.

A comparison of the empty weights of the compound version, the pure helicopter, and the same helicopters with provisions to be converted to a compound is shown in Table XXVI for a typical case. This shows the compound helicopter to have an empty weight of 7,543 pounds more than the pure helicopter and 2,621 pounds more than the helicopter having provisions for compounding.

TABLE XXVI
EMPTY WEIGHT SUMMARY - HELICOPTER,
COMPOUND HELICOPTER, AND HELICOPTER
HAVING PROVISIONS FOR COMPOUNDING

	Configuration 3 Helicopter	Configuration 5 Helicopter	Configuration 5 Compound
Fixed provisions for compounding			
Rotor	-	905	905
Structure, controls, ducting, etc	-	1,716	1,716
Removable provisions for compounding			
Wings, fans, etc	-	-	4,922
Empty weight	21,080	23,701	28,623

PERFORMANCE OF COMPOUND

Several aspect ratios and wing spans as installed on the configuration 5 compound were included in the parametric study. Table XXVII shows the effect of varying aspect ratio and wing span at both maximum continuous power and power for best range for a 200-, 300-, and 500-nautical-mile mission.

The ferry weight and empty weight are also noted. Figure 48 plots the payload versus mission radius of the compound for various hovering capabilities using an aspect ratio of 10 and a wing span of 65 feet. Also shown in this figure is the estimated curve for the pure helicopter (configuration 3) performing the optimum altitude mission with a 6,000-foot 95°F and with a sea-level standard-day hovering capability. The ferry range for the compound is 2,886 nautical miles, compared with 2,040 nautical miles for the configuration 3 helicopter.

TABLE XXVII
SUMMARY - PAYLOAD AND FERRY RANGE
(At Altitude for Best Range)

Wing Span (ft)	Aspect Ratio	Payload (Tons) for Mission Radii of 200, 300, and 500 nmi										Ferry Range (nmi)	Empty Weight (lb)		
		Hover - 6,000 ft 95° F			Hover SL Std			STOL							
		200	300	500	200	300	500	200	300	500	200				
Maximum Continuous Power															
65	8	8.14	6.42	3.00	16.74	14.30	9.46	17.01	14.55	9.73	2,226	28,315			
75	8	7.97	6.38	3.21	16.63	14.65	10.51	17.66	15.35	11.47	2,359	28,708			
85	8	7.62	6.02	2.88	16.44	14.33	10.15	19.59	17.25	13.34	2,523	29,062			
55	10	8.09	6.06	2.67	16.30	13.29	8.11	16.13	13.13	7.95	2,135	28,257			
65	10	8.15	6.42	3.05	16.81	14.38	9.58	17.03	14.59	9.79	2,886	28,669			
75	10	7.99	6.40	3.28	16.71	14.77	10.63	17.21	15.23	11.11	2,358	29,079			
85	10	7.65	6.08	2.96	16.55	14.45	10.32	18.01	15.89	11.72	2,756	29,485			
55	12	8.04	6.04	2.64	16.30	13.29	8.12	16.09	13.07	7.90	2,146	28,515			
65	12	8.10	6.40	3.02	16.81	14.38	10.23	17.01	14.57	9.81	2,255	28,976			
75	12	7.95	6.37	3.27	16.71	14.78	10.67	16.70	14.77	10.65	2,830	29,435			
85	12	7.60	6.03	2.91	16.72	14.78	10.95	17.03	15.08	11.28	2,339	29,892			
Power for Best Range															
55	6	8.14	6.24	2.92	16.29	13.42	8.48	16.48	13.61	8.64	2,252	27,708			
65	6	8.04	6.43	3.27	16.61	14.23	9.70	17.59	15.28	10.68	2,416	28,011			
75	6	7.84	6.20	3.06	16.47	14.24	10.42	19.74	17.42	12.74	2,594	28,310			
55	8	8.22	6.34	3.05	16.46	13.63	8.73	16.56	13.72	8.81	2,286	27.991			
65	8	8.21	6.57	3.46	16.38	14.48	10.03	17.34	14.97	10.48	2,436	28,315			
75	8	8.05	6.53	3.63	16.75	14.57	10.82	18.00	15.79	11.95	2,582	28,708			
55	10	8.22	6.35	3.08	16.51	13.70	8.83	16.57	13.75	8.88	2,302	28,257			
65	10	8.22	6.59	3.52	16.90	14.57	10.17	16.90	14.58	10.17	2,431	28,669			
55	12	8.18	6.32	3.06	16.51	13.71	8.86	16.53	13.73	8.88	2,310	28,515			
65	12	8.18	6.56	3.51	16.90	14.59	10.21	16.85	14.54	10.16	2,444	28,976			

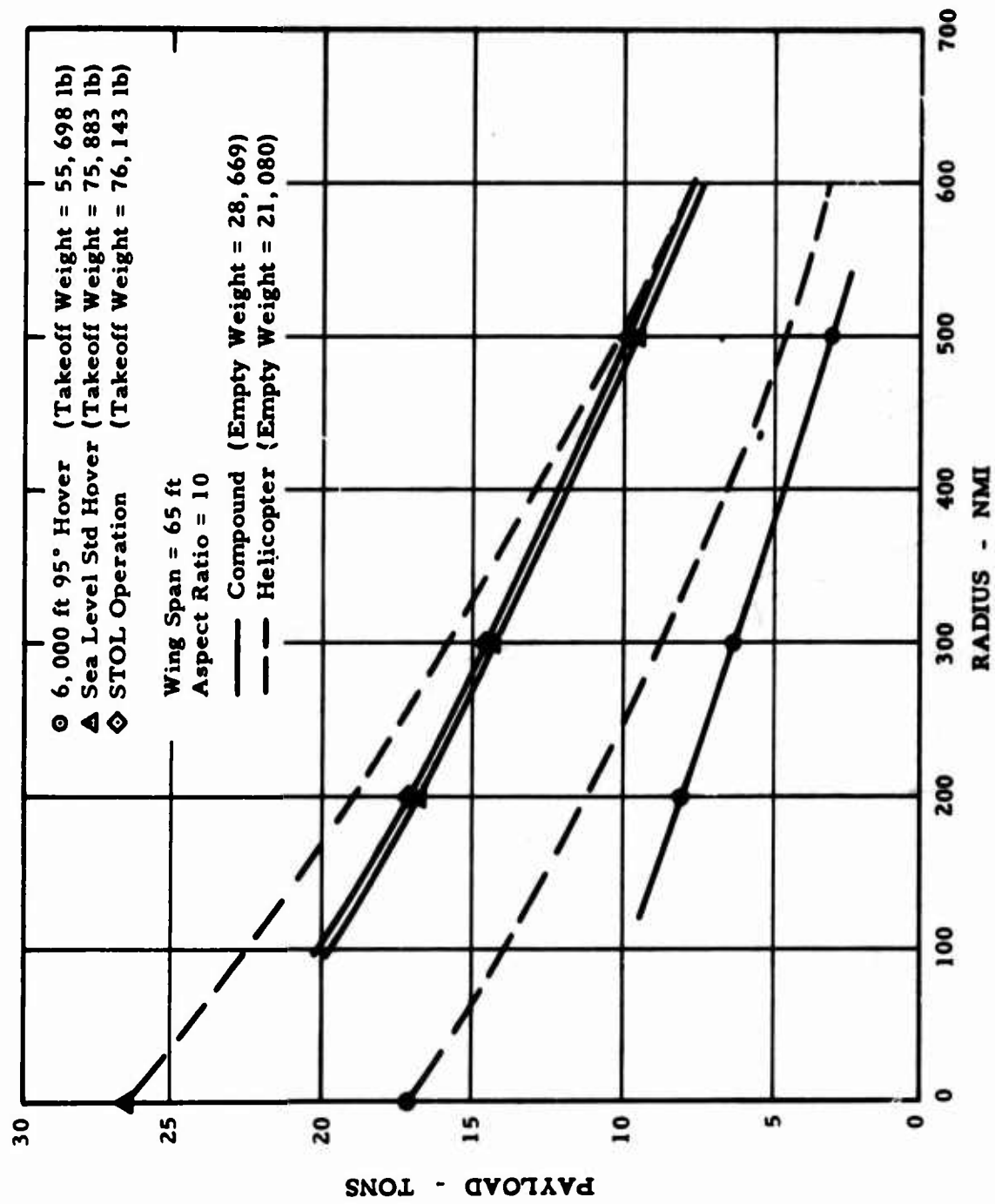


Figure 48. Payload Versus Mission Radius for Compound Helicopter.

The average cruise speed for the transport mission is approximately 225 knots at power for best range, 255 knots for maximum continuous power as a compound, and approximately 110 knots as a helicopter. A productivity parameter that takes this speed difference into account may be expressed as follows, and is shown plotted against range in Figure 49.

$$\text{Productivity} = \frac{\text{payload (lb)} \times \text{speed (kn)}}{\text{weight empty (lb)}}$$

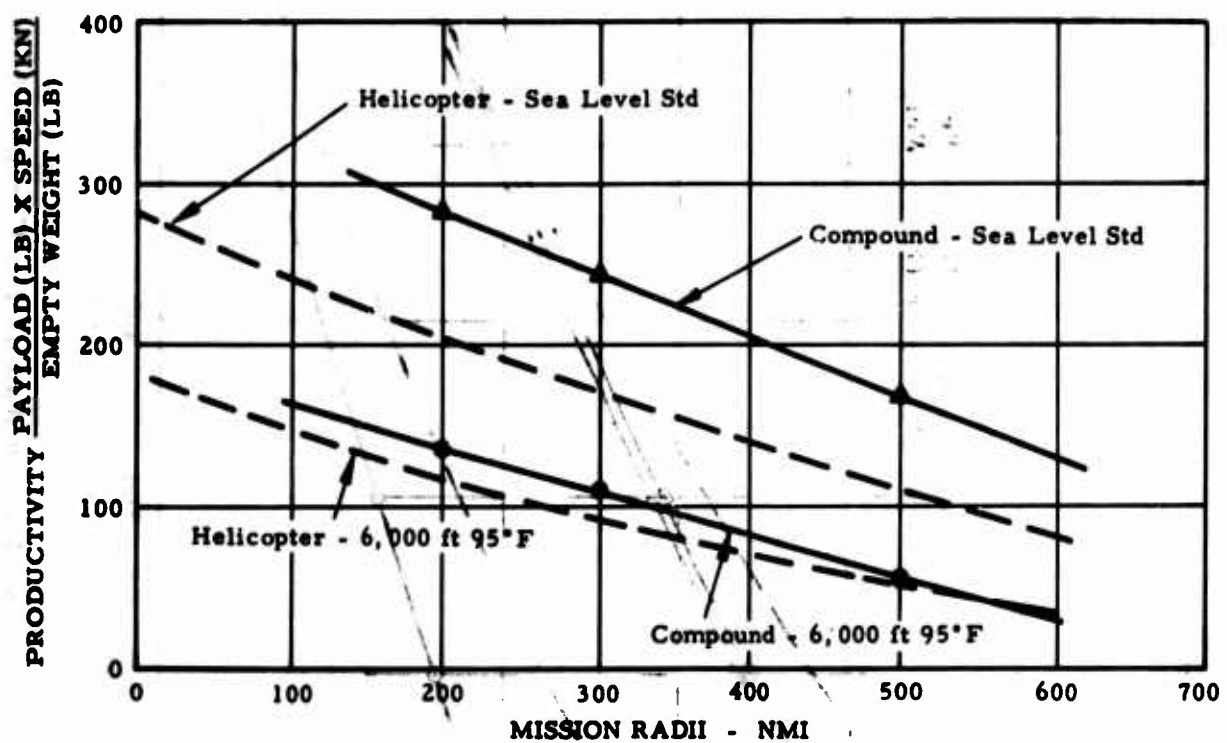


Figure 49. Productivity - Compound Helicopter.

FULLY COUPLED BLADE RESPONSE AND DYNAMIC STABILITY ANALYSIS USING SADSAM IV

INTRODUCTION

SADSAM IV is a digital computer program that was developed by the MacNeal-Schwendler Corporation under contract to the Hughes Tool Company. The development of this program has been summarized and previously submitted in Reference 1.

The program can be applied to the full range of helicopter dynamic problems, including fuselage vibration analysis and all types of rotor dynamic analysis. A nonlinear representation of blade air loads, including lift and moment hysteresis, is incorporated in the program to provide capability for fully coupled blade loads analysis in forward flight.

Problem formulation is generalized to permit application to any structural configuration. The structure is described by means of lumped elements. Problem size is limited to maximize computing efficiency by ensuring that most mathematical operations are accomplished using only high-speed core storage.

PROGRAM CAPABILITY

PROBLEM TYPES

The program is designed to treat structural dynamics problems in which the structure is described by lumped linear elements (springs, masses, dampers, and leverage devices). The user of the program specifies the manner in which the elements are connected. The program is, therefore, applicable to any structural configuration, including, for example, bridges, buildings, fixed-wing aircraft, and helicopter rotors.

In addition, a stripwise formulation of subsonic aerodynamic theory is incorporated into the program for the specific purpose of simulating, when required, the air loads on a rotor blade in hovering or in forward flight.

The following types of mathematical analysis can be performed with the program:

1. Determine vibration modes of an undamped, linear, conservative structure.

2. Determine the complex eigenvalues (or roots of the stability equation) of a damped, linear, unconservative system. The primary application of this provision is flutter analysis.
3. Determine the response of a damped or undamped, conservative or unconservative, linear system to sinusoidal excitation at a sequence of discrete frequencies.
4. Determine the response of a damped or undamped, conservative or unconservative, linear or nonlinear system to transient excitation with prescribed time history.

PROBLEM SIZE

The maximum number of degrees of freedom is 50. The maximum number of elements in each class (springs, masses, dampers, and leverage devices) is 99. These limitations are translated below into the maximum number of spanwise stations for various idealizations of a rotor blade.

Rotor Blade Idealization	Number of Stations
1. Flapwise bending only	49
2. Flapwise bending and twist	25
3. Flapwise and chordwise bending	24
4. Flapwise bending, chordwise bending, and twist (fully coupled)	16
5. Same as (4) but including chordwise shear flexibility (thereby making chordwise bending slope an independent degree of freedom)	12

MATHEMATICAL METHODS

REDUCTION OF PROBLEM TO MATRIX FORM

The first step performed by the computer in the solution of any problem is to reduce the problem to the following matrix form:

$$[M_p^2 + B_p + K] \{x\} = \{F\} \quad (47)$$

where

$$p = \frac{d}{dt}$$

[M] = mass matrix

[B] = damping matrix

[K] = stiffness matrix

{x} = vector of independent displacements

{F} = vector of applied forces including, for transient analyses only, nonlinear functions of the independent displacements

Because of the presence of leverage devices that impose constraints on components of displacement, the total number of "node" points to which elements are connected exceeds the number of independent displacements. The computer program senses this fact, selects an independent set of displacements, and refers all mass, stiffness, and damping properties to that set. The method used is substantially the same as that described in Reference 21.

DETERMINATION OF FREQUENCY RESPONSE

Frequency response is obtained by replacing p by $i\omega$, where ω is a specified real number in equation (47) and solving for {x} in terms of a given {F}. {F} may have components. The user has the option of specifying a level of structural damping by substituting $(1+ig) \cdot [K]$ for [K]. An efficient method of triangular resolution, Reference 22, is employed in solving for {x}.

EXTRACTION OF EIGENVALUES AND EIGENVECTORS

Eigenvalues and eigenvectors for both damped and undamped systems are obtained by a special algorithm developed by the MacNeal-Schwendler Corporation. The basis of the algorithm is that if {F} in equation (47) is a specified vector and if p is approximately equal to an eigenvalue ($p = r_k + \epsilon$), then all components of {x} will be large. In fact, in the neighborhood of the k^{th} eigenvalue, any particular component of {x} is approximated by

$$x_j = \frac{A_{jk}}{p - r_k} + C_{jk} \quad (48)$$

where r_k , A_{jk} , and C_{jk} are constants.

The algorithm essentially consists of the following steps:

1. Evaluate x_j for three trial values of p by solving equation (47) with $p = p_1, p_2, p_3$.
2. Solve for A_{jk}, C_{jk} , and r_k using equation (48).
3. Replace one of the p_i 's by the value r_k estimated from step (2). Replace the p_i that is farthest from r_k .
4. Repeat steps (1), (2), and (3) to convergence. In trial applications, convergence to six significant figures is obtained in approximately six iterations.

The algorithm is provided with means for sweeping previously found eigenvalues and for testing convergence. All roots within a frequency band specified by the user will be found.

EVALUATION OF TRANSIENT RESPONSE

Transient response is evaluated by direct numerical integration of the equations of motion rather than by modal decomposition. The integration algorithm has been carefully selected to avoid numerical instability while maintaining accuracy. It therefore permits the use of relatively large time steps. The algorithm is described in Reference 23.

TREATMENT OF ROTOR BLADE AERODYNAMICS

Strip theory is used; that is, the aerodynamic forces at a given station are calculated using the translations and rotations at that station. A linear, incompressible formulation is used for flutter analysis. The linear formulation, which is essentially identical with that presented in Reference 24, is summarized by the following equations for the forces and moments acting on a strip. The formulation includes mechanical Coriolis effects.

$$P_Z = \Delta r \left\{ \pi \rho (\Omega r)^2 c \left[a \frac{3}{4} + \frac{c}{4 \Omega r} (\dot{\theta} + \Omega \beta) \right] \right\} \quad (49)$$

$$P_x = \gamma_0 P_Z - \Delta r m \Omega \sin \alpha \cdot \dot{z} \quad (50)$$

$$M = \left(x_{ref} - \frac{c}{4} \right) P_Z - \left[\frac{\pi \rho}{8} \Omega r c^3 (\dot{\theta} + \Omega \beta) \right] \Delta r \quad (51)$$

$$\frac{a_3}{4} + \frac{c}{4\Omega r} (\dot{\theta} + \Omega\beta) = \dot{\theta} - \frac{1}{\Omega r} [\dot{z} + \gamma_0 \dot{x} + (c - x_{ref}) (\dot{\theta} + \Omega\beta)] \quad (52)$$

where

- \dot{x} = in-plane component of velocity, tangent to cone of rotation, positive aft
- \dot{z} = vertical component of velocity, normal to cone of rotation, positive up, on reference axis
- θ = pitch angle about reference axis, positive leading edge up
- β = spanwise slope, positive tip up
- P_z = vertical force, positive up
- P_x = in-plane force, positive aft
- M = moment about reference axis, positive leading edge up
- $\alpha_{\frac{3}{4}}$ = angle of attack at three-fourths chord
- r = distance from axis of rotation
- Δr = spanwise width of strip
- ρ = air density
- Ω = rotor speed (rad/sec)
- c = chord
- γ_0 = inflow angle
- m = mass per unit length
- a = steady coning angle
- x_{ref} = distance from leading edge to reference axis

It will be noted that:

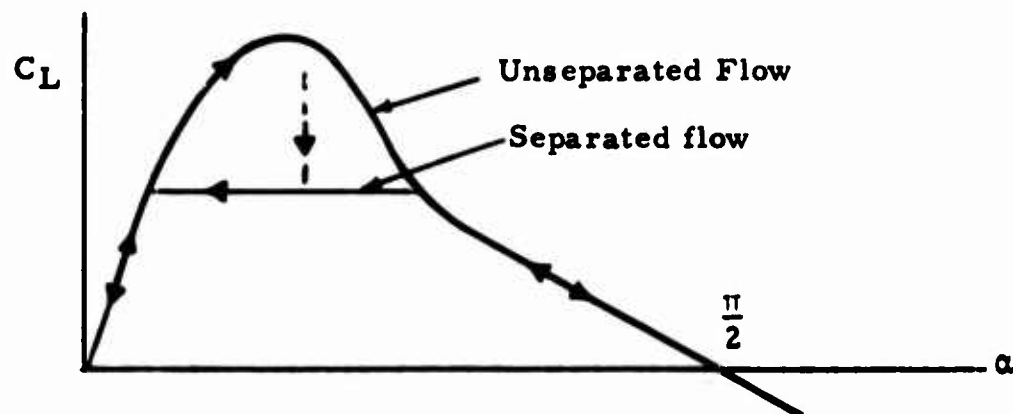
1. $C_{l\alpha}$ is assumed to be equal to 2π .
2. The center of pressure is at the one-fourth chord.
3. Lift deficiency (Theodorsen's function) is ignored.
4. $\Omega\beta$ is added to θ to obtain true pitching velocity relative to the airstream.

5. The second term in equation (50) is all that remains of the Coriolis effect after cancellation with some small aerodynamics terms.
6. The inflow angle, γ_0 , is assumed to be small.

In the nonlinear aerodynamic formulation, additional account is taken of the following:

1. The velocity of the air relative to the blade element can have any magnitude and any direction.
2. Lift, drag, and moment coefficients are nonlinear functions of Mach number and angle of attack.
3. The lift coefficient can be higher than the steady-state value in the stalled region because of rapid change of angle of attack (lift hysteresis).

Lift, drag, and moment coefficients are obtained from reported experiments on specific airfoil sections and are presented to the computer as tabular data. Lift hysteresis is accounted for in the manner shown in the sketch below.



For increasing angle of attack, the lift coefficient follows the upper curve, which is obtained either from experiments on oscillating airfoils or by reasonable extrapolation of the lift curve in the unstalled region. For decreasing angle of attack, or for any subsequent reversal of α in the stalled region, the lift coefficient follows the lower curve, which approximates the steady-state lift coefficient. The transition from the upper curve to the lower curve is abrupt. A separate pair of curves is used for each Mach number.

Moment hysteresis is accounted for by assuming that the center of pressure remains near the one-fourth chord point, as modified by Mach number effect, for unseparated flow, and that it shifts abruptly to the midchord when the flow separates. It is easily shown, incidentally, that energy is transferred from the airstream to the pitch degree of freedom during a hysteresis cycle.

PROBLEM PREPARATION

The first step that must be performed for a new problem is to formulate a lumped mathematical model of the structure using springs, masses, dampers, and leverage devices as elements. The model formulation is most conveniently accomplished by using electric circuit modeling techniques that have been developed for passive analog computers. A complete account of such techniques is given in Reference 25. A detailed application to the dynamic analysis of rotor blades is described in Reference 24.

Once the model is formulated, the elements and the nodes (degrees of freedom) to which they are connected are numbered. Cards are then punched that record the nodes to which each element is connected and the numerical values of the elements. The constants that describe the aerodynamic force coefficients and the nodes on which they act are recorded on separate cards.

Problem input is completed by listing the constants that describe the applied forces and the points at which they act, and by listing the tasks to be performed (steady-state response at specified frequencies, vibration modes in a specified frequency range, and/or transient response in a specified time range).

The model formulation step need not be repeated for a problem that is topologically similar to a previous problem, because the cards that describe interconnection data can be saved. This feature is a great convenience for rotor blade analysis where geometrical configurations tend to be quite similar. Model reformulation will be required only if it is desired to change the basic assumptions (for example, eliminate twist as a degree of freedom), to change the number of spanwise stations, or to change the hub configuration. It should be noted that model reformulation is relatively easy with the program, because it can be accomplished by changes in input data rather than by changes in program instructions.

CORRELATION OF COMPUTED LOADS AND FLIGHT TEST DATA

To verify the ability of the fully coupled rotor dynamic analysis to predict blade loads, a comparison was made of loads measured in high-speed cruise flight on the OH-6A helicopter and loads computed using SADSAM IV with an OH-6A blade model. The OH-6A was selected because it has the same hub configuration chosen for the heavy-lift helicopter; namely, a fully articulated hub with offset flapping hinges and lead-lag hinges with dampers.

For this analysis, a lift curve slope of 5.73/radian was used with a maximum C_L of 1.6. The theoretical drag coefficient of the NACA polar was also used. As the load computation was made at 103 knots, the Mach number effects on lift and drag coefficients were neglected.

The satisfactory correlation of flapwise and chordwise bending moments as computed by this program and as measured in flight on the OH-6A helicopter is shown in Figures 50 and 51. It can be seen in Figure 50 that the flapwise moment at the critical root section is matched almost exactly, and in Figure 51 that the root chordwise moment is also in exceptionally good agreement. On the outboard part of the blade, the computed flapwise moment is somewhat higher than the measured moment, perhaps as a result of the simplified aerodynamic representation used in this example case; the correlation is considered satisfactory even in this region. The computed root torsional moment is ± 124 in.-lb compared with ± 115 in.-lb measured in flight, which is also acceptable verification of torsional loads.

HEAVY-LIFT HELICOPTER BLADE AND HUB CONNECTION DIAGRAM

Having shown the ability of SADSAM IV to predict blade loads accurately, the same method of analysis was applied to the heavy-lift helicopter blade. Details of the blade and hub structure are given under the Structures section in this report. The hub is included in the problem because the root end fixity condition (hinged, cantilever, damper, and so forth) strongly influences blade loads at the root.

The blade was broken down into ten structural cells, each of the general arrangement shown in Appendix V. The blade and hub structural analog, called a connection diagram, is presented in Appendix IV. This connection diagram shows the masses, stiffness values, and lengths in the form of condensers, inductors, and transformers, as described in Appendix IV. Specific values of the elements are given in the diagram on page 347 (Appendix IV).

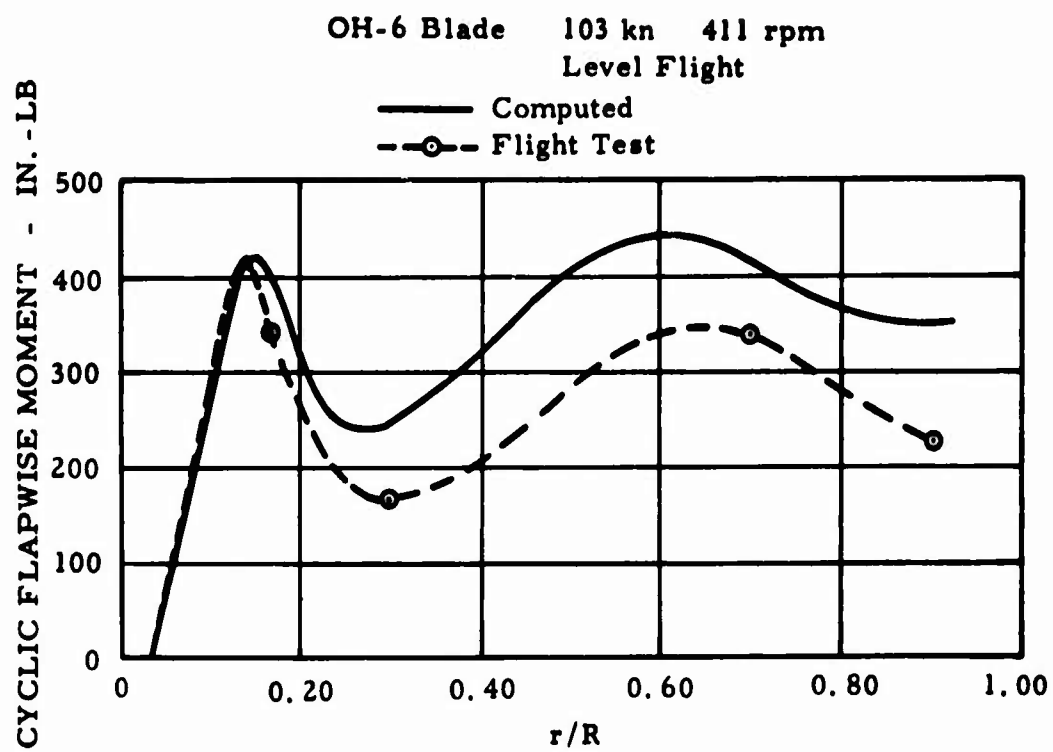


Figure 50. Flapwise Moment Distribution - Comparison of Theory and Flight Test.

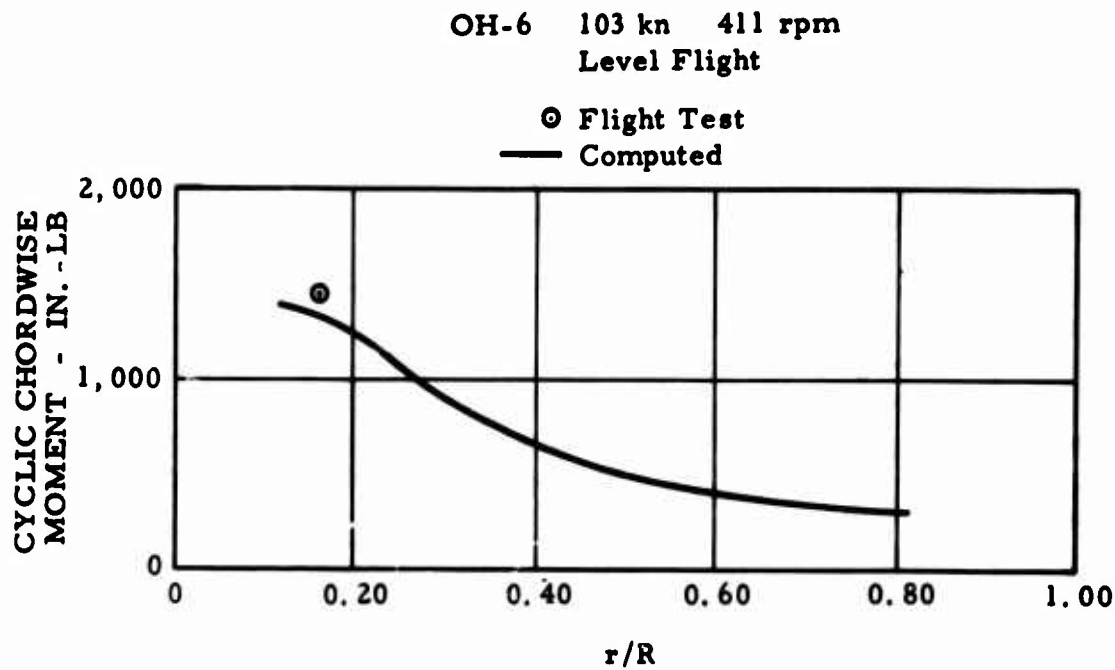


Figure 51. Chordwise Moment Distribution - Comparison of Theory and Flight Test.

RESULTS OF FULLY COUPLED HEAVY-LIFT HELICOPTER STATIC AND DYNAMIC LOADS ANALYSIS

BLADE AND CONTROL SYSTEM LOADS

The computed blade loads for static and fatigue design purposes are shown in Figures 52 through 55. Some minor modifications to these loads were made in lieu of minor adjustments to the computer program. Typical samples of the unmodified computer output may be found in Appendix VI. The cyclic flapwise bending moments were multiplied by the ratio of actual moment in the OH-6 to computed moment for the OH-6, and the result is shown in Figure 52.

Since the lead-lag damper has a constant moment independent of amplitude (for the small amplitudes encountered here), the cyclic chordwise moment at the lead-lag hinge must match the known damper moment. Figure 53 shows the result of making this adjustment.

Two sources of conservatism are present in the cyclic flapwise loads. First, chordwise-flapwise coupling causes increased flapwise moment because of the excessive chordwise moment. Second, the thrust developed in the computed condition is 60,000 pounds, compared with 52,744 pounds for the actual design condition. Cyclic flapwise moment is therefore too high by approximately the ratio of the thrusts (60,000/52,744).

Figures 54 and 55 show the maximum loads developed in a pullup to the maximum attainable load factor for this flight condition (tip speed = 675 fps, forward speed = 110 knots, gross weight = 66,000 pounds).

DYNAMIC AND EROELASTIC INSTABILITY OR FLUTTER

Examination of the transient and steady-state blade load versus time plots indicates convergence to a steady-state or decreasing load level for all structural elements. This indicates the existence of positive real parts of the eigenvalues for all modes at the flight condition studied (namely, 110-kn forward speed, 675-ft/sec tip speed, sea level standard atmosphere, 60,000-lb gross weight). Freedom from flutter is therefore substantiated at this condition.

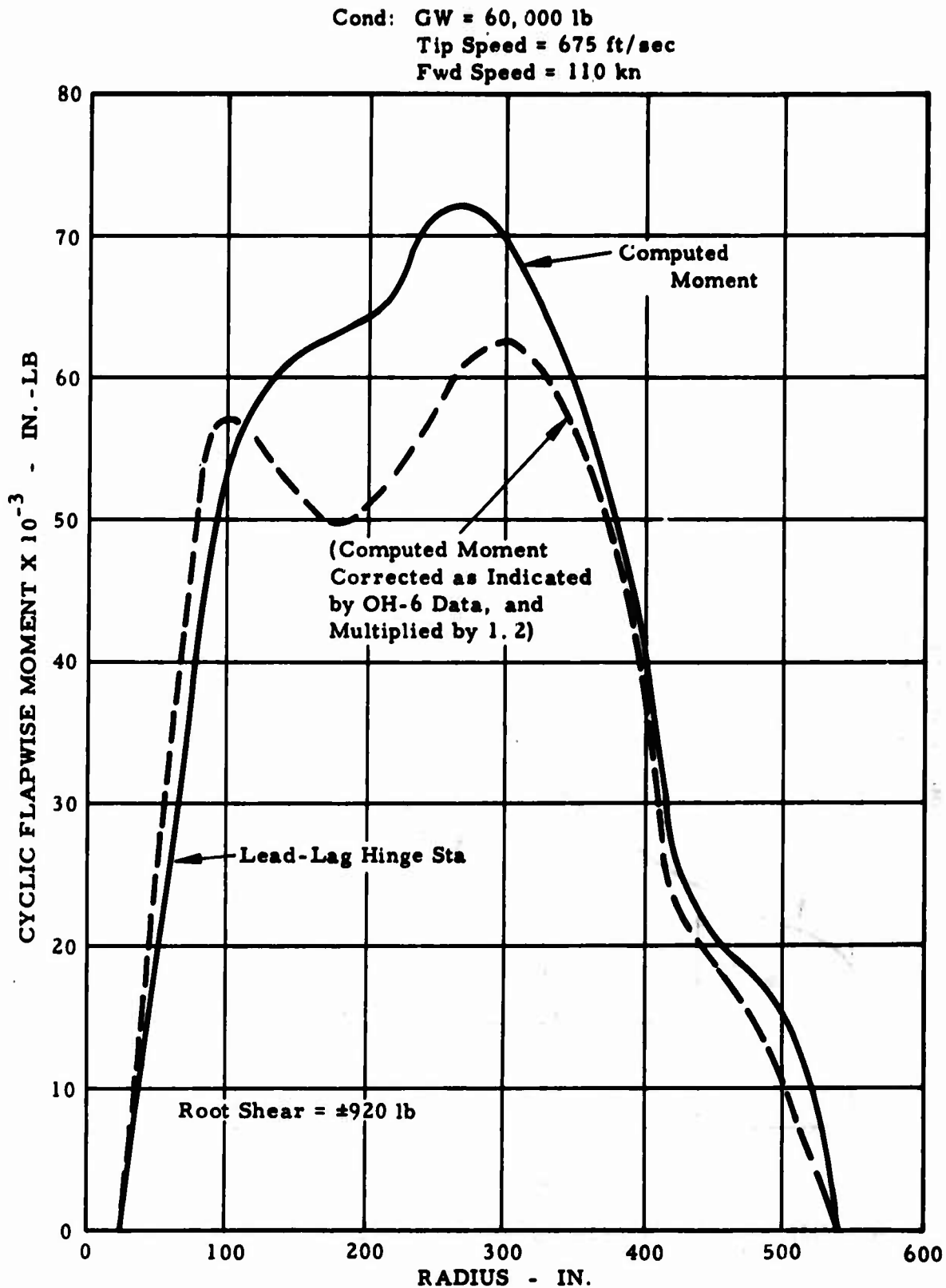


Figure 52. Cyclic Flapwise Moment Distribution.

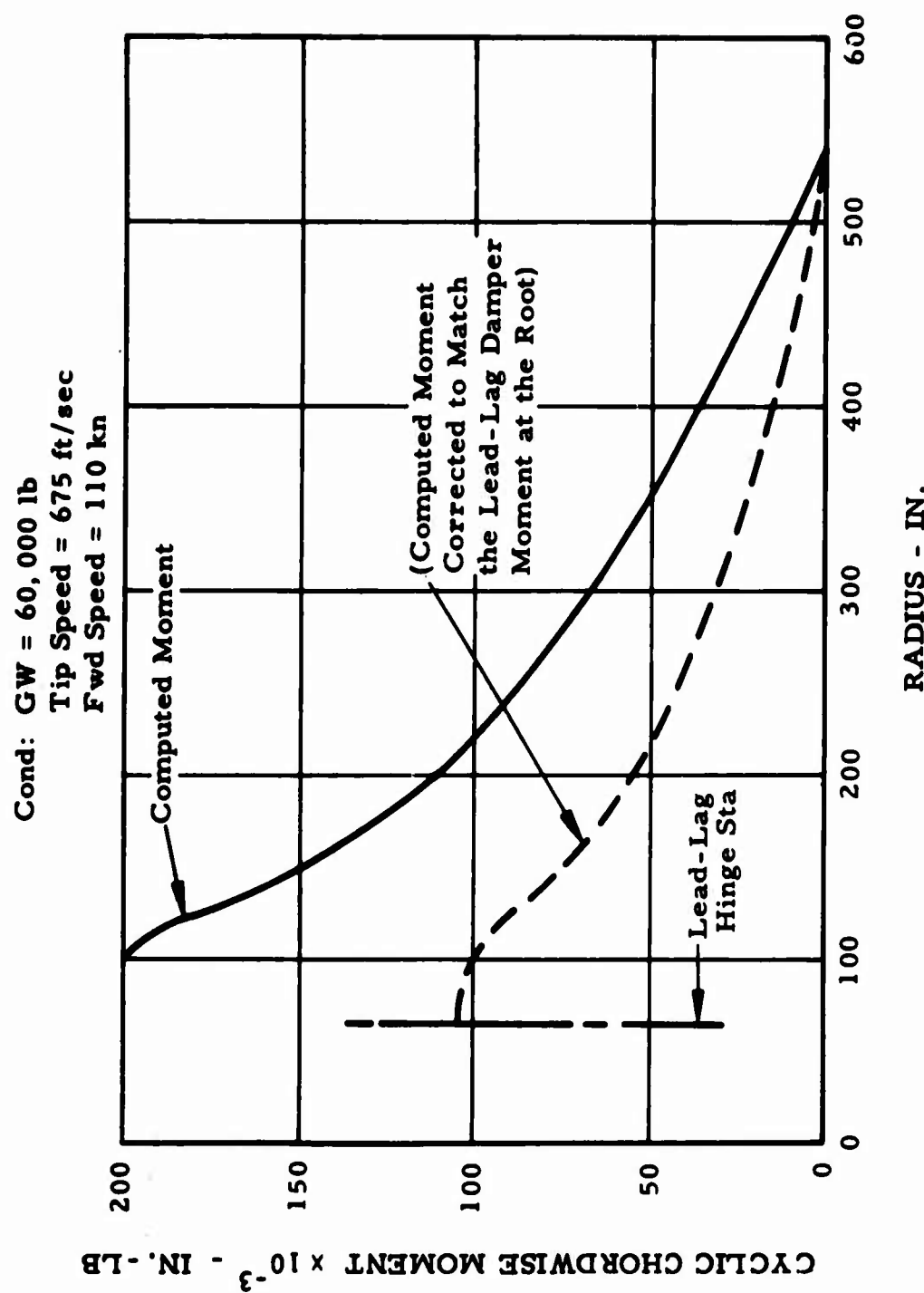


Figure 53. Cyclic Chordwise Moment Distribution.

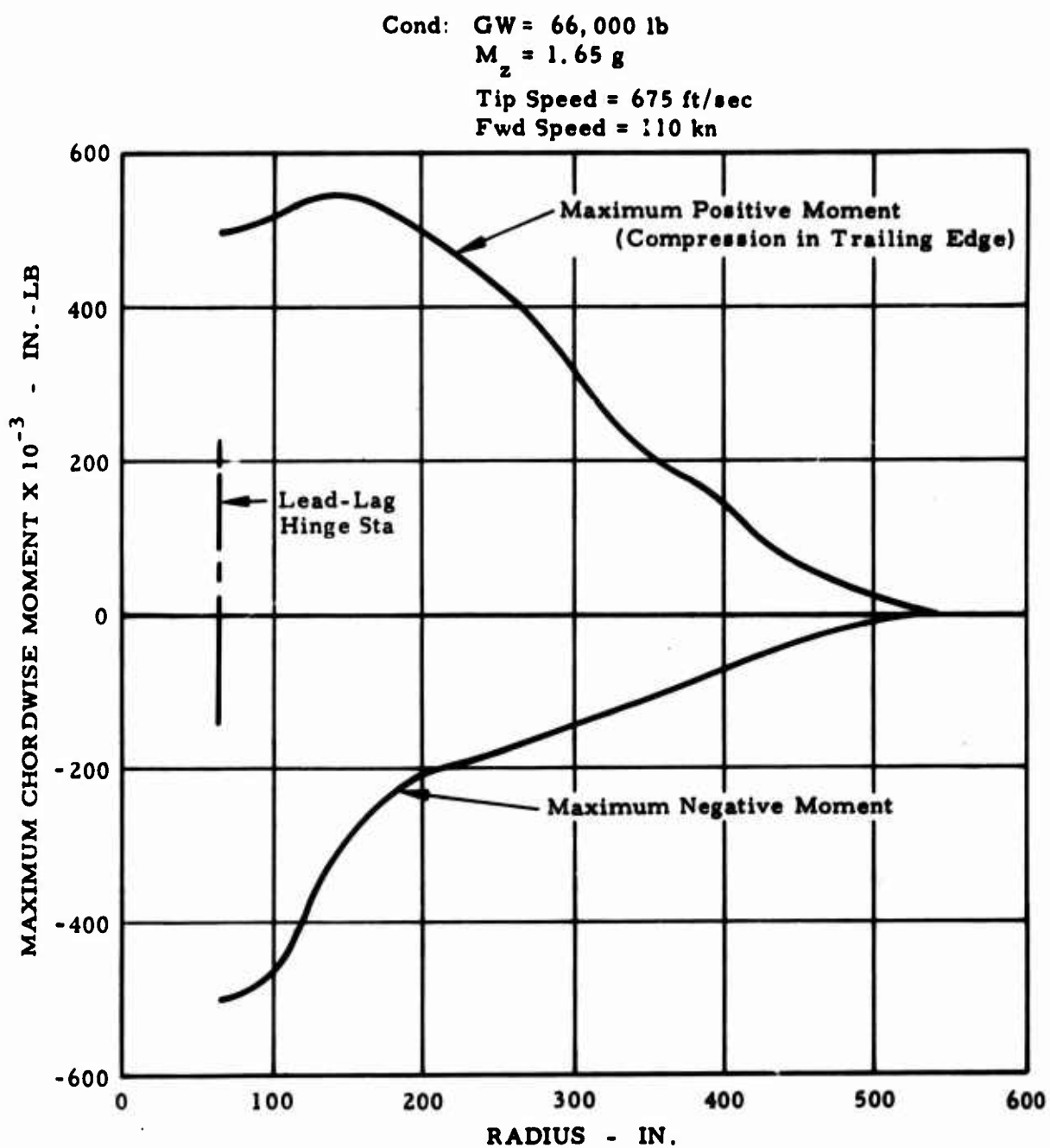


Figure 54. Maximum Chordwise Moment Distribution.

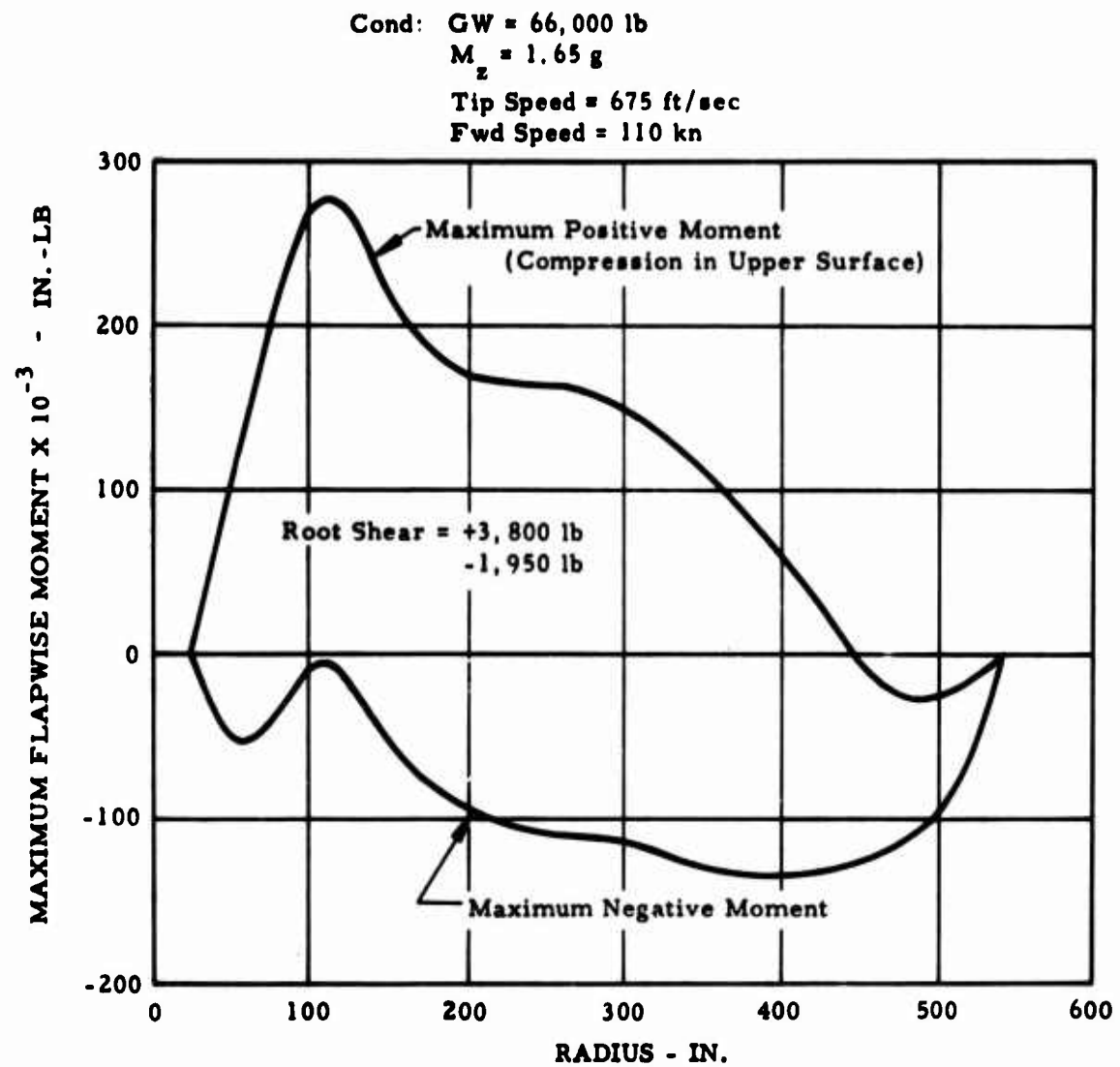


Figure 55. Maximum Flapwise Moment Distribution.

HUB MOCKUP

DESCRIPTION

A full-size mockup of the proposed Hot Cycle heavy-lift helicopter rotor hub has been designed and fabricated. The parts that have been simulated are the mast, swashplate and lift link, ducting from rotating seal to blade constant section, hub structure, torque tube, retention straps, torque flexures, lead-lag damper, and the blade transition area. The various parts have been fabricated from wood for the most part, with some plastic and sheet metal material used as required. The mockup has been built around a vertical standpipe, mounted to a platform, that supports the components in their proper relationship. The mockup has been designed and built in such a manner that components may be moved through their design motions in flapping, feathering, and lead-lag. The completed mockup is shown in Figures 56 through 64.

PURPOSE

The purpose of constructing the mockup was to check the following so that the necessary changes could be incorporated in the design:

1. Structural, control, and duct clearances through the full range and combinations of control movements and blade-hub motions.
2. Structure and controls for simplifications of load paths and fabrication.
3. Ducts for simplification of fabrication and routing for minimum duct losses.
4. Action of the retention straps, droop stops, and lead-lag hinges, stops, and dampers, if applicable.

RESULTS

As a result of constructing the mockup, the following items were accomplished.

1. The centrifugal force load path from the retention straps through the hub structure was simplified by a redesign of the lower plate.
2. Interferences between hub structure and gas ducts were determined, and the design was corrected.
3. A redesign of the torque tube was determined that permitted a more favorable routing of the gas ducts. By narrowing the

outboard end of the torque tube, it was possible to move the ducts in tighter to the feathering centerline, which results in less motion at the articulating duct seals.

4. The lead-lag damper was relocated to shorten the load path.
5. Interferences between the damper support and ducts were determined and corrected.

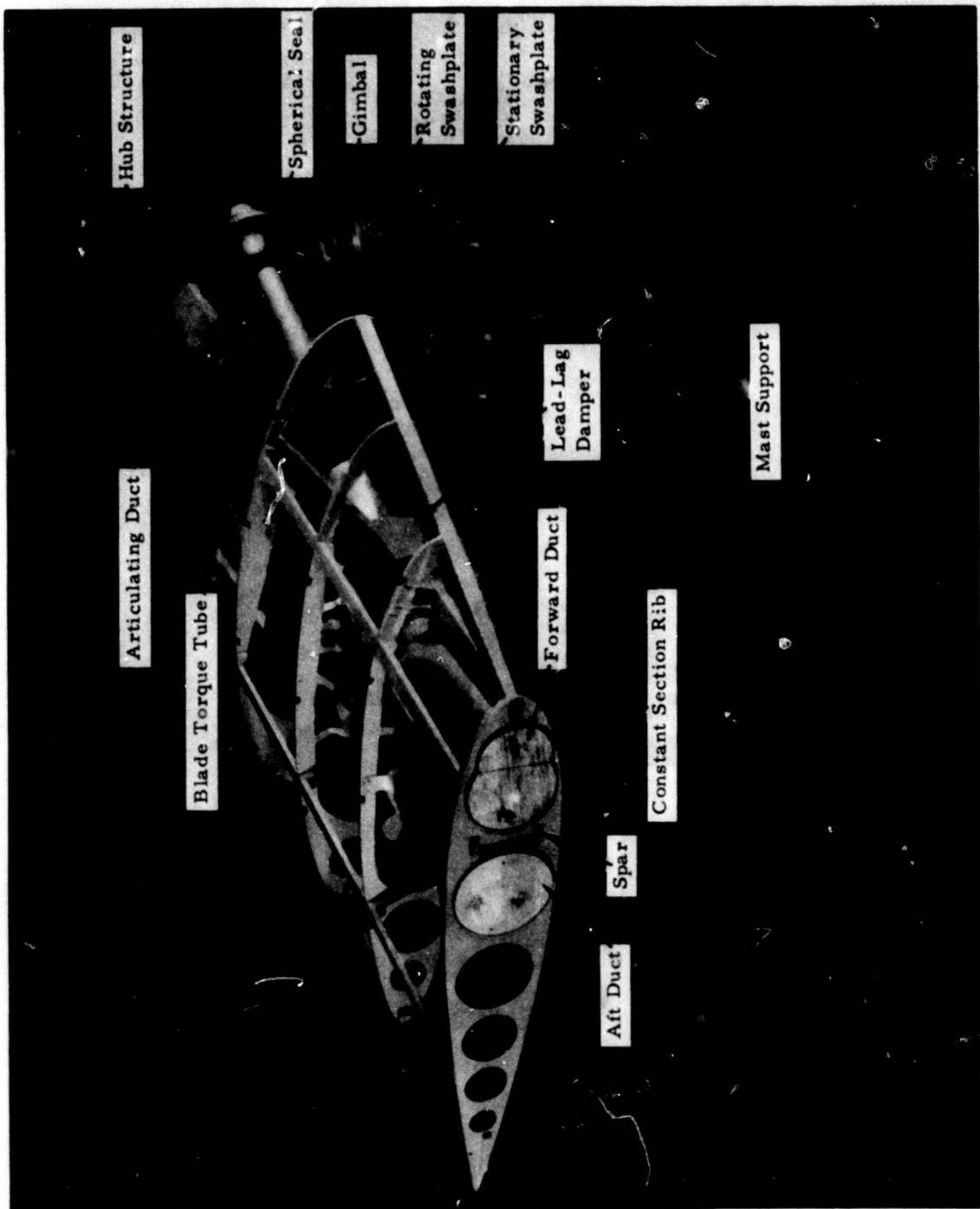


Figure 56. Plan View of Blade Transition Area.

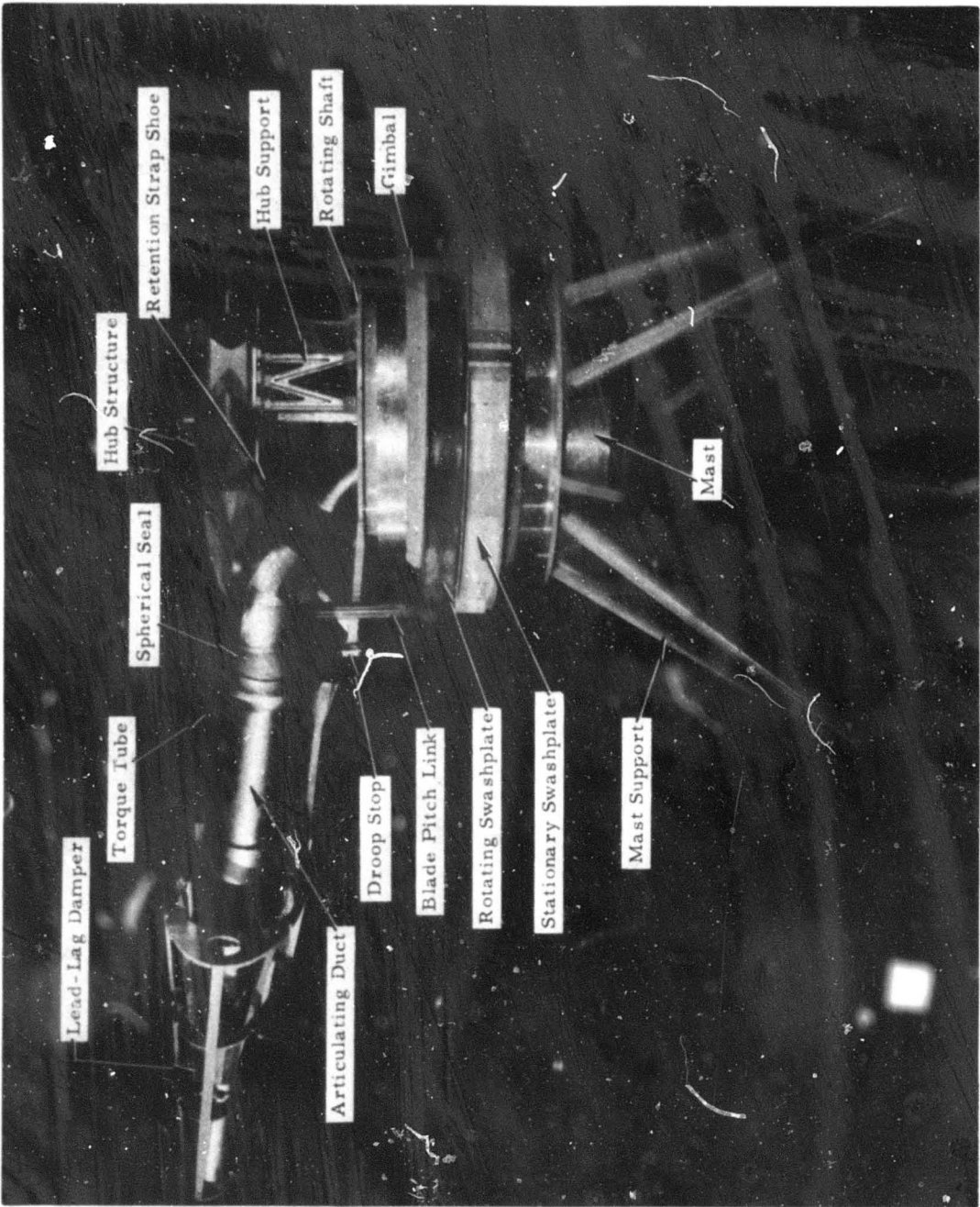


Figure 57. Blade in Cruise Coning Position.

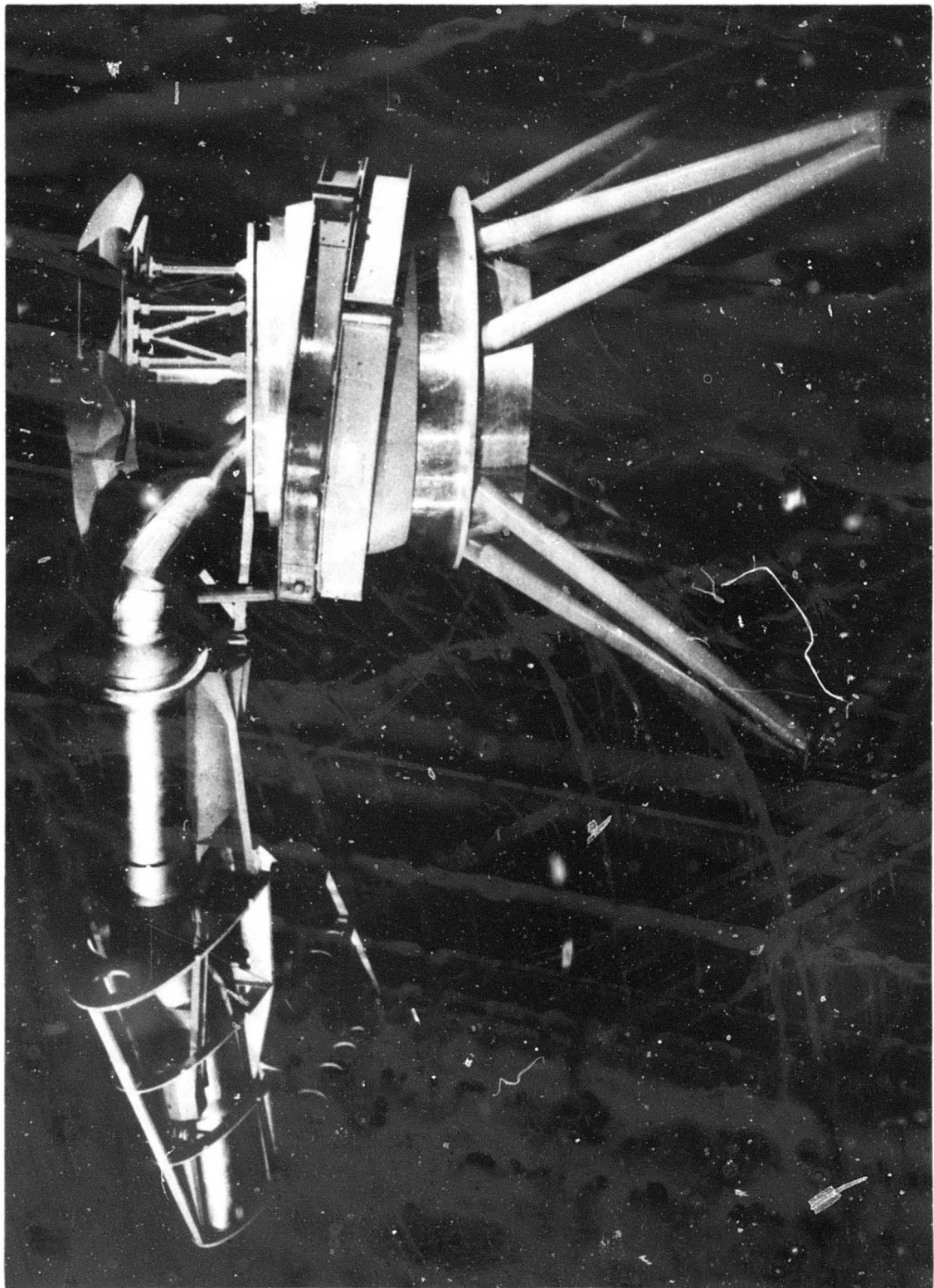


Figure 58. Blade on Droop Stop (Maximum Positive Feathering).

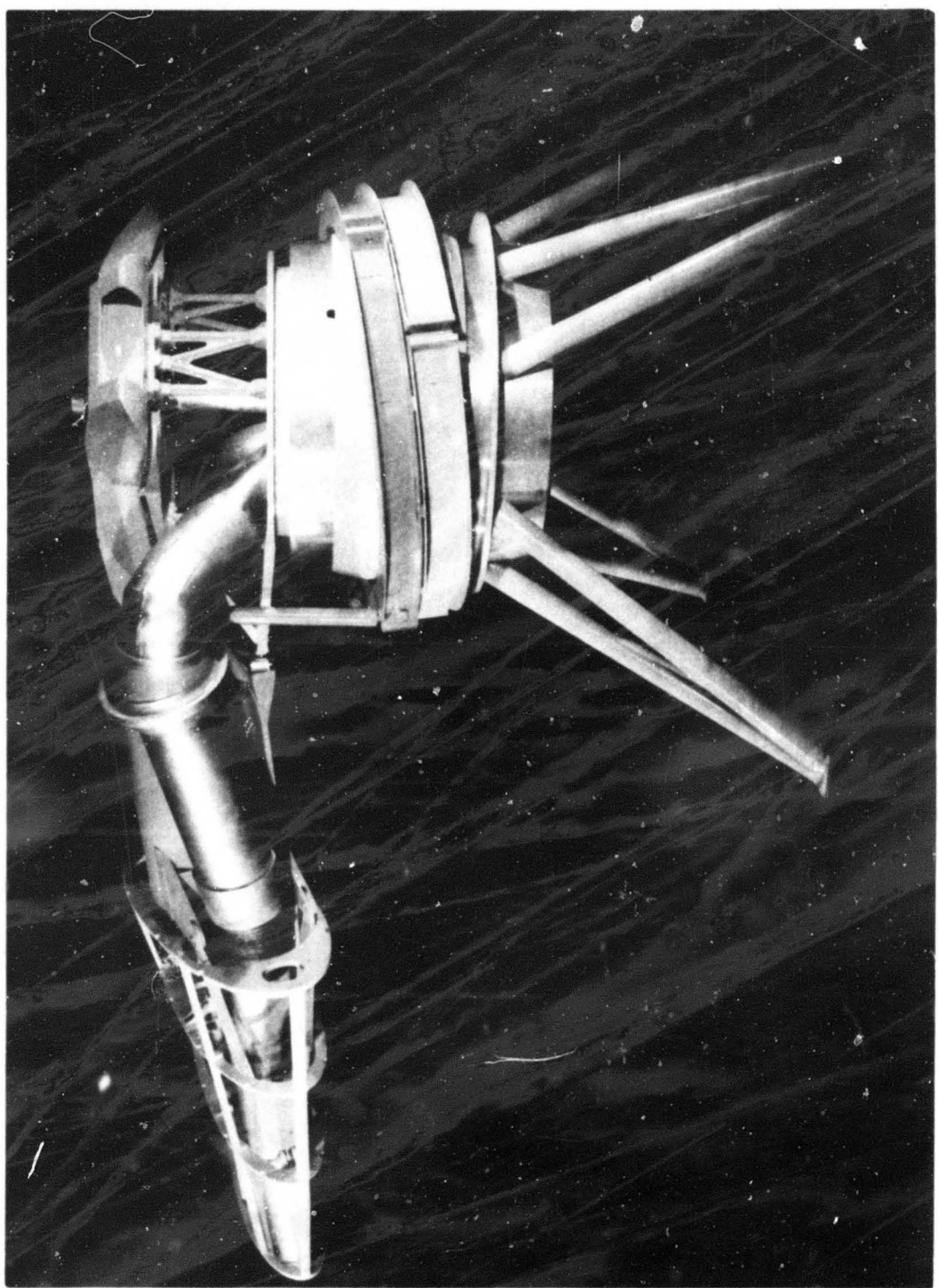


Figure 59. Blade on Droop Stop (Maximum Negative Feathering).

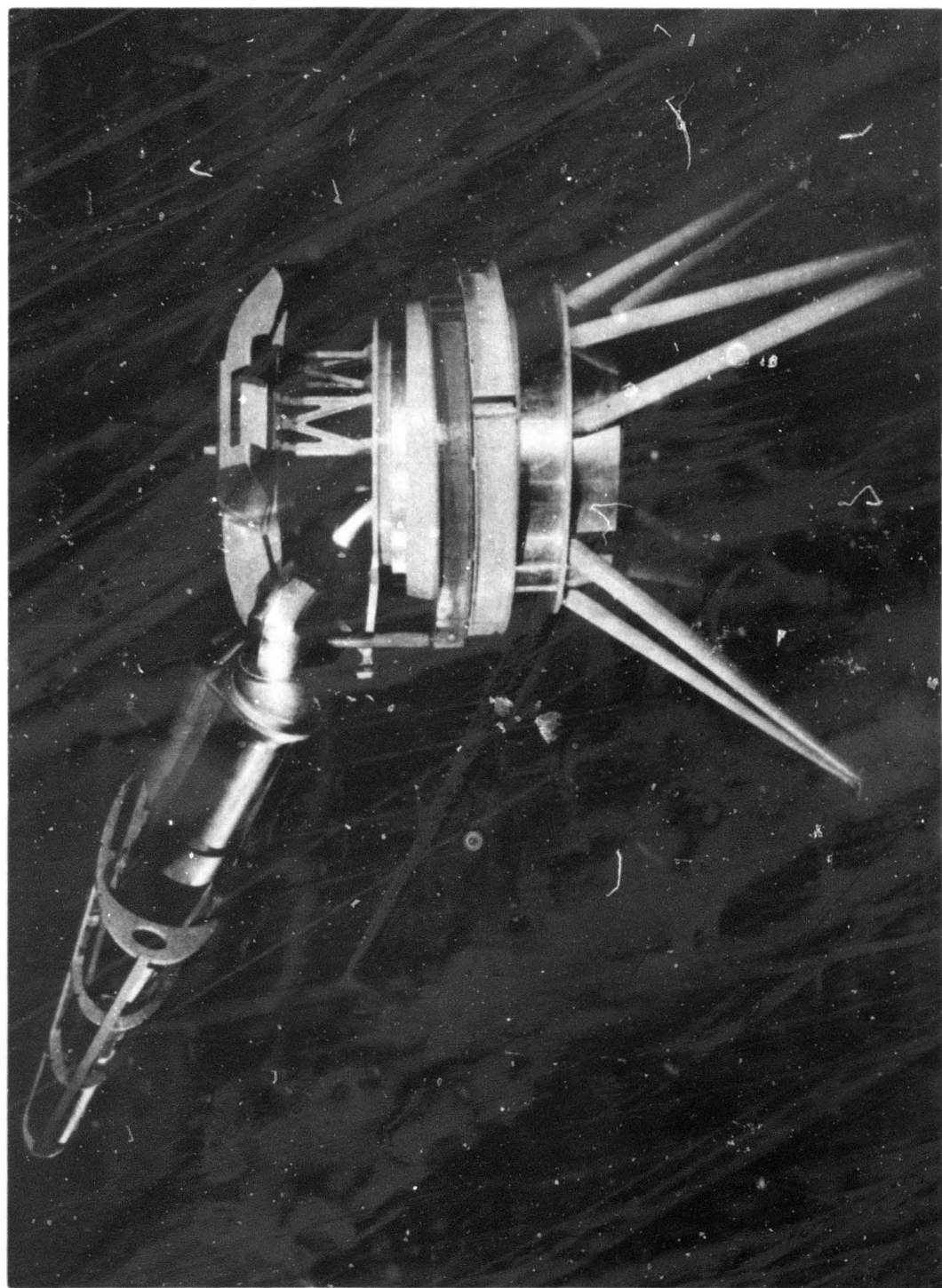


Figure 60. Blade in Maximum Up Flapping Condition.

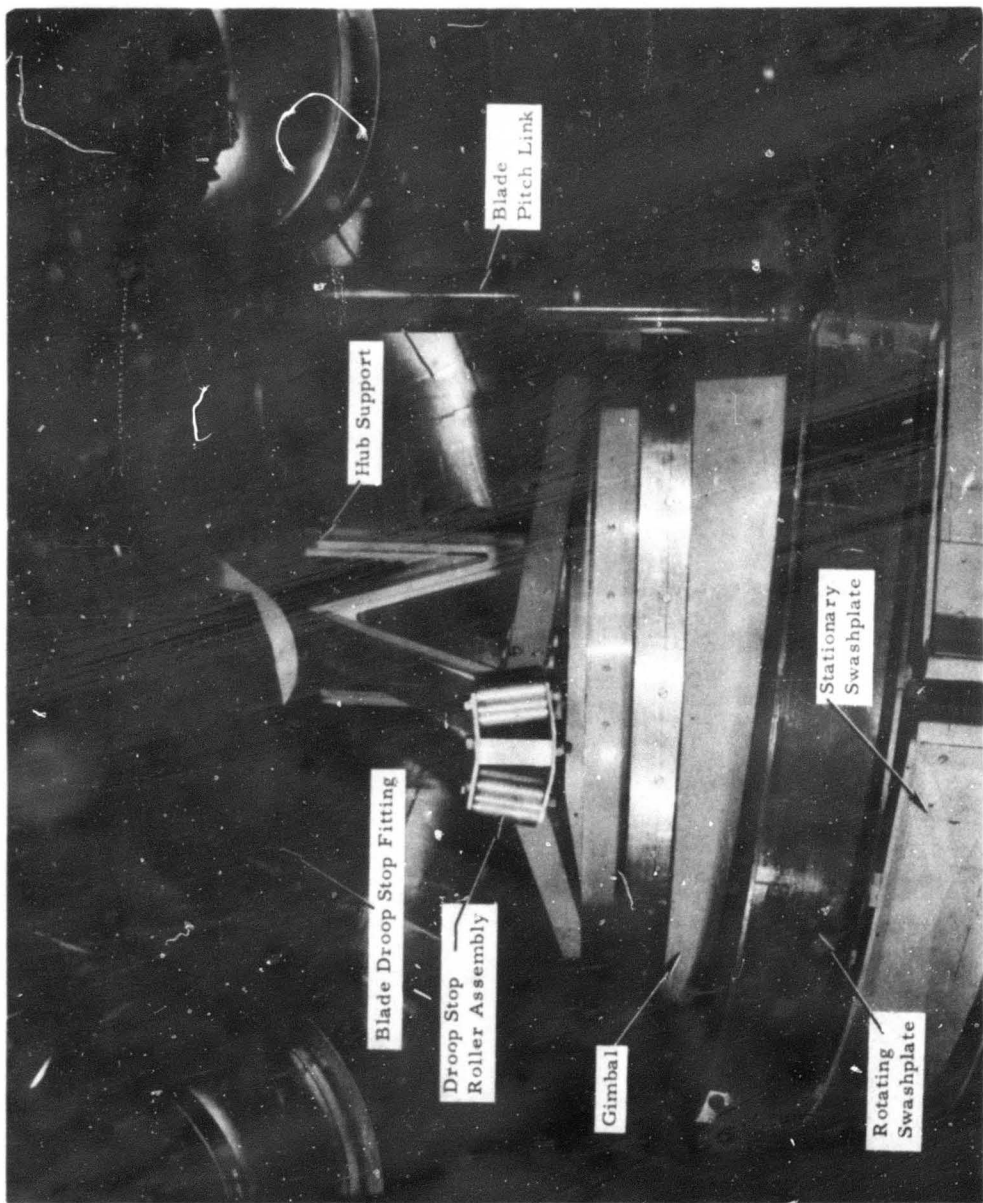


Figure 61. Droop Stop (Blade in Cruise Coning Position).

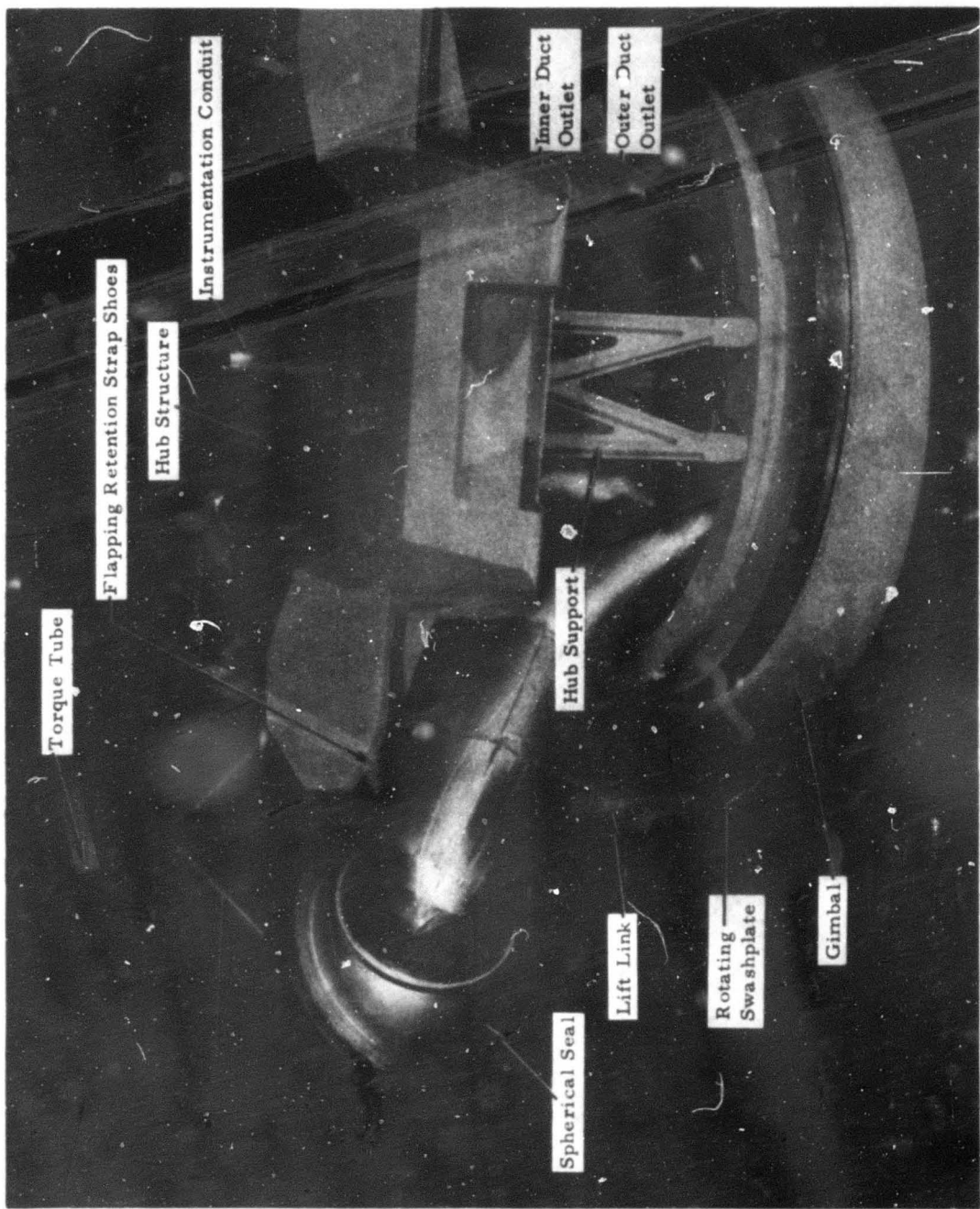


Figure 62. Hub and Duct Configuration.

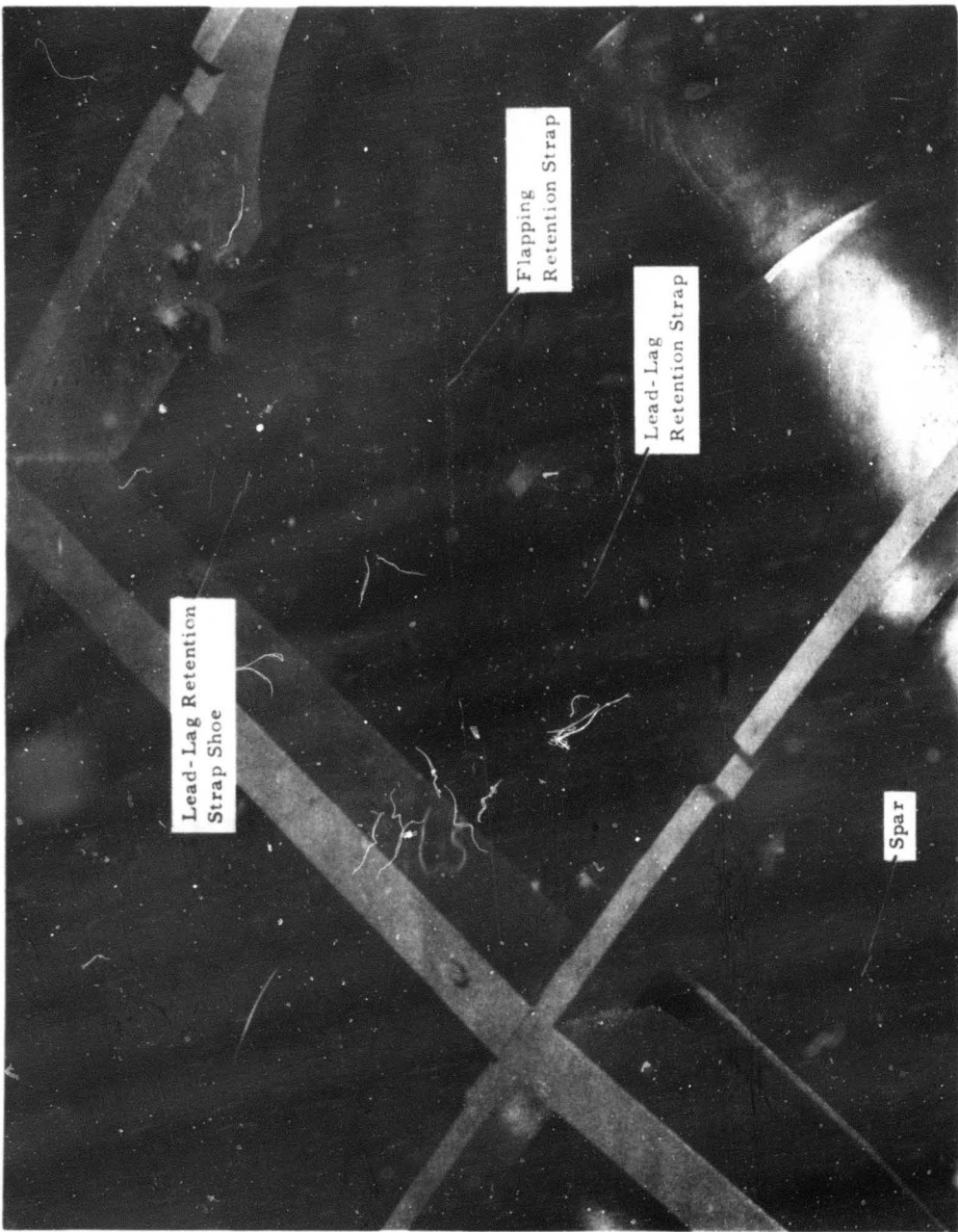


Figure 63. Lead-Lag Strap Retention.

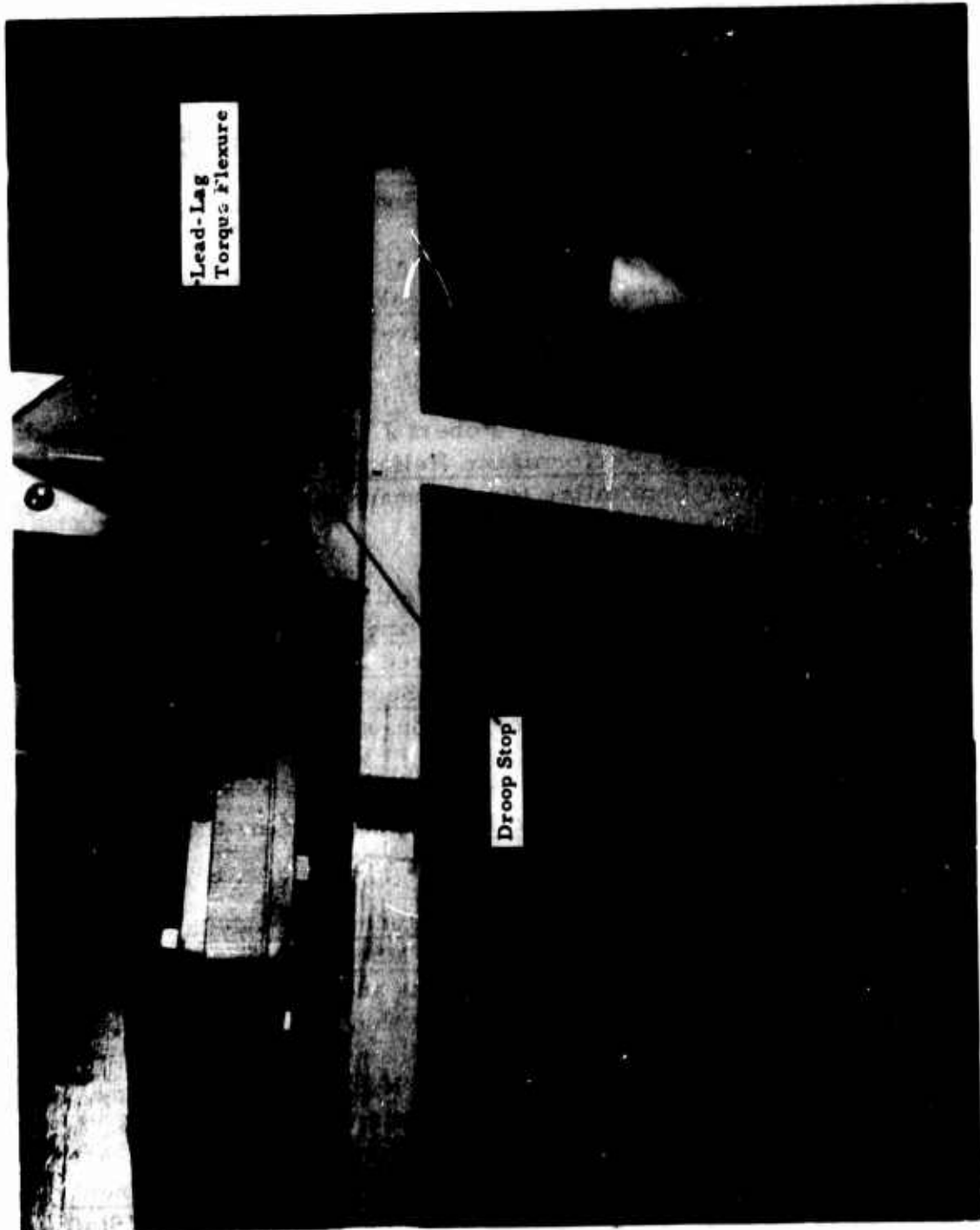


Figure 64. View Looking Up At Lead-Lag Hinge.

REFERENCES

1. A Digital Computer Program for Fully Coupled Blade Loads and Dynamic Stability Characteristics, HTC-AD 65-36, Hughes Tool Company, Aircraft Division, Culver City, California, October 1965.
2. Simpson, J. R., and Lukewille, W., Parametric Study, Hot Cycle 12- to 20-Ton-Payload Heavy-Lift Helicopter, HTC-AD 65-41, Hughes Tool Company, Aircraft Division, Culver City, California, January 1966.
3. LaForge, S. V., Performance Handbook, HTC-AD XA-8016, Hughes Tool Company, Aircraft Division, Culver City, California, January 1965.
4. Gessow, Alfred, and Tapscott, Robert J., Charts for Estimating Performance of High-Performance Helicopter, NACA TN 3323, National Advisory Committee for Aeronautics, Langley Field, Virginia, January 1955.
5. Shivers, James P., and Carpenter, Paul J., Effects of Compressibility on Rotor Hovering Performance and Synthesized Blade Section Characteristics Derived From Measured Rotor Performance of Blades Having NACA 0015 Airfoil Tip Sections, NACA TN 4356, National Advisory Committee for Aeronautics, Langley Field, Virginia, September 1958.
6. Hoerner, S. F., Fluid Dynamic Drag, published by the author, Midland Park, New Jersey, 1958.
7. Wind-Tunnel Investigation of the Longitudinal Aerodynamic Characteristics of Two Full-Scale Helicopter Models With Appendages, NASA TN-D-1364, National Aeronautics and Space Administration, Washington, D. C., July 1962.
8. FAA-Approved Flight Manual, OH-6A, Hughes Tool Company, Aircraft Division, Culver City, California, August 24, 1966.
9. Development of Medium Transport Helicopter CH-47A, Chinook, Technical Report prepared by the Army Materiel Research Staff, University of Pittsburgh for U. S. Army Materiel Command, Report 20-1-1B1, Pittsburgh, Pennsylvania, August 1963.

10. Bell UH-1D Tactical Transport Helicopter, Bell Helicopter Company Brochure, Fort Worth, Texas, (undated).
11. Sikorsky S-64A Heavy-Lift Helicopter, Sikorsky Aircraft Division Brochure SP68, Stratford, Connecticut, March 1963.
12. Carter, E. S. Jr., Technological Contributions of the CH-53A Weapons System Development Program, AIAA Paper 64-784, American Institute of Aeronautics and Astronautics, September 1964.
13. Amer, Kenneth B., Methods for Studying Helicopter Longitudinal Maneuver Stability, NACA Report 1200, National Advisory Committee for Aeronautics, Langley Field, Virginia, 1954.
14. Helicopter Configuration and Propulsion System Study, Part I, Statistical Weight Analysis, Hughes Tool Company, Aircraft Division, Culver City, California, Report 291-W-801, WADC Technical Report 57-583, November 1957.
15. Helicopter Configuration and Propulsion System Study, Part IV, Analytical Procedure for Predicting Rotor Weight, Hughes Tool Company, Aircraft Division, Culver City, California, Report 291-P-101, WADC Technical Report 57-583, November 1957.
16. Yntema, Robert T., Simplified Procedures and Charts for the Rapid Estimation of Bending Frequencies of Rotating Beams, NACA TN 3459, National Advisory Committee for Aeronautics, Langley Field, Virginia, June 1965.
17. One-Dimensional, Compressible, Viscous Flow Relations Applicable to Flow in a Ducted Helicopter Blade, NACA TN 3089, National Advisory Committee for Aeronautics, Washington, D. C., December 1953.
18. Snyder, R. C., Aerodynamic Characteristics of McDonnell Pressure Jet Rotor System at Low and at High Advance Ratios, MAC 6183, McDonnell Aircraft Corporation, St. Louis, Missouri, October 1958.
19. Full-Scale Wind Tunnel Test of a PCA-2 Autogyro Rotor, NACA TR 515, National Advisory Committee for Aeronautics, Washington, D. C., 1935.

20. Wind Tunnel Tests of 10-Foot-Diameter Autogyro Rotor,
NACA TR 552, National Advisory Committee for Aeronautics,
Washington, D. C., 1936.
21. O'Connell, R. F., "A Digital Method for Redundant Structural Analysis", Journal of Aerospace Science, December 1962.
22. McCormick, C. F., Plane Stress Analysis, American Society of Civil Engineers, Third Conference on Electronic Computation, Boulder, Colorado, June 1963.
23. Winemiller, A. F., The Stability of Numerical Integration Algorithms as Applied to Transient Dynamic Analysis, MacNeal-Schwendler Report EC-8, San Marino, California, November 1964.
24. MacNeal, R. H., "Direct Analog Method of Analysis of the Vertical Flight Dynamic Characteristics of the Lifting Rotor With Floating Hub", Journal of the American Helicopter Society, Vol 3, October 1958.
25. MacNeal, R. H., Electric Circuit Analogies for Elastic Structures, John Wiley and Sons, Incorporated, New York, New York, 1962.

APPENDIX I
SUMMARY WEIGHT STATEMENT
AND DETAILED WEIGHT CALCULATIONS

MIL-STD-451, PART I

NAME _____
DATE _____

PAGE _____
MODEL 395 Config 2
REPORT _____

SUMMARY WEIGHT STATEMENT
ROTORCRAFT ONLY
ESTIMATED - CALCULATED - ACTUAL
(Cross out those not applicable)

HOT CYCLE HEAVY-LIFT HELICOPTER
CONFIGURATION 2

CONTRACT _____
ROTORCRAFT, GOVERNMENT NUMBER _____
ROTORCRAFT, CONTRACTOR NUMBER _____
MANUFACTURED BY Hughes Tool Company - Aircraft Division

	Main	Auxiliary
Engine	Manufactured by	General Electric
	Model	GE-1
	Number	2
Propeller	Manufactured by	
	Model	
	Number	

MIL-STD-451, PART 1

NAME	ROTORCRAFT SUMMARY WEIGHT STATEMENT WEIGHT EMPTY			PAGE
DATE				MODEL 395 Config. 2 REPORT
1				
2	ROTOR GROUP			5440
3	BLADE ASSEMBLY			3806
4	HUB			1634
5	HINGE AND BLADE RETENTION			
6		FLAP	PING	
7		LEAD	LAG	
8		PITC	M	
9		FOLD	ING	
10	WING GROUP			
11	WING PANELS-BASIC STRUCTURE			
12	CENTER SECTION-BASIC STRUCTURE			
13	INTERMEDIATE PANEL-BASIC STRUCTURE			
14	OUTER PANEL-BASIC STRUCTURE-INCL TIPS		LBS	
15	SECONDARY STRUC - INCL FOLD MECH		LBS	
16	AILERONS-INCL BALANCE WTS		LBS	
17	FLAPS			
18	-TRAILING EDGE			
19	-LEADING EDGE			
20	SLATS			
21	SPOILERS			
22				
23	TAIL GROUP			1040
24	TAIL ROTOR			70
25	-BLADES			
26	-HUB			
27	STABILIZER-BASIC STRUCTURE			970
28	FIND-BASIC STRUCTURE-INCL DORRAL		LBS	
29	SECONDARY STRUCTURE-STABILIZER AND FIND			
30	ELEVATOR-INCL BALANCE WEIGHT		LBS	
31	KUDDER-INCL BALANCE WEIGHT		LBS	
32				
33	BODY GROUP			2843
34	FUSELAGE OR HULL-BASIC STRUCTURE			
35	BOOMS-BASIC STRUCTURE			
36	SECONDARY STRUCTURE-FUSELAGE OR HULL			
37	-BOOMS			
38	-DOORS, PANELS & MISC			
39				
40				
41	ALIGHTING GEAR-LAND	TYPE		2185
42	LOCATION	ROLLING	STRUCT	CONTROLS
43		ASSEMBLY		
44				
45				
46				
47				
48				
49				
50	ALIGHTING GEAR GROUP-WATER	TYPE		
51	LOCATION	FLOATS	STRUTS	CONTROLS
52				
53				
54				
55				
56				
57				

* Wheels, Brakes, Tires, Tubes and Air.

MIL-STD-451, PART I

NAME _____		ROTORCRAFT SUMMARY WEIGHT STATEMENT WEIGHT EMPTY—Continued			PAGE _____	
DATE _____					MODEL 395 Config. 2 REPORT	
1						
2	FLIGHT CONTROLS GROUP					1414
3	COCKPIT CONTROLS				33	
4	AUTOMATIC STABILIZATION				959	
5	SYSTEM CONTROLS—ROTOR NON ROTATING				260	
6	ROTATING					
7	—FIXED WING					
8					162	
9						
10	ENGINE SECTION OR NACELLE GROUP					460
11	INBOARD					
12	CENTER					
13	OUTBOARD					
14	DOORS, PANELS AND MMC					
15						
16	PROPULSION GROUP					2474
17		X	AUXILIARY	X	X MAIN	X
18	ENGINE INSTALLATION					1627
19	ENGINE					**
20	TIP BURNERS					*
21	LOAD COMPRESSOR					*
22	REDUCTION GEAR BOX, ETC					
23	ACCESSORY GEAR BOXES AND DRIVES					
24	SUPERCHARGERS—FOR TURBOS					
25	AIR INDUCTION SYSTEM					
26	EXHAUST SYSTEM					
27	COOLING SYSTEM					
28	LUBRICATING SYSTEM					64
29	TANKS					
30	BACKING BD, TANK SUP & PADDING					
31	COOLING INSTALLATION					
32	PLUMBING, ETC					
33	FUEL SYSTEM					*
34	TANKS—UNPROTECTED					
35	—PROTECTED					
36	BACKING BD, TANK SUP & PADDING					
37	PLUMBING, ETC					
38	WATER INJECTION SYSTEM					
39	ENGINE CONTROLS					60
40	STARTING SYSTEM					70
41	PROPELLER INSTALLATION					
42	DRIVE SYSTEM					653
43	GEAR BOXES					
44	LOBE SYSTEM					
45	CLUTCH AND MMC					
46	TRANSMISSION DRIVE					
47	ROTOR SHAFT					
48	JET DRIVE					
49						
50						
51						
52	AUXILIARY POWER PLANT GROUP					160
53						
54						
55						
56						
57						

*Weight for these items included in engine installation weight

**Engine weight confidential

MIL-STD-451, PART I

NAME _____ DATE _____		ROTORCRAFT SUMMARY WEIGHT STATEMENT WEIGHT EMPTY—Continued		PAGE _____ MODEL 395 Config 2 REPORT _____	
1					
2					
3					
4	INSTRUMENT AND NAVIGATIONAL EQUIPMENT GROUP				180
5	INSTRUMENTS				
6	NAVIGATIONAL EQUIPMENT				
7					
8					
9	HYDRAULIC AND PNEUMATIC GROUP				711
10	HYDRAULIC				
11	PNEUMATIC				
12					
13					
14	ELECTRICAL GROUP				742
15	A C SYSTEM				
16	D C SYSTEM				
17					
18					
19	ELECTRONICS GROUP				150
20	EQUIPMENT				
21	INSTALLATION				
22					
23					
24	ARMAMENT GROUP—INCL GUNFIRE PROTECTION			LBS	
25					
26	FURNISHINGS AND EQUIPMENT GROUP				300
27	ACCOMMODATIONS FOR PERSONNEL				
28	MISCELLANEOUS EQUIPMENT	X INCL	LBS	BALLAST X	
29	FURNISHINGS				
30	EMERGENCY EQUIPMENT				
31					
32					
33					
34	AIR CONDITIONING AND ANTI-ICING EQUIPMENT				100
35	AIR CONDITIONING				
36	ANTI-ICING				
37					
38					
39	PHOTOGRAPHIC GROUP				
40	EQUIPMENT				
41	INSTALLATION				
42					
43	AUXILIARY GEAR GROUP				
44	AIRCRAFT HANDLING GEAR				
45	LOAD HANDLING GEAR				1400
46	ATO GEAR				
47					
48					
49					
50					
51					
52					
53					
54	MANUFACTURING VARIATION				
55					
56					
57	TOTAL—WEIGHT EMPTY—PAGES 2, 3 AND 4				19,599

MIL-STD-451, PART I

NAME	SUMMARY WEIGHT STATEMENT			PAGE
DATE	USEFUL LOAD	GROSS WEIGHT	MODEL 395 Config. 2	
1 LOAD CONDITION			Transport	Heavy Lift
2			12 ton	20 ton
3 CREW--NO. 3		600	600	
4 PARACHUTED NO.				
5 FUEL	LOCATION	TYPE	GALBS	
6 UNUSABLE	FUSSEAGE	JP-4	100	100
7 INTERVAL			7881	3901
8				
9				
10				
11 EXTERNAL				
12				
13				
14				
15 BOMB BAY				
16				
17				
18				
19 OIL			30	30
20 UNUSABLE				
21 ENGINE				
22				
23				
24 BAGGAGE - Crew Kits			50	50
25 CARGO - Payload			24,000	40,000
26				
27 ARMAMENT				
28 GUNS-LOCATION	TYPE**	QUANTITY	CALIBER	
29				
30				
31				
32				
33 AMM				
34				
35				
36				
37				
38 BOMB INSTL*				
39 BOM 20				
40				
41 TOW PULL INSTR*				
42 TURBINE DRVR				
43				
44 BACKRT INSTR*				
45 IMCNETS				
46				
47 EQUIPMENT-PYTHON/IRIS				
48 -PYTHON 11880				
49				
50 -OXFORD				
51				
52 -MISC/LAUNCHES				
53				
54				
55 USEFUL LOAD			32,611	44,681
56 Weight Empty			19,599	19,599
57 GROSS WEIGHTS-PAGES 8-9			52,260	64,280

* If not specified as Weight Empty.

** Fixed, Flexible, etc.

MIL-STD-451, PART I

NAME _____
DATE _____

PAGE _____
MODEL 395 Config. 3
REPORT _____

SUMMARY WEIGHT STATEMENT
ROTORCRAFT ONLY
~~ESTIMATED - CALCULATED - ACTUAL~~
(Cross out those not applicable)

HOT CYCLE HEAVY-LIFT HELICOPTER
CONFIGURATION 3

CONTRACT _____
ROTORCRAFT, GOVERNMENT NUMBER _____
ROTORCRAFT, CONTRACTOR NUMBER _____
MANUFACTURED BY Hughes Tool Company - Aircraft Division

	Main	Auxiliary
Engines	Manufactured by	General Electric
	Model	GE-1
	Number	2
Propellers	Manufactured by	
	Model	
	Number	

MIL-STD-451, PART I

NAME _____
DATE

**ROTORCRAFT
SUMMARY WEIGHT STATEMENT
WEIGHT EMPTY**

PAGE
MODEL 395 Config 3
REPORT

• Wheat, Broken, Tires, Tubs and At.

Fixed
Retract.

MIL-STD-451, PART I

NAME _____
DATE _____

**ROTORCRAFT
SUMMARY WEIGHT STATEMENT
WEIGHT EMPTY—Continued**

PAGE
MODEL 395 Config. 3
REPORT

*Weight for these items included in engine installation weight
**Engine weight confidential

MIL-STD-451, PART I

NAME DATE	ROTORCRAFT SUMMARY WEIGHT STATEMENT WEIGHT EMPTY—Continued			PAGE MODEL 395 Config. 3 REPORT
1				
2				
3				
4	INSTRUMENT AND NAVIGATIONAL EQUIPMENT GROUP			180
5	INSTRUMENTS			
6	NAVIGATIONAL EQUIPMENT			
7				
8				
9	HYDRAULIC AND PNEUMATIC GROUP			731
10	HYDRAULIC			
11	PNEUMATIC			
12				
13				
14	ELECTRICAL GROUP			749
15	A C SYSTEM			
16	D C SYSTEM			
17				
18				
19	ELECTRONICS GROUP			150
20	EQUIPMENT			
21	INSTALLATION			
22				
23				
24	ARMAMENT GROUP—INCL GUNFIRE PROTECTION		LBS	
25				
26	FURNISHINGS AND EQUIPMENT GROUP			300
27	ACCOMMODATIONS FOR PERSONNEL			
28	MISCELLANEOUS EQUIPMENT	X INCL	LBS	BALLASTX
29	FURNISHINGS			
30	EMERGENCY EQUIPMENT			
31				
32				
33				
34	AIR CONDITIONING AND ANTI-ICING EQUIPMENT			100
35	AIR CONDITIONING			
36	ANTI-ICING			
37				
38				
39	PHOTOGRAPHIC GROUP			
40	EQUIPMENT			
41	INSTALLATION			
42				
43	AUXILIARY GEAR GROUP			
44	AIRCRAFT HANDLING GEAR			
45	LOAD HANDLING GEAR			1400
46	ATO GEAR			
47				
48				
49				
50				
51				
52				
53				
54	MANUFACTURING VARIATION			
55				
56				
57	TOTAL—WEIGHT EMPTY—PAGES 2, 3 AND 4		(Fixed Gear)	120, 570
			(Retract Gear)	21, 080

MIL-STD-451, PART I

PAGE
MODEL 395 Config. 3
REPORT

NAME _____
DATE _____

SUMMARY WEIGHT STATEMENT
USEFUL LOAD GROSS WEIGHT

	LOAD CONDITION		Transport	Heavy Lift
1				
2			12 ton	20 ton
3	CREW - NO. 3		600	600
4	PASSENGERS - NO.			
5	FUEL	LOCATION	TYPE	GALLS
6	UNUSABLE	Fuselage	JP-4	100
7	INTERNAL			6884
8				4131
9				
10				
11	EXTERNAL			
12				
13				
14				
15	BOMB BAY			
16				
17				
18				
19	OIL			
20	UNUSABLE			
21	ENGINE			30
22				30
23				
24				
25	BAGGAGE - Crew Kits			50
26	CARGO - Payload			24,000
27				40,000
28	ARMAMENT			
29	GUNS - LOCATION	TYPE**	QUANTITY	CALIBER
30				
31				
32				
33				
34	AMM			
35				
36				
37				
38	ROCKETS INSTL.			
39	MISSILES			
40				
41	TORPEDO INSTL.			
42	TORPEDOES			
43				
44	ROCKET INSTL.			
45	ROCKETS			
46				
47	EQUIPMENT - PYROTECHNICS			
48	- PYROTECHNIC			
49				
50	- OXYGEN			
51				
52	- MISCELLANEOUS			
53				
54				
55	USEFUL LOAD			31,664
56	Weight Empty (Fixed Gear)			20,570
57	GROSS WEIGHT - PAGES 3-6			52,234
				44,911
				20,570
				65,481

* If not specified as Weight Empty.

** Fixed, Flexible, etc.

NAME _____
DATE _____PAGE _____
MODEL 395 Config. 4
REPORT _____

SUMMARY WEIGHT STATEMENT
ROTORCRAFT ONLY
ESTIMATED - CALCULATED - ACTUAL
 (Cross out those not applicable)

HOT CYCLE HEAVY-LIFT HELICOPTER
CONFIGURATION 4

CONTRACT
ROTORCRAFT, GOVERNMENT NUMBER
ROTORCRAFT, CONTRACTOR NUMBER
MANUFACTURED BY Hughes Tool Company - Aircraft Division

	Main	Auxiliary
Main Engine	Manufactured by	General Electric
	Model	GE-1
	Number	2
Auxiliary Engine	Manufactured by	
	Model	
	Number	

MIL-STD-451, PART I

ROTORCRAFT SUMMARY WEIGHT STATEMENT WEIGHT EMPTY				PAGE MODEL REPORT	395 Config. 4
NAME					
DATE					
1					
2	ROTOR GROUP				5440
3	BLADE ASSEMBLY			3806	
4	HUB			1634	
5	HINGE AND BLADE RETENTION				
6		FLAP	PING		
7		LEAD	LAG		
8		PITCH	M		
9		FOLD	ING		
10	WING GROUP				
11	WING PANELS-BASIC STRUCTURE				
12	CENTER SECTION-BASIC STRUCTURE				
13	INTERMEDIATE PANEL-BASIC STRUCTURE				
14	OUTER PANEL-BASIC STRUCTURE-INCL TIPS		LBS		
15	SECONDARY STRUC-INCL FOLD MECH		LBS		
16	AILERONS-INCL BALANCE WTS		LBS		
17	FLAPS				
18	-TRAILING EDGE				
19	-LEADING EDGE				
20	SLATS				
21	SPOILERS				
22					
23	TAIL GROUP				1068
24	TAIL ROTOR			70	
25	-BLADES				
26	-HUB				
27	STABILIZER-BASIC STRUCTURE			998	
28	FINS-BASIC STRUCTURE-INCL DORSAL		LBS		
29	SECONDARY STRUCTURE-STABILIZER AND FINS				
30	ELEVATOR-INCL BALANCE WEIGHT		LBS		
31	RUDDER-INCL BALANCE WEIGHT		LBS		
32					
33	BODY GROUP				3575
34	FUSELAGE OR HULL-BASIC STRUCTURE				
35	BOOMS-BASIC STRUCTURE				
36	SECONDARY STRUCTURE-FUSELAGE OR HULL				
37	-BOOMS				
38	-DOORS, PANELS & MISC				
39					
40					
41	ALIGHTING GEAR-LAND	TYPE			2852
42	LOCATION	*	ROLLING	STRUCT	CONTROLS
43			ASSEMBLY		
44					
45					
46					
47					
48					
49					
50	ALIGHTING GEAR GROUP-WATER	TYPE			
51	LOCATION		FLOATS	STRUTS	CONTROLS
52					
53					
54					
55					
56					
57					

* Wheels, Brakes, Tires, Tubes and Air.

NAME DATE	ROTORCRAFT SUMMARY WEIGHT STATEMENT WEIGHT EMPTY—Continued	PAGE			
		MODEL 395 Config. 4 REPORT			
1					
2	FLIGHT CONTROLS GROUP				
3	COCKPIT CONTROLS				33
4	AUTOMATIC STABILIZATION				
5	SYSTEM CONTROLS—ROTOR NON ROTATING				990
6	ROTATING				269
7	—FIXED WING				
8	Intermediate Linkages				162
9					
10	ENGINE SECTION OR NACELLE GROUP				
11	INBOARD				
12	CENTER				
13	OUTBOARD				
14	DOORS, PANELS AND MISC				
15					
16	PROPELLUTION GROUP				
17		X	AUXILIARY	X	MAIN X
18	ENGINE INSTALLATION				1627
19	ENGINE				***
20	TIP BURNERS				
21	LOAD COMPRESSOR				
22	REDUCTION GEAR BOX, ETC				
23	ACCESSORY GEAR BOXES AND DRIVES				
24	SUPERCHARGERS—FOR TURBOS				
25	AIR INDUCTION SYSTEM				*
26	EXHAUST SYSTEM				*
27	COOLING SYSTEM				
28	LUBRICATING SYSTEM				64
29	TANKS				
30	BACKING BD, TANK SUP & PADDING				
31	COOLING INSTALLATION				
32	PLUMBING, ETC				
33	FUEL SYSTEM				*
34	TANKS—UNPROTECTED				
35	—PROTECTED				
36	BACKING BD, TANK SUP & PADDING				
37	PLUMBING, ETC				
38	WATER INJECTION SYSTEM				
39	ENGINE CONTROLS				60
40	STARTING SYSTEM				70
41	PROPELLER INSTALLATION				
42	DRIVE SYSTEM				638
43	GEAR BOXES				
44	LUBE SYSTEM				
45	CLUTCHES AND MISC				
46	TRANSMISSION DRIVE				
47	ROTATOR SHAFT				
48	JET DRIVE				
49					
50					
51					
52	AUXILIARY POWER PLANT GROUP				160
53					
54					
55					
56					
57					
58					

*Weight for these items included in engine installation weight

**Engine weight confidential

MIL-STD-451, PART I

NAME	ROTORCRAFT SUMMARY WEIGHT STATEMENT WEIGHT EMPTY—Continued			PAGE	MODEL 395 Config. 4
DATE				REPORT	
1					
2					180
3					
4	INSTRUMENT AND NAVIGATIONAL EQUIPMENT GROUP				
5	INSTRUMENTS				
6	NAVIGATIONAL EQUIPMENT				
7					
8					
9	HYDRAULIC AND PNEUMATIC GROUP				735
10	HYDRAULIC				
11	PNEUMATIC				
12					
13					
14	ELECTRICAL GROUP				752
15	A C SYSTEM				
16	D C SYSTEM				
17					
18					
19	ELECTRONICS GROUP				150
20	EQUIPMENT				
21	INSTALLATION				
22					
23					
24	ARMAMENT GROUP—INCL GUNFIRE PROTECTION			LBS	
25					
26	FURNISHINGS AND EQUIPMENT GROUP				300
27	ACCOMMODATIONS FOR PERSONNEL				
28	MISCELLANEOUS EQUIPMENT	X INCL	LBS	BALLAST	
29	FURNISHINGS				
30	EMERGENCY EQUIPMENT				
31					
32					
33					
34	AIR CONDITIONING AND ANTI-ICING EQUIPMENT				100
35	AIR CONDITIONING				
36	ANTI-ICING				
37					
38					
39	PHOTOGRAPHIC GROUP				
40	EQUIPMENT				
41	INSTALLATION				
42					
43	AUXILIARY GEAR GROUP^a				
44	AIRCRAFT HANDLING GEAR				
45	LOAD HANDLING GEAR				1400
46	ATO GEAR				
47					
48					
49					
50					
51					
52					
53					
54	MANUFACTURING VARIATION				
55					
56					
57	TOTAL—WEIGHT EMPTY—PAGES 2, 3 AND 4			21,105	

MIL-STD-461, PART I

NAME _____
DATE _____SUMMARY WEIGHT STATEMENT
USEFUL LOAD GROSS WEIGHTPAGE _____
MODEL 395 Config. 4
REPORT _____

	LOAD CONDITION		Transport	Heavy Lift	
1	CREW - NO.		12 ton 600	20 ton 600	
2	PASSENGERS - NO.				
3	FUEL	LOCATION	TYPE	GALS	
4	UNUSABLE	Fuselage	JF-4	100	100
5	INTERNAL			8272	4312
6					
7					
8					
9					
10					
11	EXTERNAL				
12					
13					
14					
15	BOMB BAY				
16					
17					
18					
19	OIL			30	30
20	UNUSABLE				
21	ENGINE				
22					
23					
24					
25	BAGGAGE - Crew Kits			50	50
26	CARGO - Payload			24,000	40,000
27					
28	ARMAMENT				
29	GUNS - LOCATION	TYPE*	QUANTITY	CALIBER	
30					
31					
32					
33					
34	AMM				
35					
36					
37					
38	BOMB INSTL*				
39	BOMBS				
40					
41	TORPEDO INSTL*				
42	TORPEDOES				
43					
44	ROCKET INSTL*				
45	ROCKETS				
46					
47	EQUIPMENT - PYROTECHNICS				
48	- PYROTOR 11830				
49					
50	- OXYGEN				
51					
52	- MISCELLANEOUS				
53					
54					
55	USEFUL LOAD			33,052	45,092
56	Weight Empty			21,105	21,105
57	GROSS WEIGHTS - PAGES 3-8			54,157	66,197

* If not specified as Weight Empty.

* Fixed, Flexible, etc.

MIL-STD-481, PART N

NAME	ROTOR GROUP	PAGE			
DATE	BLADE ASSEMBLY	MODEL	REPORT		
1	NACA Section	Trans.	Root		
2	.0013	.0011	Sect.	Sect.	
3					
4 FRONT SPAR-UPPER CAP					
5 -LOWER CAP					
6 -WEB & STIFFENERS					
7 -JOINTS, SPLICES & FASTNR					
8					
9 INTER SPAR-UPPER CAP @ 25% Chord	83.7	526.5	85.5		
10 -LOWER CAP					
11 -WEB & STIFFENERS					
12 -JOINTS, SPLICES & FASTNR					
13					
14 REAR SPAR-UPPER CAP					
15 -LOWER CAP					
16 -WEB & STIFFENERS					
17 -JOINTS, SPLICES & FASTNR					
18					
19 INTERSPAR STRUCTURE					
20 COVERING & STIFFENERS	186.9	503.1	39.0		
21 RIBS	40.2	124.9	112.2		
22 FILLER					
23 JOINTS, SPLICES & FASTNR					
24 Flexures	37.5	96.0	6.0		
25					
26 LEADING EDGE					
27 LEADING EDGE MEMBER					
28 COVERING & STIFFENERS					
29 RIBS					
30 FILLER					
31 JOINTS, SPLICES & FASTNR					
32					
33 TRAILING EDGE					
34 TRAILING EDGE MEMBER	3.9	12.8			
35 COVERING & STIFFENERS	39.0	103.5	14.40		
36 RIBS	8.1	24.2			
37 FILLER					
38 JOINTS, SPLICES & FASTNR	1.1	2.6			
39					
40 TIPS-17 NOT INTEGRAL + Cascade	36.0				
41 INTERNAL DUCT STRUCTURE + Insul.	124.8	327.3			
42 Articulated Duct			204.0		
43					
44 Damper		198.0			
45 Damper Arm			13.5		
46 Balance Section for Damper					
47 BALANCE WEIGHTS for 23 to 28%	124.7	155.8	14.4		
48 Lead-Lag Flexure			63.9		
49 TRIM TAB & FITTING					
50 ROOT END ATTACHMENT			78.6		
51 FITTINGS - Torque Box			277.5		
52 FASTENERS					
53 EXTERIOR FINNER					
54 Fairing			48.0		
55 Droop Stop			54.6		
56 TOTAL-BLADE ASSEMBLY	685.9	1876.7	533.7	676.2	
57					3772.5

ML-STD-451, PART H

01/66

NAME _____
DATE _____ROTOR GROUP
MOTORS AND HUBPAGE _____
MODEL _____
REPORT _____

	X HUB X X	RING & BLADE RESTRICTION				
		FLAPPING	LEAD-LAG	PITCH	ROLLING	Z
1						
2						
3						
4	HOUSING - Hub	369.0				
5	GIMBAL RING					
6	TONE					
7	UNIVERSAL JOINTS					
8	Support - Shaft to Hub	37.0				
9						
10						
11						
12	Bearings - Blade Feathering	17.0				
13	Bearings (2) - Main	285.0				
14	SEALS, SPACERS & RETAINERS	153.0				
15	BLADE GRIPS					
16	BALANCE WEIGHTS					
17	STOPs and SUPPORTS	27.0				
18	LUB BYR INCL LBS OIL					
19	PAIRINGS & DUST COVERS	24.0				
20	GREASE					
21						
22						
23						
24						
25	FITTINGS					
26	PINS					
27	LINKS					
28	DAMPERS OR RESTRAINERS					
29	DRAG BRACE					
30	TENSION STRAP ASSEMBLY	121.5				
31						
32						
33	Shaft - Fixed	286.0				
34	SHAFTS - Rotating	251.0				
35	PITCH ARMS					
36						
37						
38	BLADE FOLD-MECHANISM					
39	-ACTUATORS					
40	-CONTROLS					
41	-LOCKS					
42	-PLUMBING					
43	-CIRCUITRY					
44	-SUPPORTS					
45						
46						
47						
48						
49						
50	FASTENERS and Insulation	60.0				
51						
52						
53	EXTERIOR FINISH					
54						
55						
56	TOTAL - MOTORS AND HUB	1633.5				
57	TOTAL - ROTOR GROUP - PAGES 3 and 5					5439

* Main distribution point to actuating unit.

8/3/66

Model 205 Series 500

1000 ft. 4.25

1000 ft. 4.25

1000 ft.

1000 ft.

WEIGHT - POUNDS PER INCH

DETAILED WEIGHT CALCULATIONS

The following detailed weight calculations were made using design layouts and structural analysis of the blade, hub, and associated rotor parts. The weight of the blade nonbending material consisting of skin panels, ribs, and chordwise balance material was calculated; then the spar area required for the resulting centrifugal loads was determined and its weight calculated.

**WEIGHT CALCULATIONS FOR BLADE
SECTION (.75R TO 170)**

NACA 0014 SECTION (REF. DRAWING 395-0919)
(20" SEGMENT)

AFT SEGMENT (AL. ALLOY)

	W	WT/IN	K-L,R	$\bar{w}x$
SKIN 67.8 x 20 x .016 x .101	.178	.1028	48.93	4.7448
CHANNEL 9.3 x 20 x .012 x .101	.225	.0112	39.50	.3880
DOUBLER .8 x 20 x .016 x .101	.026	.0013	39.50	.0358
DOUBLER .8 x 20 x .012 x .101	.019	.0010	39.50	.0275
RIBS (4) 69.8 x .012 x .101 x 4	.426	.0213	36.60	.7796
END COVER 4.1 x 25.5 x .101 x .003	.053	.0017	36.60	.6682
HARDWARE (SAME AS XV-9A)	.056	<u>.0028</u>	39.50	<u>.0790</u>
TOTAL AFT SEGMENT	<u>.1481</u>	40.64	6.0044	

MAIN SEGMENT

Skin (TITANIUM)

INNER	50.6 x 18 x .012 x .17	2.152	.1076	
(.75-.8)	OUTER 50.6 x 20 x .008 x .17	(1.514)	(.0777)	
(.8-.9)	OUTER 50.6 x 20 x .007 x .17	(1.395)	(.0698)	
(.9-1.0)	OUTER 50.6 x 20 x .006 x .17	(1.195)	(.0598)	
	CORRUGATION 54.0 x 16.5 x .83 x 3.33 x .007 x .17	2.983	<u>.1466</u>	
	TOTAL SKIN (.75-.8 %R)	<u>.9354^{0.1}</u>	13.7	4.5744
"	" (.8-.9 %R)	<u>.8840^{0.1}</u>	13.7	4.4388
"	" (.9-1.0 %R)	<u>.9140^{0.1}</u>	13.7	4.9018

AFT CLOSURE WCB (HI TEMP METAL @.9" / in³)

(.75-.8)	WEB 9.0 x 20 x .020 x .3	(1.080)	(.0540) ^{0.1}	27.25	1.4715
(.8-1.0)	WEB 9.0 x 20 x .018 x .3	(.978)	(.0486) ^{0.1}	27.25	1.3204
	MID RIB (CRS) 113.8 in ² x .020 x .286	.651	.0326	13.0	.4238
	RIB DOUBLER (CRS) 30.9 in ² x .020 x .286	.177	.0088	17.0	.1496
	FWD STIFFENER (CRS) 5.8 in ² x .052 x .286	.086	.0043	3.4	.0146
	AFT STIFFENER (CRS) 7.0 in ² x .052 x .286	.104	.0052	26.3	.1368
	FWD DUCT STRAP (CRS) 17.5 in ² x .035 x .186	.175	.0087	13.5	.1174
	AFT DUCT STRAP (CRS) 19.7 in ² x .035 x .286	.187	<u>.0094</u>	16.6	<u>.1560</u>
	TOTAL RIB	<u>.0690</u>	14.67	<u>.9882</u>	

6700

**WEIGHT CALCULATIONS FOR BLADE
SECTION - 75% TO TIP (CONT'D)**

	W	WT/IN	ZPLB.	WX
BAL. WT. CLIPS (4) .20" x .020 x .226 x 4	.018	.0009"	1.0	.0009
25% WIRE 2.205" x .020 x .286 -4.50x2	.736	.0378"	15.4	.5021
UPPLATE STRP 1.95 x 18 x .040 x .286	.360	.0180"	15.16	.2227
UPPER CHANNEL 2.8 x 18 x .020 x .286	.287	.0118"	15.15	.1788
LOWER CHANNEL (SAMES AS UPPER CHANNEL)	.237	.0118"	15.16	.1788
END RIB - FWD 11.88 x .020 x .286 x 2	.227	.0113"	3.8	.0316
END RIB - MID 15.73 x .020 x .286 x 4	.360	.0180"	15.16	.2803
FLEXURE 4 x 61.5 x .025 x .30	1.345	.0922"	15.12	1.9941
FLEX. NAT 1.3 x 3.2 x .025 x .3	.031	.0016"	26.8	.0429

FWD DUCT (INFORIG)

DUCT 38.4 x 20 x .010 x .298	1.931	.0966
BELLOWS 20.8 x 3.5 x .020 x .298	.601	.0300
INSULATION .0012 x 20.8 x 20	.691	.0346
STIFFENERS 20.8 x .4 x .012 x .298 x 4	.165	.0082
TIE CHANNEL 1.3 x 4.8 x .030 x .286	.054	<u>.0027</u>
	.1721	9.0 1.5489

AFT DUCT (INFORIG)

DUCT 32.0 x 20 x .010 x .298	1.907	.0954
BELLOWS 26.8 x 3.5 x .020 x .298	.559	.0280
INSULATION .0012 x 26.8 x 20	.643	.0322
STIFFENERS 26.8 x .4 x .012 x .298 x 4	.153	.0077
TIE CHANNEL 1.3 x 4.8 x .030 x .286	.054	.0027
	.1660	21.0 3.41860

TOTAL BLADE SECTION - NO SPAR (.75-.8% R) (405-438) 1.1465 18.36 21.0461
(.8-.9% R)(438-486) 1.1312 18.36 20.9634
(.9-1.0% R)(486-540) 1.1212 18.40 20.6264

**WEIGHT CALCULATIONS FOR BLADE
CONSTANT SECTION TO .75R**

NACA 0018 SECTION (REF. DRAWING 895-0919)
(20" segment)

AFT SEGMENT (AL ALLOY)

SKIN $60.4 \times 20 \times .016 \times .101$

	W	\bar{w}	x -L.F.	$\bar{w}x$
	2.189	.1094	49.53	47.7403
	.277	.0138	22.5	.3795
	.026	.0019	22.5	.0358
	.019	.0010	22.5	.0225
	.481	.0240	36.6	.8784
	.042	.0021	36.6	.0769
	.056	.0028	22.5	.0770
TOTAL AFT SEGMENT		.1544 ^a	40.86	6.2150

MAIN SEGMENT

SKIN (TITANIUM)

INNER $60.0 \times .012 \times .17 \times .18$

2.203			
(2.244) ^{b1}	(1122)		
(1.632) ^{b2}	(0816)		
3.009	.1504		

(.2-.6) OUTER $60.0 \times .011 \times .17 \times .20$

(.6-.75) OUTER $60.0 \times .008 \times .17 \times .20$

CORRUGATION $.83 \times 3.33 \times 55.4 \times 16.5 \times .007 \times .17$

.3728 ^{b1}	13.7	5.1074
.3432 ^{b2}	18.7	4.6881

TOTAL SKIN (.2-.6)
" " (.6-.75)

AFT CLOSURE WEB

(.2-.6) WEB $11.5 \times 20 \times .022 \times .5$

(.6-.75) WEB $11.5 \times 20 \times .021 \times .3$

(1.512)	(.0759) ^{b1}	22.25	2.1683
(1.449)	(.0724) ^{b2}	22.25	1.9729

MID RIB (CRES) $150.1 \text{ in}^2 \times .020 \times .286$

.858 .0429 13.0 .5577

RIB DOUBLER (CRES) $48.4 \text{ in}^2 \times .020 \times .186$

.242 .0121 12.0 .2059

FWD STIFF (CRES) $9.2 \text{ in}^2 \times .052 \times .286$

.107 .0054 3.0 .0184

AFT STIFF (CRES) $9.2 \times .052 \times .286$

.137 .0068 26.3 .1988

FWD DUCT STRAP (CRES) $20.6 \times .035 \times .286$

.202 .0101 13.2 .1383

AFT DUCT STRAP (CRES) $22.0 \times .035 \times .286$

.220 .0110 16.9 .1859

TOTAL RIB

.0985^c 14.49 1.2798

WEIGHT CALCULATIONS FOR BLADE
CONSTANT SECTION TD, 75R (CONT'D)

	w	\bar{w}	$x - \bar{x}$	$\bar{w}x$
BAL. WT. CHIPS (4) $.8w^2 = .020 \times .286 \times 4$.015	.0009 [*]	1.0	.0009
25% WEB $10.8 \times 20.5 \times .020 \times .286$ $- .015 \times 2$	1.038	.0519 [*]	15.4	.0995
WINGPLATE STRIP $1.75 \times 18 \times .020 \times .286$.360	.0180 [*]	15.15	.0127
UPPER CHANNEL $3.8 \times 18 \times .020 \times .286$.321	.0165 [*]	15.5	.0255
LOWER CHANNEL (SAME AS UPPER CHANNEL)	.321	.0165 [*]	15.5	.0255
END RIB-FWD $.251 \times .020 \times .286 \times 2$.287	.0144 [*]	2.8	.0403
END RIB-MID $.27.2 \times .020 \times .286 \times 4$.622	.0311 [*]	15.6	.1852
FLEXURE $4 \times 6.8 \times .025 \times .3$	2.040	.1020 [*]	15.12	.1.9422
FLEXURE HAT (SAME AS 0014)	.031	.0016 [*]	26.8	.0429
 FWD DUCT (INCONEL)				
DUCT $36.6 \times 20 \times .010 \times .298$	2.141	.1090		
SELLOWS $32 \times 3.5 \times .020 \times .298$.668	.0334		
INSULATION (WV-9AWRAP) $.0012 \times 32 \times 20$.768	.0384		
STIFFENERS $12 \times .4 \times .012 \times .298 \times 4$.183	.0092		
TIE CHANNEL $1.3 \times 4.8 \times .030 \times .286$.354	.0027		
			<u>.1927[*]</u>	<u>8.0</u>
				<u>1.9416</u>
 AFT DUCT (INCONEL)				
DUCT $3.1416 \times 9.3 \times 20 \times .010 \times .298$	1.741	.0870		
SELLOWS $30 \times 3.5 \times .020 \times .298$.626	.0313		
INSULATION $.0012 \times 30 \times 20$.720	.0360		
STIFFENERS $30 \times .4 \times .012 \times .298 \times 4$.172	.0086		
TIE CHANNEL $1.3 \times 4.8 \times .030 \times .286$.054	.0027		
			<u>.1656[*]</u>	<u>8.5107</u>
 TOTAL BLADE SECTION-NO SPAR (.2-.6) (108-320) (.6-.95) (324-460)				
	1.9026	19.98	23.4183	
	1.2685	18.06	22.7036	

5700

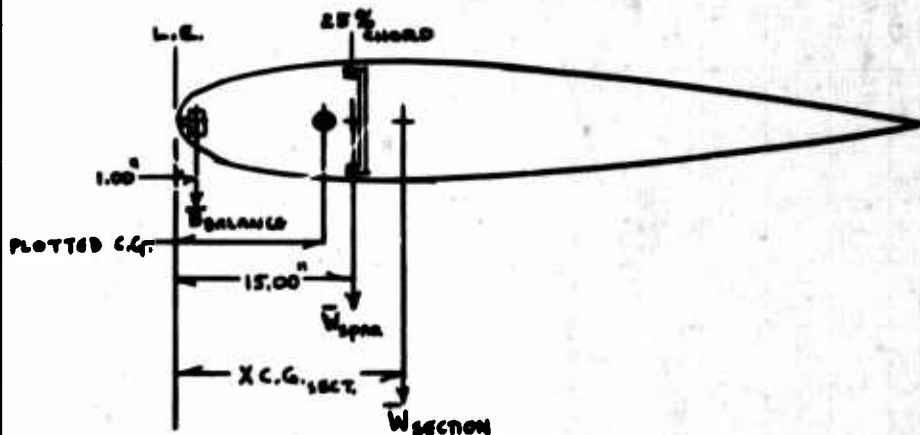
**DISCUSSION - BLADE CONSTANT SECTION
BALANCE**

Calculations for Blade Leading Edge Balance Weight.

Each typical blade section is balanced about the plotted chordwise center of gravity for that section. The plotted center of gravity was selected from the following graph at the midpoint (spanwise) of the section.

As an example:

- M = chordwise moment of item (about Leading Edge)
- W = unit weight per inch of item
- B = unit balance weight per inch



$$M_{sect} = W_{sect} \times X.C.G._{sect}$$

$$M_{spar} = W_{spar} \times 15.00$$

$$M_{balance} = B_{balance} \times 1.00 = B$$

and

$$(W_{sect} + W_{spar} + B_{balance}) \times \text{Plotted C.G.} = M_{sect} + M_{spar} + M_{balance}$$

For the blade section from station 216 to 270, the following calculations determine the unit balance required.

$$W_{section} = 1.3026 \text{#/in.}$$

$$M_{section} = 23.4183 \text{ in. #}$$

$$W_{spar} = .5900 \text{#/in.}$$

$$M_{spar} = 8.8500 \text{ in. #}$$

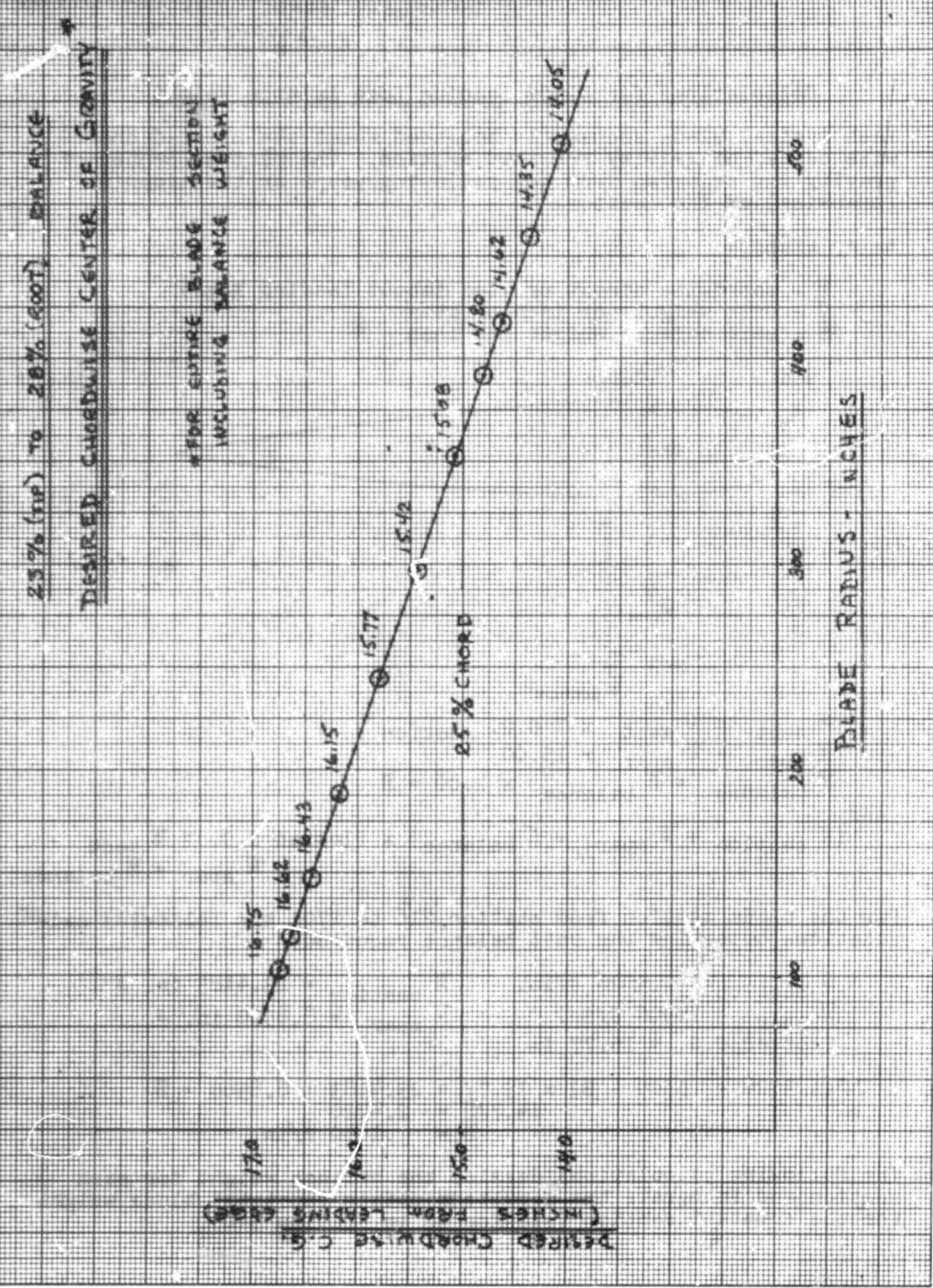
$$\text{Plotted C.G.} = 15.77 \text{ in.}$$

$$\therefore (1.3026 + .5900 + B) \times 15.77 = 23.4183 + 8.8500 + B$$

$$14.77B = 2.4220$$

$$B = .1640 \text{#/in.}$$

The following calculations develop the balance weight for each section and integrate the results to obtain the total blade weight for the constant section (station 96 to station 540).



**BALANCE CALCULATIONS FOR
29% TO 28% CHORD BALANCE**

29% TO 28% BALANCE

<u>STA</u>	<u>E</u>	<u>X(E)</u>	<u>WX</u>	<u>BALANCE CALC</u>
96-108	1.3026	17.98	23.4183	$(2.0266+B) \times 16.62 = 34.2783 + B$
SPAR	.724	15.00	10.8600	$\therefore B = .0211 \text{ ft/in}$
BALANCE	<u>.0211</u>	<u>1.00</u>	<u>.0211</u>	
	<u>2.0477</u>	<u>16.75</u>	<u>34.2994</u>	
108-135	1.3026	17.98	23.4183	$(2.0266+B) \times 16.62 = 34.2783 + B$
SPAR	.724	15.00	10.8600	$B = .0211 \text{ ft/in}$
BALANCE	<u>.0382</u>	<u>1.00</u>	<u>.0382</u>	
	<u>2.0648</u>	<u>16.62</u>	<u>34.3165</u>	
135-162	1.3026	17.98	23.4183	$(2.0266+B) \times 16.43 = 34.1983 + B$
SPAR	.705	15.00	10.5950	$B = .0654 \text{ ft/in}$
BALANCE	<u>.0654</u>	<u>1.00</u>	<u>.0654</u>	
	<u>2.0730</u>	<u>16.43</u>	<u>34.0587</u>	
162-216	1.3026	17.98	23.4183	$(1.9626+B) \times 16.15 = 33.9183 + B$
SPAR	.66	15.00	9.9000	$B = .1071 \text{ ft/in}$
BALANCE	<u>.1071</u>	<u>1.00</u>	<u>.1071</u>	
	<u>2.0697</u>	<u>16.15</u>	<u>33.9854</u>	
216-270	1.3026	17.98	23.4183	$(1.8926+B) \times 15.99 = 32.4683 + B$
SPAR	.59	15.00	8.8500	$B = .1640 \text{ ft/in}$
BALANCE	<u>.1640</u>	<u>1.00</u>	<u>.1640</u>	
	<u>2.0566</u>	<u>15.77</u>	<u>32.4323</u>	
270-324	1.3026	17.98	23.4183	$(1.8126+B) \times 15.42 = 31.0683 + B$
SPAR	.51	15.00	7.6500	$B = .2162 \text{ ft/in}$
BALANCE	<u>.2162</u>	<u>1.00</u>	<u>.2162</u>	
	<u>2.0288</u>	<u>15.42</u>	<u>31.2845</u>	
324-378	1.2685	18.06	22.9036	$(1.6985+B) \times 15.08 = 29.9536 + B$
SPAR	.43	15.00	6.4500	$B = .2656 \text{ ft/in}$
BALANCE	<u>.2656</u>	<u>1.00</u>	<u>.2656</u>	
	<u>1.9641</u>	<u>15.08</u>	<u>29.6192</u>	
378-405	1.2685	18.06	22.9036	$(1.6335+B) \times 14.80 = 28.4536 + B$
SPAR	.37	15.00	5.5500	$B = .3046 \text{ ft/in}$
BALANCE	<u>.3046</u>	<u>1.00</u>	<u>.3046</u>	
	<u>1.9431</u>	<u>14.80</u>	<u>28.7582</u>	

25% TO 27% BALANCE - (CONT'D)

<u>STA</u>	<u>W</u>	<u>X (L)</u>	<u>WX</u>	<u>BALANCE CALC</u>
405-432	1.1465	18.36	21.0461	$(1.1465 + B) \times 14.62 = 25.8461 \approx B$
SPAR	.32	15.00	4.8000	$B = .3235 \text{#/in}$
BALANCE	<u>.3231</u>	<u>1.00</u>	<u>.3235</u>	
	<u>1.7900</u>	<u>14.62</u>	<u>26.1696</u>	
432-486	1.1312	18.36	20.7634	$(1.1312 + B) \times 14.35 = 24.5134 \approx B$
SPAR	.25	15.00	3.7500	$B = .3516 \text{#/in}$
BALANCE	<u>.3516</u>	<u>1.00</u>	<u>.3516</u>	
	<u>1.7328</u>	<u>14.35</u>	<u>24.3660</u>	
486-522	1.1212	18.40	20.6264	$(1.1212 + B) \times 14.05 = 23.0264 \approx B$
SPAR	.16	15.00	2.4000	$B = .3851 \text{#/in}$
BALANCE	<u>.3851</u>	<u>1.00</u>	<u>.3851</u>	
	<u>1.6663</u>	<u>14.05</u>	<u>23.4115</u>	
522-540	.4866	7.50	3.6995	
CASCADE	.6111	15.00	9.1665	
BALANCE	<u>~</u>	<u>1.0</u>		
	<u>1.0977</u>	<u>11.68</u>	<u>12.8160</u>	
				$(13.85) \text{ for } 23\%$
				<u>19.5%</u>

**INTEGRATION TO OBTAIN TOTAL
CONSTANT BLADE WEIGHT**

INTEGRATE BLADE
23% TO 20% BALANCE

<u>STA</u>	<u>W</u>	<u>L</u>	<u>W</u>	<u>X</u>	<u>R</u>	<u>WX</u>	<u>WR</u>
96-108	2.0477	12	24.67	16.75	102.0	411.55	2506.1
108-135	2.0648	27	55.75	16.62	121.5	926.56	6773.6
135-162	2.0230	27	55.97	16.43	148.5	919.59	8311.5
162-216	2.0697	54	111.76	16.15	189.0	1804.92	21122.6
216-270	2.0866	54	111.06	15.77	243.0	1757.42	26987.6
270-324	2.0288	54	109.56	15.42	297.0	1689.42	32539.3
324-378	1.9641	54	106.06	15.08	351.0	1597.38	37227.1
378-405	1.9431	27	52.46	14.80	391.5	976.41	20538.1
405-432	1.7900	27	48.33	14.62	418.5	266.68	20226.1
432-486	1.7328	54	93.57	14.38	457.0	1342.73	42948.6
486-522	1.6663	36	59.99	14.05	504.0	842.86	30255.0
522-540	1.0977	18	19.76	11.68	531.0	230.80	10492.6
<hr/>							
TOTAL BLADE (OUTED STA 56)	848.8		15.32"	306.2"		13002.22	259908.2

$$CF@750 = 2.841 \times 259908 \times 159^2 \times 10^{-5} = 186600 \# \quad \text{HOVER}$$

$$CF @ 675 = 143^2 = 151000 \# \quad \text{CRUISE}$$

BALANCE CALCULATIONS FOR
25% CONSTANT BALANCE

85% BALANCE

STA	W	X(LB)	WX	BALANCE CALC.
96-135	1.3026	17.98	23.4183	
SPAR	.784	15.00	10.8600	
BALANCE	.2771	1.00	.2771	$\left\{ \begin{array}{l} (2.0266+B) \times 15.0 = 34.2283 + B \\ B = .2771 \frac{1}{4}/in \end{array} \right.$
	2.3037	15.00	34.5554	
135-162	1.3026	17.98	23.4183	$(2.0076+B) \times 15.0 = 33.9933 + B$
SPAR	.705	15.00	10.5750	
BALANCE	.2771	1.00	.2771	$B = .2771 \frac{1}{4}/in$
	2.2847	15.00	34.2704	
162-216	1.3026	17.98	23.4183	$(1.9626+B) \times 15.0 = 33.3183 + B$
SPAR	.660	15.00	9.9000	
BALANCE	.2771	1.00	.2771	$B = .2771 \frac{1}{4}/in$
	2.2397	15.00	33.5954	
216-270	1.3026	17.98	23.4183	$(1.8926+B) \times 15.0 = 32.2683 + B$
SPAR	.6900	15.00	8.8500	
BALANCE	.2771	1.00	.2771	$B = .2771 \frac{1}{4}/in$
	2.1697	15.00	32.5454	
270-324	1.3026	17.98	23.4183	$(1.8126+B) \times 15.0 = 31.0683 + B$
SPAR	.510	15.00	7.6500	
BALANCE	.2771	1.00	.2771	$B = .2771 \frac{1}{4}/in$
	2.0897	15.00	31.3454	
324-378	1.2685	18.06	22.9036	$(1.6985+B) \times 15.0 = 29.3536 + B$
SPAR	.430	15.00	6.4500	
BALANCE	.2769	1.00	.2769	$B = .2769 \frac{1}{4}/in$
	1.9764	15.00	29.6305	
378-405	1.2685	18.06	22.9036	$(1.6385+B) \times 15.0 = 26.4536 + B$
SPAR	.370	15.00	5.5500	
BALANCE	.2769	1.00	.2769	$B = .2769 \frac{1}{4}/in$
	1.9154	15.00	28.7905	

9700

25% BALANCE (CONT'D)

25% BALANCE (CONTINUED)

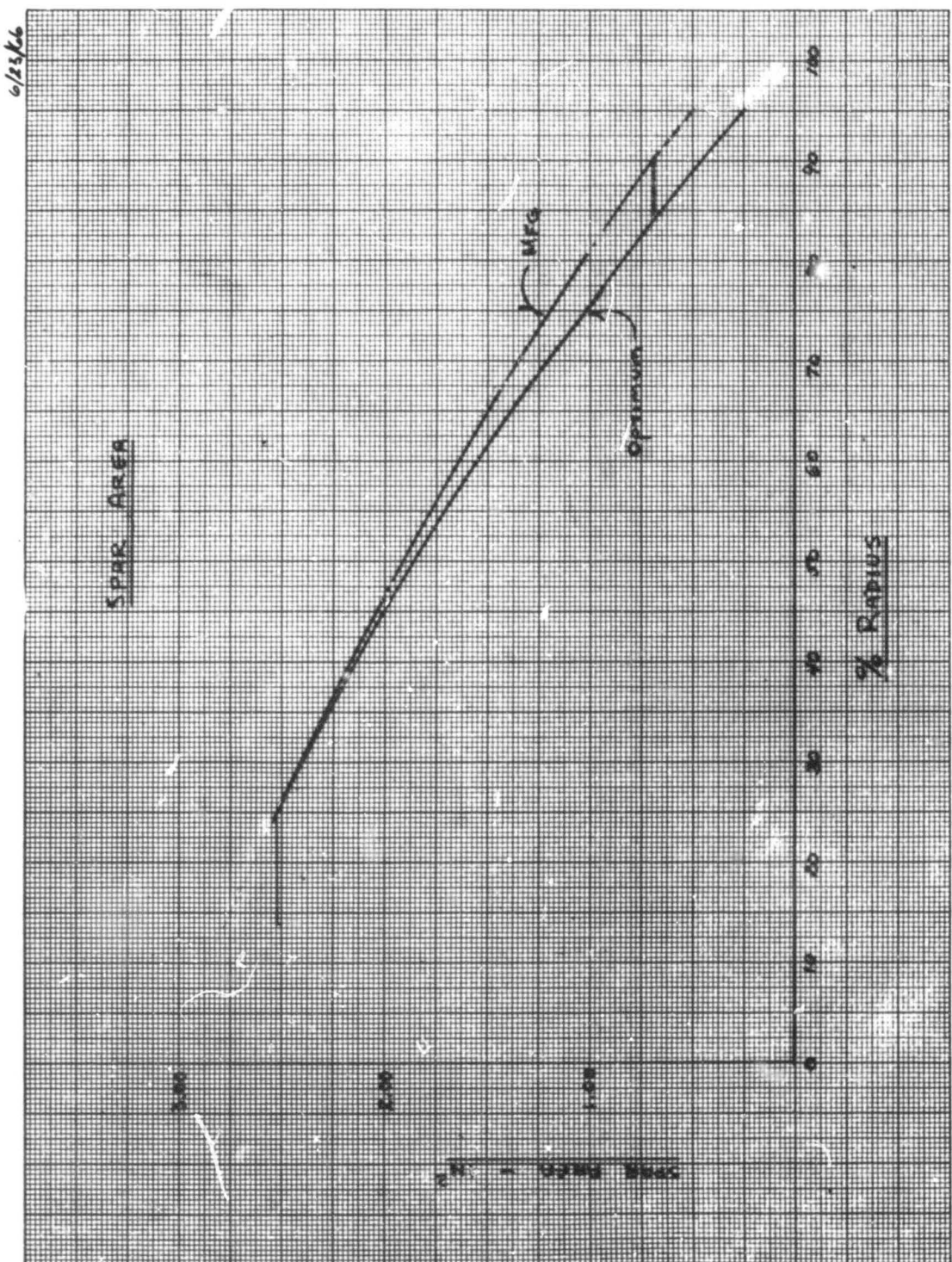
<u>STA</u>	<u>W</u>	<u>X(LE)</u>	<u>WX</u>	<u>BALANCE CALC.</u>
405-432	1.1465	18.36	21.0461	$(1.1465+B) \times 15.0 = 25.8461 + B$
SPAR	.820	15.00	4.8000	$B = .2749 \frac{\$}{in}$
BALANCE	.2749	1.00	.2749	
	<u>1.7414</u>	<u>15.00</u>	<u>26.1210</u>	
492-446	1.1312	18.36	20.7634	$(1.1312+B) \times 15.0 = 24.5134 + B$
SPAR	.2500	15.00	3.7500	$B = .2711 \frac{\$}{in}$
BALANCE	.2711	1.00	.2711	
	<u>1.6923</u>	<u>15.00</u>	<u>24.7845</u>	
486-522	1.1212	18.40	20.6264	$(1.1212+B) \times 15.0 = 23.0264 + B$
SPAR	.160	15.00	2.4000	$B = .2720 \frac{\$}{in}$
BALANCE	.2720	1.00	.2720	
	<u>1.5532</u>	<u>15.00</u>	<u>23.2984</u>	
522-540	1.4866	7.50	3.6495	
CASCADE	.6111	15.00	9.1665	
BALANCE	~	1.00	~	
	<u>1.0977</u>	<u>11.68</u>	<u>12.8160</u>	
		(19.8%)		
		(15.00% FOR 25%)		

INTEGRATION TO OBTAIN TOTAL
BLADE WEIGHT

INTEGRATE BLADE (25% BALANCE)

<u>STA</u>	<u>W</u>	<u>L</u>	<u>W</u>	<u>X(4)</u>	<u>R</u>	<u>WX</u>	<u>WR</u>
96-135	2.3037	39	89.84	15.0	110.5	1342.6	9927.3
135-162	2.2847	27	61.69	15.0	148.5	926.4	9161.0
162-216	2.2397	54	120.94	15.0	189.0	1814.1	22859.7
216-270	2.1697	54	117.16	15.0	243.0	1757.4	28469.9
270-324	2.0897	54	112.84	15.0	297.0	1692.6	33513.6
324-378	1.9754	54	106.67	15.0	351.0	1600.0	37441.1
378-405	1.9154	27	51.72	15.0	391.5	778.8	20248.4
405-432	1.7414	27	47.02	15.0	418.5	706.3	19677.9
432-486	1.6523	54	89.22	15.0	459.0	1338.3	40952.0
486-522	1.5832	36	58.92	15.0	504.0	858.8	28183.7
522-540	1.0977	18	19.76	11.68	531.0	230.80	10492.6
TOTAL BLADE (OUTBD STA 96)	872.8"	14.92"	299.0"		13026.1	260925.2	

0704



6/14/66

Spel. Weigh. Pea. Inch.

WEIGHT - POUNDS PER INCH

.0 .1 .2 .3 .4 .5 .6 .7 .8 .9 .0

ROUTE STATION

100

1400

1800

2200

1200

0

**WEIGHT CALCULATION FOR BLADE
WEIGHT (OTHER THAN CONSTANT SECT.)**

LEAD-LAG FLEXURE

$$177.6 \text{ IN}^2 \times .482 \times .286 = \underline{21.5'' \text{ EACH}}$$

L.E. BALANCE (EXTRA AREA FOR DAMPER LOADS)

.75 in² TO 0 FOR 50" - TIE IN AT R=100

BALANCE @ STA 100 = .074 in²

∴ NEED .750-.074 = .676 in² - to in² @ 150

$$\frac{.676}{\pi} \times 50 \times .286 = \underline{4.8'' \text{ PER BLADE}}$$

TIP CASCADE (.025 INCONEL) (REF. DRAWING 395-0919)

XU-9A			
STRUCTURE	5.03"	$\therefore 5.03 \times \frac{\text{Chord}}{31.5} = 5.03 \frac{6.9}{31.5} = 9.58''$	
VANES	.72"		
(31.5" CHORD)	4.10m	$.18 \times \frac{.72}{\pi} \times 7 = 2.12$	$\frac{2.12}{11.7} \text{ say } \underline{1.8''}$

FLAPPING STRAP (.50% CRES)

CONSTANT SECTION	99.9 in ²
INBOARD END	75.2 in ²
OUTBOARD END	107.0 in ²

$$\underline{282.1 \times .5 \times .286 = 40.5''}$$

DAMPER (LEAD-LAG)

369A Damper = 2.1" WITH 1" RADIUS

Per Stress HCH would require 5" radius and
1 1/4 the depth of the 369A damper.

$$\therefore 2.1 \times \frac{5^2}{12} \times 1.25 = 66'' \quad \underline{66''}$$

BLADE COMPONENTS WEIGHT
CALCULATING (CONT'D)

ARTICULATED DUCT

TRI-DUCT TO SLIP JOINT (9.5" dia - 2 REQ.)

$$XV-9A = 10.85" @ 8.5" Dia$$

$$\therefore 10.85 \times \frac{9.5}{8.5} = 12"$$

$$+ 18'L \times 9.5 = 31416 \times .02 \times .286 \times 34 \quad \left. \right\} 15" \times 2 = 30"$$

SLIP JOINT (2 REQ.)

$$XV-9A = 7.88"$$

$$\therefore 7.88 \times \frac{9.5}{8.5} = 8.8" \times 2 =$$

18"

SUP JOINT TO STA 96 (2 REQ.) L = 20"

$$28 \times 9.5 = 31416 \times .02 \times .286 = 4.8" \times 2$$

10"

BELLOWS (2 REQ.) (12" Dia)

$$XV-9A = 9.9" @ 9" Dia$$

$$\therefore 9.9 \times \frac{12}{9} = 5" \times 2$$

10"

TOTAL ARTICULATED DUCT 68"

TORQUE BOX FAIRING

ASSUME .062" BOLTIRON (SAME AS XV-9A)

$$130 \times 33 = 4380 \text{ in}^2 \times .062 \times .049 = 12"$$

$$+ 30\% \text{ LOCAL STIFFENING } \frac{4}{16}$$

16"

STUB SPAR STA 78 TO 96

$$.724" / in = 18" : 13.03 \times 1.5 = DEEP-UP$$

$$13.03 + 18.54 =$$

28.6"

**BLADE COMPONENTS WEIGHT
CALCULATIONS (CONT'D)**

TRANSITION SECTION (SEA 67 TO 96) (REF. DRAWING 395-0924)

SKIN (USE NACA 0018 SKIN)
 $.4027 \frac{1}{16} \text{ in} \times 30" = \underline{12.1}^{\#}$

CLOSURE CHANNEL
 $7 \times 30 \times .015 \times .286 = \underline{.9}$

OUTBOARD BULKHEAD
 CAP $65" \times .25" = \underline{16.25}$
 WEB $74.2 \text{ in}^2 \times .06 = \underline{4.45}$
 $20.70 \text{ in}^3 \times .284 = \underline{5.9}^{\#}$

MID STABILIZING RIBS (2)
 SAME AS OUTBD RIBS $= 5.9 \times 2 = \underline{11.9}^{\#}$

INBOARD BULKHEAD
 $316.8 \text{ in}^2 \times .06 = \underline{19.01}$
 $11 \times .6 \times 2 = \underline{13.20}$
 $34 \times 4 \times .125 \times 1 = \underline{12.00}$
 $2 \times 2.5 \times 1 \times 4 = \underline{30.00}$
 $69.21 \text{ in}^3 \times .284 = \underline{19.7}^{\#}$

TRAILING EDGE (SEE NACA 0018)

$.1611 \frac{1}{16} \text{ in} \times 30" = \underline{4.8}^{\#}$

TORSION FLEXURE (2) EST 2[#]

TOTAL TRANSITION SECTION 57.2[#]

HUB FAIRING (USE XV-9A TYPE COVER) 45'DIA 35" HIGH

XV-9A = $8.33^{\#}$ @ 3050 in^2

$8.33 \times \frac{7660 \text{ in}^2}{3050 \text{ in}^2} = \underline{20.9}^{\#}$

STIFFENING & HARDWARE 3[#]

24[#]

DOOR STOP (T1.)

$2 \text{ in}^2 \times 30$	<u>60</u>
$3 \text{ in}^2 \times 12$	<u>36</u>
$1 \text{ in}^2 \times 6 \times 3$	<u>18</u>
$\frac{114 \text{ in}^3}{\text{in}^2} \times .16 = \underline{18.2}^{\#}$	

BLADE WEIGHT CALCULATIONS (CONT'D)

DAMPER ARM (P/B TORQUE BOX)

$$\frac{39.4'' L \times .4 in^2}{8.8 \times 6.4 \times .05}$$

$$\frac{12.96}{2.82}$$

$$15.78 \times .286 =$$

$$\underline{4.5''}$$

**BLADE COMPONENTS WEIGHT
CALCULATIONS (CONT'D)**

TORQUE BOX TO HUB TRUSS (STEEL TUBING)

(1" DIA x .083 WALL) .0679 $\frac{1}{16}$ IN x 20" = 1.4 + 1.0 END FITTINGS = 2.4	
(1" DIA x .083 WALL) .0679 $\frac{1}{16}$ IN x 12" = .8 + 1.0	= 1.8
2 (2" DIA x .095 WALL) .1615 x 16" = 2.6 + 1.0 (2 REQ.)	= 3.2
4 (3" DIA x .093 WALL) .4420 x 15" = 8.1 + 1.0 (4 REQ.)	= 9.1
MISC. HARDWARE, WELD, ETC.	
	<u>2.4</u>
	<u>26.2</u>

TORQUE Box (TITANIUM)

$$\text{SKIN } 17 \times 3.1416 \times 30.5 \times .082 \times .17 = 22.2"$$

$$\begin{aligned} \text{INBOARD FRAME } & 17.26 \times 3.1416 \times 2.8 \times .1 \\ & (18.8 - 19.0) \times .7854 \times .25 \\ & 18.8 \times .7854 \times .25 \\ & 6.4 \times 4 \times 1.8 \\ & - 7.4 \times 8 \times .25 \end{aligned} \quad \left\{ \begin{aligned} & 116.65 \text{ in}^3 \times .17 = 19.8" \\ & \end{aligned} \right.$$

$$\begin{aligned} \text{OUTBOARD FRAME } & 17 \times 3.1416 \times 7.6 \times .08 \\ & - 5.6 \times 4 \times .08 \\ & 17^2 \times .7854 \times .08 \\ & 17^2 \times .7854 \times .10 \\ & - 22.8 \times 2 \times .10 \\ & - 22.8 \times 2 \times .08 \\ & 8 \times 4 \times 7 \times .4 \end{aligned} \quad \left\{ \begin{aligned} & 135.81 \text{ in}^3 \times .17 = 23.0" \\ & \end{aligned} \right.$$

$$\begin{aligned} \text{MINOR FRAMES (3)} \\ 17 \times 3.1416 \times 1 \times .08 \quad \left\{ \begin{aligned} & 22.43 \times .17 \times 3 = 11.4" \\ & 17^2 \times .7854 \times .08 \end{aligned} \right. \end{aligned}$$

$$\text{STRAP SHOES } 6.2 \times 3.6 \times 6 \times 4 \times .17 = 9.1"$$

$$\text{TRUSS TIE-IN FITTINGS (1.5" dia. x 4)} = 6.0"$$

$$\text{HARDWARE} = 1.0"$$

$$\text{TOTAL TORQUE BOX} \quad 92.5"$$

HUB & SHAFT WEIGHT CALCULATIONS

HUB AND SHAFT CALCULATIONS

HUB SUPPORT COLUMN (FIXED SHAFT) (REF. DWG. 395-0932)

SECTION

1	$.11 \times .15 \times 3.1416 \times 37.8$	19.58
2	$.35 \times .55 \times 3.1416 \times 33.0$	22.99
3	$.885 \times .4 \times 3.1416 \times 37.8$	135.36
4	$1.6 \times .5 \times 3.1416 \times 33.642$	158.32
5	$.4 m^3 \times 3.1416 \times 35.7 \times 2$	89.72
6	$24.0 \times .1 \times 3.1416 \times 38.1$	209.29
7	$.181 m^3 \times 3.1416 \times 37.6 \times 2$	28.68
8	$3.85 \times .5 \times 3.1416 \times 37.8$	198.90
9	$7.8 \times .1 \times 3.1416 \times 38.0$	93.10
10	$(44.0^2 - 38.2^2) \cdot .7854 \times .1$	27.45
11	$1.0 \times .5 \times 3.1416 \times 44.0$	67.90
12	$(36.0^2 - 35.0^2) \times .1 \times 5$	<u>27.88</u>

$$1169 \text{ m}^3 \times .286 = \underline{334.3}$$

UPPER BEARING MODEL 485 BEARING = 198" @ 48" DIA (SEE NEXT PAGE FOR CALC)

$$\text{BEARING : } 198 \times \frac{35 \text{ DIA}}{48 \text{ DIA}} = \underline{144}'' \text{ (2 REFG) } \underline{288}''$$

LOWER BEARING (SEE NEXT PAGE) 74"

UPPER RETAINER

$(39.8^2 - 33.6^2) \cdot .7854 \times .1$	95.74
$.5 \times .6 \times 3.1416 \times 35.2$	37.18
$(35.6^2 - 34.0^2) \times .7854 \times .05$	4.97

$$73.3 \text{ m}^3 \times .286 = \underline{21}''$$

UPPER FLANGE

$(39.8^2 - 37.8^2) \cdot .7854 \times .1$	12.19
$.1 \times .8 \times 3.1416 \times 38.0$	9.55

$$21.7 \text{ m}^3 \times .286 = \underline{6.2}$$

LOWER SEAL (AL. AL.)

$.28 \times 4 \times 3.1416 \times 34.4$	108.07
$1.8 \times .2 \times 3.1416 \times 37$	204.58

$$312.6 \text{ m}^3 \times .10 = \underline{31.6}$$

HUB CALCULATIONS (CONT'D)

MODEL 485 MAIN BEARING CALCULATIONS (TO RATIO TO MODEL 395)

UPPER BEARING STEEL

DIAMETER OF BEARINGS 1.625 in., 92 REQUIRED

TOTAL BEARING WEIGHT

$$\frac{3.14 \times (1.625)^3}{6} \text{ in}^3 \times 92 \times .285 \text{ lb/in}^3 = 58.6 \text{ lb}$$

INNER AND OUTER RACES

$$48 \text{ in} \times 3.14 \times 2.6 \text{ in} \times 1.25 \text{ in} \times .285 \text{ lb/in}^3 = 139.6 \text{ lb}$$

TOTAL 48" O.D. BEARING 198⁴

RE-CALC 8/23/66

LOWER BEARING (2 REQ.)

BALLS 1.375 Dia, 67 REQ

$$\frac{3.14 \times 1.375^3}{6} \times 67 \times .285 = 26.0$$

$$\text{RACES } 35 \times 3.14 \times 2.6 \times 1.25 \times .285 = 102.0$$

BEARING RETAINER

16.0

$$144^{\frac{4}{4}} \times 2 = \underline{288^{\frac{4}{4}}}$$

UPPER BEARING

BALLS .875 Dia x 94 REQ.

$$\frac{3.14 \times .875^3}{6} \times 94 \times .285 = 9.4$$

$$\text{RACES } 35 \times 3.14 \times 1.8 \times 1.0 \times .285 = 58.4$$

BEARING RETAINER

8.0

74⁴

74⁴

HUB CALCULATIONS - (CONT'D)

HUB & SHAFT (CONTINUED)

ROTATING SHAFT (TO POINT "A" ONLY) (CRESD)

SECTION

1	$1.75 \times .65 \times 3.1416 \times 32.8$	117.21
2	$(32.2^2 - 27.2^2) \times .0884 \times .1$	23.33
3	$.3 \times 1.5 \times 3.1416 \times 32.8$	38.74
4	$.5 \times .25 \times 3.1416 \times 32.8$	10.76
5	$.6 \times .4 \times 3.1416 \times 32.8$	106.18
6	$84.5 \times .18 \times 3.1416 \times 32.8$	298.62
7	$.2 \times .4 \times 3.1416 \times 32.8$	108.93
8	$(32.0^2 - 27.3^2) \times .0884 \times .1$	21.89
9	$.2 \times .5 \times .35 \times 3.1416 \times 32.8$	66.30
10	$.6 \times .25 \times 3.1416 \times 32.8$	152.68
11	$.6 \times .05 \times 3.1416 \times 32.8$	13.87
12	$.65 \times .25 \times 3.1416 \times 32.8$	13.91
13	$(32.0 - 31.0) \times .11 \times 6$	38.66
		<u>$979.4 \text{ in}^3 \times .286 = 280^4$</u>

LOWER BEARING RETAINER (CRESD)

$$\begin{array}{rcl} .42 \times 2.4 \times 3.1416 \times 33.0 & & 104.50 \\ .4 \times .6 \times 3.1416 \times 33.0 & & 25.18 \\ \hline & & 129.7 \text{ in}^3 \times .286 = 37^4 \end{array}$$

ACCESSORY DRIVE GEAR (NOT PART OF ROTOR GROUP WEIGHT)
(CRESD)

$$\begin{array}{rcl} 2.6 \times .25 \times 3.1416 \times 32.8 & & 66.98 \\ .9 \times .4 \times 3.1416 \times 34.0 & & 38.42 \\ 2.25 \times .6 \times 3.1416 \times 35.4 & & 150.10 \\ \hline & & 255.5 \text{ in}^3 \times .286 = 73^4 \end{array}$$

DROOP STOP SUPPORT (STEEL - 3 REQ)

$$\begin{array}{rcl} 1" \text{ wall} \times .083 & .0679 \times 22 \times 2 = 2.98 + .80 \text{ fitting} & : 5.0 \\ 1" \text{ wall} \times .083 & .0679 \times 30 & : 1.36 + 1.0 \text{ fitting} & : 2.4 \\ \text{Droop stop pad} & 6 \times 2 \times .5 \times .286 & \end{array}$$

$$\begin{array}{r} \frac{1.2}{9.1} \\ \times \frac{3}{3} \\ \hline 37.3^4 \end{array}$$

HUB CALCULATIONS (CONT'D)

FEATHERING BEARINGS IN HUB

$$(4.4^2 - 3.0^2) \times 7854 \cdot 2.5 \times .286 \times 3$$

17"

HUB

UPPER & LOWER PLATES	$2908.8 \text{ in}^2 \times .1 = 290.9$
STRAP TIE-IN WEB	$186.8 \text{ Long } \times .25 \text{ in}^2 \times 4 \text{ in. } 6$
CROSS-TIE	$38.4 \text{ Long } \times 1.0 \text{ in}^2 = 38.4$
CROSS-TIE	$46.6 \text{ Long } \times 2.0 \text{ in}^2 = 93.2$
CROSS-TIE	$60.0 \text{ Long } \times 1.0 \text{ in}^2 = 60.0$
STRAP WEB TIE	$1156.0 \text{ Long } \times .8 \text{ in}^2 = \underline{964.8}$

$$1289.9 \text{ in}^3 \times .286 = \underline{369"}^{\text{in}}$$

HUB SUPPORT (3 REQ.)

UPPER PAD	$3.76 \times 1.8 \times .5 \times 3$	6.768
LOWER PAD	$1.90 \times 4.2 \times .5 \times 2$	6.800
OUTER STRUT	$.7 \text{ in}^2 \times 8.75 \times 2$	12.950
INNER STRUT	$.7 \text{ in}^2 \times 9.75 \times 2$	$\underline{13.650}$

$$38.968 \text{ in}^3 \times .286 = 11.07"$$

$$\times \frac{3}{33.2}$$

+ HARDWARE $\frac{4.0}{37.2}$

$$37.2" \quad \underline{37.2}$$

PROPELLION "Y" & TRI-DUCT WEIGHT
CALCULATIONS

PROPELLION - HOT GAS DUCTING - REF. STUDY DRAWING
395-0925

TRI-DUCT

OUTER DUCT 24" - INNER DUCT 17" (STRESSED SKIN)
SIGN 1.30 lb/in^3 MATERIAL .015" THICK

DUCT	$17 \times 3.1416 \times 50 \times .015$	40.06	
	$17 \times 3.1416 \times 42 \times .015$	38.65	
	$17 \times 3.1416 \times 48 \times .006 \times 2$	26.92	
	$9 \times 3.1416 \times 30 \times .015 \times 3$	38.17	
	$9 \times 3.1416 \times 30 \times .015 \times 3$	38.17	
	$24 \times 3.1416 \times 50 \times .015$	<u>16.54</u>	
		<u>239.5 in^3</u>	<u>70.0 lb</u>

DUCT TO BLADE FLANGE - 1 $\frac{1}{2}$ " D.I.D.
 $XV-9A = 2.44" @ 10" D \therefore 2.44 \times \frac{14}{10} \times 6$

20.4 lb

STIFFENING (SAME AS XV-9A) $\times 2$

10.6 lb

LOWER FLANGE	$.25 \times 1.2 \times 17 \times 3.1416$	16.02	
	$.1 \times 1.2 \times 25 \times 3.1416$	9.42	
	$.15 \times .6 \times 25.5 \times 3.1416$	7.21	
	$.1 \times .5 \times 3.5 \times 3$	<u>.59</u>	
		<u>39.2 in^3</u>	<u>10.0 lb</u>

INSULATION	$26 \times 3.1416 \times 50$	408U	
	$9 \times 3.1416 \times 30 \times 6$	<u>52.72</u>	
		<u>9.85 in^3 $\times .0012 \text{ lb/in}^3$</u>	<u>11.2 lb</u>

TOTAL TRI-DUCT 122.2 lb

Y TO TRI-DUCT SEAL

TRI-DUCT SEAL HSNG	$53.4 \text{ in}^3 \times .286 = 15.3$	lb
Y DUCT SEAL HSNG	$52.91 \text{ in}^3 \times .286 = 15.1$	lb
SPRINGS & WASHERS	= 1.0	lb
CARBON SEALS - INNER $3.3 \text{ in}^3 \times .33 \times 2$	= 2.2	lb
- OUTER $4.9 \text{ in}^3 \times .33$	= 1.6	lb

35.2 lb

TOTAL SEAL

HOT GAS DUCTING WEIGHT CALCULATIONS
(CONT'D)

HOT GAS DUCTING - (CONTINUED)

Y DUCT (FOR CONFIGURATION #2)

17 x 3.1416 x 85 x .015	68.09	
17 x 3.1416 x 45 x .015	36.05	
24 x 3.1416 x 40 x .015	45.24	
17 x 3.1416 x 40 x .015	32.04	
17 x 3.1416 x 2 x 40 x .006	<u>25.64</u>	
	2021 in ³ x .3	62.1 #

DIVERTER VALVE ADAPTER
SAME AS XV-9A x 2

5.9 #

BELLOWS(2) (Ø 18" dia
XV-9A 3.16" @ 12"
3.16 x 18" x 2

9.5 #

FLANGE TO TRI-DUCT
SAME AS FLANGE ON TRI-DUCT

10.0 #

INSULATION

18 x 3.1416 x 45 x 2	5089.4	
25 x 3.1416 x 40	<u>3141.6</u>	
	8231 x .0012 ^{6/m³}	9.9 #

TOTAL Y DUCT

99.4 #

TOTAL HOT GAS DUCTING
(FROM DIVERTER VALVE TO
BLADE ARTICULATED DUCT)

255 #

SUMMARY - ROTATING CONTROLS
WEIGHT CALCULATIONS

SUMMARY
FLIGHT CONTROLS
(ROTATING HEAD CONTROLS)

REF. DRAWING 395-0932

STATIONARY SWASHPLATE	319.0
SWASHPLATE	249.0
ARMS	70.0
ROTATING SWASHPLATE	224.7
SWASHPLATE	184.0
ARMS	40.7
SWASHPLATE BEARINGS	200.0
SWASHPLATE BEARING BALL	75.2
TORQUE SCISSORS	11.5
VERTICAL LINKS + FITTINGS	29.3
PITCH ARM (IN TORQUE BOX WT.)	—
HYDRAULIC CYLINDERS + MOUNTS	390.0

TOTAL ROTATING CONTROLS 1250 [#]

**SWASHPLATE ACCESSORY WEIGHT
CALCULATIONS**

SWASHPLATE SUPPORT AL

$$19\text{ IN} \times 1.5(\text{STIFF}) \times 0.2\text{ IN} \times 42\text{ IN WT} \times 0.1\text{ LB/IN}^3 = 75.2\text{#}$$

TORQUE SCISSORS AL

$$8.0\text{ IN} \times 0.2\text{ IN} \times 24\text{ IN} \times 0.1\text{ LB/IN}^3 = 38.8\text{#} \quad 11.5\text{#}$$

PUSH-PULL LINKS ST
35" LONG $A = 0.82\text{ IN}^2$

$$35\text{ IN} \times 0.82\text{ IN}^2 \times 0.285\text{ LB/IN}^3 \times 3\text{ REQ} = 24.5\text{#}$$

END FITTINGS (PUSH-PULL LINKS)

$$0.8\text{ LB EA} \times 6\text{ REQ} \quad 4.8\text{#}$$

SWASHPLATE ARMS - STATIONARY ST

$$45\text{ IN} \times (2 \times 0.75\text{ IN} \times 0.25\text{ IN} + 8.0\text{ IN} \times 0.15\text{ IN}) \times 0.285\text{ LB/IN}^3 \times 3\text{ REQ} = 70.0\text{#}$$

SWASHPLATE ARMS - ROTATING ST

$$24\text{ IN} \times (2 \times 1.0\text{ IN} \times 0.175\text{ IN} + 8.0\text{ IN} \times 0.2\text{ IN}) \times 0.285\text{ LB/IN}^3 \times 3\text{ REQ} = 40.7\text{#}$$

SWASHPLATES - WEIGHT CALCULATIONS

ROTATING SWASHPLATE STEEL

$$51 \text{ IN} \times \pi \times (2.5 \times 0.7 + 3.6 \times 1.15 + 2.5 \times 0.7) \text{ IN}^2 \times 0.285 \text{ LB/IN}^3 = \underline{184^*}$$

STATIONARY SWASHPLATE ST

$$46 \text{ IN} \times \pi \times (1.25 \times 1.0 + 5.2 \times 0.1 + 1.0 \times 1.25 + 1.4 \times 0.5 + 2.3 \times 0.25 + 3.5 \times 0.5) \text{ IN}^2 \times 0.285 \text{ LB/IN}^3 = \underline{249^*}$$

SWASHPLATE BEARINGS

BALLS ST

$$\left(\frac{.75 \text{ IN}}{2}\right)^3 \times \frac{4}{3} \pi \times 0.285 \text{ LB/IN}^3 \times 300 \text{ RPM} = 18.8^*$$

BEARING RETAINERS ST

$$0.3 \text{ IN} \times 6.75 \text{ IN} \times 47.6 \text{ IN} \times \pi \times 0.285 \text{ LB/IN}^3 = 86.3^*$$

INNER AND OUTER RACES ST

$$0.25 \text{ IN} \times 7 \text{ IN} \times 47.6 \text{ IN} \times \pi \times 0.285 \text{ LB/IN}^3 = 74.6^*$$

SEALS NEOPRENE RUBBER

$$1.7 \text{ IN} \times 0.25 \text{ IN} \times 47.6 \text{ IN} \times \pi \times 0.072 \text{ LB/IN}^3 = 4.6^*$$

SEAL RETAINERS ST

$$0.55 \text{ IN} \times 0.05 \text{ IN} \times 47.6 \text{ IN} \times \pi \times 0.285 \text{ LB/IN}^3 = 1.2^*$$

GREASE

$$0.5 \text{ IN} \times 4 \text{ IN} \times 47.6 \text{ IN} \times \pi \times 0.036 \text{ LB/IN}^3 = 10.8^*$$

MISCELLANEOUS 3.7^*

TOTAL WEIGHT - SWASHPLATE BEARINGS 200^*

ACTUATORS, SWASHPLATE-WEIGHT CALCULATIONS

ACTUATORS

$P_{INIT} = 83,300 \text{ LBS}$ $STROKE = 8 \text{ IN}$ $PRESSURE = 3000 \text{ LBS}$
 BORE DIA = 6 IN $L_{CYL} = 33 \text{ IN}$ ROD DIA = 1.75 IN
 $L_{ROD} = 29 \text{ IN}$

$$(CYL WALL) \quad t = \frac{3 \times P \times B}{2 \times 160,000} = \frac{3 \times 3000 \times 6}{320,000} = .2 \text{ IN}$$

$$(ROD AREA) \quad A = \frac{15P}{\sigma} = \frac{1.5 \times 83,300}{120,000} = 1.01 \text{ IN}^2$$

$$CYL WT = B \times \pi \times C \times L_{CYL} \times 0.2854 \text{ LBS} = \\ 6 \times 3.14 \times 0.2 \times 3.8 \times 0.285 = 35.4 \text{ LBS}$$

CYL ENDS AND DIVISION ST

$$B^2 \times 0.7854 \times 1.5 \times 0.285 = 12.1 \text{ LBS}$$

ROD WT ST
 $A \times L_{ROD} \times 0.285$

$$\left(\frac{1.75}{2}\right)^2 \times \pi \times 29 \times 0.285 = 19.9 \text{ LBS}$$

PISTON VALVE WT ST

$$B^2 \times 0.7854 \times \Delta L \times 0.285 \\ 6^2 \times 0.7854 \times 1.0 \times 0.285 = 8.1 \text{ LBS}$$

SERVO VALVE 9.0 LBS

FLUID WEIGHT
 $B^2 \times 0.7854 \times L \times 0.038 \text{ LBS/IN}^3$

$$6^2 \times 0.7854 \times 2.2 \times 0.038 = 23.6 \text{ LBS}$$

MISCELLANEOUS AND MOUNTS 21.9 LBS

WEIGHT PER ACTUATOR 130.0 LBS

3 REQ 390 LBS

APPENDIX II
PRELIMINARY STRUCTURAL ANALYSIS

The preliminary structural analysis of the Heavy-Lift Hot Cycle Helicopter Rotor System is contained in this Appendix as outlined below.

- I. Basic Rotor Configuration
- II. Weight Data
- III. Temperature Data
- IV. Design Loads
- V. Materials and Allowable Stresses
- VI. Stress Analysis
 - a. Rotor Blade
 - b. Blade Retention System
 - c. Hub
 - d. Rotor Shaft Bearings
 - e. Flight Controls
 - f. Hot Gas Ducting

I. BASIC ROTOR CONFIGURATION (Figure 16 and 17)

The rotor is composed of three blades that are attached to the hub by retention straps. The retention straps transfer the blade centrifugal force to the hub. The inboard end of the blade is mounted in the hub with a feathering bearing. The retention straps provide the flexibility to allow the blade to flap and feather about the feathering bearing.

At the connection of the retention straps to the blade is located a lead-lag flexure. The lead-lag motion is controlled by a damper mounted at the leading edge of the blade.

The hub is attached to the rotor shaft by three multimember attachment fittings spaced equally about the circumference of the shaft.

The rotor shaft is supported by a lower bearing loaded by thrust and radial load and an upper bearing loaded radially.

The swashplate is mounted on the rotor shaft support between the upper and lower bearing. The rotating swashplate is attached directly to the blade pitch arm by a single tension-compression member. This design provides a short direct load path as well as a rigid control system.

BASIC DATA

Rotor radius	45.0 ft
Chord	60.0 in.
Airfoil section (blade)	
NACA 0018	Root to 3/4 radius
NACA 0014	3/4 radius to tip
Number of blades	3
Blade twist	-8°
Flapping hinge offset (% blade radius)	4.2%
Rotor shaft attitude	5° fwd
Design gross weight	65,700 lb

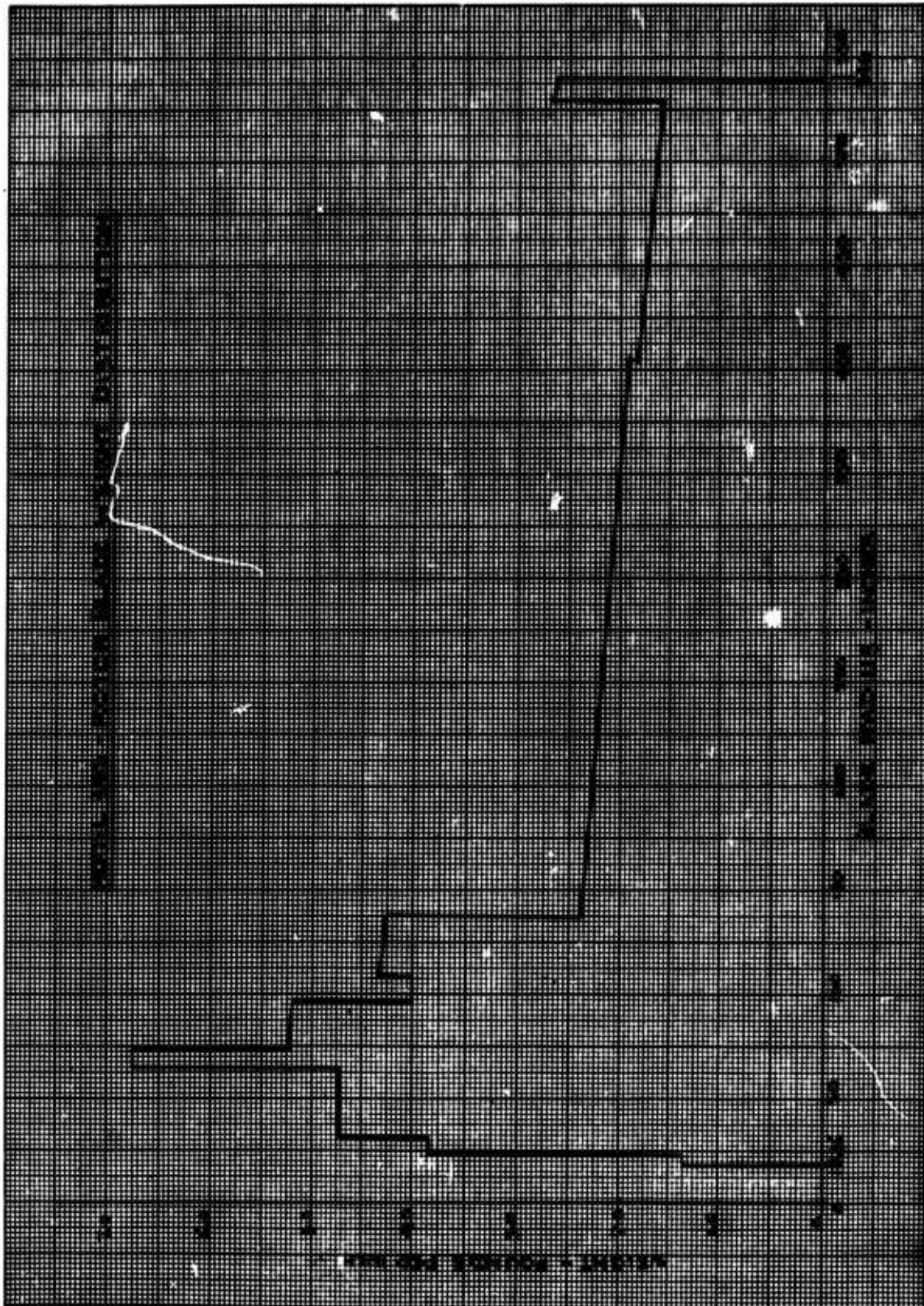
II. WEIGHT DATA

The weights used in this report were chosen early in the design program. Therefore they do not quite agree with the latest weight data based on the final preliminary design drawings.

However, the values used are conservative. The blade weight used is 1,363 pounds as against the latest value of 1,307 pounds. This results in

the blade and hub being designed for slightly higher centrifugal forces than required.

The total weight of the blades, hub, and rotor-shaft used is 5,000 pounds as against the latest value of 5,400 pounds. This results in the rotor shaft and bearings being designed for slightly higher loads than required, as the greater weight would give some additional relief to counteract the lift loads.



V.K
JULY 20, 68

III. TEMPERATURE DATA

The temperatures and gas pressures used in the analysis of the hot gas duct system are based on the engine characteristics of the General Electric GE-1 turbine engine.

The temperature spectrum for long-time operation of the ducting system is based on the mission requirements as determined from the contract. Mission requirements indicate that the gas temperatures will be below 1100°F for 80 percent of the time and below 1300°F for 95 percent of the time. Thus, the gas temperature spectrum used for structural design (see following page) is conservative.

This spectrum used for checking the ducting system for long-time operation as determined by the 0.2 percent creep allowable of the ducting material has been arbitrarily limited to a minimum gas temperature of 1300°F.

This conservatism has not caused any weight penalty, as the blade ducting gages are determined by fabrication requirements.

III TEMPERATURE DATA

GAS TEMPERATURE AND PRESSURE

SPECTRUM

CONDITION	TIME HOURS	GAS TEMP °F	DUCT* °F
EMERGENCY	.33	1490°	1390°
TAKEOFF MAX	300.00	1425°	1325°
MILITARY	1200.00	1350°	1250°
MILITARY POWER STD. DAY OR NORMAL POWER HOT DAY	2099.67	1300°	1200°
	3600.00		

* Duct Wall Temp = Gas Temp - 100°F from XV-9 DATA

T.F	T+460	t	t _{ave}	%t _{ave}
1390	1850	.33	75.	.0044
1325	1785	300.00	468.	.6410
1250	1710	1200.00	4680.	.2570
1200	1660	2099.67	23450.	.0896
		3600.00		.9920

$$(T+460)(20+6\ln_{10} t) = 40.47(10^3) \quad T=1260°F$$

T = LONG TIME EQUIVALENT DUCT WALL TEMPERATURE
FOR 3600 HOURS OF OPERATION

SUMMARY OF DUCT WALL TEMPERATURE & PRESSURE

CONDITION	Temperature Duct Wall	GAS Pressure
PEAK VALUES	1390°F	39.6 $\frac{\text{lb}}{\text{in}^2}$
3600 HOUR OPERATION	1260°F	35.0 $\frac{\text{lb}}{\text{in}^2}$

8704

IV DESIGN LOADS

The basic rotor structural design criteria has been previously shown in the Structure section of this report.

The main rotor design loads were developed from test data available from flight strain surveys on the XV-9A, OH-6, and H-34 helicopters. Since the XV-9A rotor is rigid in-plane (no lead-lag hinge), the effect of chord-flap coupling was compensated for in the use of blade loads from that helicopter.

Bending moments were scaled proportional to gross weight times rotor radius, torsional moments were scaled proportional to gross weight times blade chord, and shears were scaled proportional to gross weight. Chordwise moment was based on lead-lag damping twice as large as required to prevent ground resonance.

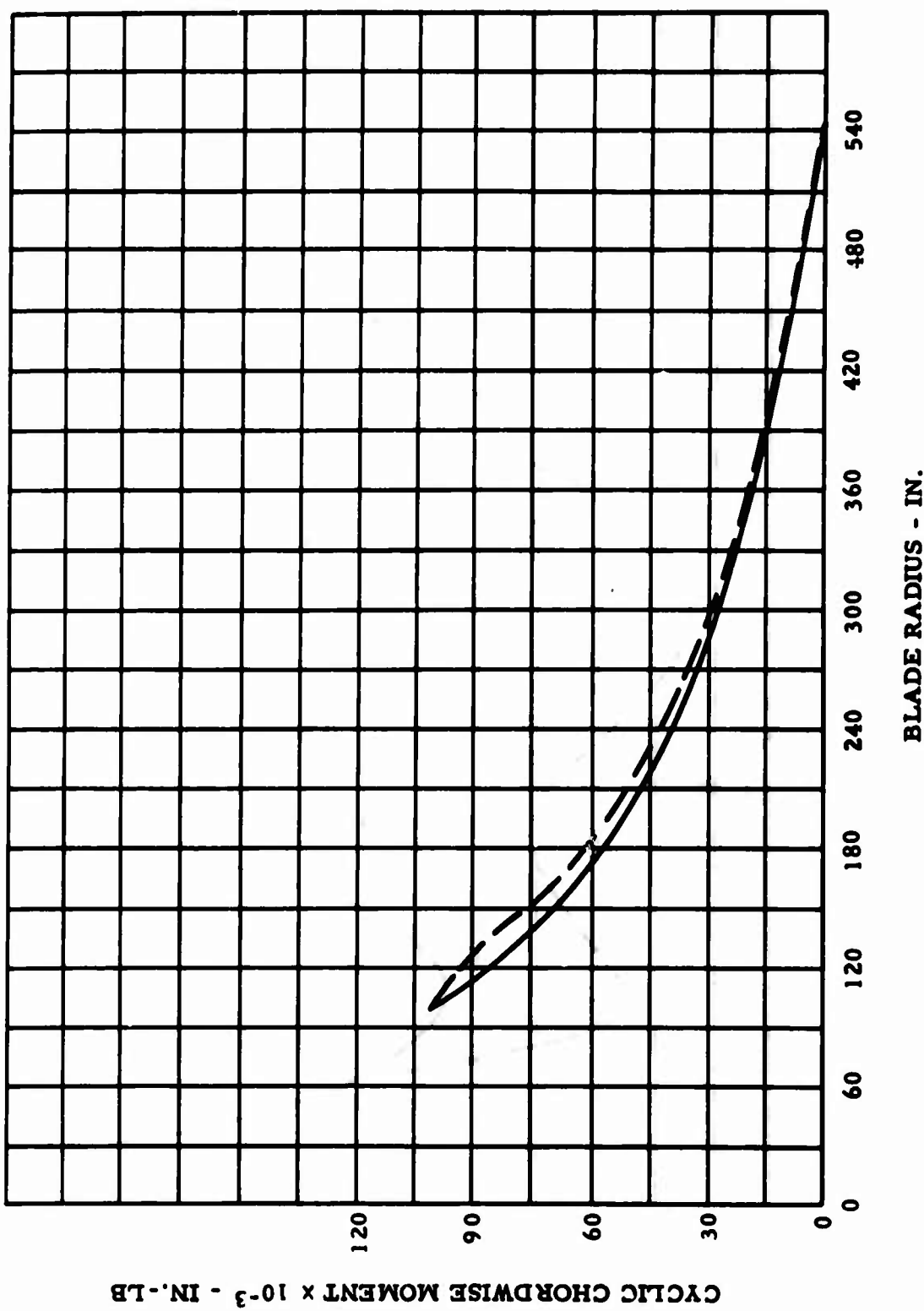
After the blade was designed to carry the loads based on the method described above, the resulting blade properties were used in a fully-coupled dynamic analysis of the design flight condition to corroborate the design loads. The satisfactory correlation of the design loads and computed loads are shown by the following two curves on the next two pages.

The cyclic chordwise moment distribution shows good agreement between the design values and the results of the coupled analysis. The cyclic flapwise moment distribution from the coupled analysis has higher values than used in design between blade station 60 to 375. However, the blade as designed has sufficient strength to accommodate these higher values as shown in the Stress Analysis section.

The structural weight data used in determining the design loads was obtained from detailed analysis of the blade and hub design.

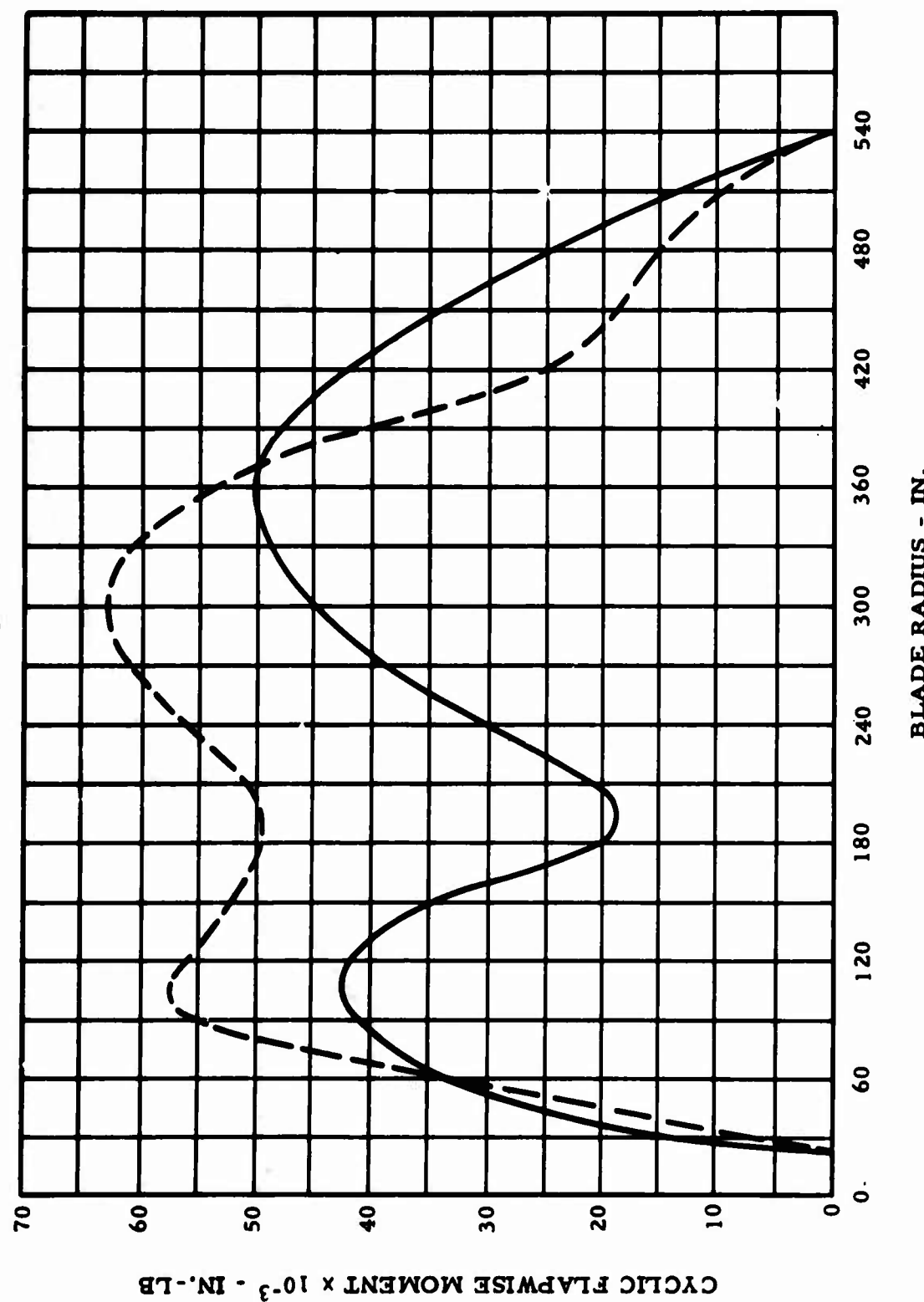
Cyclic Chordwise Moment Distribution

— — Coupled Analysis
— Design



Cyclic Flapwise Moment Distribution

— — Coupled Analysis
— Design



IV DESIGN LOADS

BLADE LOADS SUMMARY

SYMBOL	LOAD DESCRIPTION	FATIGUE CONDITION	LIMIT MANEUVER
$M_{F,2R}$	FLAPPING MOMENT	$36,011 \pm 4,213$	$110,632 \pm 110,632$
$M_{F,BR}$	FLAPPING MOMENT	$33,031 \pm 40,393$	$65,150 \pm 65,150$
V_z	FEATHERING BALL SHEAR - VERTICAL	$839 \pm 1,009$	$1,009 \pm 1,009$
$M_{C,2R}$	CHORDWISE MOMENT	$\pm 100,000$	$\pm 500,000$
$M_{C,BR}$	CHORDWISE MOMENT	± 6250	$\pm 37,500$
$V_{x,2R}$	CHORDWISE SHEAR	± 370	± 1850
$V_{x,BR}$	CHORDWISE SHEAR	± 95	± 475
$M_{T,2R}$	BLADE TORSION	$63,000 \pm 75,500$	$228,000 \pm 228,000$
$M_{T,BR}$	BLADE TORSION	$31,000 \pm 37,000$	$112,000 \pm 112,000$
$M_{T,ROOT}$	BLADE TORSION	$64,000 \pm 76,000 + M_{STAB}$	$230,000 \pm 230,000 + M_{STAB}$
β	FLAPPING ANGLE	$8^\circ + 5^\circ \cos(\psi - 30^\circ)$	$13^\circ + 10^\circ \cos(\psi - 30^\circ)$
ξ	LEAD-LAG ANGLE	$1.25^\circ \sin \psi$	$3^\circ \sin \psi$
θ	FEATHERING ANGLE	$7^\circ - 12^\circ \sin \psi$	$14^\circ - 14^\circ \sin \psi$
-	TIP SPEED	675 F.P.S	* 787 F.P.S

* SPARS, RETENTION STRAPS, ATTACHMENTS AND HUB ARE CHECKED FOR DIRECT LOAD FROM BLADE CENTRIFUGAL FORCE ONLY DUE TO 840 F.P.S TIP SPEED. (787 F.P.S = 105% OF 750 F.P.S)

A SECOND LIMIT CONDITION IS CONSIDERED IN WHICH ALL LOADS AND MOTIONS ARE THE SAME AS ABOVE, EXCEPT FLAPPING ANGLE BECOMES $15^\circ + 10^\circ \cos(\psi - 30^\circ)$ AND TIP SPEED IS 675 F.P.S

- CONT. -

IV DESIGN LOADS

BLADE MOTION CAPABILITY IS PROVIDED AS FOLLOWS:

FLAPPING — +25°
— 6.0°

COLLECTIVE PITCH (BLADE) — +14° MAX (AT 75% RAD)
+1° MIN.

COLLECTIVE PITCH (CONTROLS) — +14°
±1°

CYCLIC PITCH - FORWARD — 14°
- AFT. — 14°
- LATERAL — ± 6°

BLADE RETENTION STRAPS ARE UNTWISTED WHEN THE 75% RADIUS BLADE STATION IS AT 8°

LEAD LAG MOTION — ± 1.25° CRUISE
± 3.00° MANEUVER

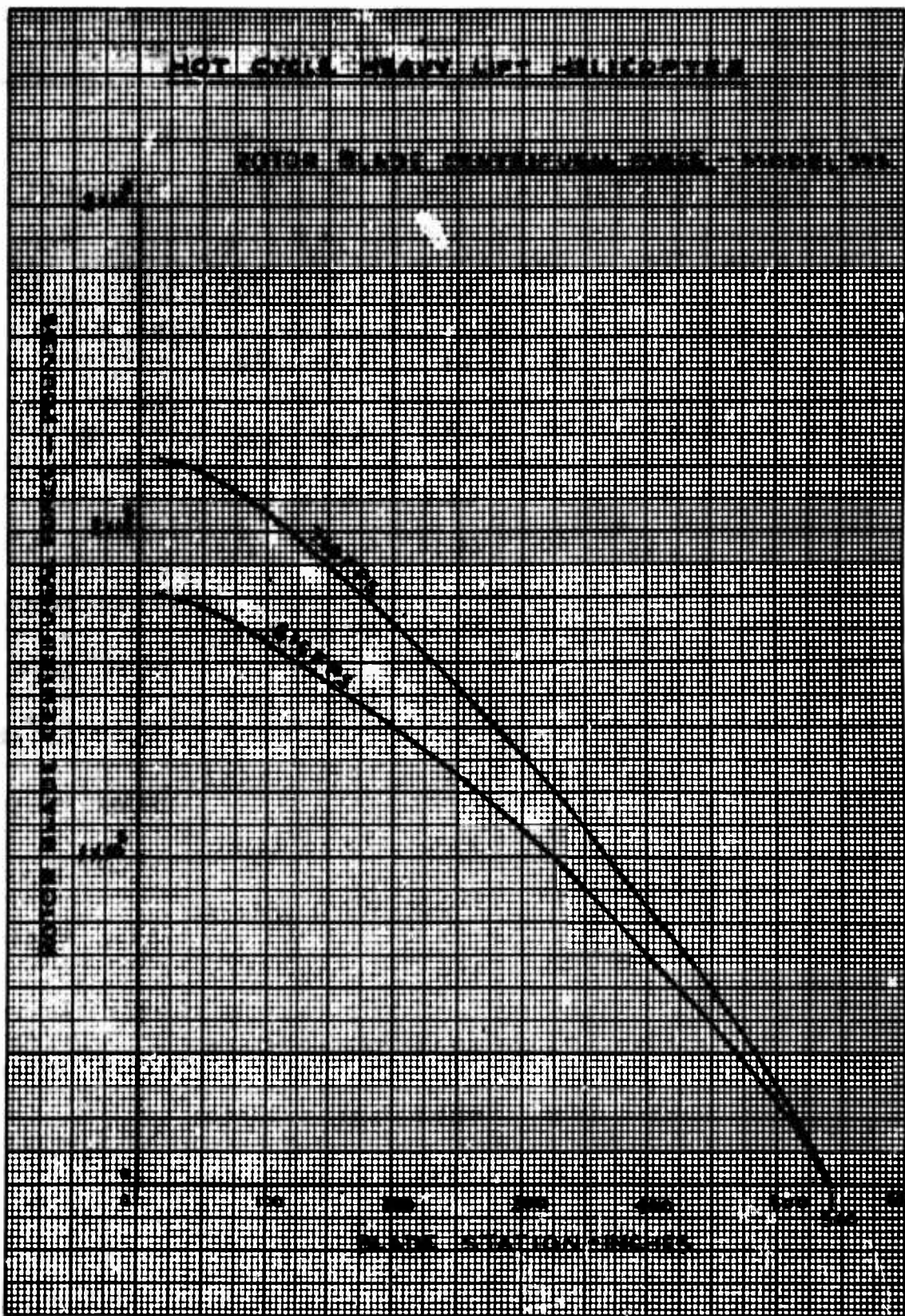
IV DESIGN LOADS

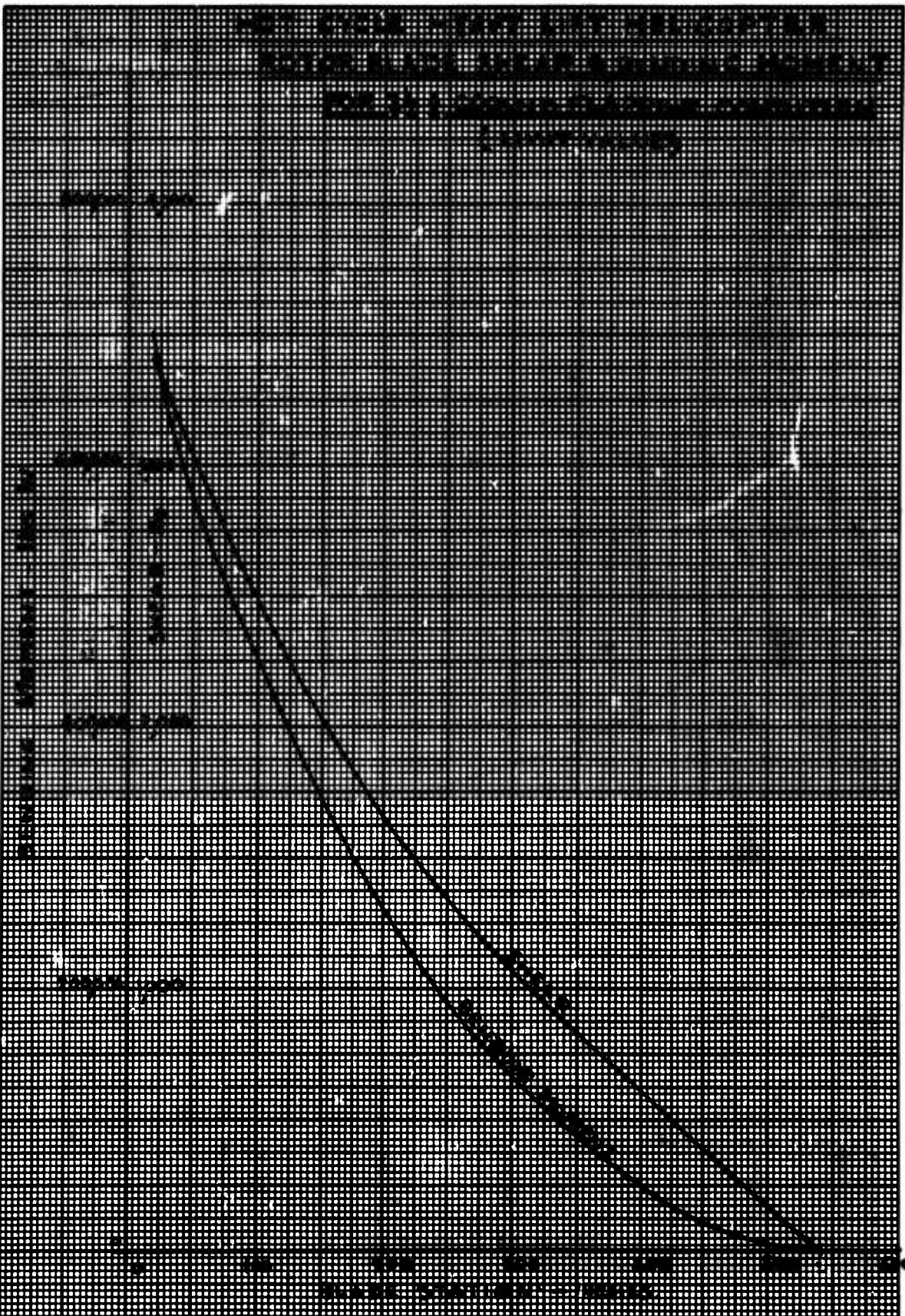
• BLADE CENTRIFUGAL FORCE AT 675 F.P.S TIP SPEED

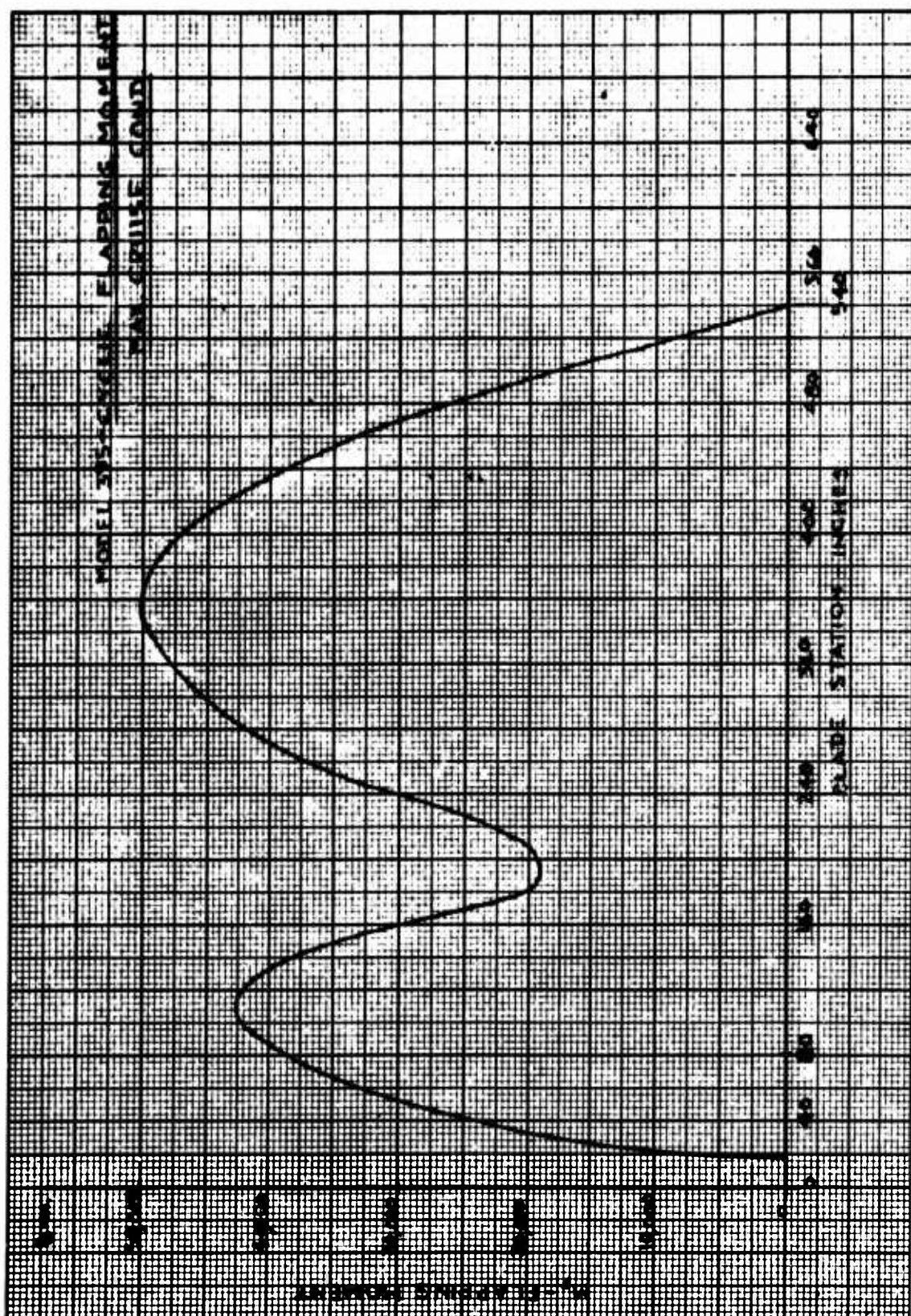
STA.	Δ STA.	#/IN AVG.	ΔWT	RADIUS TO C.G.	$\delta = \frac{\Delta W}{386}$	$\Delta C.F. = \frac{\Delta W \cdot \Delta W}{386}$	TOTAL C.F. @ 675 F.P.S	TOTAL C.F. @ 750 F.P.S
18	6	1.350	.8	21	12.20	98	180,455	222,320
24	8	3.85	30	28	16.30	484	180,357	222,199
32	33	4.72	155	48.5	28.24	4,377	179,868	221,597
65	9	6.75	60	69.50	40.50	2,430	175,471	216,205
74	23	5.20	119	85.50	49.80	59,26	173,061	213,211
97	11	4.00	44	102.50	59.43	2,615	167,133	205,910
108	34	4.30	146	125	72.82	10,632	164,520	202,687
142	160	2.25	360	222	129.40	46,580	153,888	189,590
302	73	2.02	147	338.50	197.32	29,006	167,308	132,203
375	30	1.940	58	390	227.35	13,186	78,302	96,460
405	45	1.750	76.50	427.5	248.87	19,038	65,116	80,223
450	79	1.650	130.	489.5	285	37,050	46,078	56,768
529	11	2.650	29	534.5	311.30	9,028	9,028	11,122
540							0	0
TOTAL			1362.50					

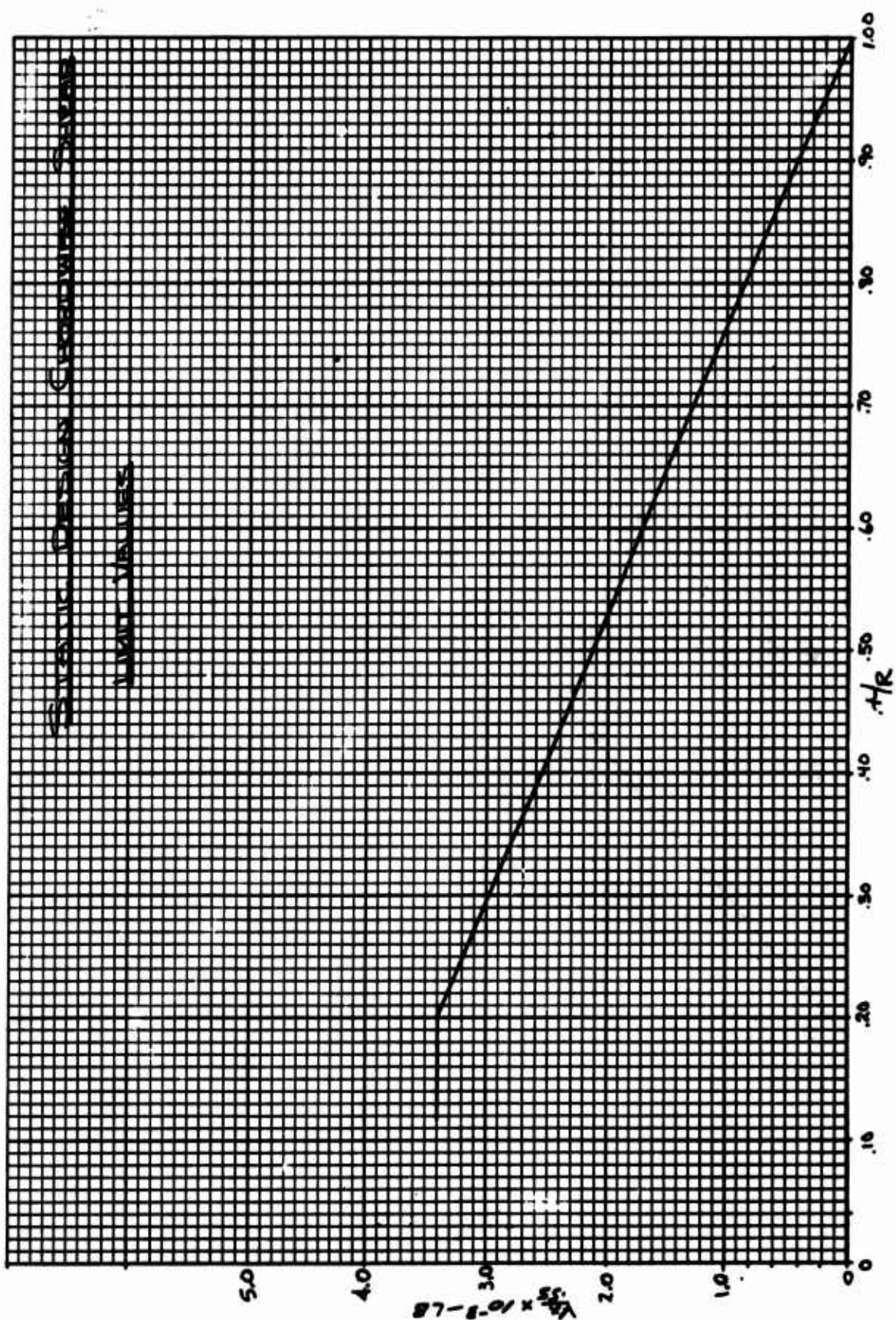
$$* \frac{675 \text{ F.P.S}}{2\pi\lambda} = \frac{675}{2\pi(45)} = 2.38 \text{ R.P.S}, \omega = 2.38 \times 2\pi = 15 \text{ Rad/sec.}; \omega^2 = 225$$

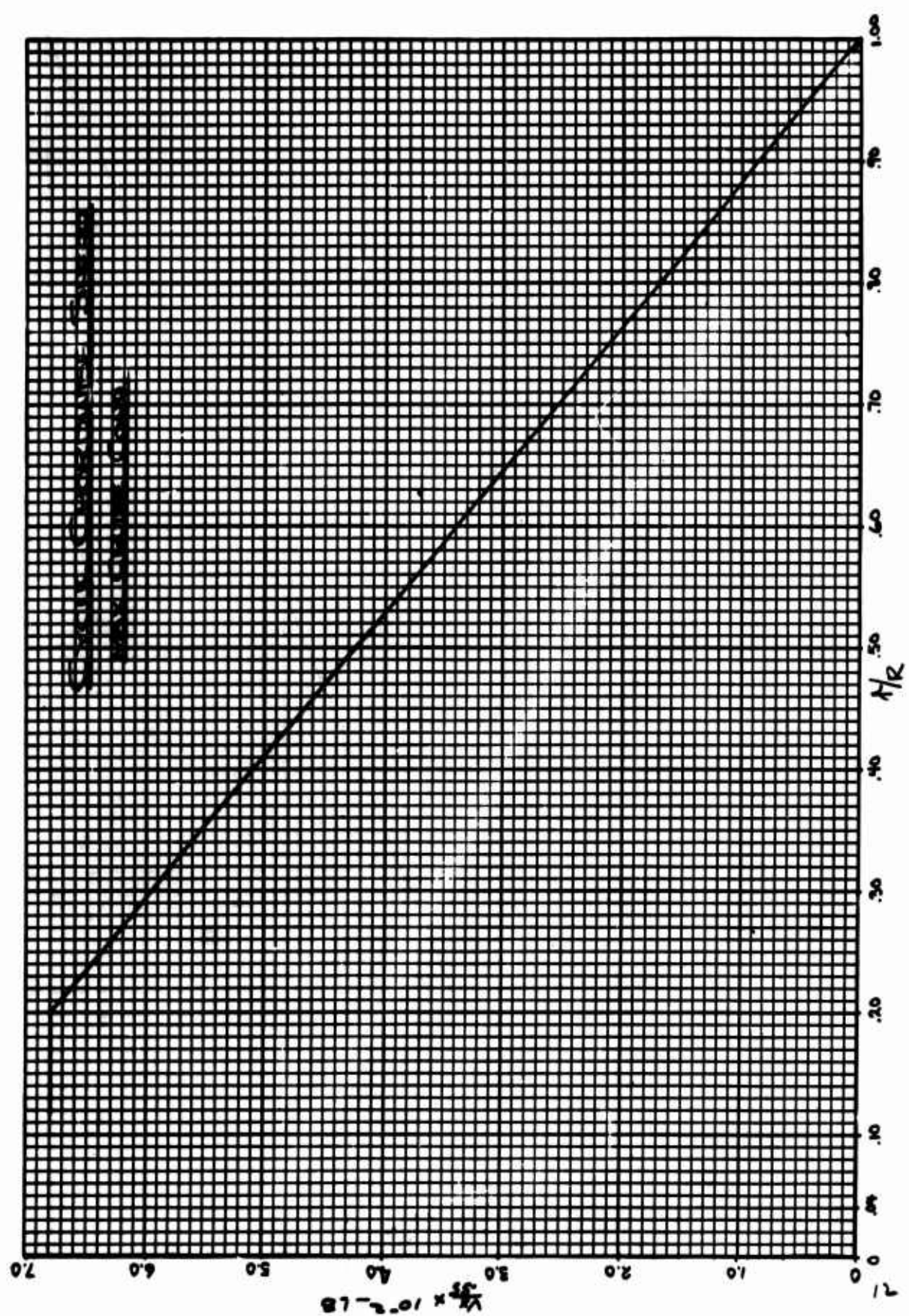
8784

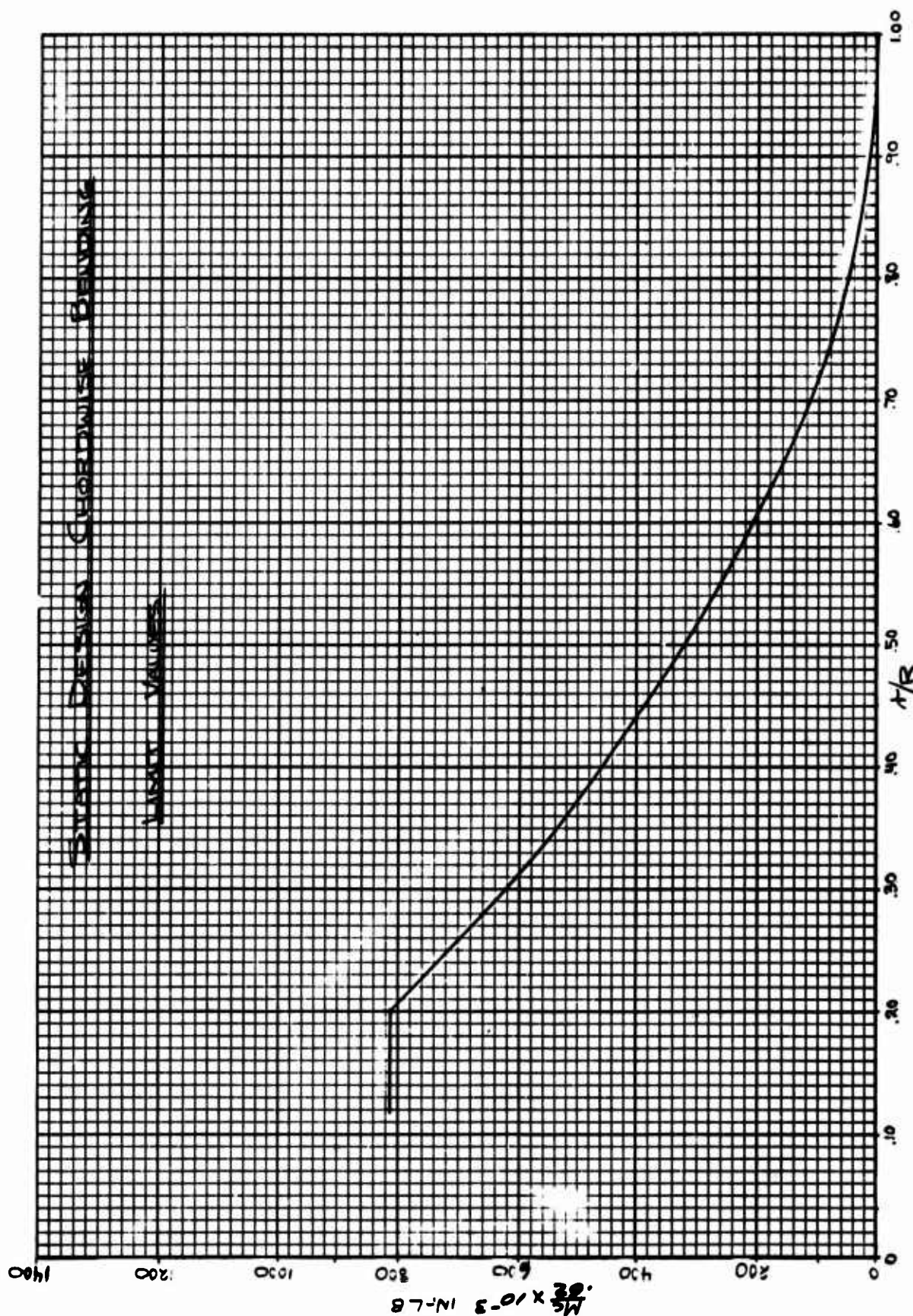


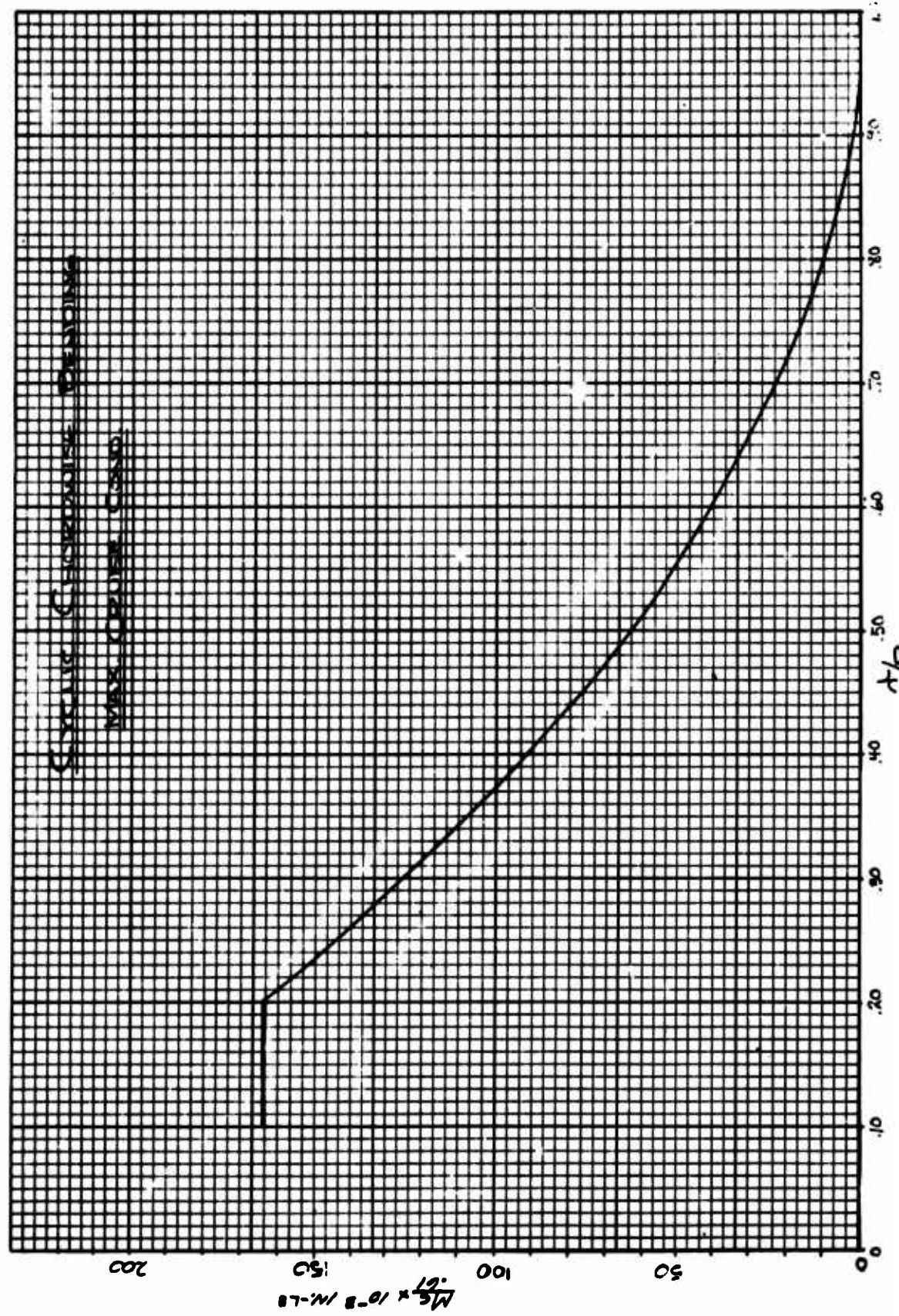


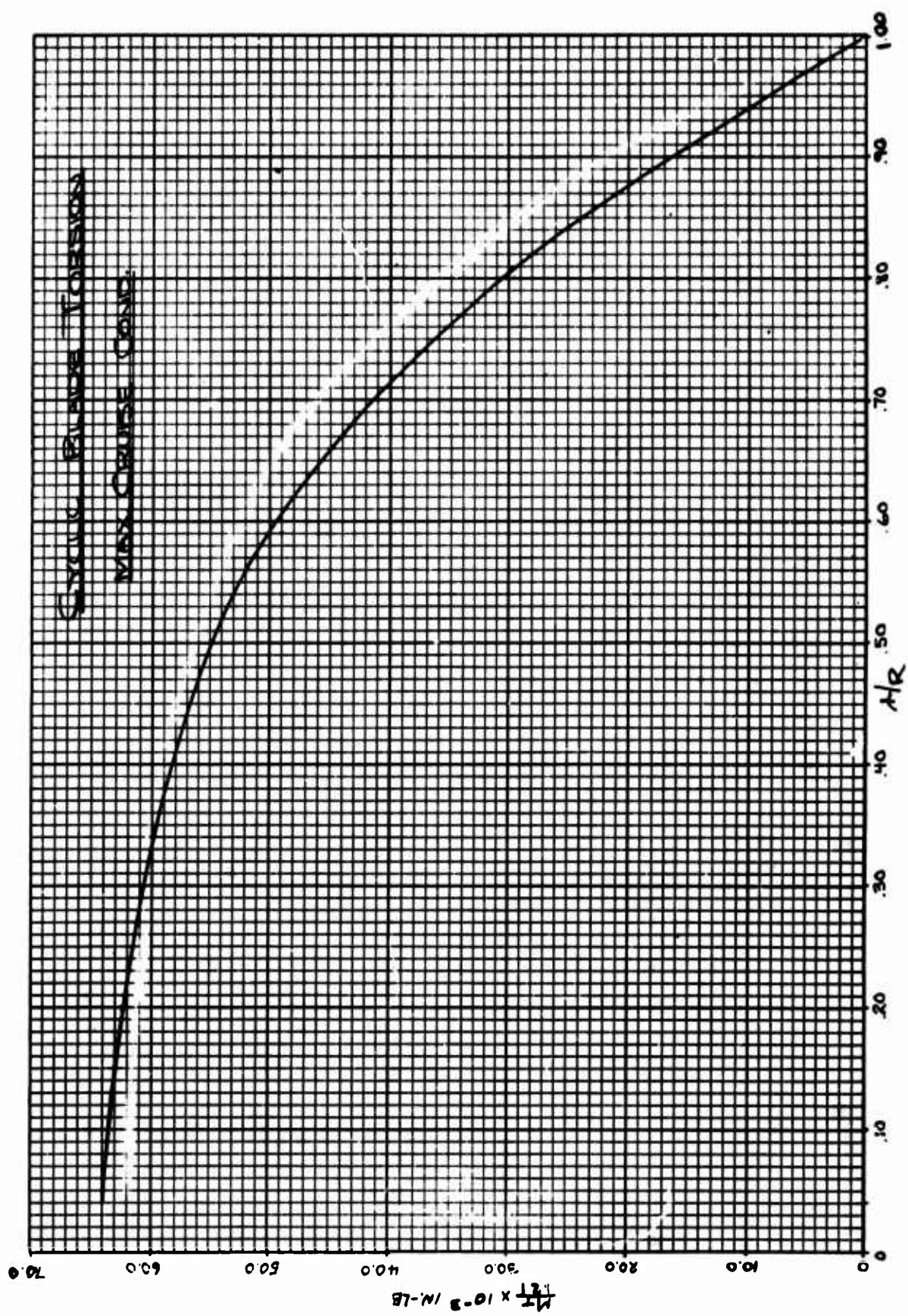


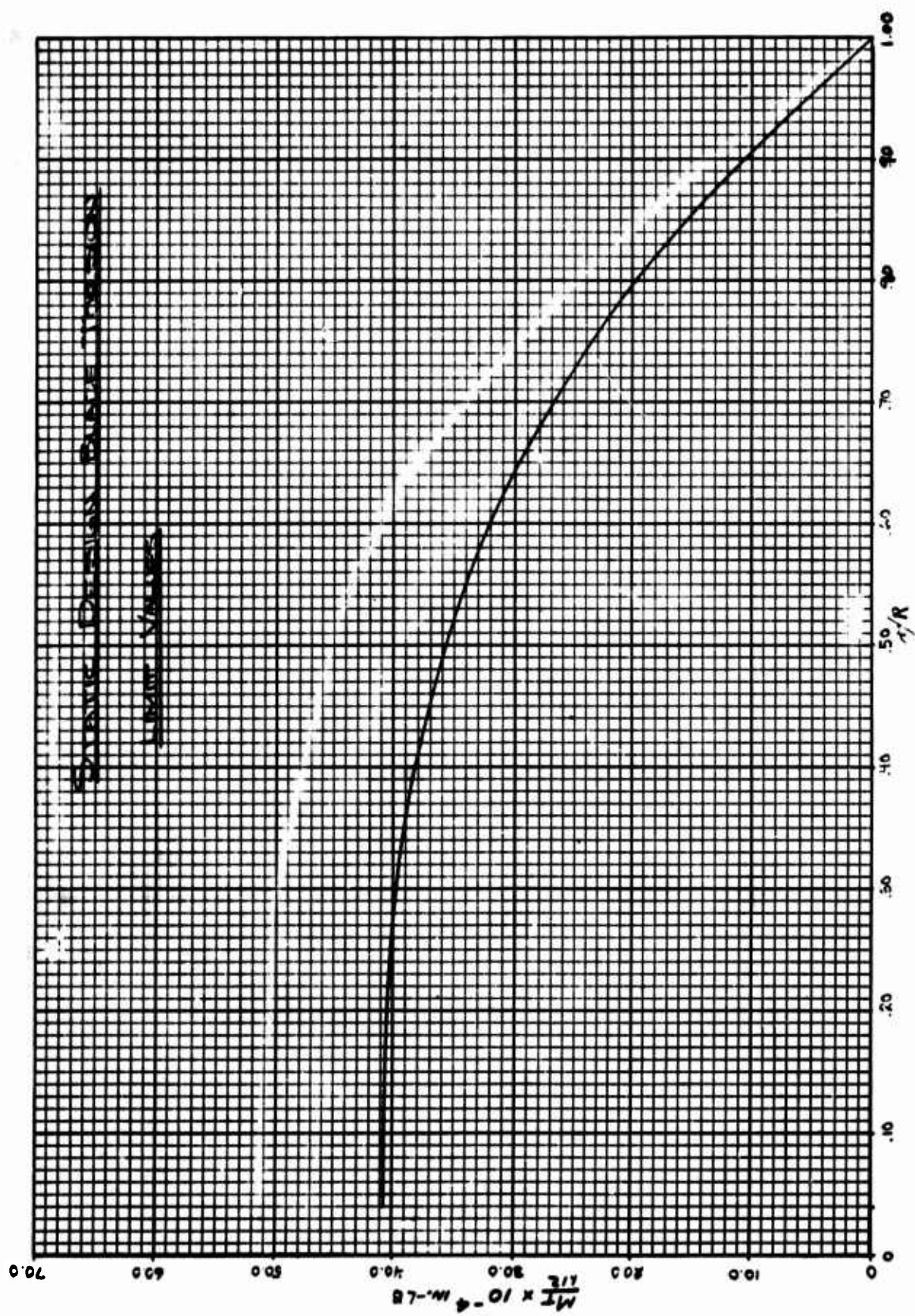


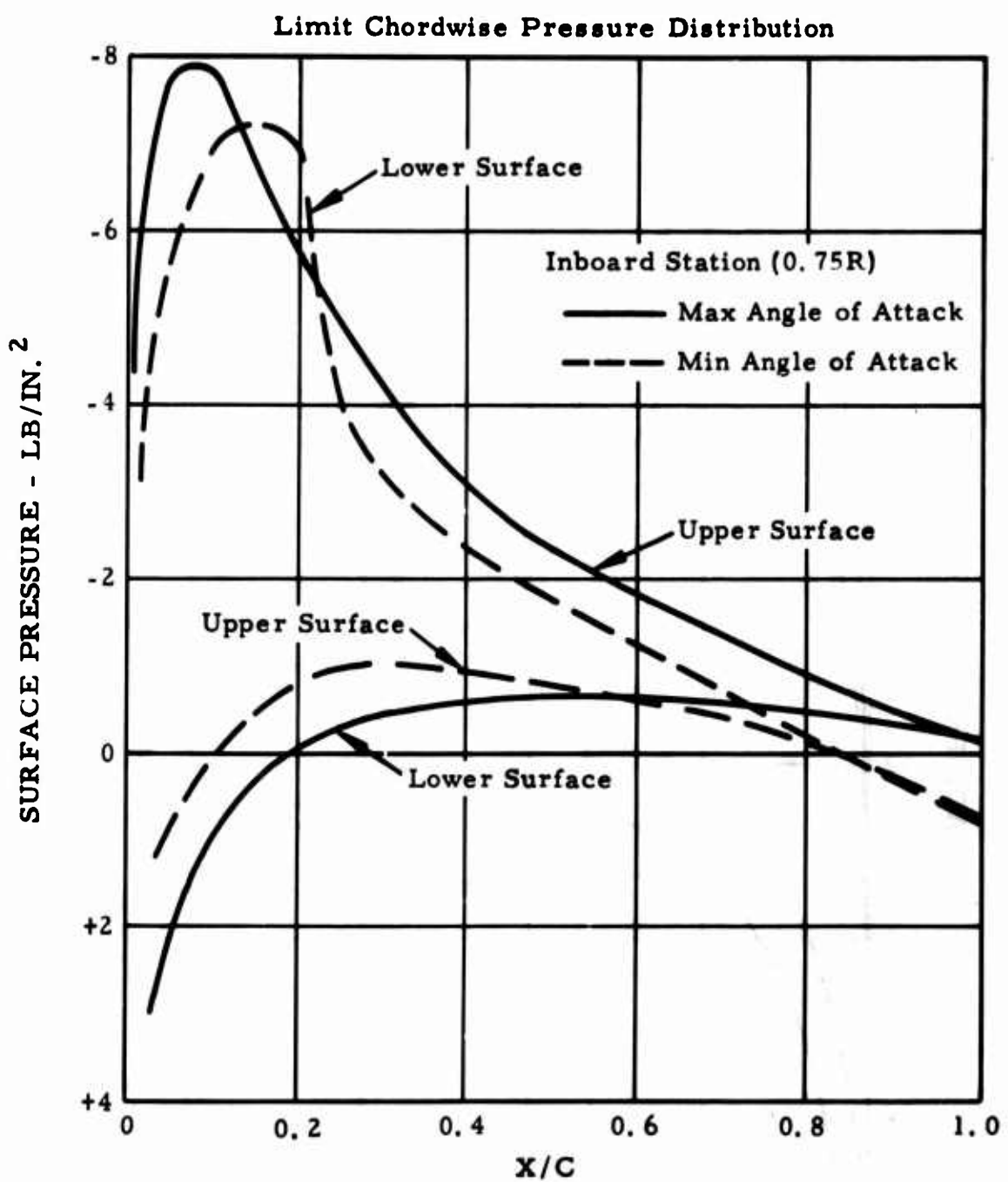


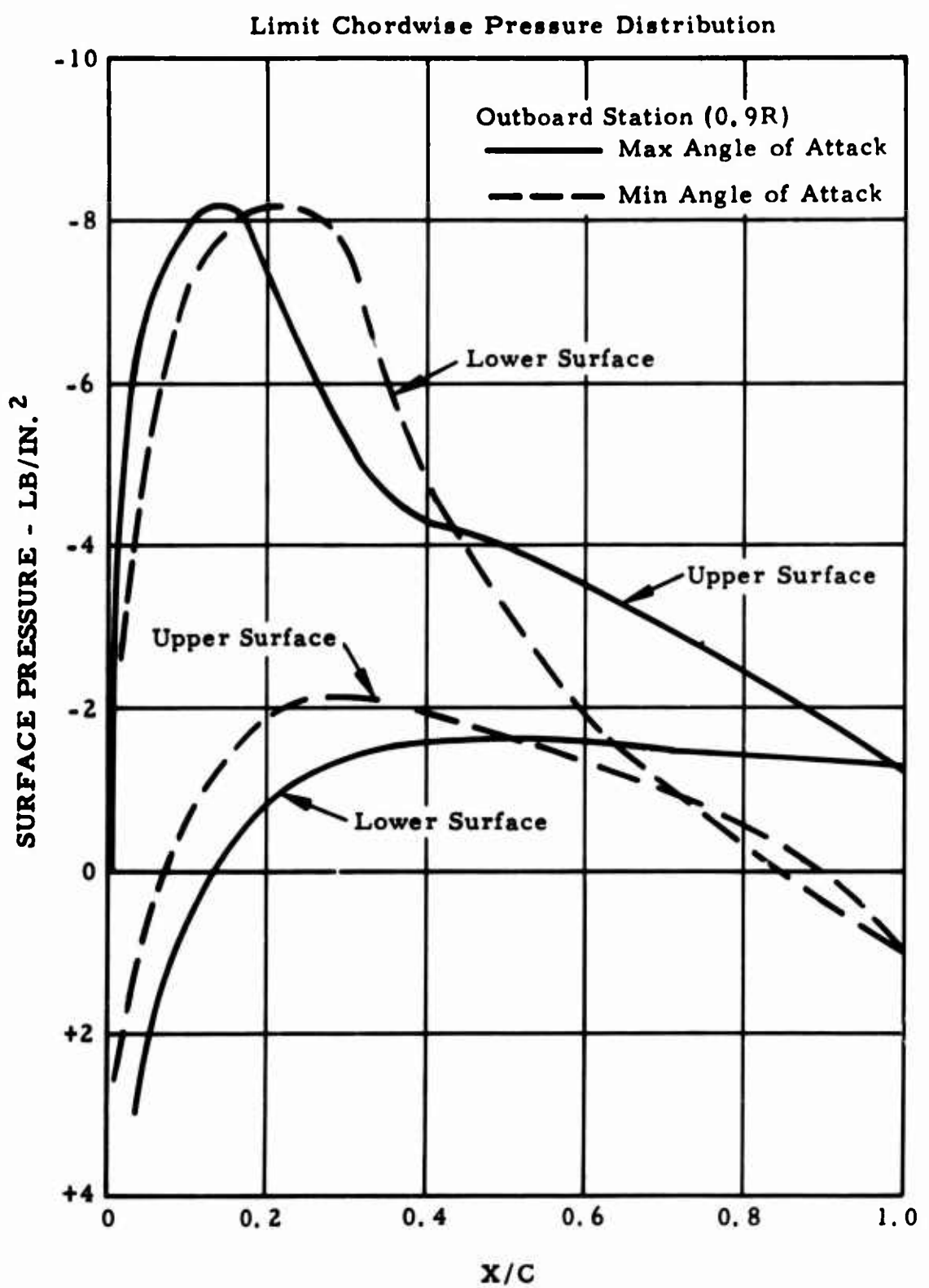


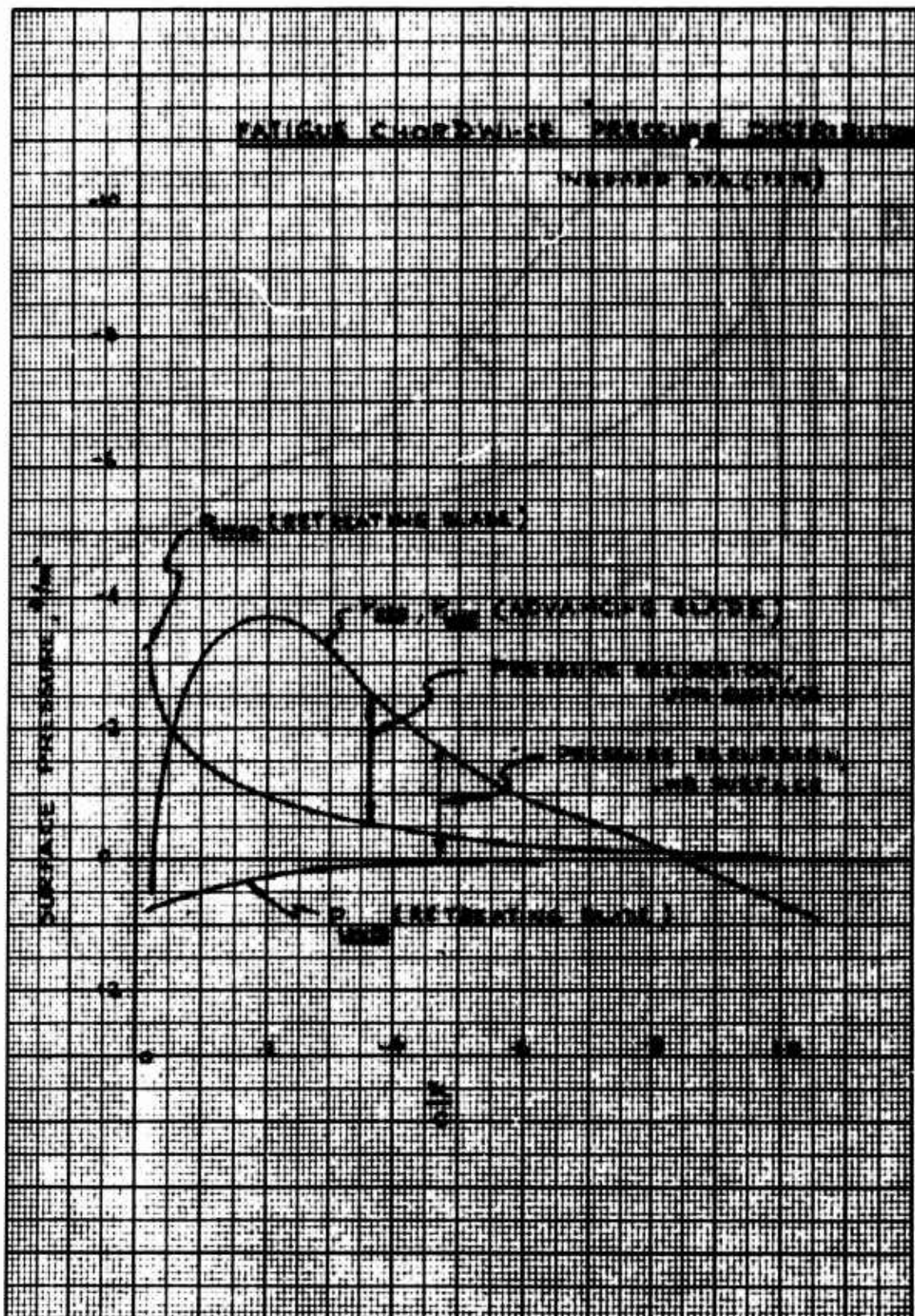


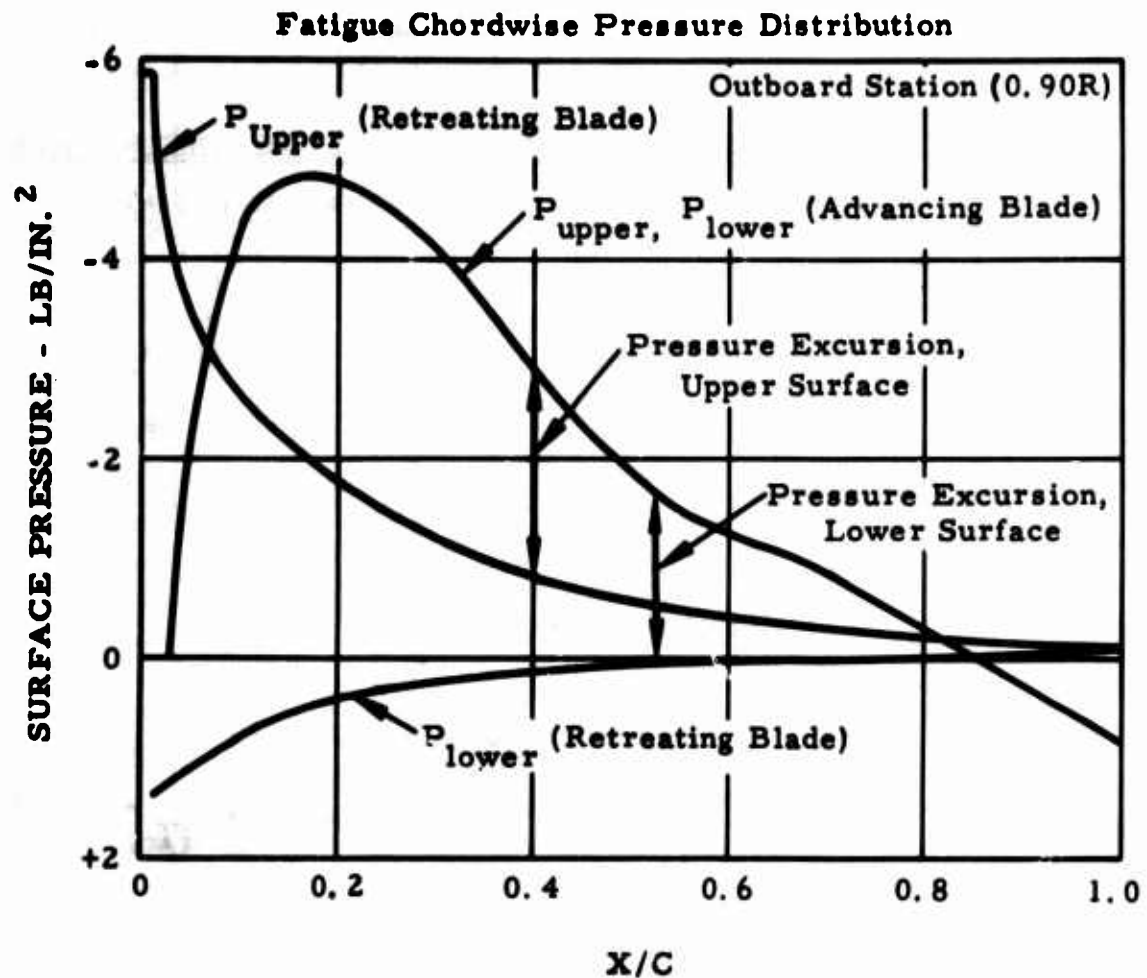






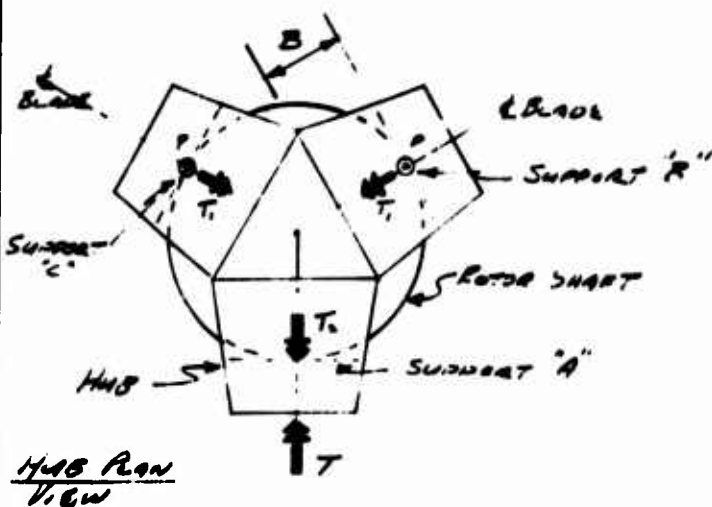






II DESIGN LOADS

ROTOR HUB LOADS

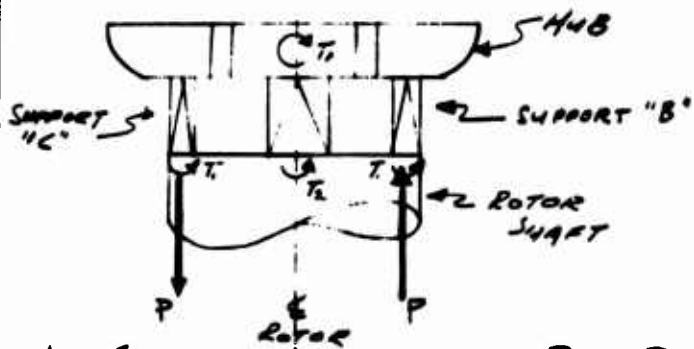


LEGEND -

T = UNBALANCED
BLADE TORQUE
ACTING ON THE
HUB.

T_1, T_2, T_3 = TORQUE REACTION
DUE TO MOMENT
STIFFNESS OF
THE SUPPORT

P = COUPLE REACTION
DUE TO AXIAL
STIFFNESS OR
THE SUPPORT



REF-Dwg 395-0936

The Rotor Hub Support Reactions are redundant for any unbalanced blade torque applied to the hub. This redundant analysis of support reactions takes into account the bending and torsional stiffness on the hub and the axial and moment stiffness at the supports.

IV DESIGN LOADS

- CONT. -

ROTOR HUB LOADS

THE FOLLOWING EQUATIONS AND PARAMETERS
ARE THE RESULT OF THE REDUNDANT ANALYSIS:

$$T_1 = T \left[\frac{1 - \left(\frac{E+2D}{E+F+2D} \right)}{\frac{E+F+D}{D} - \frac{2D}{E+F+2D}} \right]$$

$$T_2 = T \left[1 - \left\{ \frac{1 - \left(\frac{E+2D}{E+F+2D} \right)}{\left(\frac{E+F+D}{D} - \frac{2D}{E+F+2D} \right)} \right\} \left(\frac{E+F+D}{D} \right) \right]$$

$$P = \left(\frac{T - T_2 - T_1}{1.732 B} \right) ; \quad E = \frac{D}{GJ} ; \quad F = \frac{1}{K_p}$$

$$D = \frac{B}{9EI} + \frac{1}{3K_p B^2}$$

$$B = 16 \text{ IN.}$$

$$G = 11 \times 10^6 \text{ PSI}$$

$J = 94 \text{ IN.}^3$ (TORSIONAL STIFFNESS OR HUB CROSS-SECT.)

$F = \frac{1}{K_p} = 0.0222 \frac{\text{RAD}}{\text{IN.}^2}$ (TORSIONAL STIFFNESS OF SUPPORT.)

$$E = 30 \times 10^6 \text{ PSI}$$

$$I = 43.4 \text{ IN.}^4$$

$$K_p = 4.53 \times 10^6 \frac{1}{\text{IN.}}$$
 (AXIAL STIFFNESS OF SUPPORT.)

IV DESIGN LOADS

ROTOR HUB LOADS:

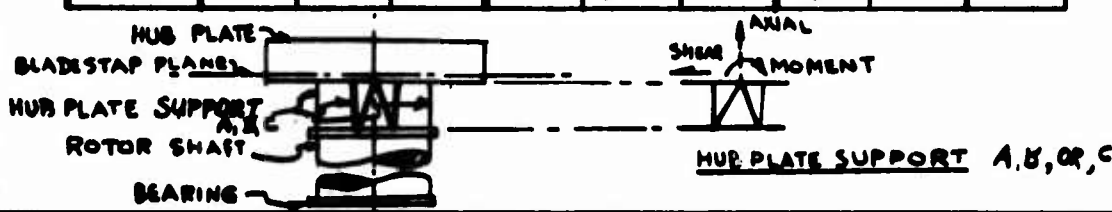
• **HUB PLATE SUPPORT LOADS:**

FATIGUE CONDITION:

LOAD ON HUB PLATE	SUPPORT A			SUPPORT B			SUPPORT C		
	MOM.	SHEAR	AXIAL	MOM.	SHEAR	AXIAL	MOM.	SHEAR	AXIAL
LIFT	-	-	35,000 $\pm 3,840$	-	-	35,000 $\pm 1,930$	-	-	35,000 $\pm 1,930$
C.F.	-	0	+	-	± 2770	-	-	± 2770	-
V_x	-	± 740	-	-	∓ 310	-	-	∓ 370	-
TORQUE	$\pm 21,186$	-	0	± 5290	-	$\pm 1,070$	± 5290	-	$\mp 1,070$
M_c	-	-	-	-	-	-	-	-	-
TOTAL	$\pm 21,186$	± 740	$35,000$ $\pm 3,840$	$\pm 5,290$	± 2400	$35,000$ $\pm 1,930$	± 5290	$\pm 3,140$	$35,000$ $\pm 2,010$

LIMIT MANEUVER CONDITION (LIMIT VALUES SHOWN)

LOAD ON HUB PLATE	SUPPORT A			SUPPORT B			SUPPORT C		
	MOM.	SHEAR	AXIAL	MOM.	SHEAR	AXIAL	MOM.	SHEAR	AXIAL
LIFT	-	-	$+192,500$	-	-	$+37,500$	-	-	$37,500$
C.F.	-	0	-	-	-11080	-	-	-11080	-
V_x	-	3700	-	-	∓ 1850	-	-	∓ 1850	-
TORQUE	$193,920$	-	-	$38,790$	-	$\mp 9,490$	$38,790$	-	$\mp 9,490$
M_c	-	-	-	-	-	-	-	-	-
TOTAL	$193,920$	3700	$192,500$	$38,790$	$9,230$	$46,990$	$38,790$	$9,230$	$28,010$

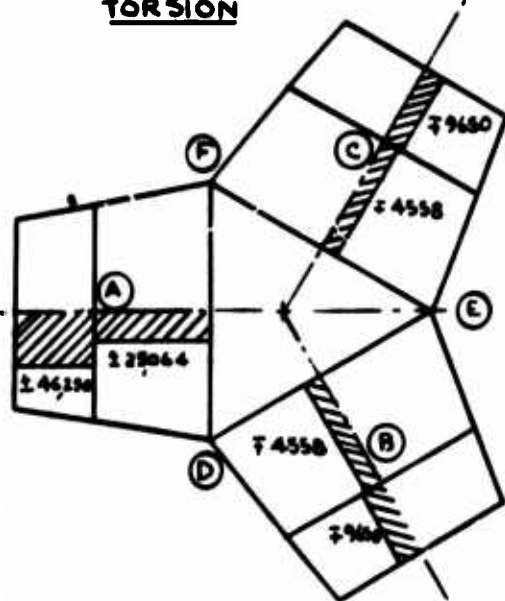


IV DESIGN LOADS

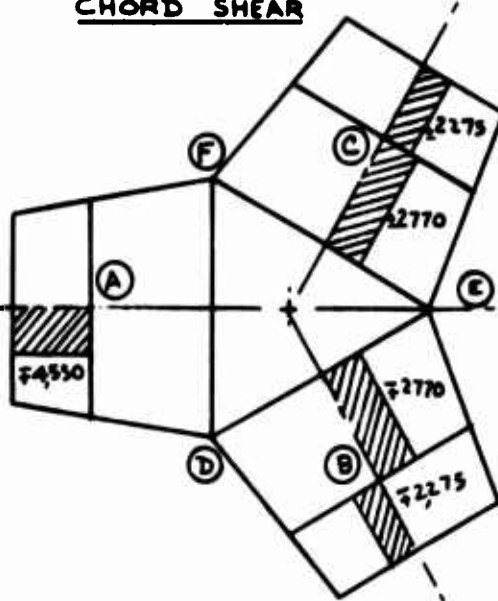
ROTOR HUB LOADS

Fatigue Condition

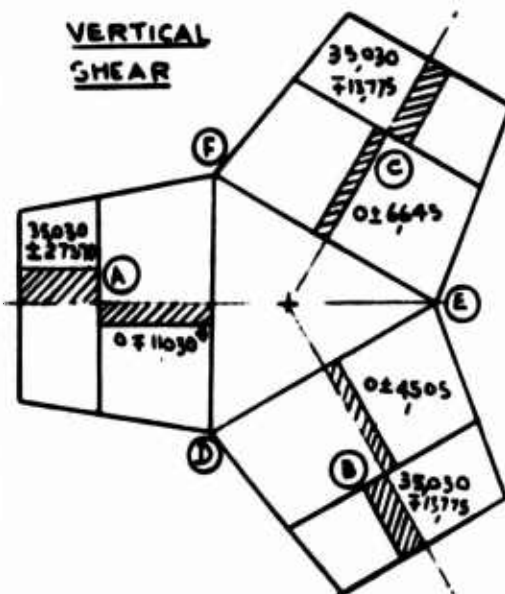
TORSION



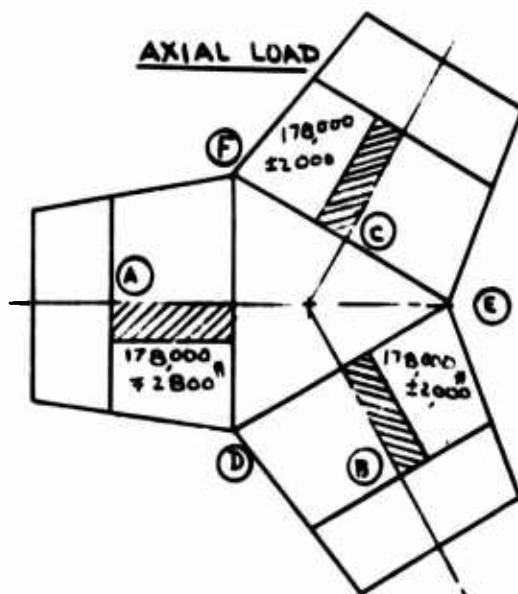
CHORD SHEAR



VERTICAL
SHEAR

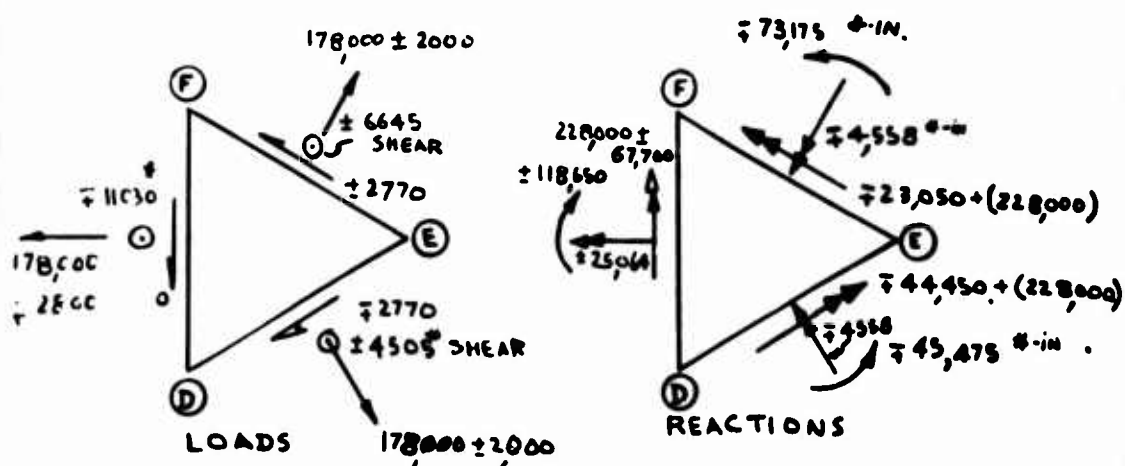
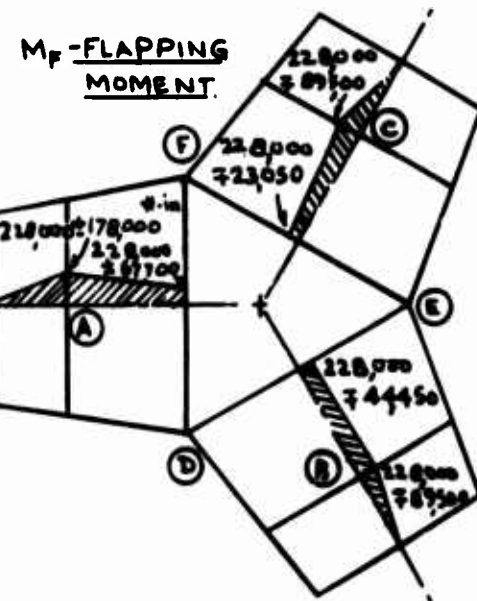
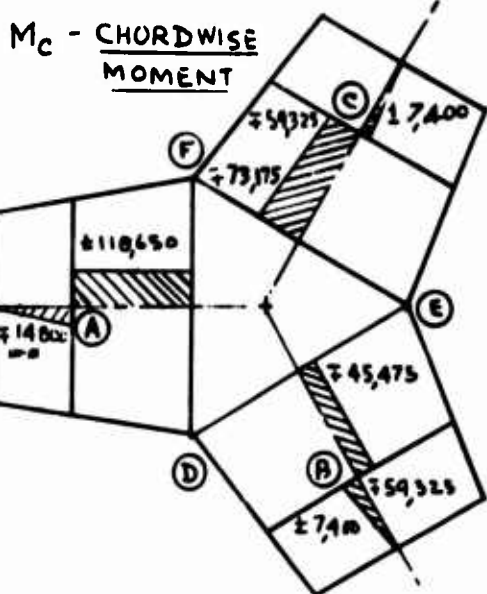


AXIAL LOAD



IV DESIGN LOADS

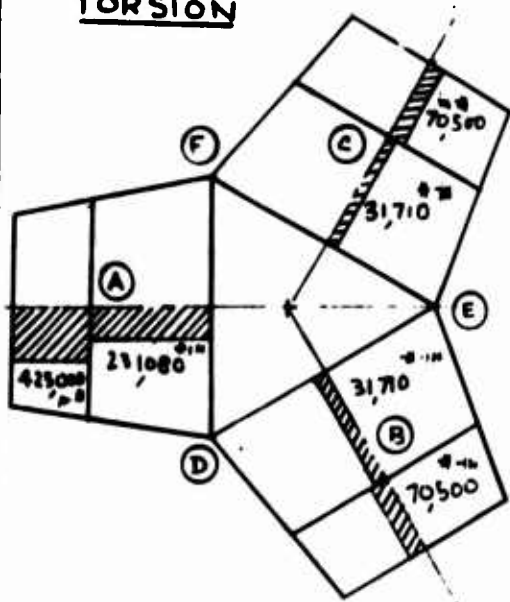
ROTOR HUB LOADS: FATIGUE CONDITION



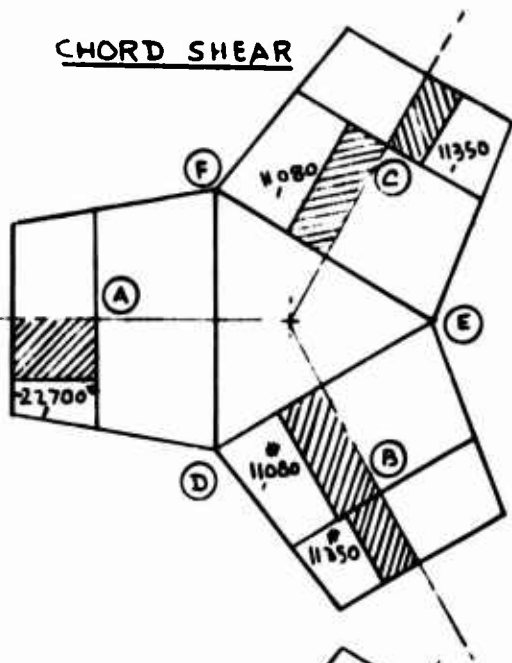
IV DESIGN LOADS

ROTOR HUB LOADS: STATIC CONDITION

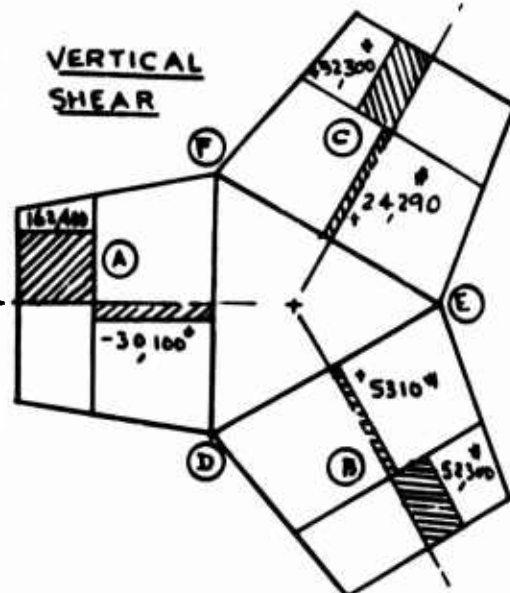
TORSION



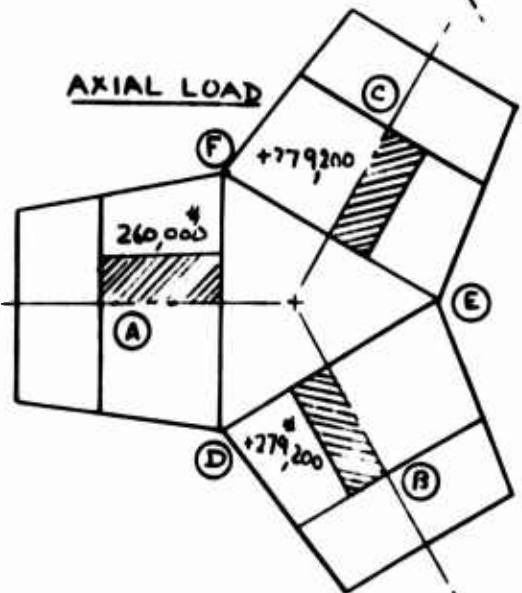
CHORD SHEAR



VERTICAL
SHEAR

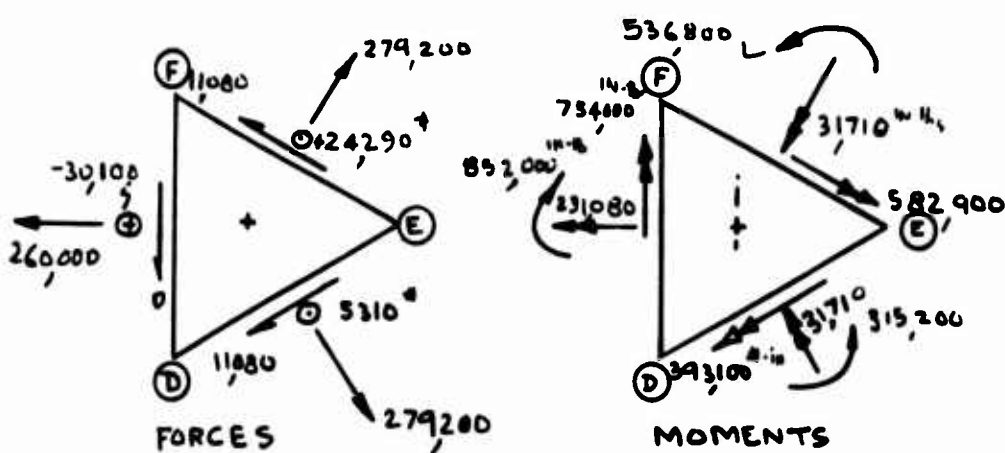
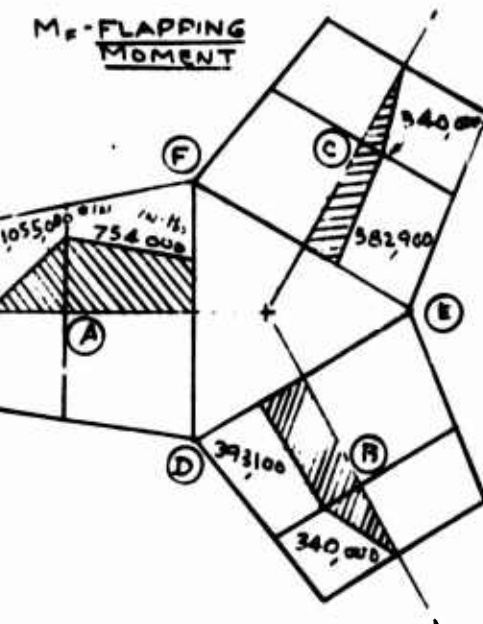
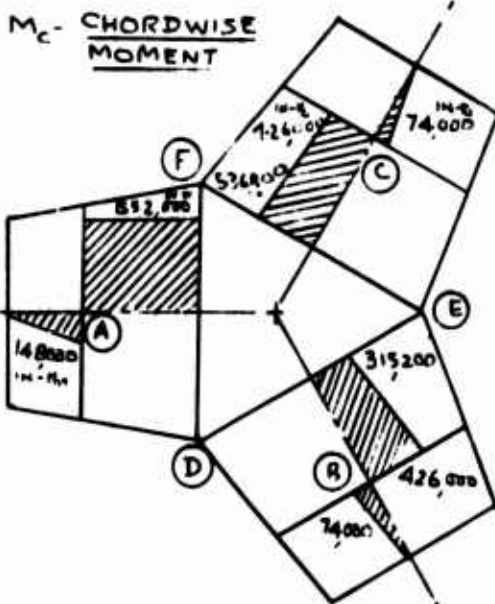


AXIAL LOAD



IV DESIGN LOADS

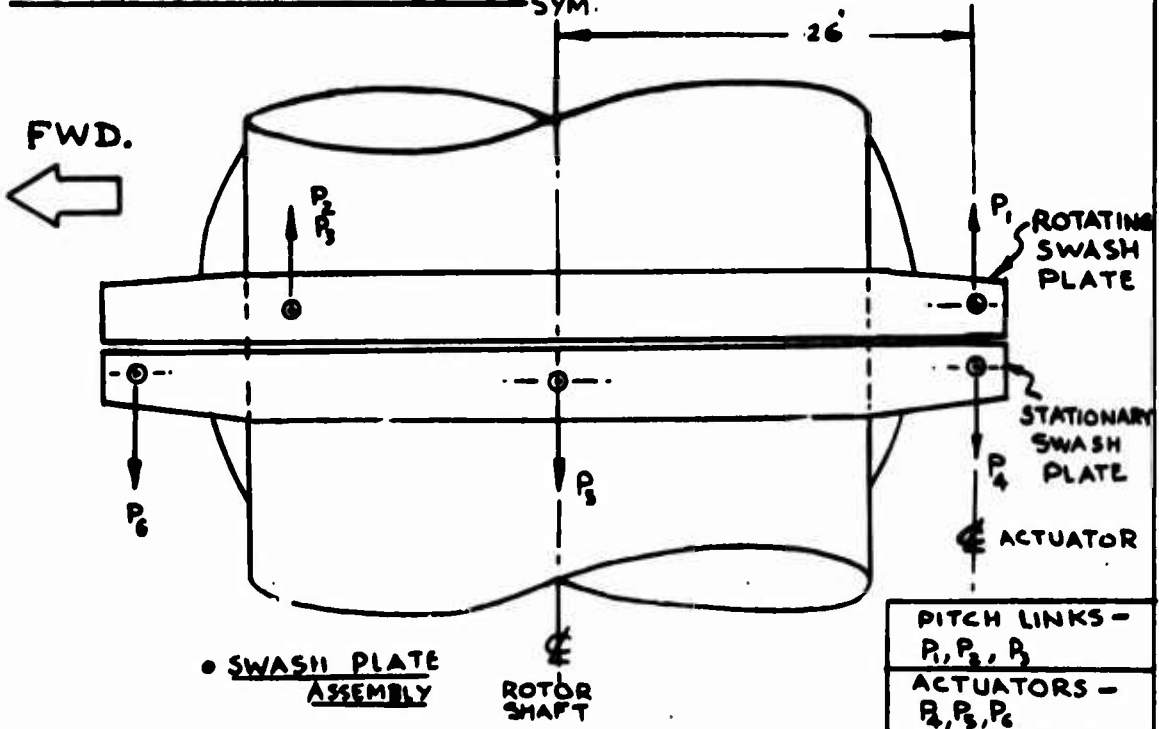
ROTOR HUB LOADS: STATIC CONDITION



9704

IV DESIGN LOADS

CONTROL SYSTEM LOADS



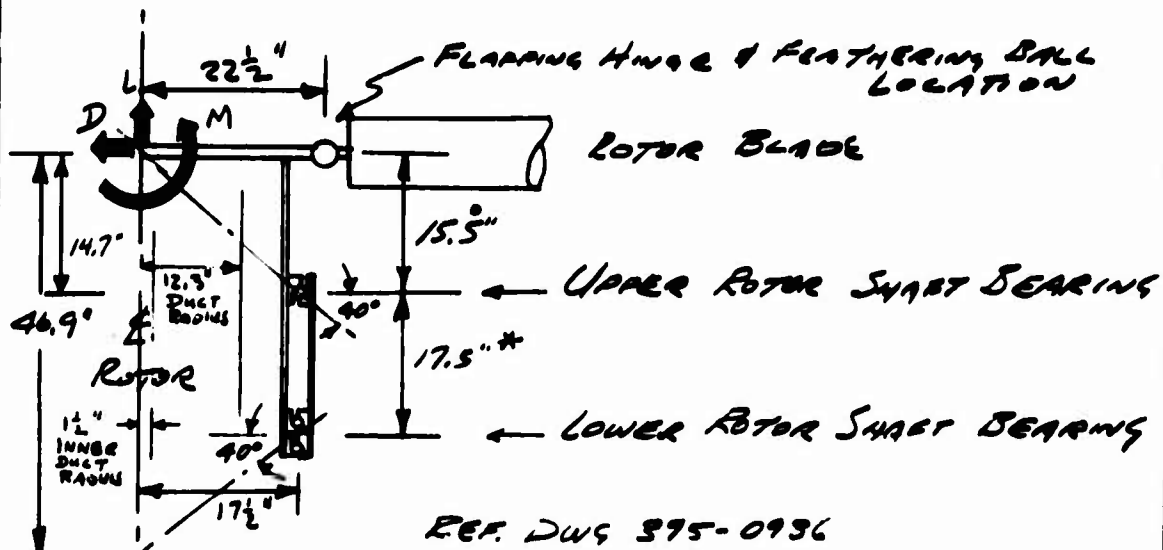
DESCRIPTION OF LOADS	FATIGUE CONDITION				LIMIT MAN. COND. *			
$M_{T,ROOT}$ - BLADE ROOT MOMENT	$64,000 \pm 9,0580$ lb-in				$242,250 \pm 252,320$ lb-in			
P_1 - PITCH LINK LOAD	$4,925 \pm 6,970$				$18,700 \pm 19,400$			
SWASH PLATE - BEARING THRUST	$14,775$ *				$56,100$ *			
SWASH PLATE - BEARING MOMENT	$271,000$ #-in				$757,000$ #-in			
ACTUATOR LOADS	LONGITUDINAL PITCHING		LATERAL PITCHING		LONGITUDINAL PITCHING		LATERAL PITCHING	
LONGITUDINAL ACTUATORS	MAX.	MIN.	MAX.	MIN.	MAX.	MIN.	MAX.	MIN.
ACTUATOR- P_6 (FWD.)	$+12,600$	$-2,200$	$12,600$	$-2,200$	$42,650$	$13,550$	$42,600$	$-2,550$
ACTUATOR- P_4 (AFT.)	$+2,200$	$-12,600$	$12,600$	$-2,200$	$13,550$	$42,650$	$42,600$	$-2,550$
LATERAL ACTUATOR - P_5	0	0	$-10,400$	$+10,400$	0	0	$-29,100$	$+29,100$

* LIMIT VALUES SHOWN

IV DESIGN LOADS

HEAVY LIFT HOT CYCLE ARTICULATED ROTOR BLADE

ROTOR SUPPORT BEARINGS LOADS



ROTOR BEARING LOADS

CONDITION	L	D	M IN O
FATIGUE COND.	94,590	5840	±530,000
LIMIT MANEUVER COND.	233,130	28,650	1,650,000

L = ROTOR LIFT - ROTOR INERTIA + GAS LOAD + LOAD FROM BLADE TORSION

CONDITION	Upper Bearing		Lower Bear. vs	
	Radial	Axial	Radial	Axial
FATIGUE COND.	5980 ± 11300	0	100 ± 11300	94,410"
LIMIT MANEUVER COND	644 ± 0	0	35,750	223,700

* * LIMIT VALUES SHOWN (NOT CRITICAL)

* THIS DIMENSION IS NOW 27 3/4" GIVING 57.13" BETWEEN BEARING CENTERS. THE EQUIVALENT BEARING LOAD, P, USED IN ANALYSIS IS 2% GREATER THAN REQUIRED, IF THIS CORRECTION IS NEGLECTED,

$$P = F_R + F_A = .5 \times 11400^2 \times \frac{44.9}{57.15} + .478(94890) = 49970 \text{ lb } \frac{50935^2}{49970} - 1 = 2\%$$

IV DESIGN LOADS

HEAVY LIFT HOT CYCLE ARTICULATED ROTOR BEARINGS

ROTOR SHAFT BEARING LOADS

LIGHT MANEUVER COND.

ROTOR RADIUS = 45' TIP SPEED = 840 F.P.S.

$$\eta = 18.65 \quad \text{BLADE C.R.} = 282,000 \text{ "}$$

$$HUB MOMENT = 1.5(\text{BLADE C.R.})r \sin \alpha,$$

$$r = 22.5 \text{ IN} \quad \alpha = 10^\circ$$

$$M = 1.5(282,000)22.5(\sin 10^\circ) = 1,655,000$$

$$L = \text{LIFT - ROTOR WEIGHT} = (66,000 - 5,000)/2 \text{ lb} = 30,500$$

$$D = 2\frac{1}{2}g/(66,000) \sin 10^\circ = 28,650 \text{ "}$$

UPPER BEARING

$$P_R = \frac{28650 \text{ "}}{46.9} \times \frac{477}{46.9} + \frac{1,655,000}{46.9} = 64,400 \text{ "}$$

$$P_A = 0$$

LOWER BEARING

$$P_L = 28650 \text{ "} \times \frac{.8}{46.9} + \frac{1,655,000}{46.9} = 34,750 \text{ "}$$

$$P_A = 152,500 + 18,550 + 52,650 = 223,700 \text{ "}$$

LOAD DUE TO GAS PRESSURE

$$[12.3^2 - 1.5^2] \pi 32.6 \text{ psi} = 185,50 \text{ "}$$

LOAD DUE TO BLADE TORSION

$$\frac{228,000 \text{ "}}{13''} = 17,550 \text{ "}$$

$$17,550 \times 3 \text{ BLADES} \\ = 52,650 \text{ "}$$

IV DESIGN LOADS

HEAVY LIFT Hot CYCLE Articulated Rotor Blade

ROTOR SHEET BEARING LOADS

FATIGUE LOADS.

$$\text{Rotor Radius} = 45' \quad \text{Tip Speed} = 675 \text{ f.p.s.}$$

$$\pi = 15 \text{ radians/sec.} \quad \text{Blade C.R.} = 180,000^{\#}$$

$$\text{Hub Moment} = 1.5(\text{Blade C.R.}) r \sin \alpha,$$

$$r = 22.5 \text{ in.} \quad \alpha, \approx 5^\circ$$

$$M = 1.5(180,000) 22.5 (\sin 5^\circ) = 530,000^{\#}$$

$$L = \text{LIFT - Rotor Wt} = 66000 - 5000 = 61000^{\#}$$

$$D = 61000^{\#} \sin 5^\circ = 5840^{\#}$$

UPPER BEARINGS

$$P_R = 5840^{\#} \times \frac{47.7}{46.9} \pm \frac{530,000}{46.9} = \underline{5940^{\#} \pm 11300^{\#}}$$

$$P_A = \frac{5840}{2} \tan 40^\circ = 2460 \pm$$

LOWER BEARINGS

$$P_L = 5840^{\#} \times \frac{8}{46.9} = \frac{530,000}{46.9} = 100 \pm 11300^{\#}$$

$$P_A = 61000^{\#} + 16400^{\#} + 14550^{\#} + 2460^{\#} \\ = \underline{94,410^{\#}}$$

LOAD DUE TO GAS PRESSURE

$$[12.3^2 - 1.5^2] \pi 35 \text{ psf} = 16400^{\#}$$

LOAD DUE TO BLADE TORSION

$$\frac{63,000^{\#}}{13} = 4849^{\#} \quad 4849 \times 386,902.5 = 14,590^{\#}$$

* Revised fact. 12 angle

V. MATERIAL ALLOWABLES

The materials to be used for the Hot Cycle Heavy-Lift Helicopter have been selected on the basis of the greatest strength-to-density ratio suitable for the temperature environments and fatigue and static loads used in this design. The design conditions are very similar to the temperature and static and fatigue conditions successfully handled by Hughes on the XV-9A Hot Cycle research aircraft.

Design allowables for the following materials are presented in this section:

Steel - Carpenter 455 maraging steel is proposed for the spar material because of its high static strength-to-density ratio. It also exhibits exceptionally consistent fatigue properties for both smooth specimens and those with holes.

It shows only a slight dropoff in strength due to temperature at the expected 300° to 400°F environment. It also performs satisfactorily for short-time temperature conditions up to 1000°F.

Titanium Alloys - Titanium alloy sandwich panels are used for the blade covering from the leading edge to the 45 percent chord. Titanium alloy is used because of the slightly elevated temperature environment of 400°F, where aluminum cannot be used, and because of its high strength-to-density ratio.

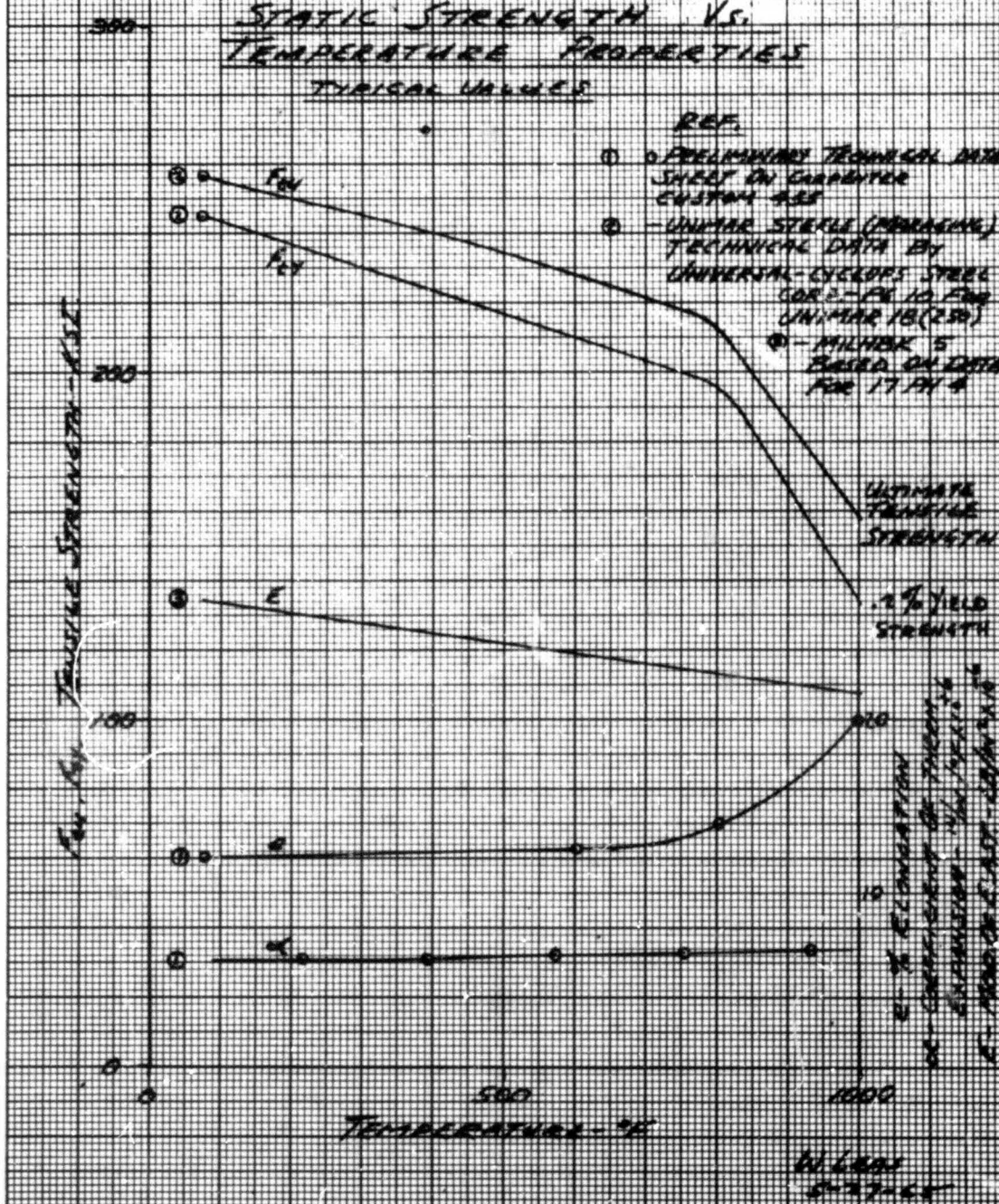
René 41 - René 41 is used as a ducting material because of its excellent static strength and creep and rupture properties in the 1200° to 1400°F range.

Inconel 718 - Inconel 718 is used in the hot gas duct system and for applications where the temperature does not exceed 1200°F. It has excellent short-time strength properties and long-time rupture and creep properties up to 1200°F.

CARPENTER CUSTOS 455

MARAGING STAINLESS STEEL

STATIC STRENGTH VS. TEMPERATURE PROPERTIES TYPICAL VALUES



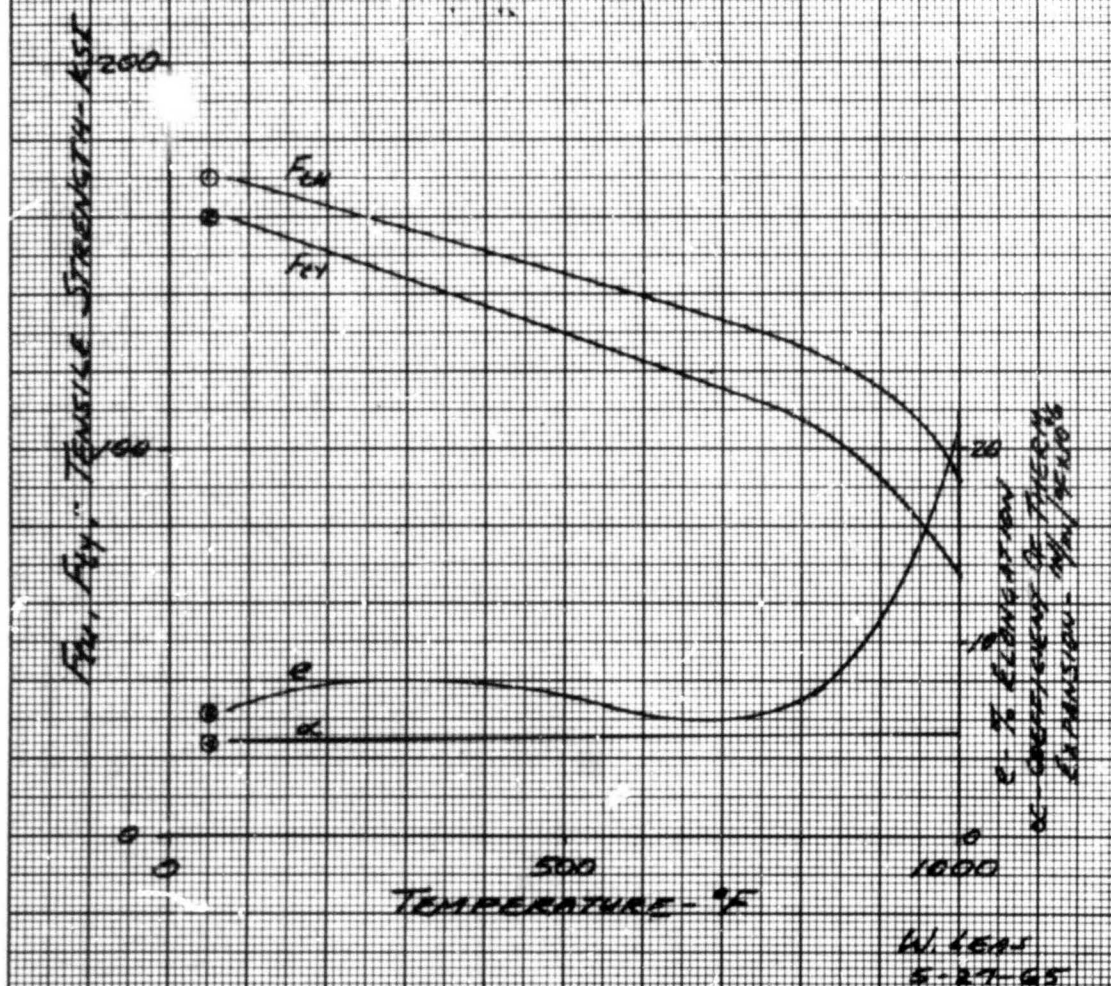
TITANIUM - Ti-6Al-6V-2Sn ALLOY

SHEET PROPERTIES

REF - AIRCRAFT DESIGNERS HANDBOOK FOR
TITANIUM AND TITANIUM ALLOYS BY
BOTTLE MEMORIAL INSTITUTE

- TABLE 5-5.1-1, FIG. 5-5.3.1-1
- TABLE 5-5.1-1, FIG. 5-5.3.1-2
- FIG. 5-5.3.1-2
- FIG. 5-5.3.1-3

MINIMUM GUARANTEED VALUES

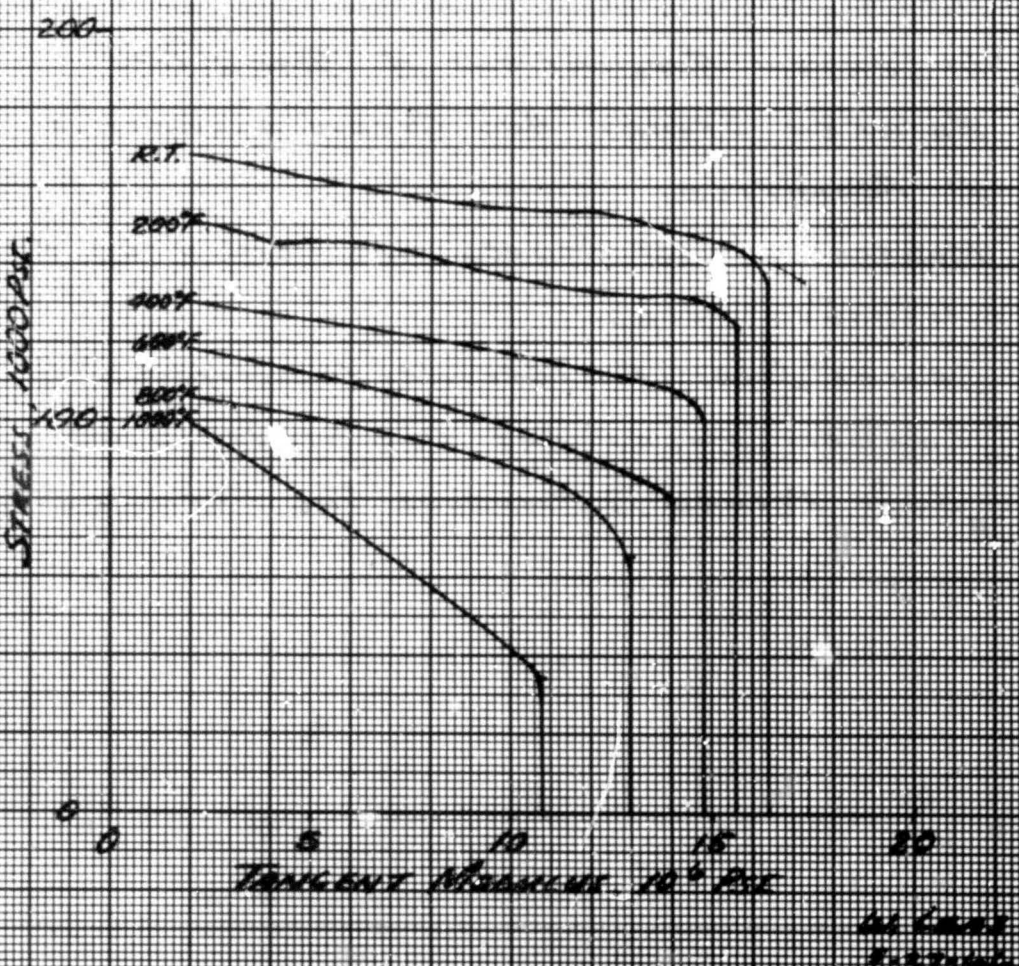


COMPRESSIVE TANGENT - MAXIMUM CURVES FOR
SOLUTION-TREATED AND AGED Ti-6Al-4V ALUMINUM ALLOY
AT ROOM & ELEVATED TEMPERATURES

LONGITUDINAL PROPERTIES

REF - AIRCRAFT DESIGNERS HANDBOOK FOR
TITANIUM & TITANIUM ALLOYS BY
BATTELLE MEMORIAL INSTITUTE
Fig. 5-9.3 3-4

MINIMUM GUARANTEED VALUES



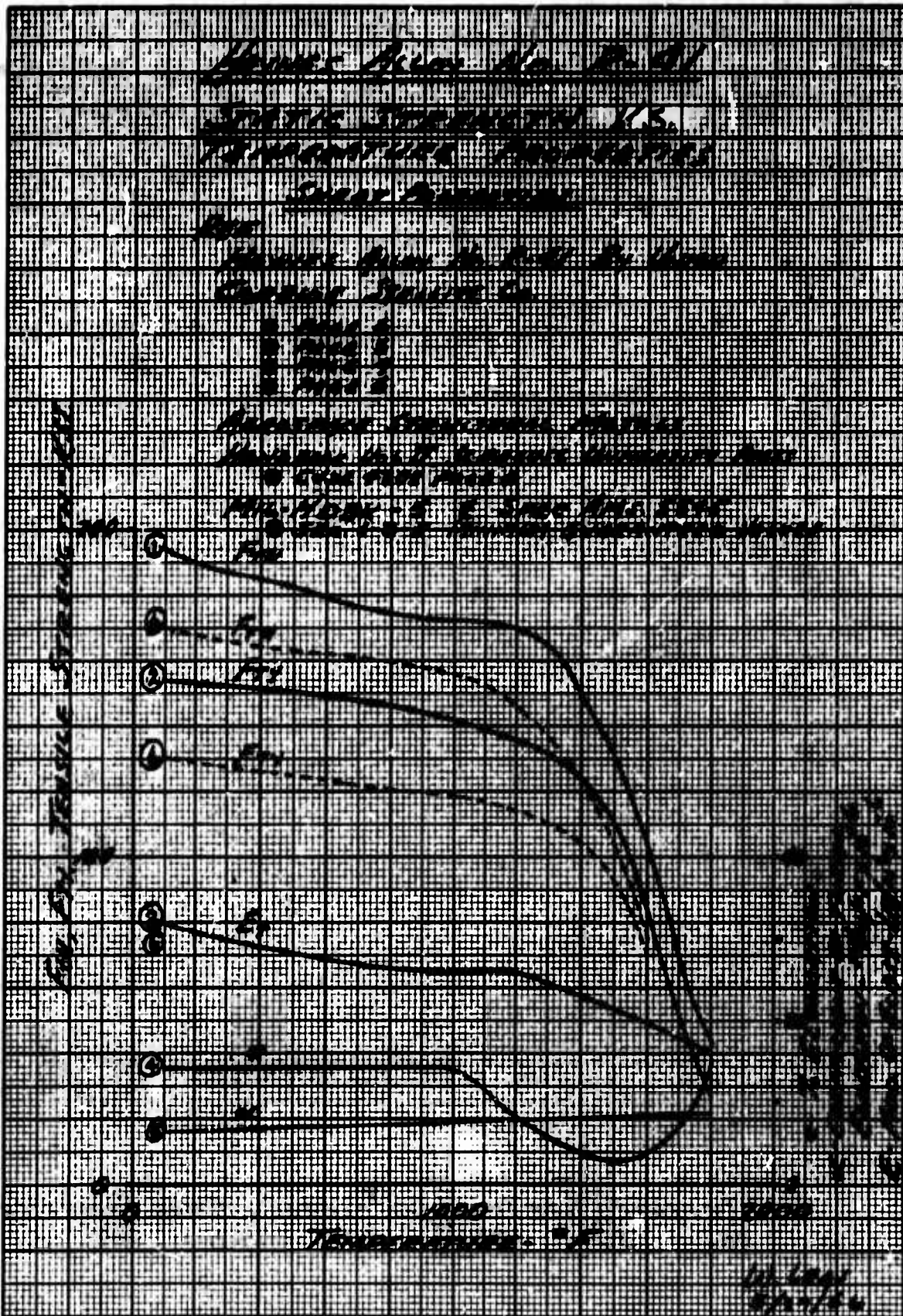
SAME ENDURANCE LIMIT FATIGUE ALLOWANCES

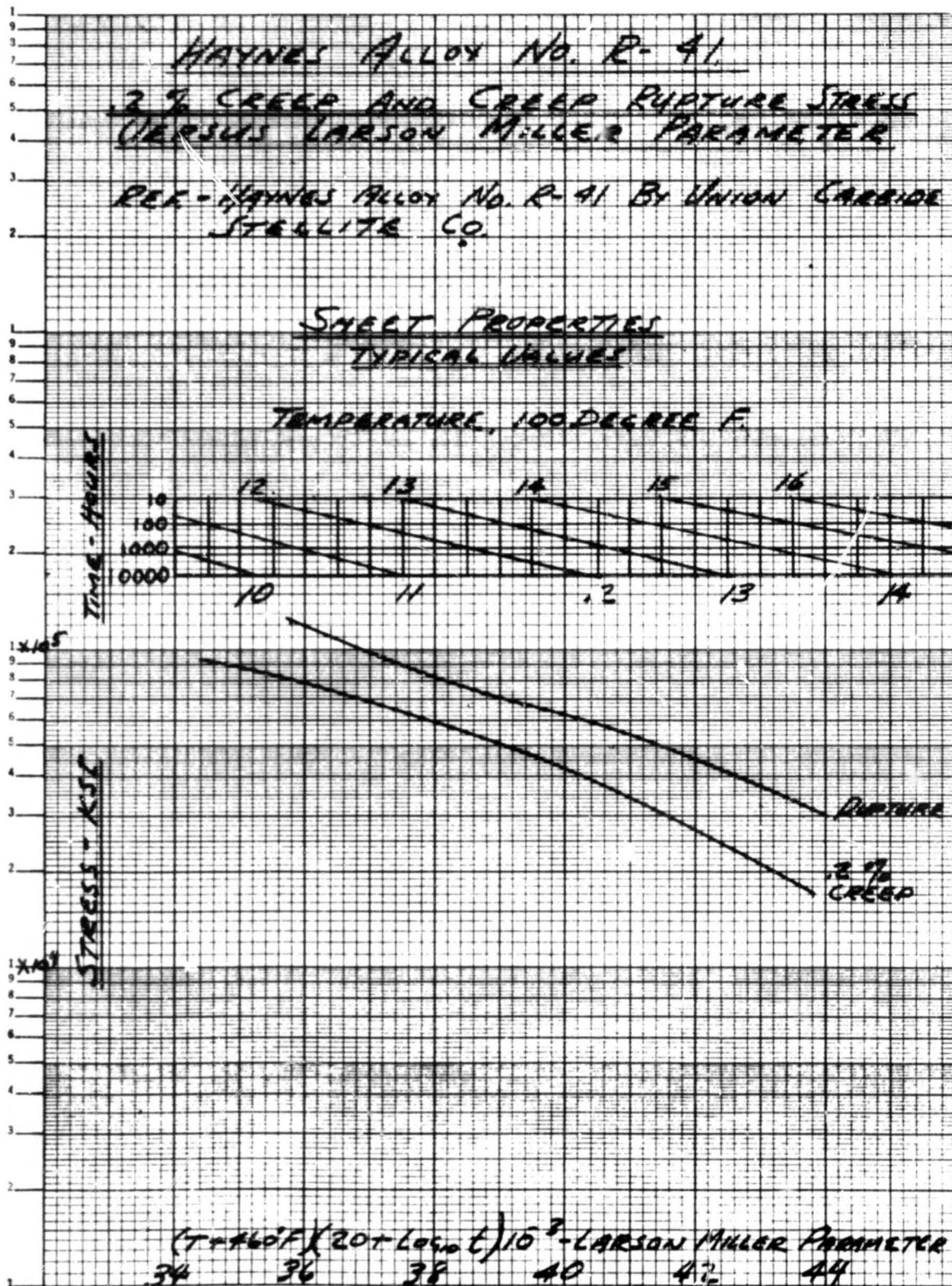
MATERIAL	F_{t_0} PSI	F_{t_1} PSI	MEAN \pm CYCLIC STRESS		
			Smooth Raises	Moderate Raises	Severe Stress Raisers
TITANIUM	170,000	160,000	25000 ± 14500	25000 ± 2000	25000 ± 5000
ALUMINUM STAINLESS STEEL	25,000	24,500	5900 ± 2500	59000 ± 1800	59000 ± 10000

IN CERTAIN APPLICATIONS A TRADE OFF
BETWEEN STEADY AND CYCLIC ALLOWANCE
IS PERMITTED.

MODERATE STRESS RAISERS ARE ITEMS SUCH AS
UNLOADED HOLES.

SEVERE STRESS RAISERS ARE LOADED HOLES. ALL
LOADED HOLES ARE PRE-STRESSED OR
SIZED REARED TO IMPROVE THE FATIGUE LIFE





Inconel 718

STATIC STRENGTH VS.
TEMPERATURE PROPERTIES

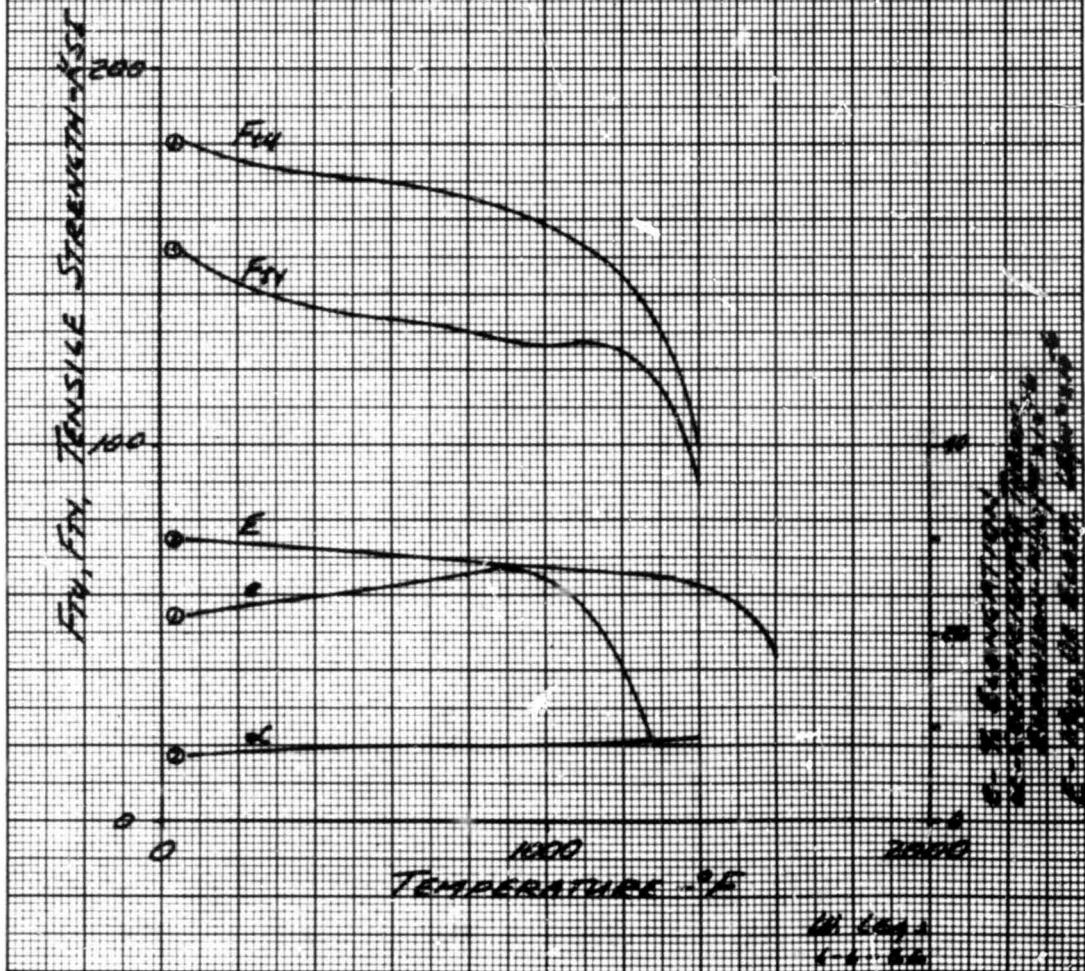
SHEET TEMPERATURE
GUARANTEED MINIMUM VALUES

Ref.

Aerospace Structural Metals
Handbook Vol II Sigma

Uniaxial Stress

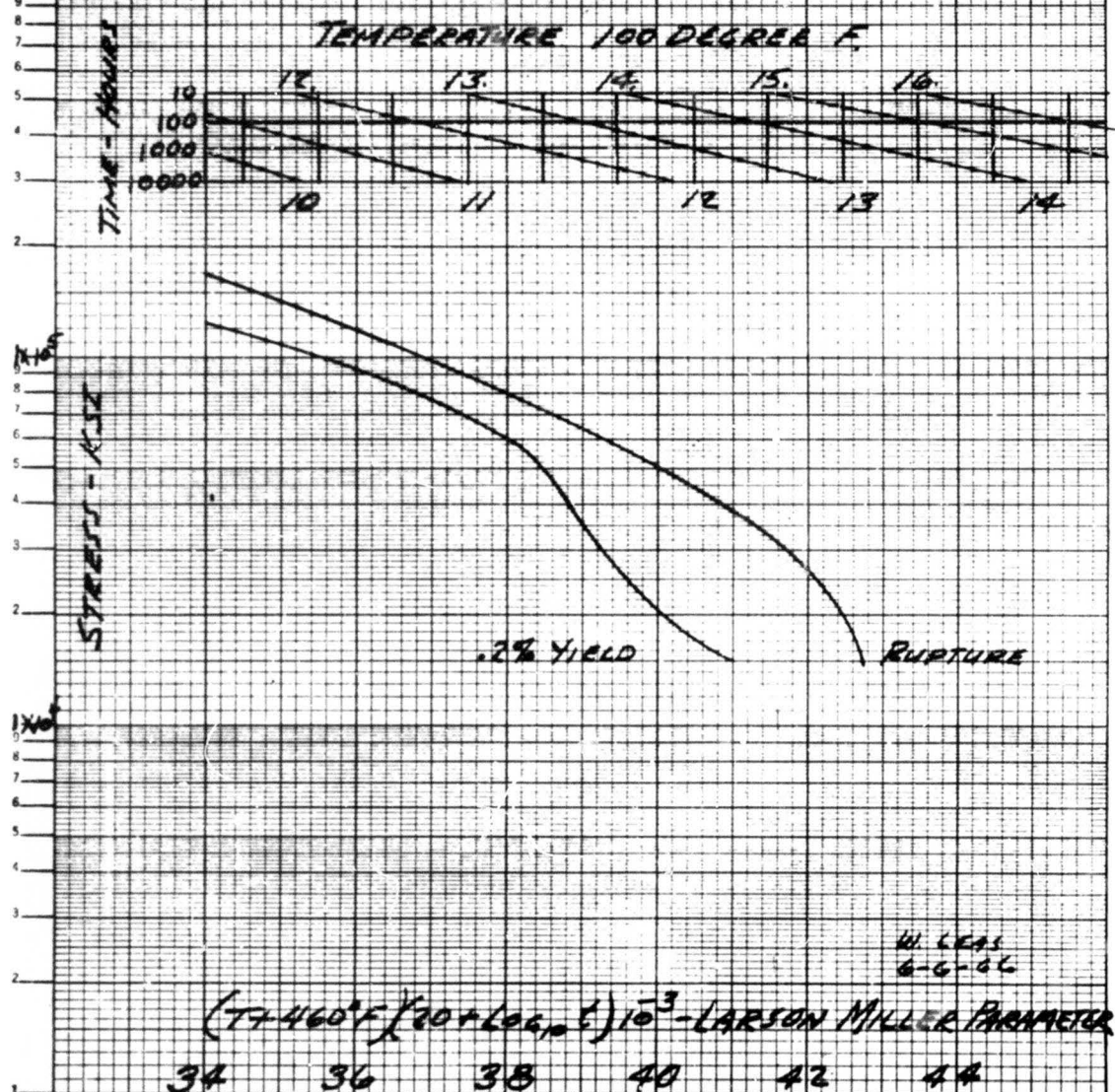
σ_{UTS} 3,430
 $\sigma_{Y0.2}$ 2,614
 σ_{E} 1,16, 3,061



INCONEL 718

.2% CREEP AND CREEP RUPTURE STRESS
VERSUS LARSON MILLER PARAMETER
MINIMUM GUARANTEED VALUES

REF - AEROSPACE STRUCTURAL METALS HANDBOOK
VOL. II SYRACUSE UNIVERSITY PRESS, FIG. 3.0431



II STRESS ANALYSIS

ROTOR BLADE

THE BLADE SKIN FROM THE LEADING EDGE TO THE 45% CHORD IS MADE UP OF TITANIUM ALLOY CORROSIONATED SANDWICH PANEL. TITANIUM IS USED BECAUSE OF THE EXPECTED 400°F. MAXIMUM TEMPERATURE ENVIRONMENT AT WHICH TEMPERATURE ALUMINUM CAN NOT BE USED. TITANIUM ALSO HAS A HIGH STRENGTH TO DENSITY RATIO.

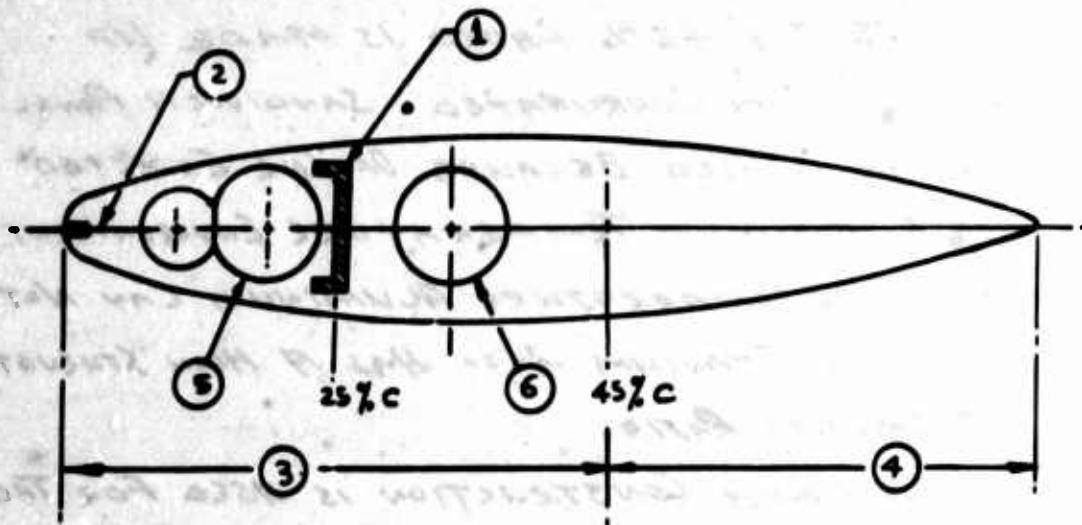
SANDWICH CONSTRUCTION IS USED FOR THE SKIN TO MINIMIZE THE NUMBER OF STIFFENERS REQUIRED TO CARRY AIR LOAD AND BLADE TORSION.

THE TRAILING EDGE OF THE BLADE AT 45% CHORD IS MADE OF LIGHT GAUGE ALUMINUM ALLOY AS IT IS OUT OF THE Elevated TEMPERATURE ENVIRONMENT AND IS LIGHTLY LOADED BY AIR LOAD.

THE BLADE SKEG IS MADE FROM CARPENTER 455 CUSTOM MACHINING STEEL. IT IS USED PRIMARILY FOR ITS EXCELLENT FATIGUE AND STATIC PROPERTIES. AT THE 400 DEGREE F. ENVIRONMENT, IT SHOWS ONLY A SLIGHT REDUCTION IN ULTIMATE STRENGTH.

II STRESS ANALYSIS

ROTOR BLADE (Ref. Dwg 395-0919)



• LOAD CARRYING ELEMENTS IN ROTOR BLADE:

- ① • THE ROTOR BLADE SPAR CARRIES THE ROTOR BLADE CENTRIFUGAL FORCE, THE FORCE FROM THE GAS PRESSURE IN THE DUCTS, VERTICAL SHEAR, ALL THE BLADE FLAPPING MOMENT AND ACTS WITH THE LEADING EDGE BALANCE WEIGHT TO CARRY THE COUPLE FORCE FROM CHORDWISE BENDING. IT PROVIDES ALL THE REQUIRED BLADE STIFFNESS NECESSARY TO LIMIT THE BLADE BENDING DEFLECTIONS DURING GROUND FLAPPING CONDITIONS.
- ② • THE LEADING EDGE BLADE BALANCE ACTING WITH THE SPAR (ITEM 1) CARRIES THE BLADE CHORDWISE MOMENT. ALSO IT CARRIES THE CHORDWISE SHEAR BETWEEN SEGMENTS.

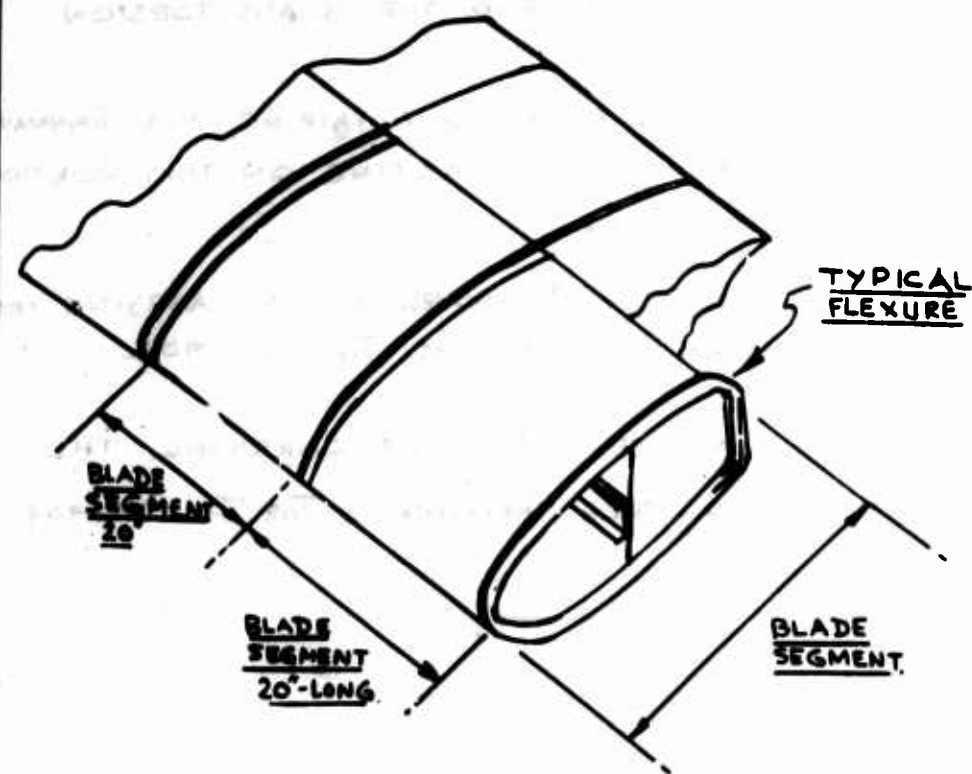
II STRESS ANALYSIS

ROTOR BLADE (CONTINUED)

- ③ • THIS SECTION OF THE BLADE CARRIES THE LOCAL AIRLOAD AND THE BLADE TORSION.
- ④ • THE TRAILING EDGE IS A FAIRING AND SUPPORTS ONLY THE AIRLOAD ACTING ON THIS PORTION OF THE BLADE.
- ⑤ • THESE ARE THE FORWARD DUCTS CARRYING HOT GAS UNDER PRESSURE TO THE TIP CASCADE.
- ⑥ • THIS IS THE AFT. DUCT CARRYING THE HOT GAS UNDER PRESSURE TO THE TIP CASCADE.

VI STRESS ANALYSIS

BLADE SEGMENT: (Ref. Dwg 395-09.9)



THE ROTOR BLADE IN THE CONSTANT SECTION IS SEGMENTED INTO 20 INCH LENGTHS, AND IN THE TRANSITION SECTION THE LENGTH OF SEGMENT VARIES SLIGHTLY FROM 20 INCHES.

THE SEGMENTS EXTEND FROM THE LEADING EDGE TO THE 45% CHORD. THE SEGMENTS ARE SEPARATED BY FLEXURES WHICH TRANSMIT TORSION FROM ONE SEGMENT TO THE NEXT, THUS PROVIDING TORSIONAL CONTINUITY TO THE BLADE. THE FLEXIBILITY OF THE

VI STRESS ANALYSIS

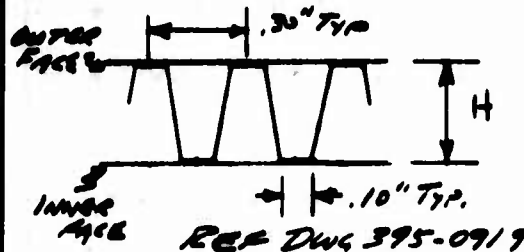
BLADE SEGMENT (CONTINUED)

FLEXURES PREVENT THE SEGMENT FROM PICKING UP ANY STRAIN FROM FLAPWISE AND CHORDWISE BENDING AND CENTRIFUGAL FORCE.

AS A RESULT, THE SEGMENT CARRIES ONLY LOCAL AIRLOAD PLUS ALL THE BLADE TORSION AND CHORDWISE SHEAR

VI STRESS ANALYSIS

BLADE SKIN PANELS



SANDWICH SKIN - TITANIUM

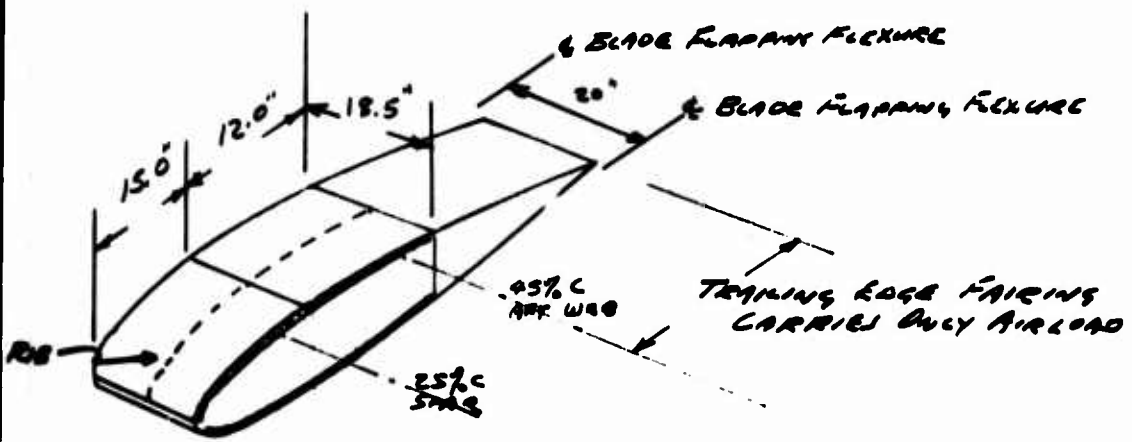
TYPE 1. FROM NOSE TO 25% C

TYPE 2. FROM 25% C TO AFT WING

TYPE	H.	CORE GAGE	INNER FACE GAGE	OUTER FACE GAGE			
				.2R TO .6R	.6R TO .8R	.8R TO .9R	.9R TO 1.05
1.	.310	.007	.012 (.22-.16) .011 (.6R-.12)	.011	.008	.007	.006
2.	.353	.008	.011	.008	.007	.006	.004

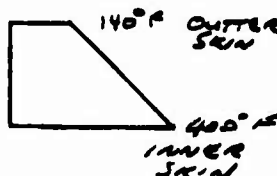
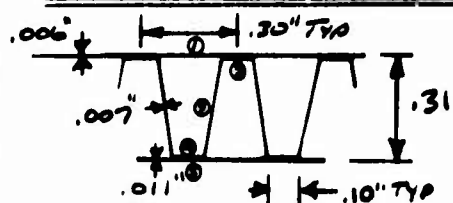
THE AIR LOADING IS HIGHEST ON THE SKIN PANELS AT THE .9R. THIS PANEL ALSO HAS THE LIGHTEST GAGE. THREE-THIRDS A SAMPLE CALCULATION FOR AIRLOADS IS SHOWN FOR THIS SECTION.

IN BOARD OF THE 2D, THE BLADE TORQUE BUILDS UP. SINCE STABILITY OF THE SKIN PANEL DESIGNS THE PANEL RATHER THAN AIR LOADINGS



VII STRESS ANALYSIS

BEDSKIN PANELS



Type I Constant
@ .9 K.

Moment of Inertia

Note - TEMPERATURE GRADIENT
BASED ON XV-90 DATA.

Thermal Stresses

E _c	AREA	t = 70°	$\alpha \times 10^6$	E _x × 10 ⁶	f = tαE	f × A	f _{therm}
1	.3(.006) = .0018	70°	4.9	16.0	54.88	9.8784	711539
2	.1(.007) = .0007	70°	4.9	16.0	54.88	3.8416	711539
3	.297(.007) = .0042	200°	4.9	15.25	149.45	62.7690	+2082
4	.1(.007) = .0007	330°	4.9	14.50	234.46	10.4122	-6419
5	.3(.011) = .0033	330°	4.9	14.50	234.46	77.3718	-6419
		.0100				170.2730	

$$\frac{170.2730}{.0100} = 17027 \text{ PSF}$$

Moment of Inertia

For .3" wide strip

E _c	AREA	$E_c/E_{c,20}$	$(E_c/E_{c,20})A$	y	YA	y^2A	I _c
1.	.0018	1.0000	.0018	.3070	.000553	.000170	—
2.	.0007	1.0000	.0007	.3035	.000212	.000064	—
3.	.0042	.9521	.0040	.1580	.000620	.000096	.000026
4.	.0007	.9062	.0006	.0065	.000004	—	—
5.	.0033	.9062	.0030	.0030	.000009	—	—
				.0101 (1384)	.001398	.000330	

$$I = .000330 + .000026 - .0101(1384)^2 - \\ = .000356 - .000193 = .000163 \text{ in}^4 \text{ for } .3 \text{ wide strip}$$

VI STRESS ANALYSIS

BLADE SKIN PANEL BENDING STRESS

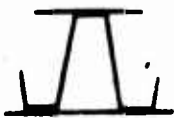
TYPE I CONSTRUCTION - MATTRESS TITANIUM

$$\text{Panel size} = 15'' \times 9.25'' \quad \gamma = 1.62 \quad \beta = .086$$

AIR PRESSURE = $8.2 \frac{\text{lb}}{\text{in}^2}$ LIMIT FROM LOADS SECTION

$$M = \rho g a^2 = .086 (8.2 \frac{\text{lb}}{\text{in}^2}) (9.25)^2 = 60.3''^3 \text{ BENDING / 1'' OF PANEL WIDTH}$$

$$f_b = \frac{Mc}{I} = \frac{(60.3 \times 1.5) \cdot \frac{.8 \text{ width}}{1.65 \times 10^6} (.1584)}{.1584} = -23056 \text{ Psi} \\ -6419 \text{ Pst} = \{ \text{TEMP} \\ -29419 \text{ Pst}$$



$$\text{ECC SKIN LENGTH} w_c = 1.97 \sqrt{\frac{E}{f_c}}$$

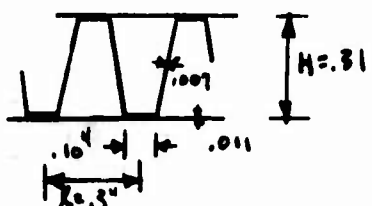
$$= 1.9 (.01) \sqrt{\frac{14.5 \times 10^6}{29419}} = .465$$

SINCE $.465 >$ CORRUGATION WIDTH

Air Type compression skin is effective = .3"

CHECK PANEL BENDING ACROSS CORRUGATIONS

$$M = \rho_{air} \cdot pa^2 = .086 (8.2 \frac{\text{lb}}{\text{in}^2}) (9.25)^2$$



$$= 34.3''^3 \text{ BENDING / 1'' OF WIDTH}$$

$$f_c = \frac{M}{w_c t} = \frac{34.3 \frac{\text{lb}}{\text{in}^2} \cdot \frac{1}{.3}}{1'' \times .011} = 4675 \text{ Psi} \\ \frac{6419 \text{ Psi}}{11094 \text{ Psi}} = \{ \text{TEMP}$$

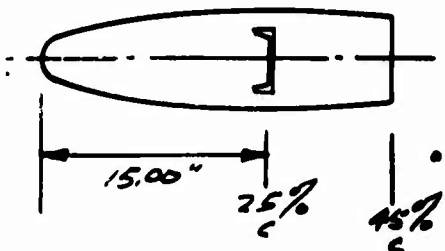
$$f_c = \frac{\pi^2 E}{(L/t)^2} \quad t = .3 \text{ ft} = .0033$$

$$= \frac{\pi^2 14.5 \times 10^6}{(.3/.0033)^2} = 17350 \text{ Psi} \quad \text{M.S.} = \frac{17350}{11094} \cdot 1 = +.57$$

PANEL STRESSES ARE LOW FOR THE MINIMUM
CHANGES SHOW AND MAXIMUM OF 20% AT THE
BLADE TIP

VI STRESS ANALYSIS

Base Skin Panels - Shear Lenses



$\frac{M_T}{240}$	$\frac{Q_x}{in^2}$
$\frac{.2R \text{ to } .75R}{.75R \text{ to } 1.0R}$	246 in^2 191 in^2

$$Q_T = \frac{M_T}{240}, \quad Q_x = \frac{V_x}{2(15)}$$

FATIGUE CONVERSION

<u>M/R Radii</u>	<u>M_T "</u>	<u>$Q_T \frac{\text{lb}}{\text{in}}$</u>	<u>V_x *</u>	<u>$Q_x \frac{\text{lb}}{\text{in}}$</u>	<u>$Q_T + Q_x \frac{\text{lb}}{\text{in}}$</u>	<u>$Q_T - Q_x \frac{\text{lb}}{\text{in}}$</u>
0	$\pm 77,440$	± 157.39	± 374	± 12.46	± 169.85	± 144.93
.2	$\pm 75,383$	± 153.22	± 374	± 12.46	± 165.68	± 140.76
.6	$\pm 59,890$	± 121.72	± 187	± 6.23	± 127.95	± 115.49
.8	$\pm 37,080$	± 97.07	± 93.5	± 3.12	± 100.19	± 93.95
.9	$\pm 19,720$	± 51.63	± 46.75	± 1.56	± 53.19	± 50.07
1.0	0	-	0	-	-	-

LIMIT MANEUVER CONDITION

<u>M/R Radii</u>	<u>M_T "</u>	<u>$Q_T \frac{\text{lb}}{\text{in}}$</u>	<u>V_x</u>	<u>$Q_x \frac{\text{lb}}{\text{in}}$</u>	<u>$Q_T + Q_x \frac{\text{lb}}{\text{in}}$</u>	<u>$Q_T - Q_x \frac{\text{lb}}{\text{in}}$</u>
0	$453,600$	922	1870	62.33	984.33	859.67
.2	$453,600$	922	1870	62.33	984.33	859.67
.6	$358,400$	728	935	31.16	759.16	697
.8	$220,600$	577.5	467	15.56	593	562
.9	$119,800$	313.61	231	7.70	321.31	306.
1.0	-	-	-	-	-	-

9704

III STRESS ANALYSIS

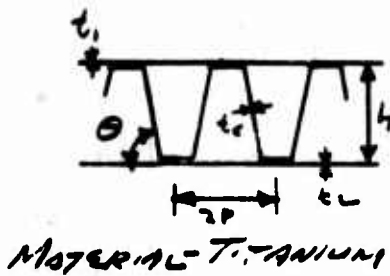
BLADE SKIN PANELS

CHEESE SHEAR STABILITY OF SKIN PANEL
IN THE CONSTANT BLADE SECTION

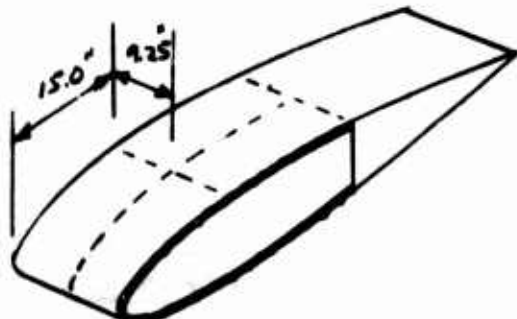
REF.- ELASTIC CONSTANTS FOR CORRUGATED
CORE SANDWICH PANELS NACA TN-2289

ANALYSIS & DESIGN OF FLIGHT VEHICLE
STRUCTURES BY E.F. BRUHN

HIGHEST SKIN SHEAR OCCURS AT THE INBOARD
END OF THE BLADE, USE VALUES AT 2 RAD/143



$$\begin{aligned} t_1 &= .011 & p &= .15 & \theta &= 85^\circ \\ t_2 &= .012 & n &= .31 & \frac{t_1}{t_2} &= .037 \\ t_c &= .007 & h_c &= .288 & \frac{p}{h_c} &= .520 \\ E_c &= 14.7 \times 10^6 & S &= 7.0 & \frac{h_c}{h_c} &= 41.2 \end{aligned}$$



$$D_{xy} = S h \left(\frac{E_c}{1 - \mu^2} \right) \left(\frac{t_c}{h_c} \right)^3 = 505$$

$$D = \frac{E_c t (h + t)^2}{\pi (1 - \mu^2)} = 91.75$$

$$J = \frac{D_{xy} b^2}{\pi^2 D} = .464$$

$$\alpha/b = \frac{15}{9.25} = 1.6 \quad K_s = 2.8$$

$$N_{xy} = \frac{K_s \pi^2 D}{2(1-\mu^2)} = \text{Panel Shear Buckling Stress}$$

$$N_{xy} = 2970 \text{ lb/in}$$

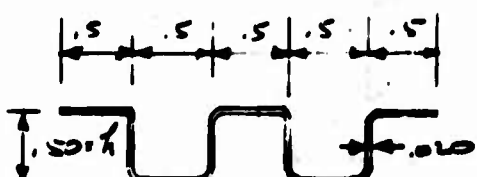
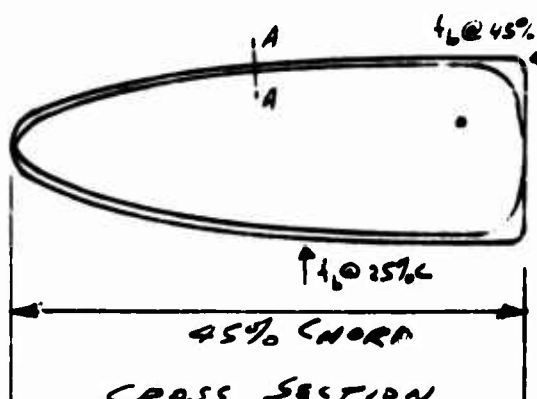
$$\text{M.S.} = \frac{2970}{984} - 1 = \underline{\underline{+2.00}}$$

FOR PANEL
BUCKLING

IV STRESS ANALYSIS

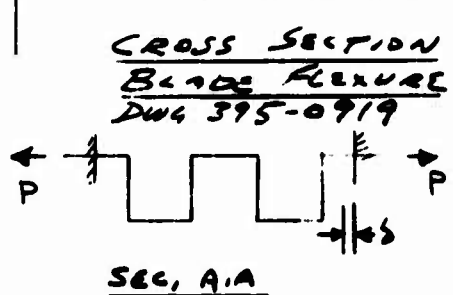
BLADE FLEXURES (BLADE SEGMENT - 1)

BLADE SEGMENT - MATERIAL - INCONEL 718



TYPICAL FLEXURE

CROSS SECTION AA



$$\delta = \frac{P}{EI} \left(\frac{h^3}{3} + \frac{h^3}{2} \right)$$

$$P = \frac{\delta EI}{\frac{h^3}{3} + \frac{h^3}{2}} \quad h = .5 \quad E = 29 \times 10^6$$

$$M = \frac{P \delta}{2} \quad f_b = \frac{Mc}{E} \quad P = \frac{SEI}{.1667}$$

$$f_b = \frac{P \delta}{2} \frac{c}{I} = \frac{SEI}{.1667} \frac{1}{2} \frac{c}{I} = \underline{\underline{3SEI \delta c}} \quad c = t_b$$

$$f_b = .75 E I S \quad t = .020 \quad f_b = 435 \times 10^3 \delta / 12$$

r/R	S		$f_b = 435 \times 10^3 \delta$		
	25% C	45% C	25% C	45% C	
.135	.0429 ± .0417	.2400 ± .0468	116.50 ± 18.40	179.00 ± 20.40	Ultimate Strength
.735	.0848 ± .0315	.0347 ± .0355	15.150 ± 18.40	15.100 ± 15.40	Ultimate Strength
.135	.284	—	123,000	—	Grounded
.735	.0663	—	21,000	—	Grounded

ULTIMATE STRENGTH CHECK
GROUNDED FLEXURE

$$M.S. = \frac{150 \times 10^6 \times 1.0 \pm 2.2}{123,000 \times 1/8}$$

S FROM BLADE STRESS CALCULATIONS

II STRESS ANALYSIS

BLADE FLEXURES (BLADE SEGMENT TO
BLADE SEGMENT - MATERIAL: INCONEL 718

CHECK SHEAR STRESS IN FLEXURE FROM
BLADE TORSION.

$$n/R = .735 \quad T = 275000 \text{ in-lb} \quad \text{LIMIT}$$

$$q = \frac{T}{2A} = \frac{275000}{2(244)} = 560 \frac{\text{lb}}{\text{in}}$$

$$q_{\text{cr}} = 53E \frac{l^3}{52} = 53(29 \times 10^6) \frac{(0.20)^3}{(1.5)^2} = 4960 \frac{\text{lb}}{\text{in}}$$

FLEXURE WILL NOT BUCKLE FROM TORSIONAL SHEAR

$$n/R = 1.35 \quad T = 458000 \text{ in-lb}$$

$$q = \frac{T}{2A} = \frac{458000}{2(244)} = 933 \frac{\text{lb}}{\text{in}}$$

$933 \frac{\text{lb}}{\text{in}} < 4960 \frac{\text{lb}}{\text{in}}$ FLEXURE WILL NOT BUCKLE

$$f_s = \frac{933 \frac{\text{lb}}{\text{in}}}{.02} = 46,500 \text{ psi}$$

$$F_{\text{st}} = 100,000 \text{ psi} \quad M.S. = \frac{100,000}{46,500 \times 1/2} - 1 = +.43$$

FATIGUE SHEAR = $\pm 75,500 \text{ in-lb}$ $f_s = \pm 7650 \text{ psi}$

$$\text{PRINCIPAL STRESS} = \frac{S_u}{2} \pm \sqrt{\frac{S_u^2}{4} + S_s^2} \quad S_u = 20400 \text{ psi}$$

$$S_s = 7650$$

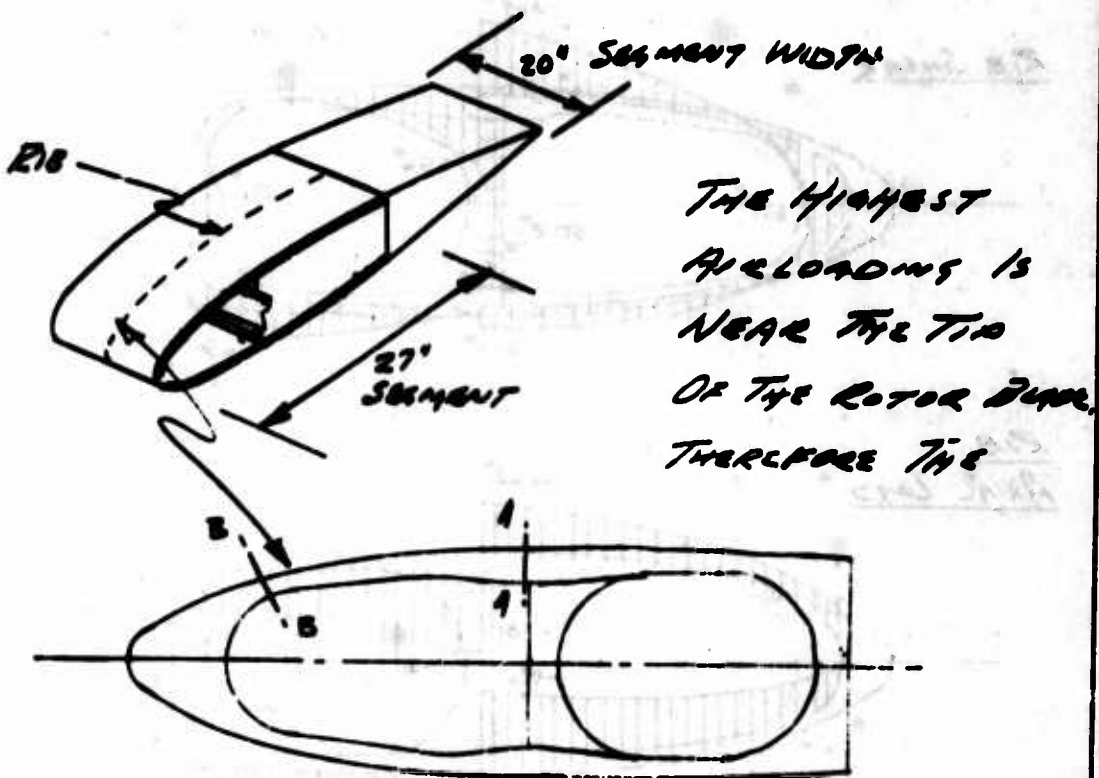
$$= 22800 \text{ psi}$$

$$\text{FATIGUE CHECK.} \quad M.S. = \frac{25000}{22800} - 1 = +.10$$

VI STRESS ANALYSIS

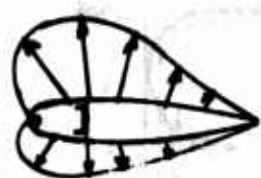
BLADE RIB ANALYSIS

REF. DWS 395-0919

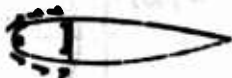


PRESSURE DISTRIBUTION AT .9 RADIUS
IS USED TO ANALYSE THE RIB. (See lower section).

RIB LOADS & REACTIONS



↓
Vertical Load
is reacted at
the base



RIB SHEAR
DISTRIBUTION
FROM GYROSCOPIC
COMPONENT OF
AIR LOAD

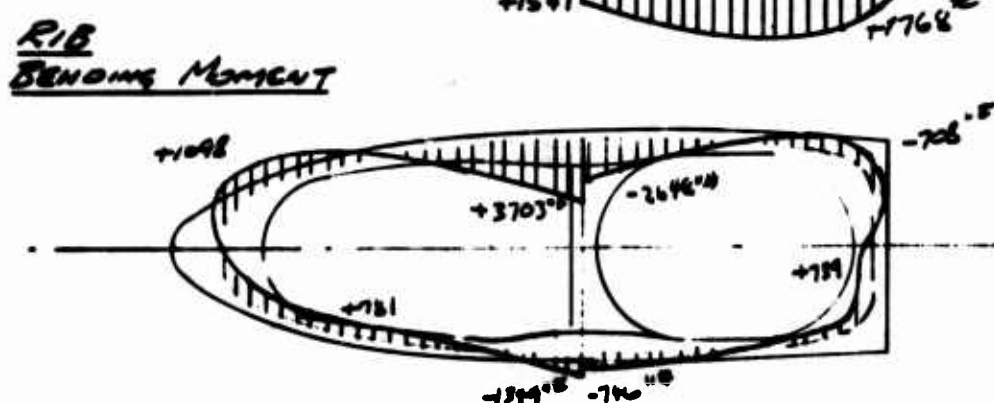
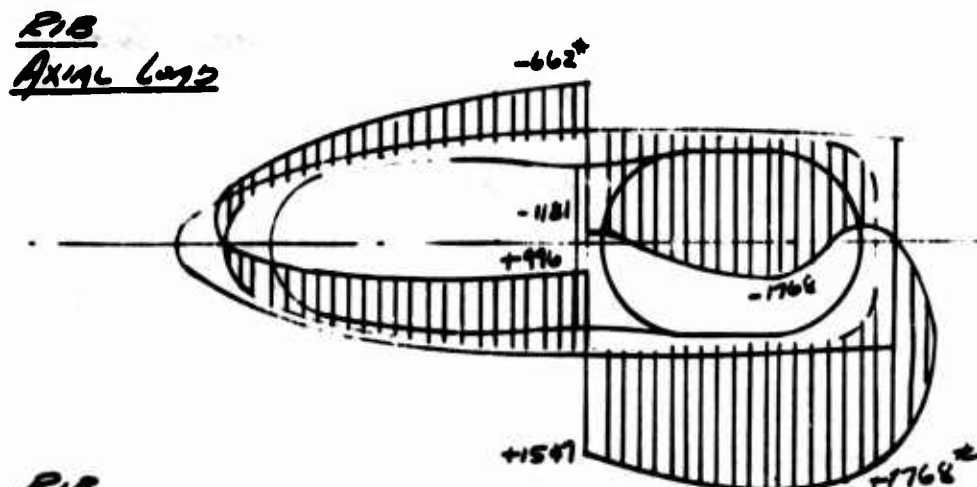
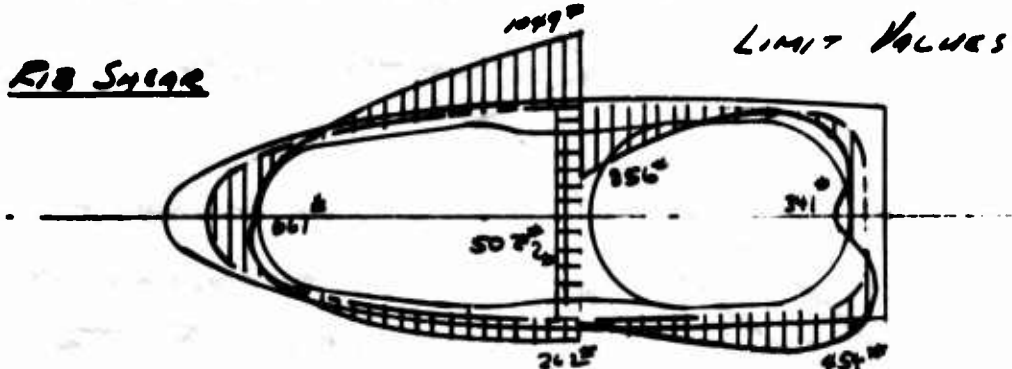


RIB SHEAR
DISTRIBUTION
FROM AIR LOAD
TORQUE

VI STRESS ANALYSIS

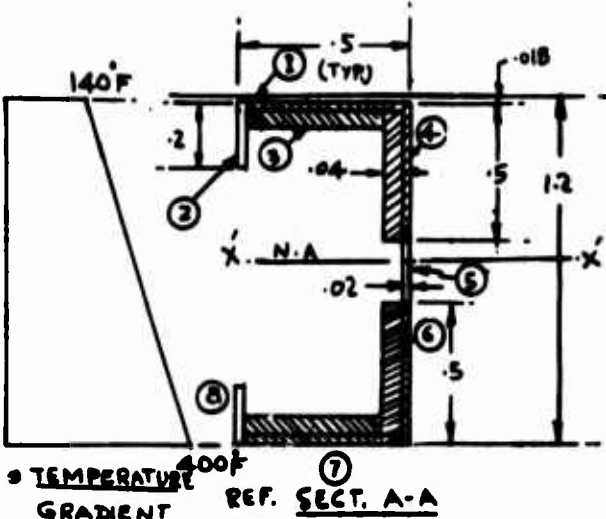
Boggs Esq Augtly 313

SHEAR AND MOMENT CURVES BASED ON AIR LOAD DISTRIBUTION AT .9 ROOMS



VI STRESS ANALYSIS

• BLADE RIB ANALYSIS



$$\begin{aligned}
 I_{xx} &= 0.030696 \text{ in}^4 \\
 (\text{in.}^4) & \\
 \bar{y} &= \frac{\Delta y}{A} = \frac{0.7983}{0.13684} = 5.824 \text{ in.} \\
 A &= 0.13684 \text{ in}^2 \\
 B.M. &= 52.37 \text{ lb-in} \\
 \text{AXIAL LOAD}(P) &= 679 \text{ lb}
 \end{aligned}$$

• TEMPERATURE GRADIENT REF. SECT. A-A

SECT. B-B TEMPERATURE STRESSES

ELEMENT	AREA	$\Delta t = T - 70^\circ$	$\times 10^6$	$E \times 10^6$	$f_t = \frac{\Delta t}{\Delta t \times E}$	ΔP	$f_{\text{RESULT.}}$
1	.0058	80°	4.6	15.4	- 5,670	- 32,38	+ 37,348
2	.004	96	7.2	30.0	- 20,700	- 82,80	+ 22,210
3	.02952	90°	7.2	30.0	- 19,400	- 573	+ 23,518
4	.0300	125	7.2	30.0	- 27,000	- 810	+ 15,918
5	.004	200	7.9	29.0	- 25,030	- 1003	+ 12,838
6	.0300	275	7.9	29.0	- 63,000	- 1890	- 20,082
7	.0295	323	7.9	28.0	- 71,500	- 2109	- 28,582
8	.004	310	7.9	28.0	- 68,500	- 274	- 25,918

$\approx .1368$

$$\frac{5,873}{.1368} = 42,918$$

$$f_b + f_a = \left[\frac{M_c}{I} + \frac{P}{A} \right] = \left[\frac{52.37 (.5834)}{0.03069} + \frac{679}{.1368} \right] \times 1.5 = \underline{155,917 \text{ psi}}$$

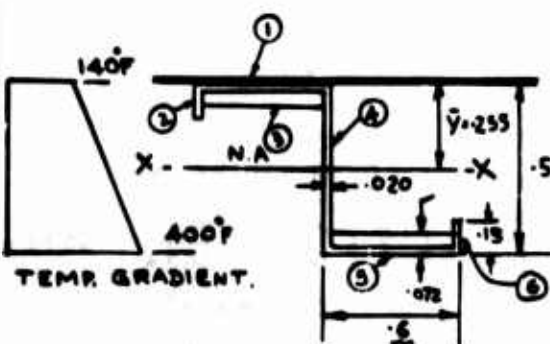
$$\text{RESULTANT STRESS (AT ITEM #1)} = (f_b + f_a) - f_t = (118,669) \text{ psi}$$

$$\text{RESULT. STRESS (AT ITEM #7)} = (f_b + f_t) - f_a = \underline{12,260 \text{ psi}}$$

$$\text{M.S.} = \frac{176000 \text{ psi}}{155,917 \text{ psi}} - 1 = +.13$$

VI STRESS ANALYSIS

• BLADE RIB ANALYSIS



$$I_{xx} (\text{in}^4) = .003983 \text{ in}^4$$

$$\bar{Y} = \frac{0.2234}{.0880} = .2538 \text{ in.}$$

$$A = .0880 \text{ in.}^2$$

$$B.M. = 1150 (\text{lb-in.})$$

$$\text{AXIAL LOAD} = 550 \text{ lb}$$

SECT. C-C TEMPERATURE STRESSES

ELEMENT	AREA IN ²	Δt = T - 70°	$\alpha \times 10^{-6}$	E X 10 ⁶	$f_b = \frac{\Delta t \times E}{I}$	ΔP	$f_t = \frac{f_b + f_a}{E}$ RESULT.
1	.0048	80°	4.6	15.4	-5,660	- 27.17	+ 46,494
2	.0030	110	7.2	30.0	-23,800	- 71.4	+ 29,354
3	.0336	90°	7.2	30.0	-19,450	- 65.35	+ 32,704
4	.0100	270°	7.9	29.0	61,800	- 618.0	- 9646
5	.0336	400	7.9	28.0	88,500	- 2973.6	- 36,346
6	.0030	370	7.9	28.0	82,950	- 246.0	- 29,846
							$\frac{4,589.6}{.088} = 52,154$

$$f_b + f_a = \left[\frac{M_c}{I} + \frac{P}{A} \right] \cdot \left[\frac{1150(2538)}{.003983} + \frac{550}{.088} \right] \times 1.5 = 119,625 \text{ psi (COMP)}$$

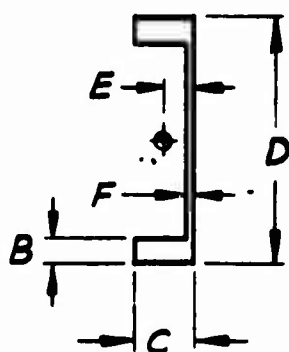
$$\text{RESUL. STRESS @ ITEM } 1. = (f_b + f_a) + f_t = (119,625) + 46,494 = 166,119 \text{ psi}$$

$$\text{RESUL. STRESS @ ITEM } 5. = (f_b + f_t) - f_a = 103,590 \text{ psi}$$

$$\underline{\underline{M.S. = \frac{175,000 \text{ psi}}{166,119 \text{ psi}} - 1 = +.04}}$$

VI STRESS ANALYSIS

BLADE SPAR DIMENSIONS AND SECTION PROPERTIES



<i>h/R</i>	<i>B</i>	<i>C</i>	<i>D</i>	<i>E</i>	<i>F</i>	<i>A</i>	<i>I</i>	<i>Z</i>
.2	.67	1.44	6.60	.53	.15	2.71	18.9	5.74
.35	.62	1.39	6.27	.53	.125	2.37	15.1	4.82
.5	.55	1.34	5.96	.52	.10	1.97	11.77	3.95
.65	.41	1.29	5.64	.47	.10	1.52	8.05	2.85
.8	.23	1.24	5.50	.35	.10	1.08	5.1	1.85
.95	.10	.50	5.00	.09	.10	.58	1.53	.612

BLADE SPAR LOADS AND STRESSES

L/R	C.F.	P_{Hc}	$\frac{M_f}{I}$	FATIGUE STRESSES		MANEUVR. LOADS		ULTIMATE STRESSES		ULTIMATE MANEUVR. STRESSES		GROUND FLAPPING*					
				($\frac{C.F.}{P_{Hc}}$)	$\frac{f_f}{A}$	f_b	$\sum f_b$	C.F.	P_{Hc}	$\frac{M_f}{I}$	$\frac{C.F.}{A}$	$\frac{P_{Hc}}{A}$	f_b	$\sum f_b$	M_p	$\frac{P_{Hc}}{A}$	f_b
.2	1.2000	7000	1960	64000	\pm	6460	66238	800	53500	8550	\pm	28200	177217	000	115000	115000	20.1
.35	1.1000	4750	1300	1080	\pm	3390	44424	10330	14500	8550	\pm	19700	28200	47500	145000	145000	22.5
.5	1.5000	2770	2920	58400	\pm	8200	69547	1400	10400	11800	\pm	12400	10000	60000	60000	60000	26.0
.65	65.00	1380	5350	56300	\pm	15200	74670	1100	12100	12100	\pm	16500	16500	16500	16500	16500	23.9
.8	52.50	441	6600	48600	\pm	18200	79330	1100	21800	22200	\pm	18600	111000	3730	51200	54900	38.8
.95	16.00	0	6060	28700	0	16200	59407	18200	18200	18200	\pm	1000	1000	1000	11400	11400	22.1

SPAR STRESSES DUE TO DUCT GAS PRESSURE:

• SPAR MATERIAL - CARPENTER CUSTOM 455

MARAGING STEEL
 $F_{tu} = 257000 \text{ psi}$ - ALLOWABLE



* ALLOWABLE UNSUPPORTED LENGTH OF
 COMPRESSION FLANGE. $L \geq 20$ REQUIRED.
 • $F_{tu} = 257000 \text{ psi}$

III STRESS ANALYSIS

STA. (in.)	DUCT CROSS-AREA (in.²)	UTM. MANEVU. (in.²)	FATIGUE (in.²)
-20	137.65	3,017	1,778
-35	137.65	3,449	2,034
-50	137.65	4,150	2,447
-65	137.65	5,379	3,170
-80	102.84	5,655	3,330
-95	102.84	10,531	6,207

• ULTIMATE MANEUVER - GAS PRESS. = $\frac{1}{2} \times 39.6 = 59.40 \text{ psi}$
 • FATIGUE - GAS PRESS. = 35.0 psi

II - STRESS ANALYSIS

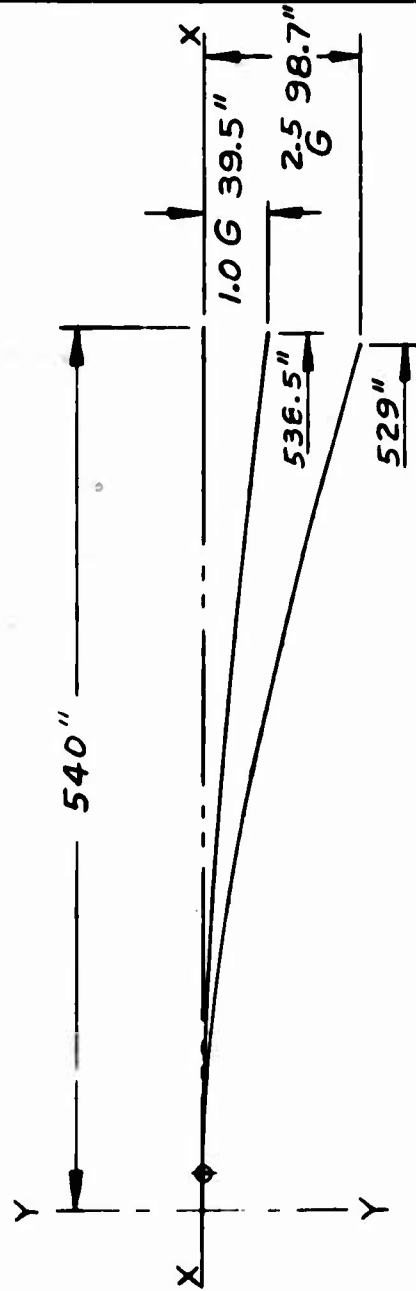
BLADE SAGE LOADS AND STRESSES

THE FOLLOWING CHART SHOWS THE ANALYSIS FOR THE FATIGUE CONDITION USING THE LOADS FROM THE COUPLED ANALYSIS. THE LOADS BETWEEN BLADE STA. 60 TO STA 375 ARE SOMEWHAT HIGHER THAN THE DESIGN VALUES, HOWEVER, THE BLADE AS DESIGNED HAS SUFFICIENT STRENGTH TO ACCOMMODATE THESE HIGHER LOADS, AS SHOWN IN THE FOLLOWING CHART.

BLADE STA. IN.	I IN ⁴	E IN ³	A IN ²	C.F. L.B.	FLAPWISE MOMENT IN. LB	GAPWISE MOMENT IN. LB	FATIGUE STRESS ± 12540	M. S.
105	18.9	5.74	2.71	162000	48000 ± 57500	± 100,000	68140 ± 12540	+ .80
190	15.1	4.82	2.37	143000	40750 ± 49,000	± 55,000	68870 ± 12580	+ .75
330	8.0	3.16	1.63	95000	62000 ± 62,500	± 23,000	74700 ± 20810	+ .03

NOTE - GAPWISE CONCave ARM IS 19"

H STRESS ANALYSIS



MAIN ROTOR BLADE

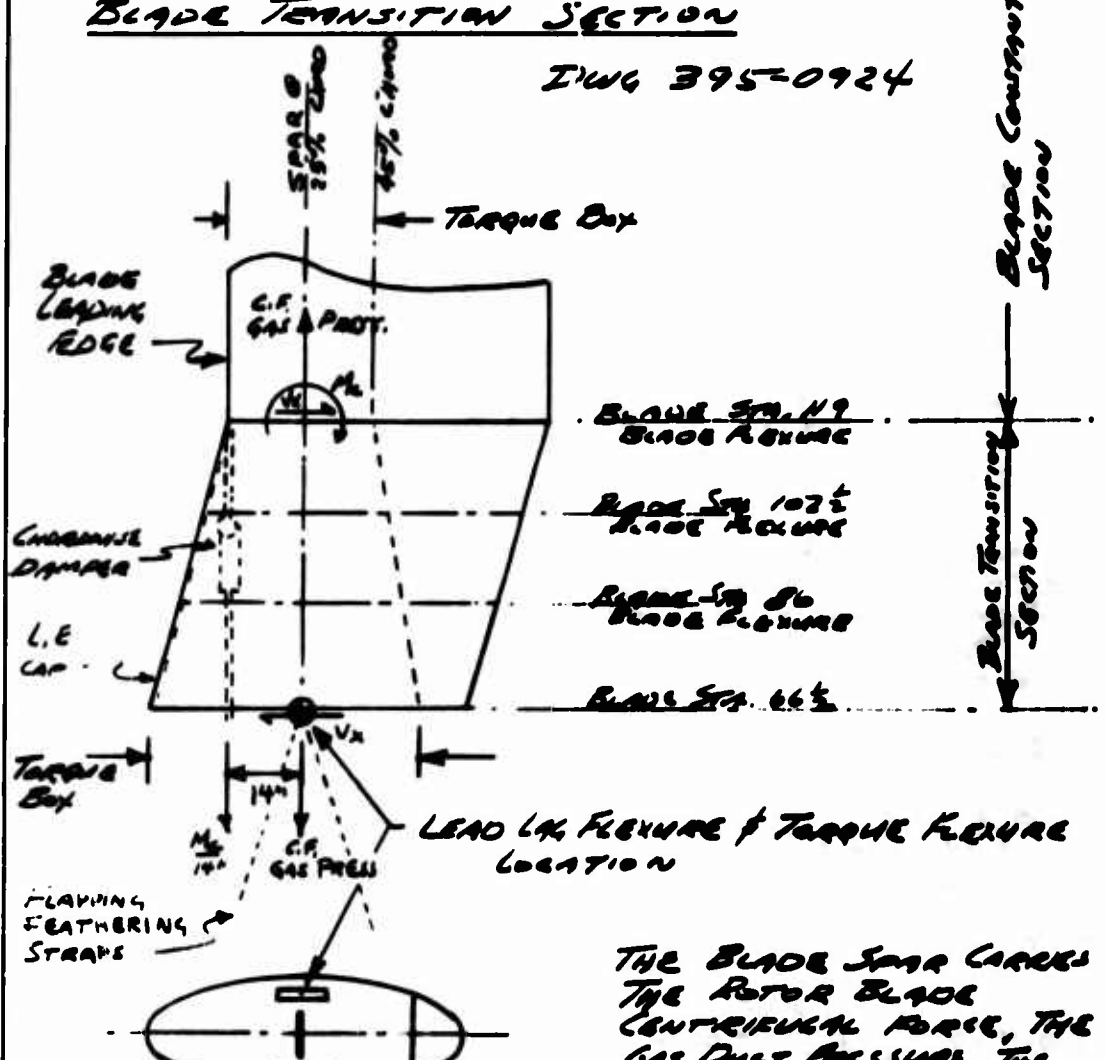
GROUNDE FLAPPING DEFLECTIONS

1.0 G	X	108	189	269.8	350.5	431	536.5
	Y	2.1	6.3	12.2	19.6	27.9	39.5
2.5 G	X	108	186.4	266	346.7	425	529
	Y	5.3	15.7	30.5	49	69.7	98.7

IV STRESS ANALYSIS

Blade Transition Section

FIGURE 395-0924



THE BLADE SPAN CARRIES THE ROTOR BLADE CENTRIFUGAL FORCE, THE GAS Duct PRESSURE, THE CHORDWISE DEMONSTRATION AND CHORDWISE MOMENT CROSS THRU THE TRANSITION SECTION TO THE LEAD Ldg FLEXURE AT STA 66 1/2 (REF. LEAD Ldg FLEXURE ANALYSIS)

THE CHORDWISE BLADE SPAN AND TORSION IS CARRIED BY THE BLADE TORQUE BOX AND REACTED BY THE TORQUE FLEXURES AT STA 66 1/2 (REF. TORQUE FLEXURE ANALYSIS)

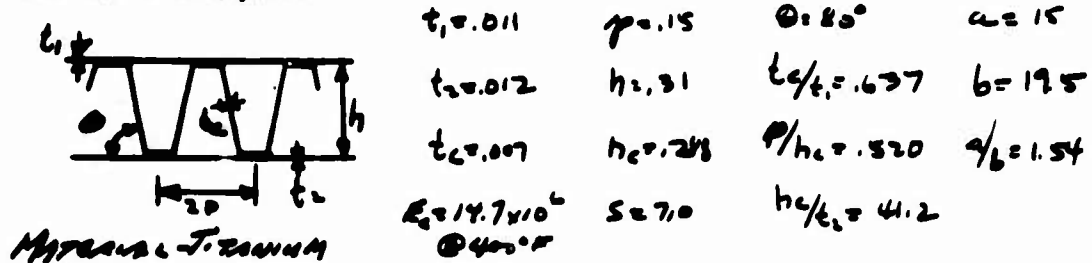
VI STRESS ANALYSIS

EDGE TRANSITION SECTION

ANALYSIS OF SKIN SHEAR FLOW LOADS

	FATIGUE	LMT. MANEUVER
V_x	$\{ \begin{matrix} \text{REP} \\ \text{LOADS} \end{matrix} \}$ $\pm 370 \text{ "}$	$\pm 1850 \text{ "}$
$M_{T,x}$	$\{ \begin{matrix} \text{REP} \\ \text{LOADS} \\ \text{SECTION} \end{matrix} \}$ $63000 \pm 25,500 \text{ "}$	$228000 \pm 228,000 \text{ "}$
$V_x/2x14" = \frac{V_x}{28}$	$\pm 13 \frac{\text{in}}{\text{in}}$	$\pm 66 \frac{\text{in}}{\text{in}}$
$M_{T,x}/24" = \frac{M_{T,x}}{5760}$	$35 \pm 43 \frac{\text{in}}{\text{in}}$	$131 \pm 131 \frac{\text{in}}{\text{in}}$
Total Shear Flow	$35 \pm 56 \frac{\text{in}}{\text{in}}$	$\pm 378 \frac{\text{in}}{\text{in}}$

Check Shear Buckling Stiffener or Panel-
R.C.-Elastic Constants for Corrugated Case
STANDARDS REQS. NASA TN-2289
ANALYSIS & DESIGN OF FLIGHT VEHICLE STRUCTURES
Dr. C. F. BRYAN



$$D_{xy} = Sh \left(\frac{E_s}{1 - \nu^2} \right) \left(\frac{t_1}{h_c} \right)^2 = 505. \quad D = \frac{E_s t / (p a t)}{2(1 - \nu^2)} = 9175$$

$$J = \frac{D_{xy} b^2}{\pi c D} = 2.06$$

$$K_3 = 3.25$$

$$N_{xy} = \frac{K_3 \pi^2 D}{2(1 - \nu^2)} = \text{Panel Shear Buckling Stress}$$

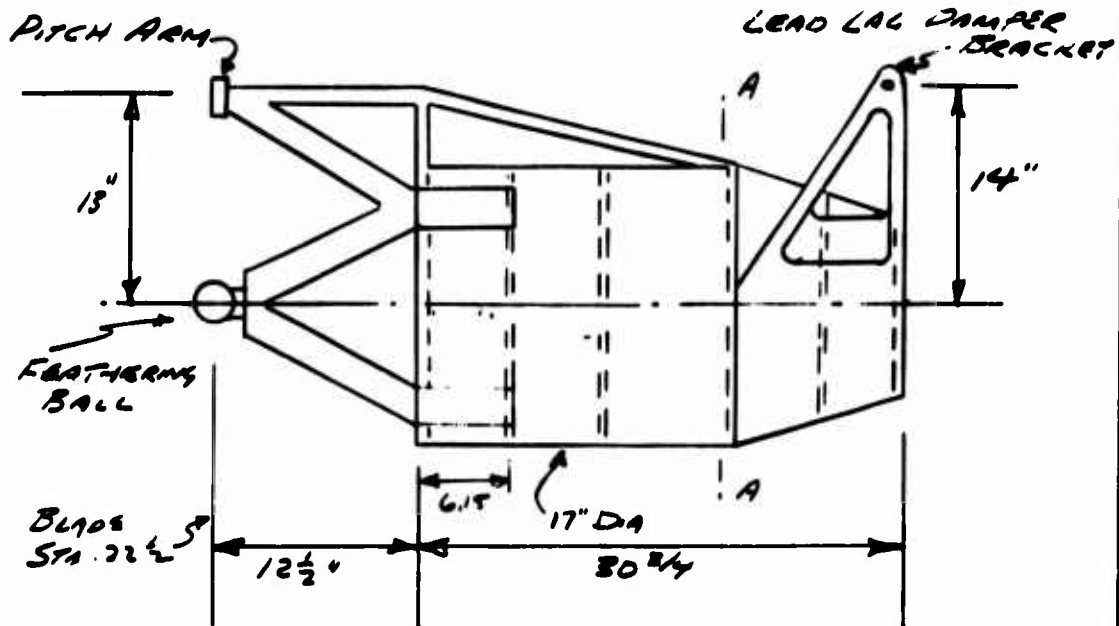
$$N_{xy} = 777 \frac{\text{lb}}{\text{in}}$$

$$\frac{M.S. \text{ for Panel}}{\text{Buckling}} = \frac{777}{328} - 1 = \underline{\underline{1.37}}$$

III STRESS ANALYSIS

BLADE TORQUE TUBE

(BETWEEN BLADE FEATHERING BALL AND
LEAD LAG HINGE) REF Dwg 395-0936



LUDOS

M_c

FATIGUE

$\pm 100,000^{\prime\prime}$

LIMIT MANEUVER

$\pm 500,000^{\prime\prime}$

M_B

$36.011 \pm 43.217^{\prime\prime}$

$110,672 \pm 119,632^{\prime\prime}$

M_T

63000 ± 75500

228000 ± 72800

CHECK SEC. AA FOR STABILITY UNDER BENDING
AND TORSIONAL SHEAR

$$R = 8 \frac{1}{2}'' \quad I = \pi r^3 t = 272 \text{ in}^4 \quad A = \pi R^2 t = 234$$

$t = .14$ ALUMINUM-TITANIUM

II STRESS ANALYSIS

BLADE TORQUE TUBE

SEC. 9A CONTINUED

RE-C-ANALYSIS & DESIGN OF FIGHT VEHICLE
STRUCTURES BY BRUHN

$$l = 6.15 \quad t = .11 \quad r = 8.5$$

CHECK BUCKLING SHEAR ALLOWABLE

$$Z_L = \frac{l^2}{kt} \sqrt{1 - \nu^2} = 38.6 \quad kt = 12. \quad \text{FIG. C8.18}$$

$$\frac{K_c \pi^2 E}{12(1-\nu^2) F_{0.7}} \left(\frac{t}{L} \right)^2 = .437 \quad F_{ce} = .44 \quad \sigma = 56000 \text{ psi}$$

FIG. C8.19

$$F_{0.7} = 127000 \text{ psi} \quad \text{Ref. A1.11}$$

BUCKLING STRESS OF CYLINDER UNDER COMPRESSION

$$\nu/t = .77 \quad Z = 38.6 \quad K_c = 8.5 \quad \text{FIG. C8.7}$$

$$\frac{K_c \pi^2 E}{12(1-\nu^2)} \left[\frac{t}{L} \right] \frac{1}{F_{0.7}} = .31 \quad \frac{F_{cr}}{F_{0.7}} = .31 \quad F_{ce} = 39000 \text{ psi}$$

REF. FIG C5.8

FOR LIMIT MANEUVER CASE

$$f_s = \frac{M_r}{2A} = \frac{\sigma (228000)}{2\pi^2(8.5)(.11)} = 9200 \text{ psi} \quad \frac{9200 \times 1^2}{56000} = .25$$

$$f_b = \frac{M_c}{I} = \frac{500000(8.5)}{214} = 20000 \text{ psi} \quad \frac{20000 \times 1^2}{39000} = .77$$

$$\left(\frac{f_s}{F_{ce}} \right)^2 + \left(\frac{f_b}{F_{ce}} \right)^2 = (.25)^2 + (.77)^2 = .65$$

$$\underline{M.S. = \frac{1}{\sqrt{.65}} - 1 = +.23}$$

VI STRESS ANALYSIS

Bending Torsion

ESTIMATED STRESSES

$$f_s = \frac{M_r}{Z} = \frac{63000 \times 75500}{2(284)} = 134 \pm 161 \text{ N/mm}$$

$= 1220 \pm 1460 \text{ Pa}$

$$f_b = \frac{M_a}{I} = \frac{4100 \times 75(45)}{214} = \pm 3960 \text{ Pa}$$

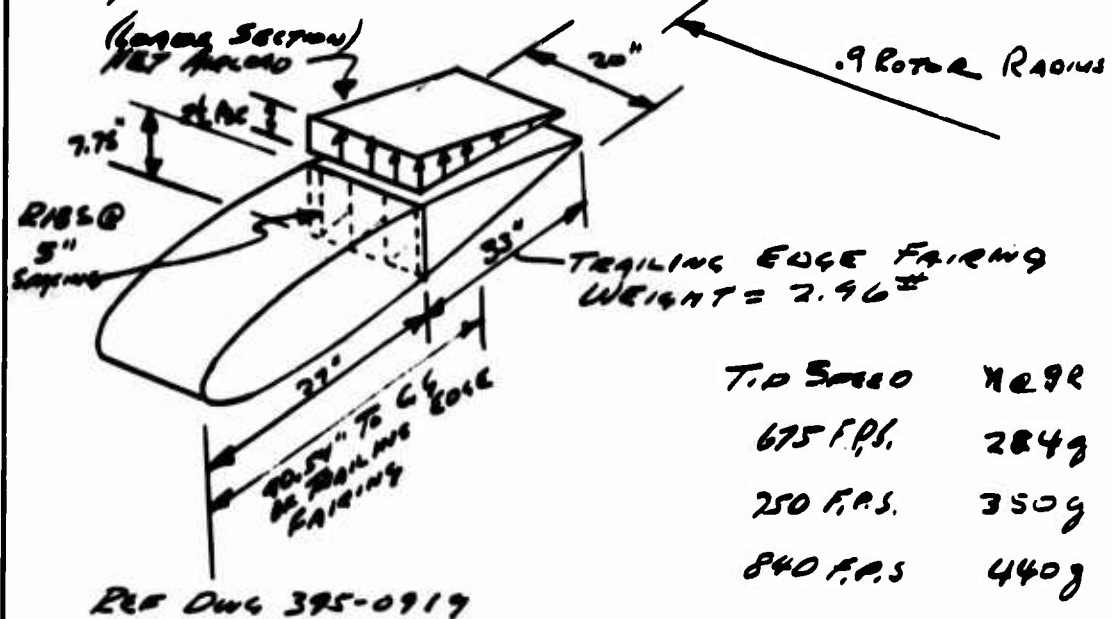
$$\text{Max. Stress} = \frac{S}{2} \pm \sqrt{\left(\frac{S}{2}\right)^2 + S_b^2} = \pm 4430 \text{ Pa}$$

$$\underline{M.S. = \frac{\pm 4430}{\pm 4430} - 1 = 0.000}$$

VII STRESS ANALYSIS

Trailing Edge Fairing

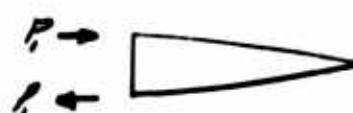
THE TRAILING EDGE FAIRING AT THE .9 ROTOR RADIUS IS CHECKED FOR ANGULAR & CENTRIFUGAL FORCE.



$$MOMENT OF INERTIA = \frac{1}{2} \rho S C \times \frac{32}{2} \times \frac{83}{3} = 453 \text{ in}^4/\text{in}$$

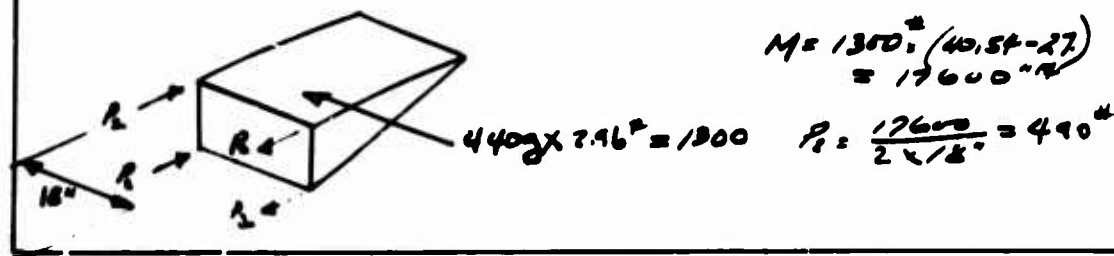
$$SHEAR = 2 \frac{1}{2} \rho S C \times \frac{22}{2} = 41.25 \text{ lb/in}$$

CHECK OUT BENDING R.I.O. OF FAIRING



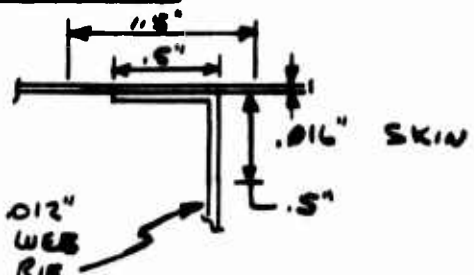
$$M = 453 \text{ in}^4 \times \frac{5}{2} = 1135 \text{ in}^5$$

$$P_e = \frac{1135}{275} = 4.17 \text{ ft}$$



III STRESS ANALYSIS

TRAILING EDGE FAIRING



SEC. AA
MATERIAL 2024 AL.

$$Area = .036 \text{ in}^2$$

$$f_{cr} = \frac{P_1 + P_2}{A} = \left(\frac{147 + 490}{0.036} \right) 1.5 = 26600 \text{ psi}$$

$$F_{cl} = 27000 \text{ psi}$$

$$M.S. = \frac{27000}{26600} - 1 = 0$$

SHEAR IN OUTSIDE SKIN DUE TO C.F. FORCE.

$$q = \frac{2.96 \times 350}{2 \times 20} = 26.5 \text{ lb/in} = 1625 \text{ psi}$$

$$F_{shear} = 5.3 E \frac{t^2}{l^2} \quad l^2 = \frac{5.3 E (.016)^2}{1625} = 8.35$$

$$l = 2.9$$

FOR NO BUCKLING OR SKIN AT HIGHLIGHT.

THE TRAILING EDGE FAIRING DESIGN IS QUITE SIMILAR TO THAT USED IN XV-9A RESEARCH HELICOPTER.

IV STRESS ANALYSIS

FLAPPING-FEATHERING BLADE STRAPS.

REF. 395-0936

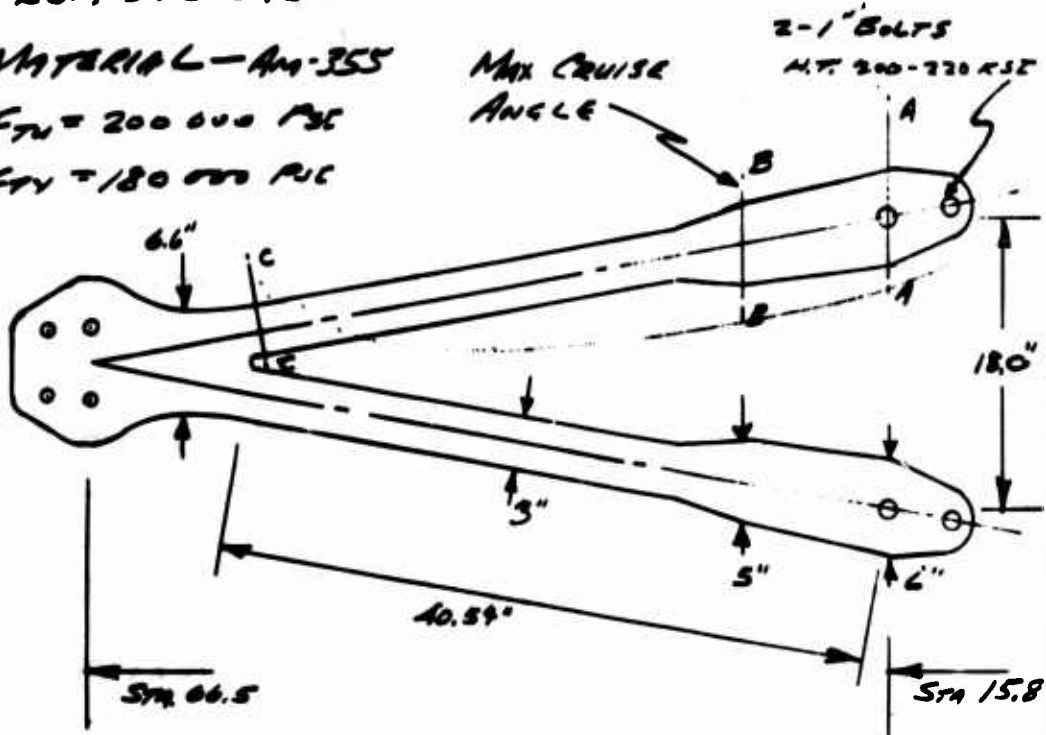
MATERIAL - Aln-355

$F_{UT} = 200,000 \text{ psi}$

$F_{UT} = 180,000 \text{ psi}$

MAX CRUISE
ANGLE

2-1" BOLTS
M.T. 200-220 KSC



LAMINATE THICKNESS = .020"

TOTAL NUMBER OF LAMINATES = 25

LOADS AND MOTIONS (Note Limit Cond = 105% of TSD FDS
TYP SPEED)

LOADS	FATIGUE COND	LIMIT MANEUVER COND
Vx, zr	$\pm 370^{\circ}$	$\pm 1850^{\circ}$
Mx, zr	$\pm 100,000^{\prime\prime \prime}$	$\pm 375,000^{\prime\prime \prime}$
C. F.	$\pm 180,000^{\#}$	$\pm 248,000^{\#}$
MOTIONS		
FLAPPING	$\pm 5^{\circ}$ (Note - STA INSTALLED (AT 8° PRE- CONING))	$+25^{\circ}$ (Note - 8° CONING) BY 1/2 IN
LEAD-LAG	$\pm 1.25^{\circ}$	$\pm 3^{\circ}$
FEATHERING	$\pm 12^{\circ}$ (STRAPS 44- 70 ARMED)	$+28^{\circ}$ (Note - +7° 18') BY 1/2 IN

II STRESS ANALYSIS

FLAPPING-FEATHERING BLADE STRAPS

SUMMARY OF STRESSES

SECTION	FATIGUE COND.			LIMIT MAX. COND.		
	AA	BB	CC	AA	BB	CC
f_1 - C.F. STRESS	+36600	+36600	+61000	+50500	+50500	-84000
f_2 - PACK BENDING	± 10150	± 10150	± 16900	± 35000	± 38000	± 57250
f_3 - LAMINATE BEND	—	7250±1250	—	—	+15000	—
f_4 - STRAP WIND UP	—	± 1200	± 5300	—	+7370	-36400
f_5 - LEAD LAG SHEAR	± 4950	± 4950	± 6250	+17000	+17000	+28400
f_6 - CHORD MOMENT	± 2625	± 2625	± 4375	+2800	+9800	+16300

$$f_{\text{TOTAL}} = f_1 + [f_2 + f_3] \cos(\psi - 30^\circ) + [f_4 + f_5 + f_6] \sin \psi$$

$$f_{\text{TOTAL MAX}} \text{ WHEN } \tan \psi = \frac{2(f_4 + f_5 + f_6) - (f_2 + f_3)}{\sqrt{3} (f_2 + f_3)}$$

MAX. STRESS FATIGUE CONDITION

SEC. AA @ BOLT HOLE = $36,600 \pm 13425$ PSC

SEC. BB IN SHOE = 43850 ± 21780 PSC

SEC CC = 61600 ± 26550 PSC

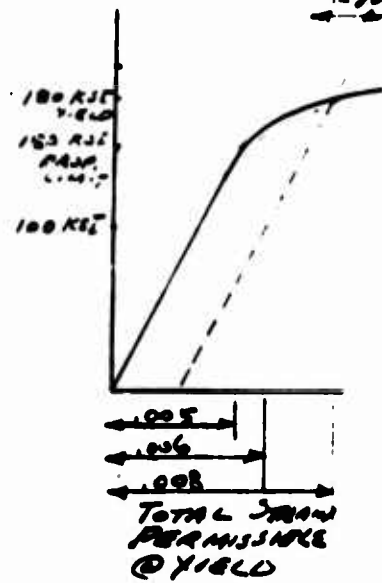
THESE STRESSES ARE RESPONSIBLE IN VIEW
ON THE FAIL-SAFE FEATURE OF THIS DESIGN.
AT THE BOLT HOLE, SEC. AA, THE LAMINATES
ARE TIGHTLY CLAMPED TOGETHER SO THERE IS
NO WORKING IN THE BOLT HOLE.

THIS STRAP DESIGN IS SIMILAR AND IS
BASED ON THE PROVEN OH-6A HELICOPTER
BLADE RETENTION STRAP CONFIGURATION.

II STRESS ANALYSIS

FLAPPING-FEATHERING BLADE STRESSES

SEC-C.C. ANALYSIS LIMIT MANEUVER LOAD.



+
3% CONCENTRATION
CHECK FOR WELD AT LIMIT LOAD

$$\frac{\sigma_f}{E} = \frac{128700 \text{ psi}}{29 \times 10^6} = .0044$$

DUE TO DIRECT LOADS

$$\frac{\sigma_f}{E} = \frac{93650 \text{ psi}}{29 \times 10^6} = .0032$$

STRAIN DUE TO MOTIONS

$$\frac{M.S.}{\text{YIELD}} = \frac{.008}{.0044 + .0032} - 1 = 4.05$$

CHECK FOR ULTIMATE STRENGTH.
 Σ STRESS FROM LOADS = $\sigma_1 + \sigma_5 + \sigma_c$
 $= 128700 \text{ psi}$

$$\frac{M.S. \cdot \frac{200000}{128700 \times 1.2}}{Wt.} - 1 = .04$$

60000 ± 30000 psi FOR SMOOTH AREAS FREE OF CONCENTRATION EFFECTS AND 40000 ± 3000 psi IN THE AREA OF A BOLTED ATTACHMENT WHICH IS CLAMPED SO TIGHTLY THAT THE LOAD IS CARRIED BY FRICTION ENTIRELY. THE STRAP SYSTEM IS MULTILPLY FAIR SAFE.

VI STRESS ANALYSIS

FLAPPING - FEATHERING BLADE STRAPS

FATIGUE CONDITION

$$f_1 = C.F. \text{ STRESS} = \frac{C.R}{\text{AREA}} \quad \begin{matrix} \text{Sec AA} \\ +36600 \text{Psi} \end{matrix} \quad \begin{matrix} \text{Sec BB} \\ +36600 \text{Psi} \end{matrix} \quad \begin{matrix} \text{Sec CC} \\ +61000 \text{Psi} \end{matrix}$$

$f_2 = P_{AC} \times \text{BENDING STRESS}$ (STEADY CURVING ANGLE BEND/IN.)

$$\theta = 15^\circ = .0872 \text{ RADIANS} \quad P_{AC} \text{ THICK.} = 25(.020) + 24(.004) = .58$$

$$\Delta = \frac{.586}{2} (.0872) = .026'' = \frac{P_L}{AE} = \frac{P_L}{WCE} \quad E = 29 \times 10^6$$

$$\frac{10.5P}{8.3tE} + \frac{27P}{3.0tE} + \frac{44P}{4tE} + \frac{8.5P}{5.5tE} = .026 \quad P = 1015 \text{#}$$

$$\text{Sec AA} = \frac{10.5}{.02} \times \frac{1}{6-1} = 10150 \text{ Psi}$$

$$\text{Sec BB} = \frac{10.5}{.02} \times \frac{1}{5} = 10150 \text{ Psi}$$

$$\text{Sec CC} = \frac{10.5}{.02} \times \frac{1}{3} = 16900 \text{ Psi}$$

$f_3 = \text{LAMINATE BENDING}$ (OCCURS ONLY AT SHOE SEC BB)

$$f_3 = \frac{Et}{2R} \quad R = \text{SHOE RADIUS}$$

$$f_3 = \frac{29 \times 10^6 \times .02}{2 \times 20} = 14500 \text{ Psi} \quad \text{SET SHOE RAD } 7250 \pm 7250$$

$f_4 = \text{STRAP WIND UP}$

$$I = \frac{.50 \times 3^3}{12} = 1.125 \text{ IN}^4 \quad \frac{EI}{P} = \frac{29 \times 10^6 \times 1.125}{91500} = .357 \times 10^3$$

$$J = \sqrt{\frac{EI}{P}} = 18.9 \quad \frac{L}{J} = \frac{40.54}{18.9} = 2.15, \quad \sinh \frac{L}{J} = 4.2342, \quad \cosh \frac{L}{J} = 4.3377$$

$$\chi_s = \frac{R_1(1-\cos\theta)}{L}, \quad R_1 = \frac{18}{2} = 9'' \quad L = 40.54 \quad \theta = 12^\circ \quad \chi_s = .00485$$

$$\delta_1 = \frac{R_2(1-\cos\theta)}{L}, \quad R_2 = 2'' \quad \delta_1 = .001080$$

II STRESS ANALYSIS

FLAPPING - FEATHERING BEFORE STRAPS

FATIGUE CONDITION

f_4 = STRAP WIND UP (CONTINUED)

$$P\delta_1 = \frac{1}{3} \left[\frac{M_2 - M_1 \cosh \frac{\delta}{2}}{\sinh \frac{\delta}{2}} \right] - \frac{1}{L} [M_1 - M_2]$$

$$99 = .0372 M_2 - .0792 M_1$$

$$P\delta_2 = \frac{1}{3} \left[\frac{M_1 - M_2 \cosh \frac{\delta}{2}}{\sinh \frac{\delta}{2}} \right] + \frac{1}{L} [M_1 - M_2]$$

$$444 = .0372 M_1 - .0792 M_2$$

$$M_1 = -4980'' \quad M_2 = -7950''$$

$$SEC. AA @ BOLT HOLE \quad f_4 = 0$$

$$SEC. BB = \frac{MC}{I} = \frac{4980(2.5)}{5.2} = 2400 \text{ PSI} \times \frac{1}{2} = \pm 1200 \text{ PSI}$$

$$SEC. CC = \frac{MC}{I} = \frac{7950(1.5)}{1.125} = 10600 \text{ PSI} \times \frac{1}{2} = \pm 5300 \text{ PSI}$$

f_5 - LEAD LAG SHEAR

$$\frac{\pm 1.35^\circ}{57.3^\circ} (180,000'') \pm 370 = \pm 4295''$$

$$f_5 = \frac{\frac{1}{2}(4295'')}{\tan 10^\circ} \times \frac{1}{\text{Area}} = \pm 8250 \text{ PSI} @ SEC. CC \\ = \pm 4950 \text{ PSI} @ SEC. AA \# 88$$

f_6 - CHORD MOMENT

$$\frac{MC_{.25}}{\text{DISTANCE FEATHER PELL} \rightarrow \text{TO LEAD LAG ANGLE}} = \frac{\pm 100,000}{44''} = \pm 2270''$$

$$f_6 = \frac{\frac{1}{2}(2270)}{\tan 10^\circ} \times \frac{1}{\text{Area}} = \pm 4375 \text{ PSI} @ SEC. CC \\ = \pm 2625 \text{ PSI} @ SEC. AA \# 88$$

II STRESS ANALYSIS

FEATHERING - FEATHERING BLADE STRINGS

ATTACHMENTS

BOLTS AT THIS END

$$M_{\text{max. C.F.}} = \frac{382000}{2 \cos 10^\circ} = +147,800^{\text{E}}$$

$$\text{DAMPER MOM. } \frac{800000}{441} \times \frac{1}{2} \times \frac{L}{\sin 10^\circ} = +32,800^{\text{W}}$$

$$\text{LL SHEAR} = \left[282000 \sin 30^\circ + 4725 \right] \times \frac{1}{2} \times \frac{L}{\sin 10^\circ} = +43,700^{\text{W}}$$

$$\frac{220,000}{220,000} = 1.0$$

USE 2-1.0" BOLTS @ 200-220 KSI H.T.

$$\text{D.S. ALLOW - 2 BOLTS} = 332000^{\text{E}}$$

$$M.S. = \frac{332000}{220000 \times 1.0} = 1.0$$

BOLT CLAMP UP REQUIRED FOR CYCLIC LOADS

$$\begin{aligned} f_2 - \text{PICK BENDING} &= \pm 10150 \text{ PSI} \\ f_5 - \text{LEAD LAG SHEAR} &= \pm 4950 \text{ PSI} \\ f_6 - \text{CHORD MOMENT} &= \pm 2625 \text{ PSI} \end{aligned} \quad \left. \right\} \text{Q SEC A.A.}$$

$$\left[\frac{\pm 10150}{2} \pm \frac{\pm 4950}{2} \pm \frac{\pm 2625}{2} \right] 5.00 \times .50 = \pm 18070^{\text{E}}$$

NET TENSILE LOAD FOR 1.0" BOLT $\frac{1.7200-220}{141000} = 1.0$

$$P_{\text{MAX}} = .3(1.6)(141000) = 25,400 > 18070^{\text{W}}$$

NOTE - ATTACHMENTS ARE CHECKED FOR
 C.F. @ 0.40 f.D.S. TOP SPEED (125 x 678)
 AND MAXIMUM DAMPER MOMENT
 AND LEAD LAG SHEAR.

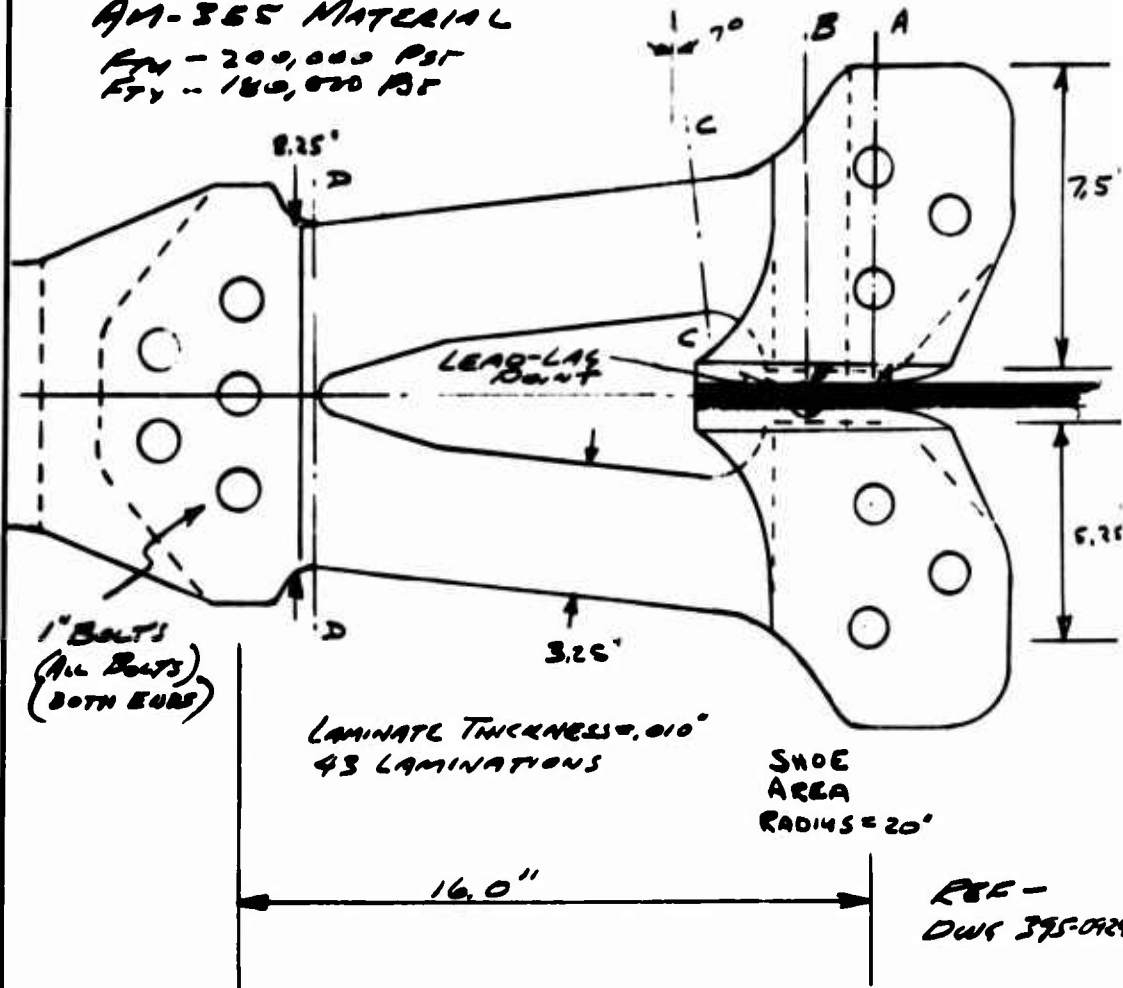
II STRESS ANALYSIS

LEAD-LAS BLADE FLEXURE

AM-365 MATERIAL

$F_{UT} = 200,000 \text{ PSF}$

$F_{Y} = 180,000 \text{ PSF}$



LOADS	FATIGUE COND.	LIMIT MANEUVER COND.
V_2	$4200 \pm 500 \#$	$5100 \pm 500 \#$
$M_{C,12}$	$\pm 100,000 \text{ "R}$	$\pm 375,000 \text{ "R}$
M_F	$43,250 \pm 52000$	134000 ± 134000
C.F	$\pm 180,000 \#$	$248,000 \#$ $\text{@ } 105\% \text{ OF } 750 \text{ F.P.S.}$
NOTIONS		
LEAD LAS	$\pm 1.25^\circ$	$\pm 3^\circ$

III STRESS ANALYSIS

LEAD-LAG BLADE FAILURE

I_{DO} MUST EQUAL 20 in^4 TO EQUAL I OF BLADE

$$\text{SPAR REQUIRED AREA} = \frac{I_{DO}}{\text{SPAN} \times \text{GEN. T.}} = \frac{20000}{8,100 \times .005} = 3.53\text{ in}^2$$

$$I = \frac{BH^3}{12} = \frac{3.53\text{ in}^2}{12} = 20 \quad H = 8.25\text{ in} \quad \frac{3.53\text{ in}^2}{8.25\text{ in}} = .43\text{ in}$$

LAMINATE THICKNESS = .010"

$$\text{PACK THICKNESS} = .43" + 42(.004) = .60"$$

FATIGUE CONDITION

$$f_1 = \text{STEADY C.F. STRESS} = \frac{CIF}{A_{\text{REB}}}$$

SEC	AA	BB	CC	DD
AREA	2.37 in^2	2.26 in^2	1.62 in^2	3.53 in^2
f_1	38000 Psi	40000 Psi	60000 Psi	51,000 Psi

f_2 - PACK BENDING STRESS

$$\Delta = \frac{b}{2} \beta = \frac{.60}{2} \left(\frac{1.25}{57.3} \right) = .0065 = \epsilon \frac{PL}{A_E}$$

$$\frac{P(2)}{4.13} + \frac{P(1.2)}{3.25} + \frac{P(2.5)}{5.25} = .0065 \epsilon t = 4.66 \epsilon, \quad P = 40300t$$

SEC.	AA	BB	CC	DD
WIDTH	(2.5-2.0)	5.25	3.25	4.13
f_2	± 7350	± 7700	± 12400	± 9750

f_3 - LAMINATE BENDING STRESS

occurs in shal only Sec B.C.

$$f_3 = \frac{st}{2E} = \frac{29 \times 10^6 \times .01}{2 \times 20} = 7500 \text{ Psi}$$

$$= 3750 \pm 3750 \text{ Psi}$$

II STRESS ANALYSIS

LEAD-LAG BLADE FIXURE

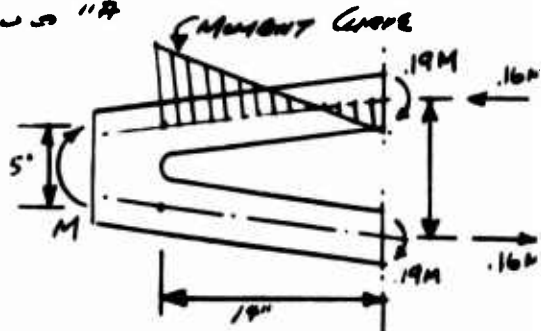
Engage Condition

f_L - Flapping Bending Stresses.

$$M_F = 43250 \pm 5200 \text{ in}^{\prime\prime}$$

$$.19M_F = 8225 \pm 990 \text{ in}^{\prime\prime}$$

$$.16M_E = 6920 \pm 8320 \text{ in}^{\prime\prime}$$



SEC.	At Dowell			
	AA	BB	CC	DD
Area	2.37 in^2	2.26 in^2	1.52 in^2	3.53 in^2
I/I	$200/14.10$	$8.68/5.19$	$1.63/1.23$	$4.13/1.00$
Moment/ A	2910 ± 3500	3060 ± 3100	4350 ± 5500	—
$\frac{.19M_F}{E}$	1170 ± 1400	4120 ± 5220	Measure =	8930 ± 1070
	4080 ± 4910	7380 ± 8920	4550 ± 5500	8950 ± 1070

f_S - Cyclic Axial Stress Due To Damper Mot.

$$M_c = \pm \frac{100,000}{14} = \pm 7150 \text{ in}^{\prime\prime} \text{ goes to Eng legs}$$

SEC.	AA	BB	CC	DD
P/A	$\pm 1500 \text{ Psi}$	$\pm 1580 \text{ Psi}$	$\pm 2350 \text{ Psi}$	$\pm 2000 \text{ Psi}$

VI STRESS ANALYSIS

LEAD-LAG BLADE FLEXURE

SUMMARY OF STRESSES

SECT.	FATIGUE COND.				LIMIT COND.			
	A A	B B	C C	D D	A A	B B	C C	D D
f ₁	+38000	+40000	+60000	+51000	+45200	+55000	+12200	+70000
f ₂	+2350	+7700	+12400	+9750	+17700	+18500	+29800	+29400
f ₃	—	+500±3750	—	—	—	+7500	—	—
f ₄	+2000	+2000	+2000	+2000	+25450	+44700	+2700	+10500
f ₅	+1500	+1600	+2350	+2000	+5650	+5900	+7800	+7500
					101,800	121,806	122,800	111,400

TOTAL FATIGUE STRESSES.

$$f_{total} = f_1 + [f_2 + f_3 + f_5] \sin \psi + f_4 \cos(\psi - 30^\circ)$$

$$\text{Max when } \tan \psi = \frac{2(f_2 + f_3 + f_5)}{\sqrt{3} f_4} - f_4$$

MAX. STRESS FATIGUE CONDITION

$$\text{Sec AA @ Bolt Hole} = +43,080 \pm 1,790 \text{ Psi}$$

$$\text{Sec BB @ Shock} = +51,30 \pm 1,800 \text{ Psi}$$

$$\text{Sec CC} = +64,550 \pm 1,8020 \text{ Psi}$$

$$\text{Sec DD} = +60,750 \pm 1,7350 \text{ Psi}$$

CHECK FOR ULTIMATE STRENGTH

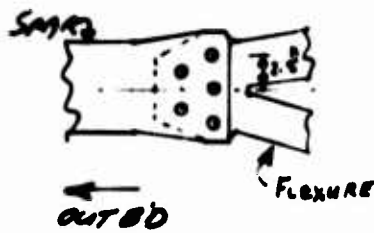
$$M.S. = \frac{200,000}{122,800 \times 1.5} - 1 = +0.08$$

VI STRESS ANALYSIS

LEAD-LAG BLADE FLEXURE

BOLT ATTACHMENT

THE OUTBOARD ATTACHMENT IS SHOWN AS THIS
ATTACHMENT IS MADE UP OF 5 BOLTS WHERE
AS THE INBOARD ATTACHMENT OR THE FLEXURE
HAD SIX BOLTS



$$A_{\text{BOLT GROUP}} = 18.9 \text{ in}^2$$

$$\sigma_{\text{MAX}, C.F.} = \frac{282000}{5 \text{ Bolts}} = 56400 \text{ psi}$$

$$\text{DAMPER MOM. } \frac{500000}{14.0 \times 5.0 \text{ in}^2} = 7150 \text{ in-lb}$$

$$\text{F. AND MOM. } \frac{M}{I} = \frac{268000(2.5)}{18.9} = \frac{35500}{99050 \text{ in}^4}$$

USE 5-1.0" BOLTS @ 200-220 KSI. HT.

$$\text{DES. ALLOWABLE} = 166000 \text{ psi}$$

$$M.S. = \frac{166000}{99050 \text{ in}^4} - 1 = +1.11$$

BOLT CLAMP UP REQUIRED FOR CYCLIC LOADS

$$\left. \begin{array}{l} f_2 - \text{PICK BENDING} = \pm 9750 \text{ psi} \\ f_5 - \text{DAMPER MOM.} = \pm 2000 \text{ psi} \end{array} \right\} \text{@ SEC DD}$$

Previous page

$$\left[\frac{\pm 9750 \text{ psi}}{2} = 200 \text{ psi} \right] 8.25 \times 4.3 \times \frac{1}{8.0 \text{ in}^2} = \pm 4870 \text{ psi}$$

DIMENSIONS
OR SEC. DD.

$$\text{CYCLIC TENS. MOM. } \frac{M}{I} = \frac{52000(2.5)}{18.9} = \pm 6400 \text{ in-lb}$$

$$\pm 11770 \text{ in-lb}$$

$$F_t(\text{ULT}) \text{ OR } 1" \text{ BOLT} = 141000 \text{ psi}$$

$$D = \mu \text{ in} = .3 (607. \text{ or } 141000) = 25900 \text{ in}$$

$$M.S. = \frac{25400}{11770} - 1 = +1.16$$

NOTE - ATTACHMENTS ARE CHECKED FOR C.G. (2000 F.P.S. 7.5 SEC.
(1.25 x 675 KAS) AND MAXIMUM DAMPER MOMENT & FRAMING MOMENT

VII STRESS ANALYSIS

BLADE TORSION FLEXURES AT LEAD LAG Hinge



FLEXURES RESIST
BLADE TORSION AND
MUST FLEX WITH
THE BLADE LEAD LAG
ANGLE.

FLEXURE 2.0" wide by 75" long
.20" thick

FATIGUE Condition

$$M_f = 63,000 \pm 75,500 \text{ in-lbs} \quad S = \pm 125^\circ \text{ lead lag}$$

$$P_c = \frac{63,000 \pm 75,500}{15.50} = 4070 \pm 4870 \text{ psi}$$

$$S = \frac{M_c}{Z_L}, \quad f_b = \frac{M_c}{J} \quad f_b = \frac{S E t}{Z_L} = \frac{125}{37.3} \times \frac{29 \times 10^6}{15} \times .482 \times 10^5 \text{ ft}$$

$$\frac{P}{A} + f_b = \frac{4070 \pm 4870}{2 \times .200} \pm .482 \times 10^5 / 200 = 10150 \pm 20590$$

$$\underline{M.S. = \frac{\pm 25500}{\pm 20590} \cdot 1 = \pm .71}$$

Limit Condition

$$M_f = 228,000 \text{ in-lbs} \pm 228,000 \text{ in-lbs} \quad S = \pm 40^\circ \text{ lead lag}$$

$$P_c = \frac{228,000 \pm 228,000}{15.50} = 14700 \pm 14700 = 29400 \text{ psi}$$

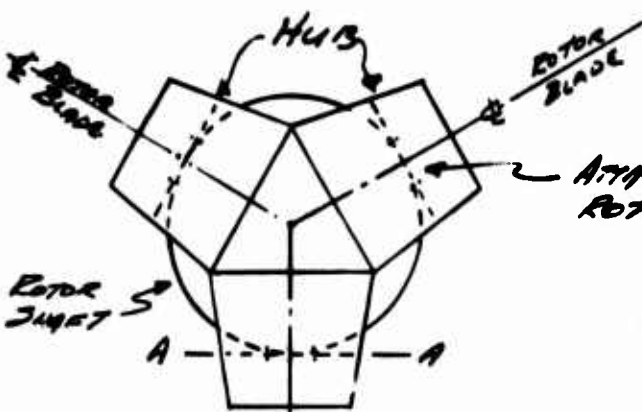
$$\frac{P}{A} + f_b = \frac{29400}{2 \times .20} + .482 \times 10^5 \times .125 \times \frac{40}{125} =$$

$$= 73500 + 27000 = 100,500 \text{ psi}$$

$$\underline{M.S. = \frac{25500}{100500} \cdot 1 = \pm .70}$$

MOTOR HUB ANALYSIS

EGF-Div, 395-0936

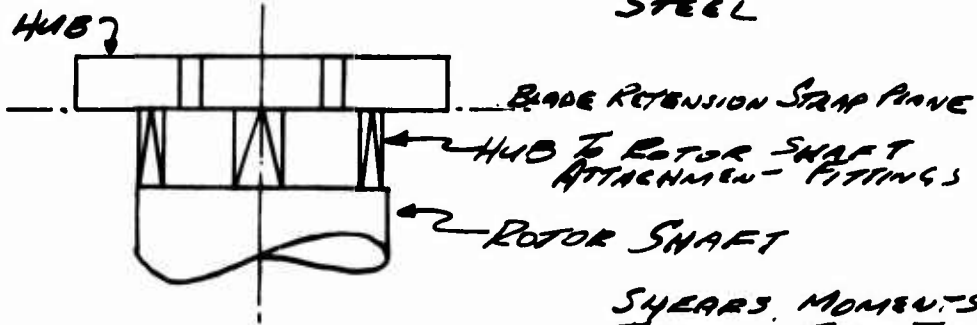


ATTACHMENT LOCATIONS TO
ROTOR SHAFT

HUB-MATERIAL

CARBONITE 455

MARAGING STAINLESS
STEEL

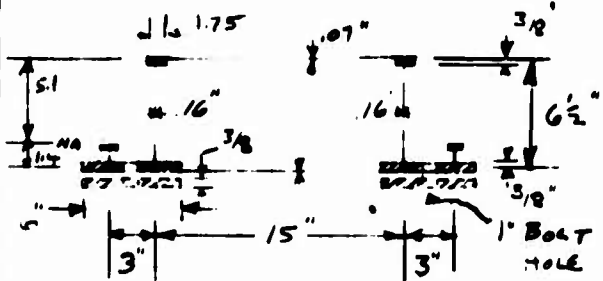
ATTACHMENT FITTINGSCONNECTING THE HUB TO
THE ROTOR SHAFT

SHREWS, MOMENTS, AND TORQUES FROM THE ROTOR BLADES ARE REACTED IN THE HUB THUS REDUCING CONSIDERABLY THE LOADS TRANSMITTED TO THE ROTOR SHAFT. THE ROTOR SHAFT EXPERIENCES ONLY THE UNBALANCED PORTION OF THESE LOADS. THE NET LOADS ARE TRANS-

MITTED TO THE ROTOR SHAFT BY THE ATTACHMENT FITTINGS WHICH PROVIDE A SHORT DIRECT LOAD PATH. THE LOADS ENTER THE ROTOR SHAFT IN THE PLANE OF THE ROTOR SHAFT WHILE TAKING ADVANTAGE IN THE AVAILABILITY STRENGTH AND STIFFNESS IN THIS DIRECTION OF THE SHAFT. RADIAL ITATING REQUIREMENTS ARE GREATLY REDUCED. AS A RESULT OF THESE SHORT LOAD PATHS AND ELLIPTICAL LOADINGS OF THE HUB AND ROTOR SHAFT, THEY ARE OPTIMIZED FOR MINIMUM WEIGHT.

II STRESS ANALYSIS

Rotor Hub Analysis



LOADS @ SECT. A-A		
	FATIGUE	LIMIT
M_C	$\pm 112,650$	852,000
M_F	$228,000 \pm 178,000$	1,055,000
M_r	$\pm 44,250$	425,000
V_x	$\pm 4,550$	22,700
V_z	$15,730 \pm 27,370$	102,000
M_{Axial}	$178,000 \pm 28,000$	260,000

BENDING SECTION OF

HUB AT A-A

$$I_{yy} = +3.4 \text{ in}^4 \text{ (for skin effective)}$$

REF LOADS FROM LOADS

SECTION

① THESE LOADS ARE APPLIED
AND REACTED IN THE
LOWER CAP MEMBERS

TOP CAP MEMBERS

$$f = \frac{M_C}{I} = 26,900 \pm 21,000 \text{ Psi}$$

$$= 124,000 \text{ Psi}$$

NOTE: THIS SECTION IS FREE OF
BOLT HOLES & OTHER STRESS CONCENTRATIONS
LOWER CAP MEMBERS

FATIGUE LOADINGS

$$M.S. = \frac{257000}{124000} - 1 = +1.9$$

$$M.S. = \frac{257000}{124000} - 1 = +1.9$$

ULTIMATE LOAD, 200,000

THROUGH BOLT HOLE ATTACHING BOLTS. RETENTION STRENGTH

$$\frac{M_C}{18} = \frac{\text{FATIGUE}}{I} = 16,600 \text{ Psi} \quad \text{LIMIT} = 67,250 \text{ Psi}$$

$$\frac{A \times M_C}{I} = \frac{89,700}{1400} = 63,000 \text{ Psi}$$

$$\text{NET AREA} = [6 - 1] \frac{3}{8} \times 2 = .375 \text{ in}^2$$

$$\% \text{ DUE TO } M_C = 1760 \text{ Psi} \quad 12,600 \text{ Psi}$$

$$\% \text{ DUE TO } M_F = 23700 \pm 373 \text{ Psi} \quad 34,700 \text{ Psi}$$

$$\frac{M_C}{I} \text{ DUE TO } M_F = \frac{7400 \pm 5750 \text{ Psi}}{31100 \pm 7885 \text{ Psi}} = \frac{34,100 \text{ Psi}}{81,400 \text{ Psi}}$$

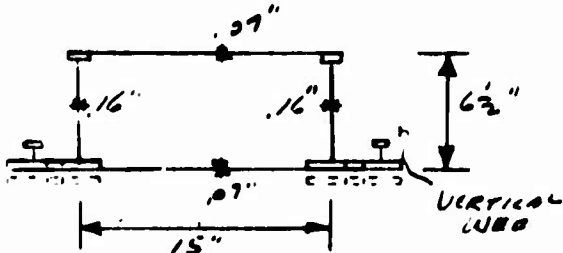
$$M.S. = \frac{\pm 10000}{\pm 7883} - 1 = +1.10 \quad \text{FATIGUE} \quad M.S. = \frac{257000}{81100} - 1 = +1.10$$

at bolt hole

9704

II STRESS ANALYSIS

ROTOR 440 ANALYSIS



$$\text{ENCLOSED AREA} = \\ 6\frac{1}{2} \times 21 = 136.5 \text{ in}^2$$

NOTE - THE VERTICAL WEBS INBOARD OF THE HUB SUPPORTS CAN BE REDUCED TO .08" AS THE SHEAR IS REDUCED TO 14485 lb/in

CHECK VERT. web Web

$$\text{TORQUE SHEAR} = \frac{M_e}{24t}$$

$$\text{FATIGUE LIMIT STRESS} \\ \pm 1485 \quad 13600$$

$$\text{VERTICAL SHEAR} = \frac{V_2}{2(0.4)t} \quad \frac{16800 \pm 13000}{16800 \pm 14485 \text{ lb/in}} \quad \frac{78,000 \text{ psi}}{91,600 \text{ psi}}$$

FATIGUE & TENSION FATIGUE
ALLOWABLE = $60\% \times 28000 \text{ psi} = 15000 \text{ psi}$

$$M.S. = \frac{15000}{14485} \approx 0$$

CHECK STRENGTH SPACING FOR LIMIT
MATERIAL CASE FOR VERTICAL WEB.

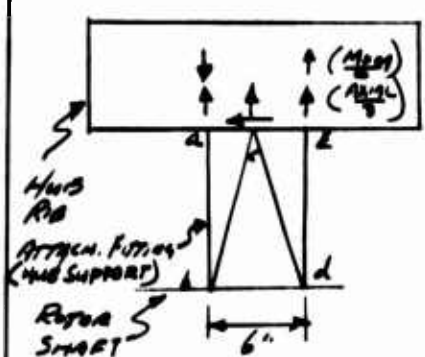
$$f_s = 5.3 \times \frac{t^2}{b^2} = 5.3 \left(27 \times 10^{-6} \right) \frac{16}{b^2} = 91600 \text{ psi}$$

$b = 6.3"$ STP. REQUIRED A-6.3" SPACING

VII STRESS ANALYSIS

ROTOR HUB ANALYSIS

RIB & ATTACHMENT FITTING TO ROTOR SHAFT



FITTING LOADS FROM
LOADS SECTION

LIMIT MAN. FATIGUE

AXIAL	192500 ⁺	3500 ± 3840
MOM	193920	± 2186
SHEAR	3200	± 740

MEMBERS → ab

LIMIT MAN. $+31880^+$

FATIGUE 11700 ± 9448

CROSS SECT
AREA

bc

$+39900^+$

6120 ± 5440

$.9^{\prime\prime} \times .9^{\prime\prime}$

cd

$+27,300$

6120 ± 7760

$.39 \times .9^{\prime\prime}$

de

$+96520^+$

11700 ± 16332

$.9^{\prime\prime} \times .9^{\prime\prime}$

$$\frac{M.S.}{U.L.T.} = \frac{25700}{\frac{96520 \times 1}{.9}} - 1 = +.60$$

$$\frac{M.S.}{FATIGUE} = \frac{25000}{\frac{79400}{.39}} - 1 = +.24$$

Note - CROSS SECTION AREA OF THESE MEMBERS IS DETERMINED BY THE STIFFNESS ANALYSIS OF THE HUB PLATE AND ATTACHMENT FITTING AND NOT BY STRENGTH REQUIREMENTS AS EXPLAINED IN THE LOADS SECTION.

ALLOWABLES FOR CARPENTER AND MACHINING STAINLESS STEEL ARE TAKEN FROM THE MATERIALS AND WORK SECTION.

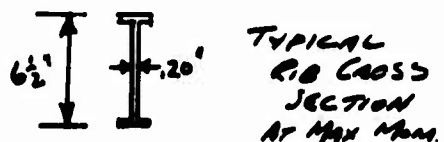
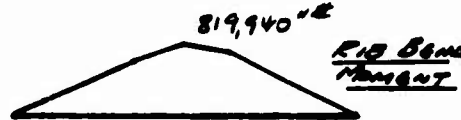
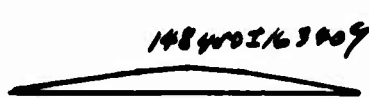
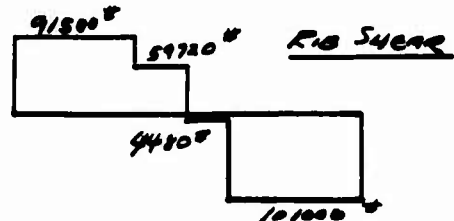
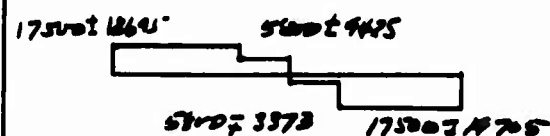
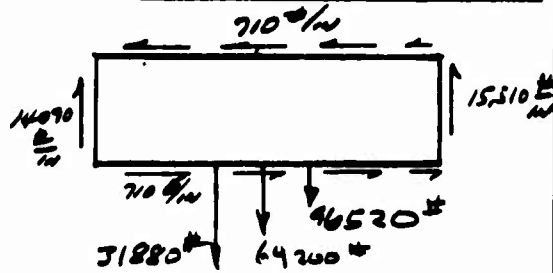
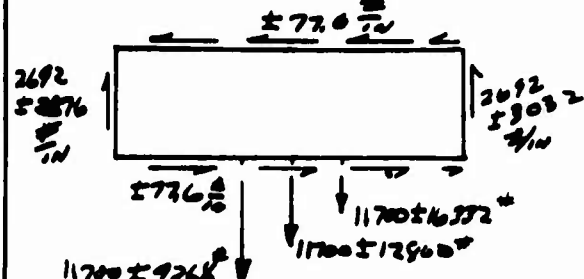
THE ANALYSIS PERTAINS TO TYPICAL MEMBER SECTIONS AND THE LOCAL AREAS AROUND ATTACHMENT BOLTS ARE REINFORCED TO REDUCE STRESSES

IV STRESS ANALYSIS

ROTOR HUB ANALYSIS

ANALYSIS OF 1/4 IN RIB 1/4 SEC. A-A
MATERIAL CONSIDERED AS MARSHAL STEEL
FATIGUE COND.

LIMIT MANOEUVRE LOAD



Web Shear Stress (Fatigue)

$$f_s = \frac{2692 \pm 303.2}{.2} = 13460 \pm 15000 \text{ psi}$$

$$M.S. = \frac{15000}{15000} - 1 = 0$$

For fatigue shear use
60% of fatigue bend allow
 $= .60 \times \pm 25000 = 15000$

Cap Stress

$$\frac{MC}{I^2} = \frac{148400 \pm 163449}{22} = 22000 \pm 24200 \text{ psi}$$

$$I = 22.0 \text{ in}^4 \quad \text{Cap Area} = .98 \text{ in}^2$$

Web Shear Stress Cap

$$f_s = \frac{15510}{.2} \times \frac{1}{L} = 11300 \text{ psi}$$

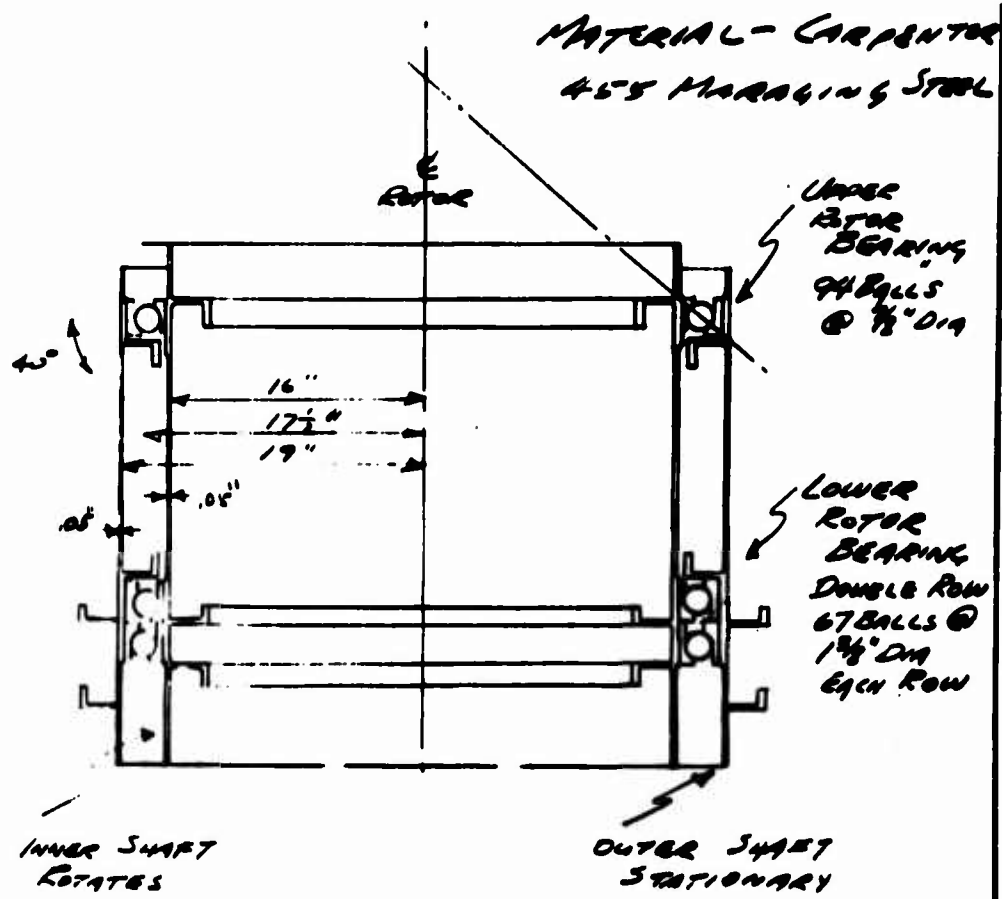
Cap Stress Cap

$$\frac{MC}{I^2} = \frac{819,940(6)}{22} = 18200 \text{ psi}$$

Critical R.I.
Stresses are
for the fatigue
condition
M.S. = $\frac{148400}{15000} - 1 = +0.03$

II STRESS ANALYSIS

ROTOR SHAFT & BEARING

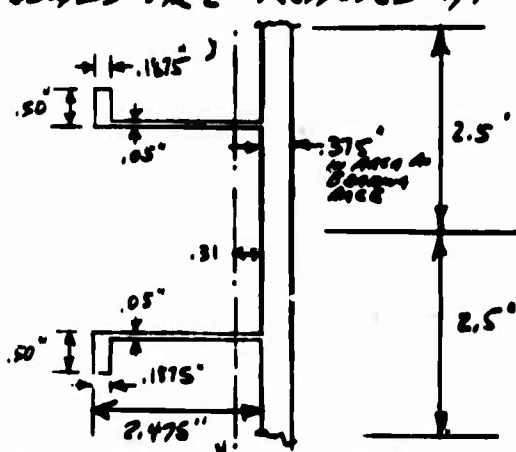


ALL LIFT LOADS ARE REACTED AT
THE LOWER BEARING.

Typical stiffening
at the bearings

$$I_{yy} = 1.22 \text{ in}^4$$

$$A = 1.72 \text{ in}^2$$



ROTOR SHAFT & BEARING - CONT'D

REFERENCE:- "BALL & ROLLER BRG. ENGINEERING"
(See pages 73 and 90) BY ARVID PALMGREN

LIFE BASED ON FATIGUE LOADING - SEE LOADS SECTION

a) LOWER BRG. $F_R = 11,400 \text{ #}$ $F_a = 94,635 \text{ #}$ $\alpha = 40^\circ$

EQUIV. LOAD $P = X F_R + Y F_a$ $X = .50$ $Y = .4 C_0 + 40^\circ$
 $= (.5 \times 11,400) + (.478 \times 94,635)$
 $= \underline{\underline{50,935 \text{ #}}}$

$f_c = 4.0$

SPECIFIC CAPACITY $C = f_c i \frac{D_w^2 Z^{2/3} \cos \alpha}{1 + .02 D_w}$ $i = 2.0$
 $D_w = \frac{(1.375)}{34.9 \text{ in/m}}$

$= \frac{4 \times 2 \times 34.9^2 \times 67^{2/3} \times .766}{1 + (34.9 \times .02)}$

$Z = 67$

$= 72,511 \text{ kg.} = \underline{\underline{159,887 \text{ #}}}$ (FOR 1,000,000 CYCLES
 B_{10} LIFE)

THEN $L_N = \left(\frac{159,887}{50,935} \right)^3 \times 10^6 \text{ CYCLES}$

$N = 143 \text{ RPM}$

$= \underline{\underline{30,929,571 \text{ CYCLES}}}$

$= 8580 \text{ Rev/Hour}$

$\therefore B_{10} \text{ LIFE IN HOURS} = \frac{30,929,571}{8580} = \underline{\underline{3605 \text{ HOURS}}}$

b) UPPER BRG. $F_R = 17,240 \text{ #}$ $F_a = 2460 \text{ #}$ $\alpha = 40^\circ$

EQUIV. LOAD $P = X F_R + Y F_a$ $X = .50$ $Y = .4 C_0 + 40^\circ$
 $= 8620 + 1176 = \underline{\underline{9796 \text{ #}}}$ $= .478$

$f_c = 4.5$

SPECIFIC CAPACITY $C = f_c i \frac{D_w^2 Z^{2/3} \cos \alpha}{1 + .02 D_w}$ $i = 1.0$

$D_w = \frac{7}{8} = 22.2 \text{ in/m}$

$= \frac{4.5 \times 492.8 \times 20.675 \times .766}{1 + .44} = 24,389 \text{ kg}$

$Z = 94$

VI STRESS ANALYSIS

UPPER BRG. - CONT'D

$\therefore C = 53,777 \text{ for } 10^6 \text{ cycles}$

$$L_N = \left(\frac{53,777}{9796} \right)^3 = 165,000,000 \text{ CYCLES}$$

$$\text{THEN } B_{10} \text{ LIFE} = \frac{165,000,000}{8580} = \underline{\underline{19,250 \text{ hours}}}$$

8704

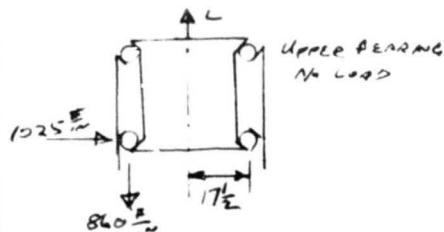
III STRESS ANALYSIS

ROTOR SHAFT & BEARING

CHECK STRESSES IN ROTOR SHAFT AND STIFF. RINGS FOR BEARING HOUSINGS.

FATIGUE CONDITION

$L = 94,590$ REF - ROTOR SHAFT BEARING LOAD TRAIL

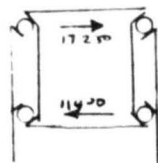


$$W_{vertical} = \frac{94590^4}{2(17\frac{1}{2})\pi} = \frac{860}{in}$$

$$W_{radial} = 860 \frac{lb/in}{in} \times \frac{1}{\tan 45^\circ} = 1025 \frac{lb}{in}$$

$$\text{HOOP TENSION (COMPRESSION)} = 1025 (17\frac{1}{2}) = \underline{\underline{18000 \frac{lb}{in}}}$$

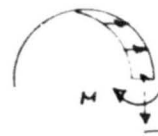
$$P_R = 5950 \pm 11300 \text{ (Upper Bearing)} \quad P_L = 150 \pm 11300 \text{ (Lower Bear.)} \\ = 17250 \qquad \qquad \qquad = 11400$$



MOMENT IN STIFFENER RING DUE TO LATERAL BEARING LOAD

$$M = .0603 KR^3, \frac{K\pi R^2}{2} = 17250 \frac{lb}{in}$$

$$K = 35.9 \frac{lb}{in^3}$$



$$M = \underline{\underline{13300 \frac{lb}{in} \text{ STRESS MOM. IN UPPER OUTER STIFF. RING}}}$$

$$M = \underline{\underline{6650 \pm 6650 \frac{lb}{in} \text{ IN UPPER INNER STIFF. RING (ROTATING)}}}$$

$$T = .75 KR^2$$

$$T = \underline{\underline{8250 \frac{lb}{in} \text{ STRESS IN LOWER OUTER STIFF. RING (NON ROTATING)}}}$$

$$T = \underline{\underline{4125 \pm 4125 \frac{lb}{in} \text{ IN LOWER INNER STIFF. RING}}}$$

$$W_{vert} = 17\frac{1}{2}(35.9) \frac{1}{\tan 45^\circ} = 750 \frac{lb}{in}$$

$$W_{vert} = +375 = 375 \frac{lb}{in} \text{ LOAD IN PLANE OF INNER SHIRT SKIN}$$

$$W_{vert} = 750 \frac{lb}{in} \text{ LOAD IN PLANE OF OUTER SHIRT SKIN}$$

For Values At Lower
Bearing Multipl. by
 $11400/17250 = .66$

$$M = 8850 \frac{lb}{in} \text{ OUTER RING}$$

$$M = 4470 \pm 4470 \text{ INNER RING}$$

$$T = 5460 \frac{lb}{in} \text{ OUTER RING}$$

$$T = 2725 \pm 2725 \frac{lb}{in} \text{ INNER RING}$$

Ref - FORMULAS FOR STRESS & STRAIN BY ROARK

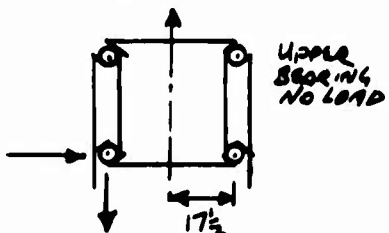
9704

IV STRESS ANALYSIS

ROTOR SHAFT BEARING

CHECK STRESSES IN ROTOR SHAFT &
STIFFENER RINGS FOR BEARING HOUSINGS
LIMIT MovEMENT Condition

$$L = 233,150 \quad \text{R.R. - ROTOR SHAFT BEARINGS
LOAD TROLL}$$

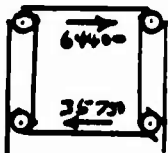


$$\text{deflection} = \frac{233,150^3}{2(7\frac{1}{2})^3} = 2120 \frac{\text{in}}{\text{in}}$$

$$W_{\text{ROUND}} = 2120 \frac{\text{in}}{\text{in}} \times \frac{1}{tan 60^\circ} = 2530 \frac{\text{lb}}{\text{in}}$$

$$\text{HOOP TENSION (compression)} = 2530 (17\frac{1}{2}) = 44250 \frac{\text{lb}}{\text{in}}$$

$$P_R = 64400 \text{ lb (lower bearing)}, P_R = 35,750 \text{ lb (upper bearing)}$$

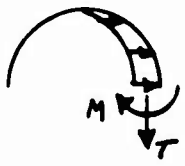


Moment in STIFFENER RING due to LATERAL BEARINGS LOAD (Upper)

$$M = .0603 KR^3, \quad \frac{KR^3}{2} = 64400$$

$$K = 134.0 \frac{\text{in}^3}{\text{in}}$$

$$M = 49700 \frac{\text{in}^4}{\text{in}} \quad \text{Peak in Both inner & Outer Ring}$$



For Upper & Lower
Bearings Multiplied
by 35750 / 6400 = .555

$$T = .75 KR^2$$

$$T = 30800 \frac{\text{lb}}{\text{in}} \quad \text{Tension in Upper Inner
Compression in Upper Outer Ring}$$

$$W_{\text{inner}} = 17\frac{1}{2} (134.0 \frac{\text{in}^3}{\text{in}}) \tan 60^\circ = 2800 \frac{\text{lb}}{\text{in}}$$

$$W_{\text{outer}} = 2800 \frac{\text{lb}}{\text{in}} \quad \text{Peak Tension in
Inner Shaft Skin}$$

$$W_{\text{outer}} = 2800 \frac{\text{lb}}{\text{in}} \quad \text{Peak Compression
Outer Shaft Skin}$$

$$M = 27600 \frac{\text{in}^4}{\text{in}} \quad \text{Peak
in Lower Inner & Outer Ring}$$

$T = 17100 \frac{\text{lb}}{\text{in}}$ Tension
in Lower Outer
Ring & Compression
in Lower Outer
Ring

R.R. - FORMULAS FOR STRESS & STRAIN BY ROSEN

II STRESS ANALYSIS

ROTOR SHAFT & BEARINGS

SUMMATION OF LOADS IN ROTOR SHAFT

		SHAFT AT LOWER BEARING			
		INNER STIFF RING (ROTATING)		OUTER STIFF RING (STATIONARY)	
		T	M	T	M
FATIGUE COND.	FROM LMT-L FORMULAS	—	—	—	—
		-4125±4125 ["]	6650±6650 ["]	+8250 ["]	13300 ["]
	TOTAL	-4125±4125	6650±6650	+8250 ["]	13300 ["]
LIMIT COND.	FROM LMT-L FORMULAS	—	—	—	—
		-30,800 ["]	49700 ["]	+30,800 ["]	49700
	TOTAL	-30,800 ["]	49700 ["]	+30,800 ["]	49700 ["]
		SHAFT AT LOWER BEARING			
		INNER STIFF RING		OUTER STIFF RING	
		T	M	T	M
FATIGUE COND.	FROM LMT-L FORMULAS	-18000 ["]	—	+18000 ["]	—
		-2725±2725 ["]	4400±4400	+5450 ["]	8800 ["]
	TOTAL	-20725±2725 ["]	4400±4400	+23450 ["]	8800 ["]
LIMIT COND.	FROM LMT-L FORMULAS	-44250 ["]	—	+44250 ["]	—
		-17100 ["]	27600 ["]	+17100 ["]	27600 ["]
	TOTAL	-61350 ["]	27600 ["]	+61350 ["]	27600 ["]
CRITICAL LOADING FOR FATIGUE T=-4125±4125 ["] M=6650±6650					
CRITICAL LOADING FOR LIMIT T=-30800 ["] M=49700 ["]					

II STRESS ANALYSIS

ROTOR SHAFT & BEARING

SUMMATION OF LOADS IN SHAFT SHELLS

INNER SHAFT WALL	FATIGUE	LIMIT
DUE TO LIFT	+260 $\frac{\text{lb}}{\text{in}}$	+2120 $\frac{\text{lb}}{\text{in}}$
DUE TO MOMENT	$\frac{+375 \text{ lb} \cdot 375 \frac{\text{lb}}{\text{in}}}{+1235 \text{ in}^2}$	$\frac{+2800 \frac{\text{lb}}{\text{in}}}{+5920 \frac{\text{lb}}{\text{in}}}$
$f_s^* \text{ (For .05")}$	$24700 \pm 7500 \text{ Psi}$	98400 Psi

OUTER SHAFT WALL

DUE TO LIFT	0	0
DUE TO MOMENT	$750 \frac{\text{lb}}{\text{in}}$	$-2800 \frac{\text{lb}}{\text{in}}$
$f_s^* \text{ (For .05")}$	$15,000 \text{ Psi}$	56000 Psi

CHECK STRESSES IN STIFFENING RINGS ON
SHAFT FOR BEARINGS.

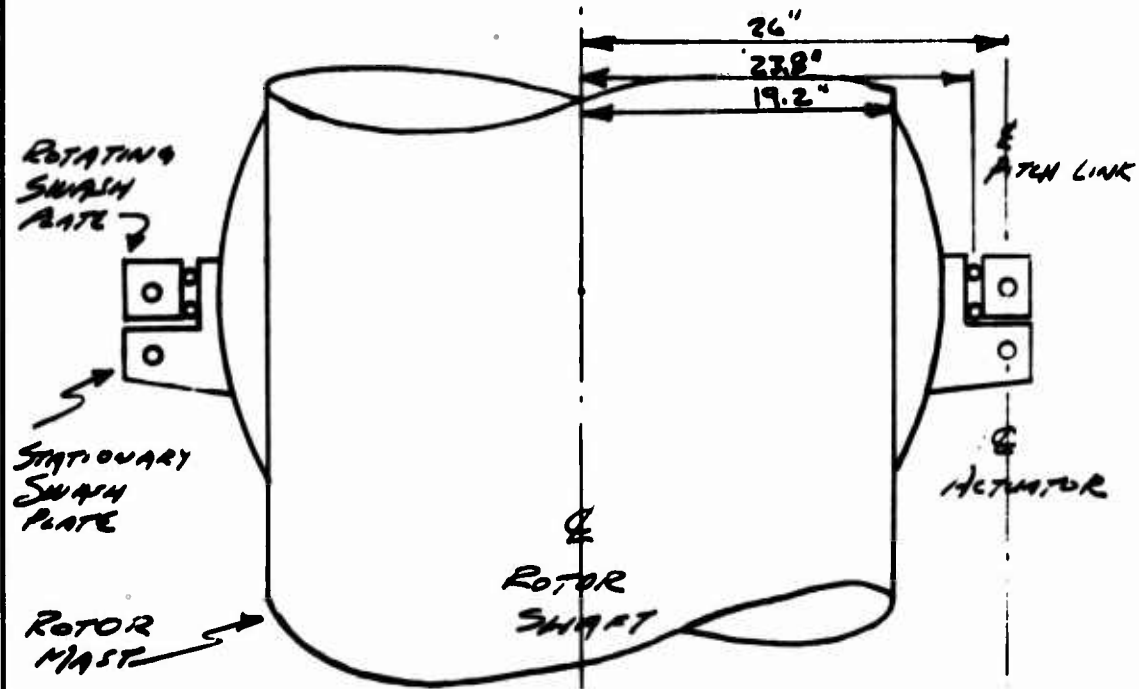
LOAD	FATIGUE	LIMIT
T - Axial Load	4125 ± 4425	30800
M - BEND. MOM.	6650 ± 6650	49700
STRESS	FATIGUE	LIMIT
$T/A = T/1.72 \text{ in}^2$	$2400 \pm 2400 \text{ Psi}$	18000 Psi
$f_s = \frac{MC}{I} = \frac{M(8.16)}{1.72}$	$11800 \pm 11800 \text{ Psi}$	78000 Psi
	$14200 \pm 14200 \text{ Psi}$	96000 Psi

$$^* \text{Follows } f_s = \frac{50000 \pm 25000 \text{ Psi}}{257000 \text{ Psi}}$$

III STRESS ANALYSIS

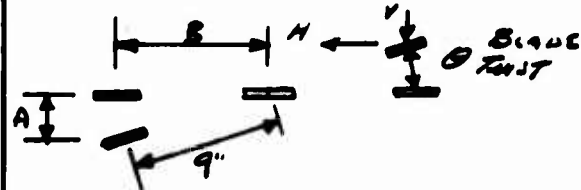
FLIGHT CONTROLS

Ref. Dwg - 395-0936



DISTANCE FROM PITCH ARM TO E FEATHERING BACK = 13"
LENGTH OF PITCH ARM = 17.8"

TORQUE DUE TO BLADE RETENTION STRAP TWIST

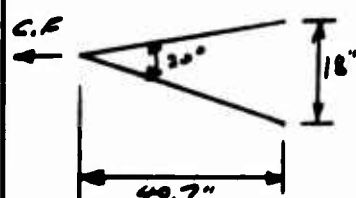


$$\text{TORQUE} = 28V - 294$$

$$A = 9'' \sin \theta \quad B = 9'' \cos \theta$$

$$H = \frac{C.F.}{2} \times \tan 10^\circ \quad V = \frac{C.F.}{2} \cdot \frac{A}{\cos \theta} = \frac{C.F.}{2} \cdot \frac{9 \sin \theta}{\cos \theta}$$

$$\text{TORQUE} = 9'' C.F. \left[\frac{\tan 10^\circ \cos \theta}{40.7} - .1736 \sin \theta \right]$$



	C.F. 1646	L.M.G.T
C.F.	180,000	240,000
G	$\pm 12^\circ$	$(14.7^\circ) \pm 14^\circ$
TORQUE	$114,580'' \text{lb}$	$12,250 \pm 22320$

NOTE: 7° OF PEDESTAL FORWARD IS ONLY IN

0704

IV STRESS ANALYSIS

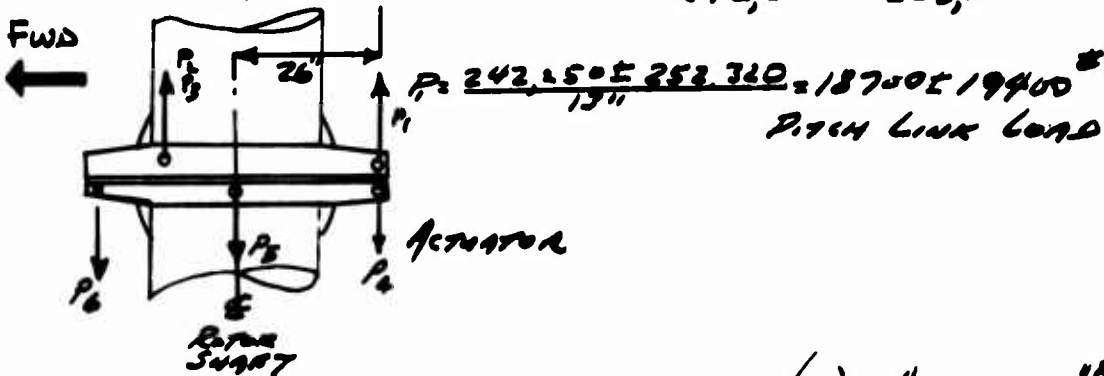
FLIGHT CONTROLS

SWASHPLATE BEARING AND ACTUATOR LOADS

LIMIT MANEUVER CONDITION

$$\text{BENDING TENSION} = M_T = 230,000 \pm 230,000 + M_{\text{TRANS}} \\ \text{AT ROOT}$$

$$M_{T_{\text{ROOT}}} = 230,000 \pm 230,000 + (12,500 \pm 2,320) \\ = 242,750 \pm 252,320 \text{ in-lb}$$



$$\text{Moment to SWASHPLATE} = \pm 19,400 \left(\frac{1}{2}\right) 26'' = 75,700 \text{ in-lb} \quad \text{LIMIT}$$

LONGITUDINAL PITCHING

LOAD TO LONGITUDINAL ACTUATORS P_y, P_c

$$= \frac{18,700 \text{ lb}}{2} + \frac{75,700 \text{ in-lb}}{2 \times 26''} = \left. \begin{array}{l} 42,650 \text{ lb MAX} \\ 1,3550 \text{ in-lb MIN} \end{array} \right\} \text{LIMIT}$$

LOAD TO LATERAL ACTUATOR, $P_5 = 0$

LATERAL PITCHING

LOAD TO LONGITUDINAL ACTUATORS P_y, P_c

$$= \frac{18,700 \text{ lb}}{2} + \frac{75,700 \text{ in-lb}}{2 \times 26''} + 42,650 \text{ lb MAX} \quad \left. \begin{array}{l} \text{MAX} \\ \text{MIN} \end{array} \right\} \text{LIMIT}$$

LOAD TO LATERAL ACTUATOR, P_5

$$= \frac{75,700 \text{ in-lb}}{26''} = 2,9100 \text{ lb either direction}$$

MAGNITUDE THRUST ON SWASHPLATE BEARINGS

$$= 3(18,700 \text{ lb}) = 56,100 \text{ lb LIMIT}$$

IV STRESS ANALYSIS

Flight Controls

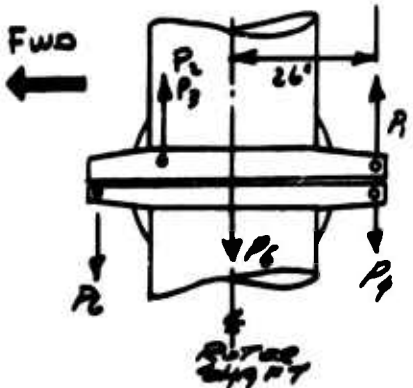
SWASHPLATE BEARING AND ACTUATOR LOADS
FATIGUE CONDITION

$$\text{Bridge Tension} = M_T = 64000 \pm 76000 \text{ ft Straps}$$

$$M_T = 64000 \pm 76000 + (\pm 14580) = 64000 \pm 90580 \text{ in}$$

$$P_t = \frac{64000 \pm 90580}{13''} = 4925 \pm 6970 \text{ lb}$$

PITCH LINK LOAD



$$\text{MOMENT TO SWASHPLATE} \\ = \pm 6970 \text{ lb/in} \times 26'' = 27,000 \text{ in-lb}$$

$$\text{MAX THRUST ON SWASHPLATE} \\ = 3(4925) = 14775 \text{ lb}$$

LONGITUDINAL PITCHING

LOAD TO LONGITUDINAL ACTUATORS, P_4, P_6

$$= \frac{4925^2 \times 3}{2} + \frac{271000}{2 \times 26''} = +12600 \text{ lb Max}$$

LOAD TO LATERAL ACTUATOR, $P_5 = 0$

LATERAL PITCHING

LOAD TO LATERAL ACTUATORS, P_4, P_6

$$= \frac{4925^2 \times 3}{2} + \frac{271000}{2 \times 26''} = +12600 \text{ lb}$$

LOAD TO LATERAL ACTUATOR

$$= \frac{271000}{26''} \approx 10,400 \text{ lb either direction}$$

III STRESS ANALYSIS

Flight Controls

PITCH LINK ANALYSIS - Fatigue Limit = 4925 ± 6970
 LENGTH = 17.8" LIMIT LOAD = $38,100^{\circ}$ LIMIT

$2'' \times .083$, A.C. 4919 P.C. 6784

$\sigma/\sigma = 26$ $F_c = 120,000$ For 150,000 H.T.

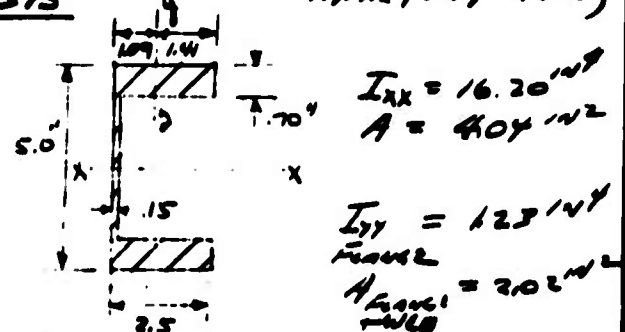
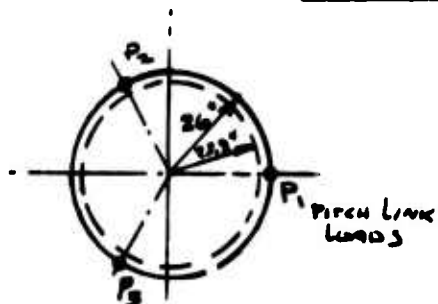
$$f_c = \frac{38,100}{4919} = 7.6200$$

$$M.S. = \frac{120,000}{7.6200 \times 1.5} = +.05$$

$$f_{\text{Fatigue}} = \frac{38,100}{4919} = 7.6200 \text{ psi}$$

FATIGUE ALLOWABLE 0.65 ± 25000 psi

ROTATING SEWING SPATHE (MATERIAL CARPENTER 455 ANALYSIS)



TRAPEZOID CROSS SECTION

CRITICAL LOADS	FATIGUE	LIMIT
M_{xx}	33000 ± 92960	152400
M_{yy} Fatigue	0 ± 7400	20700
Tension	2800 ± 0	10650
Tension only	0 ± 270	750
f_{TOTAL}	5800 ± 24190 psi	53670 psi
FOLLOWUP	± 25000 psi	237000 psi
M.S. =	$\pm .03$	± 2.10

IV Stress Analysis

Flight Controls

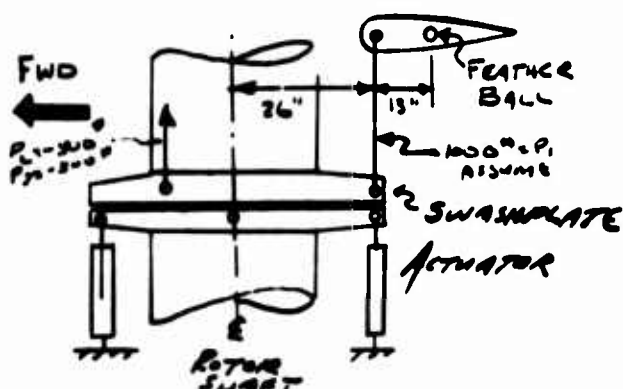
CONTROL SYSTEM STIFFNESS

ASSUMPTIONS

1. - SWASHPLATE IS RIGID

2. - USE FOR ACTUATOR DEFLECTION

$1.145 \times 10^{-5} \frac{\text{rad}}{\text{N}}$ FROM XV-9A HELICOPTER



$$M = 1000^2 (15 \times 26) = 39000^{\text{in-lb}}$$

$$\text{ACTUATOR LOAD} = \frac{39000}{5.82} = 750^{\text{lb}}$$

REF CAC 395-08C

$$\gamma_1 = \frac{\pi PL^2}{2AE} \text{ FOR PITCH LINES} = \frac{(500 \times 10^{-6})^2}{2(50/10^6) 30 \times 10^6} = .900^{\text{ in/in}}$$

$$\gamma_1 \text{ FOR SWASHPLATE ASSUMED} = 0$$

$$\gamma_1 \text{ FOR ACTUATORS} = \frac{Pd}{2} = 2 \left[\frac{750}{2} (750 \times 1.145 \times 10^{-5}) \right] = 4.90^{\text{ in/in}}$$

$$\underline{\underline{M}} = \underline{\underline{\Sigma}} \gamma_1 \quad \underline{\underline{39000}} \theta = 5.82 \quad \theta = 3.0 \cdot 10^4 \text{ RADIAN}$$

$$\frac{\text{IN. L OF}}{\text{BLADE ROOT TORQUE}} = \frac{1000^2 \times 13}{30 \times 10^6 \text{ RADIAN} \times \frac{26}{13}} = 2.17 \times 10^7$$

NOTE - VALUE OF STIFFNESS USED IN DYNAMIC ANALYSIS IS $.376 \times 10^7 \text{ Nm BLADE TORQUE/DEGREE OF BLADE DEFLECTION}$

III STRESS ANALYSIS

FLIGHT CONTROLS

SWASHPLATE BEARINGS

PAPERNO 1 - "BALL & ROLLER BEARING ENGINEERING"

By ARVID PALMGREN

LIFE BASED ON FATIGUE LOADING (REF. LOADS SECTION)

$$F_a = 14,775 \text{ lb} \quad F_R = 6,570 \text{ lb}$$

$$\text{Equiv. Load } P = .5F_R + .478F_a \\ = 3,285 + 7,388 = 10,673 \text{ lb}$$

$$\text{SPECIFIC CAPACITY } C = f_c \frac{D_{ar}^2 i E^{3/8} \cos \kappa}{1 + .02 D_{ar}}$$

$$f_c = 4.5 \\ i = 1.0 \\ D_{ar} = \frac{1}{2} (12.7\%)$$

$$\kappa = 40^\circ \\ E = 234$$

$$C = \frac{4.5 \times 161.29 \times 224^{3/8} \times .766}{1 + .254}$$

$$= 16,350 \text{ kg. (36,050 lb.)}$$

$$\therefore L = \left(\frac{36,050}{10,673} \right)^3 \times 10^6 = 38,545,966 \text{ cycles.}$$

$$N = 143 \text{ RPM} = 8580 \text{ revs/hr.}$$

$$\therefore B_{10} \text{ LIFE IN Hours} = \frac{38,545,966}{8580} = \underline{\underline{4403 \text{ hours}}}$$

VI STRESS ANALYSIS

HOT GAS DUCTING (REF-DUC 395-0909)

Duct material is Rene' 41

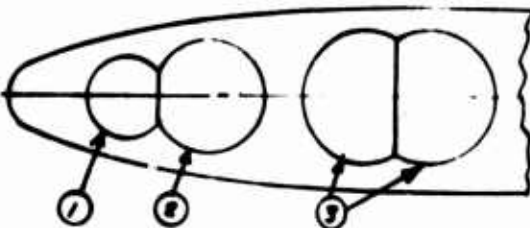
Strength Allowables

$F_{u4} = 150,000 \text{ Psi}$ @ 1395°F Peak Temperature

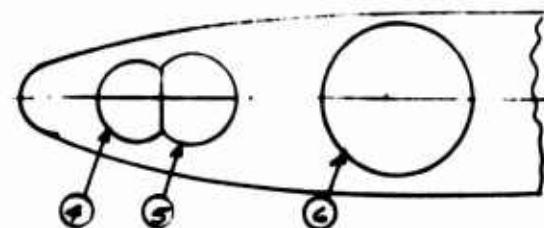
$E_t = 25.3 \times 10^6 \text{ Psi}$

$F_{c, 2\% \text{ Cyclic}} = 38000 \text{ Psi}$ @ 260°F EQUIVALENT
TEMPERATURE FOR 3600 HRS

Duct Dimensions in the blade



BLADE SECTION
OUTBOARD OR .75% R



BLADE SECTION
INBOARD OR .75% R

DUCT	DIA METER IN.	ENCLOSED DUCT AREA IN. ²	PERIMETER OF Duct IN.	THICKNESS OF Duct IN.	f_c @ SWEAT PRESS FLIN. ²	f_c @ 3600 HR OPERATION % ³
①	5.13	19.39	15.84	.007	29300	12850
②	6.46	31.85	20.14	.007	36800	16150
③	6.72	25.80	20.3	.007	38300	16800
④	6.91	23.77	19.3	.007	39800	17050
⑤	8.26	45.95	24.7	.007	47000	20700
⑥	9.30	67.93	29.22	.007	53000	23700

$$f_c @ \text{Outer Rad.} = \frac{P(1.5R)}{t} = \frac{39.6 \text{ Psi} \times 1.5 \times 1.5 \text{ R}}{.007} = 11,382 \text{ Psi}^3$$

$$f_c @ 3600 \text{ Hrs. } (.2\% \text{ Cyclic Cycles}) = \frac{PR}{t} = \frac{35 \text{ Psi}}{.007} = 5.00 \text{ R} \times 10^3$$

III STRESS ANALYSIS

HOT GAS DUCTING

BLADE DUCTS MUST WITHSTAND AN INTERNAL SPSE NEGATIVE PRESSURE. THEREFORE EXTERNAL STIRRING RINGS MUST BE ADDED.

$$\delta' = .807 \frac{EI^2}{L^3} \sqrt{\left(\frac{1}{1-\nu^2}\right)^2 \frac{t^2}{L^2}}$$

REF. FORMULAS
FOR STRESS AND
STRAIN BY POOLE
TABLE III - Q - 81

δ' = SPSE = ELASTIC BUCKLING LWT PRESS.
 L = RING STIFFENER SPACING - INCHES

Duct → ① ② ③ ④ ⑤ ⑥

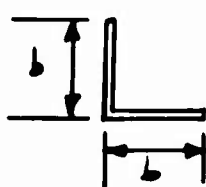
L → 4.4 3.1 2.9 2.9 2.25 1.80

EXAMPLE OF RING STIFFENER REQUIRED FOR
DUCT ①

$$\delta' = \frac{SEI}{L^3} \quad \delta' = SPSE \times L = 2.20^4 \text{ in}$$

$$I = \frac{(2.20)(2.17)^3}{3(25.3 \times 10^6)} = .493 \times 10^{-6}$$

REF. FORMULAS
FOR STRESS AND
STRAIN BY POOLE
TABLE III - 12



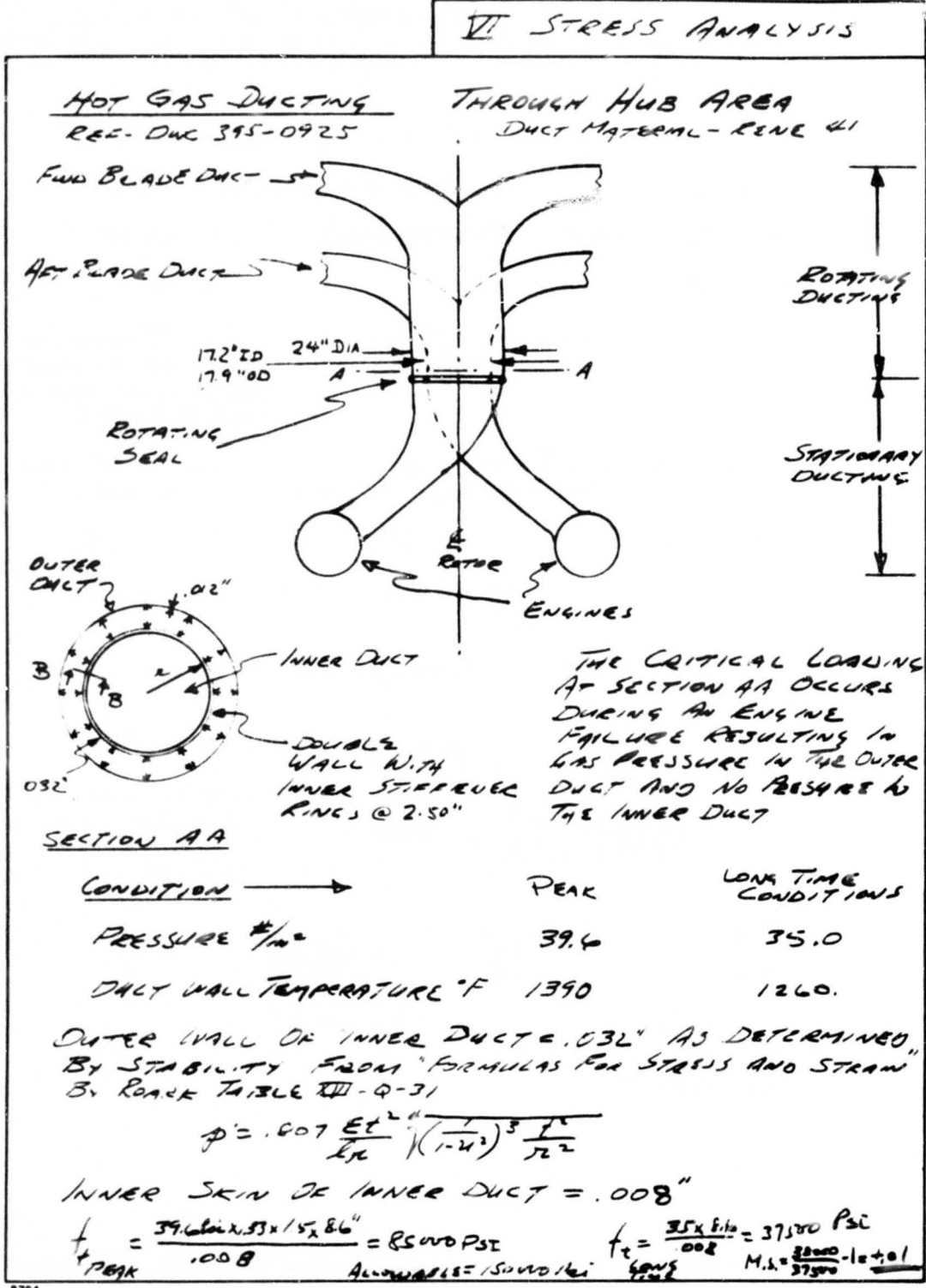
$$I = \frac{b^2 + b^3}{24}$$

$$b = \left(\frac{24I}{SE} \right)^{1/3}$$

$$b = .07"$$

RING STIFFENER
CROSS SECTION

VII STRESS ANALYSIS



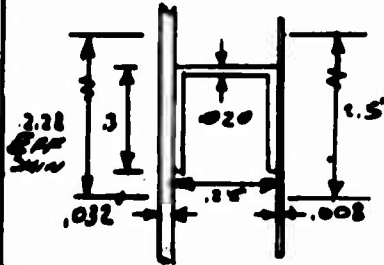
III Stress Analysis

Hot Gas Ducting Through Pipe Area

STIFFENER RING REQUIRED IN INNER DUCT

$$I_{\text{req}} = \frac{\pi r^3}{3E} \quad \text{Ref "Formulas for Stress and Strength" by Rankin Table III-12}$$

$$I = \frac{\pi r^3 (8.7)}{3(25.3 \times 10^6)} = .912 \times 10^{-3} \quad r = 37.6 \text{ mm} \times 2\frac{1}{2}'' = 91 \text{ mm}$$



$$I_{\text{available}} = .92 \times 10^{-3}$$

Outer Duct Wall Thickness

$$t = .012'' \quad \text{Ref 41}$$

$$\sigma_{\text{peak}} = \frac{39.6 B \epsilon}{.012} = 1530 \text{ psi}$$

$$= 79000 \text{ psi}$$

$$\sigma_{\text{long}} = \frac{36 B \epsilon L / 2}{.012} = 35000 \text{ psi}$$

$$M.S. = \frac{35000}{35000} = 1 \pm .08$$

SECTION 3-5

CROSS SECTION
OF INNER
STIFFENER Duct

Note - Sandwhich construction
would show a lighter
weight for the inner duct
wall.

Duct Bellows

Ref. DUC 395-0909

$$\text{MATERIAL Ref 41} \\ \alpha = 8.2 \times 10^{-6} \text{ in/in}^{\circ}\text{F} \quad E = 25.3 \times 10^6 \text{ psi}$$

Duct Wall Long Time Temp. = 1260°F
Duct Length = 20'

$$\Delta = \alpha(L) \epsilon = (1260-70)(20)8.2 \times 10^{-6} = .1950''$$

USE .040 ± .050 FOR BELLW WALL THICKNESS
NEGLIGE α THIS RELIEVES THERMAL STRAIN
 $I = 28.8 \times 10^{-9}$ LENGTH OF BELLW = $2\frac{1}{2}$ '

$$\text{Bellows} = \frac{.1950}{2\frac{1}{2}/10} = .00514$$

$$\Delta = \frac{P(l)^2}{16E} + \frac{P(l)l^2}{2EI}$$

$$.00514 = 1.582 \times 10^{-3} P$$

$$P = 3.75$$

$$M = \frac{P l}{8} = .200 \text{ in}^2 \quad \frac{M + P}{S} = \frac{.200}{8.15 \times 10^{-6} + \frac{.2}{.00514}} = 250000 \text{ psi}$$

$$M.S. = \frac{250000}{35000} = 7.14$$

STRESS ANALYSIS

Ogs Duct - Blade Mounting

Ref. Date 3/28/09/19

25% C



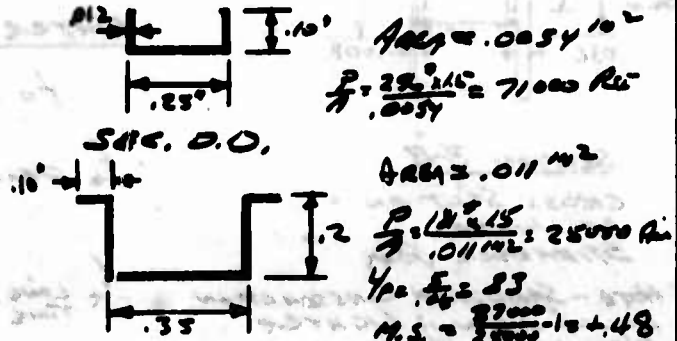
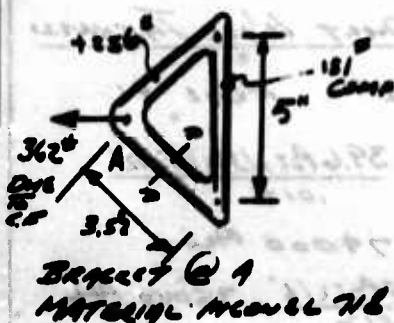
WEIGHT OF DUCT

$$(15.84 \times 20.4) / 1000 \times 20 \times 0.298 = 1.49 \text{ lb}$$

NET TURBINE WEIGHT @ 840 f.p.s. TWO SPANS

$$= 486 \text{ lbs } \text{ OVER-RUN} \text{ condition}$$

$$\text{LOAD AT PROJECTION A} = 1.49 \text{ lb} / \text{ft} \times 12 \text{ ft} = 18.1 \text{ Lb/ft}$$



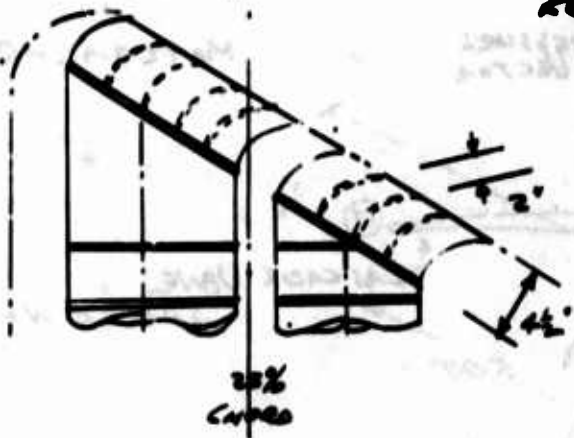
$$\text{LOAD AT ATTACHMENT B OR C} = 1.49 \text{ lb / ft} \times 12 \text{ ft} = 18.1 \text{ Lb/ft}$$

No analysis shows the loads are less.

CONTINUE

II STRESS ANALYSIS

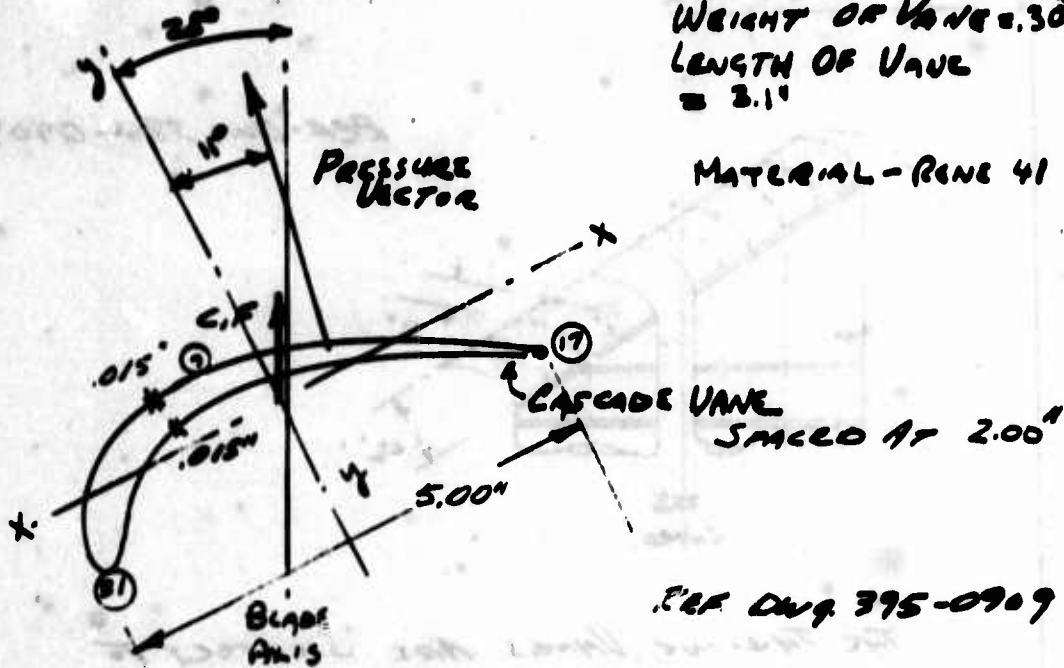
TURBINE



THE TURBINE VINES ARE SUBJECT TO
GAS PRESSURE AND CENTERLINE
LOAD. SINCE THE PERMISSIVE STRESS
FOR PEAK CONDITIONS IS 150,000 PSI
VS. 58,000 PSI FOR 3600 HOUR OPERATION.
THE ANALYSIS IS MADE FOR LONG TIME
OPERATION ONLY.

ST Stress Analysis

770 Gas Cane



CHECK FOR LONG TIME CONDITIONS

$$P = 35 \text{ psi} \quad \gamma = 315 \text{ @ } 675 \text{ F.P.S.}$$

$$C.F. = .30 \times 315 = 94.5 \text{ lb/vane}$$

$$\text{Axial load on vane} = 35 \text{ psi} / 2'' \times 5'' = 350$$

$$f_7 = \frac{M_{xx}}{Z_{xx}} + \frac{P}{A} = \frac{12900}{0.137} + \frac{350}{.30} = 13970 \text{ psi}$$

$$f_{31} = \frac{M_{xx}}{Z_{xx}} + \frac{M_{yy}}{Z_{yy}} - \frac{P}{A} = \frac{174}{.011} + \frac{61}{.050} + \frac{350}{.30} = 18020 \text{ psi}$$

$$f_{19} = \frac{M_{xx}}{Z_{xx}} - \frac{M_{yy}}{Z_{yy}} + \frac{P}{A} = \frac{174}{.011} - \frac{51}{.050} + \frac{350}{.30} = 15920$$

$$F.O. 2\% \text{ stress } 38000 \text{ psi } \text{ allowed } \text{ for } 3600 \text{ hours } M.S. = \frac{38000}{18020} - 1 = +110$$

0704

APPENDIX III
ROTOR BLADE EQUATIONS

NON-BENDING WEIGHT EQUATIONS - TIP SECTION

$$(53) \quad \bar{P}_{W_{BL}} = D_1 \left(\frac{\bar{Z}_L}{.528} \right)^{m_1} \left(\frac{\bar{E}_L}{.18} \right)^{m_2} \quad \bar{C} = .830 \left(\frac{\bar{Z}_L}{.528} \right)$$

$$D_2 = D_2 C^{m_3} \left(\frac{\bar{Z}_L}{.528} \right)^{m_3} \left(\frac{\bar{E}_L}{.18} \right)^{m_4}$$

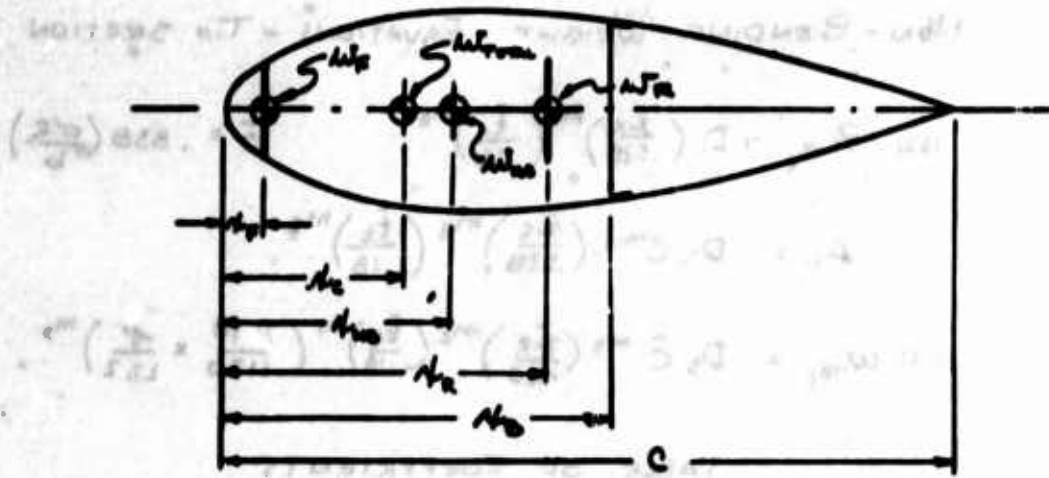
$$(54) \quad W_{W_{BL}} = D_3 \bar{C}^{m_3} \left(\frac{\bar{Z}_L}{.528} \right)^{m_3} \left(\frac{\bar{E}_L}{.18} \right)^{m_4} \left(\frac{T-70}{1180} \times \frac{1}{L^2} \right)^{m_5}$$

TABLE OF COEFFICIENTS

BLADE COEFF	XV-9A DUCTS	FIG. 'B' TWO SPAR	FIG. 'B' ONE SPAR
D ₁	.265	.236	.422
D ₂	106	98	215" 200"
D ₃	1.26	1.43	1.38
m ₁	- .31	0	.46
m ₂	2.1	2.0	2.0
m ₃	.85	0	1.20
m ₄	.95	1.0	1.69" 1.0**
m ₅	1.2	1.2	1.2
m ₆	1.34	0	.47
m ₇	.17	.35	.35
m ₈	0	0	0
m ₉	.2	0	0

* .14 ≤ t ≤ .16 ** .16 ≤ t ≤ .18

BLADE BALANCE EQUATIONS



$$w_F n_F + w_R n_R + w_{N0} n_{N0} = w_T n_C$$

$$w_F (n_F - n_C) + w_R (n_R - n_C) + w_{N0} (n_{N0} - n_C) = 0$$

$$w_R = -w_F \left(\frac{n_F - n_C}{n_R - n_C} \right) - w_{N0} \left(\frac{n_{N0} - n_C}{n_R - n_C} \right)$$

$$K_2 = \frac{n_C - n_F}{n_R - n_C}$$

$$K_3 = w_{N0} \left(\frac{n_{N0} - n_C}{n_R - n_C} \right)$$

$$w_R = K_2 w_F - K_3$$

$$w_F = \frac{w_R + K_2}{K_2}$$

$$w_T = w_F + w_R + w_{N0} = w_F (1 + K_2) - K_3 + w_{N0}$$

$$= w_R \left(\frac{1 + K_2}{K_2} \right) + \frac{K_3}{K_2} + w_{N0}$$

$$(55) \quad \bar{W}_{R_2} = \frac{S}{F_{TU}} \left\{ 1.10 V_T^2 \left[\bar{W}_{ca} \left(\frac{\bar{A}_{ca} - \bar{A}_p}{\bar{A}_a \cdot \bar{A}_p} \right) + \bar{W}_c \left(\frac{\bar{A}_c - \bar{A}_p}{\bar{A}_a \cdot \bar{A}_p} \right) \right] + p \cdot A_0 \right\}$$

$$K_{2t} = \frac{\bar{A}_{ca} - \bar{A}_p}{\bar{A}_a - \bar{A}_{ca}}$$

$$K_{4t} = 1 + K_{2t}$$

$$K_{3t} = \bar{W}_{nc_2} \frac{(\bar{A}_{nc_2} - \bar{A}_{ca})}{(\bar{A}_a - \bar{A}_{ca})}$$

$$(56) \quad \bar{W}_{F_t} = \frac{\bar{W}_{R_2} + K_{3t}}{K_{2t}}$$

$$\bar{W}_{T_t} = \bar{W}_{R_2} + \bar{W}_{F_t} + \bar{W}_{nc_2}$$

$$\bar{A}_{nc_2} = \frac{\bar{A}_p + \bar{A}_a}{2}$$

$$\bar{A}'_{nc_2} = \bar{A}_a$$

$$\Delta \bar{W}_{nc_2} = .257 C (\bar{A}_{nc_2} - \bar{A}'_{nc_2}) (\bar{A}_a - \bar{A}_p) \quad \Delta \bar{W}'_{nc_2} = .022 C (\bar{A}_{nc_2} - \bar{A}'_{nc_2})$$

$$(57) \quad \bar{W}_{nc_2} = \bar{W}_{nc_2} \left(\frac{\bar{A}_2}{\bar{A}_c} \right)^{m_1} + \Delta \bar{W}_{nc_2} + \Delta \bar{W}'_{nc_2}$$

$$(58) \quad \bar{A}_{nc_2} = \frac{\bar{W}_{nc_2} \bar{A}'_{nc_2} \left(\frac{\bar{A}_2}{\bar{A}_c} \right)^{m_1 + m_2} + \Delta \bar{W}_{nc_2} \bar{A}'_{nc_2} + \Delta \bar{W}'_{nc_2} \bar{A}'_{nc_2}}{\bar{W}_{nc_2}}$$

SPARS AT STATION 2 ARE DESIGNED BY

FATIGUE LOADS. AN INITIAL ESTIMATE FOR

DETERMINING CORIOLUS MOMENT COMPONENT IS

MADE AS FOLLOWS:

$$(w_{T_2})_c = 3.275 \cdot \delta \cdot \bar{I}_n + w_{F_1} + w_{W_2}$$

$$(\bar{M}_2)_c = \bar{d}_2^2 \left[\frac{w_{T_2}}{\bar{L}} + \frac{(w_{T_2})_c}{\bar{L}} \right] + \frac{\bar{W}_2}{\bar{N}_2} (\bar{N}_2 - \bar{L}_2)$$

$$(\bar{W}_{2_2})_c = \frac{\bar{d}_2}{2} \left[w_{T_2} + (w_{T_2})_c \right] + \frac{\bar{W}_2}{\bar{N}_2}$$

$$(\bar{M}_{t_2})_c = (\bar{M}_2)_c + (\bar{W}_{2_2})_c (\bar{L}_2 + \bar{e}_t)$$

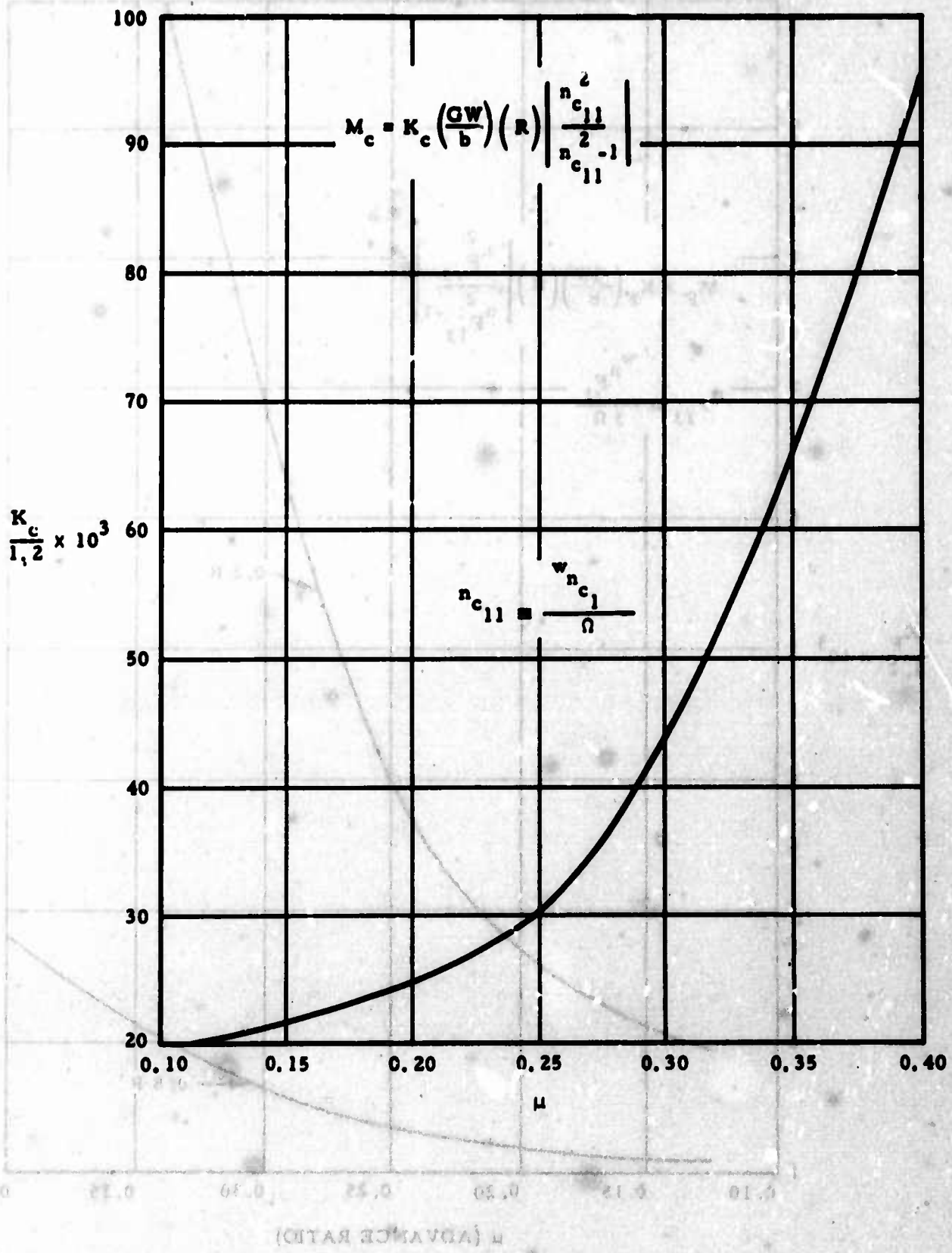
$$(I_{t_2})_c = \frac{1}{3} \left\{ w_{T_2} [1 - (\bar{L}_2 + \bar{e}_t)^2] + \left(\frac{(w_{T_2})_c - w_{T_2}}{4 \bar{d}_2} \right) \left[1 - (\bar{L}_2 + \bar{e}_t)^2 \right. \right. \\ \left. \left. [4 - 3(\bar{L}_2 + \bar{e}_t)] \right] \right\} + 3 \bar{W}_2 \bar{N}_2'$$

$$(M_{cor_2})_c = \frac{3 \lambda (N_2 - e_t) \left(\frac{W}{L} \right) \left(\frac{1}{\bar{L}} \right) (a)}{\left(w_{T_2} \right)_c \left(\frac{V_r^2}{2.68} \right) (1 + e_t) (\bar{L})} \left\{ \frac{(\bar{I}_{t_2})_c (\bar{L}_2 + 2\bar{e}_t) (\bar{M}_{t_2})_c + (\bar{W}_{2_2})_c (\bar{L}_2 + e_t) \bar{e}_t}{\left(w_{T_2} \right)_c (\bar{L})^2 \left(\frac{2+e_t}{c} \right)} \right\}$$

(59) First Approximation

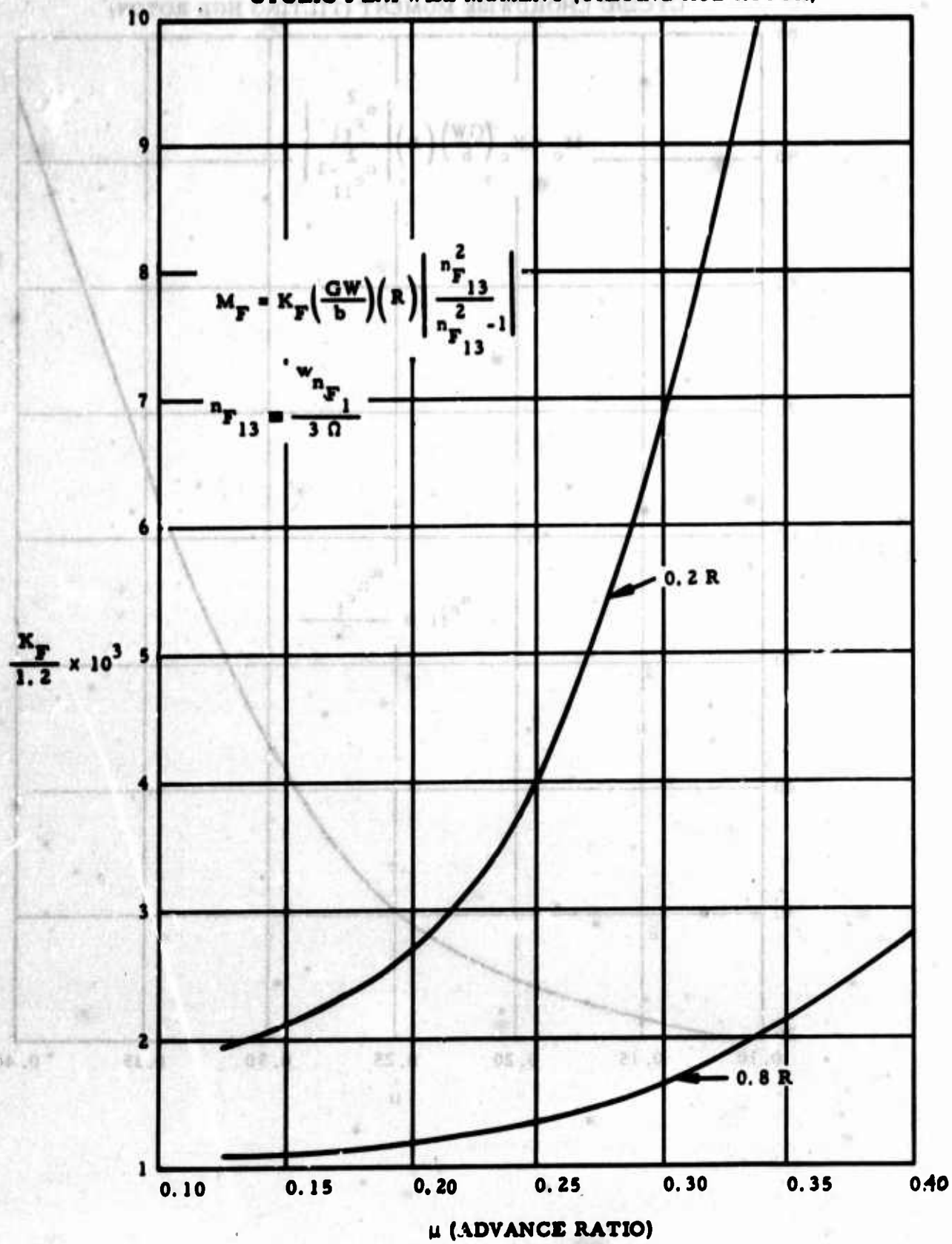
$$\left\{ \begin{array}{l} M_{C_2} = [K_{C_2} + (\bar{M}_{cor_2})_c] \left(\frac{W}{L} \right) (R) (29.4) \\ M_{F_2} = K_{F_2} \left(\frac{W}{L} \right) (R) (36.0) \\ M_{F_2} = K_{F_2} \left(\frac{W}{L} \right)^2 \left(\frac{P_e}{39.1} \right)^2 \left(\frac{w_{F_2} K_{A_2} - K_{S_2}}{w_{T_2}} \right) \left(\frac{W}{L} \right) (R) (36.0) \\ M_{C_2} = \frac{1090}{W} R^{6.4} \left(\frac{W}{L} \right)^{2.4} \left(\frac{d_2}{L + d_2} \right) \end{array} \right\} \begin{array}{l} \text{(TILTING HUB)} \\ \text{ROTOR} \\ \text{(ARTICULATED)} \\ \text{ROTOR} \end{array}$$

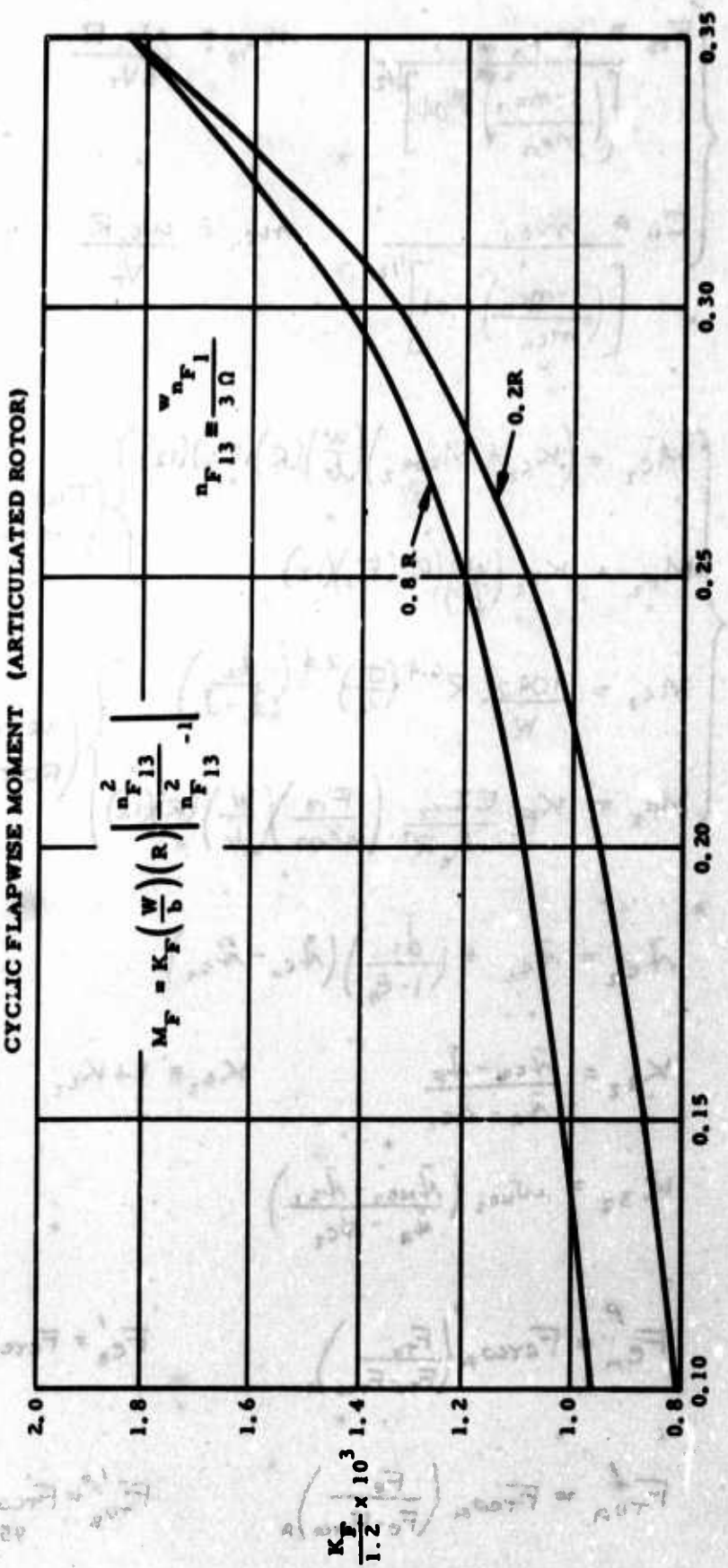
CYCLIC CHORDWISE MOMENT (TILTING HUB ROTOR)



(ОТТАЯ ГОДИНА) μ

CYCLOIC FLAPWISE MOMENT (TILTING HUB ROTOR)





$$(59a) \quad \left\{ \begin{array}{l} F_{13} = \frac{m_{F_{13}}}{\left[\left(\frac{1-m_{F_{13}}}{m_{F_{13}}} \right)^2 + .04 \right]^{1/2}} \\ C_{11} = \frac{m_{C_{11}}}{\left[\left(\frac{1-m_{C_{11}}}{m_{C_{11}}} \right)^2 + .04 \right]^{1/2}} \end{array} \right. \quad \begin{array}{l} m_{F_{13}} = \frac{\omega_{F_1} R}{3\sqrt{r}} \\ m_{C_{11}} = \frac{\omega_{C_1} R}{\sqrt{r}} \end{array} \quad c/c_e = \xi_2 = .10$$

$$(59b) \quad \text{TRANSVERSE} \quad \left\{ \begin{array}{l} M_{C_2} = \left(K_{C_2} + M_{Coz_2} \right) \left(\frac{W}{L} \right) (R)(C_{..})(12) \\ M_{F_2} = K_{F_2} \left(\frac{W}{L} \right) (R)(F_{13})(12) \\ M_{C_2} = \frac{1090}{W} R^{6.4} \left(\frac{G}{L} \right)^{2.4} \left(\frac{d_c}{d_1 + d_2} \right) \\ M_{F_2} = K_{F_2} \frac{EIx_2}{M_{T_e} R^2} \left(\frac{F_{13}}{4500} \right) \left(\frac{W}{L} \right) (R)(12) \end{array} \right\} \quad \begin{array}{l} (\text{TILT HUB}) \\ (\text{ROTOR}) \\ (\text{ARTICULATED}) \\ (\text{ROTOR}) \end{array}$$

$$\bar{\alpha}_{C_2} = \bar{\alpha}_{C_1} + \left(\frac{d_1}{1-\xi_2} \right) (\bar{\alpha}_{C_0} - \bar{\alpha}_{C_1})$$

$$K_{22} = \frac{\bar{\alpha}_{C_2} - \bar{\alpha}_P}{\bar{\alpha}_e - \bar{\alpha}_{C_2}} \quad K_{42} = 1 + K_{22}$$

$$K_{32} = \mu \bar{\alpha}_{H_2} \left(\frac{\bar{\alpha}_{H_2} - \bar{\alpha}_{C_2}}{\bar{\alpha}_e - \bar{\alpha}_{C_2}} \right)$$

$$F_{C_n}' = F_{Cnco_n} \left(\frac{F_{Tn}}{F_{Tu} - F_{Cnco_n}} \right)_n$$

$$F_{C_0}' = F_{C0co_0} \left(\frac{F_{Tu}}{F_{Tu} - F_{C0co_0}} \right)_0$$

$$F_{Tu_n}' = F_{Tuco_n} \left(\frac{F_e}{F_e - F_{Tuco_n}} \right)_n$$

$$F_{Tu_0}' = F_{Tuco_0} \left(\frac{F_e}{F_e - F_{Tuco_0}} \right)_0$$

$$a_1 = \frac{\sigma V_T^2}{2.61} \left\{ (d_1) \left[\omega_{k_1} \left(\frac{1}{2} - \frac{d_1}{L} \right) + (\omega_{m_1} - K_{31}) \left(\frac{1}{2} - \frac{d_1}{L} \right) \right] + \bar{w}_1 \right\}$$

$$a_2 = \frac{\sigma V_T^2}{2.61} d_1 K_{31} \left(\frac{1}{2} - \frac{d_1}{L} \right)$$

$$a_3 = -K_{32}$$

$$a_4 = K_{42}$$

$$a_5 = M_{F_2} \bar{k}_p \left(\frac{S}{2} \right)$$

$$a_6 = a_5 \bar{\rho}_p^2 \bar{\epsilon} (4s)$$

$$a_7 = 4s (\bar{\rho}_p^2 + K_{22} \bar{\rho}_p^2) (\bar{\epsilon})$$

$$a_8 = \frac{M_{C_2} S}{4s \bar{\epsilon} (\bar{\rho}_p - \bar{\rho}_p)}$$

$$a_9 = a_8 \left(\frac{i_E}{\bar{x}_p} \right)$$

$$a_{10} = K_{22}$$

$$A_1 = k_0 a_4 a_7 - k_1 a_7 \\ \{ (k_0 + k_1) (a_4 + a_7) + (k_0 - k_1) (a_4 - a_7) \} \frac{\partial^2 V}{\partial x^2} = 0$$

$$A_2 = k_0 (a_3 a_6 + a_4 a_5) - k_1 a_7 - k_2 a_6 - a_3 a_8 - a_4 a_9$$

$$A_3 = k_0 a_3 a_6 - k_1 a_6 - a_3 a_8 - a_4 (a_3 a_7 + a_4 a_6)$$

$$A_4 = -a_3 a_4 a_7$$

$$A_5 = k_0 a_{10} a_4 a_7 - k_1 a_7 a_{10} = k_1 a_{10}$$

$$A_6 = k_0 (a_3 a_4 a_7 + a_3 a_7 a_{10} + a_4 a_6 a_{10}) - k_1 a_7 a_{10} - k_2 a_6 a_{10} - k_3 a_4 a_7 \\ - a_4 a_9 a_{10} - a_5 a_8 a_9$$

$$A_7 = k_0 a_3 (a_4 a_{10} + a_3 a_7 + a_4 a_6) - k_1 a_6 a_{10} - k_2 a_7 a_6 - k_3 a_4 a_6 \\ - a_9 (a_3 a_{10} + a_3 a_7) - a_8 (a_3 a_7 + a_4 a_6)$$

$$A_8 = k_0 a_3^2 a_6 - k_1 a_3 a_6 - a_3^2 a_9 - a_3 a_6 a_8 = a_3^2 (k_0 a_6 - a_9) - a_3 a_6 (k_1 + a_8)$$

$$A_9 = k_3 a_4 - k_5$$

$$A_{10} = k_3 a_3 - k_4 - a_4 a_5$$

$$A_{11} = -a_3 a_5$$

$$A_{12} = k_3 a_4 a_{10} - k_5 a_{10}$$

$$A_{13} = k_3 a_3 (a_4 + a_{10}) - k_4 a_{10} - k_5 a_3 - a_4 a_5$$

$$A_{14} = k_3 a_3^2 - k_4 a_3 - a_3 a_5$$

$$k_0 = F_{c_A}$$

$$k_1 = a_1 \frac{F_{c_A}}{F'_{TU_A}}$$

$$k_2 = a_2 \frac{F_{c_A}}{F'_{TU_A}}$$

$$k_3 = F_{c_B}$$

$$k_4 = a_1 \frac{F_{c_B}}{F'_{TU_B}}$$

$$k_5 = a_2 \frac{F_{c_B}}{F'_{TU_B}}$$

$$k'_0 = F_{c'_A}$$

$$k'_1 = a_1 \frac{F_{c'_A}}{F'_{TU_A}}$$

$$k'_2 = a_2 \frac{F_{c'_A}}{F'_{TU_A}}$$

$$k'_3 = F_{c'_B}$$

$$k'_4 = a_1 \frac{F_{c'_B}}{F'_{TU_B}}$$

$$k'_5 = a_2 \frac{F_{c'_B}}{F'_{TU_B}}$$

$$\left\{ \begin{array}{l} \triangleright (\omega_{F_2})_a^3 (A_1) + (\omega_{F_2})_a^2 (A_2) + (\omega_{F_2})_a (A_3) + A_4 = 0 \\ (\omega_{F_2}')_a^3 (A'_1) + (\omega_{F_2}')_a^2 (A'_2) + (\omega_{F_2}')_a (A'_3) + A'_4 = 0 \\ \triangleright (\omega_{F_2})_b^3 (A_5) + (\omega_{F_2})_b^2 (A_6) + (\omega_{F_2})_b (A_7) + A_8 = 0 \\ (\omega_{F_2}')_b^3 (A'_5) + (\omega_{F_2}')_b^2 (A'_6) + (\omega_{F_2}')_b (A'_7) + A'_8 = 0 \\ \triangleright (\omega_{F_2})_c^2 (A_9) + (\omega_{F_2})_c (A_{10}) + A_{11} = 0 \\ (\omega_{F_2}')_c^2 (A'_9) + (\omega_{F_2}')_c (A'_{10}) + A'_{11} = 0 \\ \triangleright (\omega_{F_2})_d^2 (A_{12}) + (\omega_{F_2})_d (A_{13}) + A_{14} = 0 \\ (\omega_{F_2}')_d^2 (A'_{12}) + (\omega_{F_2}')_d (A'_{13}) + A'_{14} = 0 \end{array} \right.$$

$$f_{cr_2} = \frac{a_1 + a_2 \omega_{F_2}}{a_3 + a_4 \omega_{F_2}}$$

\triangleright If $f_{cr_2} > F_{rco}$, use primed equations.
Use largest value of $(\omega_{F_2})_{a,b,c,d}, (\omega_{F_2}')_{a,b,c,d}, \omega_{F_2}$

$$(61) \quad \bar{w}_{T_2} = K_{4_2} w_{F_2} - K_{3_2} + w_{NO_2}$$

$$\bar{w}'_{T_2} = K_{4_2} w_{F_2} - K_{3_2} + w'_{NO_2}$$

$$\Delta w_{NO_2} = .287 \bar{c} (\bar{t}_{NO_2} - \bar{t}_{NO_2}) (\bar{n}_o - \bar{n}_p)$$

$$\Delta w'_{NO_2} = .022 \bar{c} (\bar{t}_{NO_2} - \bar{t}_{NO_2}) (\frac{\bar{t}_s}{.19})$$

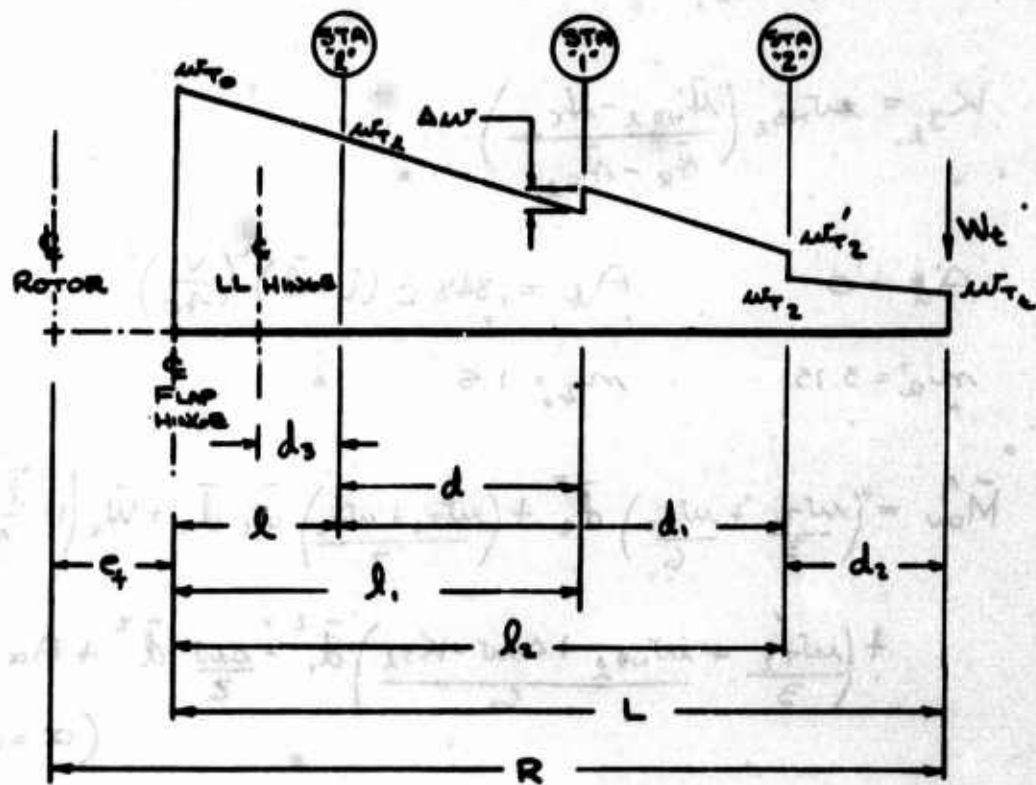
$$(62) \quad \begin{aligned} \text{RATIO T.E.} \\ \left\{ \begin{array}{l} w_{NO_2} = D_4 \bar{c}^{m_3} \left(\frac{\bar{n}_p}{.528} \right)^{m_{10}} \left(\frac{\bar{t}_s}{.19} \right)^{m_n} \left(\frac{T-70}{1130} \times \frac{P}{27.2} \right)^{m_9} + \Delta w_{NO_2} + \Delta w'_{NO_2} \\ \bar{n}_{NO_2} = \frac{(w_{NO_2} - \Delta w_{NO_2} - \Delta w'_{NO_2}) (D_5) \left(\frac{\bar{t}_s}{.528} \right)^{m_{12}} + \Delta w_{NO_2} \bar{n}_{NO_2} + \Delta w'_{NO_2} \bar{n}'_{NO_2}}{w_{NO_2}} \end{array} \right. \end{aligned}$$

$$(63) \quad \begin{aligned} \text{RATIO T.E.} \\ \left\{ \begin{array}{l} w_{NO_2} = w_{NO_2} + \Delta w_{NO_2} + \Delta w'_{NO_2} \\ \bar{n}_{NO_2} = \frac{w_{NO_2} \bar{n}_{NO_2} + \Delta w_{NO_2} \bar{n}_{NO_2} + \Delta w'_{NO_2} \bar{n}'_{NO_2}}{w_{NO_2}} \end{array} \right. \end{aligned}$$

TABLE OF COEFFICIENTS

BLADE COEF.	XV-9A DUCTS	FIG. "8" TWO SPAR	FIG. "8" ONE SPAR
D ₄	.958	.96	1.28
D ₅	.286	.298	.361
m ₁₀	.45	0	.47
m _n	.44	.35	.35
m ₁₂	.64	0	.46

SPANWISE WEIGHT DISTRIBUTION



$$(\frac{d}{dx})^m \left(x^{n_1} \frac{dy}{dx} + y \right) = x^{n_1} M(x,y) = 0. \quad (20)$$

$$\Rightarrow T_{\text{min}} = \left(\frac{1}{2} \omega_0^2 N + \frac{\omega_0^2}{4} \right) \left(\frac{4}{3} \pi^2 \right)^{1/2}$$

$$\sin x + \cos x = \sqrt{2} \sin(x + \frac{\pi}{4}) = (\text{some}).$$

$$(m - \mu m) \frac{1}{k} + \mu m \frac{1}{k} = \alpha(\tau_m)$$

$$\bar{N}_{C_2} = \bar{N}_{C_1} + \frac{1-\bar{\lambda} - \bar{\epsilon}_4}{1-\bar{\epsilon}_4} (\bar{N}_{C_0} - \bar{N}_{C_1})$$

$$K_{2_2} = \frac{\bar{N}_{C_2} - \bar{N}_F}{\bar{N}_R - \bar{N}_{C_2}}$$

$$K_{t_2} = 1 + K_{2_2}$$

$$K_{3_2} = \omega_{NO_2} \left(\frac{\bar{N}_{NO_2} - \bar{N}_{C_2}}{\bar{N}_R - \bar{N}_{C_2}} \right)$$

$$A_a = 0 \quad A_t = .848 \bar{c} (\bar{z} - \bar{l})^2 \left(\frac{v}{40} \right)^2$$

$$m_a = 3.75$$

$$m_t = 1.5$$

$$(64) \quad \bar{M}'_{ow} = \left(\frac{\omega_{T_2}}{3} + \frac{\omega_{T_2}}{6} \right) \bar{d}_2^2 + \left(\frac{\omega_{T_1} + \omega_{T_2}}{2} \right) \bar{d}_2 \bar{d}_1 + \bar{W}_t \left(1 - \frac{\bar{\lambda} + \bar{\epsilon}_4}{\bar{N}'_t} \right. \\ \left. + \left(\frac{\omega'_{T_2}}{3} + \frac{\omega_{NO_2} + \Delta\omega - K_{3_2}}{6} \right) \bar{d}_1^2 - \frac{\Delta\omega}{2} \bar{d}_1^2 + A_\alpha \right) \quad (\alpha = a, t)$$

$$(65) \quad \omega_{F_2} = \frac{6 m_a \bar{M}'_{ow} \bar{t}_R R + F_{ow} \bar{P}_R^2 K_{2_2} \pi \left(\frac{S}{\delta} \right)}{\pi \left(\frac{S}{\delta} \right) \left(\frac{F_{ow}}{\delta} \right) \left(\bar{P}_F^2 + K_{2_2} \bar{P}_R^2 \right) - m_a \bar{t}_R K_{4_2} \bar{d}_1^2 R}$$

$$(\omega_{T_2})_o = K_{t_2} \omega_{F_2} - K_{3_2} + \omega_{NO_2}$$

$$(\omega_{T_0})_o = \frac{\bar{d}_2}{\bar{d}_1} \omega_{T_2} - \frac{\bar{d}_1}{\bar{d}_2} (\omega'_{T_2} - \Delta\omega)$$

$$(\bar{W}_{\theta u})_o = \bar{d}_2 \left(\frac{\omega_{T_0} + \omega_{T_1}}{2} \right) + \frac{\bar{l}}{2} (\omega_{T_2} + \omega_{T_0} + \Delta \omega) - \bar{l} (\Delta \omega) + \frac{\bar{W}_u}{\kappa_0}$$

$$(\bar{I}_{\dot{\epsilon}_f})_o = (\bar{I}_{\dot{\epsilon}_2})_o + \frac{1}{3} \left[(\bar{l}_2 + \bar{\epsilon}_f)^3 \left\{ \omega_{T_2}' \left[1 - \left(\frac{\bar{\epsilon}_f}{\bar{l}_2 + \bar{\epsilon}_f} \right)^3 \right] + \left(\frac{\bar{l}_2 + \bar{\epsilon}_f}{\bar{l}_2} \right) (\omega_{T_2} + \Delta \omega - \omega_{T_0})' \right\} \right. \\ \left. \left[1 - \left(\frac{\bar{\epsilon}_f}{\bar{l}_2 + \bar{\epsilon}_f} \right)^3 \left(4 - 3 \frac{\bar{\epsilon}_f}{\bar{l}_2 + \bar{\epsilon}_f} \right) \right] \right\} - \Delta \omega [(\bar{l}_2 + \bar{\epsilon}_f)^3 - \bar{\epsilon}_f^3]$$

$$(\bar{M}_{\dot{\epsilon}_f})_o = (\bar{M}'_{\text{aw}})_o + \frac{K_{\dot{\epsilon}_f} \omega_{F_2} \bar{d}^2}{\zeta} + \bar{l} \left[(\bar{W}_{\theta u})_o \left(\frac{\omega_{T_0}}{2} + \frac{\omega_{T_2}}{6} \right) \bar{l} \right] + (\bar{W}_{\theta u})_o \bar{\epsilon}_f$$

$$(\bar{W}_{\theta u})_o = (\bar{W}_{\theta u})_o - \frac{\bar{l}}{2} (\omega_{T_2} + \omega_{T_0})$$

$$(\bar{M}_{\dot{\epsilon}_2})_o = (\bar{M}'_{\text{aw}})_o + \frac{K_{\dot{\epsilon}_2} \omega_{F_2} \bar{d}^2}{\zeta} + (\bar{W}_{\theta u})_o (\bar{l} + \bar{\epsilon}_f)$$

$$(\bar{I}_{\dot{\epsilon}_2})_o = (\bar{I}_{\dot{\epsilon}_2})_o + \frac{1}{3} \left[(\bar{l}_2 + \bar{\epsilon}_f)^3 \left\{ \omega_{T_2}' \left[1 - \left(\frac{\bar{l}_2 + \bar{\epsilon}_f}{\bar{l}_2 + \bar{\epsilon}_f} \right)^3 \right] + \left(\frac{\bar{l}_2 + \bar{\epsilon}_f}{\bar{l}_2} \right) (\omega_{T_2} + \Delta \omega - \omega_{T_0})' \right\} \right. \\ \left. \left[1 - \left(\frac{\bar{l}_2 + \bar{\epsilon}_f}{\bar{l}_2 + \bar{\epsilon}_f} \right)^3 \left(4 - 3 \frac{\bar{l}_2 + \bar{\epsilon}_f}{\bar{l}_2 + \bar{\epsilon}_f} \right) \right] \right\} - \Delta \omega [(\bar{l}_2 + \bar{\epsilon}_f)^3 - (\bar{\epsilon}_f + \bar{l})^3]$$

$$(\bar{M}_{\text{cor}_2})_o = \frac{4 \lambda (K_n - \bar{\epsilon}_f) (W/l_r) (h/\bar{\epsilon}_f) \gamma_0}{\left(\frac{V_f}{2.65} \right) (M_{\dot{\epsilon}_2})_o} \left[\frac{(\bar{I}_{\dot{\epsilon}_2})_o - (2\bar{\epsilon}_f + \bar{l})(\bar{M}_e)_{\text{cor}_2} (\bar{l}_2 + \bar{\epsilon}_f) (\bar{W}_{\theta u})_o}{(\bar{I}_{\dot{\epsilon}_2})_o - \bar{\epsilon}_f (\bar{M}_{\dot{\epsilon}_2})_o} \right]$$

(66) APPROXIMATION

$M_{F_2} = K_{F_2} \left(\frac{W}{l_r} \right) (R) (36.0)$	TILT. HUB ROTOR
$M_{C_2} = \left[K_{C_2} + (M_{\text{cor}_2})_o \right] \left(\frac{W}{l_r} \right) (R) (29.4)$	
$M_{F_2} = K_{F_2} \left(\frac{W}{l_r} \right) (R) (0.752) \left(\frac{\pi}{8} \right) \left(\frac{\pi}{l_r} \right)^2 D_r^2 \left(\frac{\omega_{F_2} K_{A_2} - K_{B_2}}{\omega_{T_2}} \right)$	ARTIC. (ROTOR)
$M_{C_2} = \frac{1090}{W} R^{6.1} \left(\frac{\pi}{l_r} \right)^{2.1}$	

$$\left. \begin{array}{l}
 M_{F_1} = K_{F_1} \left(\frac{W}{L} \right) (R) (F_{13}) (12) \\
 M_{C_1} = \left(K_{C_1} + \bar{M}_{C_{\text{cor},1}} \right) \left(\frac{W}{L} \right) (R) (C_{13}) (12) \\
 M_{F_2} = K_{F_2} \frac{EI \times L}{WT_e R^2} \left(\frac{F_{13}}{4500} \right) \left(\frac{W}{L} \right) (R) (12) \\
 M_{C_2} = \frac{1090}{W} R^{6.4} \left(\frac{\sigma}{L} \right)^{2.4}
 \end{array} \right\} \begin{array}{l} (\text{TILT. HUB ROTOR}) \\ (\text{ARTICULATE ROTOR}) \end{array}$$

TILT HUB ROTOR

ARTICULATE ROTOR

(66a)

$$\bar{W}'_2 = \frac{\bar{l}}{2} (\omega_{T_1} + \omega_{T_2}) + \frac{\bar{l}}{2} (\omega'_{T_2} + \Delta\omega) - \bar{l}(\Delta\omega) + \frac{\bar{W}_2}{K_2} \\ + \frac{\bar{l}}{2} (\omega_{T_2} - K_{32}) - \frac{\bar{l}}{2} (\omega'_{T_2} - \Delta\omega)$$

$$b_1 = \frac{5V^2}{2.68} \left[M_{\text{dw}} + \bar{W}'_2 (\bar{e}_1 + \bar{l}) \right]$$

$$b_2 = \frac{5V^2}{2.68} \left[\frac{d^2}{c} + \left(\frac{\bar{l} + \bar{l}_1}{2} \right) (\bar{e}_1 + \bar{l}) \right] (K_{42})$$

$$b_3 = -K_{32}$$

$$b_4 = K_{42}$$

$$b_5 = M_{T_2} \bar{l}_F \left(\frac{5}{2} \right)$$

$$b_6 = 45\varepsilon b_5 \bar{\rho}_a^2$$

$$b_7 = 45\varepsilon (\bar{\rho}_a^2 + K_{22} \bar{\rho}_a^2)$$

$$b_8 = \frac{M_{C_2} \delta}{45\varepsilon (\bar{\rho}_a - \bar{\rho}_b)}$$

$$b_9 = b_5 \left(\frac{\bar{l}_2}{\bar{l}_F} \right)$$

$$b_{10} = K_{22}$$

$$k_{11} = b_1 \frac{F_{C_2}}{F_{T_{U_2}}}$$

$$k'_{11} = b_1 \frac{F_{C_2}'}{F_{T_{U_2}}}$$

$$k_{22} = b_2 \frac{F_{C_2}}{F_{T_{U_2}}}$$

$$k'_{22} = b_2 \frac{F_{C_2}'}{F_{T_{U_2}}}$$

$$k_{44} = b_4 \frac{F_{C_2}}{F_{T_{U_2}}}$$

$$k'_{44} = b_4 \frac{F_{C_2}'}{F_{T_{U_2}}}$$

$$k_{66} = b_6 \frac{F_{C_2}}{F_{T_{U_2}}}$$

$$k'_{66} = b_6 \frac{F_{C_2}'}{F_{T_{U_2}}}$$

$$B_1 = k_0 b_4 b_7 - k_{22} b_9$$

$$B_2 = k_0 (b_3 b_7 + b_5 b_9) - k_{11} b_9 - k_{22} b_{10} - b_3 b_9 - b_4 b_7 b_9$$

$$B_3 = k_0 b_3 b_6 - k_0 b_5 - b_3 b_9 - b_5 (b_3 b_6 + b_5 b_9)$$

$$B_4 = -b_3 b_5 b_9$$

$$B_5 = k_0 b_{10} b_4 b_7 - k_{22} b_9 b_{10} = B_6 b_{10}$$

$$B_6 = k_0 (b_3 b_4 b_7 + b_3 b_5 b_{10} + b_4 b_5 b_9) - k_0 b_7 b_{10} \\ - k_{11} (b_3 b_{10} + b_5 b_9) - b_4 (b_3 b_{10} + b_5 b_9)$$

$$B_7 = k_0 b_{10} (b_3 b_{10} + b_5 b_9 + b_4 b_6) - k_{11} (b_3 b_{10} + b_5 b_9) - k_{22} b_3 b_9 \\ - b_3 b_{10} (b_{10} + b_4) - b_9 (b_3 b_9 + b_4 b_6)$$

$$B_8 = k_0 b_3^2 b_6 - k_{11} b_3 b_9 - b_3^2 b_9 - b_3 b_6 b_9$$

$$B_9 = k_3 b_3 - k_{22}$$

$$B_{10} = k_3 b_3 - k_{11} - k_4 b_9$$

$$B_{11} = -b_3 b_9$$

$$B_{12} = k_3 b_4 b_{10} - k_{22} b_{10}$$

$$B_{13} = k_3 b_3 (b_9 + b_{10}) - k_{11} b_{10} - k_{22} b_3 - b_3 b_9$$

$$B_{14} = k_3 b_3^2 - k_{22} b_3 - b_3 b_9$$

(67)

$$\begin{aligned}
 & \triangleright \left(w_{F_2} \right)_c^3 (B_1) + \left(w_{F_2} \right)_c^2 (B_2) + \left(w_{F_2} \right)_c (B_3) + B_4 = 0 \quad \left. \begin{array}{l} \\ \\ \end{array} \right\} \text{FRONT SPAN} \\
 & \left(w_{F_2}' \right)_c^3 (B'_1) + \left(w_{F_2}' \right)_c^2 (B'_2) + \left(w_{F_2}' \right)_c (B'_3) + B'_4 = 0 \\
 & \triangleright \left(w_{F_2} \right)_d^3 (B_5) + \left(w_{F_2} \right)_d^2 (B_6) + \left(w_{F_2} \right)_d (B_7) + B_8 = 0 \quad \left. \begin{array}{l} \\ \\ \end{array} \right\} \text{REAR SPAN} \\
 & \left(w_{F_2}' \right)_d^3 (B'_5) + \left(w_{F_2}' \right)_d^2 (B'_6) + \left(w_{F_2}' \right)_d (B'_7) + B'_8 = 0 \\
 & \triangleright \left(w_{F_2} \right)_e^2 (B_9) + \left(w_{F_2} \right)_e (B_{10}) + B_{11} = 0 \quad \left. \begin{array}{l} \\ \\ \end{array} \right\} \text{FRONT SPAN} \\
 & \left(w_{F_2}' \right)_e^2 (B'_9) + \left(w_{F_2}' \right)_e (B'_{10}) + B'_{11} = 0 \\
 & \triangleright \left(w_{F_2} \right)_f^2 (B_{12}) + \left(w_{F_2} \right)_f (B_{13}) + B_{14} = 0 \quad \left. \begin{array}{l} \\ \\ \end{array} \right\} \text{REAR SPAN} \\
 & \left(w_{F_2}' \right)_f^2 (B'_{12}) + \left(w_{F_2}' \right)_f (B'_{13}) + B'_{14} = 0
 \end{aligned}$$

2

$$f_{cr_2} = \frac{b_1 + b_2 w_{F_2}}{b_3 + b_4 w_{F_2}}$$

\triangleright If $f_{cr_2} > F_{rc_2}$, use primed equations.

Use largest value of $(w_{F_2})_{a,b,c,d,e,f}, (w_{F_2}')_{a,b,c,f}$.

2

SEE NEXT PAGE

2) IF FRONT SPAR IS DESIGNED BY
 STRESS REQUIREMENT ON PRECEDING
 PAGE, RECOMPUTE \bar{N}_{C_2} , USING w_{R_1} AND
 w_{P_1} AS DETERMINED BY STRESS. IF w_{R_1}
 IS CRITICAL FOR FLIGHT CONDITION, IT
 IS GIVEN BY: $w_{R_1} = w_{P_1} K_{2_1} - K_{3_1}$.

$$\bar{N}'_{C_2} = \frac{w_{F_1} \bar{N}_F + w_{R_1} \bar{N}_R + w_{W_1} \bar{N}_{W_1}}{w_{F_1} + w_{R_1} + w_{W_1}}$$

RECOMPUTE K' 'S:

$$K'_{2_1} = \frac{\bar{N}'_{C_2} - \bar{N}_F}{\bar{N}_R - \bar{N}'_{C_2}}$$

$$K'_{4_1} = 1 + K'_{2_1}$$

$$K'_{3_1} = w_{W_1} \left(\frac{\bar{N}_{W_1} - \bar{N}'_{C_2}}{\bar{N}_R - \bar{N}'_{C_2}} \right)$$

RECOMPUTE $b_2, b_3, b_4, b_7, b_{10}, b_{22}, b_{25}$,
 AND ALL B'S INVOLVED IN CRITICAL CONDITION.

RECOMPUTE CRITICAL w_{P_1} AND CONTINUE,
 USING (K') 'S.

$$(68) \quad w_{T_2} = K_{42} w_{F_2} - K_{32} + w_{NO_2}$$

$$(69) \quad w_{T_0} = \frac{\bar{L}_2}{d_1} w_{T_2} - \frac{\bar{L}}{d_1} (w'_{T_2} - \Delta w)$$

$$(70) \quad W_{BU} = 12 R \left[\frac{\bar{L}_2}{2} (w_{T_4} + w_{T_2}) + \frac{\bar{L}_2}{2} (w'_{T_2} + w_{T_0} + \Delta w) - \bar{L}_1 \Delta w + \frac{\bar{W}_1}{\bar{n}'_1} \right]$$

$$(71) \quad \left\{ \begin{array}{l} I_{x_t} = \frac{(45\bar{c})^2}{8} [w_{F_t}(\bar{\rho}_r + K_{2t}\bar{\rho}_e^2) - K_{3t}\bar{\rho}_e^2] \\ I_{x_2} = \frac{(45\bar{c})^2}{8} [w_{F_2}(\bar{\rho}_r^2 + K_{22}\bar{\rho}_e^2) - K_{32}\bar{\rho}_e^2] \\ I_{x_1} = \frac{(45\bar{c})^2}{8} [w_{F_1}(\bar{\rho}_r^2 + K_{21}\bar{\rho}_e^2) - K_{31}\bar{\rho}_e^2] \\ I_x(x) = I_{x_t} + (I_{x_2} - I_{x_t})\left(\frac{1-x}{d_1}\right) \quad \left\{ \bar{l}_1 + \bar{e}_1 \leq x \leq 1 \right\} \\ I_x(x) = I_{x_2} + (I_{x_1} - I_{x_2})\left(\frac{\bar{l}_1 + \bar{e}_1 - x}{d_1}\right) \quad \left\{ \bar{e}_1 \leq x \leq \bar{l}_1 + \bar{e}_1 \right\} \end{array} \right.$$

$$(72) \quad \left\{ \begin{array}{l} I_{Y_t} = \frac{(45\bar{c})^2}{8} (w_{F_t})(\bar{\nu}_r - \bar{\nu}_r)^2 \left(\frac{K_{2t}w_{F_t} - K_{3t}}{K_{4t}w_{F_t} - K_{3t}} \right) \\ I_{Y_2} = \frac{(45\bar{c})^2}{8} (w_{F_2})(\bar{\nu}_r - \bar{\nu}_r)^2 \left(\frac{K_{22}w_{F_2} - K_{32}}{K_{42}w_{F_2} - K_{32}} \right) \\ I_{Y_1} = \frac{(45\bar{c})^2}{8} (w_{F_1})(\bar{\nu}_r - \bar{\nu}_r)^2 \left(\frac{K_{21}w_{F_1} - K_{31}}{K_{41}w_{F_1} - K_{31}} \right) \\ I_Y(x) = I_{Y_t} + (I_{Y_2} - I_{Y_t})\left(\frac{1-x}{d_1}\right) \quad \left\{ \bar{l}_1 + \bar{e}_1 \leq x \leq 1 \right\} \\ I_Y(x) = I_{Y_2} + (I_{Y_1} - I_{Y_2})\left(\frac{\bar{l}_1 + \bar{e}_1 - x}{d_1}\right) \quad \left\{ \bar{e}_1 \leq x \leq \bar{l}_1 + \bar{e}_1 \right\} \end{array} \right.$$

$$\left\{
 \begin{aligned}
 I_{P_1} &= \frac{(45C)}{386}^2 \left\{ w_{P_1} (\bar{\lambda}_{c_1} - \bar{\lambda}_p) (\bar{\lambda}_n - \bar{\lambda}_p) + w_{N_{P_1}} \left[0.052 \left(\frac{\bar{\lambda}_p}{.528} \right) + (\bar{\lambda}_{n_{P_1}} - \bar{\lambda}_{c_1}) (\bar{\lambda}_n - \bar{\lambda}_p) \right] \right\} \\
 I_{P_2} &= \frac{(45C)}{386}^2 \left\{ w_{P_2} (\bar{\lambda}_{c_2} - \bar{\lambda}_p) (\bar{\lambda}_n - \bar{\lambda}_p) + w_{N_{P_2}} \left[0.052 \left(\frac{\bar{\lambda}_p}{.528} \right) + (\bar{\lambda}_{n_{P_2}} - \bar{\lambda}_{c_2}) (\bar{\lambda}_n - \bar{\lambda}_p) \right] \right\} \\
 I'_{P_2} &= \frac{(45C)}{386}^2 \left\{ w_{P_2} (\bar{\lambda}_{c_2} - \bar{\lambda}_p) (\bar{\lambda}_n - \bar{\lambda}_p) + w_{N_{P_2}} \left[0.052 \left(\frac{\bar{\lambda}_p}{.528} \right) + (\bar{\lambda}_{n_{P_2}} - \bar{\lambda}_{c_2}) (\bar{\lambda}_n - \bar{\lambda}_p) \right] \right\} \\
 I_{P_2} &= \frac{(45C)}{386}^2 \left\{ w_{P_2} (\bar{\lambda}_{c_2} - \bar{\lambda}_p) (\bar{\lambda}_n - \bar{\lambda}_p) + w_{N_{P_2}} \left[0.028 \left(\frac{\bar{\lambda}_p}{.528} \right) + (\bar{\lambda}_{n_{P_2}} - \bar{\lambda}_{c_2}) (\bar{\lambda}_n - \bar{\lambda}_p) \right] \right\} \\
 w_{F_1} &= w_{F_2} + (w_{F_1} - w_{F_2}) \left(1 - \frac{d}{d_1} \right) \\
 (73) \quad I_{P_1} &= \frac{(45C)}{386}^2 \left\{ w_{P_1} (\bar{\lambda}_{c_1} - \bar{\lambda}_p) (\bar{\lambda}_n - \bar{\lambda}_p) + w_{N_{P_1}} \left[0.052 \left(\frac{\bar{\lambda}_p}{.528} \right) + (\bar{\lambda}_{n_{P_1}} - \bar{\lambda}_{c_1}) (\bar{\lambda}_n - \bar{\lambda}_p) \right] \right\} \\
 I'_{P_1} &= \frac{(45C)}{386}^2 \left\{ w_{P_1} (\bar{\lambda}_{c_1} - \bar{\lambda}_p) (\bar{\lambda}_n - \bar{\lambda}_p) + w_{N_{P_1}} \left[0.028 \left(\frac{\bar{\lambda}_p}{.528} \right) + (\bar{\lambda}_{n_{P_1}} - \bar{\lambda}_{c_1}) (\bar{\lambda}_n - \bar{\lambda}_p) \right] \right\} \\
 I_p(\alpha) &= I_{P_1} + (I_{P_2} - I_{P_1}) \left(\frac{1-\alpha}{d_1} \right) \quad \left\{ \bar{\lambda}_1 + \bar{\epsilon}_1 < \alpha \leq 1 \right\} \\
 I_p(\alpha) &= I'_{P_1} + (I_{P_2} - I'_{P_1}) \left(\frac{1+\bar{\epsilon}_1 - \alpha}{d_1 - d} \right) \quad \left\{ \bar{\lambda}_1 + \bar{\epsilon}_1 < \alpha < \bar{\lambda}_1 + \bar{\epsilon}_1 \right\} \\
 I_p(\alpha) &= I'_{P_1} + (I_{P_2} - I'_{P_1}) \left(\frac{1+\bar{\epsilon}_1 - \alpha}{d} \right) \quad \left\{ \bar{\epsilon}_1 \leq \alpha < \bar{\lambda}_1 + \bar{\epsilon}_1 \right\}
 \end{aligned}
 \right.$$

$$(74) \quad \left\{ \begin{array}{l} J_1 = 17.50 \bar{L}_{\infty_1} \bar{\epsilon}^3 \left(\frac{\bar{l}_1}{\bar{L}_{\infty_1}} \right)^3 [0.951 + 2.4 (\bar{l}_0 - \bar{s})] \\ \{ l_1 + \bar{\epsilon}_1 \leq n \leq 1 \} \end{array} \right.$$

$$\left\{ \begin{array}{l} J_2 = J_1 \left(\frac{\bar{L}_{\infty_2}}{\bar{L}_{\infty_1}} \right) \left(\frac{\bar{l}_2}{\bar{l}_1} \right) \\ \{ \bar{l}_1 + \bar{\epsilon}_1 < n < \bar{l}_2 + \bar{\epsilon}_2 \} \\ J_3 = J_2 \left(\frac{\bar{L}_{\infty_3}}{\bar{L}_{\infty_2}} \right) \\ \{ \bar{\epsilon}_2 \leq n \leq \bar{l}_3 + \bar{\epsilon}_3 \} \end{array} \right.$$

$$(75) \quad \left\{ \begin{array}{l} w_T = w_{T_1} + (w_{T_2} - w_{T_1}) \left(\frac{1-n}{d_1} \right) \\ \{ \bar{l}_2 + \bar{\epsilon}_1 \leq n \leq 1 \} \end{array} \right.$$

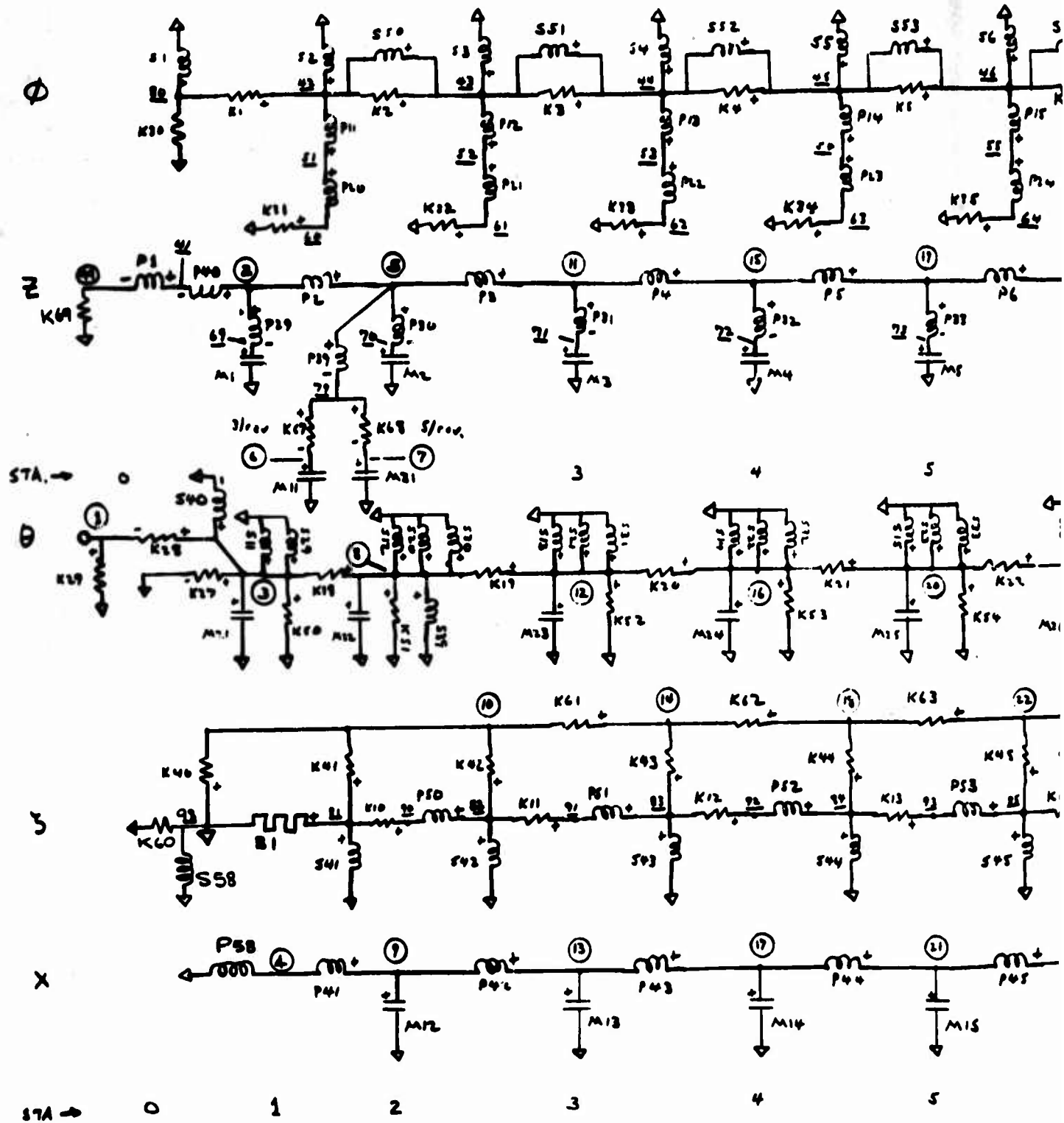
$$\left\{ \begin{array}{l} w_T' = w_{T_2}' + (w_{T_1}' - w_{T_2}') \left(\frac{\bar{l}_1 + \bar{\epsilon}_1 - n}{d_1} \right) \\ \{ \bar{l}_1 + \bar{\epsilon}_1 < n < \bar{l}_2 + \bar{\epsilon}_2 \} \end{array} \right.$$

$$\left. \begin{array}{l} w_T'' = w_{T_2}'' - \Delta w + (w_{T_1}'' + \Delta w - w_{T_2}'') \left(\frac{\bar{l}_2 + \bar{\epsilon}_2 - n}{d_1} \right) \\ \{ \bar{\epsilon}_2 \leq n \leq \bar{l}_1 + \bar{\epsilon}_1 \} \end{array} \right.$$

$$(76) \quad I_E = 1.49 R^3 \left\{ \begin{array}{l} w_{T_1} (\bar{l}^3 - \bar{l}_1^3) + \left(\frac{w_{T_2} - w_{T_1}}{4 d_1} \right) [\bar{l}^4 - \bar{l}_1^3 (4 \bar{l}^3 - 3 \bar{l}_1^3)] \\ + \bar{l}_1^3 \left(2 w_{T_2}' + \frac{w_{T_1} + \Delta w - w_{T_2}'}{4} \right) - \Delta w \bar{l}_1^3 + \frac{3 \bar{W}_s (n'_1 - \bar{\epsilon}_1)}{n'_1} \end{array} \right\}$$

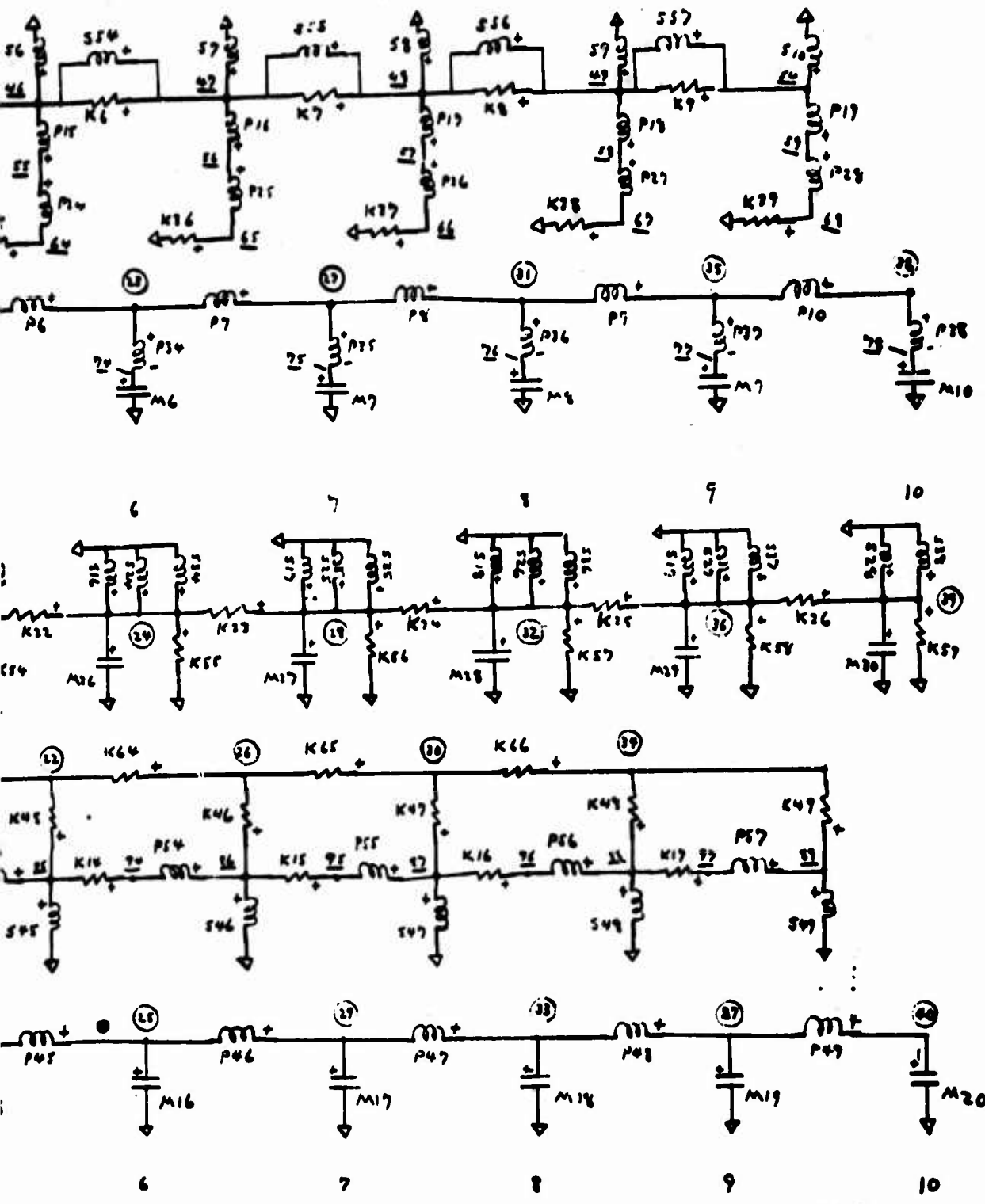
APPENDIX IV

COMPUTER CIRCUIT DIAGRAM AND INPUT DATA



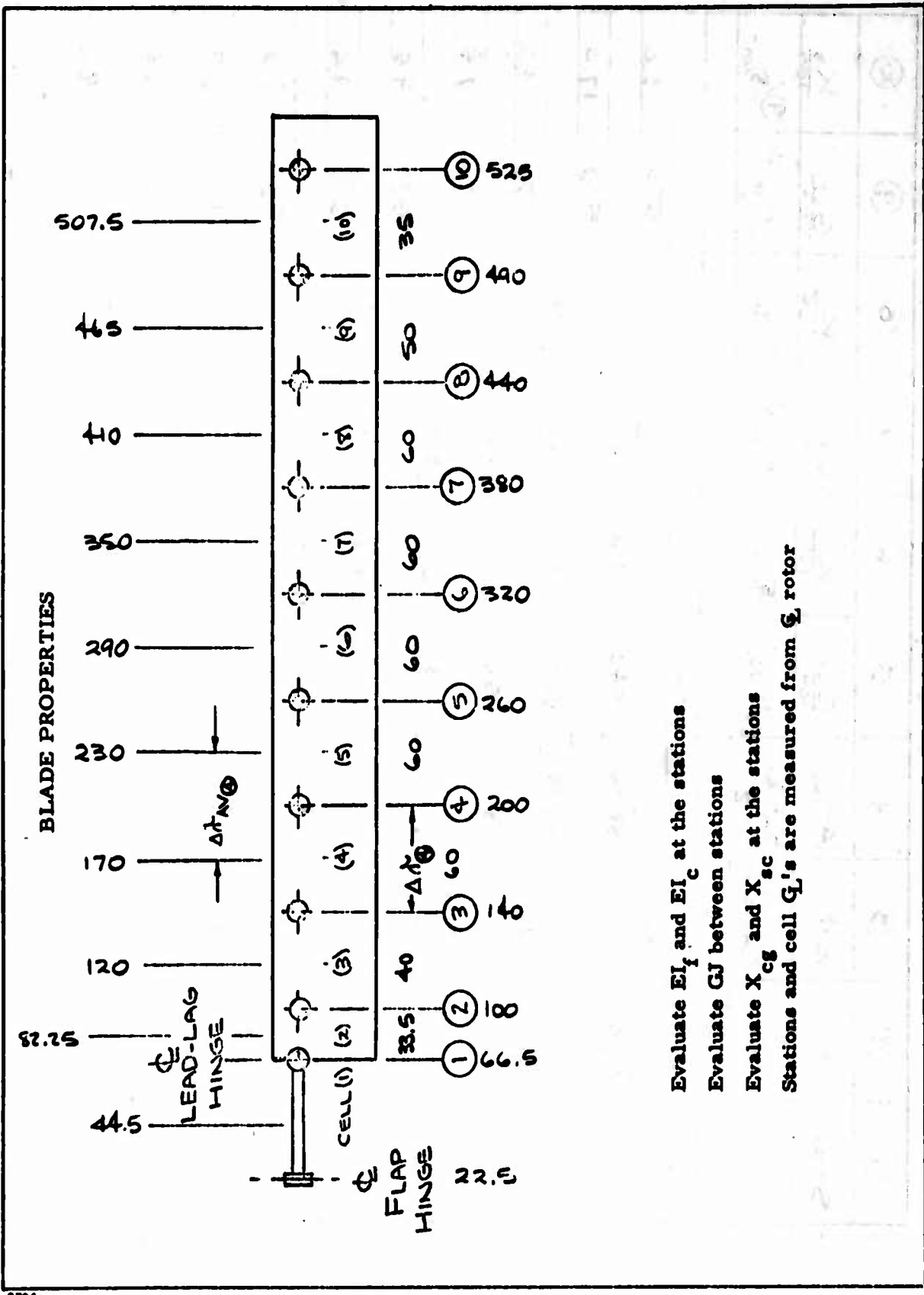
Connection Diagram - Heavy-Lift Helic

K IV
DATA FOR COUPLED ANALYSIS



Helicopter Blade Structure

B



Evaluate EI_f and EI_c at the stations

Evaluate GJ between stations

Evaluate X_{cg} and X_{sc} at the stations
Stations and cell Q's are measured from Q rotor

①	②	③	④	⑤	⑥	⑦	⑧	⑨	⑩
S_{TA}	Δt	Δt	$(\Delta t)_{AV}$	$\frac{EI}{10^6} +$	$\frac{K_{12}}{10^3}$	$\frac{EI_c}{10^6}$	$\frac{K_{21}}{10^3}$	$\frac{K_{31}}{10^3}$	K_3
(m.)	(2) \bar{x}_m	$\frac{\bar{x}_{m+1} + \bar{x}_m}{2}$	$(\# m^2)$	(# m^2)	(# m^2)	(# m^2)	(# m^2)	(# m^2)	
0	22.5	~							
1	66.5	38.75	540	13.9	0	0	570	12.0	
2	100	36.75	500	13.6	3830	104	570	17.0	
3	140	30	456	9.1	3780	76	570	14.2	
4	200	60	383	6.4	3670 :	61	570	9.5	
5	260	~	310	5.7	3480	53	570	9.5	
6	320	~	340	4.0	3210	53	520	8.6	
7	380	60	167	2.8	2860	40	400	6.7	
8	440	55	95	1.7	2380	43	320	6.4	
9	490	55	42.5	35	1790	42	300	8.6	
10	555	32.5	13	.5	1120	45			
					K_1	K_2			K_3
					P/S + P/kn				

FORM 9707

①	⑪	⑫	⑬	⑭	⑮	⑯	⑰	⑱	⑲	㉑	㉒
STA	WT	ΔW	W	m ₁	m ₂	T/2 ²	T _{Q₂} ²	η _{20%}	η _{20%}	η _{20%}	η _{20%}
(#/m.)	(#)			⑩ × ④ + ⑨	⑪ × ②	↑Σ ⑬	⑭ × ⑬ _m	(m.)	(m.)	(m.)	(m.)
0											
1	6.0		233	.604	40.2	788.6	34,100	16.44	15.00	A	
2	5.6		206	.534	53.4	768.4	25,070	16.26			
3	3.2		160	.445	52.1	695.0	21,800	16.02			
4	2.14		128	.332	66.4	636.9	38,210	15.64			
5	2.06		124	.322	83.7	510.5	34,230	15.36			
6	2.00		120	.311	99.5	496.8	29,210	15.0			
7	1.90		114	.296	112.5	387.3	23,240	14.70			
8	1.83		101	.262	115.3	274.8	16,490	14.34			
9	1.63		71	.194	90.2	139.5	7930	14.10			
10	1.56	11	51	.132	69.3	61.3	3430	13.86	15.00		
			130.4	m ₁ & m ₂							

SUMMARY

STA	P/K.	K_1 $\frac{1}{10^6}$	K_2 $\frac{1}{10^6}$	K_3 $\frac{1}{10^6}$	m.	K_4 $\frac{1}{10^6}$	P_3/S_3	P_4/S_4	P_5/S_5
1	44	13.9			.604	7.81	1.44		
2	33.5	13.6	104	17.0	.534	5.64	1.26	-.0024	-.0033
3	40	9.1	76	14.2	.415	6.26	1.02	-.0008	-.0010
4	60	6.4	61	9.5	.322	8.60	.66	+.0008	+.0013
5		5.2	58	9.5	.322	7.70	.36	.0027	.0035
6		4.0	53	9.5	.311	6.57	0	.0052	.0063
7		2.8	48	8.6	.296	5.23	-.30	.0080	.0015
8	60	1.7	43	6.7	.262	3.71	-.66	.0113	.0130
9	50	.8	42	6.4	.194	1.90	-.90	.0174	.0194
10	35			8.6	.132	.55	-1.14	.0326	.0325
						K-30 thru K-39 ✓			
						M-1 thru M-10 ✓			
						K-18 thru K-26 ✓			
						S-1 thru S-10 ✓			

STA	m_3	$\frac{K_6}{10^6}$	P_6/S_6	m_2	$\frac{K_5}{10^6}$	R/S_2	
1	136	.027			7.81		$K-27 = 24,400$
2	120	.025	.216	.534	5.64	33.5	$K-28 = 3.76 \times 10^6$
3	93	.019	.206	.415	6.26	40	$K-29 = 10^6$
4	75	.016	.191	.332	8.60	60	$K-60 = 214 \times 10^6$
5	72	.015	.177	.322	7.70		$K-67$
6	70	.015	.162	.311	6.57		$K-68$
7	67	.014	.146	.296	5.23		$M-11$
8	59	.013	.131	.262	3.71	60	$M-31$
9	41	.009	.117	.184	1.80	50	$S-39$
10	30	.007		.132	.55	33	$B-1 = 500,000$
							$S-40 = 0$
							$S-50 = 66.5$
							$K-69 = 10^6$
							$S-41 \text{ thru } S-49$
							$K-40 \text{ thru } K-49 \checkmark$
							$M-12 \text{ thru } M-20 \checkmark$
							$K-50 \text{ thru } K-59 \checkmark$
							$M-21 \text{ thru } M-30 \checkmark$

APPENDIX V
STANDARD STRUCTURAL CELL FOR THE REPRESENTATION OF
MECHANICAL EFFECTS IN HELICOPTER ROTOR BLADES

1. INTRODUCTION

A standard structural cell for rotor blades is described for use in conjunction with the digital computer program, SADSAM IV, developed for Hughes Tool Company by the MacNeal-Schwendler Corporation. Structures are represented in SADSAM IV by combinations of simple springs, masses, dampers and generalized leverage elements (otherwise called "constraints" or "transformers"). In general, the user selects a combination of simple structural elements to represent each particular structure, so that the program is suitable for a very broad range of applications.

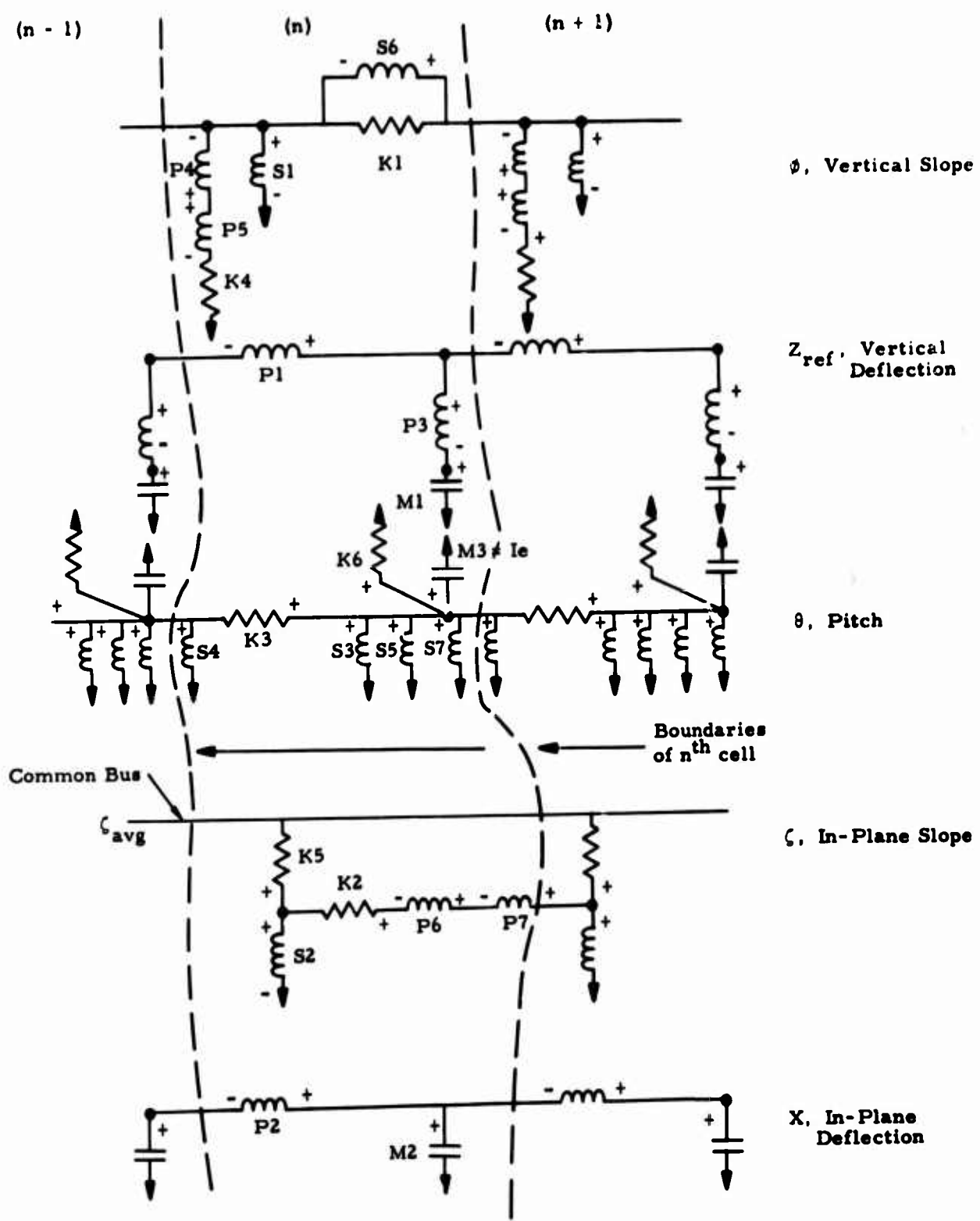
Since the analysis of rotors is a primary application of the program, and since most rotor blades are similar in their primary structural behavior, it is both desirable and feasible to describe a standard structural cell for rotor blades that can be used in rotor blade analysis. The major differences between rotor designs are usually confined to the hub and control system; these are elements which will require separate treatment for each type of rotor system and which can be conveniently treated by the basic computer program due to its flexibility.

The arrangement of elements for the standard structural cell is shown in the diagram on the following page. The electrical circuit notation employed in the diagram is described in the users manual for SADSAM IV and also in References 24 and 25. The identification of the elements in the model, formulas for their calculation, and interpretation of results obtained from the model are described in detail in section 3 of this appendix. The mathematical derivation of the standard structural cell is discussed in the following paragraphs.

2. DEVELOPMENT OF STANDARD CELL FOR REPRESENTATION OF
MECHANICAL EFFECTS IN BLADES

The standard cell for the representation of mechanical effects in blades is similar to that developed in Reference 24. The present treatment differs in the following respects:

1. A finite-difference beam model is used rather than a "Russell" beam model.



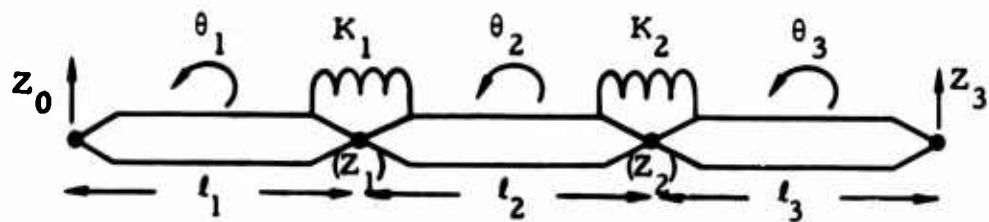
STANDARD STRUCTURAL CELL FOR BLADE

2. Mass coupling between pitching and flapping is treated by chordwise levers rather than by mutual mass coupling.
3. The arrangement of elements to represent coupling between vertical and in-plane bending due to blade pitch is different in order to facilitate measurement of flapwise bending moment.
4. The centrifugal force coupling between pitching and flapping is treated in a more correct manner.

Since the discussion in Reference 24 is quite detailed, only the manner of treating the differences listed above will be described here.

2.1 Finite Difference Beam Model

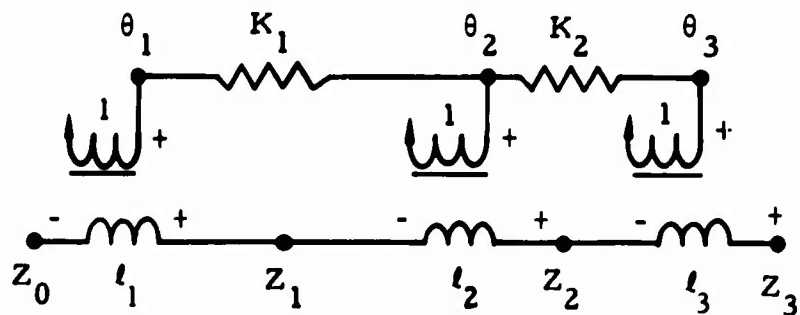
The finite-difference beam model is equivalent to the following arrangement of rigid levers and springs:



The springs resist rotation between adjacent levers. Their values are given by:

$$K_n = \frac{2EI}{l_n + l_{n+1}}$$

The formal circuit diagram for the finite-difference model is shown below:

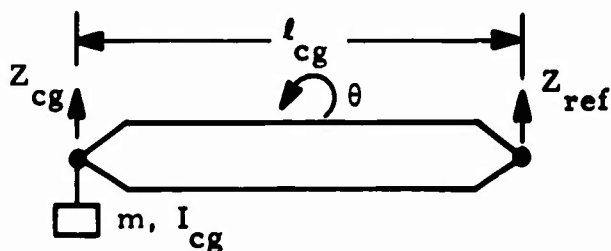


Internal forces in the springs K represent bending moment. Internal forces in the transformers represent shear.

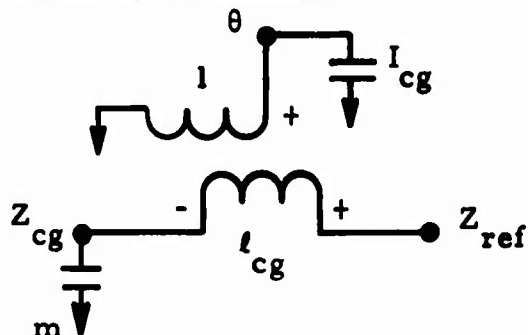
A comprehensive treatment of the finite-difference beam model, including a discussion of finite-difference errors in both static and dynamic analysis, is given in Reference 25. The finite-difference beam model has been chosen for the standard cell because it eliminates rotations as independent degrees of freedom, which is desirable due to the limitation of SADSAM IV to 50 independent degrees of freedom. Note that transverse shear flexibility in the beam is also eliminated for the same reason.

2.2 Mass Coupling Between Pitching and Flapping

Mass coupling between pitching and flapping is treated by means of a lever that locates the chordwise position of the center of gravity of a blade section relative to the elastic axis as shown below:

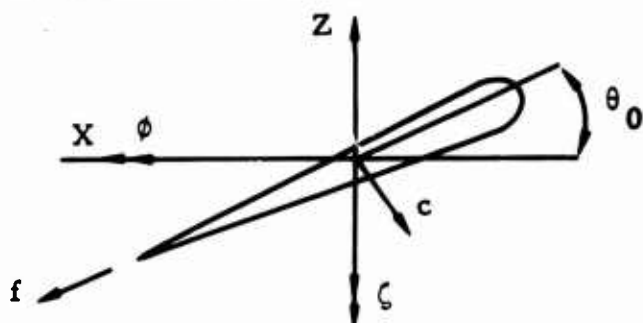


The formal circuit diagram is as follows:



2.3 Elastic Coupling Between Vertical and In-Plane Bending

Consider a blade section that is rotated through an angle θ_0 with respect to a horizontal axis as shown below:



The principal axes, f and c, are also rotated through the angle θ_0 . The relationship between moments and curvatures about the vertical and inplane axes may easily be shown to be:

$$\begin{Bmatrix} M_\phi \\ M_\zeta \end{Bmatrix} = \begin{bmatrix} K_{\phi\phi} & K_{\phi\zeta} \\ K_{\phi\zeta} & K_{\zeta\zeta} \end{bmatrix} \begin{Bmatrix} \Delta\phi \\ \Delta\zeta \end{Bmatrix} \quad (77)$$

where

$$K_{\phi\phi} = \frac{(EI_f \cos^2 \theta_0 + EI_c \cdot \sin^2 \theta_0)}{\Delta l} \quad (78)$$

$$K_{\phi\zeta} = \frac{[-\sin \theta_0 \cos \theta_0 (EI_c - EI_f)]}{\Delta l} \quad (79)$$

$$K_{\zeta\zeta} = \frac{(EI_c \cos^2 \theta_0 + EI_f \cdot \sin^2 \theta_0)}{\Delta l} \quad (80)$$

Two simplifying approximations will be made:

1. θ_0 is small so that $\sin \theta_0 \approx \tan \theta_0$ and $\cos \theta_0 \approx 1$.
2. $I_c \gg I_f$ so that EI_f may be ignored in equations (79) and (80). Note that when this assumption is not valid, EI_f should be retained in equation (79).

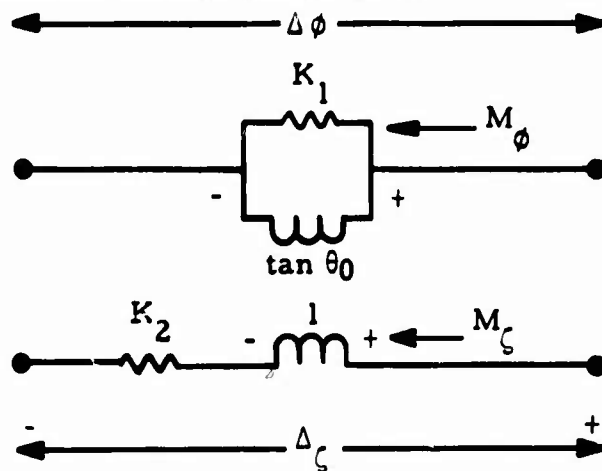
With these simplifications the above equations may be written:

$$K_{\phi\phi} = \frac{(EI_f + EI_c \cdot \tan^2 \theta_0)}{\Delta l} \quad (78a)$$

$$K_{\phi\zeta} = \frac{(-\tan \theta_0 \cdot EI_c)}{\Delta l} \quad (79a)$$

$$K_{\zeta\zeta} = \frac{EI_c}{\Delta l} \quad (80a)$$

An equivalent circuit model that satisfied equation (77) with these values is as follows:



where $K_1 = EI_f/\Delta l$ and $K_2 = EI_c/\Delta l$.

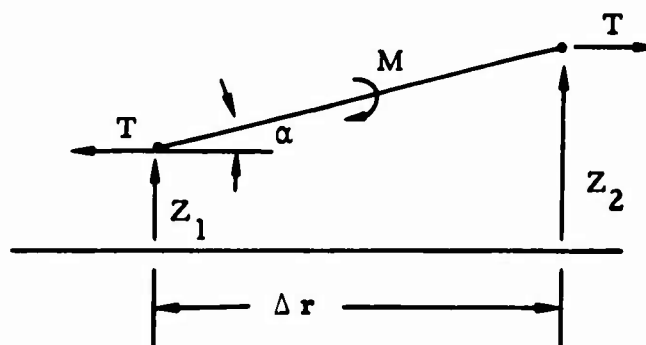
The internal force in K_1 is

$$M_{K_1} = M_\phi + \tan\theta_0 \cdot M_\zeta \quad (81)$$

which is approximately equal to the flapwise bending moment (moment about the chord axis).

2.4 Centrifugal Force Coupling Between Pitching and Flapping

The idealized element to represent centrifugal force stiffening is a tensioned string that resists rotations about axes normal to the string. Consider a tensioned string element of length Δr with tension T as shown below:



The restoring moment is

$$M = T \cdot \Delta r \cdot \alpha \quad (82)$$

which is equivalent to a couple force

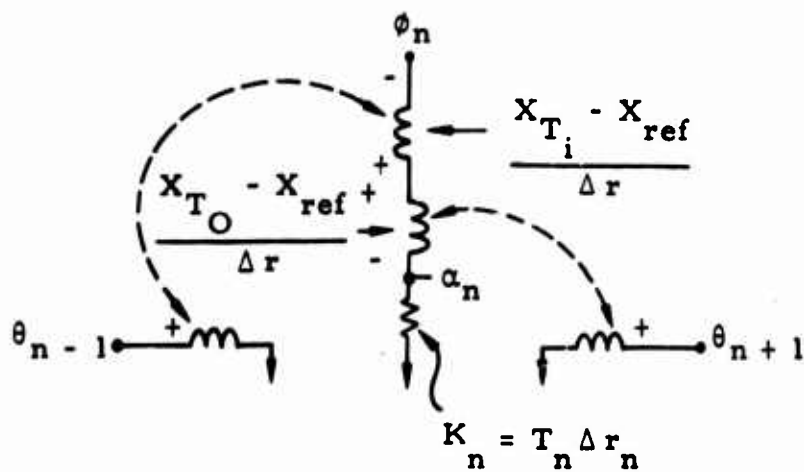
$$F_{Z_2} = -F_{Z_1} = \frac{M}{\Delta r} = \frac{T}{\Delta r} (Z_2 - Z_1) \quad (83)$$

Stiffness coupling between pitching and flapping occurs because the string is not located on the shear center of the blade and therefore the displacements Z_2 and Z_1 include contributions from both pitching and flapping. The location of the string is indicated in the diagram on page 364 as the "tension axis". The tension axis at any spanwise station is located at the centroid of spanwise tension over the blade cross section and includes contributions from steady aerodynamic chordwise bending as well as from centrifugal force. The tension axis is discontinuous due to the concentration of mass at discrete points.

Referring to equation (83) and the diagram on page 364, the rotation θ_n for the n^{th} cell is

$$\begin{aligned} \alpha_n &= \frac{Z_2 - Z_1}{\Delta r} \\ &= \frac{1}{\Delta r} \left[\phi_n - \frac{x_{T_O} - x_{ref}}{\Delta r} \theta_n + \frac{x_{T_i} - x_{ref}}{\Delta r} \theta_{n-1} \right] \end{aligned} \quad (84)$$

This relationship and the spring restraint are represented by the following equivalent circuit model.

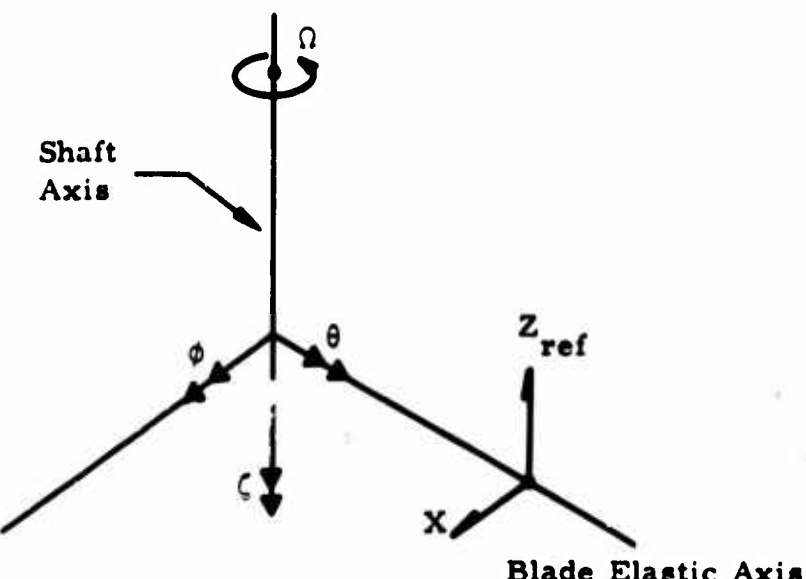


The elements in this model are represented by K_4 , P_4/S_4 and P_5/S_5 in the diagram on page 355.

Formulas for computing the magnitude of the tension force and the inboard and outboard locations of the tension axis are given in section 3.4.

3. DESCRIPTION OF STANDARD STRUCTURAL CELL

3.1 Identification of Coordinate Directions



X : Blade motion perpendicular to shaft axis and to blade elastic axis; positive aft.

Z_{ref} : Blade motion parallel to shaft axis. Measured at elastic axis; positive up.

ϕ : Local vertical blade slope; normal to shaft axis and to elastic axis; positive tip up.

ζ : Local in-plane blade slope; parallel to shaft axis; positive tip aft.

θ : Local blade pitch angle; parallel to blade elastic axis; positive leading edge up.

NOTES:

1. θ does not include built-in twist; θ may or may not include collective pitch, depending on whether collective pitch is included in the blade root boundary condition or in the specification of aerodynamic forces. θ includes cyclic pitch and elastic twist.
2. If the effect of static coning on coupling between pitch and lead-lag motion is included in the analysis, ζ is measured perpendicular to

the statically deformed blade elastic axis ; i.e., the ζ axis is rotated in a vertical plane through an angle equal to the local blade slope.

3. 2 Identification of Internal Forces

In the diagram on page 355:

Element K1: Flapwise bending moment, that is, bending moment about an axis parallel to the blade chord; positive for tip bending up. Computed at mass stations.

Element K2: In-plane bending moment, that is, bending moment about the ζ axis. Positive for tip bending aft. In-plane bending moment does not coincide with chordwise bending moment if blade pitch is not zero. Computed at mass stations.

Element K3: Twisting moment about blade elastic axis; positive for tip twisting up. Computed between mass stations.

Element P1: Total shear force in a vertical plane including elastic shear force and the vertical component of blade tension. Positive for tip up. Computed between mass stations.

Element P2: Total shear force in the in-plane direction, that is, in a plane perpendicular to the ζ axis. Positive for tip aft. Computed between mass stations.

3. 3 Identification of Elements in the Model

Masses

M_1 : Vertical component of lumped mass.

M_2 : In-plane component of lumped mass.

M_3 : Polar moment of inertia of blade section mass about the center of gravity ($= I_p$).

Springs

$$K_1 = \frac{2EI_f}{\Delta r_n + \Delta r_{n+1}} : \text{Flapwise bending stiffness. Located at mass stations.}$$

$$K_2 = \frac{2EI_c}{\Delta r_n + \Delta r_{n+1}} : \text{Chordwise bending stiffness. Located at mass stations.}$$

$$K_3 = \frac{GJ}{\Delta r_n} :$$

Torsional stiffness. Located between mass stations.

$$K_4 = T_n \cdot \Delta r_n :$$

Centrifugal force stiffening for vertical motions. Located between mass stations.

$$K_5 = T_n \Delta r_n :$$

Centrifugal force stiffening for in-plane motions. Located between mass stations.

$$K_6 = \Omega^2 (I_Z - I_X) :$$

Centrifugal force stiffening for pitch (tennis-racket effect). Located at mass stations.

Transformers

$$\frac{P_1}{S_1} = T_1 = \Delta r_n = \text{Spanwise lever for vertical bending.}$$

$$\frac{P_2}{S_2} = T_2 = \Delta r_n = \text{Spanwise lever for in-plane bending.}$$

$$\frac{P_3}{S_3} = T_3 = X_{cg} - X_{ref} : \text{Chordwise lever for location of blade center of gravity relative to elastic axis.}$$

$$\frac{P_4}{S_4} = T_4 = \frac{X_{T_i} - X_{ref}}{\Delta r_n} : \text{Chordwise lever for location of the tension axis at the inboard end of the cell. (See diagram on page 364.)}$$

$$\frac{P_5}{S_5} = T_5 = \frac{X_{T_O} - X_{ref}}{\Delta r_n} : \text{Chordwise lever for location of the tension axis at the outboard end of the cell.}$$

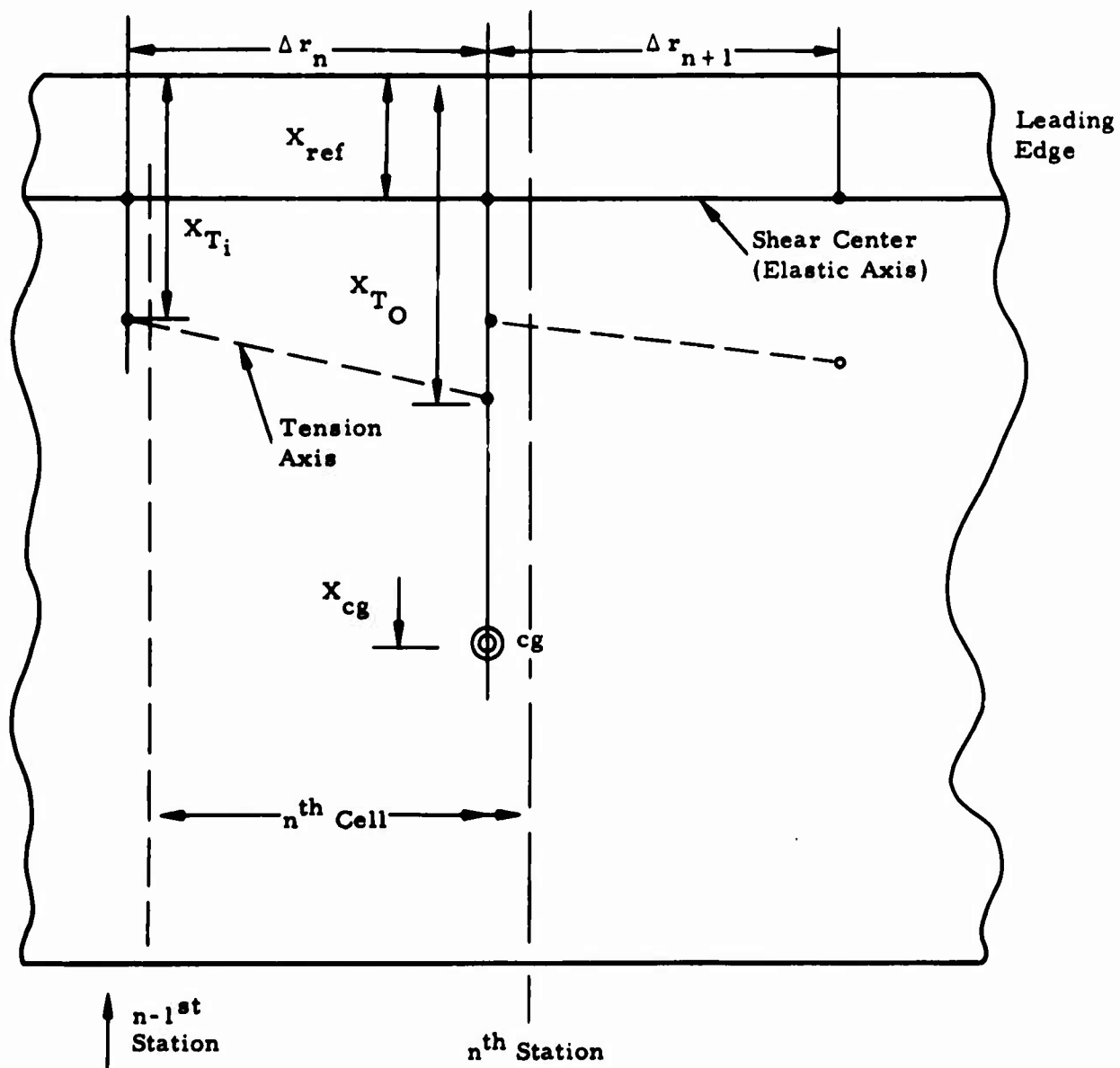
$$\frac{P_6}{S_6} = T_6 = \tan \theta_0 : \text{Elastic coupling between vertical and in-plane bending due to rotation of the blade principal axes about the pitch axis.}$$

$$\frac{P_7}{S_7} = T_7 = \sin(\Delta a_n)$$

Change in direction of the ζ coordinate due to spanwise increment in static blade coning.

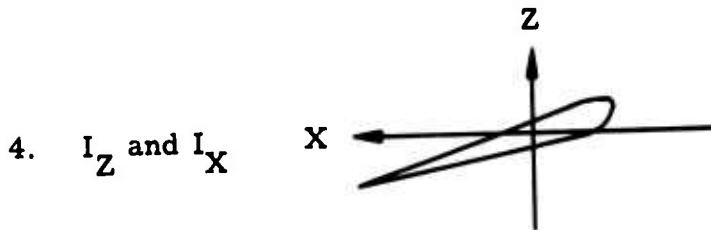
3.4 Definitions of Mechanical Qualities

Geometrical Qualities



Other Terms

1. EI_f : Flapwise bending stiffness
2. EI_c : Chordwise bending stiffness
3. GJ : Torsional stiffness



I_Z = Mass moment of inertia through cg about vertical axis

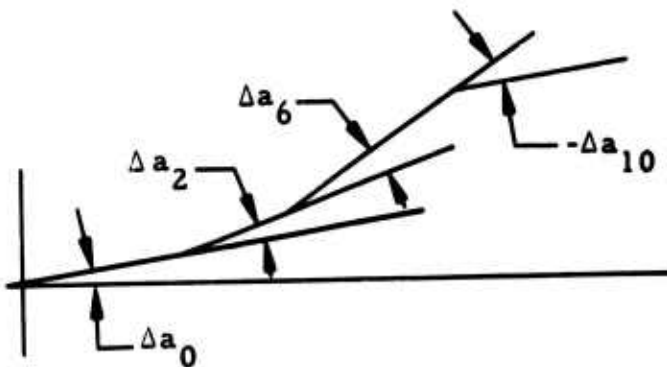
I_X = Mass moment of inertia through cg about horizontal axis

For flat blades: $I_Z - I_X \approx I_p \cos(2\theta_0)$

where I_p = Mass moment of inertia of blade about cg

5. θ_0 = Local pitch angle of blade relative to cone of rotation

6. Δa_n = Change of (static) spanwise blade slope.
 Δa_n may be changed at about 4 points. For example:



7. T_n : Tension in blade

$$T_n = \Omega^2 \sum_{i=n}^N m_i r_i$$

where

m_i = mass at i^{th} station

r_i = radius from axis to i^{th} station

Ω = rotation frequency

N = last station (at tip)

NOTE: It is important that the number and location of stations used in computing T_n be identical to those used in the idealized model.

8. X_{T_i} : Inboard tension axis

X_{T_O} : Outboard tension axis

$$X_{T_i} = - \frac{M_{\zeta_i}}{T_n} \quad X_{T_O} = - \frac{M_{\zeta_O}}{T_n}$$

M_{ζ_i} is the (static) chordwise bending moment about the reference axis just outboard of the $n-1^{\text{st}}$ station.

M_{ζ_O} is the (static) chordwise bending moment about the reference axis just inboard of the n^{th} station.

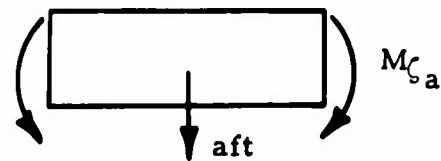
Formulas for computing X_{T_i} and X_{T_O} :

$$X_{T_i} = X_{fa} + r_{n-1} \frac{\sum_{i=n}^N m_i (X_{cgi} - X_{fa})}{\sum_{i=n}^N m_i r_i} - \frac{M_{\zeta_{a, n-1}}}{T_n}$$

$$X_{T_O} = X_{fa} + r_n \frac{\sum_{i=n}^N m_i (X_{cgi} - X_{fa})}{\sum_{i=n}^N m_i r_i} - \frac{M_{\zeta_{a, n}}}{T_n}$$

where X_{fa} = location of blade feathering axis, that is, the axis that passes through the center of rotation.

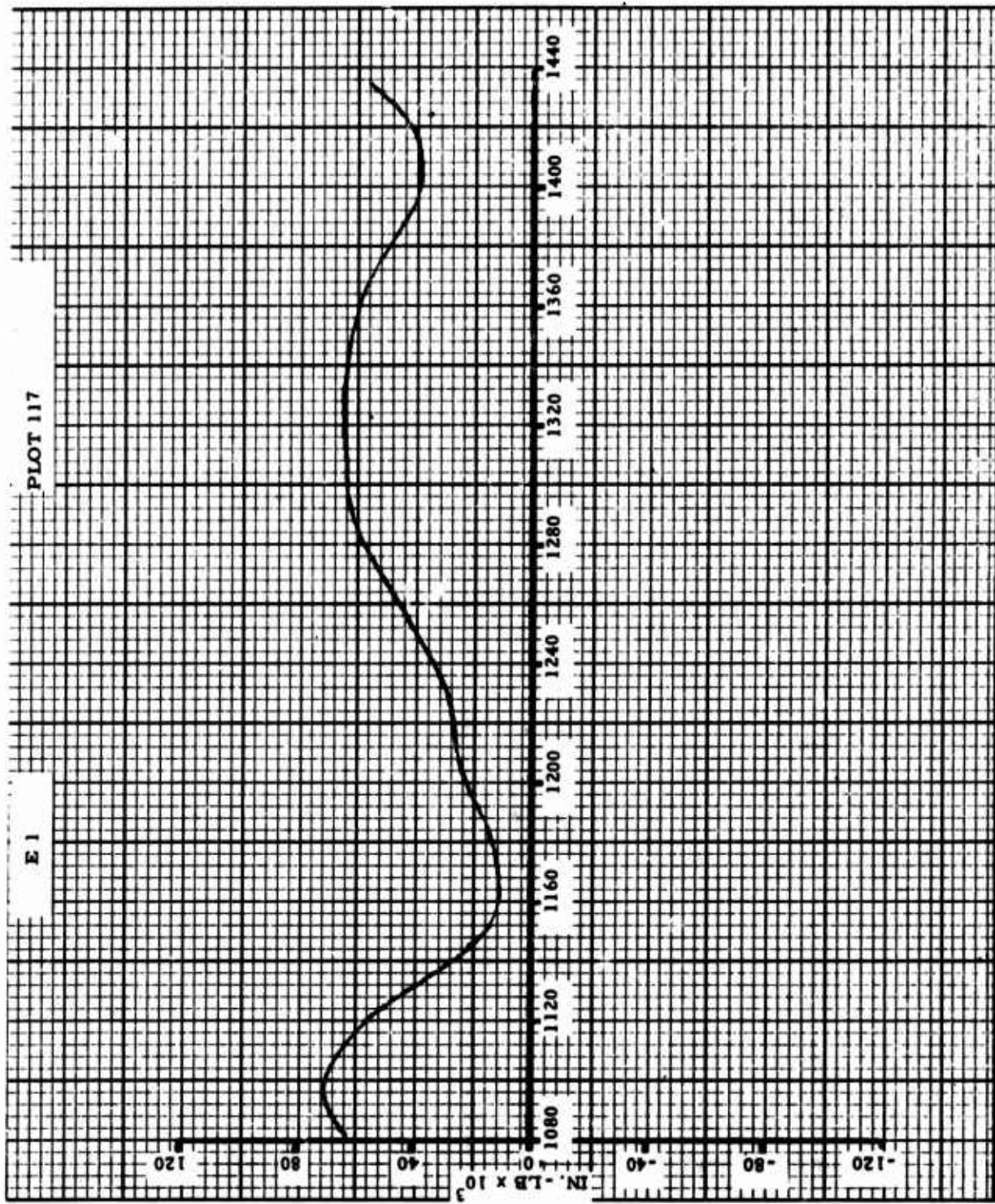
$M_{s,a,n}$ is the (static) chordwise bending moment due to aero-dynamic drag about the reference axis, at the n^{th} station.

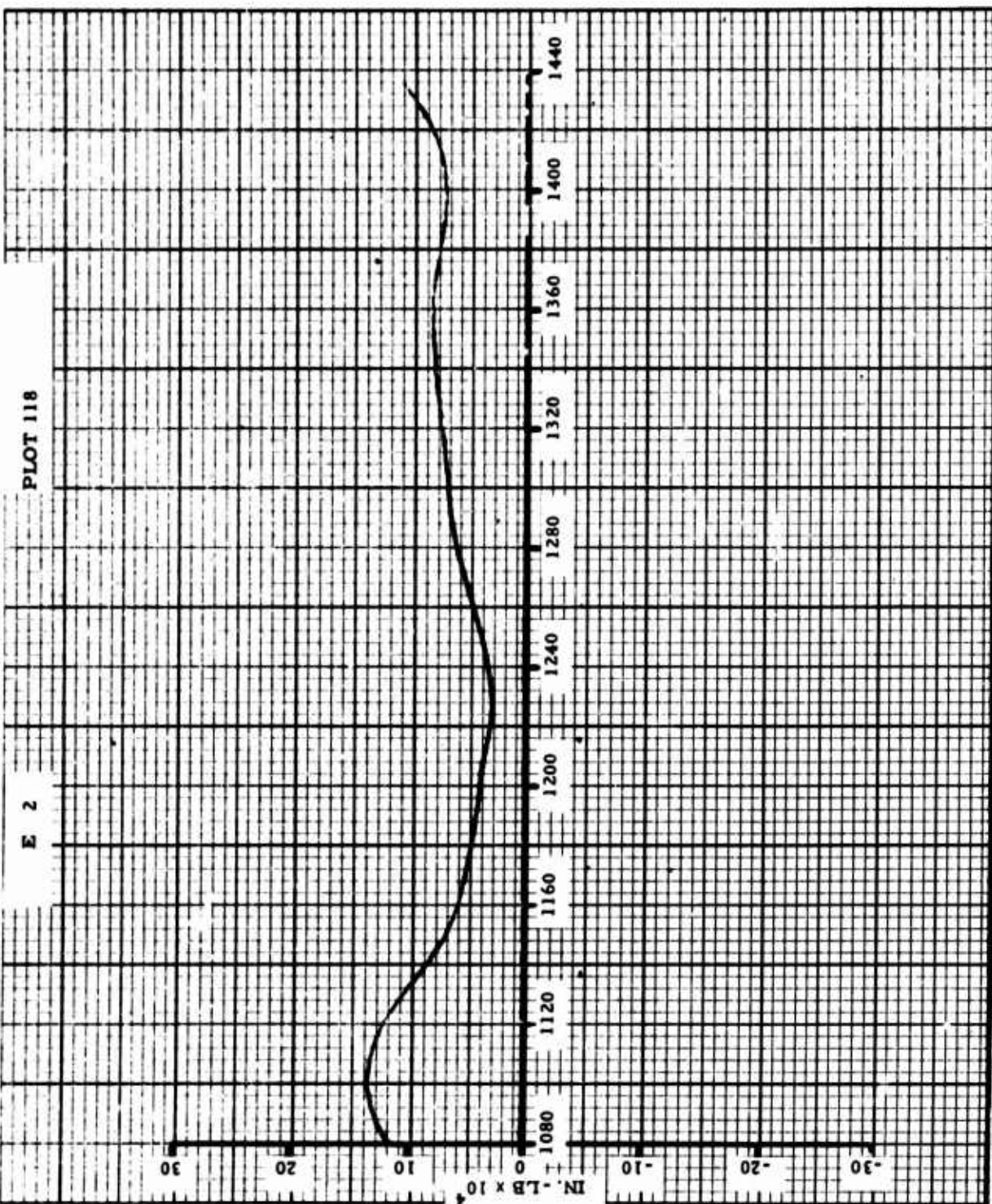


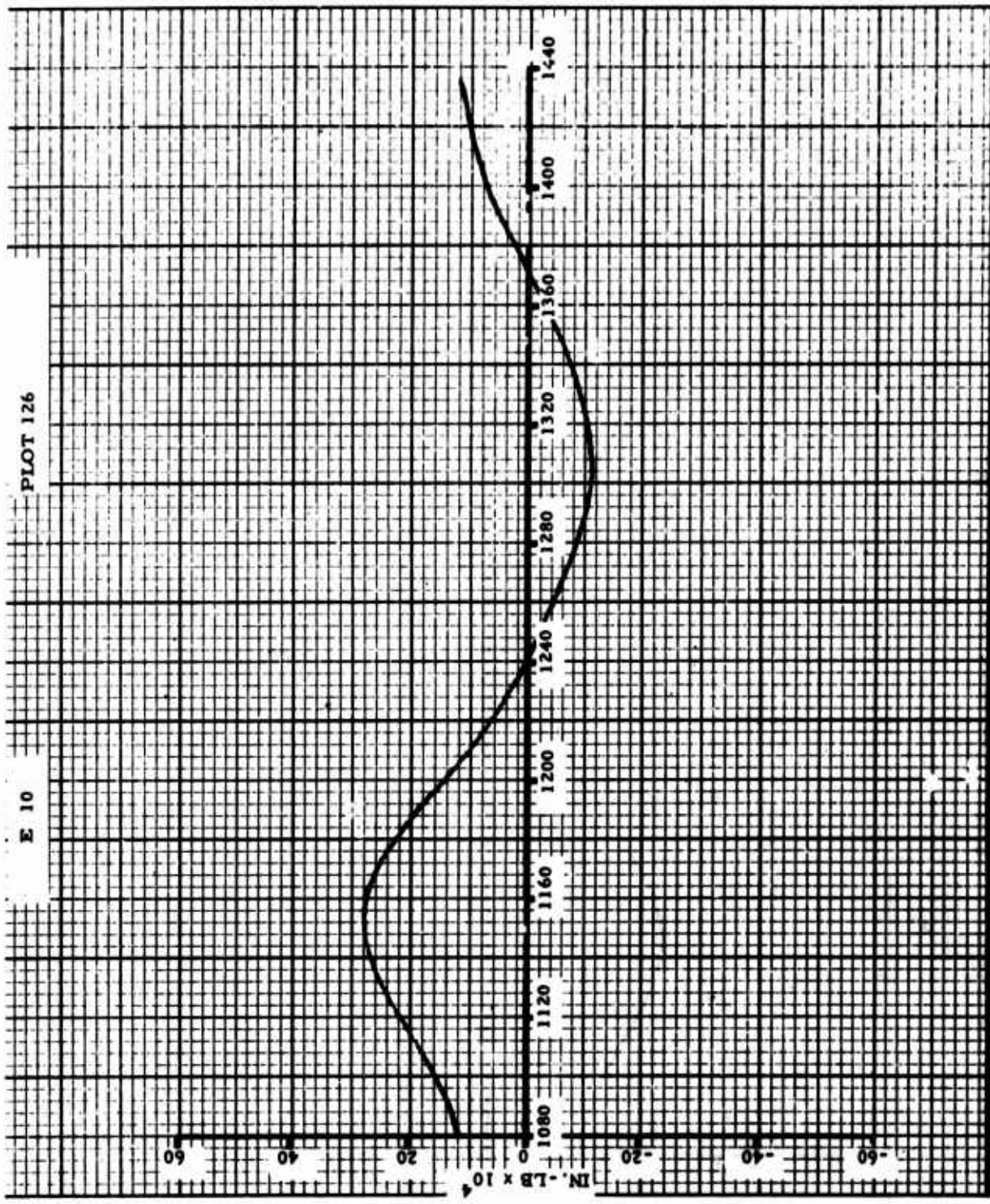
NOTE: It is important that the number and location of stations used in computing $M_{s,i}$ and $M_{s,O}$ be identical to those used in the idealized model.

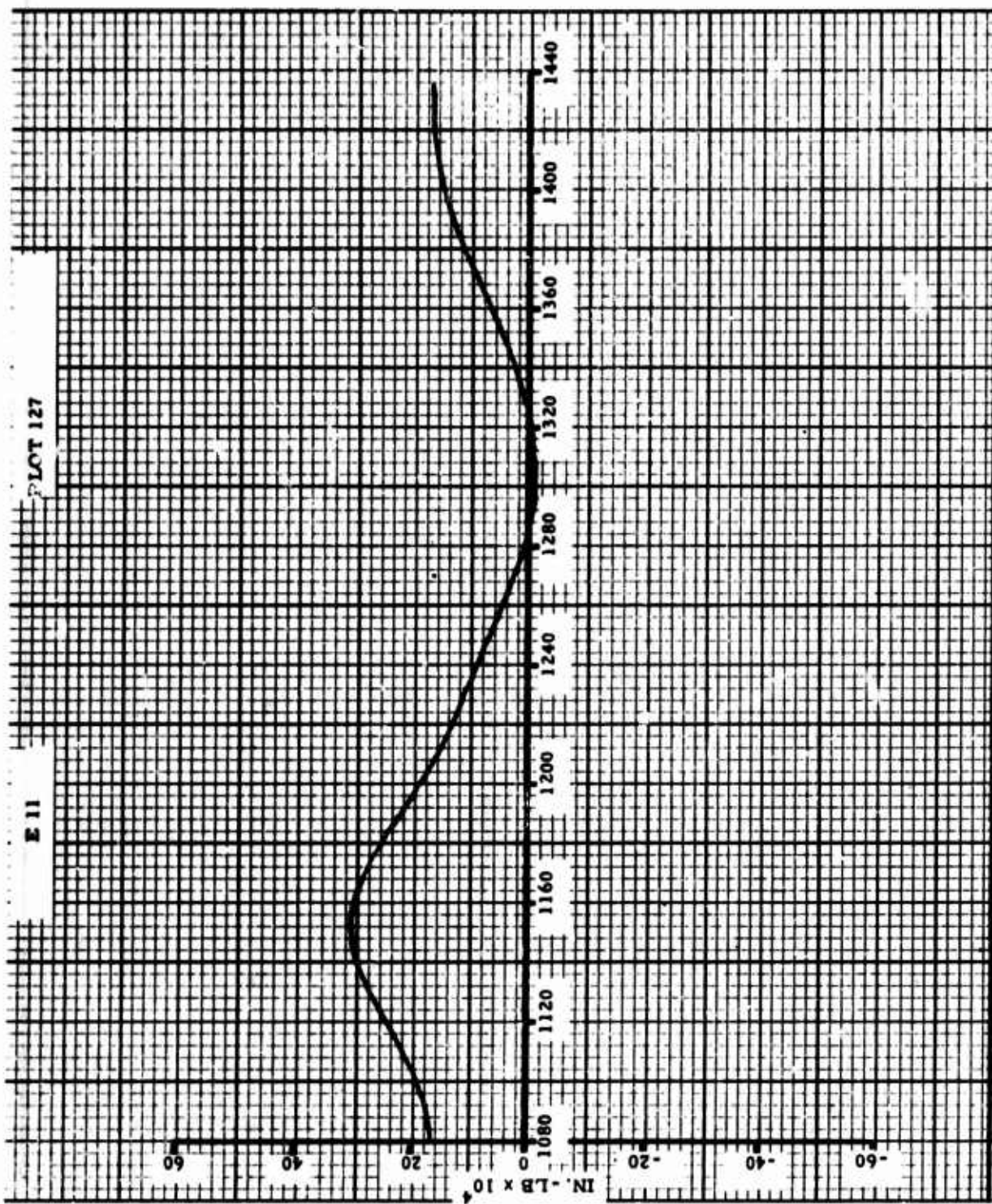
APPENDIX VI
TYPICAL SAMPLES OF COUPLED ANALYSIS
UNMODIFIED COMPUTER OUTPUT

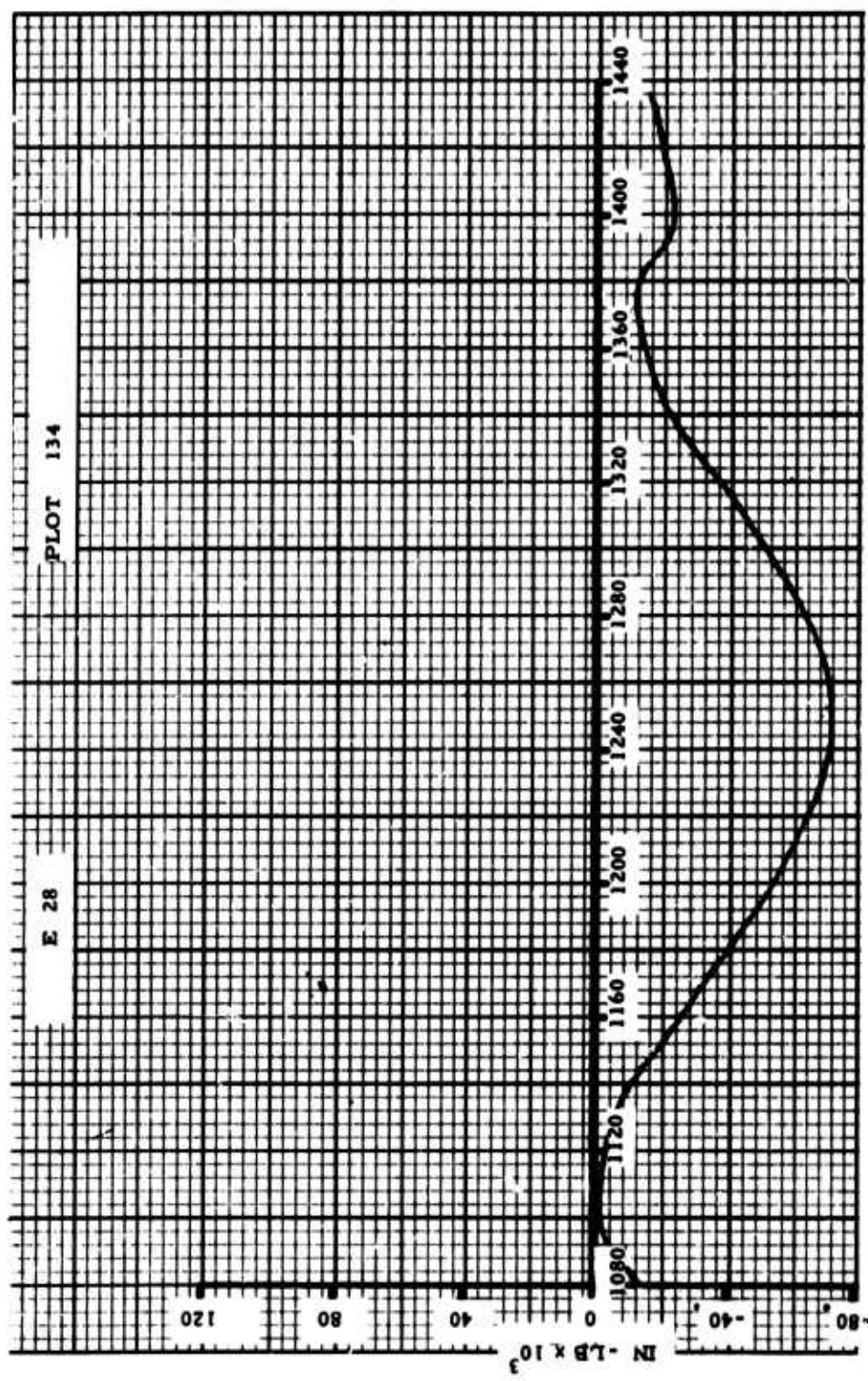
This appendix presents six typical unmodified computer output plots of loads versus azimuth angle (in degrees) for a series of blade stations. Spanwise plots presented as Figures 51 through 54 in the section of this report titled Fully-Coupled Blade Response and Dynamic Stability Analysis Using SADSAM IV were derived from these computer plots. The flight condition represented is level, unaccelerated cruise at 110 knots, 675-fps tip speed, 60,000-pound gross weight, and sea level standard atmosphere. Plots are numbered the same as the elastic elements (K's) in the Connection Diagram - Heavy-Lift Helicopter Blade Structure in Appendix IV, page 345. For example, plot E-69 is the load element K-69 (total vertical force per blade), and plot E-28 is the moment in element K-28 (blade root torsion).

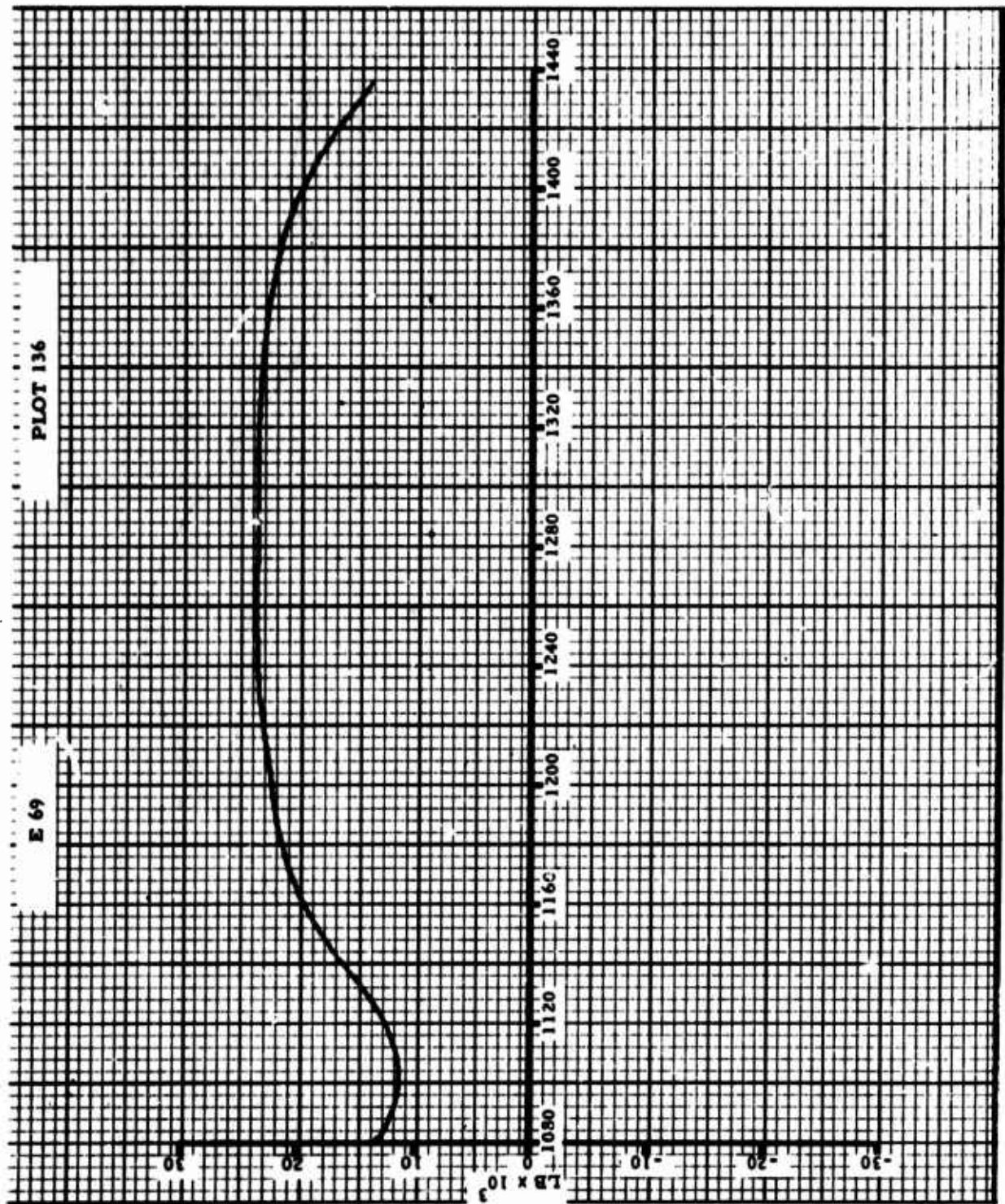












UNCLASSIFIED

Security Classification

DOCUMENT CONTROL DATA - R&D

(Security classification of title, body of abstract and indexing annotation must be entered when the overall report is classified)

1. ORIGINATING ACTIVITY (Corporate author) Hughes Tool Company - Aircraft Division Culver City, California		2a. REPORT SECURITY CLASSIFICATION Unclassified
2b. GROUP		
3. REPORT TITLE PRELIMINARY DESIGN OF A ROTOR SYSTEM FOR A HOT CYCLE HEAVY-LIFT HELICOPTER		
4. DESCRIPTIVE NOTES (Type of report and inclusive dates) Final Report, 17 March 1965 through 31 August 1966		
5. AUTHOR(S) (Last name, first name, initial) Simpson, John R.		
6. REPORT DATE March 1967	7a. TOTAL NO. OF PAGES 393	7b. NO. OF REFS 25
8a. CONTRACT OR GRANT NO. DA 44-177-AMC-225(T) Task II	8a. ORIGINATOR'S REPORT NUMBER(S) USAABLabs Technical Report 67-1	
8b. PROJECT NO. Task 1F131001D15701	8b. OTHER REPORT NO(S) (Any other numbers that may be assigned to this report) HTC-AD 66-17	
10. AVAILABILITY/LIMITATION NOTICES Distribution of this document is unlimited.		
11. SUPPLEMENTARY NOTES	12. SPONSORING MILITARY ACTIVITY U.S. Army Aviation Materiel Laboratories Fort Eustis, Virginia	
13. ABSTRACT In a preliminary design study of a rotor system for a Hot Cycle heavy-lift helicopter, the following items were accomplished. (1) An analytical procedure was developed that permitted calculation of fully coupled blade response and dynamic stability characteristics; (2) parametric and configuration studies involving basic characteristics of the rotor system were conducted; (3) design layouts, structural design studies, and detailed weight analyses were made (design and analysis were limited to the integrated lift-propulsion system with emphasis on the rotor system); (4) preliminary design was completed, and performance of the optimum rotor for the heavy-lift mission requirements was determined; (5) a fully coupled blade loads analysis of the optimum rotor was made; and (6) a full-scale mockup of the rotor hub area was constructed. ()		

UNCLASSIFIED

Security Classification

14. KEY WORDS	LINK A		LINK B		LINK C	
	ROLE	WT	ROLE	WT	ROLE	WT
Hot Cycle Rotor System Heavy-Lift Helicopter						
INSTRUCTIONS						
1. ORIGINATING ACTIVITY: Enter the name and address of the contractor, subcontractor, grantee, Department of Defense activity or other organization (corporate author) issuing the report.	10. AVAILABILITY/LIMITATION NOTICES: Enter any limitations on further dissemination of the report, other than those imposed by security classification, using standard statements such as:					
2a. REPORT SECURITY CLASSIFICATION: Enter the overall security classification of the report. Indicate whether "Restricted Data" is included. Marking is to be in accordance with appropriate security regulations.	(1) "Qualified requesters may obtain copies of this report from DDC."					
2b. GROUP: Automatic downgrading is specified in DoD Directive 5200.10 and Armed Forces Industrial Manual. Enter the group number. Also, when applicable, show that optional markings have been used for Group 3 and Group 4 as authorized.	(2) "Foreign announcement and dissemination of this report by DDC is not authorized."					
3. REPORT TITLE: Enter the complete report title in all capital letters. Titles in all cases should be unclassified. If a meaningful title cannot be selected without classification, show title classification in all capitals in parentheses immediately following the title.	(3) "U. S. Government agencies may obtain copies of this report directly from DDC. Other qualified DDC users shall request through _____."					
4. DESCRIPTIVE NOTES: If appropriate, enter the type of report, e.g., interim, progress, summary, annual, or final. Give the inclusive dates when a specific reporting period is covered.	(4) "U. S. military agencies may obtain copies of this report directly from DDC. Other qualified users shall request through _____."					
5. AUTHOR(S): Enter the name(s) of author(s) as shown on or in the report. Enter first name, first name, middle initial. If military, show rank and branch of service. The name of the principal author is an absolute minimum requirement.	(5) "All distribution of this report is controlled. Qualified DDC users shall request through _____."					
6. REPORT DATE: Enter the date of the report as day, month, year; or month, year. If more than one date appears on the report, use date of publication.	If the report has been furnished to the Office of Technical Services, Department of Commerce, for sale to the public, indicate this fact and enter the price, if known.					
7a. TOTAL NUMBER OF PAGES: The total page count should follow normal pagination procedures, i.e., enter the number of pages containing information.	11. SUPPLEMENTARY NOTES: Use for additional explanatory notes.					
7b. NUMBER OF REFERENCES: Enter the total number of references cited in the report.	12. SPONSORING MILITARY ACTIVITY: Enter the name of the departmental project office or laboratory sponsoring (paying for) the research and development. Include address.					
8a. CONTRACT OR GRANT NUMBER: If appropriate, enter the applicable number of the contract or grant under which the report was written.	13. ABSTRACT: Enter an abstract giving a brief and factual summary of the document indicative of the report, even though it may also appear elsewhere in the body of the technical report. If additional space is required, a continuation sheet shall be attached.					
8b. 8c. & 8d. PROJECT NUMBER: Enter the appropriate military department identification, such as project number, subproject number, system numbers, task number, etc.	It is highly desirable that the abstract of classified reports be unclassified. Each paragraph of the abstract shall end with an indication of the military security classification of the information in the paragraph, represented as (TS), (S), (C), or (U).					
9a. ORIGINATOR'S REPORT NUMBER(S): Enter the official report number by which the document will be identified and controlled by the originating activity. This number must be unique to this report.	There is no limitation on the length of the abstract. However, the suggested length is from 150 to 225 words.					
9b. OTHER REPORT NUMBER(S): If the report has been assigned any other report numbers (either by the originator or by the sponsor), also enter this number(s).	14. KEY WORDS: Key words are technically meaningful terms or short phrases that characterize a report and may be used as index entries for cataloging the report. Key words must be selected so that no security classification is required. Identifiers, such as equipment model designation, trade name, military project code name, geographic location, may be used as key words but will be followed by an indication of technical context. The assignment of links, rules, and weights is optional.					

UNCLASSIFIED

Security Classification